

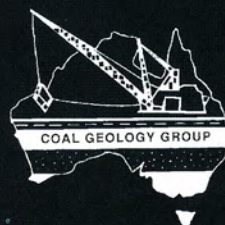
BOWEN BASIN SYMPOSIUM 2010

BACK IN (THE) BLACK



EDITED BY JW BEESTON

MACKAY ENTERTAINMENT AND CONVENTION CENTRE QUEENSLAND
6-8 October 2010



BOWEN BASIN SYMPOSIUM 2010

BACK IN (THE) BLACK

JW BEESTON
Editor

**ORGANISED BY
THE BOWEN BASIN GEOLOGISTS GROUP
AND
THE GEOLOGICAL SOCIETY OF AUSTRALIA INCORPORATED
COAL GEOLOGY GROUP**

MACKAY, QUEENSLAND 6-8 OCTOBER 2010

Organised by:

Bowen Basin Geologists Group and
GSA Inc Coal Geology Group

Organising Committee:

POSITION	INCUMBENT
Chairman	Todd Harrington
Secretary	Joan Esterle
Treasurer and Venue Coordinator	Renate Sliwa
Paper and Media Coordinator	Wes Nichols
Poster Paper Coordinator	Mark Biggs
Proceedings Publisher/Editor	Jim Beeston
Workshop Coordinator	Merryl Peterson
Sponsorship and Booth Coordinator	Troy Peters
Entertainment Coordinators	Warwick Smith, Mark Hayward
Satchels and Merchandise Coordinator	Adrian Buck
Flyer Coordinator	Chris McMahon
Active committee members covering numerous items	Doug Dunn, Jason Moultrie, Simon Brady, Peter Crosdale
Silent but willing committee members	Georgina Rees, Nick Gordon

Representing the GSA Coal Geology Group:

Wes Nichols (Chairman, GSA Coal Geology Group)
Mark Biggs (Secretary, GSA Coal Geology Group)
Peter Crosdale (Treasurer, GSA Coal Geology Group)
Jim Beeston (Editor, GSA Coal Geology Group)

Proceedings prepared by: JW & SA Beeston

Proceedings published by: GSA Coal Geology Group

(This proceedings volume is a peer-reviewed publication of the Coal Geology Group of the Geological Society of Australia Inc)

© Geological Society of Australia Inc

Issued: October 2010

ISBN: 978-0-646-54347-5

Printed by: Impulse Digital Printing

Reference guides:

BEESTON, J.W. (Editor), 2010: *Bowen Basin Symposium 2010 — Back in (the) Black*. Geological Society of Australia Inc. Coal Geology Group and the Bowen Basin Geologists Group, Mackay, October 2010.

ZHOU, B., HATHERLY, P., PETERS, T. & SUN, W., 2010: Seismic imaging of coal seam structure under basalt cover. *In* Beeston, J.W. (Editor): *Bowen Basin Symposium 2010 — Back in (the) Black*. Geological Society of Australia Inc. Coal Geology Group and the Bowen Basin Geologists Group, Mackay, October 2010, 139–148.

CONTENTS

COAL QUALITY

- 1 Beamish & Beamish Self-heating rate of torbanite from the Bowen Basin, Queensland
- 7 Comino, Warren & O'Brien Applying the Coal Grain Analysis (CGA) method on liberation studies in coal
- 17 O'Brien, Meyers & Cameron Standardised washability through advances in borecore data unification
- 27 Permana, Ward, Li, Gurba & Davison Mineral matter in the high rank coals of the South Walker Creek area, Northern Bowen Basin
- 35 Lambert, Campbell, Ryan, Rooker, McLennan & Coffey Further refinement of the clean process technologies ultimate froth flotation test
- 43 McMahon Coal quality reconciliation and quality assurance/quality control
- 49 de Jongh & Smith Extracting value from coal remnants and pillars — quality modelling in previously mined coal seams
- 57 Metcalfe, Nicoll, Crowley, Mundil, Denyszyn, Schmitz & Foster Application of high-precision CA-IDTIMS U-Pb zircon dating to Permian – Lower Triassic stratigraphy in eastern Australian coal basins

COAL SEAM GAS

- 59 Burra Application of domains in gas-in-place estimation for opencut coal mine fugitive gas emissions reporting
- 65 Pinetown, Sherwood & Saghafi The influence of coal maceral composition on gas contents in the Hunter Coalfield

DATABASE AND MODELLING

- 73 Bax Inheriting a deficient and defective database — the repair challenge
- 77 Williams, Noppe & Carpenter Coal quality estimation error — Ordinary kriging challenges inverse distance
- 89 Martinez Strategic coal mine planning project using an integrated real options model approach
- 97 Yacopetti & Mundell Improving the quality of geoscientific information

ENVIRONMENTAL MANAGEMENT

- 101 Saghafi A Tier 3 method for estimating fugitive emissions from open cut coal mining: application to Bowen Basin Coalfields
- 111 Thomson Gas layering in the subsurface: implications for greenhouse gas emissions

EXPLORATION

- 117 Ferenczi Bowen Basin coal exploration and mine developments 2005–2010

GEOPHYSICS

- 123 Peters, Rich & Strong Seismic reflection, a useful tool to assist underground coal gasification (UCG)

- 131 Dirstein & Fallon Automated Interpretation of 3D seismic data using genetic algorithms
- 139 Zhou, Hatherly, Peters & Sun Seismic imaging of coal seam structure under basalt cover
- 147 Hatherly & Medhurst Additional opportunities for geophysical log analysis
- 153 Opperman A new workflow for high-resolution fault imaging delivers groundbreaking insights into resource operations and recoveries

GEOSTATISTICS

- 159 Casley, Bertoli, Mawdesley & Dunn Drill hole spacing analysis for coal resources
- 163 Casley, Bertoli, Mawdesley, Davies & Dunn Benchmarking estimation methods for coal resource estimation

GEOTECHNICAL

- 169 Rosengren, Simmons, Maconochie & Sullivan Geotechnical investigations for open pit mines — 250m and beyond
- 181 Maconochie, Soole & Simmons Validation of a simple one person method for structural mapping using Sirovision
- 185 Thomson Imaging systems for geotechnical boreholes – Slim Borehole Scanner

MINING GEOLOGY

- 191 Harding, Hernandez & Fleming A geological solution at Cerrejón, Colombia

SAFETY

- 201 Nichols Implementing a Stepchange in Safety Culture — a Case Study in Managing Safety

DIAMOND SPONSORS



acQuire is the premier Geoscientific Information Management System (GIMS) in the marketplace. Our solution is designed to assist mining businesses with the capture, management, interrogation and delivery of original observations and measurements. Resource estimates and sub-surface models all depend on quality information. These, in turn, are used to underpin the intrinsic value of the geological asset. Fundamentally, data integrity starts in the field and acQuire provides innovative technologies to encourage validation of geological information at the point of capture. The acQuire solution can assist the mining business in the asset discovery, asset development and asset production phases. acQuire is utilised by people and businesses that demand confidence in their data assets and who need consistent standards coupled with a flexible, robust and efficient system.

Anglo American's metallurgical coal business unit is one of Australia's leading producers and exporters of metallurgical coal, with extensive coal mining interests in Queensland and New South Wales. We are committed to creating value from coal responsibly, pursuing growth through our attractive project pipeline and investing in the communities in our areas of operation. We strive to achieve gender diversity within our workforce, and women are strongly encouraged to apply for all vacant positions. A part of Anglo American, we are helping to build the leading global mining company.



BHP Billiton Mitsubishi Alliance

BHP Billiton Mitsubishi Alliance (BMA) is the world's largest seaborne coking coal supplier. BMA operates seven mine sites and a coal loading port in Central Queensland. Located in both Brisbane and our Central Queensland Office near Moranbah, the Resource Development Group (RDG) is committed to adding value to BMA's operations by providing expertise in Exploration and Geological Services, Strategic Mine Planning, Underground Strategy, and Development and Research. The RDG includes our high performing Geological Services team: geologists and support staff that operate as internal consultants, providing centralised exploration services and geological support to our operating mines, as well as development and grassroots exploration projects. The size and magnitude of our business provides significant opportunity for professional development, attractive salary packages with performance based bonuses, unique BHP Billiton employee share programs and access to the BHP Billiton superannuation program.

The **Moultrie Group** of companies provides contracting and consulting services in the fields of geology, surveying, database & modelling, safety & training, site rehabilitation, polyethylene pipe and gas developments and underground mining and maintenance. We also hire out compressors, earth moving and underground equipment. We pride ourselves on the range and quality of our services and expertise, the meticulous servicing of our mine compliant equipment, and our safety record. Moultrie Group's service quality has been recognised through expanded business opportunities with a number of major mining houses. We service all of the major coal and coal seam gas producing areas including Central Queensland (Bowen Basin), the Darling Downs, northern New South Wales and the Hunter Valley region of New South Wales through Moultrie Group's offices in Mackay, Brisbane and Newcastle. Moultrie Group – quality and experience you can rely on.



Macarthur Coal (ASX: MCC) is a Queensland success story. The Company's vision is to be an independent, growth focused coal company delivering long-term shareholder value. Listed in 2001, it is now the world's largest producer of seaborne low volatile pulverised coal injection (LV PCI) coal. The Company's focus is on high margin or low cost coal assets with a strong market demand and product diversification capability. The principal activities of the Company are exploration, project evaluation, project development and coal mining activities in Queensland's Bowen Basin. Coal sales and marketing are undertaken globally. The Company's goal is to double its 2009 production to achieve sales of 9.2mtpa by 2014. To achieve this, Macarthur Coal will focus on two strategic objectives – operational excellence and sustainable growth. Macarthur Coal's major assets are: a 73.3% share in Coppabella Mine and Moorvale Mine through the Coppabella and Moorvale Joint Venture (CMJV), and a 72.48% share of the Middlemount Mine project.

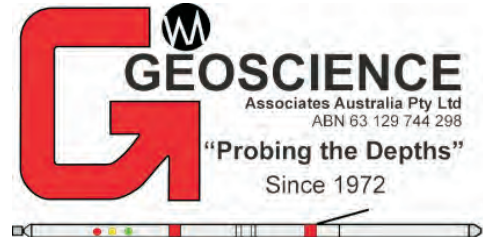
Velseis Pty Ltd is a highly experienced Australian seismic contractor, offering fully integrated seismic services to the coal, petroleum and mineral industries locally and overseas. Providing comprehensive 2D and 3D seismic data acquisition services, Velseis utilises dynamite, Mini-SOSIE and 'Envirovibe' Vibroseis techniques. Additionally, Velseis acquires multi-component, heli-portable, and shallow marine data as well as providing a specialised shot hole drilling service through its Seisdrill division. With a highly experienced seismic processing and interpretation division, Velseis delivers high-quality 2D and 3D onshore, transition and marine processing and interpretation services to the coal and petroleum sectors. Velseis maintains its competitiveness with a proactive commitment to research and development. The R&D division engages in focussed research projects, and provides technical support to production divisions. Velseis is Australia's only fully integrated seismic service company.





Xstrata Coal is the world's largest exporter of thermal coal and one of the largest producers of hard coking coal, producing both premium quality hard coking coal and semi-soft coal. Headquartered in Sydney, Australia, Xstrata Coal has interests in over 30 operating coal mines throughout Australia, South Africa and Colombia. It is a wholly owned subsidiary of Xstrata plc. The Xstrata Coal business is world scale, with consolidated production of more than 100 million tonnes in 2009, of which about 80% is exported. Approximately 75% of revenue is earned from Australian businesses. Xstrata Coal has an unmatched pipeline of competitive coal projects across all of its geographies, with the potential to approximately double the scale of the business. The Company employs more than 16 000 people (including contractors) across its underground and open cut mines, the majority of which are located in the NSW Hunter Valley, QLD's Bowen Basin and the Witbank area in South Africa. Xstrata Coal contributes to a broad range of education, health, arts, environmental and skills development initiatives within each of the countries in which it operates, to make a positive and significant difference to the communities that support its local and regional operations.

Geoscience Services QLD has been established since 1972 and exclusively offers downhole wireline services to the Exploration and Mining Industry. In 2009 our company was purchased by UXA, an ASX listed Company. With our Head office in Mt Barker SA, we have now extended our operation into Queensland, with offices in Rockhampton and Moranbah, and a field presence in Emerald. Geoscience Services is the choice logging service provider to the coal industry, combining the provision of 'state of the art' quality logs with dependable timely delivery. Capable of wireline logging up to depths of 1800 metres we offer an extensive range of tools including, Density, Natural Gamma, Bulk Density, Full way Sonic, Electrical logs, Calliper, Neutron, Verticality, Acoustic Televiwer Imaging, Gyro, Temperature, Interpretation and Processing Services



Ultramag Geophysics is an industry leader in applying potential field geophysics to coal exploration and mining. Ultramag pioneered high-resolution ground magnetic surveys in the coal industry in 1995, shortly to be followed by our Ferret 1 & 2 borehole magnetometers. These instruments are used to map a wide range of occluded geological hazards including dykes, plugs, sills, faults, siderite, paleo-channels, diatremes and burn zones. Ultramag is now pioneering high-resolution ground based radiometrics for mapping acidic/non-magnetic intrusions and faults. We also offer regional and micro gravity surveys for a wide range of coal related applications including: mapping basin shape, locating near surface thick coal pods, faults, rolls, dyke density (harness) and looking beneath surface basalts where seismic surveys flounder. Ultramag Geophysics develops in-house geophysical instrumentation and software and is known as an innovator in the industry. Our new iPhone magnetometer is setting a new benchmark in instrument portability and safety with secure real-time data reporting capability (including operator location) to any computer on the internet. Complementing our geophysical survey service, Ultramag Geophysics offers a range of customised geophysical data processing services and most importantly a quality interpretation service where experienced geophysicists integrate 'your' geology.

Bureau Veritas is synonymous with quality, professionalism and integrity. We are global leaders in Minerals Services, Asset Integrity & Reliability Services, Risk & Safety Engineering, HSE Services and Management System Certification. Certified to ISO 9001 for all of its activities globally, Bureau Veritas is well known for its ability to adapt to changing client environments and situations and for its commitment to providing leading solutions through quality service. With a network of 900 locations and 39 000 employees in more than 140 countries, Bureau Veritas provides solutions to over 370 000 clients throughout the world across a diverse range of industries. The core competency of the Bureau Veritas Minerals Group (Coal Services) is to service the technical needs of the Australian minerals industry by providing analytical facilities, technical support and consulting services. Our expert local and worldwide network helps our Australian and international clients achieve their objectives.



GeoConsult is a progressive and multi-disciplinary company of consulting geoscientists and affiliated industry professionals offering a complete range of project management, field, analytical and reporting services in: Mining, Mineral and Petroleum Resource Exploration; Geotechnical Site Investigation and Mining Geology; Geophysics, Coal Quality, Resource Analysis, and Geological Modelling; Coal Seam Gas, Well Site Geology and Laboratory Services; and Research and Development. GeoConsult is a Queensland based Australian-owned company, established in 1994, with services extending throughout Australia and South East Asia. GeoConsult can provide experienced, qualified and reliable consultants who are capable of using the most advanced geological methods and computing facilities to maintain a high standard of technical excellence and efficiency to our clients. Recognition of our experience and competence in a broad spectrum of projects has established long-standing relationships and a respected reputation with a wide range of operators and managers, project developers, exploration and mining industry leaders. GeoConsult's Quality Assurance System is endorsed to AS/NZS ISO 9001:2008, and its laboratory is NATA accredited. The company is responsive to the personal aspirations of its staff and group affiliates and is dedicated to providing a technically stimulating work environment. The benefits of this philosophy are reflected in the high degree of innovation and professionalism applied to projects.

GRAPHITE SPONSORS

Santos

ANTHRACITE SPONSORS



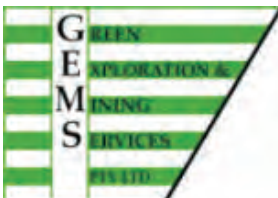
BITUMINOUS SPONSORS



Rio Tinto



LIGNITE SPONSORS



TRADE EXHIBITORS

BMA
MOULTRIE GROUP
VELSEIS
ACQUIRE TECHNOLOGY
XSTRATA COAL
GEOSCIENCE ASSOCIATES AUSTRALIA
GEOCONSULT
BUREAU VERITAS
ANGLO AMERICAN
ULTRAMAG GEOPHYSICS
GEOIMAGE
DOWNUNDER
RUNGE - GEOGAS
ADVANCED LOGIC TECHNOLOGY
SNOWDEN
GOLDER ASSOCIATES
MAPTEK
ALS
TERREX
EARTH DATA
SALVA
WEATHERFORD
PEARSON COAL PETROGRAPHY
COFFEY MINING
DOUGLAS PARTNERS
DATAMINE
PITNEY BOWES BUSINESS INSIGHT
SIGRA
MICROMINE

B Basil Beamish and Debra E Beamish

Self-heating rate of torbanite from the Bowen Basin, Queensland

Adiabatic oven tests provide a simple and accurate measure of the intrinsic spontaneous combustion propensity of coal. Results from these tests on coal samples from the Bowen Basin and Callide Basin show that coal rank, mineral matter and coal type have significant effects on self-heating rate. As rank increases from sub-bituminous A to medium volatile bituminous, the R_{70} self-heating rate index value decreases by a factor of 50. Increasing amounts of mineral matter in coal often lower the self-heating rate due to a simple heat sink effect, although there are instances where the mineral matter has a more complex physico-chemical effect due to pore structure interference. Torbanite (boghead coal) has a much lower R_{70} self-heating rate index value (approximately one fifth) than its humic coal rank equivalent. In addition, torbanite does not readily produce coal fines, which also contributes to lowering the propensity for spontaneous combustion.

INTRODUCTION

The self-heating of coal is due to a number of complex exothermic reactions that occur as soon as the coal is exposed to air. If there is a sufficient air supply and the heat produced is not dissipated thermal runaway is possible leading to spontaneous ignition. Relationships between coal properties (rank, mineral matter content and composition, maceral composition, and moisture content) and self-heating indices have been published from a number of studies (Humphreys, Rowlands & Cudmore, 1981; Moxon & Richardson, 1985; Singh & Demirbilek, 1987; Barve & Mahadevan, 1994; Beamish, Barakat & St George, 2001; Beamish, 2005; Beamish & Blazak, 2005; Beamish & Hamilton, 2005; Beamish & Clarkson, 2006; Beamish & Arisoy, 2008a; Beamish & Sainsbury, 2008; Beamish & Schultz, 2008; Beamish & Beamish, 2010).

However, to date there have been no reported self-heating studies of torbanite (boghead coal) despite their importance as sources of oil shale.

Torbanite, which is a form of sapropelic coal is distinguishable from humic coal by a more uniform, compact fine-grained texture and non-banded appearance that commonly displays conchoidal fractures (Han & others, 1999). The dominant maceral group of torbanite is liptinite, with the dominant maceral type being alginite. Previous research has suggested that the presence of liptinite in coal leads to a higher spontaneous combustion propensity (Walters, 1996).

However, Beamish, Barakat & St George (2001) were able to show that resin bodies present in low rank Waikato coals from New Zealand showed no self-heating propensity. More recent laboratory test work on liptinite-rich Surat Basin coals has shown that these coals have lower self-heating rates than their inertinite-rich rank equivalents.

A recent drilling program in the Bowen Basin has provided the opportunity to conduct self-heating tests on fresh cores of torbanite and coal from the same deposit. This paper presents a detailed analysis of the results of this work and compares the torbanite self-heating rate values against other coals from the Bowen and Callide Basins.

COAL SAMPLES AND R_{70} TESTING PROCEDURE

Sample characteristics

The coal samples tested in this study have been supplied as fresh cores from exploration and mining areas. They cover a rank range from sub-bituminous A to medium volatile

Table 1: Analytical and rank data for coal samples

Coal Sample	IM (%, adb)	Ash (%, db)	VM (%, dmmf)	CV (Btu/lb, mmmf)	ASTM Rank	Suggate Rank
Bowen Basin Torbanite	4.6	14.0	70.1	15003	hvCb	8.6
Bowen Basin hvCb	12.1	14.2	40.8	11205	hvCb	8.6
Trap Gully	10.5	9.8	27.6	11460	subA	7.1
Aries Seam	9.6	11.9	27.8	13027	hvBb	12.7
German Creek Seam	2.6	12.6	36.5	14700	hvAb	13.0
Goonyella Middle Seam	1.4	11.4	30.3	15391	mvb	14.3

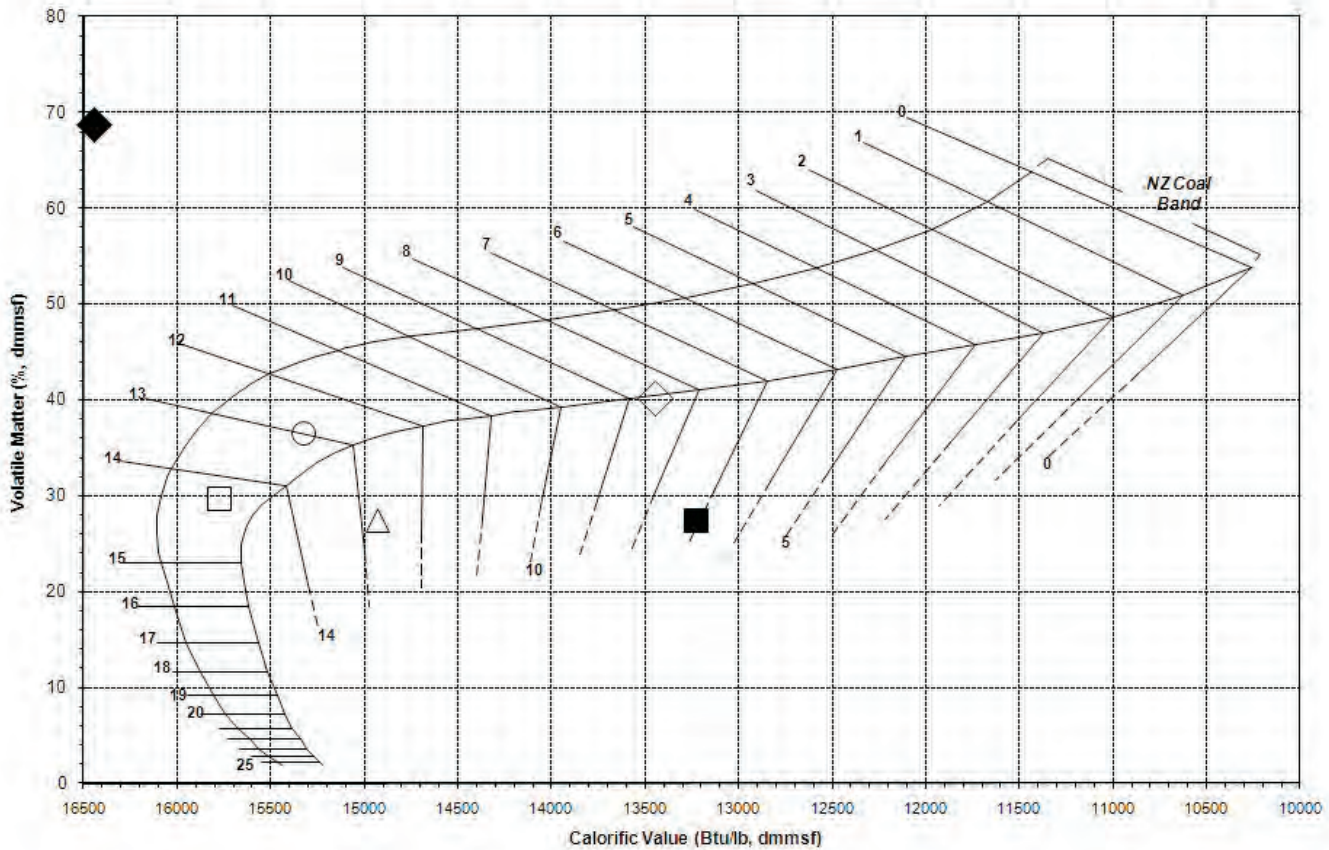


Figure 1: Suggate rank plot of Bowen and Callide Basin coal samples (see Figure 3 for legend)

bituminous (Table 1) and incorporate a mix of thermal and coking coal products. When viewed on a Suggate rank plot (Suggate; 1998, 2000) the samples range from 7.1 to 14.3 (Figure 1). This plot also shows the substantial differences in coal type between each sample. The Trap Gully and the Aries Seam samples plot below the New Zealand coal band, indicating they are inertinite-rich and are therefore mined as thermal coals. The German Creek Seam and Middle Goonyella Seam samples plot within the New Zealand coal band and are therefore vitrinite-rich coking coals. The Bowen Basin high volatile C bituminous (hvCb) coal sample plots at the lower boundary of the New Zealand coal band and is also a thermal coal product. The torbanite rank equivalent of this sample, from the same deposit, plots well above the New Zealand coal band due to its high liptinite content.

R₇₀ test procedure

The R₇₀ test procedure essentially involves drying a 150g sample of <212µm crushed coal at 110°C under nitrogen for approximately 16 hours. Whilst still under nitrogen, the coal is cooled to 40°C before being transferred to an adiabatic oven. Once the coal temperature has equilibrated at 40°C under a nitrogen flow in the adiabatic oven, oxygen is passed through the sample at 50mL/min. A data logger records the temperature rise due to the self-heating of the coal. The average rate at which the coal temperature rises between 40°C and 70°C is the initial self-heating rate index (R₇₀), which is in units of °C/h and is a good indicator of the intrinsic coal reactivity towards oxygen.

RESULTS AND DISCUSSION OF R₇₀ TESTING

Examples of R₇₀ determination

The self-heating rate curves for the Bowen Basin high volatile C bituminous coal and the sample from the adjacent torbanite layer are shown in Figure 2 along with their respective R₇₀ values and tie lines showing how these values have been determined. R₇₀ values for the other samples have been determined in the same manner and the full set of results is contained in Table 2. The R₇₀ values range from 0.32 to 16.22°C/h. The lowest value corresponds to the highest rank coal and the highest value corresponds to the lowest rank coal, which is consistent with the general perception of coal rank effect on spontaneous combustion propensity.

Intrinsic spontaneous combustion propensity classification

Interpreting the significance of the R₇₀ value for determining spontaneous combustion propensity has often been problematical for mining operations in the Bowen and Sydney Basins, particularly as there is a wider range of coals being mined than when the test was first developed for Queensland coals in the late 70s (Humphreys & others, 1981). Moreby (1997) reports that a coal with an R₇₀ value below 0.5°C/h is considered to be low propensity, 0.5–0.8°C/h medium propensity, while coals with an R₇₀ value higher than 0.8°C/h are considered to be highly prone to spontaneous combustion.

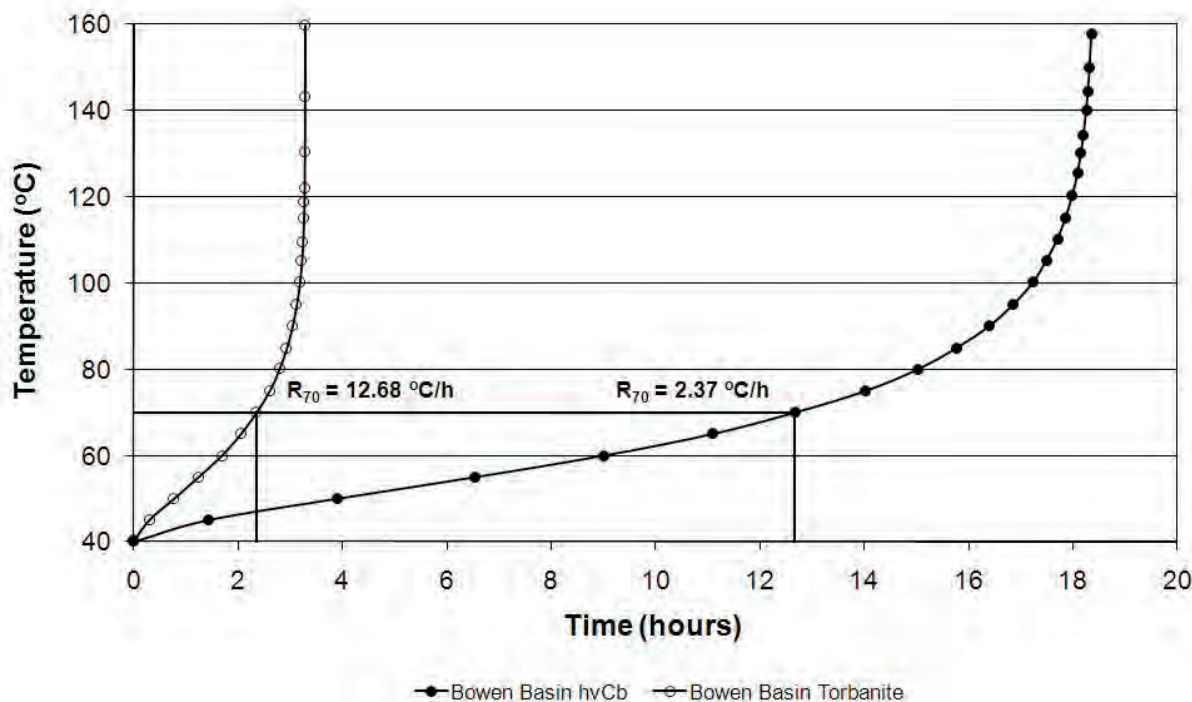


Figure 2: Examples of adiabatic self-heating curves obtained for R_{70} value determination

Table 2: R_{70} values of Bowen and Callide Basin coal samples

Coal Sample	R_{70} (°C/h)
Bowen Basin Torbanite	2.37
Bowen Basin hvCb	12.68
Trap Gully (9.8% ash, db)	16.22
Trap Gully (28.4% ash, db)	9.31
Trap Gully (39.1% ash, db)	5.98
Aries Seam	3.01
German Creek Seam	0.99
Goonyella Middle Seam	0.32

Using this classification would indicate that all the samples in this study except the Goonyella Middle Seam have a high propensity for spontaneous combustion. R_{70} values in the UQ database have been measured as high as 74.72°C/h for an Indonesian low rank coal. Therefore, a more refined classification scheme is needed to cover this range.

A simple scheme is shown in Table 3, which uses a self-heating rate doubling to distinguish between intrinsic spontaneous combustion propensity classes. This doubling effect of self-heating rate is somewhat analogous to the Arrhenius kinetics often applied to coal oxidation modelling. Table 3 also shows a distinction between Bowen Basin and Sydney Basin conditions to take into account the different ambient temperature of the operations, namely Bowen Basin ambient temperature conditions will be higher and therefore the coal self-heating will effectively have a head start.

As the R_{70} value is obtained on a dry basis, the best way to graphically represent the data is to plot it against the ash content (on a dry basis, Figure 3). The ash content is closely related to the mineral matter in the coal, which is the inorganic constituents of the coal that modify the coal behaviour in many combustion processes. In the case of the coal self-heating, the mineral matter often acts as a diluent, effectively creating a heat sink due to its heat capacity (Smith, Miron & Lazzara, 1988).

Mineral matter may also create blockage of access to oxidation sites, lowering the self-heating rate of the coal even further (Beamish & Arisoy, 2008a; Beamish & Sainsbury, 2008). A general trend of decreasing R_{70} value with increasing ash content can be seen in Figure 3 for the Trap Gully coals tested. The non-linearity of the trend (note the y-axis is logarithmic) was reported by Beamish & Blazak (2005) and further kinetic analysis by Beamish & Arisoy (2008b) showed that physico-chemical processes were most likely contributing to the self-heating behaviour of the samples.

Boundaries for each of the intrinsic spontaneous combustion propensity classes have been superimposed on Figure 3 to show which class each of the coals falls into. While the rank association with self-heating rate is strongly evident in Figure 3, the coal type effect is also very apparent.

The torbanite has a much lower self-heating rate than the humic coal rank equivalent (R_{70} of 2.37°C/h cf 12.68°C/h). This may be due to either the torbanite having a lower number of reactive sites for oxidation or access to the reactive sites is hindered due to the pore structure arrangement (for example pore blockages or an ultra fine pore structure). It should be noted that the torbanite is still classified as having a high intrinsic spontaneous combustion propensity under Bowen Basin conditions.

Table 3: Intrinsic spontaneous combustion propensity classification (ISCP), based on Queensland and New South Wales coal conditions

ISCP Class	Propensity rating	Queensland	New South Wales
		R_{70} value ($^{\circ}\text{C/h}$)	R_{70} value ($^{\circ}\text{C/h}$)
I	low (L)	$R_{70} < 0.5$	$R_{70} < 1$
II	low-medium (LM)	$0.5 \leq R_{70} < 1$	$1 \leq R_{70} < 2$
III	medium (M)	$1 \leq R_{70} < 2$	$2 \leq R_{70} < 4$
IV	high (H)	$2 \leq R_{70} < 4$	$4 \leq R_{70} < 8$
V	very high (VH)	$4 \leq R_{70} < 8$	$8 \leq R_{70} < 16$
VI	ultra high (UH)	$8 \leq R_{70} < 16$	$16 \leq R_{70} < 32$
VII	extremely high (EH)	$R_{70} \geq 16$	$R_{70} \geq 32$

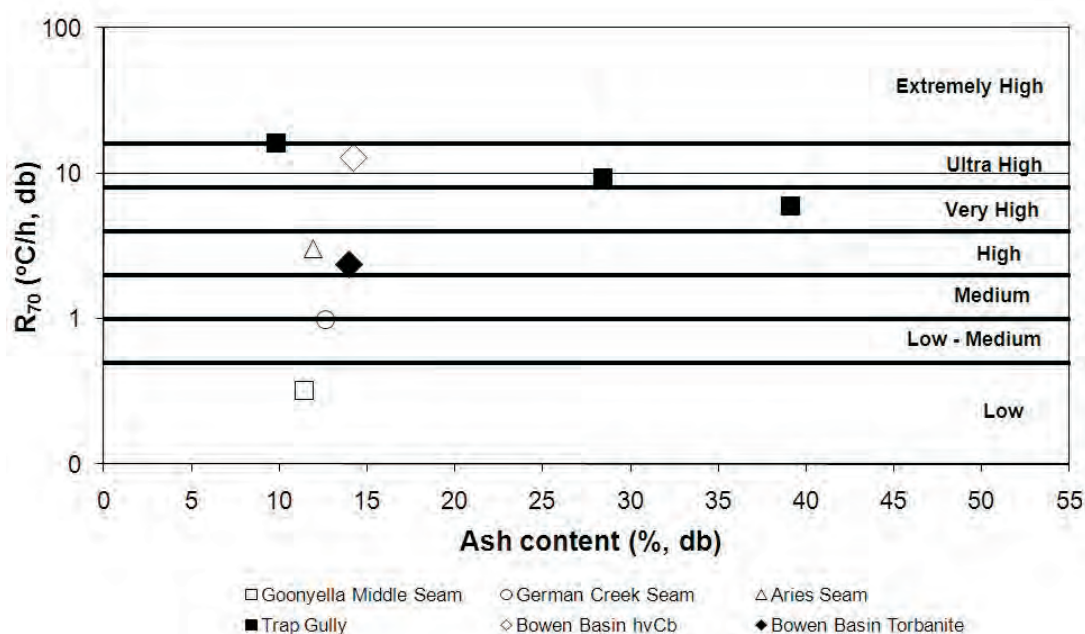


Figure 3: Relationship between ash content, coal rank and R_{70} self-heating rate for Bowen and Callide Basin coals with intrinsic spontaneous combustion propensity classes superimposed.

Other modifying influences on spontaneous combustion risk

The risk of self-heating generating a hot spot that leads to a spontaneous ignition event is moderated by various coal physical properties and mine site factors. The most important coal physical property from a mining and coal handling perspective is the ability of the coal to generate fines. Production of coal fines will enhance the reactivity of the coal through greater access of air to oxidation sites as a result of the increased surface area available for reaction to take place.

The ease of fines production is a property of the coal, which is best measured by the Hardgrove Grindability Index (HGI) value. High volatile C bituminous coals have low HGI values, generally somewhere between 45 and 55 (Mutton, 2003). Trimble & Hower (2003) showed that for coals of this rank with high liptinite contents the HGI value was even lower than 40. Hence the production of fine coal is significantly reduced for torbanite. This was evident in the preparation of the torbanite sample for adiabatic testing as it required

considerable energy to size reduce the core that was supplied. The tough nature of the torbanite therefore acts as a major moderating influence on its spontaneous combustion propensity.

CONCLUSIONS

Adiabatic self-heating tests show significant differences exist in the reactive nature of coals in terms of spontaneous combustion. The effect of coal rank on coal self-heating is readily apparent, but other factors such as coal type and mineral matter effects are also important. A large range of samples have now been tested from the Bowen Basin, including torbanite for the first time. The perception that liptinite-rich coals have a higher spontaneous combustion propensity is not supported by the results of this work. In fact the exact opposite has been established.

The R_{70} self-heating rate of a torbanite sample with an ash content of 14% (dry basis) has been determined to be

2.37°C/h. This compares with a humic coal rank equivalent value of 12.68°C/h. Such a considerable difference in self-heating rate can either be attributed to a reduction in reactive sites in the torbanite or lack of access to the reactive sites due to pore structure properties of the torbanite (for example blocked pores or an ultra fine pore structure).

Torbanite does not readily produce fines, primarily due to its high liptinite content. When this is combined with the lower self-heating rate it indicates torbanite has a reduced overall spontaneous combustion propensity.

ACKNOWLEDGEMENTS

The authors also would like to thank Dane Haukohl for going out of his way to supply the torbanite sample for testing.

REFERENCES

- BARVE, S.D. & MAHADEVAN, V., 1994: Prediction of spontaneous heating liability of Indian coals based on proximate constituents. In, *Proceedings of 12th International Coal Preparation Congress*, Cracow, Poland, 557–562.
- BEAMISH, B.B., 2005: Comparison of the R₇₀ self-heating rate of New Zealand and Australian coals to Suggate rank parameter. *International Journal of Coal Geology*, **64** (1-2), 139–144.
- BEAMISH, B.B. & ARISOY, A., 2008a: Effect of intrinsic coal properties on self-heating rates. In, *Proceedings 12th US/North American Ventilation Symposium, The Society of Mining, Metallurgy and Exploration Inc.*, 149–153.
- BEAMISH, B.B. & ARISOY, A., 2008b: Effect of mineral matter on coal self-heating rate. *Fuel*, **87** (1), 125–130.
- BEAMISH, B. & BEAMISH, R., 2010: Benchmarking moist coal adiabatic oven testing. In *Proceedings 10th Underground Coal Operators' Conference*, University of Wollongong and The Australasian Institute of Mining and Metallurgy, 264–268.
- BEAMISH, B.B. & BLAZAK, D.G., 2005: Relationship between ash content and R₇₀ self-heating rate of Callide coal. *International Journal of Coal Geology*, **64** (1-2), 126–132.
- BEAMISH, B. & CLARKSON, F., 2006: Self-heating rates of Sydney Basin coals — The emerging picture. In *Proceedings 36th Sydney Basin Symposium*, University of Wollongong, 1–8.
- BEAMISH, B.B. & HAMILTON, G.R., 2005: Effect of moisture content on the R₇₀ self-heating rate of Callide coal. *International Journal of Coal Geology*, **64** (1-2), 133–138.
- BEAMISH, B.B. & SAINSBURY, W., 2008: Development of a site specific self-heating rate prediction equation for a high volatile bituminous coal. In *Proceedings 8th Underground Coal Operators' Conference*, University of Wollongong and The Australasian Institute of Mining and Metallurgy, 161–165.
- BEAMISH, B.B. & SCHULTZ, T.J., 2008: Moisture content impact on self-heating rates of a highly reactive subbituminous coal. In *Proceedings 8th Underground Coal Operators' Conference*, University of Wollongong and The Australasian Institute of Mining and Metallurgy, 155–160.
- BEAMISH, B.B., BARAKAT, M.A. & ST GEORGE, J.D., 2001: Spontaneous-Combustion propensity of New Zealand coals under adiabatic conditions. In Lindsay, P. & Moore, T.A. (Editors): Geotechnical and environmental issues related to coal mining. *Special Issue, International Journal Of Coal Geology*, **45** (2-3), 217–224.
- HAN, Z., KRUGE, M.A., CRELLING, J.C. & BENSLEY, D.F., 1999: Classification of torbanite and cannel coal. 1. Insights from petrography analysis of density fractions. *International Journal of Coal Geology*, **38**, 181–202.
- HUMPHREYS, D., ROWLANDS, D. & CUDMORE, J.F., 1981: Spontaneous combustion of some Queensland coals. In *Proceedings Ignitions, Explosions and Fires in Coal Mines Symposium*, The Australasian Institute of Mining and Metallurgy: Illawarra Branch, 5-1 – 5-19.
- MOREBY, R., 1997: Dartbrook coal — Case study. In *Proceedings 6th International Mine Ventilation Congress, Society of Mining, Metallurgy and Exploration Inc.*, 39–45.
- MOXON, N.T. & RICHARDSON, S.B., 1985: Development of a self-heating index for coal. *Coal Preparation*, **2**, 91–105.
- MUTTON, A.J., 2003: *Queensland Coals 14th Edition*, Queensland Department of Natural Resources and Mines, Brisbane.
- SINGH, R.N. & DEMIRBILEK, S., 1987: Statistical appraisal of intrinsic factors affecting spontaneous combustion of coal. *Mining Science and Technology*, **4**, 155–165.
- SMITH, A.C., MIRON, Y. & LAZZARA, P., 1988: *Inhibition of Spontaneous Combustion of Coal*. US Bureau of Mines Report of Investigation, RI 9196.
- SUGGATE, R.P., 1998: Analytical variation in Australian coals related to coal type and rank. *International Journal of Coal Geology*, **37**, 179–206.
- SUGGATE, R.P., 2000: The Rank (S_r) scale: its basis and its application as a maturity index for all coals. *New Zealand Journal of Geology and Geophysics*, **43**, 521–553.
- TRIMBLE, A.S. & HOWER, J.C., 2003: Studies of relationship between coal petrology and grinding properties. *International Journal of Coal Geology*, **54** (3-4), 253–260.
- WALTERS, A.D., 1996: Joseph Conrad and the spontaneous combustion of coal – Part 1. *Coal Preparation*, **17**, 147–165.

Penny Comino, Karryn Warren, and Graham O'Brien

Applying the Coal Grain Analysis (CGA) method on liberation studies in coal

Coal Grain Analysis (CGA) is an optical microscopic imaging method that is used for routine coal petrography assessments (maceral composition and coal rank) and for obtaining compositional information on individual coal grains, enabling coal grain analysis. This method was used to evaluate two coal exploration areas within the Bowen Basin, Central Queensland for liberation improvements by further crushing.

The first case study investigated the liberation potential of five individual coal ply samples, collected from the LD 200mm diameter core, to assess whether a low ash coking product could be produced. It was surmised that if the mineral component was able to be liberated by crushing, then the ash content could be lowered, thereby producing a low ash coking coal product. Therefore a detailed knowledge of the maceral and mineral associations using CGA, could identify coals that are more economically suited to produce low ash coking coals.

The second study investigated the liberation potential of a coal seam to assess whether the sulphur content could be reduced at a target ash 8%. Samples of three different seams from six boreholes were taken from a mine in the Bowen Basin, Central Queensland. CGA was used to determine if the sulphur could be liberated from other mineral and maceral associations within the coal, therefore enabling a reduction of sulphur content in the product.

Both studies showed that there was modest liberation potential to produce a low ash coking coal product and to reduce the sulphur content of the coal. The limited liberation of the coals produced very minor increases in yield when washability curves were examined at a targeted ash of approximately 8%.

Key words: liberation, target ash, coal grain analysis, yield, sulphur, washability

INTRODUCTION

New areas for coal mining are regularly assessed to determine the quantity and quality of potential resource by drilling boreholes to provide samples for evaluation. One assessment traditionally difficult with bore core samples is the prediction of the size distribution and washability characteristics of the expected feed to the preparation plant. A certain amount of

comminution occurs during mining and some liberation of coal from minerals will occur. However, further size reduction, for example from grinding, can liberate more minerals which can then be removed through beneficiation processes.

A principal focus of borecore treatment and subsequent analysis is to predict the size distribution and washability characteristics of the coal so that reliable estimates of plant yield and product quality can be made. Due to the cost involved, there is a trend towards drilling slim cores (generally 63mm in diameter), instead of the large diameter (LD) cores (generally 150mm in diameter). Assessment of individual plies within the seams in these cores can be limited due to the small amount of sample available.

The difficulty in performing washability studies with slim bore cores samples comes from the sample having a finer topsize (typically 12.5mm for slim cores) than what would eventually be used in the coal preparation plant (typically 50mm). Hence, there would be more liberation than would be present in normal run of mine coal. LD cores provide better predictions as they have a coarser size distribution.

For economic reasons coal is generally beneficiated at 50mm or coarser topsizes. However, when the coal exhibits poor washability at these topsizes a reduction in topsize may be required to improve the washability characteristics. The amount of mass required to undergo washability studies of a raw coal are linked to the size of particle being assessed. At a top size of 12.5mm, a minimum of 10kg of sample is required (Standards Australia, 1994).

This means that plies may need to be combined to get enough sample mass at the desired top size to do the study. This is often not ideal as plies generally form the sampling basis for coal quality assessment across a deposit or mine site (Esterle & others, 2000). If topsize is reduced then a smaller sample mass can be used, and hence information can be obtained on the individual plies. At the smallest recommended topsize (0.5mm) a minimum of 800g of sample or 20g of sample per density fraction is required (Standards Australia, 1994).

This paper explores two case studies from the Bowen Basin during which an alternate method, Coal Grain Analysis (CGA), was used to obtain washability information on plies from bore core samples. This information was used to assess the liberation potential of these samples.

BACKGROUND

Coal Breakage and Liberation

Coal consists of both organic and inorganic matter. The organic matter consists of the maceral groups vitrinite, inertinite and liptinite, whilst the inorganic material consists of intrinsic (entrained) and adventitious (inherent) minerals. Intrinsic minerals are intimately associated with the macerals whilst the adventitious material occurs as discrete partings. To improve the overall quality of a particular coal, and to realise its utilisation potential, liberation of the inorganic material may be needed. Liberation occurs when parent particles consisting of multi-component grains are broken to produce daughter particles with a high degree of single component grains (Figure 1).

A certain amount of breakage and liberation already occurs during the mining process. Some coals may benefit from further crushing to a size that achieves sufficient liberation of the inorganic material from maceral associations. However, only coals that show compositionally different daughter particles to parent particles will have liberation benefits from a reduction in particle size. Hence detailed knowledge of the mineral maceral associations in the parent coal particles and the daughter particles produced by crushing is critical for selecting coals that may benefit from further size reduction.

The correlation between density and the amount of mineral matter in a particle has long been recognised, and is the basis of most current coal cleaning processes (Partridge, 1994). The density distribution of particles form a significant part of the characterisation of a coal sample, commonly known as its 'washability', and it is typically determined by float/sink analysis with liquids of varying densities (Partridge, 1994).

Each coal will have differing washability characteristics; these are determined by the unique associations of macerals and minerals within the individual coal particles. The amount of each constituent within the coal determines the coal grains density. Coal particles comprising organic (vitrinite, inertinite, liptinite) and inorganic (minerals) material will generally have relative densities (RDs) ranging from 1.20–.00. Traditional washability characteristics of coal are determined using float sink testing using organic fluids with known RDs that contain varying amounts of white spirit (RD 0.77), perchlorethylene (RD 1.61), tetrabromoethane (RD 2.96) and bromoform (RD 2.79) (Partridge, 1994). As there are significant HSE issues associated with the use of these chemicals alternate methods for obtaining this information are preferred. Products from the float sink testing can be analysed in the laboratory for ash, sulphur, etc.

Coal Grain Analysis

The Coal Grain Analysis (CGA) method (detailed in O'Brien & others, 2003) may be used to obtain washability

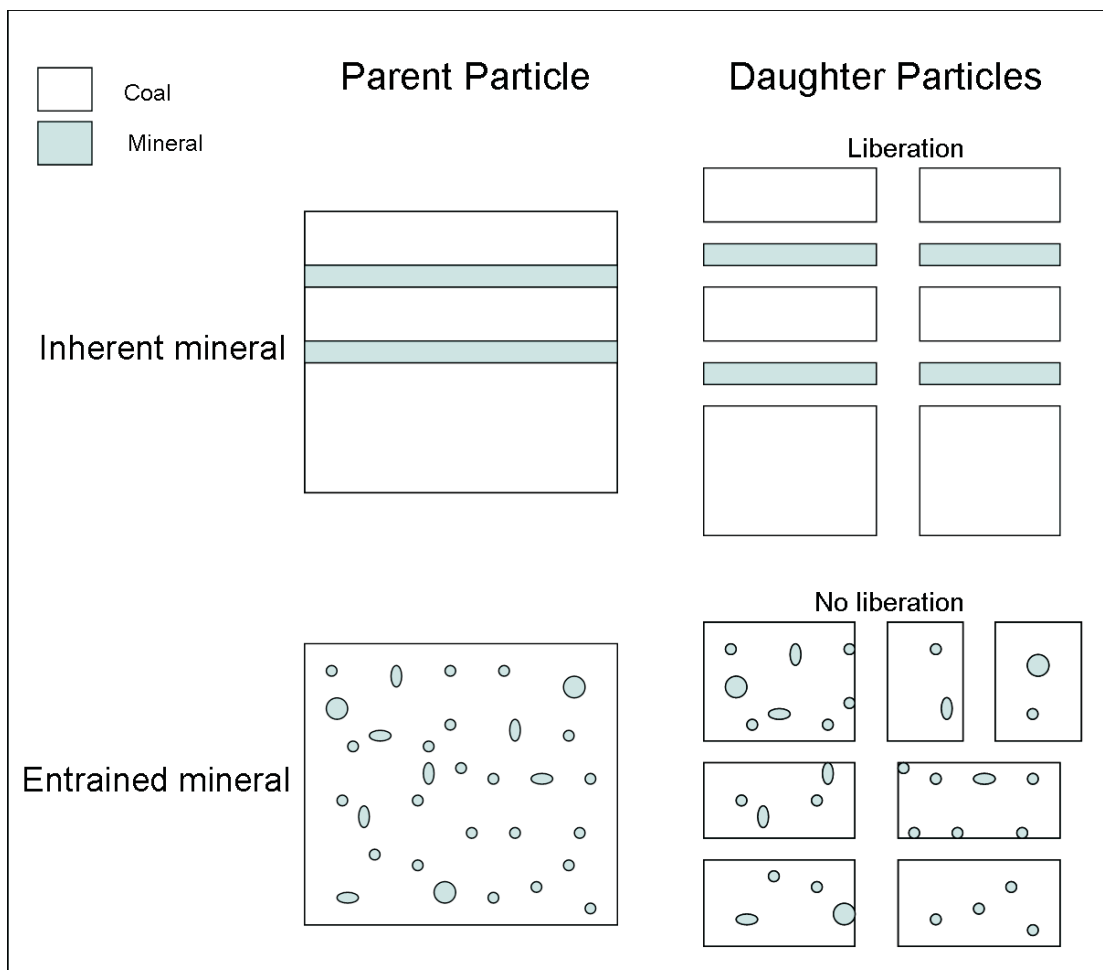


Figure 1: Coal breakage showing liberation is dependant on parent particle

Table 1: The four classes of liberated grains (Vitrite, Inertite, Liptite and Minerals) and the four non-liberated classes (Vit Rich, Inert Rich, Lip Rich and Min Rich)

	Grain Class
Single component grains	Vitrite (>95% vitrinite)
	Inertite (>95% inertinite)
	Liptite (>95% liptinite)
	Minerals (>95% mins)
Composite component grains	Vit rich (V>I, L, mins)
	Inert rich (I>V, L, mins)
	Lip rich (L>V,I, mins)
	Min rich (Mins>V, I, L)

information on fine coal samples. It is an optical imaging method that can be used for routine coal petrography assessments (maceral composition and coal rank) and for obtaining compositional information on individual coal grains.

Analyses are conducted on polished grain-mounts using an oil immersion lens fitted to a reflected-light microscope. Microscopic images are captured using MACE[®] 300 software that was developed by Jenkins Kwan Technology (Jenkins & Kwan, 2003). This system produces bulk petrographic information, including maceral abundance and maceral reflectance data and compositional information on individual particles. The area and composition of each grain is used to estimate grain volume, and when combined with component density information enables the density and hence mass of each grain to be estimated (O'Brien & others, 2007).

The ash % of the grains can be estimated using an experimentally determined relationship between mineral abundance and ash value. Hence the CGA method can estimate the ash % of each grain, and washability curves can be created from the cumulative yield % (or cumulative recovery %) verse ash %, and /or verse grain density information (O'Brien & others, 2005).

The grains were classified into eight classes consisting of four liberated (single component) and four non-liberated (composite) grains (Table 1). The macerals can be represented as either a single component (> 95% vitrinite, inertinite, mineral and liptinite) or composite components (< 95% vitrinite, inertinite, mineral and liptinite) that will determine the functional characteristics of the coal, and the coal grain particle size.

The proportion of grains that are present as pure components or as composites will be a function of the characteristics of the coal and the grain size. Samples that have good liberation will have a higher proportion of single component grains. This process is detailed in O'Brien & others (2007).

For exploration samples CGA is done on samples that are crushed to -1mm and only requires 10g per sample. Hence they can provide washability information on individual plies or the whole seam composite (O'Brien & others, 2006). This can provide information on a ply by ply basis, which can show which plies have a significant amount of liberation potential and/or highlight pyrite or other mineral associations (O'Brien & others, 2010). Individual plies information can also be mathematically combined into any theoretical composite to give washability information on that composite. If liberation of the maceral and mineral components in the coal are realised then significant improvements in overall yield, as well as reducing impurities in the coal namely ash and sulphur can result.

COAL ASSESSMENT

The CGA method provides the theoretical best degree of liberation within coal by examining the daughter particles after the sample is ground to <1mm. These case studies will outline two examples of liberation to (1) assess the potential to reduce high ash in coal plies and (2) to reduce sulphur in coal seam samples.

CASE STUDY ONE:

A liberation study was conducted for a resources client in the Bowen Basin, Central Queensland, using Coal Grain Analysis (CGA) on 5 coal ply samples. The coal ply samples were collected from a 200mm diameter core in the Bowen Basin, Central Queensland. This study was conducted to establish if additional crushing of these ply samples would result in improved liberation and therefore increase in yield.

Four of these plies, (B, C, D, E), had been composited and then screened into size fractions. Float sink testing had been conducted on the 31.5 x 9.5mm and the 9.5mm x 0.707mm fractions and froth flotation testing had been conducted on the 0.707 x 0.0mm fraction. This data was used to construct yield verse ash% curves for each size fraction and for the weighted average of the 4 plies at a 31.5mm topsize (Figure 2), which benchmarked the yield characteristics at this topsize.

The yield ash curves for the -0.707mm showed significantly better washability than the 31.5mm x 9.5mm and 9.5mm x 0.707mm fractions. This is consistent with results obtained for other coal samples.

Reflectogram Results

The reflectograms of the 5 plies shown in Figure 3, confirm that the plies were of similar rank as they exhibited similar vitrinite reflectance ranges. The coals were of sufficient rank that they did not contain liptinites. Hence the portions of the reflectograms below the vitrinite reflectance range are attributed entirely to dark minerals (predominately clays). Ply A contained most minerals and ply C contained least minerals, and more vitrinite and inertinite.

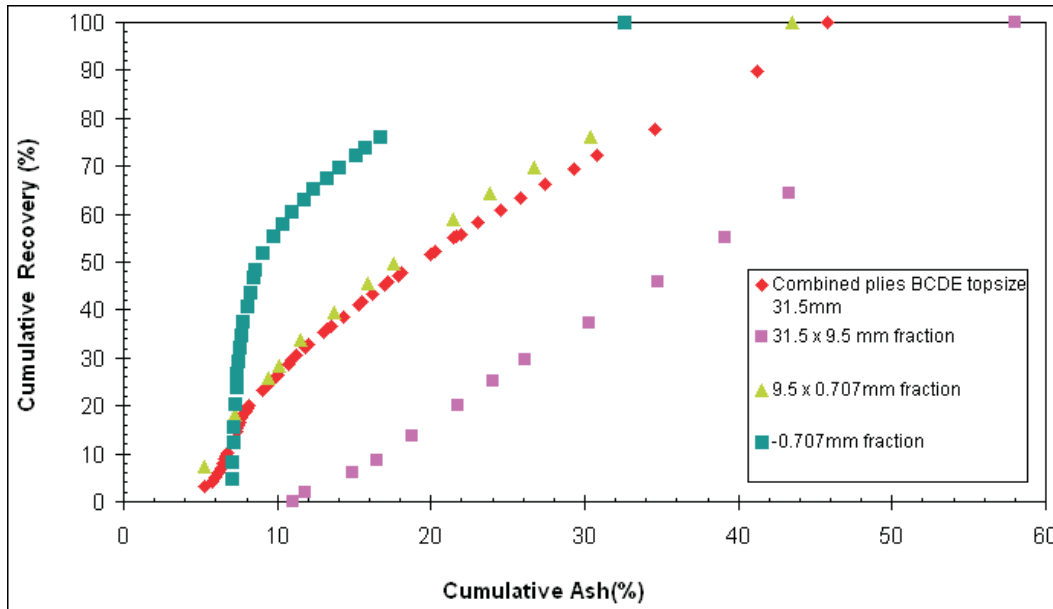


Figure 2: Yield ash curves for the combined BCDE size fractions and combined BCDE at 31.5mm topsize

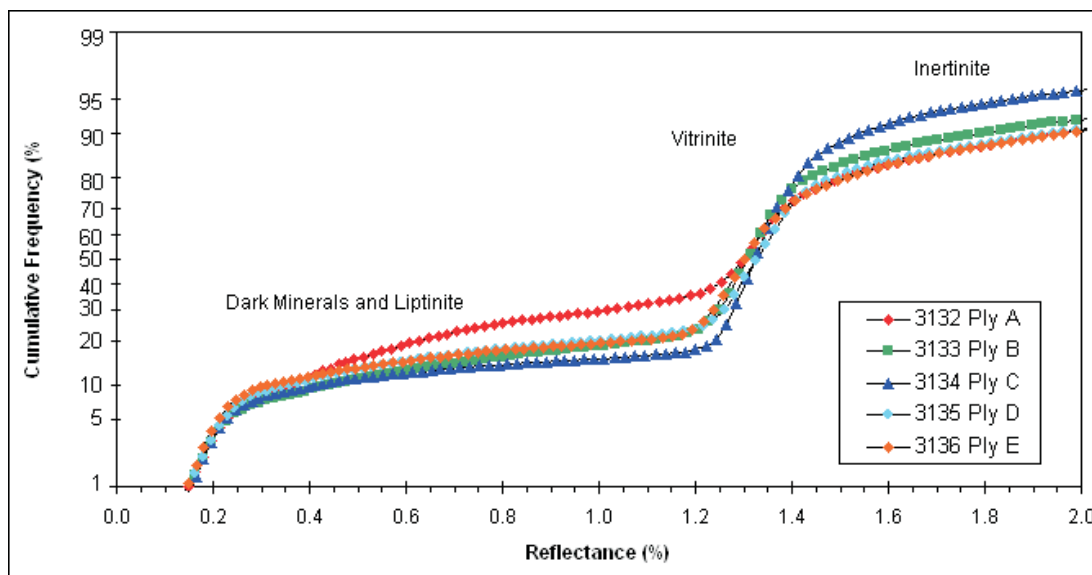


Figure 3: Representation of all sample reflectograms for Plies A, B, C, D and E

Grain Data Analysis (CGA) Results

The mass abundances for the grain classes present in each ply (A, B, C, D and E) are shown in Table 2.

Samples that have good liberation will have a higher proportion of single component grains. Therefore, the single component organic constituents, in this case predominately vitrinite, should report to the clean product and the single component mineral grains should report to the high density rejects.

The CGA information was used to construct the yield versus ash% curves for each of the plies (Figure 4).

When looking at the individual plies at a topsize of 1mm, as shown in Figure 4, plies B, C and D exhibit the best overall recovery percentages. At an ash of 8%, recoveries for all plies varied between 12–28%. At a slightly higher target ash value of 10% recoveries varied between 16 and 34%.

When examining the yield ash curve for the combined plies BCDE, in Figure 4, plies B, C and D exhibit better recoveries than ply E, whilst Ply A shows very poor recovery.

Figure 5 shows the comparative yield versus ash% curves for combined plies BCDE at topsizes of 31.5mm and 1mm. The 1mm curve shows some increase in the amount of low (5% ash) material present when compared with the 31.5mm curve.

However the yield increase is not maintained at higher product ash% values, which suggests that clean coal is being liberated from the intermediate ash % (perhaps 10% to 30%) fraction. It would appear that when the topsize is reduced from 31.5mm to 1mm, recoveries are improved at ash values below 8%, mostly occurring at 5%. Ash values above 10% show very little improvement in recovery. Hence it would appear unlikely that for these samples further crushing would result in significant yield increases, for a target ash% above 8%.

Table 2: Mass abundances for individual plies are categorised into single and composite grain classes

	Grain class	Mass Abundances %				
		Ply A	Ply B	Ply C	Ply D	Ply E
Single component grains	Vitrite (>95% vitrinite)	8.5	16.9	18.3	15.0	12.8
	Inertite (>95% inertinite)	0.7	0.0	0.1	0.1	0.1
	Liptite (>95% Liptinite)	0.0	0.0	0.0	0.0	0.0
	Minerals (>95% mins)	8.8	23.4	3.6	0.7	3.1
Composite grains	Vit rich (V > I, L, mins)	13.9	30.3	41.2	29.6	30.2
	Inert rich (I > V, L, mins)	6.9	6.6	1.5	5.5	10.9
	Liptinite rich L(>V,I, mins)	0.0	0.0	0.0	0.0	0.0
	Min rich (M > V, I, L)	61.2	22.8	35.4	49.1	42.8
	Total	100.0	100.0	100.0	100.0	100.0

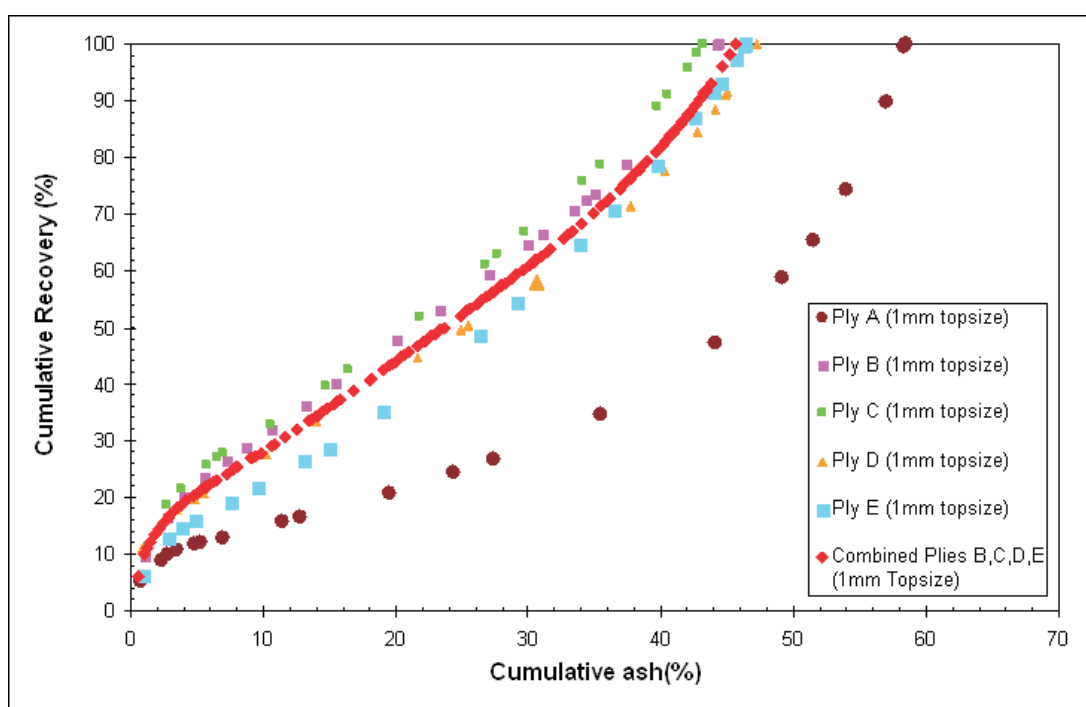


Figure 4: Washability curves for individual plies at 1mm topsize and combined plies BCDE at 1mm topsize

In summarising, the CGA analyses conducted on the coal ply samples collected from the 200mm diameter core suggest that there is limited potential for liberation and yield improvement for a coking coal product by crushing alone. If a low ash coking coal product is to be produced then other ash reduction strategies would need to be investigated.

CASE STUDY TWO:

A resources client in the Bowen Basin asked CSIRO to investigate the potential for sulphur reduction, through grinding and targeting a lower ash% product, in two of their coal seams (Seam 1 and 2) and compare them to a currently mined seam that produces a low sulphur product (Seam 3). Samples of the three different seams were taken from six boreholes and subsamples of each of these (total of 10

samples), crushed to <1mm, were sent to CSIRO to undertake Coal Grain Analysis (CGA).

Reflectogram results shown in Figure 6 demonstrate that Seam 3 samples were of lower rank (R_{vmax} 0.97–0.98%) than Seam 1 (R_{vmax} 1.12–1.20%) and Seam 2 (R_{vmax} 1.17–1.22%). Seam 2 samples were of equal or higher rank (greater R_{vmax}) than corresponding Seam 1 samples from the same borehole. This illustrates that the coal seams are from different deposits and that the seams vary in rank and composition with depth and location around the mine site.

CGA methodology can accurately determine dark and bright mineral contents within individual coal grains. Pyrite is the main constituent of the bright mineral class and hence volume abundance of pyrite in each individual grain can be estimated. When using pyrites molecular formula (FeS_2), the mass of

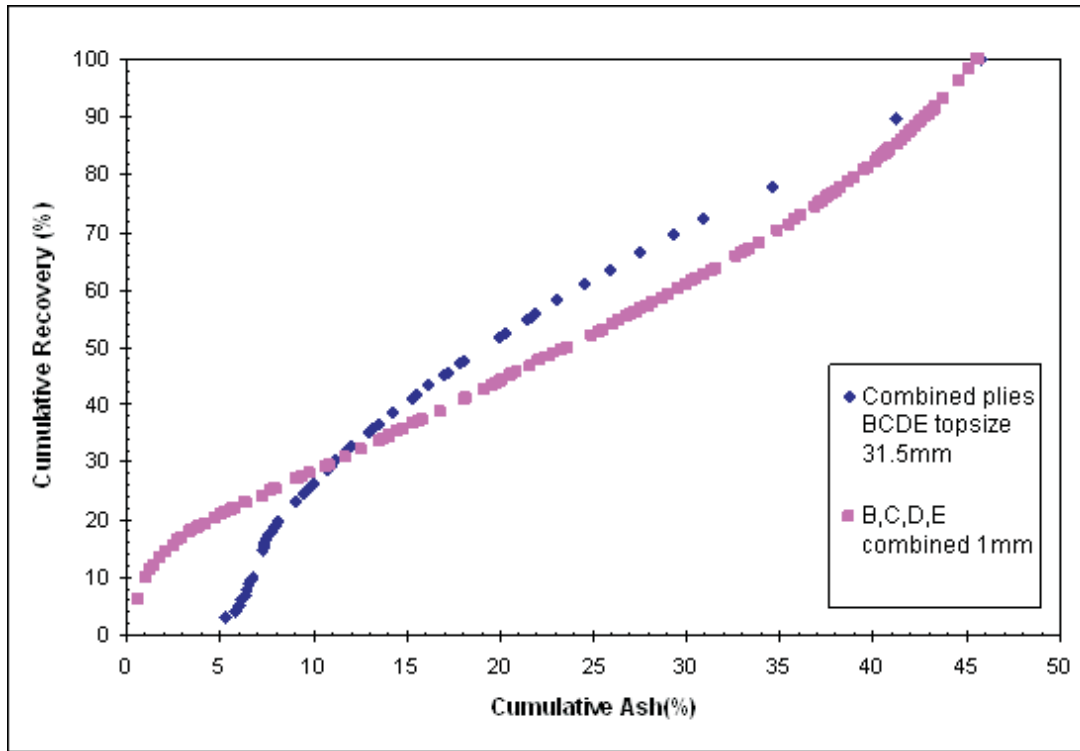


Figure 5: Washability curves for combined plies BCDE at 31.5mm topsize and 1mm topsize

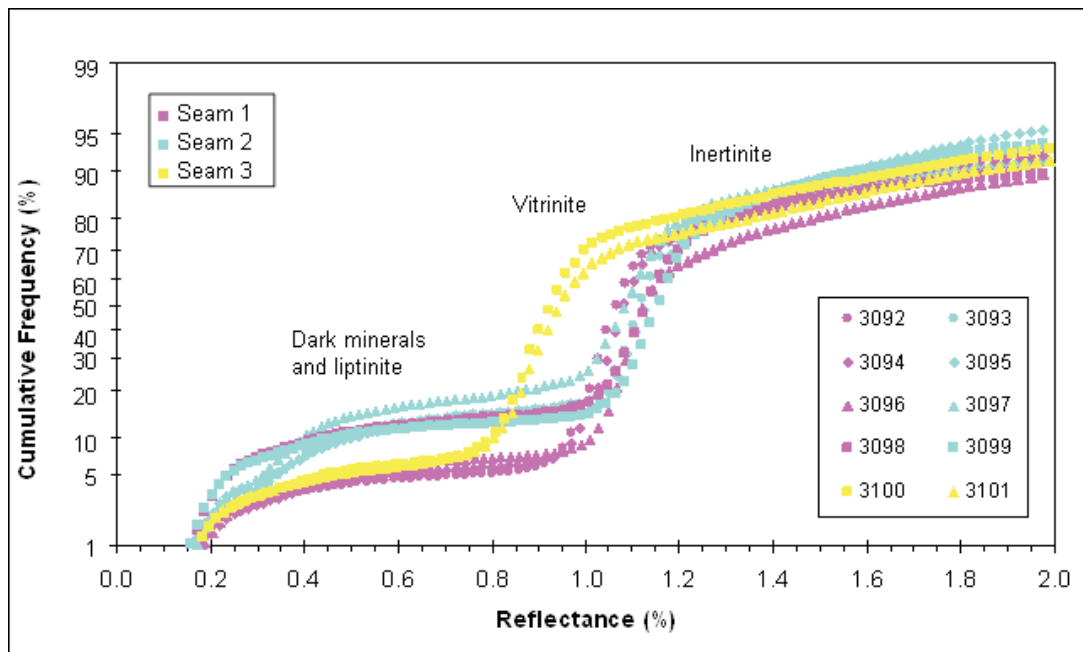


Figure 6: Reflectogram comparisons for all samples

pyritic sulphur can be determined and hence the mass % of pyritic sulphur can be estimated for each grain.

An example of the grain data results is shown in Table 3 for Sample 3092. For this sample, approximately one third of the bright mineral is associated with vitrinite rich grains, while the rest is associated with mineral and mineral rich grains. As vitrinite has a greater propensity to float, any bright mineral (pyritic sulphur) associated with vitrinite rich grains is likely to float and be carried through to the product. The bright minerals for the rest of the samples were also distributed mainly in the vitrinite rich, minerite and mineral rich grains (Table 4).

Washability information for each of the samples was generated in the form of yield-ash% curves from the grain data. The yield-ash% curve for Sample 3093 is shown in Figure 7. This figure shows the predicted yield-ash% curve for each grain type as well as the overall recovery curve of all grain types. This shows that for the vitrinite, inertite and vitrinite rich grain types, a low ash product could be produced. It also shows the proportion of grain types that will report to the product or rejects at certain target ash%. For example at a target ash of 8% the product would consist of vitrinite, vitrinite rich, inertite and half the inertinite rich grains, the rejects would consist of the other half of the inertinite rich, minerite and mineral rich grains.

Table 3: Example grain data results for Sample 3092 showing grain compositions, density and ash%

	Grain class	Vitrinite	Inertinite	Liptinite	Dark mineral	Bright mineral	Grain Volume abundance	Grain density	Grain mass abundance	Grain Ash %	Contact angle
Single component grains	Vitrinite (>95% vitrinite)	20.6	0.3	0.0	0.1	0.0	21.0	1.24	17.3	1.0	62.6
	Inertite (>95% inertinite)	0.0	2.8	0.0	0.0	0.0	2.8	1.31	2.5	1.4	40.0
	Liptite (>95% Liptinite)	0.0	0.0	0.0	0.0	0.0	0.0	0.00	0.0	0.0	0.0
	Minerals (>95% mins)	0.0	0.0	0.0	1.5	0.2	1.7	2.91	3.3	70.3	4.7
Composite grains	Vit rich (V > I, L, mins)	42.8	8.6	0.2	2.0	1.2	54.8	1.39	50.7	11.4	57.5
	Inert rich (I > V, L, mins)	3.1	9.7	0.0	1.4	0.1	14.3	1.45	13.8	18.2	43.7
	Liptinite rich L(>V, I, mins)	0.0	0.0	0.0	0.0	0.0	0.0	0.00	0.0	0.0	0.0
	Min rich (M > V, I, L)	0.8	0.6	0.0	2.0	1.9	5.3	3.51	12.4	70.3	26.6
	Total	67.3	22.0	0.2	6.9	3.5	100.0	1.47	100.0	17.5	54.5

Table 4: Bright mineral distribution within the grain types

	Grain class	Seam 1				Seam 2				Seam 3	
		3092	3094	3096	3098	3093	3095	3097	3099	3100	3101
Single component grains	Vitrinite (>95% vitrinite)	0.0	0.0	0.0	0.0	0.0	0.0	0.0	0.0	0.0	0.0
	Inertite (>95% inertinite)	0.0	0.0	0.0	0.0	0.0	0.0	0.0	0.0	0.0	0.0
	Liptite (>95% Liptinite)	0.0	0.0	0.0	0.0	0.0	0.0	0.0	0.0	0.0	0.0
	Minerals (>95% mins)	0.2	0.1	0.9	3.2	0.2	0.0	1.2	0.4	0.1	0.2
Composite grains	Vit rich (V > I, L, mins)	1.2	0.7	0.6	0.6	0.1	0.1	0.2	0.2	0.1	0.1
	Inert rich (I > V, L, mins)	0.1	0.1	0.1	0.0	0.0	0.0	0.0	0.0	0.0	0.1
	Liptinite rich L(>V, I, mins)	0.0	0.0	0.0	0.0	0.0	0.0	0.0	0.0	0.0	0.0
	Min rich (M > V, I, L)	1.9	1.7	0.4	3.2	0.0	0.0	0.4	0.3	0.0	0.3
	Total	3.5	2.6	2.0	7.0	0.4	0.2	1.9	1.0	0.3	0.7

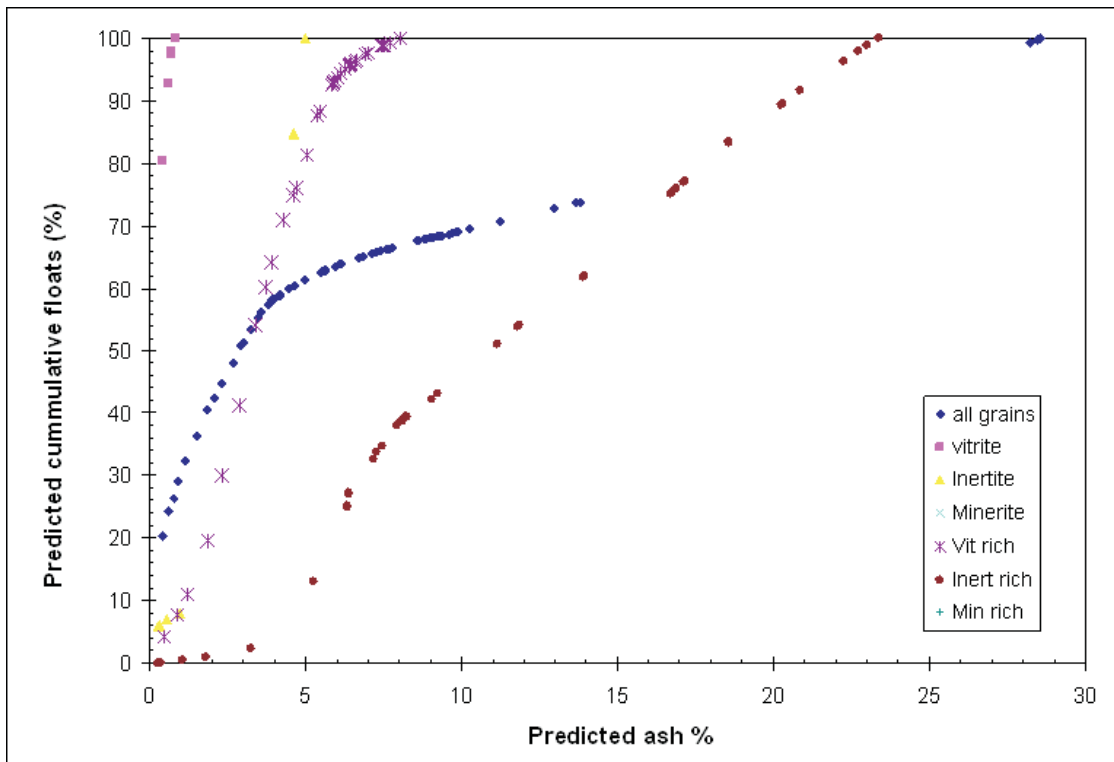


Figure 7: Predicted yield ash curve for Sample 3093

As part of the reconciliation process in CGA, ash% data generated is compared to laboratory ash% data. For seams one and three there was good agreement between the CGA estimated ash values and the client lab assay ash values but the agreement, whilst still acceptable, was not as good for the Seam 2 samples. This may be due to mineralogy differences between the seams as the relationship between mineral abundance and ash value that is used to estimate the ash value of each grain does not yet incorporate mineral abundance information. Hence mineral species such as clays and quartz, which produce different amounts of ash, are currently grouped together as dark minerals. Imaging refinements to provide mineral identification is currently being undertaken by CSIRO.

The CGA data was also used to estimate sulphur contents. Sulphur in coals is present as pyrite, sulphates and organic sulphur. Most Australian coals contain very little sulphate, therefore total sulphur can be considered to be comprised of organic sulphur and pyritic sulphur. Organic sulphur content has been estimated as being 0.5% (Average value for Queensland coals taken from Queensland Coal Board, 1993). Hence total sulphur can be estimated for each individual grain by using the pyritic sulphur content obtained by CGA and adding the chemically determined organic sulphur results or 0.5%.

The forms of sulphur data were available for four samples and reconciliations with the CGA data were performed for these samples. The data was comparable for one of the samples, however the other three did not agree. There appeared to be a transcription error with the laboratory results (the sulphate and pyritic sulphur values appeared to be transposed), as they showed minor amounts of pyritic sulphur but significant amounts of sulphate sulphur, which is highly unusual for Australian coal. However there was a good correlation between the CGA total sulphur results and those determined

by the laboratory analysis for all four samples. These reconciliations give confidence in the CGA results.

As CGA determined the ash and sulphur content for each grain, it is possible to estimate sulphur content of the raw coal and the product coal at different target ash% values. In this instance estimates were made at 9.4% and 8% (Table 5).

The CGA results showed that pyritic sulphur content was significantly higher in Seam 1 than the other two seams. For Seam 1 Sample 3098 contained most pyritic sulphur (10.5% by mass) and Sample 3096 contained least (3.8% by mass). Seam 2 samples had less than 3% pyritic sulphur, with half being less than 1%. Seam 3 samples had pyritic sulphur contents less than 2%.

It is noted that by reducing the ash% from 9.4% to 8.0% there is negligible further reduction in sulphur for Seams 2 and 3. The sulphur reduction in Seam 1 is significant, with only a minor drop in yield.

The total sulphur content of the raw and 9.4% target ash product coals are compared in Figure 8. The raw coals sulphur content is shown first in the darker shade of the colour and the 9.4% product ash's sulphur content is shown to its immediate right in a lighter shade of that colour. Note that the product sulphur content for Seam 2 is comparable to that of Seam 3, i.e. the total sulphur content is reduced to below 1.1%.

The majority of the bright mineral present in the samples is in the mineral, mineral rich and vitrinite rich grains, with minimal amounts in the inertinite rich grains. This implies that while during washing much of the bright mineral, hence the pyritic sulphur, should be removed from the sample, what remains will most likely be present in the vitrinite rich grains. If the fine coal was processed using flotation, the sulphur present in these vitrinite rich grains will most likely be carried

Table 5: Comparison of total sulphur content between raw and products of different target ashes

	Sample No.	Raw Coal	9.4% Target Ash		8.0% Target Ash	
		Predicted Total Sulphur (mass %)	Predicted % Yield	Predicted Total Sulphur (mass %)	Predicted % Yield	Predicted Total Sulphur (mass %)
Seam 1	3092	6.9	85.6	2.4	81.7	1.9
	3094	5.2	80.5	1.8	77.2	1.8
	3096	4.3	86.6	1.8	84.0	1.3
	3098	11.0	52.3	1.4	49.3	1.1
Seam 2	3093	1.1	68.4	1.0	66.4	0.9
	3095	0.9	81.5	0.9	77.9	0.9
	3097	3.4	64.3	0.9	61.8	0.9
	3099	2.2	65.5	1.0	62.4	1.0
Seam 3	3100	1.1	96.7	0.9	95.2	0.9
	3101	1.9	95.0	1.1	94.2	1.1

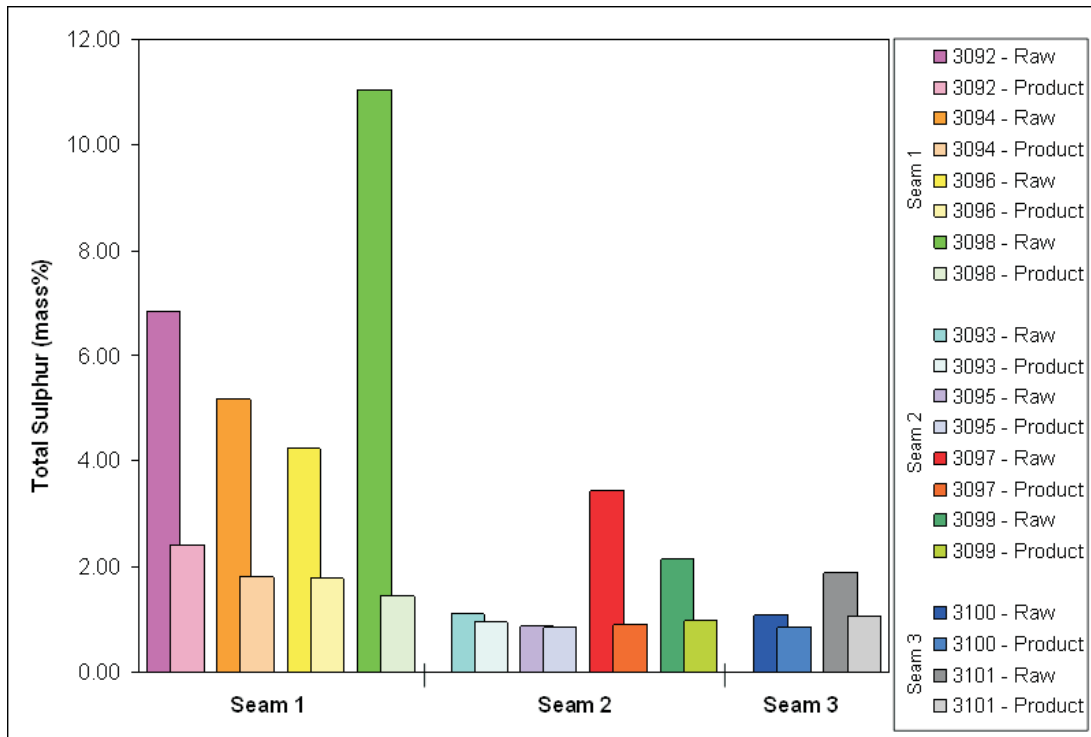


Figure 8: Comparison of total sulphur content between raw and 9.4% target ash product coal

through to the product as these have a higher flotation potential, as determined by their contact angle.

The predictions of sulphur content at 8% product ash suggest that there may be some merit in lowering the product ash specification for Seam 1 and sacrificing some yield to reduce the product coal's total sulphur content. However for Seams 2 and 3, there appears to be little merit in lowering the product ash below 9.4% to further reduce product sulphur as the sulphur remaining in the sample is attached to low ash and density particles.

DISCUSSION

Many coal producers are interested in using selective crushing to recover a lower ash% and reduced sulphur product. To achieve this means that liberation must occur and that daughter particles must be compositionally different to the parent particles. Coal Grain Analysis (CGA) provides a unique method of assessing daughter particles to determine if liberation has occurred and in conjunction with traditional washability studies can predict parent particles and provide a more reliable prediction of the washability attributes at a higher topsize as encountered in washability plants.

Currently borecore analysis programs are used to determine washability and to prepare a clean coal composite for coal quality assessment. Coal petrography, when performed is undertaken at this final stage of assessing exploration samples. Whilst this provides an assessment of the utilisation performance of the coal we believe that there is significant merit in undertaking the petrographic assessment on the raw coal rather than on the clean coal composite. As the analyses require minimal amounts of sample they can be performed on individual plies when required. This means that yield

predictions can be made on the entire seam or with one or more plies excluded. This may highlight early in the exploration program if selective mining of plies may be applicable.

Undertaking CGA testing on raw coal samples enables yield and petrographic information to be predicted at different target ash values. In addition, other coal quality parameters such as sulphur can be estimated at these ash values. It is thought that in the future maceral chemistry information may also be able to be reported on a grain by grain basis. If this capability is developed then other quality attributes such as the proximate and ultimate composition may also be able to be obtained at different product ash values from the single analysis of the raw coal sample.

As the CGA determinations are generally undertaken on the material after it has been crushed to a 1mm topsize this method has the capability of benchmarking the "ultimate washability" from a bore core ply and/or seam. Traditional washability testing on the selected plies could then be used to establish if these results would be obtained at coarser topsize. It is also possible for the CGA data to be used in conjunction with the traditional method of bore core treatment to work back and predict the yield at the top size the material will report to the preparation plant with more accuracy. In addition, the technique can be used to investigate if a coal will benefit from additional crushing and hence improve yield at the required product ash value.

The case studies that have been conducted suggest that the degree of liberation that is obtained is coal specific. For case study 1, the results obtained from the CGA analyses suggest that there is limited potential for liberation and yield improvement for a coking coal product by crushing alone. If a low ash coking coal product is to be produced then other ash

reduction strategies would need to be investigated. CGA would be a useful diagnostic tool for any studies that tried other ways of reducing product ash. The second case study showed that mineral maceral associations influence the processing options that were available for reducing sulphur. For the samples analysed the majority of the bright mineral was present in the mineral, mineral rich and vitrinite rich grains, with minimal amounts in the inertinite rich grains. This implies that during washing much of the bright mineral, hence the pyritic sulphur, should be removed from the sample, what remains will most likely be present in the vitrinite rich grains. If the fine coal was processed using flotation, the sulphur present in these vitrinite rich grains would most likely be carried through to the product as these have a higher flotation potential, as determined by their contact angle.

As further crushing will result in increasing the proportion of the coal that would require flotation beneficiation, knowledge of the mineral maceral associations is a valuable tool for deciding crushing and beneficiation strategies. This information can only be obtained by this analysis method.

CONCLUSIONS

Coal Grain Analysis provides compositional information that cannot be obtained by any other analytical method. CGA provides summary maceral abundance information on a coal sample and compositional information on a grain by grain basis. This grain information can be used to generate industry standard washability information and additional information such as an estimate of the total sulphur content and sulphur distribution on a grain by grain basis of coal samples.

The case studies reported on in this paper highlighted that washability is coal and grind specific. Hence reduction in topsize will result in different amounts of improvement in yield for different coals. As CGA tests are conducted on coals at a 1 mm topsize they benchmark the ultimate practical washability that could be obtained.

When used to analyse raw coal samples CGA can be used to obtain washability information from a standard petrographic sample. From analysis of raw exploration samples it enables yield and product quality (petrographic composition, sulphur content, etc.) predictions to be calculated for any nominated product ash. As analyses only require a small amount of sample, this means that tests can be conducted on individual plies if required.

Industry uptake of this technique will minimise and potentially replace the need for petrographic analyses of exploration samples to be conducted on “clean coal composite” samples. It also allows the prediction of product coal quality parameters.

REFERENCES

- ESTERLE, J.S., THORNTON, D., O'BRIEN, G. & COCKER, A., 2000: Optimising Coal Fragmentation for Improved Recovery, ACARP Project C6046 Final Report.
- JENKINS, B. & KWAN, H., 2003: Calibration of the MACE300™ System. 55th Meeting of the International Committee for Coal and Organic Petrology, Utrecht, The Netherlands.
- O'BRIEN, G., JENKINS, B. & BEATH, H., 2003: Coal Grain Analysis, ACARP Project C10053 Final Report.
- O'BRIEN, G., FERGUSON, K., KELLY, J. & JENKINS, B., 2005: Bore Core Washability by Coal Grain Analysis. In Beeston, J.W. (Editor): *Bowen Basin Symposium 2005 – the future for coal – Fuel for thought*, Geological Society of Australia Inc. Coal Geology Group and the Bowen Basin Geologists Group, Yeppoon, October 2005, 51–55.
- O'BRIEN G., OFORI P. FIRTH, B. & JENKINS, B., 2006: Flotation Diagnostics by Coal Grain Analysis, ACARP Project C13059 Final Report.
- O'BRIEN, G., JENKINS, B., OFORI, P. & FERGUSON, K., 2007: Semi-automated petrographic assessment of coal by coal grain analysis. *Minerals Engineering*, **20**(5), 428–434.
- O'BRIEN, G., FIRTH, B. & ADAIR, B., 2010: The Application of the Coal Grain Analysis Method to Coal Liberation Studies. *International Coal Preparation Congress 2010 Conference Proceedings, Society for Mining, Metallurgy, and Exploration Inc., Littleton, Colorado*, 922–930.
- PARTRIDGE, A., 1994: Principles of Separation. In Swanson, A. & Partridge, A. (Editors): *Advanced Coal Preparation Monograph Series, Volume 1 Part 2*, Australian Coal Preparation Society.
- QUEENSLAND COAL BOARD, 1993: *Queensland Coals Physical and Chemical Properties, Colliery and Company Information, 9th Edition*. Queensland Coal Board, Brisbane, Queensland, Australia.
- STANDARDS AUSTRALIA, 1994: *Australian Standard 4156.1 Coal Preparation Part 1: Higher rank coal – Float and sink testing*. Standards Australia, Homebush, New South Wales, Australia.

John O'Brien, Andy Meyers and Don Cameron

Standardised washability through advances in borecore data unification

Coal borecores are typically subjected to drop shatter and wet pretreatment in the laboratory to simulate the natural breakage that occurs during mining and CHPP processing. It is an unfortunate fact that most resource databases contain legacy coal quality data which has been crushed. Crushing does not simulate natural breakage and crushed borecores are often rejected when undertaking CHPP simulations due to the significant errors in the predicted product yield and quality.

Other investigators established that similar coal preparation data could be obtained from a channel sample crushed to pass 19mm or drop shattered to pass 150mm. This paper will demonstrate that the subtle variations in the washability characteristics of a coal across a resource are retained even after crushing. The washability analysis of a crushed core can be transformed through a series of models into washability data that aligns with correctly pretreated data. The required 'Liberation' and 'Circuit Segregation' models are built around the predictable relationship between ash and density. Successfully applying liberation and circuit segregation models will have significant implications for resource evaluations. Crushed data previously considered unsuitable for CHPP simulation may be transformed to provide reliable yield predictions. This will potentially increase data density providing a more reliable assessment of product yield and quality, as well as an improved indication of inherent variability throughout a resource. This is a cost effective and technically robust alternative to re-drilling and analysing new borecores in areas where crushed data and suitable reference pretreated data is currently available.

This paper explains how 'Liberation' and 'Circuit Segregation' models are built and evaluates their effectiveness through comparisons with adjacent pretreated data and two alternative approaches.

INTRODUCTION

In recent years coal borecores have typically been subjected to drop shatter and wet pretreatment in the laboratory to simulate the natural breakage that occurs during mining and CHPP processing. The laboratory washability analysis is typically designed to match the circuit configuration of the proposed or installed CHPP. It is an unfortunate fact that most resource databases contain legacy coal quality data which does not align with the circuit configuration of the proposed or currently installed CHPP. This is most pronounced when crushing is implemented instead of drop shatter and wet pretreatment.

Crushing generates an unnatural liberation state, whereby coal particles of varying size and density are forced into size fractions where they would not normally exist in a ROM state (Meyers & Leach 2000). Using crushed data for CHPP simulations can result in significant yield and ash errors as the relative proportions assigned to circuits and product streams are incorrect (Meyers & Leach 2000) (Esterle & others, 2000). This is why crushed washability data is often rejected when completing a resource evaluation.

Unifying this legacy crushed data to generate a standardised washability dataset is a cost effective and technically robust alternative to drilling and analysis of new exploration samples. This paper demonstrates a proof of concept for such advanced data unification techniques.

Terminology

Liberation models are used to transform crushed washability data into pseudo pre-treated washability data. This transformation factors in the variation in the liberation state and inherent ash between neighbouring crushed and pre-treated core.

Circuit Segregation models are used to align washability data with a nominated CHPP configuration. This transformation factors in the variation in the washability characteristics with size, which may be a function of either inherent ash or the by-size distribution of dilution material.

PROJECT DATA

Liberation models and circuit segregation models are built around the predictable relationship between ash and density. Appropriate reference data is required to build these models.

For the proof of concept 8 HQ cores were drilled to intersect the target seam. These 8 holes were drilled adjacent to historical HQ cores which had been crushed to pass 12.5mm. An additional 2 HQ holes drilled adjacent to historical crushed HQ cores were used to validate the liberation and circuit segregation models. The locations of the 8 holes used to build the liberation and circuit segregation models and the 2 holes used to validate the model are presented in . A summary of the treatment procedures applied to new and historical cores is detailed in .

There were significant differences in the raw coal ash between the adjacent crushed and pretreated holes (average difference 3.0%). This could be attributed to core erosion, where the coal

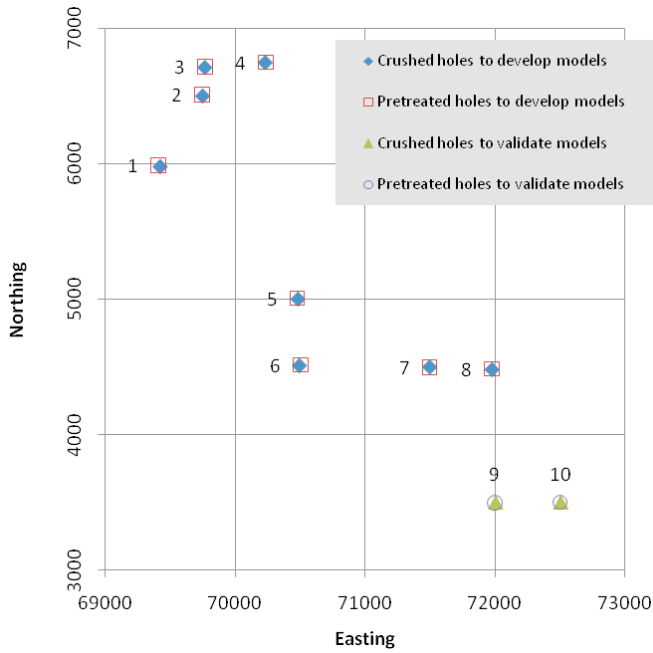


Figure 1: Location of the crushed and pretreated holes

Table 1: Summary of the borecore treatment procedures

Procedure	Historical HQ Core	New HQ Core
Pre-treatment	Crush to pass 12.5mm	Drop shatter 20 times Hand knap to pass 50.0mm Wet-tumble with cubes for 5 minutes
Float/Sink Analysis	-12.5 + 0.5mm	+12.5mm -12.5 + 1.0mm -1.0mm + 0.25mm
Float/Sink Densities	1.30, 1.35, 1.40, 1.45, 1.50, 1.55, 1.60, 1.70, 1.80, 1.90 & 2.00	1.30, 1.35, 1.40, 1.45, 1.50, 1.55, 1.60, 1.70, 1.80, 1.90 & 2.00

plies were preferentially eroded during drilling of the historical HQ cores. To remove the sampling and analysis variability the raw coal ash for adjacent crushed and pretreated holes were aligned. This was achieved through the addition of generic dilution to the hole with the lower raw coal ash. Average generic dilution washability for both crushed and pretreated holes were calculated from the resource database.

LIBERATION MODELLING

Development of the Liberation Model

A liberation model was built on the relationship between adjacent crushed and pretreated washability for 8 target holes. Fractional ash (Figure 2) and cumulative ash (Figure 3) relationships were developed between crushed washability (-12.5+0.5mm) and adjacent pretreated washability (-50.0+0.25mm). The polynomial equations developed from these relationships are the basis for the liberation model. These equations are applied to the crushed washability data to generate pseudo pre-treated washability data. A flow diagram of the liberation model process is presented in (Figure 4).

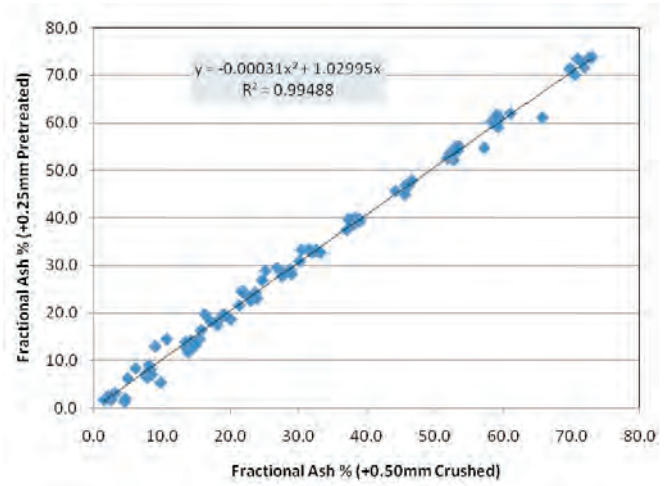


Figure 2: Relationship between crushed and pretreated fractional ash for 8 holes

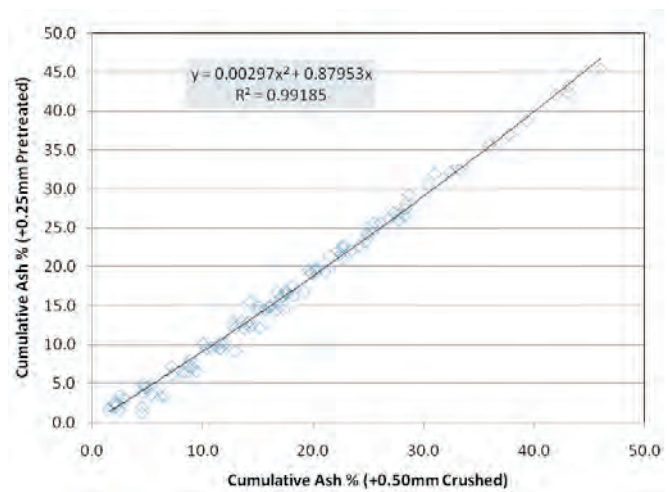


Figure 3: Relationship between crushed and pretreated cumulative ash for 8 holes

The liberation model, developed from the relationship between adjacent crushed and pretreated data points, is only as good as the reference data it is built from. A robust model is dependent upon the adjacent crushed and pretreated data points being within close proximity. The more variable the resource the closer the holes need to be. Ideally adjacent crushed and pretreated data points should be within 20m. For this paper the 8 crushed cores used to build the liberation model were all within 15m of the adjacent pretreated core.

Application of the Liberation Model

The first step in applying a liberation model is to predict a pseudo pretreated +0.25mm head ash for the crushed data series. This was predicted for the crushed dataset using the relationship between the pretreated raw coal ash and the pretreated +0.25mm head ash (Figure 5).

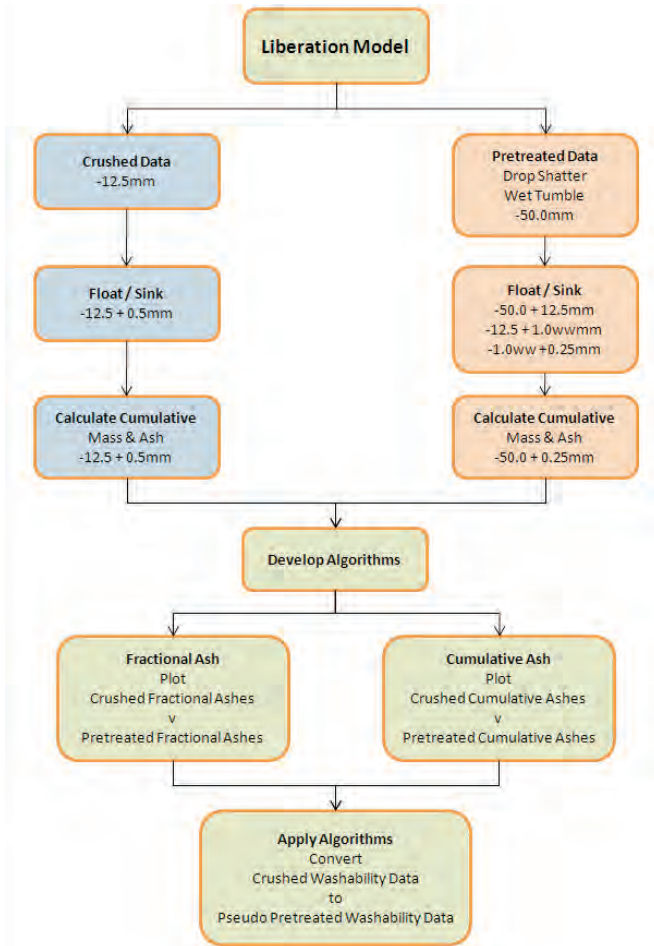


Figure 4: Flow diagram of the Liberation Model applied to crushed coal

The crushed washability data was transformed to pseudo pretreated washability by applying the liberation model algorithms for fractional and cumulative ash. An example of how the crushed washability changes when the liberation model is applied is provided in the following theoretical ash yield curve (Figure 6).

Crushed washability data typically has less low density material than correctly pretreated washability data (Figure 6). This can be attributed to inadequate liberation during crushing compared to correct pretreatment (drop shatter / wet tumble).

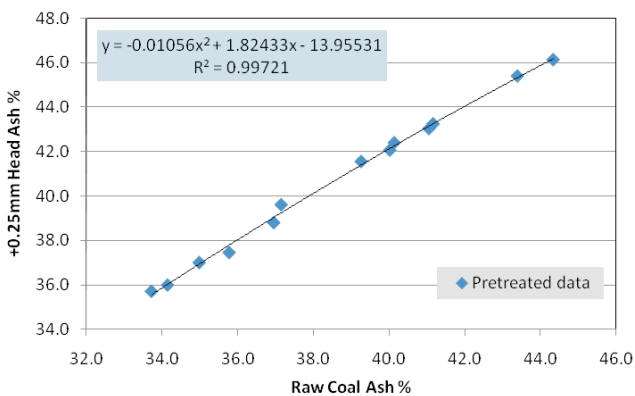


Figure 5: Relationship between raw coal ash and +0.25mm head ash for the 8 pretreated holes

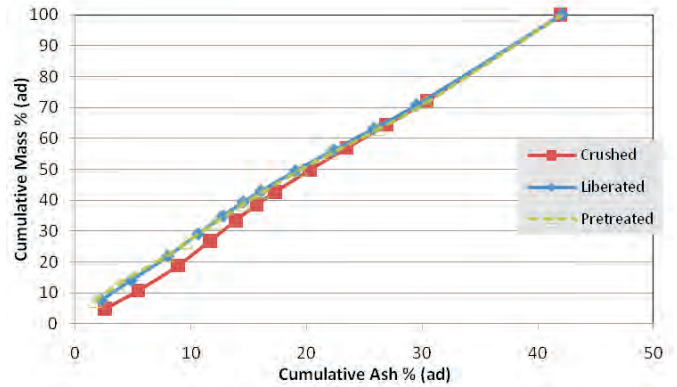


Figure 6: Comparison of crushed, liberated and pretreated washability for hole #2

Applying the liberation model to the crushed data series effectively aligned the crushed washability with the adjacent pretreated washability (Figure 6). For the liberation model to be effective the offset between crushed data and pretreated data must be consistent, e.g. crushed data must always have less low density material than correctly pretreated washability data.

CIRCUIT SEGREGATION MODELLING

Development of the circuit segregation model

Washability characteristics of a coal vary by size. The circuit segregation model was built to assign washability characteristics to the following size fractions:

- +12.5mm
- -12.5 + 1.0wwmm
- -1.0ww + 0.25mm

The circuit segregation model is based on the relationship between correctly pretreated washability by size for 8 holes. Fractional ash (Figure 7) and cumulative ash (Figure 8) relationships were developed between the combined washability (-50.0+0.25mm) and fractional washability (+12.5mm, -12.5+1.0wwmm & -1.0ww+0.25mm) for the

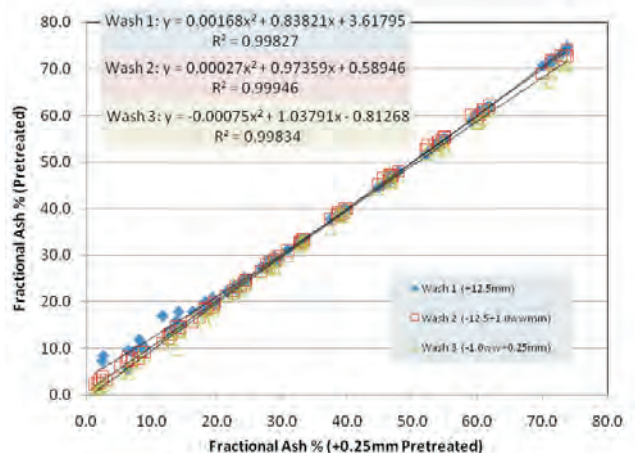


Figure 7: Comparison of crushed, liberated and pretreated washability for hole #2

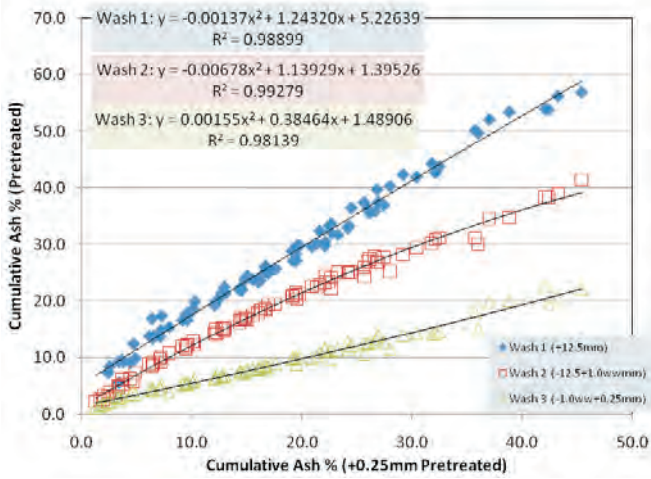


Figure 8: Relationship between combined and fractional ash for 8 correctly pretreated holes

correctly pretreated data. The polynomial equations developed from these relationships are the basis for the circuit segregation model. These equations are applied to the 'pseudo pretreated washability data' (+0.25mm washability produced from applying the liberation model to the crushed data) to generate washability data by size. A flow diagram of the circuit segregation model process is presented in (Figure 9).

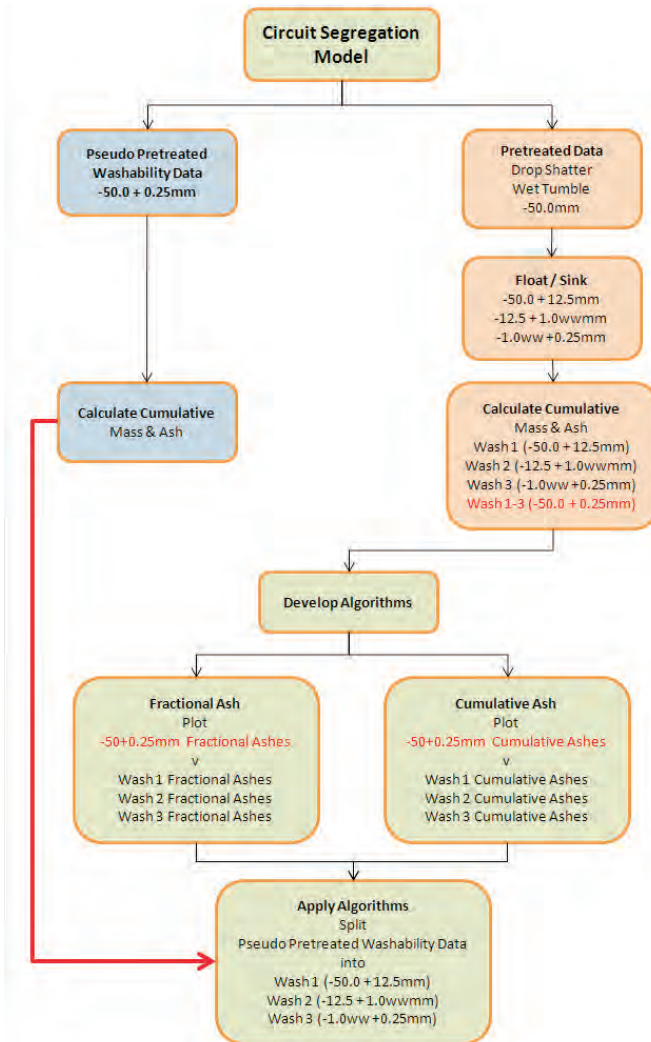


Figure 9: Flow diagram of the Circuit Segregation Model applied to crushed coal

Application of the circuit segregation model

The washability for three different size fractions was predicted by applying the circuit segregation model algorithms for fractional and cumulative ash to the pseudo pretreated washability data. Figure 10 provides a comparison between the liberated and circuit segregated data (crushed) and the adjacent pretreated washability for hole #2.

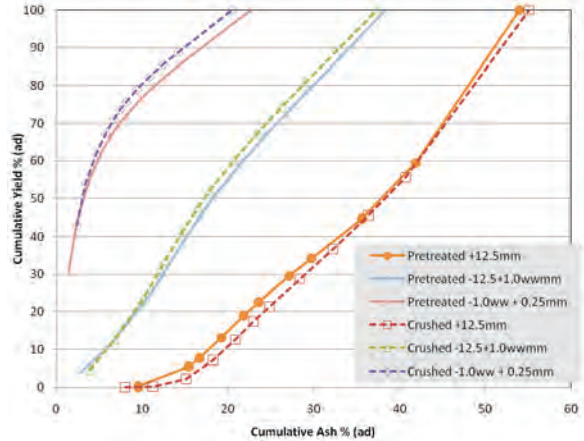


Figure 10: Comparison between predicted and actual theoretical ash yield curves by size (hole #2)

Applying the circuit segregation model to the pseudo pretreated washability data, (i.e. crushed washability processed through a liberation model) effectively distributed washability to three size fractions. There was a significant difference between the washability characteristics for these three size fractions. For the circuit segregation model to be effective the offset between the relevant size fractions must be consistent, e.g. coarse washability must always be inferior to fine washability.

Prediction of the pseudo pretreated size distribution

Application of the liberation and circuit segregation models generated pseudo pretreated washability by size. The size distribution to apply this washability data to needed to be predicted. An average size distribution could have been applied or the average slope from a Rosin Rammler plot used to predict a pretreated size distribution. For this paper the relationships between the pretreated head ashes (Figure 11) were used to calculate the mass % +0.25mm and -0.25mm. The relationships between the pretreated head ashes and circuit masses (Figure 12) were used to calculate the mass % required for the remaining circuits to maintain the raw coal ash. These relationships were not ideal and may not be applicable to other resources. A universal approach using multivariable analysis is currently being investigated to provide a definitive model for predicting a pretreated size distribution for crushed data.

The predicted size distribution for the crushed data set was applied to the predicted washability by size to generate feed files for CPP simulations.

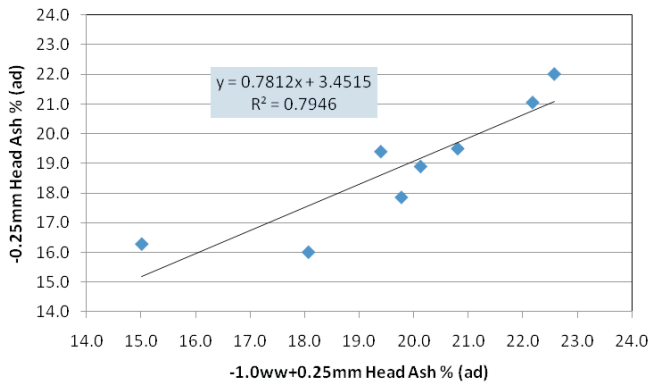


Figure 11 : Relationship between $-1.0ww+0.25mm$ head ash and $-0.25mm$ head ash

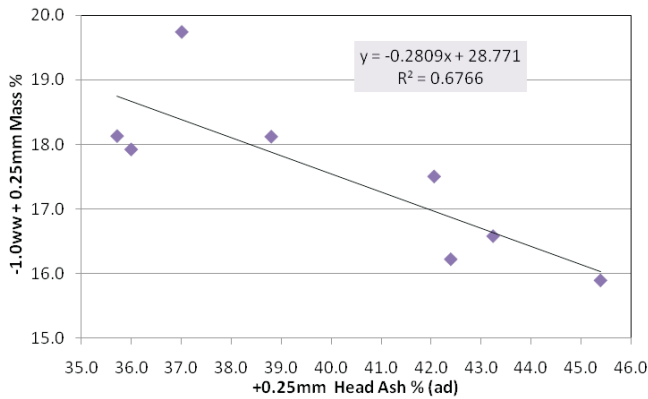


Figure 12: Relationship between $+0.25mm$ head ash and $-1.0ww + 0.25mm$ mass %

COMPARATIVE YIELD ESTIMATION

To measure the success of the liberation and circuit segregation modelling a series of fixed ash simulations were undertaken to predict primary and secondary product yields using the modelled sizing and washability data. These predicted yields were compared with the following:

- Predicted yields from fixed ash simulations on actual pretreated data from an adjacent HQ hole.
- Predicted yields from ROM ash yield equations which were developed from the relationship between ROM ash and simulated yield at dilution levels ranging from 0-15%. The ROM ash equations to predict primary and secondary product yields are detailed in Figure 13.
- Predicted yields from fixed ash simulations on size unified crushed data. Size unification assumes the washability characteristics for each size fraction are equivalent to the crushed washability. A size distribution is applied to each crushed data point and the crushed washability is replicated across all circuits. This is a methodology that has been used in the past to estimate product yield. Esterle & others (2000) applied this methodology to slim cores (63mm) crushed to -12.7mm and found it produced a poor estimation of product yield and ash. To counter this problem a yield offset based upon the relationship between correctly pretreated yield and size unified yield was applied to align the size unified yields with the correctly

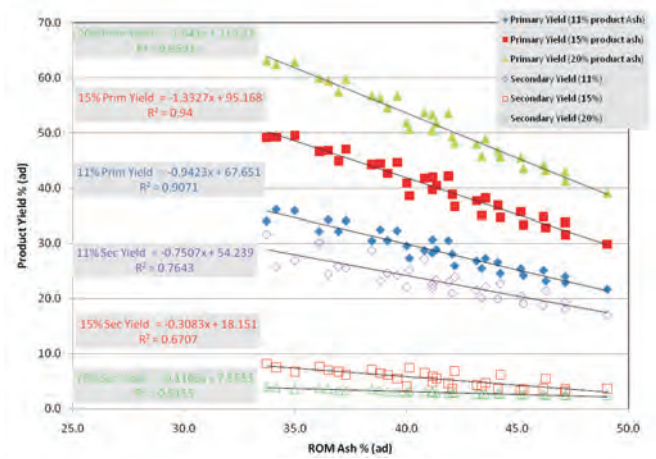


Figure 13: Relationship between ROM ash and primary and secondary product yield

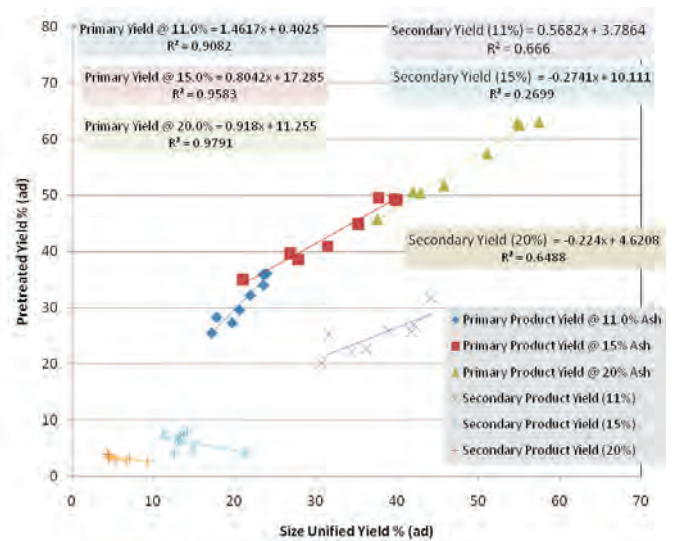


Figure 14: Relationship between correctly pretreated yields and size unified yields

pretreated yields. The size unified offsets developed to predict primary product yield are detailed in Figure 14.

CPP simulation parameters

Using the **RESOURCE_MASTOR™** plant simulation software, the following operating parameters were employed to predict primary and secondary yields.

DMC	+12.5mm	Variable SG of 1.35 – 1.85
DMC	-12.5 + 1.0wwmm	Variable SG of 1.35 – 1.85
Spirals	-1.0ww + 0.25mm	Fixed SG 1° 1.75 & 2° 1.95
Flotation	-0.25mm	Pseudo Density

Industry benchmark plant efficiency parameters were used to undertake the simulations.

Simulation outputs

To provide a measure of performance with a low, medium and high DMC cut-point three different ashes were targeted for the primary product. Secondary product yield was generated from a fixed ash target of 30% with a variable DMC rewash and a fixed spirals middling fraction (S1.75 - F1.85SG).

The estimated primary and secondary product yields are presented in Table 2 and Table 3 respectively. The difference between the actual pretreated yield and the yields for the crushed data alternatives were used to calculate the standard errors (standard deviation of the differences).

Compared to the correctly pretreated data, the liberation and circuit segregation modelling produced primary product yields with the lowest standard errors (Table 2). As the primary product target ash increased (higher cut-points) the predicted liberation and circuit segregation modelled yields were more reliable with a noticeable reduction in the standard errors. As the primary product target ash increased there was no improvement in the standard errors for the ROM ash and size unified primary product yields. Figure 15 provides a graphical representation of the variability in primary product yield for a 15% primary product ash.

The liberation and circuit segregation modelling, ROM ash yield equation methodology and size unified offsets produced similar secondary product yields which were comparable to the correctly pretreated secondary yields (Table 3). As the primary product target ash increased the predicted secondary yields were more reliable, with a noticeable reduction in the standard errors.

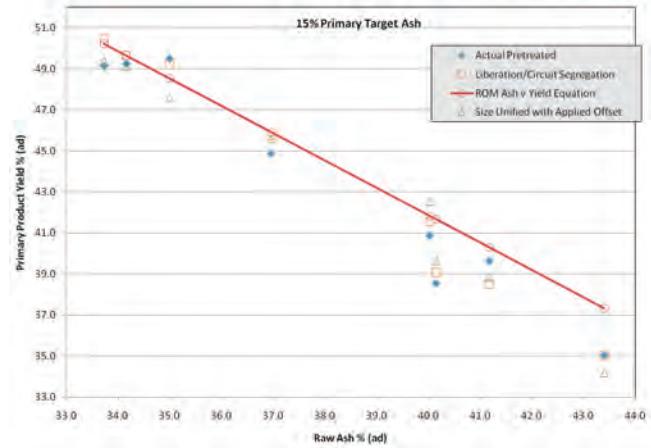


Figure 15: Variability in predicted primary product yield at 15% primary product ash

VALIDATION OF THE LIBERATION AND CIRCUIT SEGREGATION MODELS

Two crushed HQ cores were selected to validate the liberation and circuit segregation models. Correctly pretreated HQ holes were drilled adjacent to these two historical crushed HQ cores. The liberation model was applied to the crushed HQ washability to generate pseudo pretreated washability. The circuit segregation model was applied to the pseudo pretreated washability to generate washability for three size fractions. A comparison between the by size theoretical ash yield curves for liberated and circuit segregated data (crushed) and the adjacent pretreated washability is presented in Figures 16 and 17. To measure the success of the liberation and circuit segregation modeling a series of fixed ash simulations were undertaken to predict primary and secondary product yields.

Table 2: Predicted primary product yields from fixed ash simulations

Hole ID	Raw Ash % (ad)	Primary Product Target Ash % (ad)	Primary Product Yield % (ad)				Difference from Actual Pretreated Yield % (ad)			Standard Error		
			Actual Pretreated	ROM Ash v Yield Equation	Size Unified with Applied Offset	Liberation & Circuit Segregation	ROM Ash v Yield Equation	Size Unified with Applied Offset	Liberation & Circuit Segregation	ROM Ash v Yield Equation	Size Unified with Applied Offset	Liberation & Circuit Segregation
#1	33.7	11.0	34.0	35.9	34.8	36.4	-1.9	-0.8	-2.4	1.2	1.2	1.1
#2	40.0		29.6	29.9	30.5	29.9	-0.4	-0.9	-0.4			
#3	43.4		25.5	26.8	25.5	24.9	-1.3	0.0	0.6			
#4	40.1		27.3	29.8	29.2	28.6	-2.5	-1.9	-1.3			
#5	41.2		28.3	28.9	26.4	27.7	-0.6	1.9	0.6			
#6	34.2		36.1	35.5	35.3	36.5	0.6	0.8	-0.4			
#7	37.0		32.2	32.8	32.4	33.2	-0.7	-0.2	-1.1			
#8	35.0		35.9	34.7	34.8	35.1	1.2	1.1	0.8			
Average	38.1	31.1	31.8	31.1	31.5	-0.7	0.0	-0.5				
#1	33.7	15.0	49.1	50.2	49.4	50.5	-1.1	-0.3	-1.3	1.2	1.1	0.8
#2	40.0		40.9	41.8	42.5	41.5	-0.9	-1.6	-0.7			
#3	43.4		35.0	37.3	34.2	35.0	-2.3	0.8	0.0			
#4	40.1		38.6	41.7	39.6	39.1	-3.1	-1.0	-0.5			
#5	41.2		39.6	40.3	38.8	38.5	-0.7	0.8	1.1			
#6	34.2		49.3	49.7	49.1	49.7	-0.4	0.2	-0.4			
#7	37.0		44.9	45.9	45.6	45.7	-1.0	-0.7	-0.9			
#8	35.0		49.5	48.5	47.6	49.2	1.0	1.9	0.3			
Average	38.1	43.4	44.4	43.4	43.7	-1.1	0.0	-0.3				
#1	33.7	20.0	63.0	63.9	63.9	64.6	-0.8	-0.9	-1.6	1.1	1.0	0.6
#2	40.0		51.8	53.6	53.2	52.6	-1.7	-1.4	-0.8			
#3	43.4		45.8	48.0	45.7	46.2	-2.2	0.1	-0.4			
#4	40.1		50.7	53.4	49.7	50.8	-2.7	1.0	-0.1			
#5	41.2		50.4	51.7	50.5	50.2	-1.3	-0.1	0.2			
#6	34.2		62.5	63.2	61.7	62.6	-0.7	0.8	-0.1			
#7	37.0		57.4	58.6	58.1	58.0	-1.2	-0.7	-0.6			
#8	35.0		62.8	61.8	61.5	62.5	1.0	1.3	0.4			
Average	38.1	55.6	56.8	55.5	55.9	-1.2	0.0	-0.4				

Table 3 : Predicted secondary product yields from fixed ash simulations

Hole ID	Raw Ash % (ad)	Primary Product Target Ash % (ad)	Secondary Product Yield % (ad)				Difference from Actual Pretreated Yield % (ad)			Standard Error		
			Actual Pretreated	ROM Ash v Yield Equation	Size Unified with Applied Offset	Liberation & Circuit Segregation	ROM Ash v Yield Equation	Size Unified with Applied Offset	Liberation & Circuit Segregation	ROM Ash v Yield Equation	Size Unified with Applied Offset	Liberation & Circuit Segregation
#1	33.7	11.0	31.6	28.9	28.9	29.0	2.7	2.8	2.6	1.8	2.0	1.9
#2	40.0		22.2	24.2	23.3	22.7	-2.0	-1.1	-0.5			
#3	43.4		20.2	21.7	21.2	22.6	-1.5	-1.0	-2.4			
#4	40.1		25.2	24.1	21.7	22.3	1.1	3.5	3.0			
#5	41.2		22.6	23.3	24.3	23.6	-0.7	-1.7	-0.9			
#6	34.2		25.8	28.6	27.5	25.3	-2.8	-1.7	0.4			
#7	37.0		25.9	26.5	25.9	24.8	-0.6	0.0	1.1			
#8	35.0		26.9	28.0	27.6	28.3	-1.0	-0.7	-1.4			
Average	38.1		25.1	25.7	25.1	24.8	-0.6	0.0	0.2			
#1	33.7	15.0	8.2	7.8	6.2	8.9	0.4	2.0	-0.7	1.0	1.4	1.1
#2	40.0		4.1	5.8	6.7	5.2	-1.7	-2.6	-1.1			
#3	43.4		4.1	4.8	4.3	4.9	-0.6	-0.1	-0.8			
#4	40.1		7.4	5.8	6.4	5.8	1.6	1.1	1.6			
#5	41.2		4.9	5.5	6.0	6.7	-0.6	-1.2	-1.8			
#6	34.2		7.5	7.6	7.0	6.9	-0.1	0.5	0.6			
#7	37.0		6.7	6.8	6.5	6.9	-0.1	0.1	-0.2			
#8	35.0		6.7	7.4	6.5	7.7	-0.6	0.3	-1.0			
Average	38.1		6.2	6.4	6.2	6.6	-0.2	0.0	-0.4			
#1	33.7	20.0	4.0	3.8	3.6	3.9	0.2	0.4	0.1	0.2	0.3	0.1
#2	40.0		2.9	3.1	3.4	3.1	-0.2	-0.5	-0.2			
#3	43.4		2.6	2.8	2.5	2.6	-0.1	0.1	0.0			
#4	40.1		3.2	3.1	3.0	3.3	0.1	0.2	-0.1			
#5	41.2		2.9	3.0	3.1	3.0	-0.1	-0.2	-0.1			
#6	34.2		3.9	3.8	3.6	4.1	0.1	0.3	-0.2			
#7	37.0		3.3	3.5	3.6	3.4	-0.1	-0.3	-0.1			
#8	35.0		3.5	3.7	3.6	3.7	-0.2	0.0	-0.2			
Average	38.1		3.3	3.4	3.3	3.4	0.0	0.0	-0.1			

These simulations were replicated using the actual pretreated data. The ROM ash yield equations were also applied to each raw coal ash to predict primary and secondary product yield. The primary and secondary product yields generated from these simulations and calculations are presented in and respectively. The difference in predicted yield between actual pretreated and each of the crushed data alternatives was used to calculate the standard errors (standard deviation of the differences).

Compared to the correctly pretreated data, the liberation and circuit segregation modelling produced more reliable primary product yields with lower standard errors than the ROM ash yield equations (Table 4). As the primary product target ash

increased (higher cut-points) the predicted liberation and circuit segregation modelled yields were less reliable with a noticeable increase in the standard errors. This trend was the opposite of that observed for the original eight bore cores from which the models were developed. This variation could be due to the limited number of samples used to validate the model.

The liberation and circuit segregation modeling also produced reliable secondary product yields with lower standard errors than the ROM ash yield equations (Table 5). As the primary product target ash increased the predicted secondary yields were more reliable, with a noticeable reduction in the standard errors.

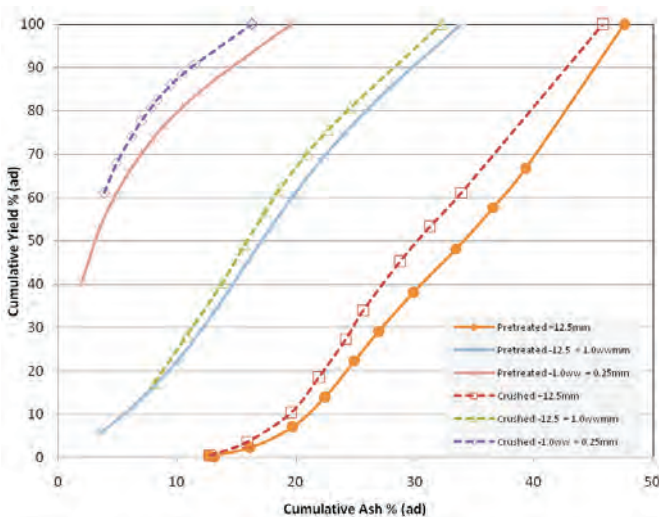


Figure 16: Comparison between predicted and actual theoretical ash yield curves by size for Hole #9

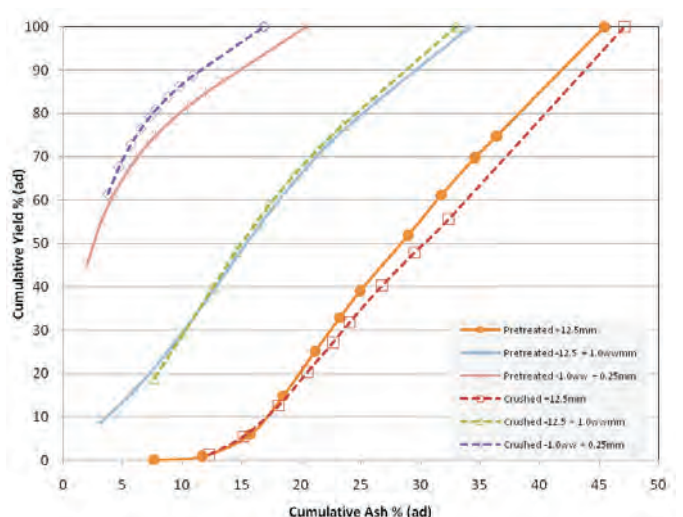


Figure 17: Comparison between predicted and actual theoretical ash yield curves by size for Hole #10

Table 4: Predicted primary product yields from fixed ash simulations

Hole ID	Raw Ash % (ad)	Primary Product Target Ash % (ad)	Primary Product Yield % (ad)			Difference from Actual		Standard Error	
			Actual Pretreated	ROM Ash v Yield Equation	Liberation & Circuit Segregation	ROM Ash v Yield Equation	Liberation & Circuit Segregation	ROM Ash v Yield Equation	Liberation & Circuit Segregation
#9	32.1	11.0	35.4	37.4	35.9	-2.1	-0.6	2.7	0.4
#10	33.1		38.1	36.4	38.1	1.7	0.0		
#9	32.1	15.0	50.0	52.4	50.7	-2.4	-0.6	2.7	0.6
#10	33.1		52.4	51.0	52.2	1.4	0.2		
#9	32.1	20.0	64.8	66.6	65.9	-1.8	-1.0	2.3	1.6
#10	33.1		66.4	64.8	65.2	1.5	1.2		

Table 5 : Predicted secondary product yields from fixed ash simulations

Hole ID	Raw Ash % (ad)	Primary Product Target Ash % (ad)	Secondary Product Yield % (ad)			Difference from Actual		Standard Error	
			Actual Pretreated	ROM Ash v Yield Equation	Liberation & Circuit Segregation	ROM Ash v Yield Equation	Liberation & Circuit Segregation	ROM Ash v Yield Equation	Liberation & Circuit Segregation
#9	32.1	11.0	31.7	30.2	32.4	1.5	-0.7	2.4	1.2
#10	33.1		27.6	29.4	26.5	-1.8	1.0		
#9	32.1	15.0	9.2	8.3	10.6	0.9	-1.4	1.6	0.8
#10	33.1		6.6	7.9	6.9	-1.3	-0.3		
#9	32.1	20.0	4.1	4.0	4.3	0.1	-0.2	0.2	0.1
#10	33.1		3.7	3.9	4.0	-0.2	-0.3		

CONCLUSIONS

- Applying the liberation model to the crushed data series effectively aligned the crushed washability with the adjacent pretreated washability. For the liberation model to be effective the offset between crushed data and pretreated data must be consistent, e.g. crushed data must always have less low density material than correctly pretreated washability data.
- Applying the circuit segregation model to the pseudo pretreated washability data, (i.e. crushed washability processed through a liberation model) effectively distributed washability to three size fractions. There was a significant difference between the washability characteristics for these three size fractions. For the circuit segregation model to be effective the offset between the relevant size fractions must be consistent, e.g. coarse washability must always be inferior to fine washability.
- To measure the success of the liberation and circuit segregation modelling a series of fixed ash simulations were undertaken to predict primary and secondary product yields. Compared to the correctly pretreated data, the liberation and circuit segregation modelling was in line with or better than several alternative approaches with the lowest standard errors. The real benefit over the alternative approaches however is the flexibility offered by the liberation and circuit segregation modelled data. Alternative approaches rely upon the redevelopment of models for every new permutation. For example if the primary target ash was changed to 13% a new ROM ash yield equation would have to be developed or a new offset developed for the size unified data. The liberation and circuit segregation

modelled data however requires no further adjustment to reliably predict product yields.

- It is apparent that subtle variations in the washability characteristics of a coal are still retained after crushing. These subtle variations are maintained throughout the liberation and circuit segregation modelling, which are reflected in the simulated product yields. The ROM ash yield equations do not account for these subtle variations which do not impact on ROM ash (Figure 15). Liberation and circuit segregation modelling provides an effective means of capturing the subtle variability in the washability characteristics of a crushed coal. The predicted yields for crushed coals are therefore more reliable when liberation and circuit segregation modelling has been undertaken.
- Successfully applying liberation and circuit segregation modelling will have significant implications for resource evaluations. Data previously considered unsuitable for CPP simulation may be transformed to provide reliable yield predictions. This will potentially increase data density providing a more reliable assessment of product yield throughout a resource. This is a cost effective and technically robust alternative to re-drilling and analysing new borecores in areas where crushed data and suitable reference pretreated data is currently available.
- With appropriate reference data it is possible to apply circuit segregation models to a resource database to generate washability data for different CPP configurations. This would enable a whole of resource assessment to be undertaken to determine the optimum CPP configuration for a particular resource. It would also facilitate CPP circuit option / upgrade studies for brown field operations, such as the investigation of midsize circuit alternatives.

REFERENCES

- ESTERLE, J.S., CLARKSON, C., O'BRIEN, G., SWANSON, A.R. & FLETCHER, I.S., 2000: Predicting plant performance from small and large diameter bore cores. *Proceedings, Eighth Australian Coal Preparation Conference, Port Stephens 2000*, Paper A4.
- MEYERS, A .D. & LEACH, K.R., 2000: Realistic sizing and washability data from slim cores. In Beeston, J.W. (Editor): *Bowen Basin Symposium 2000 - The New Millennium - Geology*. Geological Society of Australia Inc. Coal Geology Group and the Bowen Basins Geologists Group, Rockhampton, October 2000, 365–370.
- SWANSON, A.R., STAINLAY, R., FLEMING, C. & WOOD, D.L., 1988: A further study into utilizing slim bore cores to provide detailed coal preparation data, *Proceedings of the Fourth Australian Coal Preparation Conference, Gladstone, 1988*, Paper 5A.

John O'Brien, john@abmylec.com.au (mailto:john@abmylec.com.au)

Andy Meyers, andy@abmylec.com.au (mailto:sam@abmylec.com.au)

Don Cameron, don@abmylec.com.au (mailto:sam@abmylec.com.au)

A&B MYLEC PTY LTD

A.K. Permana, Colin Ward, Z. Li, L.W. Gurba and S. Davison

Mineral matter in the high rank coals of the South Walker Creek area, Northern Bowen Basin

The coal of the South Walker Creek area, with a vitrinite reflectance ($R_{v_{max}}$) of 1.7 to 1.95% (semianthracite), is one of the highest rank coals currently mined in the Bowen Basin. The coal occurs in a single seam, split in places, and is dominated by inertinite (mainly semifusinite) with minor vitrinite, together with a small proportion of bituminite as a secondary maceral component. The minerals in the coal are represented mainly by fine grained cell cavity and pore infills (e.g. kaolinite, phosphates), with some nodules (mainly sideritic) and cleat infilling materials (mainly ankerite or kaolinite).

X-ray diffraction analysis of ply-by-ply samples shows that the mineral matter of the coal is dominated by kaolinite and interstratified illite/smectite in the top and bottom of the seam, along with typically a small proportion of quartz. In the middle of the seam, however, this is replaced by an illite-chlorite assemblage, with no quartz. Diaspore ($Al(OH)_3$) also occurs in some of the mid-seam coal plies. The kaolinite-bearing assemblages at the top and bottom of the seam are probably related to the depositional processes that formed the roof and floor strata, with additional kaolinite, quartz and phosphates being formed by authigenesis within the peat swamp. The illite-chlorite assemblages in the middle part of the seam, however, resemble a metamorphic association, and appear to have formed from interaction of the kaolinite assemblages and the organic matter with rank advance and/or hydrothermal fluid migration.

The XRD pattern of the illite, with an [001] peak at around 10.3\AA rather than the more usual 10.0\AA , indicates that the mineral is an ammonium illite, and this is confirmed by indications of nitrogen in the material when studied by SEM-EDS techniques. The mode of occurrence of the illite suggests that it was formed by incorporation of N (as NH_4^+) and possibly K^+ from the organic matter into the kaolinite structure with rank advance.

Keywords: Mineralogy, metamorphism, Bowen Basin, Australia

INTRODUCTION

The South Walker Creek coal mine is located near Nebo in Central Queensland, on the north-eastern flank of the Bowen Basin (Figure 1). The mine works one of the highest rank coals currently extracted from the Bowen Basin, mainly for the pulverized coal injection market. Previous studies carried out at UNSW (Fraser & others, 2006) identified significant variations in the nature and abundance of different minerals within a vertical section of the coal seam. Illite-chlorite



Figure 1: Location map (adapted from Davis & others, 2006)

assemblages resembling a metamorphic association were found in the middle parts of the seam section while kaolinite-rich assemblages suggesting more normal sedimentary origin were found in the upper and lower sections. The reason for this vertical variation is unknown, providing the prime focus for the present study.

Such changes in clay mineralogy within a coal seam may be a result of sedimentary processes in the original peat or derived from post-depositional interactions developed during rank advance. Daniels & Altaner (1990), for example, report the metamorphic development of ammonium illite (NH_4 -illite) in high-rank coals of the Anthracite Region in Pennsylvania, and Ward & Christie (1994) describe similar minerals in semi-anthracites of the Baralaba area in the southern Bowen Basin. However, the changes at South Walker Creek, if metamorphic, might also be due to more localised effects, such as igneous intrusions or injection of hot fluids into the coal seam (Kisch, 1966, 1968; Usyal & others, 2000; Susilawati & Ward, 2006).

The aim of this paper is to investigate the geological factors responsible for mineral matter occurrence and the mineralogical variation within the coals of the South Walker Creek deposit. It is based on examination of mineralogical profiles from different parts of the open-cut operation, using XRD, XRF, SEM and optical microscopy techniques.

COAL GEOLOGY

The South Walker Creek deposit is located on the eastern flank of the Carborough Syncline, within the Nebo Synclinorium in the northern Bowen Basin. The coal-bearing sequence is part of the Rangal Coal Measures, which are conformably underlain by the Fort Cooper Coal Measures and overlain by the Rewan Formation. The Rangal Coal Measures in the area are approximately 150m thick and comprise light grey, cross bedded, fine to medium grained labile sandstone, grey siltstone, mudstone and coal seams. Elsewhere in the region the Rangal Coal Measures contain two economic seams, the Elphinstone and the Hynds, with the latter containing the Yarrabee Tuff. At South Walker Creek the most economic coal bed is the Main seam, which splits to the north and the south to form the Main Tops and Main Bottoms. The Main seam may be equivalent to the Elphinstone seam and the top part of the Hynds. The remainder of the Hynds seam at South Walker Creek is represented by an uneconomic, thin and banded carbonaceous horizon.

The strata at South Walker Creek are moderately structurally deformed, due to a compressional stress regime. Several major faults have been exposed in the pits; NNE normal faults are the dominant type, but thrust faults are also found in places. Slickensides with coatings of dickite and nacrite are a common feature in the fault zones, and shearing also occurs within the coal seam. A sub-vertical dolerite dyke and associated sill have been exposed in ramp G of the Mulgrave Pit, and dolerite intrusives were intersected at Ramps Y and Z of the Walker Pit area.

SAMPLING AND ANALYTICAL TECHNIQUES

A series of 338 coal samples from 21 boreholes in the Mulgrave and Walker Pit areas of the South Walker Creek mine were made available by the company to facilitate the study, covering most of the strike length available in the deposit (Figure 2). The seam section in each bore had been sampled by the company in successive increments of 0.5 m, providing a basis for evaluating the mineralogical profile at each individual site. Lithologic logs and down-hole geophysical data for each hole were also made available to assist the study.

Individual core samples around 100 mm long, taken from specific depths in the borehole (Borehole 11424) studied by Fraser & others (2006), were added to the sample suite and subjected to more comprehensive chemical, petrographic and SEM evaluations. Hand specimens of coal were also collected



Figure 2: Location of pits and boreholes studied at the South Walker Creek mine.

from the exposed mine workings (Walker & Toolah Pits), and used for similar mineralogical and microscopic studies.

Representative portions of the coal samples were powdered and subjected to low-temperature oxygen plasma (radio-frequency) ashing, following Australian Standard procedures. The mineralogy of the low-temperature ash (LTA), and also of associated non-coal rock samples where available, was evaluated by X-ray powder diffraction, with quantification using the Rietveld-based Siroquant™ data processing system (Taylor, 1991). The clay (<2 micron) fractions of each LTA and rock sample were separated by settling and prepared as oriented aggregates, which were then subjected to more detailed mineralogical analysis using ethylene glycol and heat treatment. Selected coal samples were also ashed at 815°C, and along with the non-coal rocks the ashes were subjected to X-ray fluorescence analysis to determine chemical composition.

Twenty four polished sections of the coal samples from Borehole 11424 were examined using optical microscopy techniques, including vitrinite reflectance measurement and maceral evaluations. Selected coal samples from this borehole were also analysed under a Hitachi S3400-I scanning electron microscope (SEM), equipped with an energy-dispersive X-ray spectrometer (EDS), to identify more clearly the modes of mineral matter occurrence within the coal seam.

RESULTS AND DISCUSSION

Coal petrology

Polished section observations indicate that the coal at South Walker Creek is dominated by inertinite, with minor vitrinite. A small proportion of bituminite occurs as a secondary maceral component, filling cleats in the vitrinite and displaying an orange to yellow fluorescence. The bituminite was probably formed from light and heavy oils which were polymerized as bitumen in vitrinite cleats after diffusion through inertinite cavities. The occurrence of this secondary maceral is generally associated with hydrothermal systems (Simonit, 1994; Glikson & others, 2000).

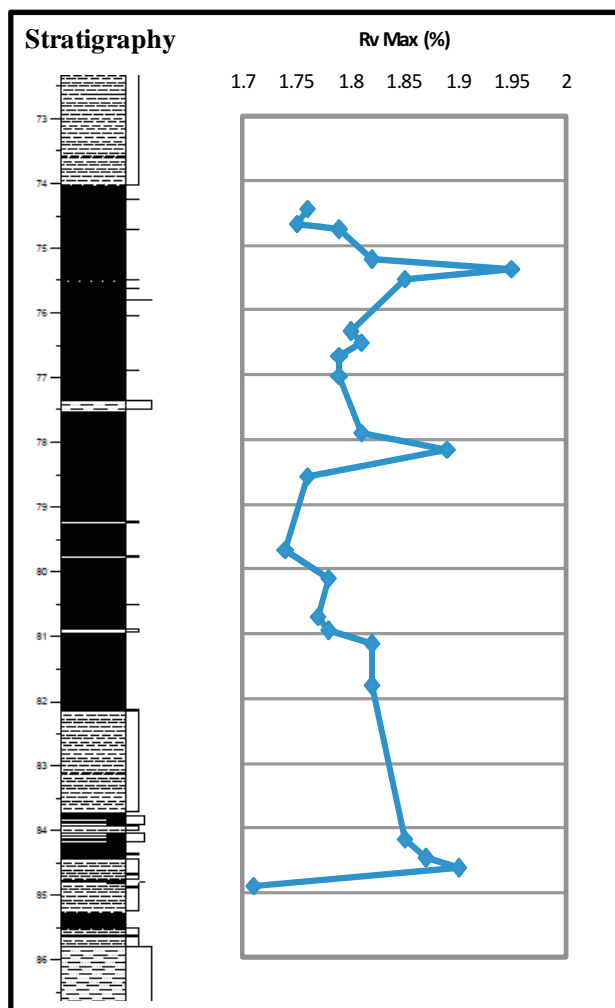


Figure 3: Profile showing variation in reflectance ($R_{v_{max}}$) with depth in the coal seam from Borehole 11424 in the Mulgrave Pit at South Walker Creek.

Vitrinite reflectance data for samples from Borehole 11424 indicate $R_{v_{max}}$ values ranging from 1.70 to 1.95%, representing a semianthracite level of rank advance. The values for the individual samples show an irregular pattern from the top to the bottom of the seam (Figure 3), possibly representing a response in the organic matter to uneven heat distribution from a hydrothermal system (cf. Glikson & others, 2000). Thus, although the overall rank of the coal is relatively high, the irregular reflectance profile may possibly be a result of hydrothermal processes associated with fluid injection superimposed on more uniform burial effects.

Coal mineralogy

XRD analysis shows that the mineral matter in the coal seam consists mainly of clay minerals (kaolinite, illite, illite/smectite, chlorite and diaspore), with varying proportions of carbonate minerals (calcite, ankerite, siderite) and quartz. Minor proportions of rutile, anatase, apatite, goyazite and bassanite are also present in the LTA of many coal samples, along in some cases with paragonite, dickite and/or nacrite. The relative abundance of the main minerals within the LTA or rock samples varies considerably through the seam, with a typical mineralogical profile indicated in Figure 4.

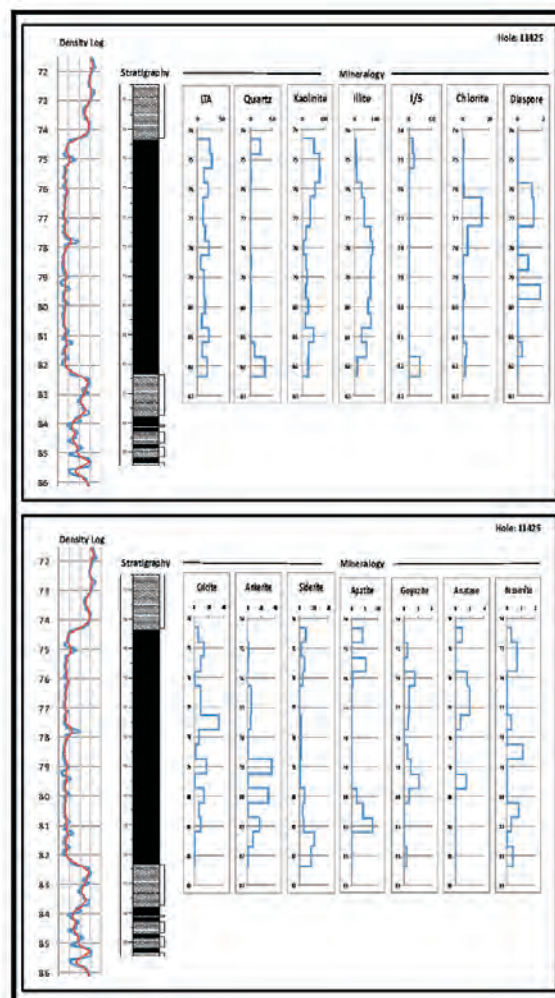


Figure 4: Distribution of minerals in LTA for a vertical sequence through the Main coal seam (Borehole 11425). Depth values are in metres.

Quartz and the clay minerals

Clay minerals are the dominant components in the mineral matter of the coal seam. Kaolinite and interstratified illite/smectite are very abundant in the top and bottom parts of the seam, associated with a small proportion of quartz. In the middle of the seam, however, the LTA is dominated by an illite-chlorite assemblage, with almost no quartz being present. Diaspore is also commonly associated with the illite and chlorite components.

XRD studies indicate that the illite in the LTA has a $d[001]$ crystal spacing of around 10.3\AA , in contrast to the more usual spacing of 10.0\AA . This and other features of the XRD pattern suggest that the material is ammonium illite (NH_4 -illite) rather than the more common potassium illite (K-illite), although in some cases NH_4 -illite and K-illite may both be present. Ammonium illite is commonly thought to be formed by substitution of NH_4^+ for K^+ in the original mica or illite structure (Juster & others, 1987; Ward & Christie, 1994). However, Daniels & Altaner (1993) and Sucha & others (1994) suggest that the mineral can also be formed at relatively high temperatures ($> 200^\circ\text{C}$) by interaction of kaolinite with nitrogen released from the organic matter in coal seams during metamorphism or rank advance.

SEM-EDS studies suggest that the kaolinite in the South Walker Creek coal generally occurs as layers, lenses and fine dispersed particles in the maceral components, particularly the relatively abundant inertinite macerals. In some cases kaolinite infills cell lumens or pore spaces, associated with apatite, and in other cases it occurs as a cleat infilling along with anatase. This suggests that kaolinite in the coals at South Walker Creek occurs as both a syngenetic and an epigenetic phase within the coal seams.

Illite typically occurs as lenses and finely dispersed material, and in some instances is found in thin layers associated with interstratified illite/smectite minerals. Although the element is inherently difficult to identify by SEM-EDS analysis, there is some indication that nitrogen is present in some of the illite, particularly the illite intimately associated with the maceral components. The inverse relationship between illite and kaolinite abundance within the seam (Figure 4), coupled with the SEM-EDS observations, suggests that the ammonium illite in the South Walker Creek coal may have been formed by interaction of kaolinite with N released from the organic matter under high temperatures associated with fluid injection or rank advance.

In addition to ammonium illite, XRD analysis indicates that chlorite is also abundant in the middle parts of the coal seam. SEM-EDS observations show that chlorite occurs as small lenses, finely dispersed particles and infillings of cell lumens in the maceral components. Renton (1982) indicates that chlorite is unstable in peat-forming environments, and thus the association of chlorite with illite in the middle parts of the seam (Figure 4) could possibly indicate chlorite formation in association with rank advance. Sanguesa & others (2000) and Susilwati & Ward (2006) have suggested that chlorite in similar cases was formed by interaction of kaolinite with Fe^{2+} and Mg^{2+} released from the organic matter or carbonate minerals and Si from quartz that may also be present.

Although not strictly a clay mineral, the bauxite mineral diaspore ($\text{Al}(\text{OH})_3$) occurs in some of the mid-seam coal plies (Figure 4), often in association with abundant illite and chlorite. SEM-EDS observation indicates that the diaspore occurs as tabular shaped particles in the vitrinite macerals. As well as being formed by deep weathering, diaspore may also be formed by hydrothermal alteration of aluminous minerals (Deer & others, 1992). Its association in the present study with decreases in the abundance of kaolinite and interstratified illite/smectite may indicate that the diaspore, like the chlorite, is a product of kaolinite alteration due to heat-induced changes within the coal seam.

Dickite has been reported as cleat and fracture infills or coatings on slickenside surfaces associated with the fault zone in the South Walker Creek area. XRD analysis of slickensided coal from the Toolah Pit also indicates that nacrite occurs in a similar way. The formation of the kaolinite polymorphs dickite and/or nacrite in other settings has been related to the influence of hot fluid circulation associated with tectonic deformation (Lin & Wang, 1997; Buatier & others, 1997; Goemaere, 2004), and a similar mechanism is suggested for the occurrences in the South Walker Creek deposit.

XRD analysis show that quartz mostly occurs in the top and bottom of the seam (Figure 4) associated with kaolinite and mixed layer illite-smectite. It is virtually absent from the middle part of the seam, where illite, chlorite and diaspore are typically the main clay mineral components. The quartz in the top and bottom of the seam appears to be mainly of detrital origin (Figure 5B). However, especially in the middle of the seam, quartz also occurs in cell lumens and pore spaces (Figure 5A), suggesting formation by authigenic processes.

Carbonates, phosphates and other minerals

The carbonate minerals in the coal primarily consist of calcite and ankerite, along with lesser proportions of siderite. The siderite is most abundant in the top and bottom parts of the seam, occurring as nodules in inertinite (Figure 5C) and as fine grained syngenetic lenses. Calcite and ankerite, by contrast, occur mainly in the cleats or as veins in the vitrinite macerals (Figure 5D), especially in the middle part of the seam, and appear to be of epigenetic origin. However, in some instances they also infill cell lumens in inertinite.

Small proportions of apatite and goyazite are indicated from XRD analysis, mostly making up less than 5% of the mineral matter. Goyazite has a varying abundance in the vertical sequence, but apatite appears to be most abundant in the top and bottom of the seam (Figure 4). Apatite and goyazite commonly infill cell lumens of the inertinite macerals, associated with kaolinite (Figure 5E), but may also occur as cleat infillings associated with kaolinite and calcite. This suggests that phosphate minerals may be both authigenic and epigenetic in origin. Davis & others (2006) have suggested that epigenetic apatite in the South Walker Creek coal was formed by low-temperature fluid migration through permeable zones at locations where faults intersect the coal seam.

Rutile and/or anatase occur as spherical particles in the vitrinite macerals and clay minerals. In some instances they also occur as euhedral crystals cross cutting kaolinite in veins (Figure 5F). This indicates that rutile and anatase formed mostly as a product of weathering in detrital minerals or during early coalification. At a later stage, however, some rutile and/or anatase also crystallized to infill cleat fractures, associated with deposition of epigenetic kaolinite minerals.

Relation of mineralogy and ash chemistry

Figure 6 provides a comparison of the chemical composition for Borehole 11424 of the coal ash implied by the mineralogy derived from the XRD analysis to the chemical analysis of the coal ash (815°C) as determined directly by XRF analysis. The comparisons for each major oxide are expressed as graphic plots, with a diagonal line on each plot to indicate equality in the percentages indicated by the two techniques.

The graphic plots for most elements (SiO_2 , Al_2O_3 , CaO , MgO , Fe_2O_3) have a relatively high correlation, with the data points plotting close the equality line. The percentages of these major oxides inferred from the Siroquant data are thus close to

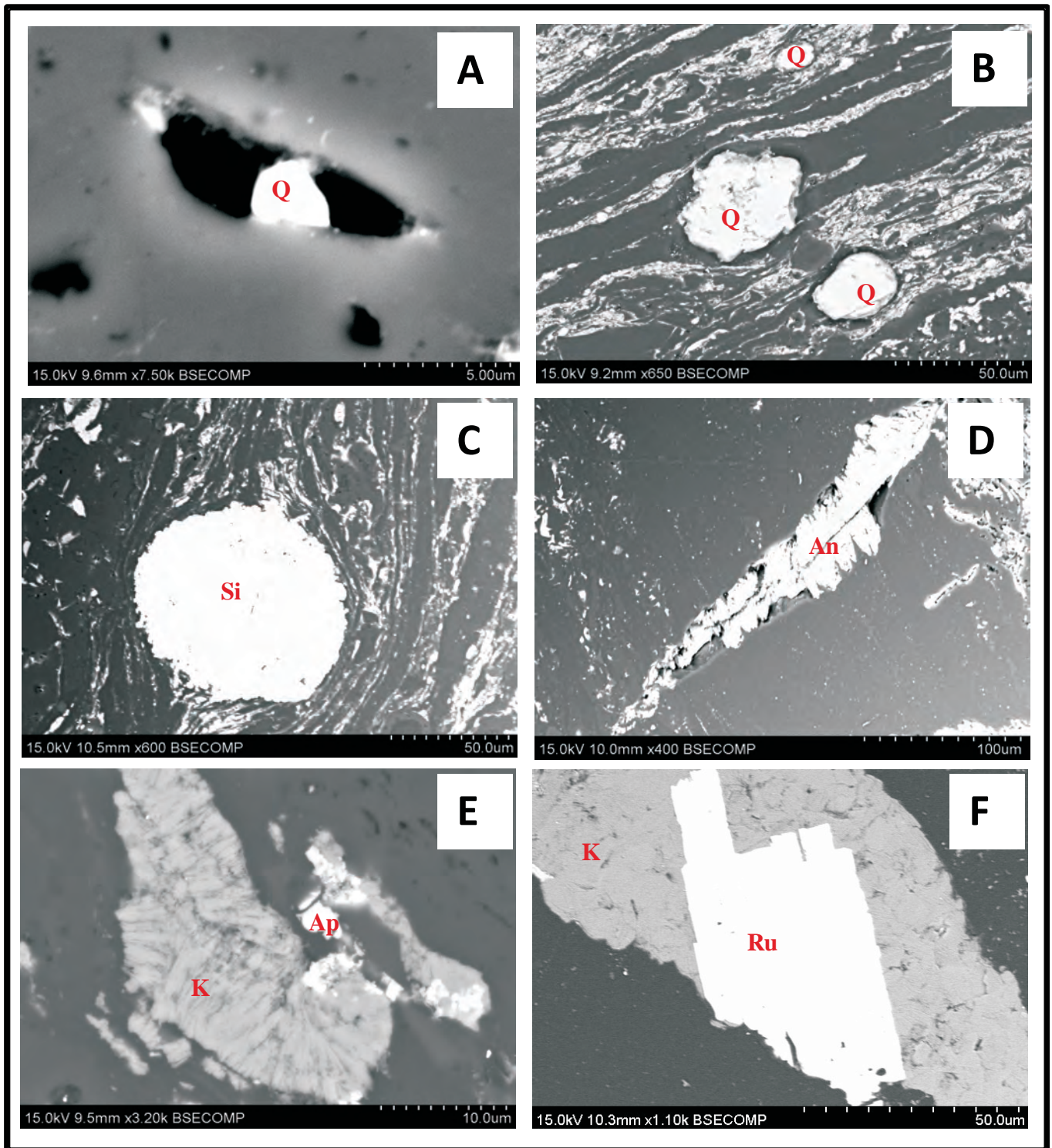


Figure 5: Photomicrographs showing modes of mineral occurrence in coal from South Walker Creek. A: Subrounded quartz (Q) in pore space; B: Rounded particles of detrital quartz (Q); C: Siderite nodules (Si); D: Ankerite (An) infilling cleat in vitrinite; E: Association of kaolinite (k) and apatite (Ap); F: Prismatic crystals of rutile (R) cross cutting kaolinite in a vein.

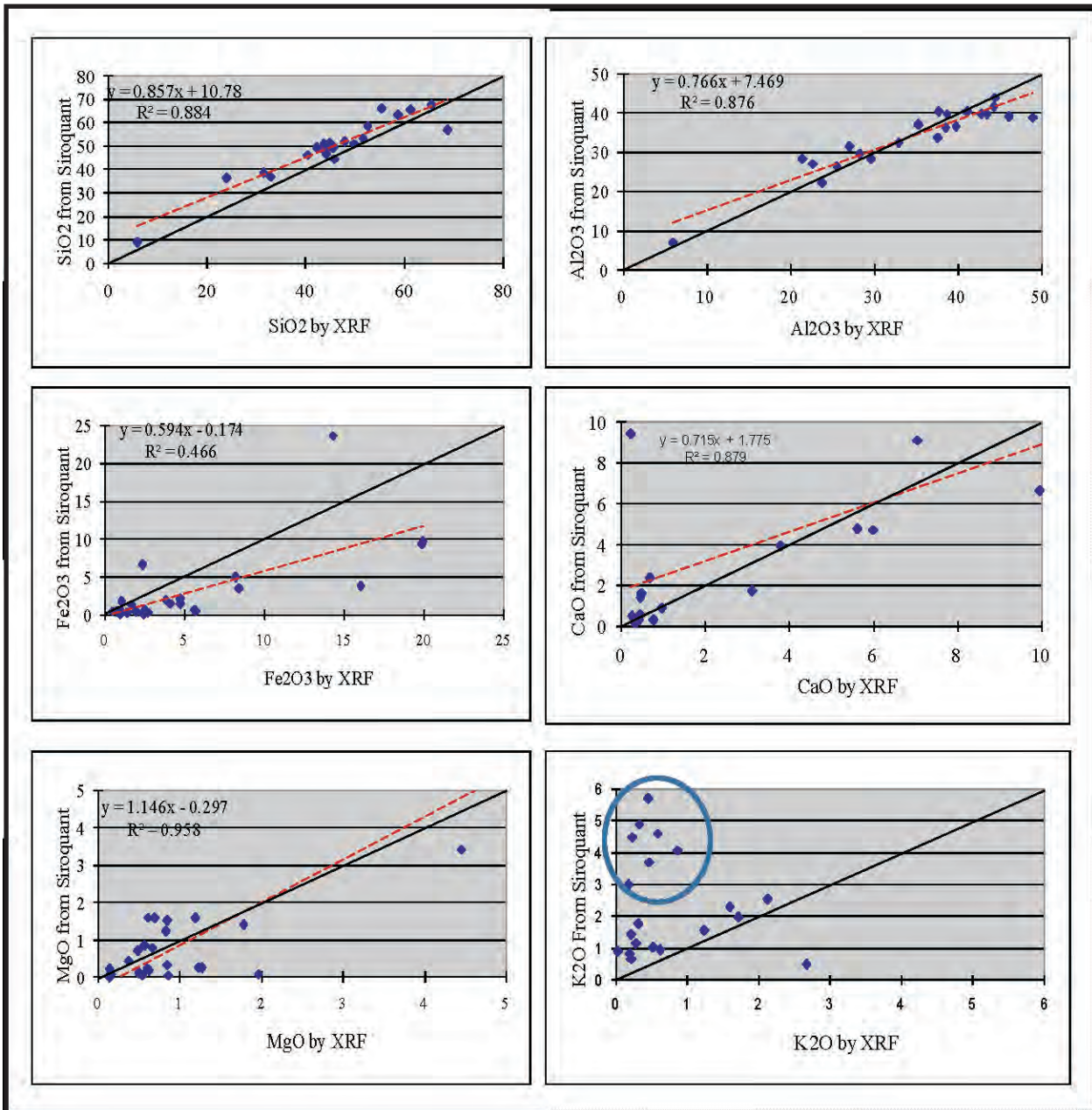


Figure 6: Relation between proportions of major element oxides observed from XRF (x-axis) and inferred from XRD data (y-axis) for ash of the South Walker Coal (Borehole:11424). Full square shape in the circle area shows an over-estimation of K₂O proportion by Siroquant, it is indicate that high illite but low K₂O percentages are consistent with ammonium (NH₄) illite rather than potassium (K) illite

actual percentages of each oxide indicated by XRF analysis. However, the plot for K₂O suggests an over-estimation by Siroquant, compared to the direct determination in conventional ash analysis. The proportion of K₂O inferred from the Siroquant data, however, is based on a potassium illite. The contrast between the high proportion of K₂O inferred from the XRD and the low proportion of K₂O indicated by the actual ash chemistry are therefore consistent with the presence of abundant NH₄-illite rather than K-Illite in the coal samples.

If allowance is made for the occurrence of Ca, Mg and Fe in carbonates, phosphates or sulphates, the normalised chemistry of the coal ash shows very little variation over the main part of the coal seam, despite the changes from a kaolinite-rich to an illite-rich clay mineral assemblage (Figure 7). The coals at the top and bottom of the seam, which have significant

percentages of quartz in the mineral matter, have ashes with higher proportions of SiO₂. However, the ashes from the other plies in the seam all have approximately equal proportions of SiO₂ and Al₂O₃ on a normalised basis, and all plies, regardless of the illite percentage, have ashes with low K₂O percentages. This suggests that, although nitrogen may have been remobilised from the organic material, the changes in the silicate fraction of the coal took place without an associated change in the balance between SiO₂, Al₂O₃ and K₂O in the mineral matter.

CONCLUSIONS

The inertinite rich coal in the South Walker Creek deposit contains minerals of syngenetic, diagenetic and epigenetic origin. Quartz, siderite and clay minerals occur at the top and

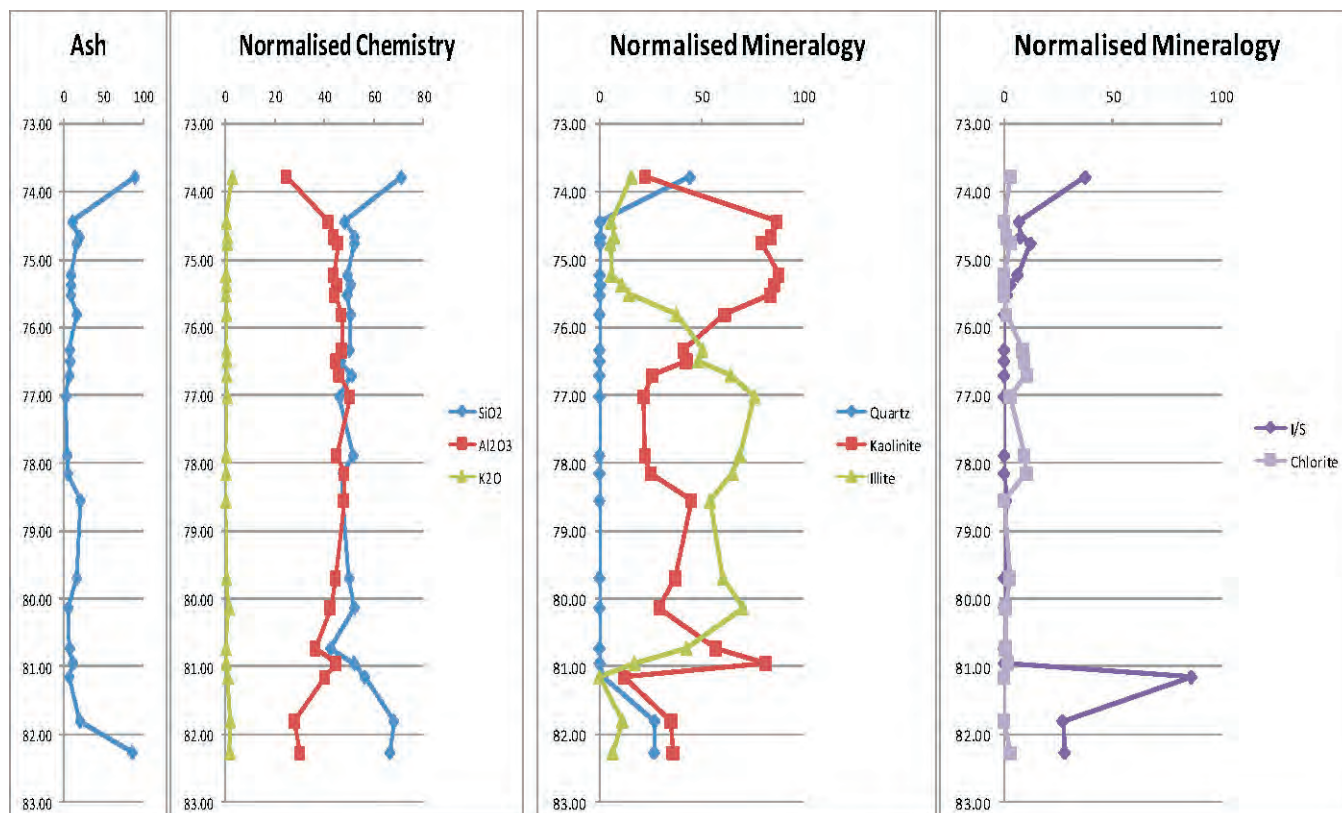


Figure 7: Relation between proportions of normalised chemistry and normalised mineralogy for ash coal of the South Walker Coal (Borehole:11424).

bottom of the seam, mainly derived from sediment input to the original peat swamp combined with early diagenetic remobilisation and pore-filling processes. Minerals such as calcite and ankerite, along with additional kaolinite and in some cases rutile and apatite, were precipitated in cleats and fractures at a later stage as a result of epigenetic activity.

Mineralogical studies indicate that a mixture of kaolinite, illite/smectite and quartz occurs in the upper and lower parts of the seam, but that an assemblage dominated by ammonium illite, chlorite and diaspore is developed in the middle part of the coal bed. This change appears to have been brought about by interactions among the quartz and other silicates at relatively high temperature, probably with addition of nitrogen released from the organic matter. Decreases in the abundance of kaolinite and quartz, coupled with increases in illite, chlorite and diaspore, suggest that the kaolinite was the main precursor for generation of the other clay minerals.

An irregular pattern of reflectance distribution through the seam may indicate the influence of hydrothermal fluids on the coal, superimposed on the overall process of rank advance due to burial effects. Cleats and fractures within the coal probably enhanced permeability and fluid circulation, further influencing illitization and chloritization in the middle of the seam. The cleats and fractures were also mineralized with dickite, nacrite, kaolinite, calcite, ankerite and some apatite, probably by precipitation from hydrothermal solution. The ammonium illite, in particular, was probably formed by interaction of kaolinite with nitrogen derived from the organic matter in response to thermal impacts from a combination of rank advance and fluid circulation.

ACKNOWLEDGEMENTS

This study forms part of an MSc research program supported by a scholarship from ADS (Australian Development Scholarship). Thanks are expressed to BHP Billiton Mitsubishi Alliance (BMA) Coal Pty Ltd for provision of the coal samples and other data and for permission to conduct the investigation. Thanks are also expressed to Irene Wainwright of UNSW for the chemical analyses, and to Joanne Wilde at UNSW for preparation of the polished sections.

REFERENCES

- BUATIER, M., TRAVE, A., LABAUME, P. & POITEVIN, J.L., 1997: Dickite related to fluid-sediment interaction and deformation in Pyrenean thrust-fault zones. *European Journal of Mineralogy*, **9**, 875–888.
- DANIELS, E.J. & ALTANER, S.P., 1990: Clay mineral authigenesis in coal and shale from the Antrachite region, Pennsylvania. *American Mineralogist*, **79**, 825–839.
- DANIELS, E.J. & ALTANER, S.P., 1993: Inorganic nitrogen in anthracite from eastern Pennsylvania, USA. *International Journal of Coal Geology*, **22**, 21–35.
- DAVIS, B., ESTERLE, J. & KEILAR, 2006: Determining geological controls on the spatial distribution of phosphorus within coal seams mined at South Walker Creek Mine, Bowen Basin, Central Queensland, Australia. In: Griffin, J. (Editor): *Proceedings of the Thirty-sixth symposium on Advances in the study of the Sydney Basin*, 27–35.

- DEER, W.A., HOWIE, R.A. & ZUSSMAN, J., 1992: *An introduction to the rock-forming minerals*. John Wiley and Sons Inc. New York.
- FRASER, S., ESTERLE, J., WARD, C., HENWOOD, R., MASON, P., HUNTINGTON, J., CONNOR, P., SLIWA, R., COWARD, D. & WHITBOURN, L., 2006: Automated Mineralogical Logging of Coal and Coal Measure Core. End of Grant Report, ACARP Project C13014, CSIRO Exploration and Mining Report P2005/281.
- GLIKSON, M., GOLDING, S.D., BOREHMAN, C.J. & SAXBY, J.D., 2000: Mineralization in eastern Australia coals: a function of oil generation and primary migration. In: Glikson, M. & Mastalerz, M. (Editors): *Organic Matter and Mineralisation*. Kluwer Academic Publishers, 327–358.
- GOEMAERE, E., 2004: Dickite and nacrite from the Liege Coal Basin, Belgian Coal Measures Group, Westphalian, Upper Carboniferous. *Geologica Belgica*, **7**(3–4), 285–311.
- JUSTER, T.C., BROWN, P.E. & BAILEY, S.W., 1987: NH₄-bearing illite in very low grade metamorphic rocks associated with coal, north-eastern Pennsylvania. *American Mineralogist*, **72**, 555–565.
- KISCH, H.J., 1996: Chlorite-illite tonstein in high-rank coals from Queensland, Australia. Notes on regional epigenetic and coal rank. *American Journal of Science*, **264**, 386–397.
- KISCH, H.J., 1998: Coal rank and lowest grade regional metamorphism in the southern Bowen Basin, Queensland, Australia. *Geologie en Mijnbouw*, **47** (1), 28–36.
- LIN, S.B. & WANG, Y.R., 1997: Mineralogy and tectonic implication of the dickites from Hung-Chun Peninsula, Southern Taiwan. *Acta Geologica Taiwanica*, **27**, 19–32.
- RENTON, J.J., 1982: Mineral matter in coal. In: Meyers, R.A. (Editor): *Coal Structure*. Academic Press, New York, 283–325.
- SANGUESA, F.J., AROSTEGUI, J. & SUAREZ-RUIZ, I., 2000: Distribution and origin of clay minerals in the lower cretaceous of the Alava Block (Basque-Cantabrian Basin, Spain). *Clay Minerals*, **35**, 393–410.
- SIMONIET, B.R.T., 1994: Organic matter alteration and fluid migration in hydrothermal systems. In: Parnell, J. (Editor): *Geofluids: origin, migration and evolution of fluids in sedimentary basins*. Geological Society, London, *Special Publication*, **78**, 261–274.
- SUCHA, V., KRAUS, I. & MADEJOVA, J., 1994: Ammonium illite from anchimetamorphic shales associated with antrachite in the Zemplinicum of the Western Carpathians. *Clay Minerals*, **29**, 369–377.
- SUSILAWATI, R. & WARD, C.R., 2006: Metamorphism of mineral matter in coal from the Bukit Asam deposit, south Sumatra, Indonesia, *International Journal of Coal Geology*, **68**, 171–195.
- TAYLOR, J.C., 1991: Computer programs for standard less quantitative analysis of minerals using the powder diffraction profile, *Powder Diffraction*, **6**, 2–9.
- USYAL, I.T., GOLDING, S.D. & AUDSLEY, F., 2000: Clay mineral authigenesis in the Late Permian Coal Measures, Bowen Basin, Queensland, Australia, *Clays and Clay Minerals*, **48**, 351–365.
- WARD, C.R. & CHRISTIE, P.J., 1994: Clay and other minerals in coal seams of the Moura-Baralaba area, Bowen Basin, Australia, *International Journal of Coal Geology*, **25**, 287–309.

N. Lambert, M. Campbell, G. Ryan, E. Rooker, K. McLennan and A. Coffey

Further refinement of the clean process technologies ultimate froth flotation test

A new test method was developed which gives a result closer to the theoretical flotation yield across a range of coal types in ACARP project C14068. This method has since been further refined to give a closer flotation response curve to the possible theoretical curve. It removes much of the inconsistency that occurs with the use of the current AS 4156.2.2-1998 Part 2.2: Higher rank coal – Froth flotation – Sequential procedure.

The Ultimate Flotation Test (UFT) involves floating a 400g sample of coal sequentially to produce a number of concentrates and tailings. The 400g sample is sized into a coarse and fines fraction, which are then floated separately producing several concentrate and tailing samples. The concentrate is successively refloats until it has been split into smaller fractions that are in turn refloats. Each new concentrate and tailings is then dried and analysed for mass, moisture and ash. Both yield and ash are reported on a dry basis. The advantage of sizing before flotation is to have the coarse material completely slimes free. The original UFT has been described in literature as a method of estimating the outcome of a flotation circuit installation.

The further development of the UFT has led to the development of a method to calculate a partition curve for an operating plant flotation cell. It should be noted that at the time of the writing of this report further improvements had been made to both the UFT (CPT UFT 2010 method) and the partition curve calculation method and that development is expected to continue. It is proposed that this method is analogous to a float-sink test for the fines fraction of a coal resource.

INTRODUCTION

The Australian Coal Association Research Program (ACARP) commissioned a study to develop a new test procedure that would determine the best possible flotation performance for a wide variety of coal samples, with varying characteristics and feed ash values. This requires the production of a cumulative mass yield versus ash curve that is as close as possible to the ultimate flotation response.

The UFT was presented in a paper at the 12th Australian Coal Preparation Conference. Since the presentation of the original method, the test has been refined to improve the flotation response curve even further than was originally possible with the UFT.

Through successive trials of the various methods and subsequent analysis of the results achieved on the same

flotation feed sample, it is possible to show how different methods perform in their prediction of flotation response.

Four methods were assessed during the ACARP project. They were:

- AS 4156.2.2-1998
- ISO 8858-3:2004(E)
- ACARP Project C10044
- CPT UFT

Four coal samples of different types and regions of Australia were tested. These were:

- Hunter Valley Coal
- Bowen Basin Coal
- Newcastle Lake Macquarie Coal
- Illawarra Coal

The UFT Method was shown to be the most comprehensive test of the four methods trialled in ACARP project C14068. In summary, the findings of ACARP Project C14068 were that the UFT froth flotation method performed better than the current industry standard procedures. In particular, the major advantages with this method were considered to be:

- Improved flotation response curves
- Total elimination of slimes entrainment from coarse concentrate fractions
- Detailed operator instructions that define reagent additions
- Improvements to flotation test equipment and setup
- The requirement that mass yield and ash be reported on a dry basis
- No new specialised equipment needed
- Small (400g) sample mass required

Froth flotation testing is carried out on both bore core samples and samples taken from a plant situation. During the development of the UFT an investigation was undertaken into the different methods that were being used in laboratories across Australia. It was found that there were over 100 methods being used that claimed conformity to AS 4156.2.2-1998 Part 2.2: Higher rank coal – Froth flotation – Sequential procedure. As part of the ACARP Project C14068 it was found that the results from the current Australian Standard AS 4156.2.2 – 1998 were dramatically underestimating the potential yield from fine coal flotation, particularly for high clay samples such as thickener underflow. It was found in one case that the Australian Standard method gave a mass yield of 50 (% d/d) at an ash of

25 (% d), where as the UFT test gave a mass yield of 50 (% d/d) at an ash of 13.5 (% d) (see Figure 8).

The current Australian Standard AS 4156.2.2 (1998) method does suffer from a number of issues such as a high degree of operator dependency (for example selection of reagent dosage rates). Operators require a very high level of training and experience as various stages of the test necessitate operator judgement which will impact directly on the results. In addition to this operator dependency issue, the lack of froth washing in existing procedures leads to the entrainment of slimes in the concentrates. These issues may not only contribute to poor reproducibility of the test but also accuracy as it may underestimate the flotation yield and overestimate product ash. The method also relies on a high number of sample transfer steps, each one running the risk of incomplete sample recovery. Any loss of sample will affect sample integrity and may impact on both yield and ash value.

Another factor in the inconsistency of the tree test is the myriad of client defined "modified froth flotation methods" that have become common, where a very small number of fractions, often as low as five, are requested for analysis. The curves produced from such methods may still be used for plant comparisons but in all probability would show an inferior flotation response which may in turn contribute to a poor reputation for AS4156.2.2.

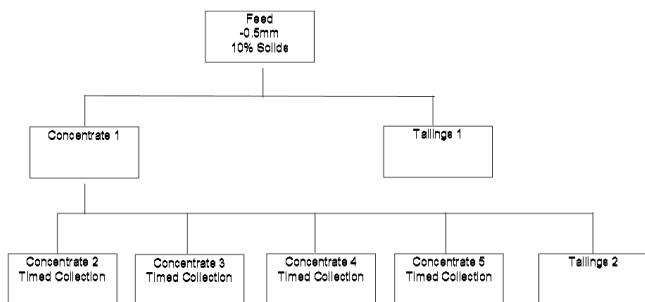


Figure 1: Example of modified tree flotation method

This method recommends that mass and ash for each of the flotation fractions be reported on an air-dried basis. The influence of moisture variations between samples will distort the flotation response (Lambert & others, 2008), and as such a dry basis reporting standard should always be used. Dry basis reporting is currently mandatory in AS 4156.2.2, but it is seldom used.

Sampling of flotation streams is often difficult and can be subject to bias. As an example, sampling slurry from the bottom of horizontal pipes may result in samples which are over representative of the coarse particles. Fast flowing vertical slurry streams may over represent the coarse particles if the 'boiling effect' results in the loss of fine particles from hand held ladles. The feed can be the most difficult of the streams to sample due to the high variability in the average ash value of the stream. Flotation circuits are challenging due to their high volume. They are generally sampled manually, and the sampling points do not normally comply with the requirements for correct sampling practice. The accurate sampling and testing of these streams is critical as the ash

values of the feed, concentrate and tailings are then used to estimate flotation yield using the equation

$$MY_a = \frac{t-f}{t-p} \times 100 \quad (1)$$

Where MY_a is the mass yield calculated from ash (% d/d), t is the tails ash value (% d), f is the feed ash value (% d) and p is the product ash value (% d). Consider the following:

Feed Ash =	20.0 % (d)	} Calculated Yield = 75.0 %
Concentrate Ash =	10.0 % (d)	
Tailings Ash =	50.0 % (d)	

If the feed ash had been biased high due to difficulties in sampling, then the actual recovery would have been:

Feed Ash =	22.0 % (d)	} Calculated Yield = 70.0 %
Concentrate Ash =	10.0 % (d)	
Tailings Ash =	50.0 % (d)	

It is demonstrated in this simple calculation that a 2.0 % (absolute) change in the feed ash has resulted in a 5.0 % change in mass yield.

If the laboratory flotation test and a plant audit are to be compared accurately, then the feed ash for both needs to be identical and all results reported on a dry basis. For accurate results, the feed sample should be the same as that used for flotation testing and any sub-division accurately performed to ensure that all samples are representative.

A recent sampling study performed on a coal slurry system in a pilot plant installation (Lambert & others, 2010) has demonstrated that currently prevalent CPP sampling standards appear to be woefully inadequate in accurately representing the nature of slurry streams. The example demonstrating the effects of a 2 % variation in feed composition due to poor sampling is in the authors' opinions an optimistic estimate, and most slurry sampling installations would operate at a minimum of ± 20 % relative uncertainty in ash value determination. If all slurry streams – not just the feed – vary by this amount, then the calculation uncertainty increases further. In many cases the potential errors in downstream calculations become so large as to make the data essentially meaningless.

Poor sampling practice has a significant impact on the effectiveness of the UFT as a plant performance auditor. The increased precision of the UFT compared with more traditional flotation testing allows UFT data of a feed, product and tails sample to be used to generate an ash-based partition curve. This makes the UFT analogous to a float sink test.

The partition curves can be developed in three ways: Taking the mass to product as a fraction of the mass in the feed, taking the mass in the feed minus the mass in the tails as a fraction of the mass in the feed, and taking the mass of the product as a fraction of the mass of the reconstituted feed (the product mathematically recombined with the tails). In this manner it becomes immediately apparent when samples are not accurate, as negative or greater than 100 % recoveries will be recorded for particular fractions in the partition curves that

use the feed composition as an input value. When the reconstituted feed is compared to the actual feed sample the reasons for the discrepancies become apparent. It has been demonstrated in testwork performed on samples from a Hunter Valley CPP that in some cases as much as 85 % of the material in the product and tails samples of a working flotation cell was not evident in the feed sample.

It can be suggested from a thorough review of the sample data available that significant improvements must be made to the current methods of acquisition and analysis. It is the authors' opinion that the complete potential of the UFT as both a resource evaluation tool and a method of plant performance auditing will not be reached until concurrent advances in sampling practice are implemented. CPT has developed a range of samplers that address this issue. These samplers are available for installation in operating CPPs.

METHODOLOGY

It should be noted that samples collected for laboratory testing may suffer deterioration in flotation properties due to storage time and/or sample preparation procedures. This may in itself lead to discrepancies, if compared directly to the flotation response from "fresh" flotation feed that is constantly delivered to industrial plant equipment. Regardless of the similarity in feed ash values the laboratory sample may have quite different surface properties. This may be especially true for borecore type samples that undergo the effects of drilling, lengthy pre-treatment stages followed by numerous air-drying steps.

To achieve the closest ultimate flotation response curve to the theoretical flotation response curve for any coal sample, the entrainment of slimes into the concentrates has to be minimised. There are various ways of achieving this, such as using wash water as in the C6044 froth flotation method (Atkinson, Blanchard, 1999). Using wash water however does not eliminate all slimes from the concentrates.

Sizing

The concentrates are sized into coarse and fines to remove any slimes contamination from the coarse fraction, this ensures that little or no slimes contamination is present in the coarse fraction.

The sizing step helps show a more accurate flotation response for the coarser particles. Observation shows that some of these coarser particles tend to remain in the flotation cell on refloating. This appears to be due to the hydrodynamics of the cell. The coarse particles are visibly caught in eddies within the centre of the unit. Numerous refloats of concentrates are often required to remove the entrained slimes, but each time that a refloat is performed, it appears that a proportion of these coarser particles are lost due to them being caught in these eddies, irrespective of particle hydrophobicity. Sizing the sample completely removes the entrained slimes from the coarse concentrate, meaning that only two refloats are required before the material is split into smaller higher and

lower ash fractions. This reduces the loss of the coarser material to tails.

To size the flotation products for the purpose of slimes removal may at first be considered inappropriate, however it is merely a tool to help give the true theoretical flotation response. This test is to find the theoretical yield from a sample, not to replicate exact plant practice. Sizing guarantees the removal of slimes from the flotation products. In some circumstances, plant sizing is performed to maximise flotation yield. Hydrocyclones may be used prior to flotation and either the underflow floated only (this has a reduced slimes loading) or both the underflow and overflow floated separately. Cycloning is an imperfect plant practice, whilst laboratory sieve sizing ensures perfect desliming. Even if deliberate desliming of flotation feed is not performed within the plant, any flotation process itself involves desliming. Froth drainage will occur as soon as there is a froth depth. This froth drainage, combined with wash water addition, is a form of desliming.

Flotation

Following sizing, the coarse and fine fractions are floated separately.

The coarse fraction is floated 2–3 times producing a concentrate and subsequent tails each time before being floated a final time where the concentrate is split into small discrete concentrate samples. The smaller concentrate samples are then floated individually splitting these into a number of concentrates and tails sample.

The above procedure is repeated for the fine fraction.

Slimes entrainment is inevitably collected with the concentrate due to the ultra fine clays (less than 2 μ m) being entrained in the froth water. Dependent on coal type, this very low ash material may even float with just the addition of air to the cell. The use of low reagent dosage rates allows for greater control, with low ash material floating with the least amount of reagent possible. Frother is therefore dosed at 5 μ L of laboratory grade MIBC per L of slurry, and collector at 1mg of dodecane per kg of dry solids. The air rate is set at 4L/min and the vacuum pressure recorded. Laboratory grade dodecane must be used, not diesel which is highly variable in composition from one batch to the next.

Sample Preparation

The coarse concentrate samples are dried and then inspected for slimes contamination. If visible slimes contamination exists, the coarse concentrates are refloats. Following the success of the visual inspection, sample preparation can proceed. All fractions are to be air dried and the mass, moisture content, and ash of each determined. The mass and ash are calculated on a dry basis, all concentrate and tailings fractions are sorted into ascending ash order and flotation response is shown graphically by plotting the cumulative ash (%d) versus cumulative mass yield curve % (d/d).

Equipment Recommendations

The use of a clear plastic flotation cell allowed the operator greater visual control over the UFT. The operator can now visually see what is happening in the flotation cell throughout the UFT test as well as for the first time, the ability to continually monitor the froth depth. The disadvantage of a stainless steel cell is that only the surface of the froth can be seen.

The placement of the air control valve (refer Figure 8) after the rotameter ensures a true reading of the airflow, as the rotameter reads at atmospheric pressure, not at partial vacuum. A vacuum gauge must also be installed. If the vacuum pressure is not stable then there is a problem with the flotation system.

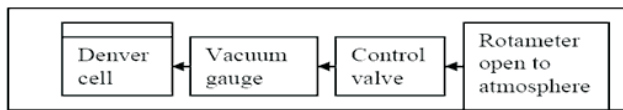


Figure 2: Placement of air control valve

Cell level is adjusted by the operator. The transparent cell allows the level to be clearly seen and the level is adjusted by manual additions of water. The operator should use this water to wash the material that adheres to the deflector block and the cell walls adjacent to the deflector block, back into the slurry. It was found that having a 3mm gap between the deflector block and cell allowed the particles to be easily washed down and was the reason for increasing the gap from the currently used distance of < 1mm.

RESULTS

The different methods were compared to each other using yield-ash graphs produced for each coal type. The four samples were chosen in such a way that the test methods could be evaluated across a range of coal types. The ISO 8858-3:2004(E) method was only trialled on the Hunter Valley sample with the results showing the method was inadequate.

The UFT Method used in ACARP Project C14068 has undergone further refinement and is now known as the CPT UFT 2010 method.

The CPT UFT 2010 method was recently used on a plant audit of a Bowen Basin Coal Handling Preparation Plant. Samples were taken from around the flotation circuit, these included: flotation feed, flotation cell product and flotation tails. The results from the CPT UFT 2010 were then used to mathematically generate a partition curve for the flotation cell. This curve can be used to investigate the cut point of the flotation cell as it is operating during the sample period.

The CPT UFT 2010 method was compared to a modified tree flotation test method (See Figure 8). The modified tree method is a very common variation that is performed by commercial labs in Australia. This method involves placing the sample into the cell and then successively collecting five

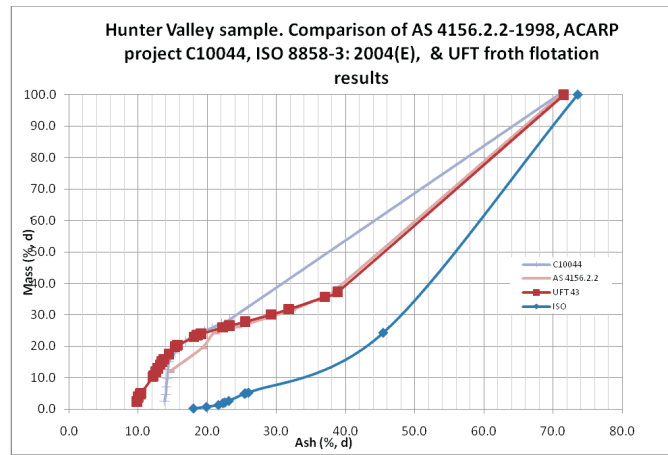


Figure 3: Hunter Valley sample – Comparison of methods

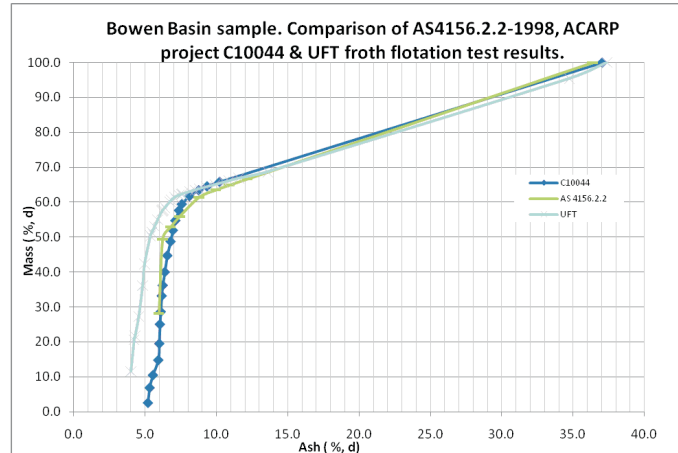


Figure 4: Bowen Basin Sample – Comparison of Methods

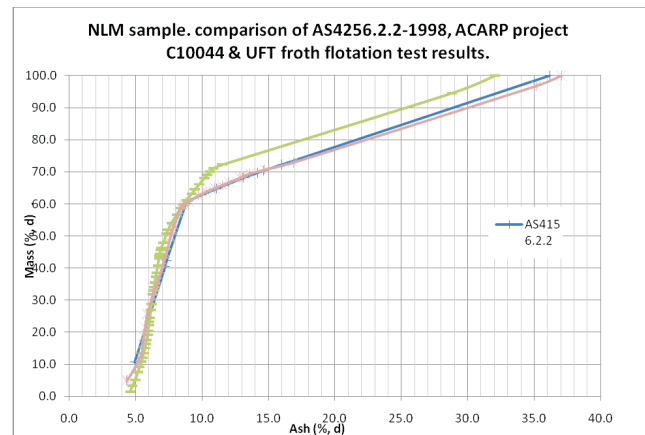


Figure 5: Newcastle Lake Macquarie Sample – Comparison of Methods

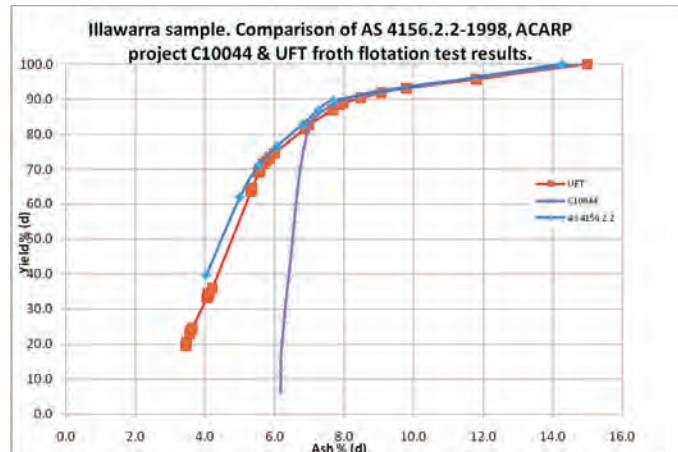


Figure 6: Illawarra Coal Sample – Comparison of Methods

Table 1: Sample feed ash (%_d) & Flotation response comparison.

Sample	Ash (% _d)	Relative Flotation Response				Reference
		AS4156.2.2	C10044	UFT	ISO	
Hunter Valley (HV)	72	X	√	√√	X	Figure 3
Bowen Basin (BB)	37	√	√	√√	-	Figure 4
Newcastle Lake Macquarie (NLM)	35	√√	X	√√	-	Figure 5
Illawarra (I)	15	√√	X	√√	-	Figure 6

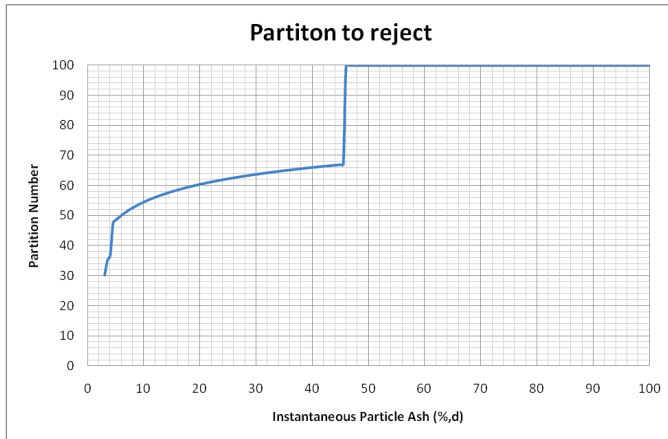


Figure 7: Partition curve for the primary flotation cell

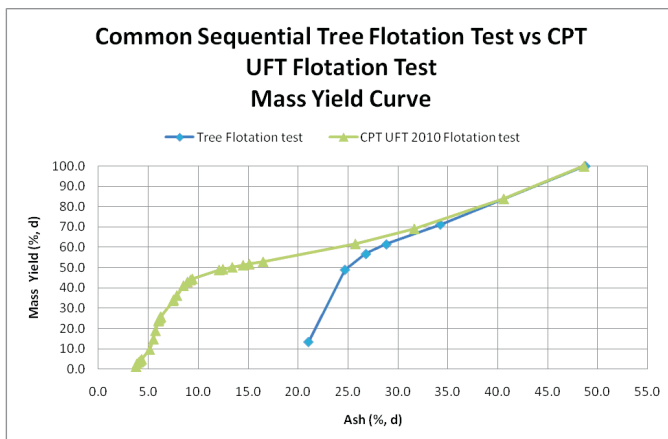


Figure 8: Comparison of CPT UFT 2010 vs “common sequential tree flotation test.”

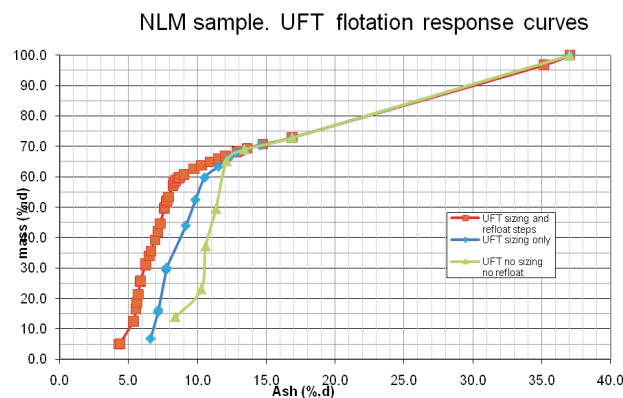


Figure 9: UFT – Effect of sizing and refloat steps

concentrate samples and producing a final tails sample. This “common” method suffers from slimes contamination in the concentrates. The tails sample produced from the common tree method is very good showing a high ash indicating that all the coal appears to have been recovered from the flotation feed. The UFT curve shown in the same figure gives a very different assessment of the recoverable coal remaining in the plant tailings.

DISCUSSION

The UFT method developed utilises a sizing step to show a more accurate assessment of the flotation response of the coarse fraction of the particles. Observation shows that some of the coarser particles tend to remain in the flotation cell on refloating due to the hydrodynamics of the cell.

A major advantage of using the UFT method is that it allows for the mathematical recombination of the results so that the affect of the desliming or sizing step and the affect of the refloating of the size fractions can be easily identified. This is shown in Figure 8, where it is clearly seen that without the desliming step and the refloat step, the resultant yield-ash curve would be dramatically to the ‘right’ and further away from the theoretical yield-ash curve for the sample being tested.

A number of the methods tested have their own benefits and have a range over which they seem to give the closest yield ash curve to the theoretical response curve for the four samples tested. The method developed in C10044 uses wash water to remove slimes from the froth concentrates and as expected it performed well on the high ash Hunter Valley and the Bowen Basin samples. The C10044 method has limitations which are observed in the results of the low feed ash Illawarra sample shown in figure 5. The resultant yield ash curve substantially understated the possible flotation response for the coal. Additionally, method C10044 requires specialised laboratory equipment as well as a sample mass of 800 g, much larger than the 400 g required for the Australian Standard and UFT methods.

The AS 4156.2.2-1998 modified tree method showed some limitations, in that it performed well on low ash 15 (%_d) Illawarra flotation feed sample, giving 40 % (d/d) mass yield at an ash value of 4 (%_d) for the NLM sample. However, on the high ash 72 (%_d) Hunter Valley sample it missed the ‘knee’ of the flotation response curve. The AS 4156.2.2

method produced the poorest (but only slightly) resultant yield ash curve for the Bowen Basin sample. This is most likely due to slimes collection in the concentrates. In general this method was found to perform reasonably well.

The UFT Froth Flotation method was the best performing test, particularly on the high ash Hunter Valley sample and the Bowen Basin sample. This is likely due to the sizing step which removes the slimes contamination from the coarse fraction and the multiple refloats of both fractions to remove slimes contamination from the concentrates. The UFT performed very well on the NLM sample giving a yield-ash curve equivalent to the AS 4156.2.2 method. For the low ash 15 (% d) Illawarra sample the UFT method was able to show a flotation response at lower ash values than the other comparable methods. A product ash of 3 (% d) with a yield of 20 (% d/d) was produced from the UFT method whereas the AS 4156.2.2 method did not show any response until a 4 (% d) ash was produced and method C10044 indicated that there was no flotation response at all below 6 (% d) ash.

The CPT UFT 2010 method in comparison to the common tree method, shown in Figure 7, demonstrates how the tree flotation test can dramatically underestimate the potential yield from a coal resource. The CPT UFT 2010 results showed that a 50 % (d/d) yield at an ash of 13 (% d) could be achieved from the thickener underflow, which is a very saleable product. The tree flotation test showed that there is essentially no valuable material exiting the plant in the thickener underflow, and gave the erroneous impression that plant is performing well.

The CPT UFT 2010 method can allow a plant to quantify what is being lost to the tailings stream and instigate a plant optimisation or expansion program to reduce the clean coal losses. The results from the CPT UFT 2010 method have now been used to generate a partition curve for a flotation cell. This is a major step forward in being able to quantify the cut point that is able to be achieved from flotation and can have a major impact on the operation of the plant.

The results of the CPT UFT 2010 versus the common tree flotation test have also shown major discrepancies for bore core samples. The common tree flotation method is used in the initial modelling of a coal resource and the results are used in the design of the CHPP, in some situations it can even lead to flotation not being considered in the design due to poor flotation response curves.

Reporting of Results

It is important that yield and ash results from flotation studies are reported on a dry basis. This removes variations due to moisture when comparing the different fractions or when comparing one sample to another. As well, some understanding of the mineral matter would be a significant advantage when interpreting flotation results.

To calculate to a dry basis the equations:

$$A_d = \frac{100 \times A_{ad}}{100 - M_{ad}} \quad (2)$$

$$m_d = m_{ad} \frac{100 - M_{ad}}{100} \quad (3)$$

were used, where A_d is the ash (% d), A_{ad} is the ash (% ad), M_{ad} is the moisture (% ad), m_d is the mass (g, d) and m_{ad} is the mass (g, ad). After converting the masses to a dry basis the mass percent was calculated for all samples.

Australian Standard AS2418 (Standards Australia, 1995) defines ash as "the inorganic residue after the incineration of coal to constant mass under standard conditions". Ash as determined in laboratory testing of coal samples, can sometimes be misleading if it is interpreted as being representative of the total inorganic portion of coal. The mineral matter present in coal undergoes many chemical changes during high temperature heating which will directly affect the ash and mineral matter relationship. For example, consider Table 2 which shows the tailings ash from a UFT sample.

Table 2: Comparison of ash results at different moisture basis

Size Fraction	Moisture%(a d)	Ash%(ad)	Ash%(d)
+0.106 mm	1.4	92.4	93.7
-0.106 mm	7.0	84.7	91.1

On viewing the air-dry results only, it would be incorrect to assume that the flotation process has been more efficient with the coarse coal in separating the organic and inorganic components as it could be wrongly interpreted that there is 15.3 % organic matter remaining in the fine fraction and only 7.6 % organic matter remaining in the coarse fraction. The flotation results on a dry basis however show the two ash values being similar. If mineral matter was to be determined then the two values may even be identical and perhaps very close to 100.0 %.

Tailings Ash

As a general rule, the tailings ash (dry basis) should be a good indicator of plant performance and yield. If the tailings ash is lower for actual plant circuit samples than the tailings ash attained in the laboratory sequential tests, then plant performance is likely to be giving lower yields than the laboratory tests showed. If this is not the case, then the feed ashes may be different and as such no direct comparison between the two could be made with any confidence.

CONCLUSIONS AND RECOMMENDATIONS

The UFT method gave a flotation response curve closest to optimum when compared against other known methods using a variety of coal types. Analytical results indicate the most marked improvement in flotation response curves was for coals high in clay. The UFT method is less operator dependent than the current Australian Standard method

AS 4156.2.2-1998 with tight control over reagent dose rates, flotation cell design and setup, control of air rates and desliming procedures.

The refined UFT method, now known as CPT UFT 2010, gives the closest currently available laboratory flotation response to the theoretical flotation response curve. The combination of the desliming and refloat steps ensure that the final flotation concentrates produced are slimes and contamination free. The further development of the CPT UFT 2010 has led to the results from a plant audit being used to produce a partition curve for a flotation cell in an operating plant. This quantification of the operational cut point of a flotation cell could allow the plant to modify the operation of the cell to increase their flotation yield.

The use of the CPT UFT 2010 froth flotation method for the analysis of bore core samples can facilitate the more accurate modelling of a coal resource, most particularly the fines fraction. This improved data can then be used in the design of the fines processing circuit within the CPP to maximise the recovery of the valuable material in such a way that it is not wasted by being rejected to the plant's tailings disposal system.

While the method is the best currently available, there is still further improvement that can be made to move the response curve closer to what is theoretically possible. With the improvements that have been made, this procedure is to be considered analogous to a float sink test.

REFERENCES

- AUSTRALIAN STANDARDS ASSOCIATION, 1995: *Coal and Coke Glossary of Terms*, **AS 2418**.
- AUSTRALIAN STANDARDS ASSOCIATION, 2004: *Coal preparation Part 2.2: Higher rank coal – Froth flotation – Basic Test*, **AS 4156.2.1**.
- AUSTRALIAN STANDARDS ASSOCIATION, 1998: *Coal preparation Part 2.2: Higher rank coal – Froth flotation – Sequential procedure*, **AS 4156.2.2**.
- ATKINSON, B. & BLANSHARD, S., 1999: *Improved measure of ultimate flotation performance*, **ACARP C6044**.
- CAMPBELL, M. & LAMBERT, N., 2008: (2008), *Ultimate Froth Flotation Performance Test*, **ACARP 14058**.
- INTERNATIONAL STANDARDS ORGANISATION, 2004: *Hard coal – Froth flotation testing – part 3: Release evaluation*, **ISO 8858-3**.
- LAMBERT, N., COX, N. & RYAN, G., 2010: Slurry Sampling – A Case Study. In Atkinson, B.A. (Editor): *Proceedings of the Thirteenth Australian Coal Preparation Conference*, 86-99.
- LAMBERT, N., CAMPBELL, M., MCLENNAN, K. & COFFEY, A., 2008: An Improved Laboratory Flotation Method. In Mathewson, D.J. (Editor): *Proceedings of the Twelfth Australian Coal Preparation Conference*, 396-408.

Chris McMahon

Coal quality reconciliation and quality assurance/quality control

Coal quality can be effectively used as a tool for reconciling predicted and actual tonnages and coal qualities at operating coal mine sites. The definition of 'predicted' and 'actual' coal tonnages and quality is usually difficult to accurately reconcile.

This paper details various methods and examples of reconciliation processes using coal quality as the controls. It shows how to utilise data routinely collected by mines on a daily, weekly and monthly basis. That is, minimal additional data and processes are enacted to get a system up and running.

MCQR has constructed several innovative models and tools to examine the predicted and actual data in a valid statistical fashion that will be discussed in the paper.

Predictions from models and their correlation to coal handling plant outputs (actual values) with mine life coal movements, crushing, stockpiling and blending can obscure firm conclusions when comparing against actual results. Additionally, accuracy of measuring devices (belt weighers, truck counts, mechanical and manually sampling, etc), can further complicate findings.

The role and importance of stockpile management, tracking and modelling and the use of methods to define such from existing coal mining data are also discussed. Examples will be given from open cut, underground and multi mine / pit operations along with various options for assessing the data in these environments.

The installation of a reconciliation system creates a number of checks which can form part of a mine sites QA/QC (Quality Assurance / Quality Control) process, which inevitably creates greater efficiencies and bottom line gains. The results from enacting a coal quality based reconciliation system give better predictions for critical issues such as market expectations in coal quality, mined tonnages and estimates of mining contamination and loss.

INTRODUCTION

Reconciliation of prediction and actual tonnages and quality values at coal mines can be a difficult process. Some of the typical issues involve the following.

1. Definition of desired outcomes.

What part of the process is to be measured and evaluated? From the mine to the coal handling and preparation plant (CHPP)? To the port? Can we measure by pit area or can

we measure the mining output as a whole? Do we use spatially based (planned mining block) or time period based criteria for reconciliation?

2. The myriad of potential inputs and outputs for evaluation.

Such evaluation parameters include various predictions for tonnage and coal quality and actual, results from manual sampling, coal handling plant and shipping data.

3. The existence of parallel and conflicting data.

Examples of potentially parallel / conflicting data for example include truck weighers versus belt weighers.

4. Comparing 'apples with apples' for predictions and actual data.

Coal quality and tonnage is often predicted by mine area, whereas tonnage and coal quality are often not measured until the coal is processed or washed. There are often several phases of stockpiling and blending between estimates of these two measures.

In order to show how some of these difficulties can be overcome, MCQR supplies in this paper some examples and methods for reconciling predicted and actual tonnages and qualities at coal mining sites.

METHODS

Coal Mining and Processing

Often management desires reconciliation by mine area, from certain pits and strips. This can often be done reasonably readily for tonnage reconciliations. However for coal quality reconciliations, this is much more difficult, as often times several mine sources combine for subsequent processing, and good measurement of the coal quality is not possible until some time after mining. An example of a mining to coal handling plant process setup is given following.

Figure 1 shows the following features.

1. Multiple pit area operations, underground, opencut and other purchased / supplied coals.
2. The coal once mined has several stockpiling and blending opportunities prior to being washed and quality measured.

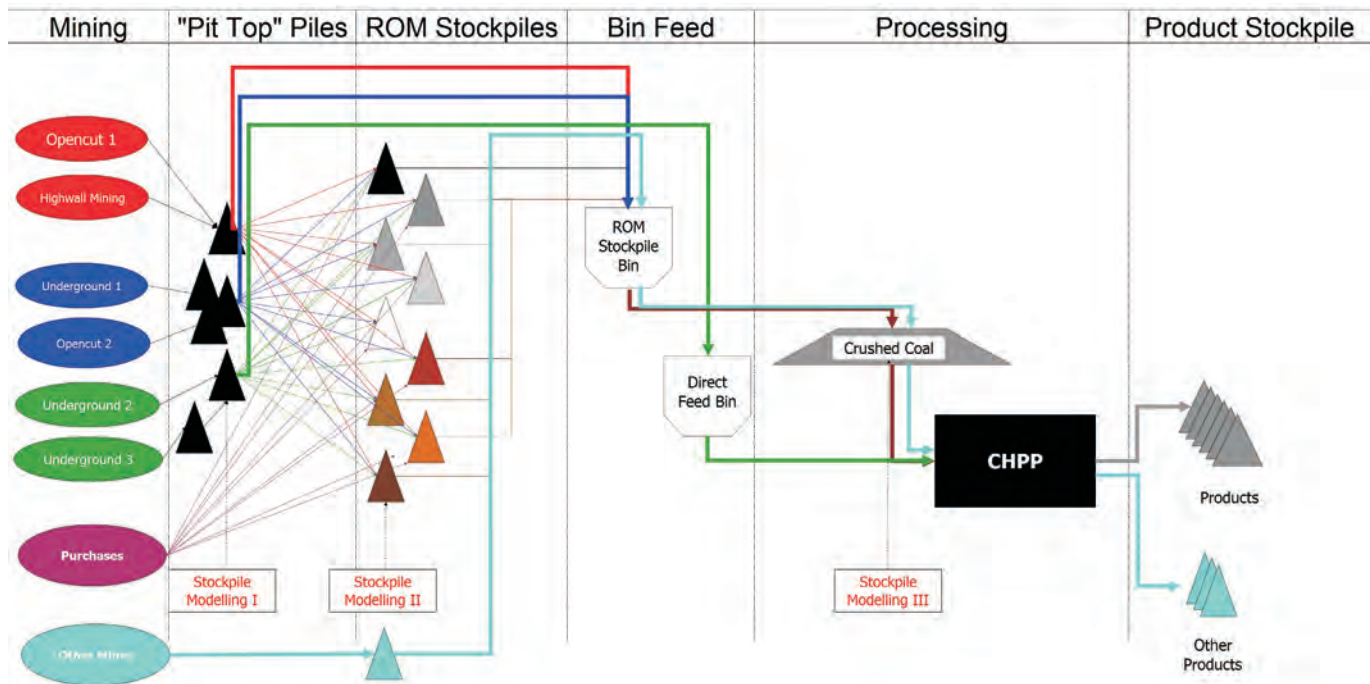


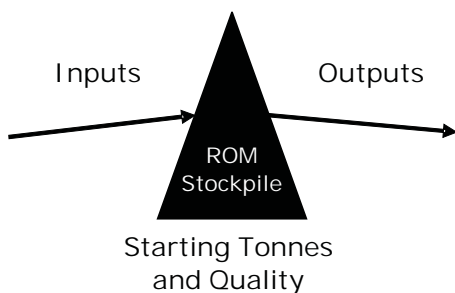
Figure 1: Coal processing flow diagram example.

- Multiple avenues for each coal type exist and are periodically altered.
- Several products are formed from the wash plant.

In order to properly reconcile mined tonnage and coal qualities predictions (which are usually "as mined" or directly from the resource) against actual data from the coal handling and preparation plant, movements between stockpiles need to be properly mapped and accounted for. Basic and advanced stockpile models exist or can be created to account for these movements. A basic stockpile modelling scenario is given following.

There are several models or methods for estimating quality values from stockpiles to best suit the process. Some form of open and close position of each stockpile via estimates of the quality moved from and to the stockpiles is required on a (tonnage) weighted basis.

Coal tonnages need to be utilised at all stages to 'weight' coal quality information correctly.



Weighted average calculations for stockpile accounting for starting tonnage and quality, inputs and outputs of tonnage by area

Figure 2: Simple stockpile modelling example.

Time Based Modelling

Mine area based coal quality reconciliation is usually impractical, accurate sampling devices (on belt samples) to attain sufficiently accurate samples for preparation and measurement not being available until the coal handling and preparation plant.

MCQR has created an alternative 'time based' scenario, utilising monthly accounting reporting period data. Mines usually report on a monthly basis, so most of the information for coal quality reconciliation could be attained from processes that were completed as part of mining life. That is, minimal additional processes were required - just data collation and modelling for comparison.

The effect of processing on a monthly basis gives a reasonable number of data points by year's end (12) that can form the basis of some reasonable statistical comparisons and reasoning.

Inputs

In order to compare the predicted and actual values for tonnage and coal quality, inputs are required from mine sites. These usually include the following.

- Year ahead predictions (Budgets).
- Month ahead predictions.
- Tonnage movements to and from mining areas and stockpiles.
- Coal handling and preparation plant tonnage and quality data for plant feed and products.

This data can then be collated and put into a model that corrects for coal movements and compares predicted and actual data on an equal basis.

RESULTS

Following are a series of charts that display outcomes from processing time based monthly data on a routine basis.

Tonnage Comparisons

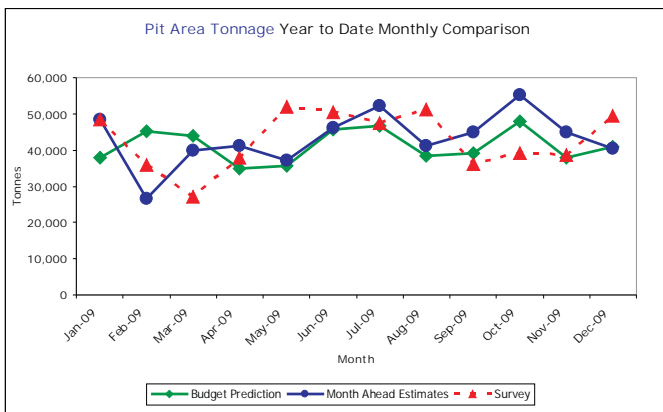


Figure 3 – Tonnage Tracking by Month – pit specific.

Figure 3 shows tonnage tracking on a monthly basis for a particular pit area. There are three comparisons.

1. A Budget Prediction.

The Budget Prediction is the predictions made at the start of the calendar year.

2. A Month Ahead Estimate.

The Month Ahead Estimate is the prediction made just before each month’s starts based on the most recent data and mining.

3. A Survey Result.

The Survey result is that which the surveyors estimate the coal extracted to be, based on volume and factors for density, moisture and stone contamination.

Variations of $\pm 20\%$ were observed in the above example between predicted (Budget, Month Ahead Estimate) and Actual (Survey) results.

Comparisons of individual pit areas can also be also coalesced into an “All Pits” comparison as follows.

Figure 4 shows that in this instance the Month Ahead Estimate results were in reasonable agreement with actual results (survey) most of the time. Budget figures were significantly variable.

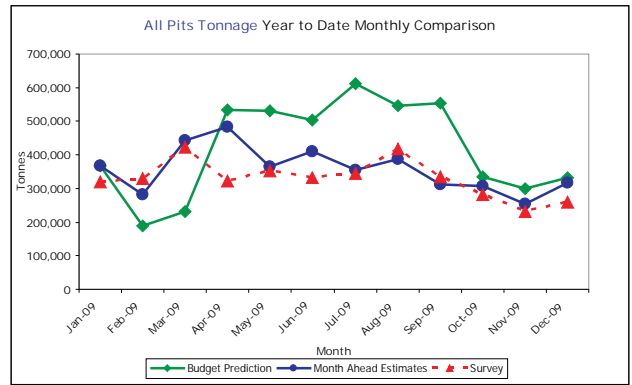


Figure 4: Tonnage Tracking by Month – overall results, raw ash%.

Coal Quality Comparisons — Raw Ash and Yield

Raw Ash: As raw (plant feed) ash increases, yield generally decreases.

Figure 5 shows raw ash tracking on a monthly basis for all pits (coal handling plant feed).

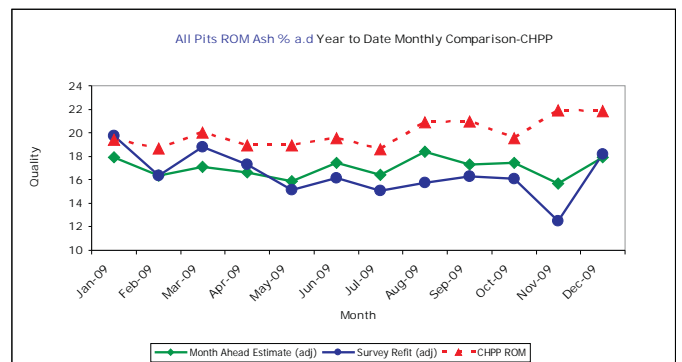


Figure 5: Quality Tracking by Month – overall results, raw ash%

There are three comparisons in the above chart.

1. A Month Ahead Estimate (adj).

The Month Ahead Estimate (adj) is the prediction made just before each month’s starts based on the most recent data and mining. The “(adj)” suffix indicates that the mining estimates have been modified in line with stockpile movements.

2. A Survey Refit result (adj).

The Survey refit result is that attained when using the surveyors spatial points fitted into the predictive coal quality model from the mine modelling package. The surveyor’s estimate of stone contamination is also utilised. The “(adj)” suffix indicates that the mining estimates have been modified in line with stockpile movements.

3. The 'CHPP ROM' result.

The CHPP ROM result is the plant result attained from sampling the plant feed.

The above chart shows the CHPP ROM (plant feed) data consistently has higher raw ash values than the Month Ahead Estimate and the Survey Refit. This indicates that both the Month Ahead Estimate and the Survey Refit underestimate the amount of contamination (and likely loss) that is occurring in reality.

Raw Ash 'Spot' Samples and Contamination: The following chart gives supporting evidence of increased contamination from "spot" samples attained on the rare occasion when a single source (pit area) coal was sampled at the coal handling and preparation plant.

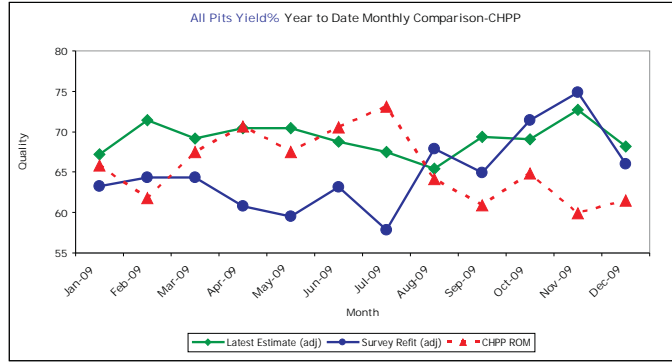


Figure 8: Quality Tracking by Month – overall results, yield%.

1. Contamination only was factored into estimates rather than contamination and loss. Yield being mass based reduces less quickly where only a contamination value and not mass is accounted for, resulting in higher predicted yields.
2. 'Basic' bore cores that did not have allowance for breakage were sometimes included in the model, increasing the yield.

Further discussion of the effects of 'basic' bore core data processing follows.

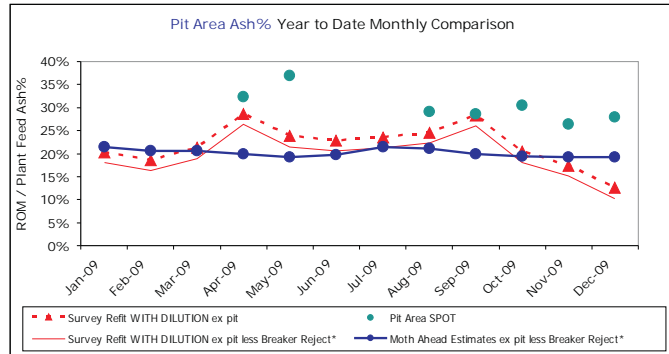


Figure 6: Spot samples quality comparison – pit specific.

The spot sample values for raw ash (actual data values) were generally higher than the Month Ahead Estimates and Survey Refit data.

Correspondingly, contamination (and loss) estimates from Survey and for predictions (Budget Prediction and Month Ahead Estimates), were still generally too low. The following chart shows the comparable contamination estimate for the ROM ash predictions in the prior chart.

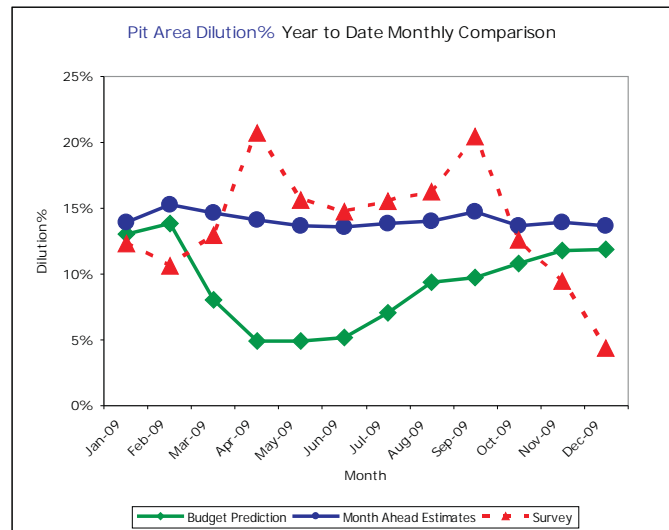


Figure 7: Contamination estimates – pit specific.

Yield Comparisons: Higher ash values as observed above generally mean lower yield. This should have been reflected in the following chart of yield on a monthly basis.

The above chart does not show an overall bias between the predicted and actual results. This was likely due to two factors in the opinion of MCQR.

DISCUSSION AND INTERPRETATION

The above charts indicated two primary data processing difficulties that are discussed following.

Raw Ash Indicating Contamination and Loss

The raw ash values indicated that contamination and loss can at times not be adequately accounted for in predictions.

The following table (Table 1) shows an ash value for a coal seam and how that value changes with increasing levels of contamination and loss (measured in centimetres or cm and %).

The ash value starts at 17%* for zero contamination and zero loss. The value from the coal handling plant was 25%. Values for 25% have been highlighted in the above table for different levels of contamination and loss. The tabulation shows that the coal seam could have had between 6 and 12% contamination and 0 and 34% loss to achieve the observed product ash. Reality lies in the midst of these values, probably at the higher contamination, lower loss end (10 to 12%)

*(ash values were rounded to no decimal places for clarity of reporting in this section).

Using Table 1, if in pit measurements show a 120mm contamination (11%), based on the ash value (25%), the loss will be about 4% (75mm) over a two metre seam as is used above.

Table 1: Raw ash change with loss and contamination example

Ash%		Loss (cm / %)															
Contamination		0	75	150	225	300	375	450	525	600	675	750	825	900	975	1050	1125
cm	%	0%	4%	7%	10%	13%	16%	18%	21%	23%	25%	27%	29%	31%	33%	34%	36%
0	0%	17	17	17	17	17	17	17	17	17	17	17	17	17	17	17	17
10	1%	18	18	18	18	18	18	18	18	18	18	18	18	19	19	19	19
20	2%	19	19	19	19	19	19	19	19	19	19	19	20	20	20	20	20
30	3%	19	19	20	20	20	20	20	20	20	20	21	21	21	21	21	22
40	4%	20	20	20	20	20	21	21	21	21	21	22	22	22	22	23	23
50	5%	21	21	21	21	21	21	22	22	22	22	22	23	23	24	24	24
60	6%	21	21	22	22	22	22	22	23	23	23	23	24	24	25	25	26
70	7%	22	22	22	22	23	23	23	23	24	24	24	25	25	26	26	27
80	8%	22	23	23	23	23	24	24	24	24	25	25	26	26	27	27	28
90	9%	23	23	24	24	24	24	25	25	25	26	26	27	27	28	28	29
100	9%	24	24	24	24	25	25	25	26	26	26	27	27	28	29	29	30
110	10%	24	24	25	25	25	26	26	26	27	27	28	28	29	30	30	31
120	11%	25	25	25	26	26	26	27	27	28	28	29	29	30	31	31	32
130	12%	25	26	26	26	27	27	27	28	28	29	29	30	31	31	32	33
140	13%	26	26	26	27	27	28	28	28	29	29	30	31	31	32	33	34
150	13%	26	27	27	27	28	28	29	29	30	30	31	31	32	33	34	35

Basic Bore Cores and Processing – ‘Too High’ Yields

Bore core processing difficulties for yield can be encountered for 'basic' bore cores that did not have extensive washability testing and processing performed, resulting in higher than expected yield values.

The following chart shows an example of differences that can be observed in predicting bore cores via different preparation and processes.

The above chart shows typical yield value differences between preparation and processes as well as the variability that could typically be expected when using the different data sets*.

*Comparison is made between the two noted data sets in each column in the chart above, thus the “Contam Wash” variability is slightly different between the two columns.

The 'Core Yield' values were yield values derived from simple crush / cut point bore cores with no contamination.

The 'Contam / Wash' bore cores had contamination added and a washability simulation process performed. These values are significantly lower in yield (74% average compared with 85% average).

The 'CHPP Sim' bore cores include additional breakage to simulate mining reality (reconciled against coal handling and preparation plant performance - which can also be attained by drop shatter testing, and drum tumble testing of bore cores). These give lower yield values again on average (68%).

In the above example, a 'Core Yield' reported as 85% yield, would have a most likely yield value of about 74% if the 'Contam Wash' data was used, with a +/- 4% precision. Thus the expected value has a 95% chance (± two standard deviations) of occurring between 70 to 78% in yield.

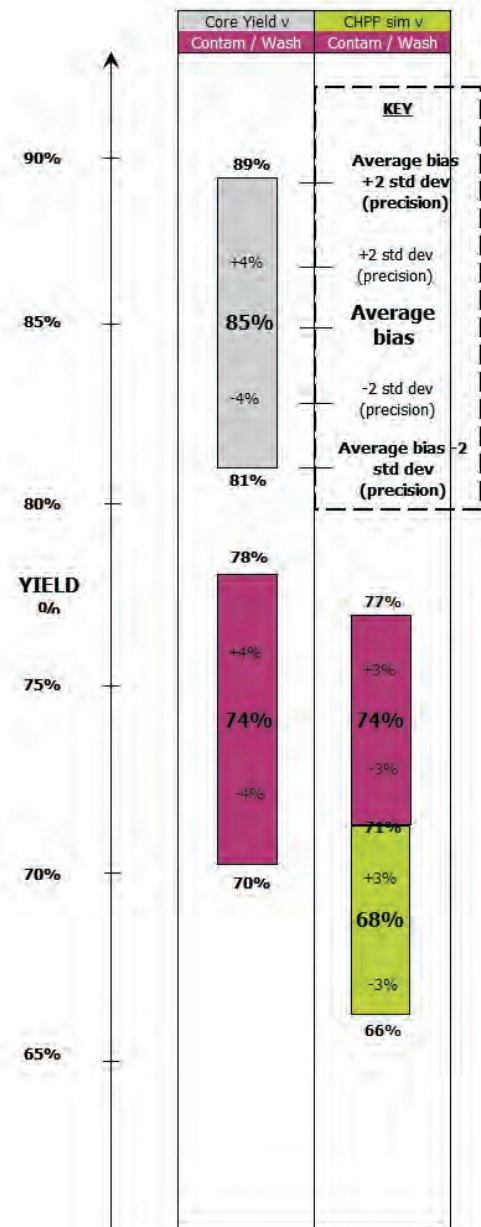


Figure 9: Differences in bore core predictions via processes.

CONCLUSIONS

The following conclusions can be drawn from the above methods and outcomes for reconciliation systems.

- Reconciliation systems can be set up on available monthly mine site data to reconcile predicted and actual tonnages and coal quality.
- Coal contamination and loss is often underestimated until measured in a program such as a reconciliation system, which can affect yield estimates, tonnage and other coal quality estimates.
- The measures of contamination and loss from an implemented reconciliation system can be used to better predict future mining.
- Reconciliation points to the need to account for contamination, loss and coal handling and preparation plant practice in bore core predictions for accurate planning.

OTHER APPLICATIONS

The processes described in this paper by MCQR gave examples from some of the work done in reconciling predicted and actual data produced by mine sites. Further studies have been conducted by MCQR including the following.

- Mine area to port reconciliation.
- Other coal quality parameters including product ash, (total) moisture, energy, sulphur and petrographic constituents.
- Special cases where coking properties may deteriorate from bore cores to product samples, including fluidity.

Using the principles in this paper, reconciliation of any coal quality parameter can be performed, allowing better control and assurance of process predictions.

Iwan de Jongh and Marius Smith

Extracting value from coal remnants and pillars - quality modelling in previously mined coal seams

The coal deposits of South Africa are contained within the Karoo Sequence and are preserved in a number of Basins throughout South Africa. In recent years most of the coal mining has been concentrated in the Witbank, Highveld and Ermelo coal fields due to the proximity to infrastructure as well as the quality of the coal. The other basins have been exploited to a far lesser extent due to the lack of infrastructure in these areas.

XCSA's mines are situated in the Witbank and Ermelo Coal Fields. These coal fields have been actively mined for the last 120 years. Very little remain in terms of large virgin blocks of coal resources. Mining in these coal fields have become severely challenging. The "eyes have been plucked out" by companies chasing short term incentives.

Although XCSA is developing a number of large virgin coal blocks and is doing exploration on some virgin coal prospects, the XCSA mines operating in these coal fields are facing the same challenges as the rest of the industry. XCSA has become one of the industry leaders in innovative ways to unlock the last ounce of value from these remnant resources.

XCSA has especially distinguished itself in 2 areas, remnant mining and pillar mining. Both of these areas represent numerous challenges in terms of the entire technical value chain, ranging from exploration all the way through to the mine planning level. This paper focuses on the geological portion of the technical value chain and addresses exploration and geological modelling in particular as well as resource estimation and management of these remnant and pillar resources.

With many of the coal resources in the Witbank area located in underground pillars remaining from bord and pillar mining, the opportunity exists where these resources can add significant life to the established operations. Many of these pillar resources are extracted through underground stooping methods, with the geotechnical parameters being the biggest consideration. In many operations the pillars are successfully extracted through opencast methods as well, but these present a myriad of challenges that need to be addressed, from spontaneous combustion to blasting optimization in order to limit fines creation, but to name a few.

From a geological modelling and planning perspective the most challenging aspect of opencast pillar mining is the parameters to be used when attempting to simulate the mining process and estimate the reserves. XCSA have developed a simulation model which considers many physical characteristics such as pillar size, the nature of

the void collapse, quality distribution and additional contamination. Using the simulation model, various mining scenarios can be studied in an attempt to predict the impact of mining decisions on the reserve value.

INTRODUCTION

General Geology

The coal deposits are contained within the Karoo Sequence which unconformably overlies rocks of the Basement Igneous Complex. The stratigraphy of the Karoo Sequence consists of the Dwyka Formation at the contact with the Basement Igneous Complex, overlain by the Vryheid Formation (Figure 1a). Formerly known as the Middle-Ecca-Stage, this fluvio-deltaic formation consists of a cyclic series of upward-coarsening sedimentary units, each capped by a coal seam. The coal Seams are numbered from No. 1 Seam at the base to No. 5 Seam at the top of the sequence. In the Witbank Coalfield the maximum thickness of the Vryheid Formation is estimated at 120m.

The majority of the Xstrata Coal SA collieries are located near the northern margin of the Witbank Coalfield which is clearly defined by pre-Karoo granite and felsite hills (Figure 1b).

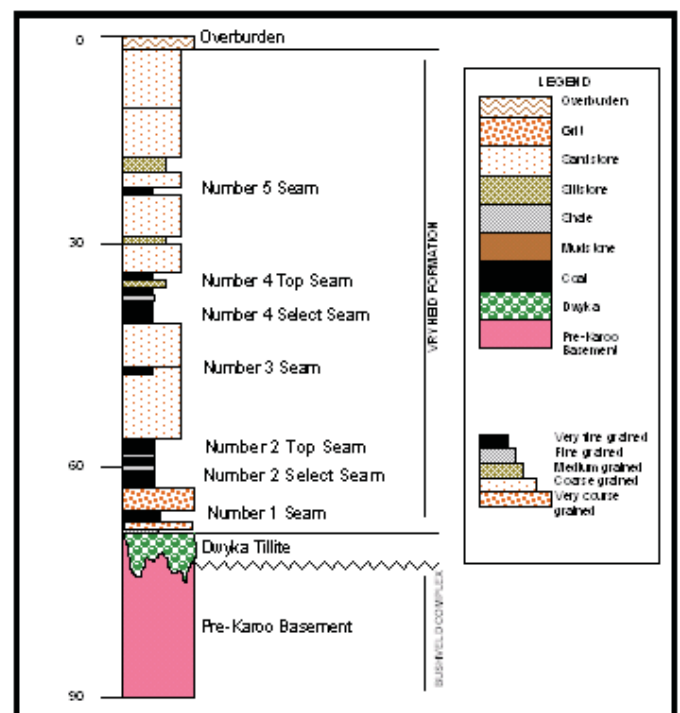


Figure 1a: Generalised Stratigraphic column of the southern margin of the central portion of the Witbank Coalfield

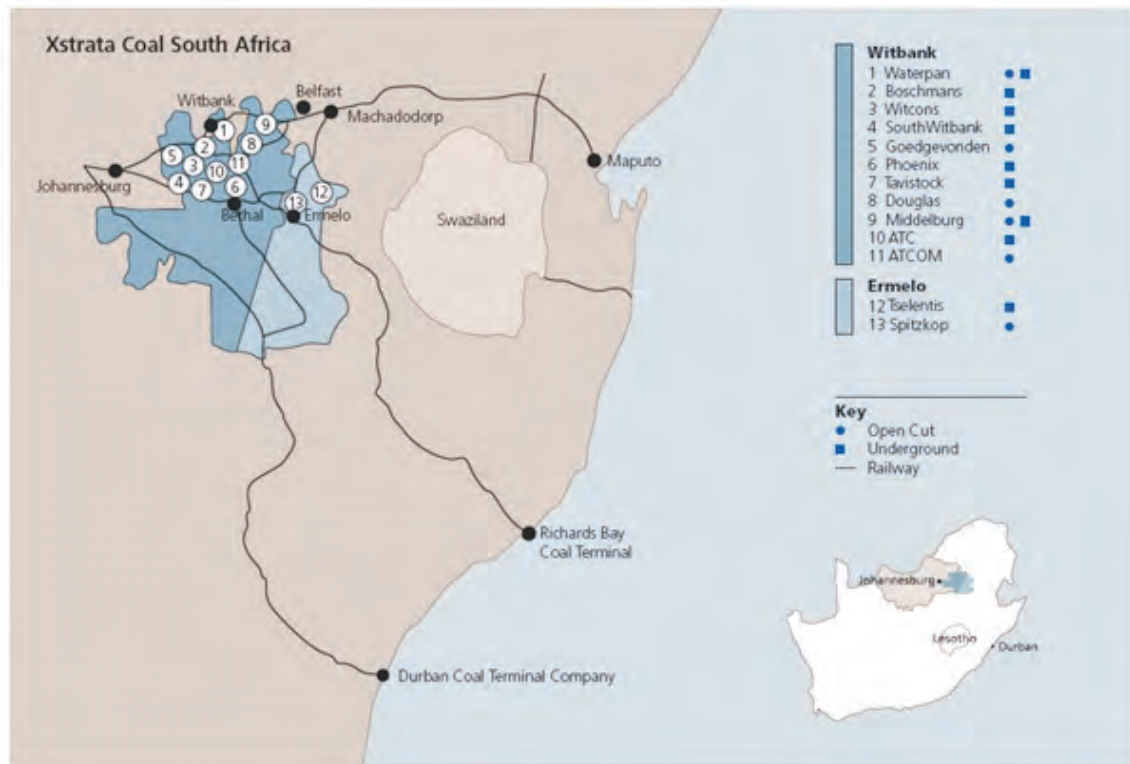


Figure 1b: Witbank and Mpumalanga Coalfields showing the locality of the collieries.

Pre-Karoo

The Pre-Karoo rocks consist of felsites and gabbros of the Bushveld igneous complex, which are locally collectively termed as a “Basement”.

The limited knowledge of these rocks is derived from boreholes. The palaeo-topography shows great elevation contrasts, due to the effects of the Dwyka glaciation, and is thus characterised by deep northwest-southeast trending palaeo-valleys separated by basement highs.

A prominent range of felsites, granites and diabase, the Smithfield-Ridge, outcrops in various areas throughout the coalfields.

Dwyka Formation

The Dwyka glaciation and the northerly retreat of the glaciers resulted in the deposition of poorly sorted glacial tillite over most of the area. Basement highs were glacially scoured and palaeo-weathered, but the tillite was usually not deposited on these areas. The Dwyka sediments overlie the basement rocks unconformably.

The palaeo-valleys and their flanks, however, have relatively thick tillite (or diamictite) deposits. The diamictite varies from dark to light grey to a distinctive pink. The clasts within range from angular to well rounded from small pebble to boulder in size, and consist of a variety of pre-Karoo rock types. The clasts are supported by a muddy to sandy matrix. The tillite was deposited unevenly and local damming created lakes in which fine mud and silt were deposited. These form the rhythmically banded mudstone/siltstone sequences most often found in the deeper palaeo-valleys. These units typically

display alternating millimetre to centimetre thick light and dark bands which represent seasonal fluctuations in the rate and type of sedimentation. Soft-sediment deformation structures are often present.

Vryheid Formation

Formerly known as the Middle-Ecca-Stage, this formation consists of a series of upward-coarsening sedimentary units, each capped by a local coal seam. The coal seams are numbered from No. 1 Seam at the base to No. 5 Seam at the top of the sequence.

In the Witbank Coalfield the maximum thickness of the Vryheid Formation is estimated at 120 m. The Lower and Upper Ecca stages (Pietermaritzburg) Formation and Volksrust Formation), are not present in the Witbank area.

Post-Karoo Dolerite

Post-Karoo dolerite intrusions are present over most of the Witbank Coalfield. In general the thicker dykes trend east-west and the thinner dykes north-east and west-south-west.

Coal Seams

Not all five coal Seams present in the Vryheid Formation are fully developed across the XCSA deposits. The Number 1 seam at the Base is of average quality and is best developed in the paleo low areas. The No. 2 Seam is the most extensively developed seam and consists of a basal bright band overlain by lustrous to dull lustrous coal with thin bright bands. The thin uneconomic No.3 Seam is developed between the No. 2

and No. 4 Seams. The No. 4 Seam being closer to surface is more influenced by weathering and is subsequently not as extensively preserved as the No. 2 Seam. The No. 4 Seam consists of a basal bright band overlain by a zone of dull and dull lustrous coal with thin bright bands and carbonaceous shale/mudstone partings. The No. 5 Seam is preserved as erosional remnants on the higher ground and consists of a bright, well-banded, vitrain rich coal.

No. 1 Seam

The distribution of the No. 1 Seam is determined by paleo topography, being best developed in the paleo low areas and thinner or absent over the paleo high areas. It averages at 1.1m in thickness. Typically the No. 1 Seam consists of three zones of coal; a basal bright laminated zone, a middle dull lustrous zone with occasional bright bands and an upper zone of dull massive coal. The Seam was deposited in unstable conditions and lenses of sediment are common but unpredictably distributed. The floor and roof are competent and the mining cut is the whole Seam. The No.1 Seam underlying Tweefontein has been mined in the past predominantly on Waterpan.

The separation between the No. 1 and No.2 Seams varies between 1.0 and 3.5m and consists predominantly of sandstones and grits.

No. 2 Seam

The No. 2 Seam varies in thickness between 0m and 13.7m where thick in Seam partings occur. Seven distinct bands or zones are recognized although some of these may be locally absent. The 2L seam is made up of the Zone A, B and C while the 2U seam is made up of Zone D, E, F and G (F and G zones are not uniformly well developed across the XCSA resources). The basal Zone A is thin impersistent and dull; zone B is bright coal; zone C is usually dull overall and can be locally further split by sandstone partings; Zone D is bright coal; Zone E is dull lustrous coal; Zone F is carbonaceous mudstone or siltstone and the uppermost Zone G consists dull coal with occasional bright bands. In very localized positions Zone A splits off the main 2 Seam and can have a parting between it and the 2 Seam of approximately 3m. Separate from the 2 Seam, Zone A is uneconomic to consider.

The No. 2 Seam Zones are readily recognized on down-hole geophysical traces which are used to control the sampling and selection of mining cuts. The No. 2 Seam mining cuts selected are determined by the relative thickness of the in Seam partings. The 2L seam height varies in thickness from 0m to 12.2m and has an average thickness of 3.66m.

The No. 2 Seam is overlain by a prominent carbonaceous siltstone, which grades upwards into a highly micaceous, bioturbated sandstone. An interlaminated siltstone/sandstone, and a cross bedded sandstone follow, and the thin uneconomic No.3 Seam forms a capping. This is overlain by coarse grained channel sandstone and a medium grained highly micaceous sandstone on which the No. 4 Seam forms a capping to the sequence.

No. 4 Seam

The No. 4 Seam group consists of a lower zone (No. 4Lower) which consists of a basal bright band overlain by dull and dull lustrous coal with thin bright bands. No. 4 Lower Seam varies but has an average thickness of 3.33m. The 4L Seam is overlain by a fissile siltstone parting (4P) which varies widely from zero to approximately 5.0m, but has an average thickness of 0.79m.

The overlying No. 4 Upper Seam varies between 0.3m and 2.5m is generally of low quality and is split by several mudstone partings. The lowermost coal in the No.4U zone is referred to as No.4U1. The No. 4 Seam mining cut is determined by the stability of the 4P parting. Where the parting is sufficiently thick and competent enough to form a stable roof the mining cut used is the No.4L; where the parting is unstable then a mining cut consisting of 4L + 4P + 4U1 used.

Locally a No. 4A Seam may occur above the No.4 Upper but is invariably too thin to be mined. The interburden thickness between the No. 4 Seam and the No. 5 Seam ranges from 18.0 to 25.0m.

No. 5 Seam

The No. 5 Seam is preserved as erosional remnants on the higher ground. It varies in thickness between 0.01 m and 5.94m and is a bright well-banded coal. A cm- scale mudstone band referred to as the 'false floor' occurs some 10 to 25cms above the soft mudstone floor. One or more 'floating stone' bands are frequently present in the upper portion of the Seam. The No. 5 Seam mining cut includes the 'false floor' and roof.

Resources

Most of these coal seams have been actively mined by bord and pillar method for the last 120 years. With a large portion of the coal resources in the Witbank area located in underground pillars remaining from bord and pillar mining, the opportunity exists where these resources can add significant life to the established operations. Very little remain in terms of large virgin blocks of coal resources and mining in these coal fields have become severely challenging. Most of XCSA's current resource areas are affected by previous mining and most of the operations are undertaking remnant mining, stooping or pillar extraction to some degree.

The total resource base for XCSA consists of 3.4 billion tonnes of measured and indicated and 0.76 billion tonnes of inferred resources (see table 1 below). The areas that are unaffected by any previous mining include the green fields projects, consisting of Elandspruit, Zonnebloem, Mooifontein, Sterkfontein, Sara Buffels, and Paardekop. The other resource areas have all be mined extensively and although large virgin blocks of coal are still present reserves are impacted on by previous mining in most cases.

Table 1: XCSA Resources as at 30 June 2009 (XCSA Resources and Reserves, 2009)

Name of Operation	Ownership	Commodity	Coal Resources			Competent Person
			Measured (Mt)	Indicated (Mt)	Inferred (Mt)	
Coal - June 2009						
XCSA Coal Resources						
Tweefontein Division	79.8%	Thermal Coal	750.4	23.0	10	MS
			750.4	23.0	10	
SouthStock Division	79.8%	Thermal Coal	269.0	44.0	17	MS
			269.0	44.0	17	
Goedgevonden Division	74.0%	Thermal Coal	522.9	27.7	63	MS
iMpunzi Division	79.8%	Thermal Coal	381.1	37.3	13	
iMpunzi		Thermal Coal	258.4	1.7	1	MS
ATCOM East		Thermal Coal	122.7	35.6	12	MS
Mpumalanga Division	79.8%	Thermal Coal	224.8	7.6	5	MS
Tselentis			57.0	3.1	2	
Spitzkop			167.7	4.5	3	
New Projects	100.0%	Thermal Coal	212.4	825.4	454	
Elandspruit			30.5	-	0	
Zonnebloem			103.0	20.6	6	
Mooifontein / Sterkfontein			36.7	31.2	3	
Sara Buffels			6.8	13.7	7	
Paardekop			-	450.5	399	
Oogjesfontein			35.5	17.6	40	
Consbrey			-	291.8	0	
Undeveloped	100.0%	Thermal Coal	-	45.3	194	MS
Subtotal - South Africa			2 360.6	1 010.4	757	

Definitions

- OC = opencut; UG = Underground
- Salable Coal Reserve is the tonnage and coal quality that will be available for sale, either in the raw ROM state at a specific moisture content or after beneficiation of the ROM Coal Reserve has produced materials at specified qualities, moisture contents and size ranges.

Notes:

- The Coal Resource and Coal Reserve figures tabulated have been stated on a total mine basis as at 30 June 2008.
- The Measured and Indicated Mineral Resources are inclusive of those modified to produce Mineral Reserves.
- The estimates of Coal Resources and Coal Reserves presented in this table have been estimated according to the SAMREC Code (South African Code For The Reporting Of Exploration Results, Mineral Resources And Mineral Reserves).
- minority interests in controlled entities and the interests of joint venture partners. Figures are subject to rounding and therefore totals may not add up.
- Coal Resources and Recoverable Coal Reserves are quoted on an air dried moisture basis. Extractable Coal Reserves are reported as
- High grade Salable Coal Reserves were based on a 6000kCal NAR product. Atcom East based on a 5800kCal NAR product with a secondary, 21.5Mj/kg CV domestic power station (Eskom), product.
- Low grade Salable Coal Reserves are based on a primary 21.5/22MJ/kg (Air-dried) product.
- Product yields used to estimate Salable Reserves were derived from the "Limn Model" software. Inputs to this model are coal ply and in-seam dilution data, processed in the model. The model takes into account plant efficiencies to calculate practical yields. The model is calibrated to historical plant performance and where applicable, large diameter borehole data is used.
- Reserves are reported on an extractable and saleable basis.
- Valid prospecting rights have been issued for all the undeveloped Coal Resources. Some prospecting rights are being renewed, while application has been made for a number of mining rights.

The Life of Mine plan for XCSA includes 51 million tonnes of pillar resources to be mined by opencast dragline methods at the Atcom East and Atcom North mines. A further 54 million tonnes of resources are to be mined through truck and shovel opencast methods at the Tweefontein opencast operation.

The pillar resources will augment the life and profitability of these collieries significantly but the challenge lie in accurately predicting the amount of coal that is contained in the pillars. Many of these old workings were mined in the early 1900s before it became a statutory requirement to offset pillars in order to draw accurate survey plans. Both the position and

size of the old pillars may vary from what is indicated on the survey plans. For the areas that were mined more recently the survey plans were used to create de-rating grids to reduce the *in situ* resources according to the coal that was extracted. In the old areas where the accuracy of the survey plans is questionable a more conservative approach is used where a specific extraction percentage is applied to the calculated resources.

Obtaining coal quality information in these old pillar areas is also challenging as the exact position of the pillars and bords are not known, making drilling extremely challenging. With minimal coal intersections it is still possible to make an

Table 2: XCSA Reserves as at 30 June 2009 (XCSA Resources and Reserves, 2009)

Name of Operation	Ownership	Commodity	Coal Reserves			Competent Person (aa)
			Probable (Mt)	Proved (Mt)	Salable Probable (Mt)	
Coal - June 2009						
XCSA Coal Reserves						
Tweefontein Division	79.8%	Thermal Coal	-	86.3	-	IPD
SouthStock Division	79.8%	Thermal Coal	-	38.1	-	IPD
Goedgevonden Division	74.0%	Thermal Coal	-	195.4	-	IPD
iMpunzi Division	79.8%	Thermal Coal	26.3	99.3	12.6	
iMpunzi		Thermal Coal	-	44.5	-	IPD
ATCOM East		Thermal Coal	26.3	54.8	12.6	IPD
Mpumalanga Division	79.8%	Thermal Coal	-	18.7	-	IPD
Subtotal - South Africa			26	438	13	

Definitions

- OC = opencut; UG = Underground
- Salable Coal Reserve is the tonnage and coal quality that will be available for sale, either in the raw ROM state at a specific moisture

Notes:

- The Coal Resource and Coal Reserve figures tabulated have been stated on a total mine basis as at 30 June 2008.
- The Measured and Indicated Mineral Resources are inclusive of those modified to produce Mineral Reserves .
- The estimates of Coal Resources and Coal Reserves presented in this table have been estimated according to the SAMREC Code
- Coal Resources and Coal Reserves stated on a total mine basis include interests in Coal Resources and Coal Reserves attributable to minority interests in controlled entities and the interests of joint venture partners. Figures are subject to rounding and therefore totals may not add up.
- Coal Resources and Recoverable Coal Reserves are quoted on an air dried moisture basis. Extractable Coal Reserves are reported as Recoverable Coal Reserves.
- High grade Salable Coal Reserves were based on a 6000kCal NAR product. Atcom East based on a 5800kCal NAR product with a secondary, 21.5Mj/kg CV domestic power station (Eskom), product.
- Low grade Salable Coal Reserves are based on a primary 21.5/22MJ/kg (Air-dried) product.
- Product yields used to estimate Salable Reserves were derived from the "Limn Model" software. Inputs to this model are coal ply and in-seam dilution data, processed in the model. The model takes into account plant efficiencies to calculate practical yields. The model is calibrated to historical plant performance and where applicable, large diameter borehole data is used.
- Reserves are reported on an extractable and saleable basis.
- Valid prospecting rights have been issued for all the undeveloped Coal Resources. Some prospecting rights are being renewed, while

inference regarding the quality as these old pillar areas represent the high grade eyes that was picked out by the earlier miners. Mining was suspended as soon as coal quality dropped off, thus these old workings represent consistent high quality coal zones.

Most of the historic mining took place within the high grade plies of the No. 2 Seam and to a lesser extent in the high grade plies of the No. 4 Seam and the upper low grade plies were left behind. The mining height of the old workings is indicated on even the oldest plans making it possible to determine the exact mining horizon if it is assumed that the floor of the mining horizon coincided with the coal seam floor. Where borehole intersections can be obtained the quality of the coal seam is then determined by weight averaging the quality of the pillars by the tonnes that remain in the pillars with the quality and the tonnes off the coal left in the roof.

Reserves

Converting resources into reserves in the pillar areas is dependent on the mining method that will be utilised. Whether the coal will be mined through opencast dragline or mini pit truck and shovel methods determine the amount of contamination, coal losses, dilution and the mining horizon which in term will have a direct impact on the reserve estimation. The product yield and qualities of the saleable reserves is also dependant on the above factors.

47 million tonnes of pillar reserves are included in the Atcom East and Atcom North Life of Mine plans. A further 49 million tonnes of pillar reserves are included in the Tweefontein opencast operation's Life of Mine. This is a total of 69 million tonnes out of a reserve base of 833 million tonnes (see Table 2).

Reserve estimation risk

When determining the financial viability of extracting pillar resources through opencast methods there are many factors, from the coal condition and quality to the proposed mining method that will impact on the profitability and ultimate feasibility of extracting the coal seams. Some of these factors are:

1. Previous workings

The old bord-and-pillar mining was done on a select horizon within the major coal seam. The mining height was driven by this, but was also constrained by the capabilities and limitations of the mining equipment. The shallower coal seams allowed for high extraction limiting the amount of high grade coal for future extraction. Extraction of the deeper coal seams required larger pillars to be left for increased safety factors, resulting in more high-grade coal still available for future projects. The mining height, pillars centres and pillar sizes are required for further investigation.

2. Inherent coal quality

As the coal will undergo beneficiation in order to create a specific coal product, the washability of the coal is very important. Due to the extreme stratified nature of the Witbank coal seams, where sufficient samples were taken and analysed, the incremental quality of the coal sub-seams (or plies) must be analysed to determine the effect of various mining practices.

3. Nature of the proposed extraction

When considering the manner in which the different plies should be combined the mining practice plays a crucial part. The blasting method could either collapse the pillar in the void resulting in greater fines generation but lower top-seam contamination, with the reverse true as well, where the blast-holes are drilled short of the pillars, the fines generated are much less, but the potential for coal loss and/or contamination is much greater as the overlying coal seams (and subsequent waste) collapses into the voids.

The post-blasting cleaning of the coal surface should be considered as well, as a balance between coal loss and contamination must be found.

METHODOLOGY

Data gathering

In order to complete the investigation the following information is needed:

1. Basic geological information. The borehole data with the seam picks and quality analyses results are needed to determine the nature of the coal seams.

2. Detailed mining plans indicating mining heights, pillar sizes and centres. These plans are used to determine the extraction and subsequent percentage coal remaining in the mining horizon, which will in turn be used to de-rate the weighting of those plies in the combined quality model.
3. Details on the proposed mining method/s. Various mining methods can also be considered when evaluating the quality of the coal seams, but the impact of each of these mining methods must be well understood as the quality modelling is only as good as the basic assumptions.
4. Beneficiation methods must be understood as the various plant designs will have an impact on the export coal produced. XCSA uses LIMN plant simulation software for the simulation of the coal washing process. The plant design is considered by using a plant flow chart replicating the components of the wash plant in LIMN.

Quality compositing

The entire simulation is driven by the fact that the quality information is combined using weights derived from the ply thicknesses; through altering these thicknesses, by considering the mining practices, the correct mix of material can be created to estimate the yield of the reserve blocks. Thus for the following mining methods the simulation data was created in the following manner:

1. Pillar blasting

If the pillars are charged and blasted, collapsing the old workings, less ingress of air will be allowed reducing the chances for spontaneous combustion of the coal. This will also allow the voids (bords) to be filled with coal ensuring less collapsed roof material blending with the coal. The swell of the blasted coal and fill of the void will depend not only on the nature of the blast but also the effectiveness thereof, and is thus very unpredictable. The estimate uses 50% pillar material to fill the void, resulting in the remaining 50% of the void to be filled with material from above the previous mining horizon. The roof material is incrementally added to fill the void. If the coal seams above the pillars are thin, waste material is added to fill the void.

This method does however generate more fines, and appropriate sizing envelopes are used in LIMN to cater for the additional loss of coal during de-sliming.

2. No pillar blasting

If the blast-holes are drilled short of the workings, the pillars do not collapse well and the above method is also used, but with only 20% of the void filled with pillar material, resulting in 80% of the void filled with material from above, resulting in higher contamination figures reducing the coal qualities and yields. This method generates fewer fines during the blasting and less coal is lost during de-sliming.

3. Coal roof scalping

If the roof quality becomes very poor, or the contamination becomes very high resulting in poor coal qualities, the option exists for the dragline to scalp a certain amount of material from the roof of the desired mining horizon. The above technique is still used, but a specific amount of roof material is removed from the simulation. This will decrease the ROM but will increase the coal quality.

The new mining horizon thicknesses are then used to composite the various plies with their washabilities and simulated using LIMN. The plant yields simulated in LIMN are used with the ROM estimation and a basic cost/benefit calculation will indicate the most profitable option that must be undertaken.

DISCUSSION AND RESULTS

Quality compositing

The methods were applied to the planned opencast operations, and the following are the results from the Atcom East colliery. The operation mainly mines No. 2 Seam (of which a select horizon was previously extracted through bord-and-pillar mining) and virgin No. 1 Seam. Some small areas contain No. 4 Seam.

1. Basic short drilling

By drilling the blast-holes short of the workings and not collapsing the pillars, the mining horizon contamination reached 12%, this resulted in an average export yield for the No. 2 seam of 52.7%. See Figure 2.1 for the yield contours.

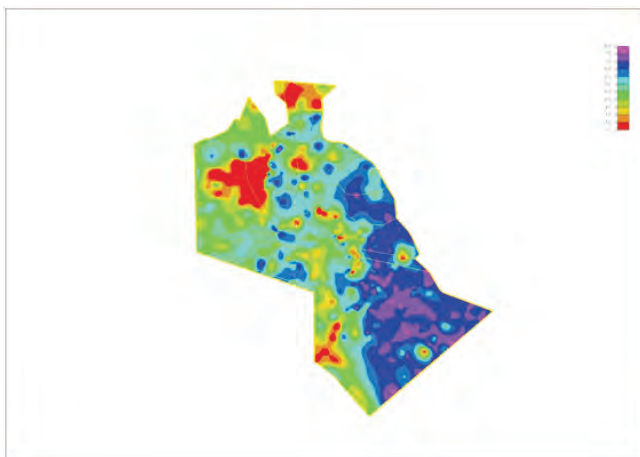


Figure 2.1: Yield contours for a basic short drilling simulation

2. Short drilling with 75% of the roof coal removed

As with the previous simulation, the voids aren't collapsed, but to increase the export yield 75% of the roof coal material with the waste collapsed into the mining horizon is scalped off by the dragline. The mining horizon contamination is reduced to 5% with the average export

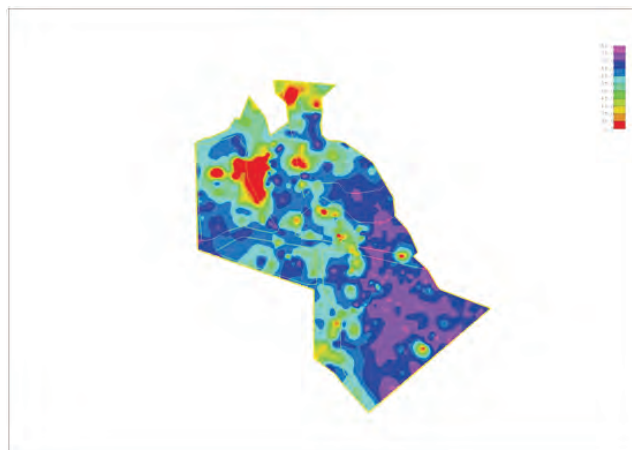


Figure 2.2: Yield contours for a short drilling simulation with 75% roof coal removed.

yield for the No. 2 seam increasing to 55.7%. See Figure 2.2 for the yield contours.

3. Drilling and collapsing the pillars

By drilling into and collapsing the pillars the contamination was reduced from the initial 12 % to 6%. Compositing for the fines that are increased by blasting the actual pillars, the yield of the No. 2 seam is 53.5%. See Figure 2.3 for the yield contours.

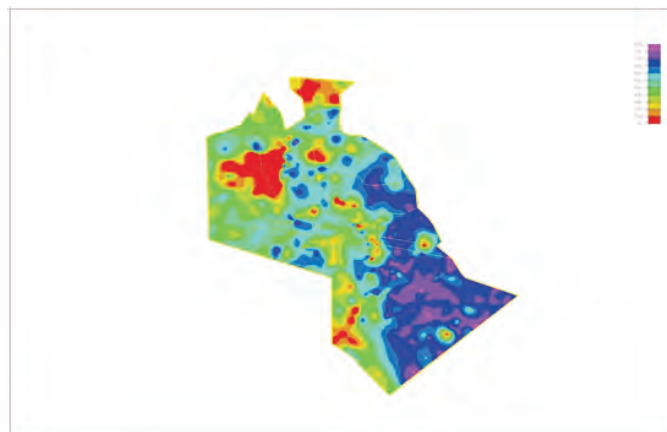


Figure 2.3: Yield contours for pillar collapsing scenario.

CONCLUSIONS

In the simulation of the Atcom East reserve the financial evaluation indicated that the best option was to drill into the pillars as the quality of the coal in the areas allowed for the fines to be added to the export product. This resulted in little reduction of the yield while ensuring high reserve extraction. This combination ensured maximisation of the saleable reserve and the greatest value benefit.

This methodology is very useful to evaluate a large area when considering the impact of various mining practices on the value of a reserve, or it can be used to determine the most profitable practice in a given block. The method does not consider the impact of sending different coal sources to the plant, which will be the next focus of the project.

In the simulation discussed here, the impact of mining practices on the yield, is but one of the many complexities that need to be investigated. The impact of source mixing and ply-optimization should also be considered, to name but a few.

With so much of the resources in the Witbank coalfield remaining as remnants or pillars, greater focus must be placed on increasing coal recovery and decreasing, losses, dilution and contamination to maximize the mine life and value for the existing operations. Using a financial approach to increase value can assist in maximising the true extractable reserve base by evaluating the most profitable manner of extraction.

These types of paradigm shifts are crucial to the continual successful extraction of remnant and pillar reserves. Many of the better known challenges are studied and considered during mine planning, but with coal quality and mining conditions deteriorating as the last remnants and pillars are mined, greater emphasis must be placed on the precision of the

planning process. With expectations of greater precision, additional information acquisition might be required, but the planning process itself must be augmented with detailed simulations of various conditions that might impact on the vital variables that drive the value of the reserve.

ACKNOWLEDGEMENTS

Xstrata Coal South Africa for the use of the data and geological models.

REFERENCES

XSTRATA COAL SOUTH AFRICA, 2009: Resources and Reserves as at Jun 2009, viewed 10 Aug 2010, http://www.xstrata.com/assets/pdf/x_reserves_resources_coal_200910.pdf

Ian Metcalfe, Robert S. Nicoll, James L. Crowley, Roland Mundil, Steven W. Denyszyn, Mark D. Schmitz and Clinton B. Foster

Application of high-precision CA-IDTIMS U-Pb zircon dating to Permian – Lower Triassic stratigraphy in eastern Australian coal basins

Zircons obtained from ashfall tuff beds, abundant in the Guadalupian and Lopingian (middle and upper Permian coal-bearing basins of eastern Australia, yield new high-precision U-Pb ages that provide robust international timescale calibration for the Middle Permian-Lower Triassic of eastern Australia. Initial results from 16 ashfall tuff beds in the Bowen (BB) and Sydney (SB) basins provided eruptive ages with uncertainties as low as $\pm 0.02\text{Ma}$ (2 sigma), and are considered to be accurate if uncomplicated by factors of inheritance or extended dwell time in the magma chamber. Samples from the Gunnedah Basin are awaiting analysis and plans are in preparation to obtain core samples from the Galilee Basin. Ashfall tuff beds are also associated with Permian coal beds in Tasmania. A research program is in place to expand the study to additional stratigraphic units in the Permian and Triassic basins of both eastern and western Australia.

Initial results (Figure 1) include an Early Guadalupian (Roadian) age for the Rowan Formation (SB, Greta Coal Measures) and a Late Guadalupian (Late Capitanian) age for the Broughton Formation (SB). The mid Lopingian (mid Wuchiapingian) is represented by the Ulan C marker bed (SB), Ingelara Formation (BB), Nobbys Tuff (SB) and Platypus Tuff (BB). A Late Lopingian (Early Changhsingian) date was obtained from the Awaba Tuff and Late Lopingian (Changhsingian) dates were obtained from Farmborough Formation (SB) and the Kaloola Member at the base of the Bandanna Formation (BB). A date of $252.2 \pm 0.4\text{Ma}$ at the top of the Bandanna Formation (BB) indicates that the late Changhsingian mass extinction and Permian-Triassic boundary levels are very close to the boundary between the Bandanna Formation and overlying Rewan Group. Early Triassic (Late Olenekian, Late Spathian) dates were obtained from the Garie Formation in the southern Sydney Basin.

Ages from this program are designed to provide important calibration tie points for largely endemic eastern and western Australian biozonation schemes. By tying them to the biozones, we hope to resolve questions related to the synchronicity of palynological biozones between eastern and western Australia and their correlation to regions beyond

Australia. Age will also be used to correlate brachiopod, conodont and foraminiferal biozones, also highly endemic, to similar biozones outside Australia.

The precision of the ages allows more accurate stratigraphic correlation within and between sedimentary basins and provide a better time framework for event analysis and depositional studies. Initial results from the Bowen Basin indicate that deposition of the Bandanna Formation with an average thickness 100m occurred over c. 0.65Ma (deposition rate of 154m/Ma). The interval between the Platypus and Kaloola tuff horizons is c. 3.35Ma and is represented by a sediment package that averages 200m (60m/Ma). The stratigraphic package of c. 160m between the Ingelara Formation and Platypus Tuff was deposited over c. 1Ma (160m/Ma).

In the northern Sydney Basin, the sediment package between the Fairford Formation of the Wittingham Coal Measures (mid Lopingian, Middle Wuchiapingian) and the Awaba Tuff of the Newcastle Coal Measures (Late Lopingian, Early Changhsingian) has a thickness of c. 465m and was deposited over 3.8Ma (122.35m/Ma). Preliminary analyses also indicate that the Fairford Formation of the Muswellbrook Area is roughly equivalent in age to the Ulan C Marker Bed Tuff of the Ulan–Gulgong area.

In the southern Sydney Basin, the sediment package of about 170m between the Broughton Formation and the Bargo Claystone (Huntley Claystone Member) was deposited over c. 8.64Ma (19.67m/Ma) from the late Guadalupian (Capitanian) to the mid Lopingian (late Wuchiapingian). The 50m of sediment between the Huntley Claystone Member and Wongawilli Coal (Farmborough Claystone Member) was deposited over 1.29Ma (38.75m/Ma) from the late Wuchiapingian to the early Changhsingian. The 160m of sediment between the Farmborough Claystone Member and top of the Bulli Coal, the presumed level of the Permian - Triassic boundary, was deposited over 1.22Ma (131.14m/Ma). The 243m of sediment between the Coal Cliff Sandstone (Griesbachian/basal Induan) and the Garie Formation (late Spathian/late Olenekian) represents c. 4.25Ma (57.17m/Ma).

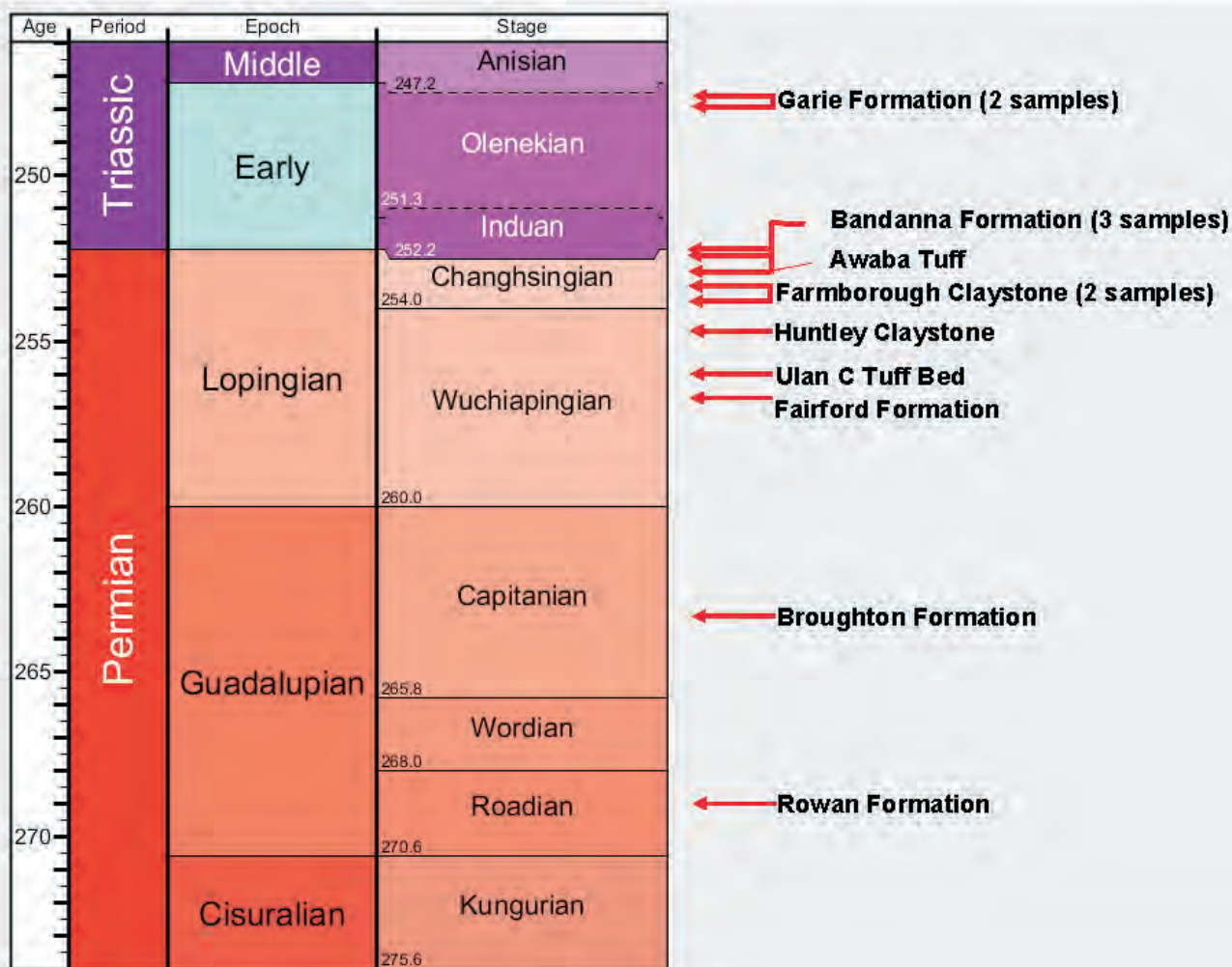


Figure 1: Permian – Triassic timescale, modified from Gradstein & others (2004) and Ogg & others (2008) showing relative stratigraphic and time correlation of selected stratigraphic units in the Sydney and Bowen Basins.

Ian Metcalfe, Earth Sciences, School of Environmental & Rural Science, University of New England, Armidale, NSW 2351, Australia

Robert S. Nicoll, Geoscience Australia, PO Box 378, Canberra City, ACT 2601, Australia, and Research School of Earth Sciences, Australian National University, Canberra, ACT 200, Australia

James L. Crowley, Isotope Geology Laboratory, Department of Geosciences, Boise State University, 1910 University Drive, Boise, ID, USA, 83725-1535

Roland Mundil, Berkeley Geochronology Center, 2455 Ridge Rd. Berkeley, CA, USA, 94709

Steven W. Denyszyn, Berkeley Geochronology Center, 2455 Ridge Rd. Berkeley, CA, USA, 94709

Mark D. Schmitz, Isotope Geology Laboratory, Department of Geosciences, Boise State University, 1910 University Drive, Boise, ID, USA, 83725-1535

Clinton B. Foster, Geoscience Australia, PO Box 378, Canberra City, ACT 2601, Australia.

Agi Burra

Application of domains in gas-in-place estimation for opencut coal mine fugitive gas emissions reporting

Estimating fugitive gas emissions from opencut coal mines has been a topical subject in the last couple of years. Since the National Greenhouse Gas Emissions Reporting (NGER) guidelines were released in 2007 (and more recently updated in 2009), increasing number of coal mining companies have aimed to start accounting for their emissions using the NGER Method 2 utilising site specific field data instead of the Method 1 state default figures. Initial methods focussed on borehole by borehole interpretation of gas data and attempted to then extrapolate such data to the whole mine site. This approach, while may be valid at some deposits, does not always capture the vast amount of in-depth geological understanding available in most coal mining areas and that are actually part of the gas distribution setting that is observed in the field today. This paper aims to present a geological and gas domain based approach to gas-in-place estimates that form the basis for the fugitive emissions calculations as per the guidelines. The method is designed to honour regional and local gas domains and associated trends with depth by establishing gas zones within domains to form a framework that is subsequently populated by data obtained from coal seam gas exploration.

INTRODUCTION

This study presents a methodology for fugitive emissions estimation for opencut coal mines, focussing on the gas-in-place (GIP) estimation for NGER reporting, particularly as to how to interpret and incorporate information from multiple boreholes within an area.

Coal mine fugitive gas emission estimation has become an eagerly debated topic recently in Australia. Of particular interest is how these emissions from opencut mining activities are best estimated. The 2009 NGER technical guidelines based originally around the Tier 3 method work of Saghafi & others (2008), provide the reporting framework, however, it does not offer guidance on the implementation of this method across a whole deposit, such as interpolation between and extrapolation beyond known data points.

Other current methodologies focus on developing relationships with gas from geophysical logs (eg Fu & others, 2009) or other coal quality or petrographic parameters (Scott & others, 2008). These methods ultimately aim to derive a technique to predict gas content and/or composition in other boreholes that have not been sampled for gas. In this way,

they would be able to develop a dataset covering the area of interest and then be able to treat the gas parameters as they would treat coal quality variables such as ash or density. However, as will be discussed later, such correlations are not always straight-forward and they are often unable to accommodate other key reservoir characteristics such as gas saturation that influence gas distribution in shallow coal fields.

The strength of the method presented here is that it proposes to utilise regional geological understanding and existing site-specific geological models for the interpretation of gas domains and gas zones. These domains and zones provide the framework for the population of the data obtained from exploration drilling allowing the integration of a 3D gas regime into the geological model and the GIP estimation.

PROJECT BACKGROUND

The concept for this estimation method originated from the analysis of results from a regional gas exploration program that was carried out by Xstrata Coal NSW in the Hunter Valley Coalfields of the Sydney Basin from 2008–2010. The program consisted of 26 boreholes drilled over Xstrata leases in the Lower and Central Hunter Valley, and an area west of Muswellbrook in the Upper Hunter (Figure 1).

The data collection strategy for these 26 boreholes was to contiguously sample all coal and carbonaceous layers in the borehole for a complete picture of the emissions profile for the proposed (or existing) opencut mine. In addition to gas content and composition testing, selected samples were

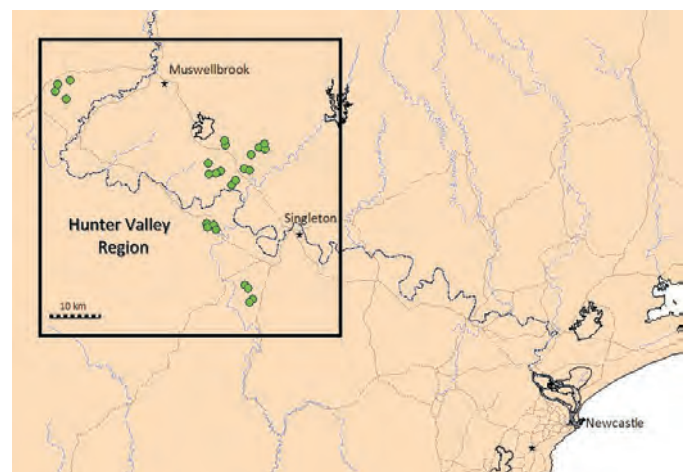


Figure 1: Location of 2008–2010 Xstrata gas boreholes.

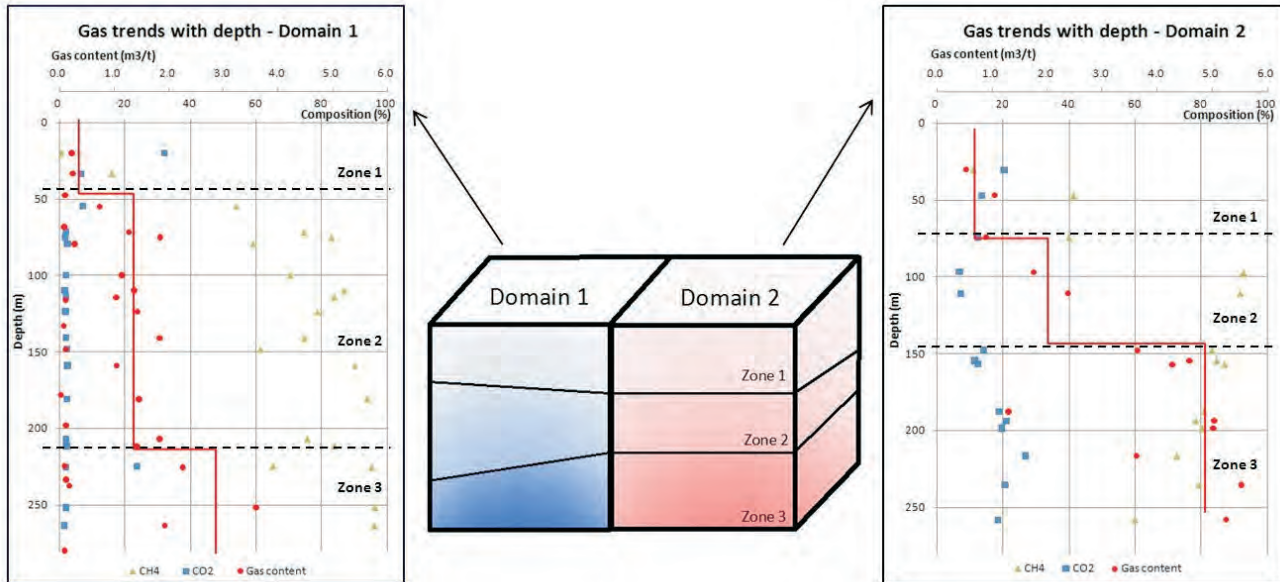


Figure 2: Schematic of the approach for gas domains and zones that define the block model framework that is populated by exploration data.

additionally subjected to coal quality (proximate and ultimate) analyses, petrophysical studies, and desorption isotherm testing.

Total depths of boreholes were between 250–380m and in many areas this represented the deepest coal seams in the particular Coal Measures in the area. In this sense, the expansive dataset permitted the investigation of the trends beyond the opencut mine limits, and this in turn allowed for the interpretation of gas domains with increased confidence.

The results (that will be detailed later) showed that there are a number of major gas domains in the Hunter Valley that appear to be bound by significant regional geological features. Within each of these regional domains, further sub-domains may exist that are limited by more localised structures or geological strata discontinuities such as faults, folds, dykes, sandstone channels or unconformities. For the purposes of this GIP methodology description, however, all of these sub-domains will also be referred to as gas 'domains'.

Additionally, it is apparent that each domain has its particular trend of gas content and composition change with depth. These changes happen in particular depth intervals which are referred to here as gas 'zones'.

DISCUSSION OF METHODOLOGY

Overview

Essentially, this GIP estimation method aims to build a 3D gas model that is bound by gas domains spatially, and by gas zones vertically to create a gas block model (Figure 2). These blocks can then be populated by data that estimates the gas parameter values (or relationships) to complete the 3D gas distribution model. The gas model can subsequently be applied to a geological model to derive the GIP estimate for the area.

Domaining

Gas domaining here refers to the delineation of areas where the downhole gas trends observed are similar. This is often an iterative process as not all obvious geological domains host different gas regimes. If the pore pressures are similar in regions, then the gas regime will likely be similar as well. For example, an area can be split by a major fault zone but if there is communication across the fault, then the gas regime may not change at all. This has been observed at numerous locations in the Hunter Valley. Conversely, a seemingly homogeneous area (ie no major structures observed) was shown to have 2 different gas domains which, upon closer inspection, showed a disparity based around a change in sedimentological characteristics in each area. In particular, this phenomenon was related to different horizontal and vertical stresses in one of the domains due to differential compaction originating from a significant increase in the presence of sandstone channels in the strata sequence on one side of the 'invisible' gas domain boundary (Figure 3).

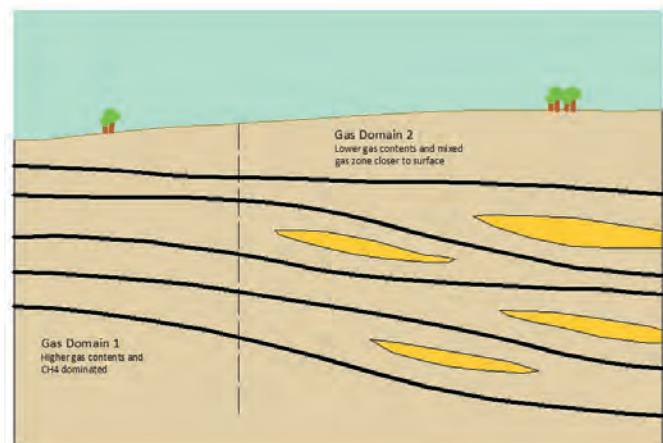


Figure 3: Schematic diagram illustrating soft boundary between gas domains that are associated with changes in sedimentological features.

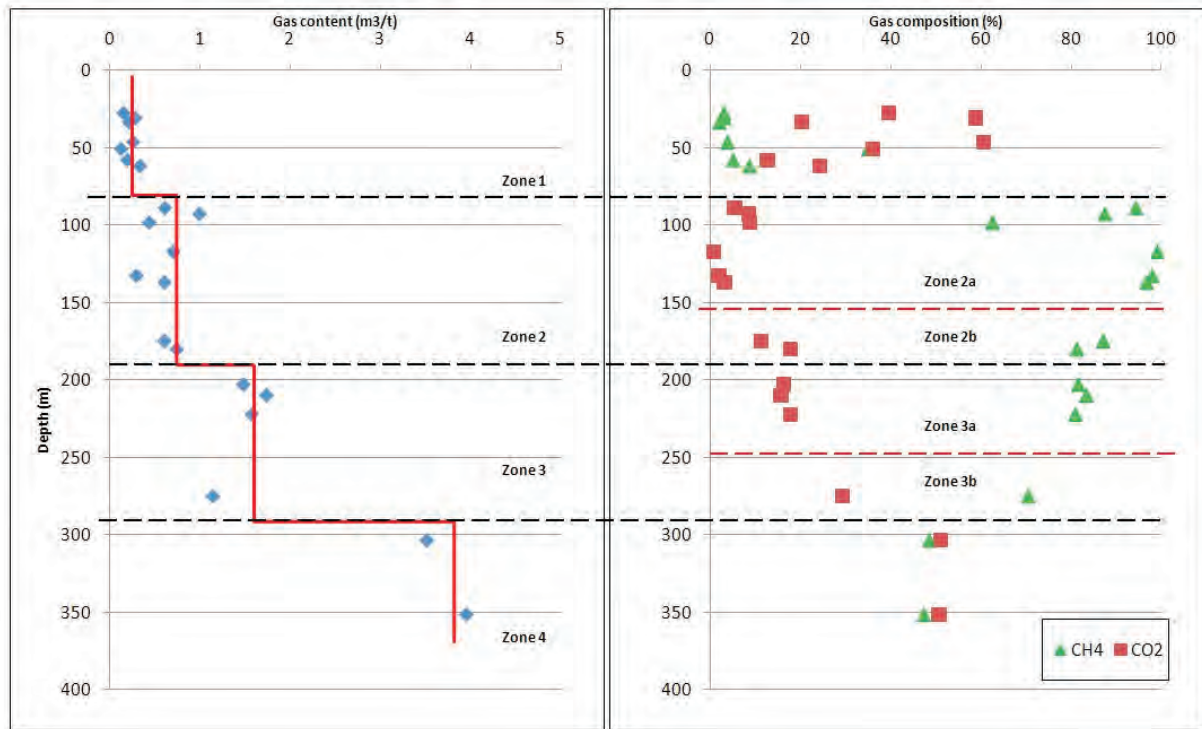


Figure 4: An example where sub-zoning may be warranted due to rapidly changing gas composition layering within regional gas content zones.

Gas zones

Gas zones for the purposes of this GIP estimation methodology are defined in the vertical strata as intervals of similar gas characteristics, particularly relating to gas content values. Often these zone boundaries also coincide with gas composition changes, however this is not always the case. It should be noted that other researchers in this field have referred to these, or similar, zones as “layers” (eg Thomson & others, 2008). It is thought that this term may imply that these zones are horizontal regions coinciding with coal seam or other sedimentological bedding planes and this is not always the case. For this reason, the term “gas zone” is used in association with this methodology.

In general, the main gas zones in the Hunter Valley with increasing depth can be observed as (for example, Figures 2 and 4):

1. Shallow, no or very low gas horizon from surface to about 70–90m depth
2. Low gas zone characterised by gas contents of about 1–3m³/t for coals, ranging from 100–150m depth
3. Moderate gas zone with gas contents of 4–6m³/t, from 150–250m depth
4. High gas zone 6–15m³/t around 250–350m depth
5. Occasionally, there is a deep, moderate or low gas zone again with around 3–6m³/t around 350–800m below surface (depending on the particular domain).

Appreciably, these depth ranges and the actual gas content values change across domains, however, the relative trends across zones remain across all major domains. A full domain and zone analysis of the Hunter Valley is beyond the scope of this paper (for related discussions on these topics, see Thomson & others (2008) and Pinetown (2010)).

The other gas characteristic input in to the fugitive emission estimation considerations is the gas composition within these gas zones. This is an important factor because methane has 21 times the global warming potential (GWP) of carbon dioxide, and hence has a major impact on the actual CO₂-equivalent tonnes emissions reported.

Gas composition zonation also occurs in the coal measures sequences. The typical ‘layering’ often coincides with the above-mentioned gas content zones, however, these can vary from domain to domain. In general, the following zones can be observed with depth:

1. Shallow, no gas horizon
2. Low gas horizon, usually dominated by CO₂, can show mixed compositions during the ‘crossover’ from the CO₂ to CH₄ rich zone. However, most often there is a rapid change from CO₂ dominated to CH₄ dominated zones
3. Moderate to high gas zones are predominantly CH₄ dominated, with the deeper segments occasionally seeing the mixed gas zone (CH₄ and CO₂) Thompson & others (2008) described.

Although these gas composition boundary depths vary between areas, the sequence and approximate depths are similar in each domain. Interestingly (and conveniently!), the shallow gas composition zones tend to coincide with the gas

content zones described above. This trend is often valid down to the start of the moderate to high gas content zones. Below this, the composition zones are either CH₄ dominated or a mixed gas zone may have developed. Where the gas content and gas composition zones do not coincide, the gas zones can be broken down to further 'sub-zones' for the purposes of emissions estimation (Figure 4). In either case, once the horizons in the boreholes (and hence, the zoning for the domain or area) are established, the framework is set for establishing the gas distribution model for the deposit.

Gas Model

The model framework generated by the domaining and zoning processes, can now be populated by actual or predicted gas data. Since all potentially gas-bearing strata was sampled in these boreholes, it is possible to separate the gas data within each zone to comprise of coal-only and carbonaceous rock-only samples. This level of detail may not be required in all coal basins, but in the Hunter Valley carbonaceous materials can be abundant in some strata sequences and often contain some gas (aka shale gas). Figure 5 shows the gas dataset for one of the boreholes with the coals samples and the carbonaceous samples separated (and displayed in different symbols). It is apparent that the coal samples in all domains show higher gas values than the carbonaceous samples. In this sense, it would be possible to process these 2 different types of samples separately (where appropriate) in the gas value assignment stage. Incidentally, the gas composition values for both coals and carbonaceous rocks are the same in each gas zone.

It can also be observed from this dataset that the variance of gas contents and composition values within each domain and zone pairing is small, particularly when the dataset is split into coal-only and carbonaceous units (Figure 5). In this instance, it is possible to average the gas values within each zone, for each rock-type as appropriate, and establish a table of input values into the estimation model for further use in the gas emissions tonnes estimations. In some zones or domains, it may be more appropriate to develop a linear relationship with depth or some other parameter instead of the averaging shown here, or even apply a more stringent statistical method (such as kriging) for deriving representative gas content and composition values for each zone. In this paper, the averaging

Table 1: Representative gas content values for coals and for carbonaceous materials in each gas zone.

Gas Zone	Average gas content for coal (m ³ /t)	Average gas for carbonaceous (m ³ /t)	CH ₄ %	CO ₂ %
Zone1	0.84	0.00	67.02	13.65
Zone2	3.24	0.77	78.33	16.51
Zone3	5.80	1.42	67.27	28.57
20m below pit floor	2.50	1.00	65.74	32.81

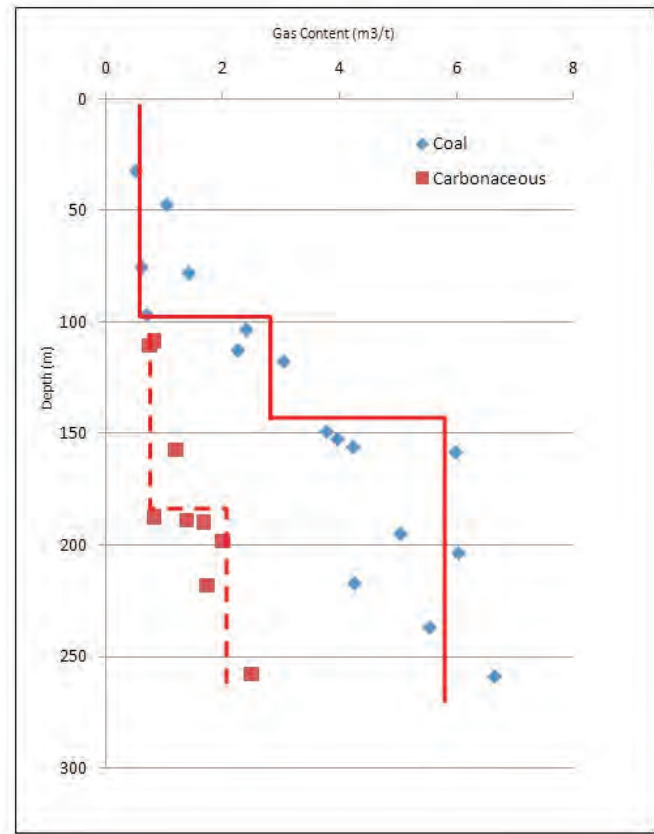


Figure 5: Cross plot of gas content and depth highlighting that carbonaceous shales have significantly less gas content than coals, even in high gas zones or domains.

method within zones was employed. Essentially, the aim is to arrive at a series of representative gas content values for coals and for carbonaceous materials in each gas zone in preparation for applying the gas model to the site geological model (Table 1).

Estimating gas bearing strata masses

The site geology model is a 3D representation of the coal seam geology at a particular deposit. These models form the basis for coal resource estimation and mine planning purposes at most operations. Coal tonnages reported from such models are directly applicable to gas in place estimation, particularly when combined with the gas model blocks as described in the preceding sections. It should be noted that NGER requires coal emissions to be reported from 20m below the pit floor, and hence, this should be treated as an additional "gas zone" for the purposes of opencut fugitive gas emissions estimations.

In the case of the Hunter Valley where carbonaceous materials can form a notable percentage of the rock mass, it is possible to establish the percentage of carbonaceous rocks not captured in the coal geological model utilising geophysical logs such as density. The amount of carbonaceous materials are calculated from the geophysical log and then converted into a percentage of total strata (for example, to the base of the pit floor) for an opencut emissions estimation. The carbonaceous tonnes can be estimated by multiplying the waste material tonnages by the percentage of carbonaceous rocks present in the strata. In

Table 2: Data derived from gas and geology models forms the basis for the GIP, and subsequent CO₂-e emission estimation.

Depth	Fugitive Emissions Estimation Detail				Total GHG emissions (tonnes CO ₂ -e)
	Total CH ₄ emissions (m ³)	Total CO ₂ emissions (m ³)	Total CH ₄ emissions (tonnes)	Total CO ₂ emissions (tonnes)	
Zone 1	460 320	159 600	313	298	6870
Zone 2	2 239 380	471 900	1522	882	32 851
Zone 3	3 358 270	1 427 140	2283	2669	50 611
20m below pit floor	200 385	100 345	136	188	3048
TOTAL	2 158 985	2 158 985	4254	4037	93 380

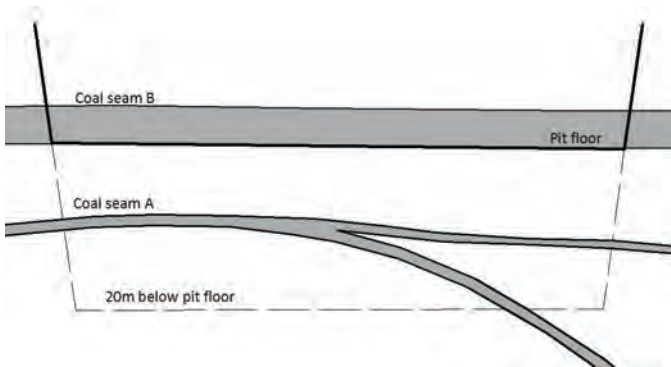


Figure 6: Coal seam geometry in the 20m zone below pit floor may introduce complexity in the estimation of release factor that the NGER methodology does not address.

the Hunter Valley, carbonaceous materials comprise about 2–5% of the non-sampled, non-coal strata. These include carbonaceous shales, claystones and mudstones that may be too thin or inconsistent across the deposit to be adequately sampled or correlated, in some instances, mixed lithology gas samples such as partial coal, partial siltstone and partial carbonaceous shales.

For floor emissions, NGER guidelines advise that percentages of influence be calculated for each coal seam based on its thickness, gas content and proximity to the pit floor. This means that a thin gassy seam that is close to 20m below the floor will likely have less influence than a thicker, moderately gassy seam in the immediate pit floor.

The calculation for the floor emission release factor shown in the NGER guidelines, however, this is designed to be carried out on a borehole by borehole basis. This is not directly transferrable to the gas domain and zone concept because in a 3D model approach, seam dip needs to be accounted for and this means that in some parts of the pit, seam A will be in the immediate floor, whilst in other parts, it may no longer be within the 20m floor horizon (Figure 6). For the domain estimation method, however, it is recommended that an approximation for the amount of coal and carbonaceous material in the floor be made from the geological model. In this sense, it is possible to report the actual coal tonnes that occur in the pit floor, and investigate the “vicinity” of these tonnes to the pit floor so that an emission factor can be estimated. As a general observation, there is unlikely to be

significant coal seams left behind in the 20m below the pit floor, as these would have been captured in the mineplan and pit design wherever possible.

Estimating gas in place

This section illustrates a worked example of the fugitive emission estimations that would be produced for a hypothetical coal mining production of 3.1Mt pa using the gas data listed in Table 1. For this example it is assumed that the productions will disturb 1Mt in each of the 3 gas zones with 0.1Mt in ‘Zone 4’ which is the 20m of strata below pit floor. Table 2 shows the results of the estimations.

In this example, the reported coal tonnes for each zone (including 20m below the pit) can be multiplied by the gas content, gas composition and the density of the particular gases to arrive with 2 sets of numbers, one for CH₄ tonnes, and the other for CO₂ tonnes (Table 2).

- CH₄ tonnes = $\sum (\text{coal tonnes} \times \text{average gas content} \times \text{average CH}_4 \% \times \text{CH}_4 \text{ density})_{\text{zone}}$
- CO₂ tonnes = $\sum (\text{coal tonnes} \times \text{average gas content} \times \text{average CO}_2 \% \times \text{CO}_2 \text{ density})_{\text{zone}}$

This GIP estimation can be taken further in the fugitive emissions estimation context and converted to CO₂-equivalent tonnes as per the NGER guidelines (Table 2).

- Thus, CO₂-e tonnes = $\sum [(\text{CH}_4 \text{ tonnes} \times 21) + \text{CO}_2 \text{ tonnes}]$

The fugitive gas emissions originating from *in situ* gas-bearing strata in the hypothetical opencut coal mine is 93 380t CO₂-e.

CONCLUSION

A domain-based gas-in-place estimation methodology for opencut fugitive gas emissions reporting has been presented here. The method is designed to capture regional and site-specific geological understanding to delineate domains and gas zones associated with those domains to form a

framework that is subsequently populated by data obtained from coal seam gas exploration.

The advantage of such an estimation method is that it places the gas distribution observations into a 3D geological context which allows for a realistic estimation of gas occurrence in the particular domains and zones even with limited gas data.

The shortcomings of such a method is that it requires an adequate dataset and regional geological understanding to be able to define these domains and zones, and this may not always be available, particularly in the case of small or isolated deposits. It may also be the case that some aspects of the strata may not be well understood or documented such as carbonaceous rocktype distribution, or associated gas content trends. However, on-going exploration programs allow for datasets to be improved and it is hoped that the findings presented here assist with the collation of datasets in an effective manner.

ACKNOWLEDGEMENTS

The author would like to thank Jim Sandford of Xstrata Coal NSW for his support in developing this methodology and for the permission to release information as part of this paper. I would also like to thank Joan Esterle of the University of QLD who provided much valued feedback and guidance in the presentation of this paper.

REFERENCES

- FU, X., QIN, Y., WANG, G. & RUDOLPH, V., 2009: Evaluation of gas content of coalbed methane reservoirs with the aid of geophysical logging technology. *Fuel* **88**, 2269–2277.
- DEPARTMENT OF CLIMATE CHANGE, AUSTRALIAN GOVERNMENT, 2009: *National Greenhouse and Energy Reporting (Measurement) Amendment Determination (No1) Technical Guidelines 2009*. Australian Government, Canberra ACT.
- PINETOWN, K., 2010: Delineation of Coal Seam Gas Domains in the Hunter Coalfield, Sydney Basin. In Hutton, A., Ward, C. & Bowman, H, (Editors): Thirty-seventh Symposium on the Geology of the Sydney Basin, Hunter Valley, Pokolbin, NSW May 6-7, 2010 (Abstracts).
- SAGHAFI, A., ROBERTS, D., FRY, R., QUINTANAR, A., DAY S., LANGE, T., HOARAU, P., DOKUMCU, C. & CARRAS, J., 2008: Evaluating a Tier 3 Method for Estimating Fugitive Emissions from Open Cut Coal Mining. ACARP Report 15076.
- SCOTT, S., RUNGE, C., ROSS, T. & STACKHOUSE, Z., 2008: How much methane gas can shales contribute to a producing coal seam gas well? *1st Asia Pacific CBM Symposium*, Brisbane.
- THOMSON, S., HATHERLY, P., HENNINGS, S. & SANDFORD, J., 2008: A model for gas distribution in coals of the Lower Hunter, Sydney Basin. In *PESA Eastern Australasian Basins Symposium III*.

Kaydy Pinetown, N. Sherwood and A. Saghafi

The influence of coal maceral composition on gas contents in the Hunter Coalfield

A variety of factors are likely to contribute to the generation and retention of coal seam gas (CSG), and these factors include coal maceral composition and rank. In a previous study, the Hunter coalfield was divided into 'gas domains' on the basis of geology, gas content and composition distributions. Studies on organic petrology, and gas contents, compositions and origins, for coals of two gas zones occurring within two of the 'gas domains' enable insights into controls on gas distribution. Between ~200m and ~500m depth, *in situ* gas contents vary between ~0.5m³/t and ~10m³/t in Zone 1, and between ~3m³/t and ~11m³/t in Zone 2. More than ~80% of the CSG in Zone 1 consists of methane (CH₄), whereas the CSG in Zone 2 consists of a mixture of CH₄ and carbon dioxide (CO₂). CH₄ concentrations generally decrease with increasing depth for Zone 2 between ~200m and ~500m, but do not systematically vary with depth for Zone 1. Stable carbon isotope data indicate that the CH₄ in both zones, in part, is of biogenic origin, although thermogenic sources are also apparent for Zone 1 and to a lesser extent for Zone 2. The coals in both zones are generally rich in vitrinite (>50%), but more so in Zone 1. Coals in Zone 1 contain more liptinite, whereas coals in Zone 2 are richer in inertinite and minerals. Comparisons between *in situ* gas contents and maceral compositions for the two zones show that high *in situ* gas contents are commonly associated with liptinite-rich coals for Zone 1, down to about 480m depth. The coals in Zone 1 that have high gas contents contain higher proportions of suberinite than those of Zone 2 having high gas contents. The suberinite is intimately associated with telovitrinite in these coals.

It is likely that geological structures in each zone have influenced the migration of groundwater, and thus perhaps the extent to which biogenic gas has been generated. Dipping strata could provide preferential pathways along bedding planes for microbial communities to access coals irrespective of maceral composition. Microbial activity in some sections of the coal seams in Zone 1 may explain the variation in gas contents between seams and within the same seams in this zone.

INTRODUCTION

Previous studies have shown that relationships between CSG reservoir and coal properties are complex, and disagreement commonly exists in interpretations of these relationships. For example, Gurba & Weber (2001) has shown that elevated CH₄ contents are associated with coals rich in specific macerals, whereas Hackley, Warwick & Breland (2007) suggests that there is no significant relationship between maceral composition and gas content. This study aims to enhance the

understanding of these relationships. Studies on the occurrence of natural gas in various coal seams have been used to gain an understanding of the behaviour of gas in coal with respect to methane (CH₄) extraction, carbon dioxide (CO₂) sequestration potential and fugitive greenhouse gas emissions estimations (e.g. Faiz & others, 2006; Golding & others, 2009; Saghafi, 2010).

The origin of natural gases in coal has been extensively investigated (e.g. Hargraves 1986; Smith & Pallasser 1996; Whiticar 1996; Kotarba & Lewan 2004; Gurgey & others 2005). CH₄ (along with C₂ to C₄ hydrocarbons) and CO₂ are the two main gases occurring in coal (Clayton 1998). Biogenic gas is produced by the decomposition of organic matter or pre-existing gas, by micro-organisms, whereas thermogenic gas is produced during devolatilisation of coal at high temperatures generally associated with deep burial (Rice, 1993). Gas can also be generated by contact metamorphism associated with igneous intrusions, and in many instances coals in close proximity to igneous bodies have high concentrations of CO₂. Throughout geological time significant volumes of gas may be lost from coal, and migrate and accumulate due to a range of geological processes (Rice, 1993). The present day distribution of CSG is mainly related to the burial history, geological structure, depth, source rock type, rank, hydrogeology and proximity to igneous intrusions of the seams concerned (Smith, 1999; Scott, 2002).

PREVIOUS WORK

Research literature on the influence of coal maceral composition and rank on gas stored in coal indicates varying relationships. According to Crosdale (1989), Lamberson & Bustin (1993), Bustin & Clarkson (1998) and Crosdale, Beamish & Valix (1998), bright, vitrinite-rich coals seem to have a greater adsorption capacity than dull, inertinite-rich coals of a similar rank. In contrast to these observations, however, Ettinger & others (1966) suggested that, at low ranks, fusinite-rich coals have a greater CH₄ adsorption capacity than vitrinite-rich coals. Furthermore, Faiz & others (1992; 2007) found that maceral composition did not exert any systematic influence on gas adsorption capacity and that other effects prevail. Similar to the findings of Karacan & Mitchell (2003) and Chalmers & Bustin (2007), Laximinarayana & Crosdale (1999) concluded that an evaluation of coal type alone is complicated by rank influences.

From a study on coals in central Queensland, Walker, Glikson & Masteralerz (2001) observed that vitrinite-rich coals desorb CH₄ faster than inertinite-rich coals, hence facilitating gas

drainage. This contradicts findings by Laximinarayana & Crosdale (1999), who noted that dull coals desorb more rapidly than bright coals. A study by Gurba & Weber (2001) on some Australian coals shows that elevated CH₄ contents for most of the samples studied are associated with a specific type of vitrinite, desmocollinite. Gurba & Weber (2001) also observed that slits and cleats in another vitrinite, telocollinite, served to enhance adsorption capacity and permeability. Contrary to these observations, however, Hackley, Warwick & Breland (2007) found no significant influence of maceral composition on gas content.

Contrasting observations have also been made for the influence of coal rank on CSG. Studies by Crosdale (1989), Faiz & others (1992) and Chalmers & Bustin (2007) amongst others, indicate that the gas adsorption capacity for coal increases with increases in coal rank. Bustin & Clarkson (1998) found little or no correlation between coal rank and CH₄ adsorption capacity nor a consistent variation in modal micropore size and size distribution with rank. Low volatile bituminous coals generally adsorb approximately twice as much CO₂ than CH₄ at a given pressure and constant temperature than lower rank coals.

Generally, a negative correlation exists between mineral content and gas adsorption capacity (Faiz & others 1992; Laximinarayana & Crosdale 1999), and the presence of minerals in coal is commonly associated with low gas contents. In a study on the impact of coal properties on gas drainage efficiency, Gurba & others (2001) observed distinct differences in petrology between coal of normal and difficult drainage areas. It was found that gas migration may be impeded by micro-cleat mineralisation, the presence of oil and solid bitumen in cell cavities, as well as siderite nodules (Gurba & others 2001). In an investigation on the adsorption of hydrocarbon gases in coals, organic-rich shales and clays, Cheng & Huang (2004) observed that adsorption in the coals and organic-rich shales is greater than on clays such as kaolinite and montmorillonite. Further information on the effects of maceral composition, rank and minerals on CSG can be found in Faiz, Aziz & Hutton (1996), Levy, Day & Killingley (1997) and Bustin & Bustin (2008).

Scott (2002) mentioned that some controlling factors are interrelated and together affect CSG characteristics. Periods of deep burial are associated with increased gas storage capacity whereas present day gas contents are controlled by the gas generation history (Hildenbrand & others, 2006). The amount and types of coal gases generated during coalification are a function of tectonic history, geothermal gradient, maceral composition, and coal distribution within the thermally mature parts of a basin (Scott, 2002). In addition, the presence and geometry of folds and faults may strongly influence recharge of meteoric water, and therefore, the generation of biogenic gases (Scott, 2002). Depositional fabric strongly influences migration pathways and the distribution of gas. Gas contents may vary laterally within individual coal seams, vertically among coals within a single well, and laterally and vertically within thick coal seams (Scott, 2002).

Scott (2002) and Pashin (2007) studied the hydrogeologic factors affecting CSG reservoirs. Carbon isotope data of coal

seam gases provide evidence that significant bacterial activity takes place in zones of meteoric recharge. Water chemistry in such zones are characterised by low total dissolved solids contents, and can extend from the basin margins to the interior. Pashin (2007) suggested that meteoric flow can effectively be confined within coal seams and that thick marine shales separating coal seams can limit cross-formational flow. Similar studies by Lamarre (2003) have shown that coals can act as aquifers within stratigraphic traps. Two effects may apply for gas contents in such areas: gas contents increase in areas where hydrodynamic trapping is present and decrease where there is active recharge (Scott, 2002).

STUDY AREA

The Sydney Basin (Figure 1) is a foreland basin and forms part of the Permo-Triassic, Sydney-Gunnedah-Bowen Basin system, which extends for 1700km from southern NSW to central Queensland (Scheibner 1999). The Hunter Coalfield, in the north-eastern region of the Sydney Basin, hosts the Newcastle, Wittingham and Greta Coal Measures. Most of the sediments of the Sydney Basin were sourced during rising of the New England Fold Belt (Glen & Beckett, 1989). Sedimentation in the Hunter Coalfield is characterised by four major episodes of deltaic to fluvial deposition separated by three marine transgressive events.

Pinetown (2010) delineated a number of 'gas domains' in the Hunter Coalfield on the basis of geological setting and gas properties and distribution. The present study involves the study of two subzones within the domains. A 'gas zone' is a subdivision of a 'gas domain' characterised particularly by gas composition trends, although having gas contents consistent with the general trend for the domain (Saghafi, 2010). 'Gas Zone 1' is located within 'Domain 2' as defined by Pinetown (2010) and is located within a syncline. The lowermost coal seams of the Jerry's Plains Subgroup (the upper subgroup of the Wittingham Coal Measures) as well as

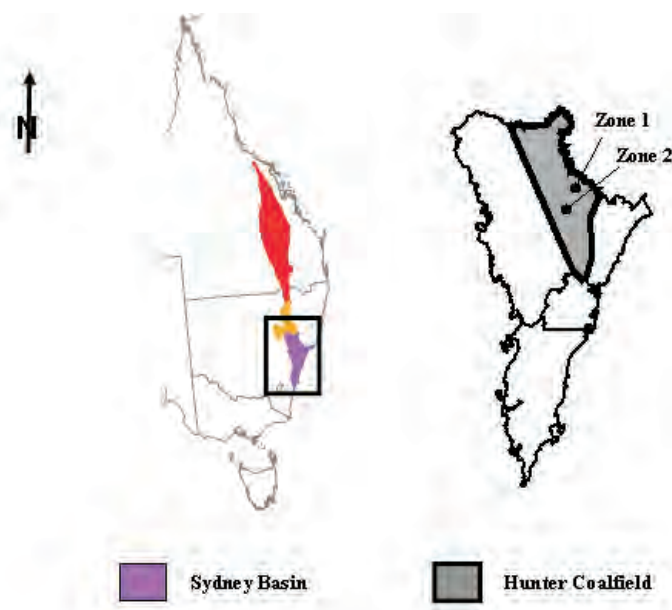


Figure 1: Location of the Sydney Basin and the Hunter Coalfield

coal seams of the Foybrook Formation of the Vane Subgroup (the lower subgroup of the Wittingham Coal Measures) are present in this zone between the depths of ~200m and ~500m. Zone 2 forms part of 'Domain 1' as defined Pinetown (2010), which is an area south of the Hunter River Cross Fault. This zone is located within a monocline and coal seams of the Jerry's Plains Subgroup are present between the depths of ~200m and ~500m.

For the purposes of comparison, observations and interpretations presented in this study are restricted to coal seams occurring between ~200m and ~500m depth, and to areas where data are available. Coal seams in both zones are present at variable depths due to geological structure. CSG distribution from the ground surface down to ~150m to ~200m depth is commonly affected by surface mining and weathering.

METHODS

Existing data were provided by mining companies operating within Zones 1 and 2. The data include information on previously drilled boreholes, such as coordinates, collar elevation, total depth, seam thickness, lithology, gas content, gas composition, adsorption isotherms, permeability, coal density, maceral analysis and reflectance, proximate and ultimate analysis, and structure data. Seventy-nine coal and twenty-five gas samples were collected from 11 vertical boreholes within Zones 1 and 2. Maceral composition and vitrinite reflectance analyses (VR) were conducted on all coal samples according to the Standards Association of Australia (1998; 2000). Gas molecular composition and stable carbon isotope ratio analyses for all gas samples provided were performed on a gas chromatography-combustion-isotope ratio mass spectrometer (GC-C-IRMS) at the CSIRO gas geochemistry laboratory in North Ryde according to established internally developed procedures. All gas samples were measured in duplicate with a standard deviation of $\leq 0.5\%$ for most samples.

RESULTS

Organic petrology and CSG distribution in Zone 1

As shown in Figure 2, *in situ* gas contents in Zone 1 have a wide range varying between $\sim 0.5\text{m}^3/\text{t}$ and $\sim 10\text{m}^3/\text{t}$ between ~200m and ~500m depth. Given the geometry of the syncline, the same seam within this zone can be present at different depths. In cases where the same seam is present at a similar depth but at another locality, variation in gas contents exist but within a narrower range than for the seam in total. For example, Seam F is present between ~230m and ~515m depth, and at a depth of ~435m gas contents vary between $\sim 4\text{m}^3/\text{t}$ and $\sim 7\text{m}^3/\text{t}$, whereas for the total seam they vary from $\sim 3\text{m}^3/\text{t}$ to $\sim 10\text{m}^3/\text{t}$. The dominant gas in the CSG in all seams is CH_4 ; more than ~80% of the CSG volumes within this zone consist of CH_4 . $\delta^{13}\text{C}$ values for CH_4 range between -74.8% and -47.6% (Vienna Pee Dee Belemnite, VPDB).

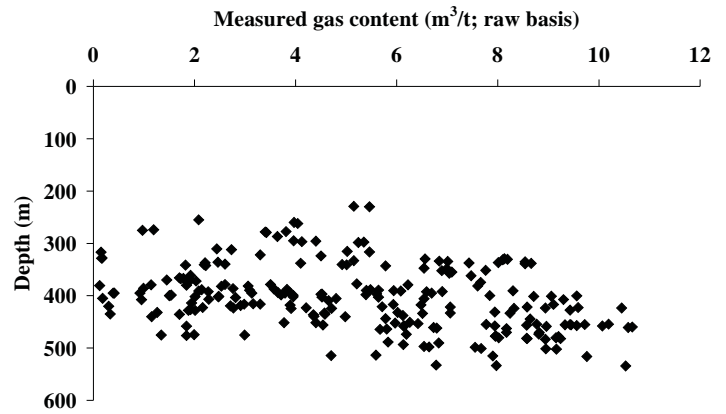


Figure 2: Gas content distribution with depth for Zone 1.

Figure 3 shows the distribution of VR with depth, with VR data for the coals from 6 individual wells specifically shown to indicate variation for the given intersections. For a single depth, $R_{v,max}$ may vary by up to 0.2% (absolute); and for samples taken vertically from the same seam (generally between 3 and 4 samples) the variation in $R_{v,max}$ is between 0.02 and 0.06%.

The average maceral composition for each seam, from Seam A to Seam G, is shown in Figure 4. Coals in Zone 1 are rich in vitrinite with average vitrinite contents for each seam greater than ~60%. Data in Figure 4 shows that vitrinite contents are higher for the deep seams than for the shallowest two. In comparison to the other seams, Seam A has the greatest proportion of inertinite, whereas Seam B has the greatest proportion of minerals (Figure 4).

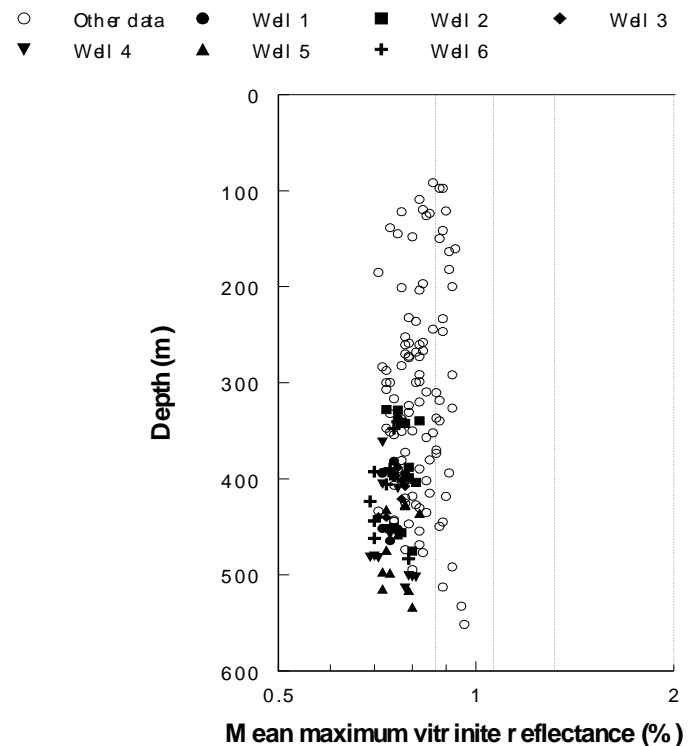


Figure 3: Variation in vitrinite reflectance (VR) with depth for Zone 1

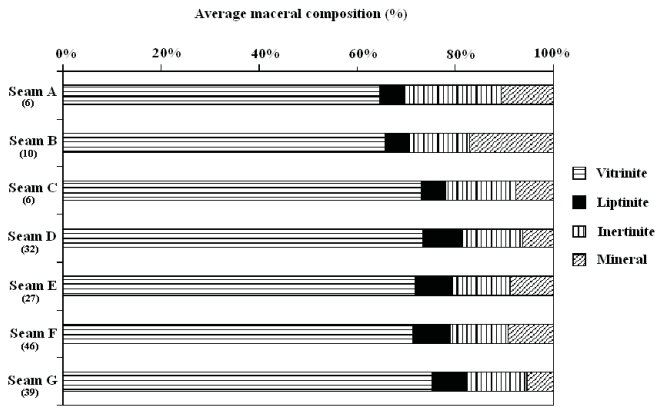


Figure 4: Variation in average maceral composition for seams in Zone 1 between the depths of ~200m and ~500m (number of samples shown in brackets)

For individual samples liptinite contents vary between ~1.5% and ~20%, and, on average, they tend to be greater for Seams D to G, than for Seams A to C (Figure 4). In samples where liptinite contents are greater than ~3%, sporinite is generally the dominant maceral of the liptinite group; however, in some coal suberinite, which is intimately associated with telovitrinite, is the main liptinite.

For purposes of comparison, liptinite contents (on a mineral-free basis) are plotted alongside corresponding measured gas contents for samples from Wells 2, 4 and 6 in Figure 5. Apart from the uppermost samples liptinite contents generally appear to be directly proportional to gas contents for Well 2. This relationship also appears to apply for samples from Wells 4 and 6, with the exception of the shallowest sample from Well 6 and the samples from below ~480m from both wells, all of which have anomalously high gas contents with respect to liptinite contents (Figure 5). Similar variations are observed for Wells 1, 3 and 5 (not shown), but do not apply for the other maceral groups.

To evaluate relationships between liptinite contents and measured gas contents, Figure 6 presents a plot for all samples studied from Zone 1 where data for both variables are available. Coals containing liptinite contents lower than ~5%, but having $>5\text{m}^3/\text{t}$ measured gas contents are all from deeper than ~480m depth. With the exception of these samples, preliminary interpretations show that a general trend of increasing gas contents with liptinite contents exists, although additional data would be required to substantiate the relationship.

Organic petrology and CSG distribution in Zone 2

Measured gas contents for Zone 2 vary between $\sim 3\text{m}^3/\text{t}$ and $\sim 11\text{m}^3/\text{t}$, between ~200m and ~500m depth, as shown in Figure 7. In this zone, gas contents seem to generally increase with increasing depth, which is also common in other regions of the coalfield, although this trend is different than for the coals studied from Zone 1.

The uppermost seams contain some high concentrations of CO_2 (e.g. $>40\%$); however at ~200m depth CH_4 is the

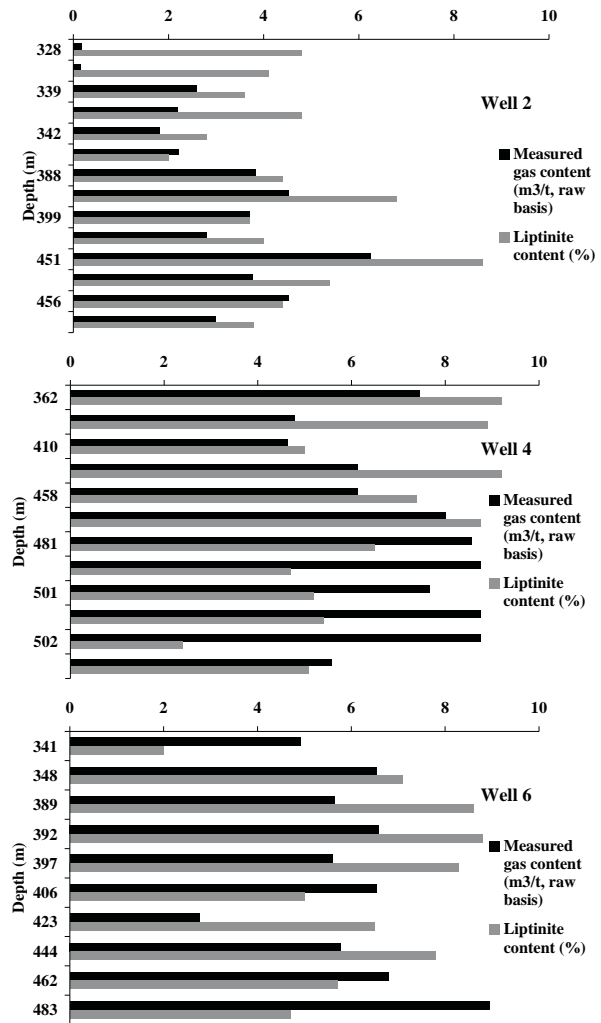


Figure 5: Distribution of liptinite content and measured gas content for Wells 2, 4 and 6 in Zone 1

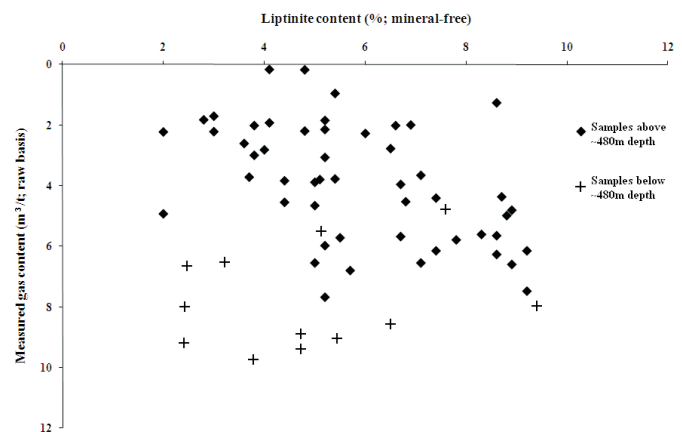


Figure 6: Plot of liptinite content versus measured gas content for 6 wells in Zone 1

dominant gas component. Below this, CH_4 concentration decreases and CO_2 increases gradually with increasing depth. Stable carbon isotope ratios for the CH_4 vary between -68.6‰ and -39.0‰ (VPDB), whereas $\delta^{13}\text{C}$ values for CO_2 range between 2.3‰ and 8.1‰ .

Although the dataset acquired for this zone is smaller than for Zone 1, VR shows an increase with depth, with $R_{v,\text{max}}$ values ranging between 0.73% and 0.84% (Figure 8). Coals in

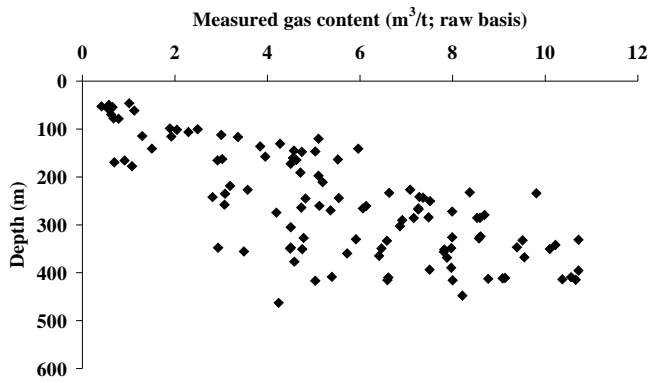


Figure 7: Gas content with depth distributions for Zone 2

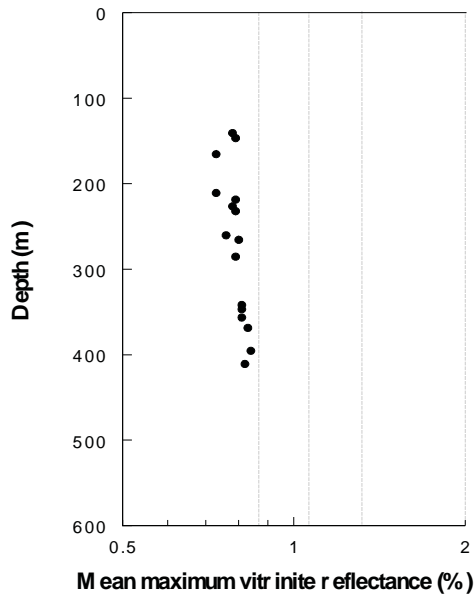


Figure 8: Variation in vitrinite reflectance (VR) with depth for Zone 2

Zone 2 are rich in vitrinite, generally containing greater than ~40%, but generally contain less vitrinite and more inertinite than coals in Zone 1. Figure 9 shows that the liptinite contents, which vary between ~1.5% and ~5.1% for seam averages, are significantly lower than those in Zone 1. Sporinite is the dominant liptinite group in these coals. Figure 10 indicates that liptinite contents are not directly related to gas content.

DISCUSSION AND INTERPRETATION

To understand gas content distribution within the gas zones evaluated in this study, an integrated approach is required, recognising all parameters that could possibly have contributed to present day distributions and the varying degrees to which each parameter has influenced gas content distribution in each zone. For example, a schematic diagram for Zone 1 is presented in Figure 11 to illustrate the possible influences of biogenic activity on gas distribution (black dots represent the average gas content for that section of the seam).

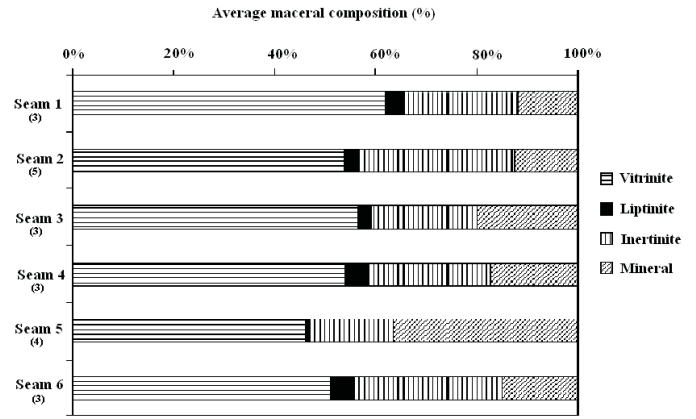


Figure 9: Variation in averaged maceral composition for seams in Zone 2 between the depths of ~200m and ~500m (number of samples shown in brackets)

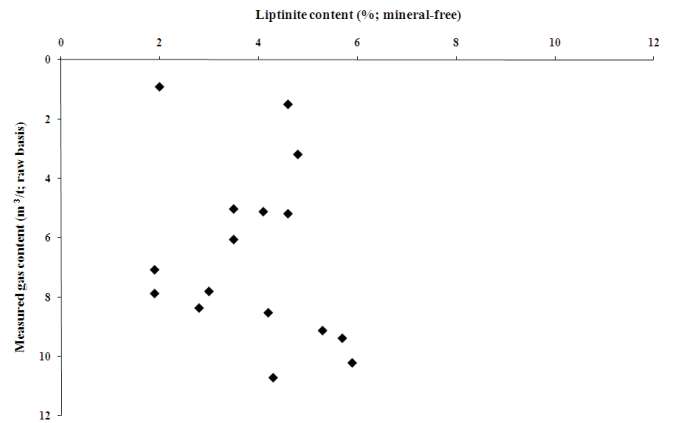


Figure 10: Plot of liptinite content versus measured gas content for Zone 2

As Scott (2002) and Pashin (2007) have shown, regions of active flow of meteoric water through coal seams are commonly associated with increased biogenic activity, and thus the production of significant volumes of biogenic gas. Stable carbon isotope ratio data for Zone 1 show that gases are predominantly biogenic in origin. However, as shown in Figure 11, the most enriched $\delta^{13}\text{C}$ value applies to the deepest part of the structure, suggesting mixing with thermogenic sources. In a recent study on the connectivity of groundwater aquifers within the Hunter Coalfield, Bryant & others (2010) concluded that there is no migration of groundwater between shallow (mainly alluvial sediments) and deep (coal seam) aquifers. Thus meteoric recharge within coal seams appears to take place via surface outcrops with migration along bedding planes. However, the degree of biogenic influence is not simply related to meteoric water access, and therefore it appears that other factors also affect the amount of biogenic activity.

The production of biogenic CH_4 takes place mainly through the reduction of CO_2 (Faiz, 2004), whereas the degradation of coal is a less preferred pathway. If CO_2 has been absent from the coals in Zone 1 during its history as well as presently, the organic matter would be the main available source of carbon required for metabolic processes. In particular, perhydrous hydrocarbons generated from liptinite-rich coals may act as energy sources (Faiz & Hendry, 2006).

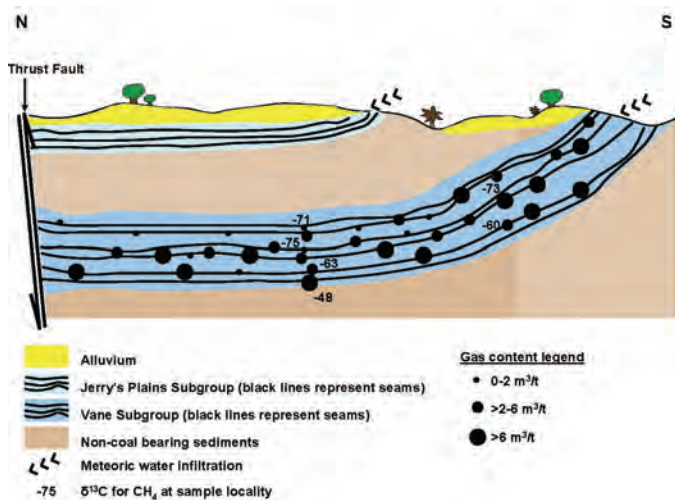


Figure 11: Schematic diagram showing relationship between geological structure and measured gas content for Zone 1

The multiple potential mechanisms of CH₄ generation would explain the complex distribution in gas content, especially for the shallow coals. For example, high gas contents in the shallow coals may be influenced mainly by biogenic activity and appropriate substrates. For the deeper coals the main influence could be related to limited uplift and depressurisation, in comparison to the shallower coals, and thus limited volumes of lost gas.

A similar schematic diagram is presented for Zone 2 in Figure 12. From the stable carbon isotope data for CH₄ in Zone 2, gases along the zones of meteoric recharge can still be regarded as biogenic in origin. If CO₂ was present in the past as well as currently, it is likely that the preferential pathway for CH₄ production was via CO₂ reduction. The isotopically 'heavy' δ¹³C values for CO₂ in Zone 2 are consistent with the gas being residual from biogenic activity. The general increase in gas contents with depth indicates that the main influence on gas contents in Zone 2 may be pressure.

CONCLUSIONS

Previous studies in CSG have shown that the controls on gas contents and other reservoir properties are numerous, and that an integrated approach needs to be considered in order to understand variations in gas distribution. The distribution of CSG in the Hunter Coalfield is compartmentalised, with the gas in each compartment mainly influenced by either local geology or coal properties or both. Gas Zone 1 is a unique setting where gas content appears to be related to coal maceral composition, groundwater migration and microbial activity, geological structure, and to a lesser extent depth. Preliminary observations from this study have shown that enhanced biogenic activity in liptinite-rich coals could be a possible reason for increased gas contents. In Zone 2, depth seems to be the overriding influence, and gas contents and compositions have distributions more consistent with other regions in the coalfield.

The two gas zones investigated in this study have provided insights into the extent to which various properties may influence gas content distribution. This study has highlighted

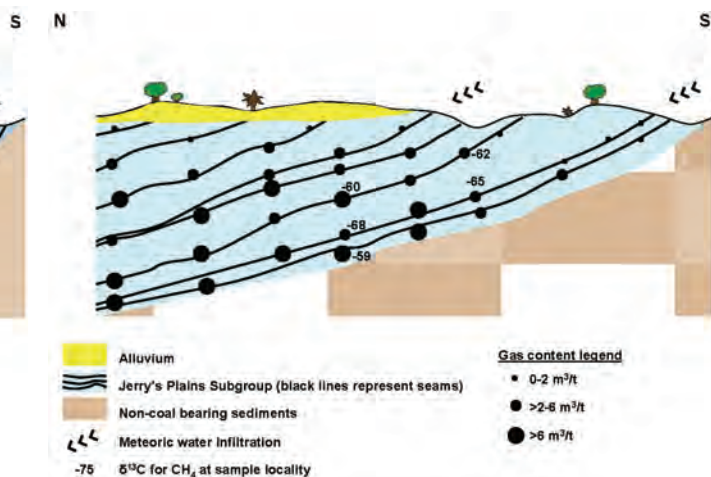


Figure 12: Schematic diagram showing relationship between geological structure and measured gas content for Zone 2

the importance of assessing a number of possible factors when evaluating CSG reservoirs, including studies related to CH₄ extraction, CO₂ sequestration and fugitive gas emissions estimations.

ACKNOWLEDGEMENTS

The authors wish to thank Vale Australia and Rio Tinto Coal Australia for their continued support during this study and previous studies relating to CSG in the Hunter Coalfield.

REFERENCES

- BRYANT, N., MCLEAN, W., ROSS, J. & SCARFF, S., 2010: Use of environmental isotopes for aquifer characterisation and connectivity assessment during CSG exploration in the Hunter Valley, NSW. In Hutton, A., Ward, C. & Bowman, H. (Editors): Thirty-seventh Symposium on the Geology of the Sydney Basin, Hunter Valley, Pokolbin, NSW May 6-7, 2010 (Abstracts).
- BUSTIN, R. & CLARKSON, C., 1998: Geological controls on coalbed methane reservoir capacity and gas content, *International Journal of Coal Geology*, **38**, 3–26.
- BUSTIN, A. & BUSTIN, R., 2008: Coal reservoir saturation: Impact of temperature and pressure, *AAPG Bulletin*, **92**, 77–86.
- CLAYTON, J., 1998: Geochemistry of coalbed gas – A review, *International Journal of Coal Geology*, **35**, 159–173.
- CHALMERS, G. & BUSTIN, R., 2007: On the effects of petrographic composition on coalbed methane sorption, *International Journal of Coal Geology*, **69**, 288–304.
- CHENG, A. & HUANG, W., 2004: Selective adsorption of hydrocarbon gases on clays and organic matter, *Organic Geochemistry*, **35**, 413–423.
- CROSDALE, P. 1989: Mixed CH₄/CO₂ sorption by coal. In *Proceedings of the 23rd Sydney Basin Symposium on Advances in the Study of the Sydney Basin, April 1989*, Newcastle, 167–173.

- CROSDALE, P., BEAMISH, B. & VALIX, M., 1998: Coalbed methane sorption related to coal composition, *International Journal of Coal Geology*, **35**, 147–158.
- ETTINGER, I., EREMIN, I., ZIMAKOV, B. & YANOVSKAYA, M., 1966: Natural factors influencing coal sorption properties. I. Petrography and sorption properties of coals', *Fuel*, **45**, 267–275.
- FAIZ, M., AZIZ, I., HUTTON, A. & JONES, B., 1992: Porosity and sorption capacity of some eastern Australian coals in relation to coal rank and composition. In *Symposium on Coalbed Methane Research and Development in Australia, April 1992*, Townsville, 9-20.
- FAIZ, M., AZIZ, I. & HUTTON, A., 1996: The influence of coal composition on gas emission rates and some implications on mining in the southern Sydney Basin. In *Symposium on Geology in Longwall Mining*, November 1996, Sydney, 41–46.
- FAIZ, M. 2004: Microbial influences on coal seam gas reservoirs - A review. In *BAC-Min Conference Proceedings, November 2004*, Bendigo, 133–142.
- FAIZ, M. & HENDRY, P., 2006: Significance of microbial activity in Australian coal bed methane reservoirs - a review, *Bulletin of Canadian Petroleum Geology*, **54**, 261–272.
- FAIZ, M., BARCLAY, S., SHERWOOD, N., STALKER, L., SAGHAFI, A. & WHITFORD, D., 2006: Natural accumulation of CO₂ in coals from the southern Sydney Basin - Implications for Geosequestration, *The APPEA Journal*, **46**, 455–473.
- FAIZ, M., SAGHAFI, A., SHERWOOD, N & WANG, I 2007, 'The influence of petrological properties and burial history on coal seam methane reservoir characterisation, Sydney Basin, Australia', *International Journal of Coal Geology*, vol. 70, pp. 193-208.
- GLEN, R. & BECKETT, J., 1989: Thin-skinned tectonics in the Hunter Coalfield of New South Wales, *Australian Journal of Earth Sciences*, **36**, 589–593.
- GOLDING, S., UYSAL, I., FENG, Y., BAUBLYS, K. & ESTERLE, J., 2009: Natural analogues for storage of CO₂ in coal systems, Gunnedah and Bowen Basins, Australia, *Geochimica et Cosmochimica Acta*, **73**, A448.
- GURBA, L. & WEBER, C., 2001: The relevance of coal petrology to coalbed methane evaluation, using the Gloucester Basin, Australia as a model. In *International Coalbed Methane Symposium*, Tuscaloosa, 371–382.
- GURBA, L., GURBA, A., WARD, C., WOOD, J., FILIPOWSKI, A. & TITHERIDGE, D., 2001: The impact of coal properties on gas drainage efficiency. In *Geological hazards – The Impact to Mining, November, 2001*, Newcastle, 215–220.
- GURGEY, K., PHILP, R., CLAYTON, C., EMIROGLU, H. & SIYAKO, M., 2005: Geochemical and isotopic approach to maturity/source/mixing estimations for natural gas and associated condensates in the Thrace Basin, NW Turkey, *Applied Geochemistry*, **20**, 2017–2037.
- HACKLEY, P., WARWICK, P. & BRELAND, F., 2007: Organic petrology and coalbed gas content, Wilcox Group (Paleocene-Eocene), northern Louisiana, *International Journal of Coal Geology*, **71**, 54–71.
- HARGRAVES, A. 1986: Seam gases in major Australian coalfields. In *Proceedings of the 13th CMMI Congress Volume 3 - Mining, May 1986*, Singapore, 103–112.
- HILDENBRAND, A., KROOSS, B., BUSCH, A. & GASCHNITZ, R., 2006: Evolution of methane sorption capacity of coal seams as a function of burial history - a case study from the Campine Basin, NE Belgium, *International Journal of Coal Geology*, **66**, 179–203.
- KARACAN, C. & MITCHELL, G., 2003: Behaviour and effect of different coal microlithotypes during gas transport for carbon dioxide sequestration into coal seams, *International Journal of Coal Geology*, **53**, 201–217.
- KOTARBA, M. & LEWAN, M., 2004: Characterizing thermogenic coalbed gas from Polish coals of different ranks by hydrous pyrolysis, *Organic Geochemistry*, **35**, 615–646.
- LAMBERSON, M & BUSTIN, R 1993, 'Coalbed methane characteristics of Gates Formation coals, Northeastern British Columbia: Effect of maceral composition', *AAPG Bulletin*, vol. 77, pp. 2062-2076.
- LAMARRE, R., 2003: Hydrodynamic and stratigraphic controls for a large coalbed methane accumulation in Ferron coals of east-central Utah, *International Journal of Coal Geology*, **56**, 97–110.
- LAXIMINARAYANA, C. & CROSDALE, P., 1999: Role of coal type and rank on methane sorption characteristics of Bowen Basin, Australia coals, *International Journal of Coal Geology*, **40**, 309–325.
- LEVY, J., DAY, S. & KILLINGLEY, J., 1997: Methane capacities of Bowen Basin coals related to coal properties, *Fuel*, **76**, 813–819.
- PASHIN, J., 2007: Hydrodynamics of coalbed methane reservoirs in the Black Warrior Basin: Key to understanding reservoir performance and environmental issues, *Applied Geochemistry*, **22**, 2257–2272.
- PINETOWN, K., 2010: Delineation of coal seam gas domains in the Hunter Coalfield, Sydney Basin. In Hutton, A., Ward, C. & Bowman, H, (Editors):Thirty-seventh Symposium on the Geology of the Sydney Basin, Hunter Valley, Pokolbin, NSW May 6-7, 2010 (Abstracts).
- RICE, D., 1993: Composition and Origins of Coalbed Gas. In Law, B. & Rice, D. (Editors): *Hydrocarbons from coal – AAPG studies in Geology*.
- SAGHAFI, A., 2010: A tier 3 method for estimating fugitive emissions from open cut coal mining: Application to Hunter Coalfield. In Hutton, A., Ward, C. & Bowman, H, (Editors):Thirty-seventh Symposium on the Geology of the Sydney Basin, Hunter Valley, Pokolbin, NSW May 6-7, 2010 (Abstracts).
- SCHEIBNER, E., 1999: *The Geological Evolution of New South Wales – A Brief Review*, Geological Survey of New South Wales, Sydney.
- SCOTT, A., 2002: Hydrogeologic factors affecting gas content distribution in coal beds, *International Journal of Coal Geology*, **50**, 363–387.
- SMITH, J. & PALLASSER, R., 1996: Microbial Origin of Australian Coalbed Methane, *AAPG Bulletin*, **80**, 891–897.

- SMITH, J., 1999: The development of an understanding of the origins of the Sydney and Bowen Basin gases. *In* Mastalerz, M., Glikson, M. & Golding, S., (Editors): *Coalbed Methane: Scientific, Environmental and Economic Evaluation*, Kluwer, Dordrecht.
- STANDARDS ASSOCIATION OF AUSTRALIA, 1998: Australian Standard: Coal petrography – Part 2: Maceral analysis, (AS2856.2-1998), Standards Australia, North Sydney.
- STANDARDS ASSOCIATION OF AUSTRALIA, 2000: Australian Standard: Coal petrography – Part 3: Method for microscopical determination of the reflectance of coal macerals, (AS2856.3-2000), Standards Australia, North Sydney.
- WALKER, R., GLIKSON, M. & MASTERALERZ, M., 2001: Relations between coal petrology and gas content in the Upper Newlands Seam, central Queensland, Australia, *International Journal of Coal Geology*, **46**, 83–92.
- WHITICAR, M., 1996: Stable isotope geochemistry of coals, humic kerogens and related natural gases, *International Journal of Coal Geology*, **32**, 191–215.

Danique Bax

Inheriting a deficient and defective database – the repair challenge

In February 2007, the Jeebropilly mine closed and geological data was archived; in early 2008, the decision was made to recommence operations. This triggered the process of ensuring the geological models were up to date.

Due to the time consuming task of collating and validating historical information, the decision was made to “go with what you’ve got” and geological modelling commenced. When these models were produced, they overestimated the resources compared to previous models. The reasons for this are numerous, but mostly reflected a lack of accurate data, related to the limited amount of geophysical data available at the time to support or deny the existence of the coal. After several modelling attempts, all with unfavourable results, a concerted effort to recover all of the outstanding data was made. Once the geophysics had been located and loaded, several corrections had to be made to the lithology logs as there were problems with seam picks and most of the correlations did not match from hole to hole, let alone across the deposit.

Over a two-year period, the Jeebropilly database has evolved into a warehouse where all known electronic data is stored. The Company has also been able to report JORC resources for Jeebropilly for the first time in its history, mostly due to the recovery and validation of historical data, and some further exploration drilling. The life of mine has also been extended significantly, considering that operations had shut down in 2007. Although there has been a vast improvement in the data volume and accuracy, there is still missing data, which is possibly no longer retrievable, due to its age and/or the medium it was stored on.

INTRODUCTION

The Jeebropilly mine is situated approximately 15km by road west of Ipswich, Queensland, Australia (Figure 1). The mine uses thin seam extraction techniques to recover coal from the Lower Walloon Coal Measures of the Clarence-Moreton Basin. The mine has had a long history, originally commencing open cut operations in 1983 and closing down due to economic constraints in February 2007. At this time, all the data was archived; however, due to a shift in the economic climate, Jeebropilly recommenced operations in August 2008. The reopening of the mine instigated a need to ensure that the geological models were up to date and accurately reflecting the predicted resources. It was also proposed that the exploration drilling would occur in order to bring the Jeebropilly deposit up to JORC status.

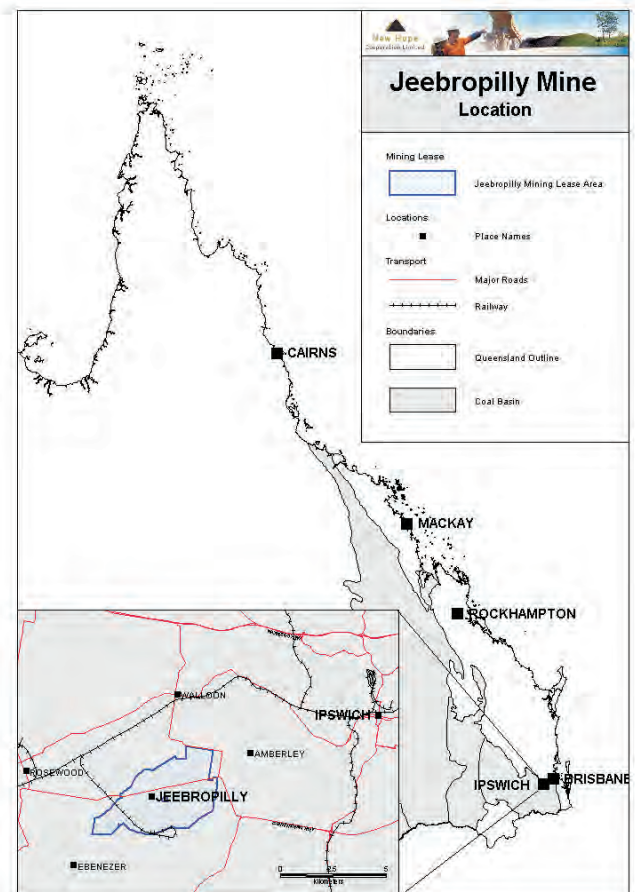


Figure 1: Location of Jeebropilly Coal Mine

THE HISTORY OF DATA AT JEEBROPILLY

Prior to September 2003, New Hope Coal Australia was not a publicly listed company, and was not required to collect and report information in accordance with the Australian Securities Exchange (ASX) rules. Regardless of this, a number of holes were geophysically logged, and core holes were drilled with laboratory analysis carried out on most coal intersections. The ASX references the JORC Code, which requires a competent person to sign off on resource/reserve statements — the competent person within New Hope Coal has stipulated that the holes which are deemed to be valid include (in order of priority): core holes with geophysics; chip holes with geophysics; or core holes without geophysics. All other data is considered unreliable. Therefore, in order to be included in a geological model, these conditions must be met. Historically, this was not the case, and all data was modelled, regardless of its validity.

THE EVOLUTION OF THE JEEBROPILLY DATABASE

The modelling package being used is Mincom's MineScope, and the standard practice is to ensure all drilling data is loaded into GDB and modelled using Stratmodel. Until 2008, no GDB database existed for Jeebropilly, and data was recovered from a variety of sources, including, but not limited to:

- Archive box reclamation, which involved manual data entry of some borehole data
- 3½" floppy disks, many of which were corrupt and data was unattainable
- New Hope Coal's network drives
- Unix-based Silicon Graphics computers, which are now obsolete

Geological Modelling – Early Attempts

Due to increasing pressure relating to re-opening the mine in August 2008 a "go with what you've got" approach was adopted when creating the geological model. This effectively resulted in variations in product tonnage estimations, and around five attempts were made to model the relatively small area which would be the first operational pit when the mine reopened. Each of these attempts overestimated what had been predicted previously. One attempt even replicated the old model and achieved a different result. From the first model review, the reliability of the geological models was questionable.

Investigations into the cause of these modelling misrepresentations began and the findings were as follows:

- The models being used by the mining engineers had been constructed using invalid data
- There was an underlying assumption that all data that had been entered into the Unix systems had been corrected to geophysics
- The expedited time frame meant that not all data could be reformatted and loaded into GDB before the model was built
- Specific boreholes from the 1990s' drilling programs were missing from the model, and these were drilled in areas where there were data gaps in the model
- Very little geophysical information was available to confirm or deny the presence or thickness of the coal seams
- Where geophysics was available, it was mostly microdensity, which has been found to overestimate the coal seam thickness for this thin seam deposit and others like it
- Time constraints halted the process of entering all of the known electronic data into GDB, and therefore there was a lack of survey, lithology, geophysics and coal quality available to use in the validation and construction of the geological model
- Coal seams were correlated based on seam and interburden thickness trends, as no other information was available (Figure 2)

- Several coal horizons had not been named as seams, and it appeared that those unpicked horizons fit better with the coal seam trends
- Many seam names had been incorrectly assigned (Figure 2), or were placed on waste rock lithotypes, rather than the coal horizon itself, leaving the coal horizons nameless (Figure 3)

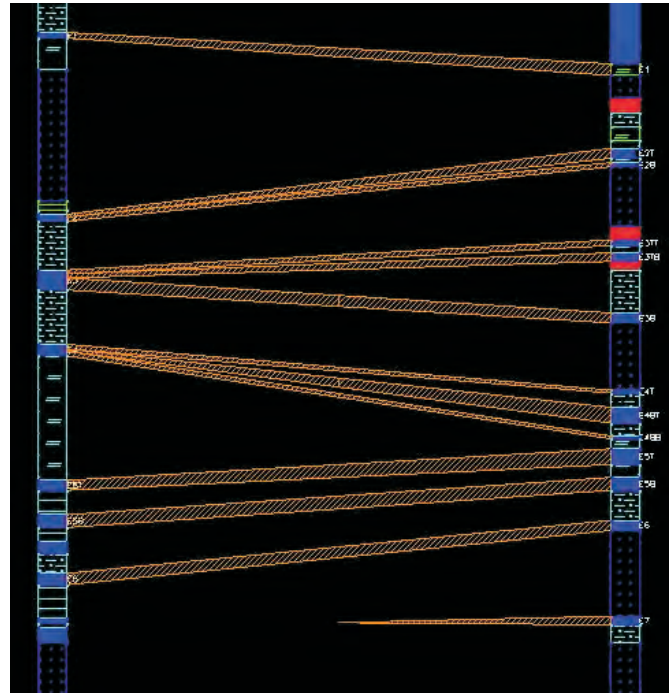


Figure 2: Coal seams miscorrelated

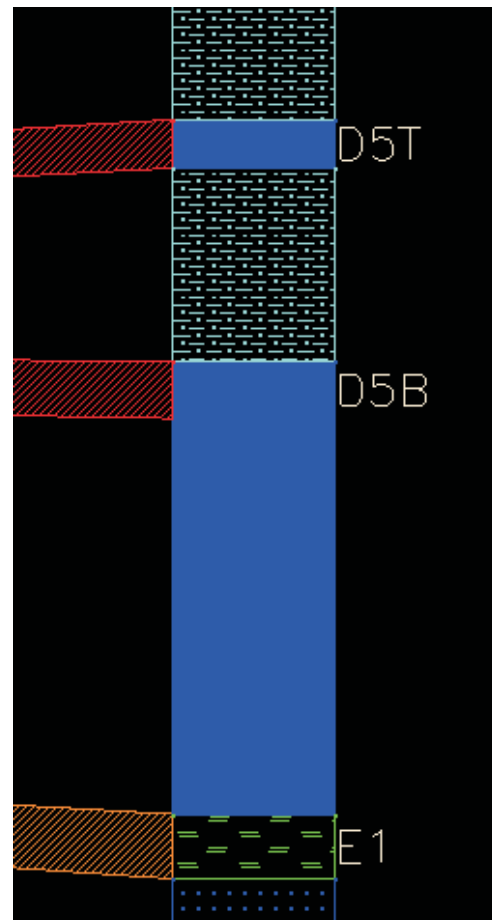


Figure 3: Coal not corrected to geophysics, and seam names assigned to non-coal lithotypes

The recommendations from this investigation included:

- Checking the correlations on all of the boreholes to be used in the model
- Using annotated highwall photography to ensure seams have been named correctly
- The seam names would be assigned by two of the most experienced people at the Jeebropilly's mine — the senior mining engineer and the open-cut examiner (OCE) at the time
- Ensured that the boreholes along the highwall crest (at the time the photograph was taken) matched the annotations, and tied these into the rest of the boreholes in the area
- Locating more historical data which could help to validate the drilling information and correlations

Geological Modelling – Later Attempts

As per the recommendations from the early modelling attempts, more data was required to ensure the accuracy of the models, and in particular, locating borehole geophysics files became a priority. 3½" floppy disks and the New Hope network drives were searched for these files. Several raw geophysical run files were recovered, and converted to LAS using ALog. The only problem with this ALog conversion was that it generated V1.2 format LAS, and to load it into GDB, it had to be converted to V2.0 format. This was done using software developed specifically for New Hope Coal.

The following steps were taken to update the database on this attempt:

1. Loaded extra data from MineScape design files into GDB
2. Loaded over 550 more holes of historical geophysics into GDB
3. Normalised geophysics so that all geophysics would display at the same scale

Once the geophysics had been loaded into GDB, it was found that the majority of the holes had errors in their geophysical corrections, and seam names differed between the drill holes.

To correct the seam thicknesses and naming, the following steps were taken on each individual borehole separately:

1. The coal seams were corrected so that the lithology matched the roof and floor elevations of the geophysical signature
2. Ensured that lithotypes were corrected to geophysics, using the gamma, caliper and density curves (predominantly microdensity) in combination with each other
3. The corrections were conservative, ensuring that when a seam was picked that the pick reflected the gamma signature as well as the density signature
4. All valid data had a model flag applied to the header data, so that any data that showed data discrepancies would not be modelled.

A model flag is a code placed in the header information for each borehole. When developing the template of holes to model, the search query looks for this code, and these flagged holes are the only holes used in the model.

Once the boreholes were checked, the following process occurred:

1. A cross-section of the holes which contained a combination of core holes and chip holes (with and without geophysics) were used to correlate the coal seams – those which were incorrectly named were adjusted so that the section showed correct correlations (once again incorporating the annotated highwall photograph in this process) (Figure 4)
2. If the geophysics displayed stone bands in a seam, then the seam was split into its plies (e.g. D2 into D2T and D2B) and, in most cases, only the coal was picked as the seam

The geological model was then produced, this time constructed only with the holes where a model flag existed. As a result, the model was accepted by the mining engineers, and reconciliations carried out on the operating pit produced a 3% difference when comparing actual product tonnes to modelled tonnes.

Although the result of this model was accepted and deemed to be satisfactory, over half of the lithology logs for the Jeebropilly boreholes were still unaccounted for. On top of that, no coal quality model existed, creating room for further improvement.

Geological Modelling — Further Improvements

Over the next eighteen months, several small-scale exploration programs were conducted in areas which were identified as possibly economic to mine. Although each of the potential areas were subset into separate geological models, they were produced based on the same set of rules as stated previously, and all of these were accepted by the mining engineers.

In recent times, it was decided that producing separate models was an inefficient process, and all of these should be combined into one model for the entire deposit. In this case, checking the seam correlations across the entire mine became essential. Throughout this process, it became apparent that more data was needed to ensure that the entire deposit was represented in this 'super' model, and the old Unix systems were searched again for borehole files. Extra survey data, lithology logs and coal quality files (proximate analysis and washability) were recovered, reformatted and loaded into GDB. below shows the evolution of the data from December 2008 to its current state in July 2010.

In eighteen months, the number of borehole headers in the database increased from 1496 to 1833 – a change of 18% (Figure 5). Although this is significant, it is not a large change compared to the 67% increase in the number of holes with lithology data (584 holes to 1788 holes); the number of holes

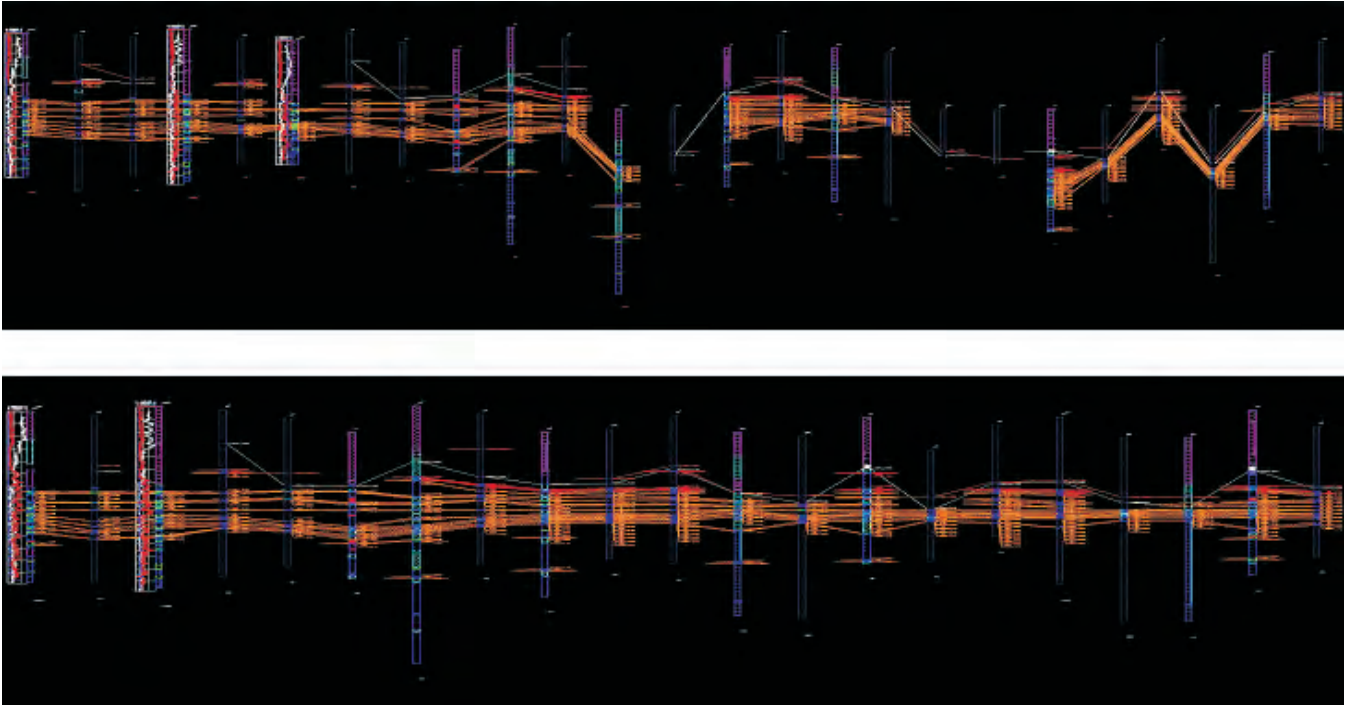


Figure 4: Cross section showing the state of the correlations in the Jeebropilly database. Top: before correlations; Bottom: after correlation.

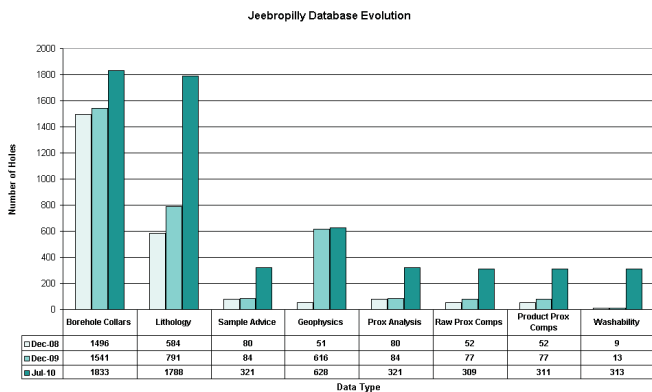


Figure 5: Evolution of the Jeebropilly Database

with sample advice increased by 75% (80 holes to 321 holes); and most importantly, holes with geophysical data increased by 91% (51 holes to 628 holes).

After the extra lithology data was loaded, the holes with geophysics were checked to ensure the correct thicknesses had been picked for coal seams, as well as having the correct seam name. Coal quality sample numbers had to be added into the lithology table for the majority of the boreholes, and once this was complete, the seam depths were compared in the sample advice table and the lithology table, to ensure they matched. As a result, a coal quality model was produced, with the number of holes composited for raw and product proximate analysis increasing by 83% and washability composites increasing by 97% () between December 2008 and July 2010. Only 3% of the holes with coal quality were not composited; this was due to poor sampling.

This model is currently in the process of being completed and reviewed, and the results are yet to be determined, however, given that it's a combination of four previously accepted models, the outlook is promising for the Jeebropilly model.

CONCLUSION

At a maximum New Hope product cut-off ratio of 14:1, the Jeebropilly mine closed in 2007, marking the “end of an era” for coal mining in Ipswich. At that time, the nearby New Hope owned Oakleigh mine was due to close within the next 2 years (by the end of 2009). Although several resource areas still existed, the ratios were too high to economically mine the remaining coal. However, since then, an increase in coal prices meant the mine could start operating again, mining coal to a cut-off ratio of 17:1. Three main areas of the deposit were suggested for further mining potential, totalling approximately 5 million product tonnes.

After creating the GDB database, and performing resource modelling on valid data, along with confirmation drilling of resource areas, the life of mine has extended at Jeebropilly, with a potential mineable resource of 7.4 million product tonnes in four areas of the deposit. There are also several outlying areas which have not been mined in the deposit, and these have not been taken into consideration at this point in time. However, with the new geological model now covering the entire deposit, these areas can be examined with confidence, although some of these outlying areas are underexplored and data poor, and confirmation drilling is recommended to constrain the model if these areas are to be developed in the future. Furthermore, 2010 was the first time in the company's history that it reported JORC resources. This is a valuable reporting statistic for the Company, and enforces that geophysically logged and corrected data needs to be used and uploaded to a database, if the data exists. It makes a significant difference to accuracy of geological model, and every attempt should be made to ensure that only geophysically corrected holes and core holes are being used. As seen in the Jeebropilly case, there is significant value in spending time to ensure all relevant data is in the geological database, and ensuring that all of the data is backed up on an appropriate storage medium.

C.M. Williams, M. Noppe and J. Carpenter

Coal quality estimation error — Ordinary kriging challenges inverse distance

The use of inverse distance weighted (IDW) interpolation methods to estimate coal quality attributes from coal deposit drillhole data is widespread in the industry. This paper examines the performance of IDW against the most commonly used geostatistical estimation method, ordinary kriging (OK), in order to investigate the relative performance of these two interpolators. Two raw coal quality test data sets are used and the performance of each interpolator is examined relative to the original sample data set using the ‘leave-one-out’ or ‘jack-knife’ method. A variety of sample configurations are tested by randomly excluding samples from each of the original data sets prior to each run.

IDW estimates have proved robust for coal deposits that are drilled on regular grids and where coal quality is relatively homogenous. However, where a regular grid of drilling has not been possible, and/or the coal quality has high local variability, estimation errors can be very large. This paper identifies four main factors which have an effect on the degree of estimation error introduced during the estimation of coal quality attributes. These are drilling density/regularity, domain stationarity, the global statistics of the quality attribute and the local variability/continuity of the quality attribute as defined by the semivariogram.

This study shows that estimation error can vary widely between quality attributes in the same data set, depending on the degree of variability exhibited by the attribute. This has important implications for the use of standard distances between points of observation during the classification of Coal Resources.

INTRODUCTION

The aim of this paper is to look at the influence of a number of factors on coal quality estimation error. These factors are:

- Drilling density/regularity
- Domain stationarity
- Global statistical properties of the coal quality attribute
- Geostatistical properties of the coal quality attribute

The second objective of this paper is to investigate the relative performance of the IDW versus the OK interpolator. Both interpolators have therefore been used in a range of different estimation scenarios in which the above four factors were systematically changed, in order to define the scenarios where one interpolator performs better than the other.

The contribution of the above four factors to the accuracy of the interpolation is considered by comparing the estimated results of a number of raw coal quality attributes to the original values used in the interpolation. This is achieved by using the ‘leave-one-out’ or ‘jack-knife’ method whereby each sample point within a data set is estimated, leaving out the sample point in question from the estimate for that point. This is done for each point in the data set, enabling the original sample point to be used as the ‘truth’ data set to evaluate the relative performance of the estimate.

The overall accuracy of each estimate is determined using the Mean Absolute Percentage Error (MAPE) for each estimate, the formula for which is shown below.

$$M = \frac{1}{n} \sum_{i=1}^n \left| \frac{A_i - F_i}{A_i} \right|$$

http://en.wikipedia.org/wiki/Mean_absolute_percentage_error

where: M= MAPE, A_i = actual value for that point, F_i = interpolated value for that point

It should be noted that the MAPE is not the actual estimation error for the point in question as in a normal estimate the point being left out would be used in the estimate as well. However the MAPE does give a good measure of the relative level of estimation accuracy between a number of estimation runs and as such is commonly used to fine tune estimation parameters.

In order to obtain information on the relative effect of the above four factors on coal quality estimation error, two raw coal quality data sets have been selected which contain coal quality attributes with a range of statistical and geostatistical properties. Coal quality attributes have been selected for estimation so as to test the effect of both global and local variability on the accuracy of the estimate as well as sample spacing and domain stationarity.

Domain stationarity with regard to spatial variables such as coal quality attributes can be defined as the consistency of both the mean and variance over sub-regions, typically described as panels, of a larger region or population. Deviation from stationarity is achieved within the test data sets in some scenarios, in the case of the raw ash attribute, by the inclusion sub-regions where the seam contains a high proportion of mudstone parting.

For Case Study 1 (Case1), raw ash (%) for two seams together with raw volatiles (%) and raw sulphur (%) for one of these seams has been used. For Case Study 2 (Case 2), the raw ash (%) alone for a single seam has been examined.

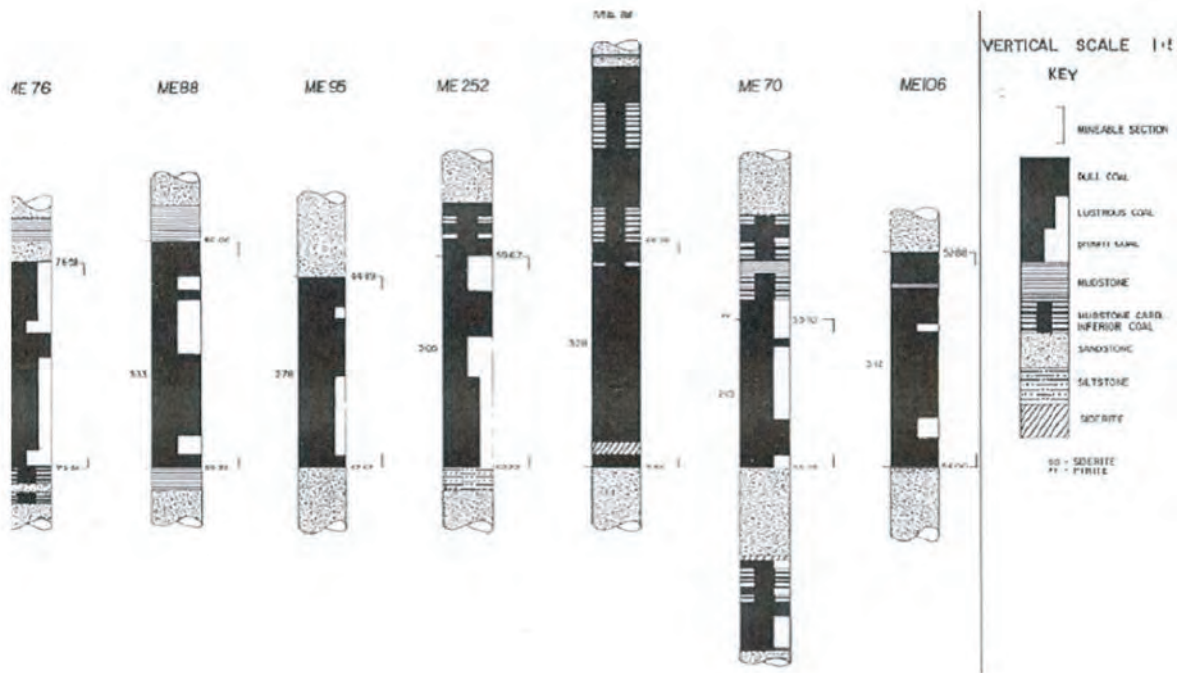


Figure 1: Lithological logs for a few typical M2 seam sections at Mookane (CIC Energy, 2006)

GENERAL GEOLOGY

The Case 1 data set comes from the Mmamabula coal field in Southern Africa (Botswana) published in open file on the TSX stock exchange SEDAR website (CIC Energy, 2006). The raw coal quality data for two coal seams within the Mookane area of this coal field was obtained from the appendices to this report. Two seams of interest are present in this area, namely the upper D1 seam and the lower M2 seam.

The D1 seam is the basal coal seam to a succession of up to 60 m of interbedded coal seams and mudstones. The D1 seam ranges in thickness from 1m to 12m in the Mookane area. The M2 seam is found about 20m below the D1 seam and has a competent sandstone roof and floor. The M2 seam ranges in thickness from 0.5m to 6.5m in the Mookane area. Thicker intersections of both the D1 and M2 seam are related to the presence of internal mudstone partings within the seam (Figure 1). The presence of these mudstone partings causes the overall raw ash (%) of both seams to increase.

Sulphur occurs in both seams mainly in pyritic form. The inherent nuggetty mode of occurrence of this form of sulphur

results in a high local variability in the concentration of sulphur in both seams.

The Case 2 data set comes from a single seam located elsewhere in Southern Africa. The exact location is confidential; however the geological control on the raw ash (%) is similar to that seen for the Case 1 data set.

GLOBAL STATISTICS

The coal quality attributes chosen for estimation exhibit a range of global statistical properties as well as local variability/continuity. Histograms for the coal quality attributes used for the two case studies are shown below in Figure 3. These histograms show the data distribution for the first scenario in each case study, namely that of the closest spaced (largest) data sets. A summary of the global statistics for each case study and each scenario is given in Table 1 and Table 2. In general the global means and variances for the various coal quality attributes remain the same for successive scenarios (i.e. for successive smaller wider spaced and/or irregularly spaced data sets). Exceptions to this rule occur for two scenarios, namely the Case 1, 1000 m random data set

Table 1: Global statistics for Case 1

Data set	Number of Samples M2 Seam	Number of Samples D1 Seam	M2VOL Mean(%)	M2VOL VAR	M2ASH Mean(%)	M2ASH VAR	M2SUL Mean(%)	M2SUL VAR	D1ASH Mean(%)	D1ASH VAR
500 m	186	165	23.75	1.88	21.13	18.02	1.93	1.19	23.76	19.46
1000 m	50	43	23.44	2.00	21.68	19.31	1.88	0.94	23.91	21.58
1000 m random	56	43	23.77	2.19	21.78	44.36	2.09	1.21	23.96	10.89
2500 m	11	10	23.76	1.13	21.40	8.7	1.62	0.43	25.71	17.4

Table 2: Global statistics for Case 2

Data set	Number of Samples	ASH Mean(%)	ASH VAR
250m	256	26.25	87.96
250m CUT<38% ash	227	23.60	26.58
500m CUT<38% ash	79	25.03	34.17
1000m CUT<38% ash	24	23.67	44.51

M2ASH and the Case 2, 250 m unfiltered data set for raw ash. In these two scenarios, domain stationarity has not been maintained for raw ash due to the presence of samples in the data set which have sampled areas of the seams in question which contain unusually high proportions of internal mudstone parting. This is manifest by very high global population variances in both these instances although the global means are not significantly affected.

In general, the skewness of the distributions increases in Case 1 from M2 volatiles through to D1 ash. In Case 2, the removal of the high ash domain (samples above 38% ash, Figure 2) reduces the skewness of the distribution from 1.52 to 0.24 and the variance is greatly reduced.

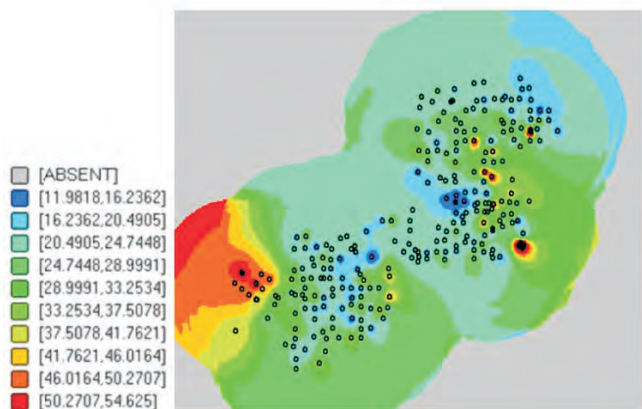


Figure 2: Location of high ash samples (>38% ash) for Case 2 250m spaced data

M2 sulphur shows the lowest variance of all attributes but this is not directly comparable with the variance of the other attributes due to its low mean concentration (1.19). M2 sulphur does exhibit one of the most skewed distributions, which is indicative of the high local variability of this attribute. A better measure of variability for M2 sulphur, which is comparable with the other attributes, would be the coefficient of variation (CV) which is the variance divided by the mean value (Figure 3). M2 volatiles exhibits the next lowest variance of 1.88, which in this case is very low relative to its mean value of 23.7%.

SPATIAL DATA AND VARIOGRAPHY

The original data spacing for the two parent data sets has been regularised to 500m, 1000m, 1000m-random and 2500m for Case 1 and 250m, 500m and 1000m for Case 2, by leaving out sample points from the initial parent data sets that do not fall on a regular N-S, E-W grid. In the single random sampling scenario for Case 1 (1000m-random), samples were randomly selected from the parent data set so that the number of samples left over, divided by the total area, is equal to an average 1000 m grid spacing. As a result, a single high ash sample was selected for the M2ASH 1000 m random data set. This high ash sample, which imparts non-stationarity to the M2ASH 1000 m random data set, is not present in the other M2ASH data sets.

The original 250m Case 2 raw ash data set contained some areas of unusually high ash (raw ash >38%) (Figure 2). Samples from these areas, which impart non-stationarity to the original 250m Case 2 raw ash data set, were removed for successive Case 2 scenarios. The sample configurations for each of the two test cases are shown in Figure 4.

Variography was conducted for each coal quality attribute selected for estimation using data sets for the first (closest spaced) scenario in each case study. Semivariogram models obtained for each attribute from these data sets (Figure 5) were used to perform OK estimates for the scenario concerned and for all successive scenarios. The exception to this is Case 2, where the semivariogram was remodelled after the high ash material was domained out. This remodelled raw ash semivariogram was used for all successive Case 2 scenarios.

In general the variography for Case 1 attributes is considered to be poor and suboptimal due to the absence of sample pairs below 500m. This results in the nugget being poorly constrained for these semivariograms. In the case of M2 sulphur (M2SUL) the variography is particularly poor and it is debateable as to whether this attribute exhibits any continuity at all. The range of continuity for this attribute is the lowest at 550m, followed by D1ASH (1700 m) and M2ASH and M2VOL which both have the longest range of the Case 1 attributes at 2000m.

The poor variography shown by the Case 1 coal quality attributes is the main reason for incorporating the second case study. The semivariograms obtained for Case 2 are much better constrained, with sample pairs obtained down to just below 250m. Hence Case 2 allows the influence of better variography on the OK estimation error to be investigated. Even for Case 2 however, the selection of an appropriate nugget is still open to some interpretation with a range of nuggets between 0.1 and 0.3 all possible (Figure 5). In this situation an initial suboptimal semivariogram using a nugget of 0.13 was modelled. Optimisation of the semivariogram nugget, by evaluating the mean squared error (MSE) defined below, was possible after the completion of the first scenario estimate for Case 2, which used the suboptimal semivariogram.

$$MSE = \text{mean}(X_{\text{est}} - X_{\text{true}})^2$$

Using the 'leave-one-out' paired true and estimated point data set following the first Case 2 OK estimate, it was found that the mean kriging variance produced by the estimate was too low. The kriging variance is a function of both the semivariogram and the sample spacing around the point being estimated, but is independent of the actual sample values. The kriging variance is however highly sensitive to the nugget used in the variogram model. As a general approximation, the following relationship can be used to determine if the semivariogram used is optimal;

$$MSE \sim \text{kriging variance} \pm 10\%$$

The mean kriging variance of all the blocks in the estimated model was found to be about half the MSE of the paired leave-one-out data set. The semivariogram was then adjusted by increasing the nugget to 0.3 (Case 2 optimal semivariogram) and the 250m spaced data estimate was re-run (Case 2, scenario 2).

Analysis of the paired estimated and true data following this second scenario estimate for Case 2 showed the MSE and average kriging variance to be within 10% of each other, indicating that the semivariogram used was optimal. In the third Case 2 scenario, the high ash samples were domained out and the semivariogram was again remodelled using the domained (low ash) data set. The nugget was now reduced to 0.2 due to the reduced local variability in the domained data set. The range of continuity was also reduced and the first structure was steepened as well. Analysis of the MSE and kriging variance showed that the scenario 3 semivariogram remained optimal. This third Case 2 (optimal) semivariogram was then used for all successive Case 2 scenarios incorporating domained (low ash) but wider spaced raw ash data sets.

SUMMARY OF INTERPOLATION METHODS USED

One of the aims of this paper was to examine the relative performance of IDW in coal quality estimation as opposed to the use of OK. The IDW estimator is a form of weighted average whereby the weights applied to samples used in the estimate have an inverse relationship with distance between the sample in question and the point being estimated. Commonly this inverse relationship is an exponential one with inverse distance squared ($1/d^2$) or IDW2 and inverse distance cubed ($1/d^3$) or IDW3 relationships commonly used. The use of the inverse exponential relationship when assigning weights is based on the logic that the closer the point being estimated is to the known sample value, the more similar the value of the estimated point is likely to be.

The use of IDW has long been preferred for the estimation of coal quality for a number of reasons, these being;

- It is quick and easy to set up the estimation parameters (search radius and maximum and minimum number of samples to use in each estimate of an unknown) with no need for lengthy kriging neighbourhood analysis as is the case for OK.
- Once the estimation parameters have been set up, they can normally be used again and again for numerous similar deposits. This lends the method to use in software packages designed for minimal user intervention in the interpolation process as commonly seen in many stratigraphical modelling software packages.
- A related issue which lends itself to use in stratigraphical modelling software packages is that there is no requirement for semivariogram modelling as in the case of OK. Semivariogram modelling can also become very onerous where large numbers of coal quality attributes need to be estimated.
- There is no general limitation on the block size or grid spacing to use when using IDW whereas the use of small block sizes is generally not supported in the case of OK. This again lends itself to stratigraphical modelling where the estimation of quality grids is common practice. Estimation of coal qualities into a block model with small block sizes is equivalent to building a gridded model for the coal quality attribute concerned.

OK is similar to IDW in that it is also a form of weighted average estimator. However in the case of OK, the sample weights are obtained by solving a series of simultaneous equations designed to minimise the MSE between the estimated value and the known sample values used in the estimate. The weighting by distance used by OK is a function of the semivariogram, which is itself a function of the continuity of the attribute, rather than the arbitrary distance function used in the case of IDW. Unlike IDW however, OK is highly sensitive to the selection of estimation parameters such as the optimal search ellipse and the minimum and maximum number of samples to use in each estimate. It is also highly sensitive to the semivariogram model used in the estimate. Another factor with OK is that it has a strong tendency to smooth out the input (point based) data distribution (i.e. make it less variable), since OK is designed to estimate the average value within a block rather than at a point.

As mentioned above, the use of small blocks typically less than 1/3rd the drill spacing, is strongly discouraged in the case of OK. This may be perceived as a problem in the case of coal quality with typically widely spaced data. Due to the fact that the leave-one-out method of determining the relative accuracy of both IDW and OK estimates used in this paper is a point estimation based method, the effect block size is not taken into account when comparing OK to IDW in this paper. It should be noted however when considering the results of this test work comparing IDW to OK, that block kriging is vastly more accurate (lower errors) than point kriging. The effect of increasing the block size on the estimation error obtained during OK is explored in the Case 1 example by conducting the OK estimate twice, firstly using a small block size commonly used for coal quality estimates (grids) and secondly

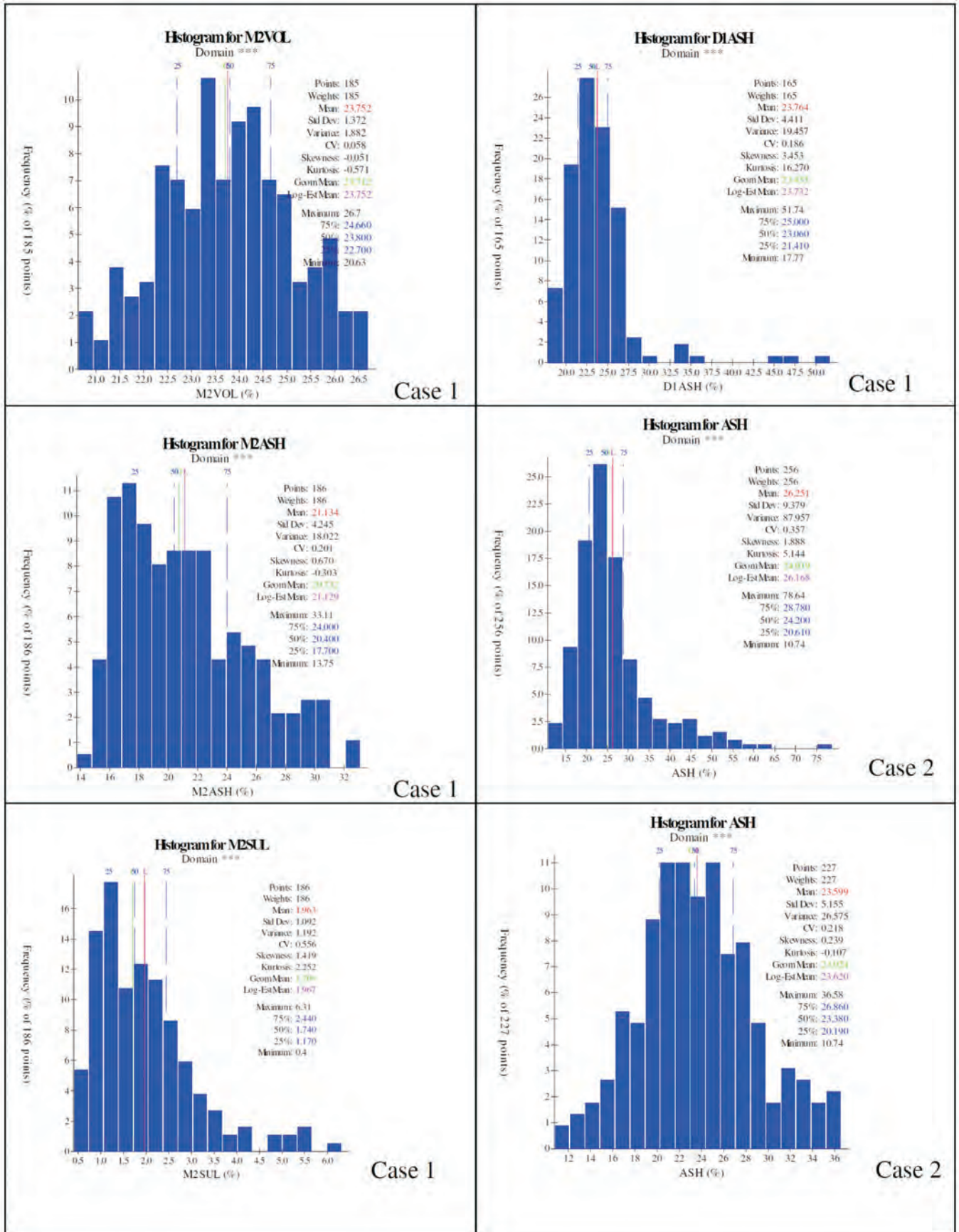


Figure 3: Histograms for raw coal quality attributes, 500 m spaced samples used in Case 1 (M2VOL, M2ASH, M2SUL and DIASH) and 250 m spaced samples used in Case 2 (ASH and ASH <38% ash)

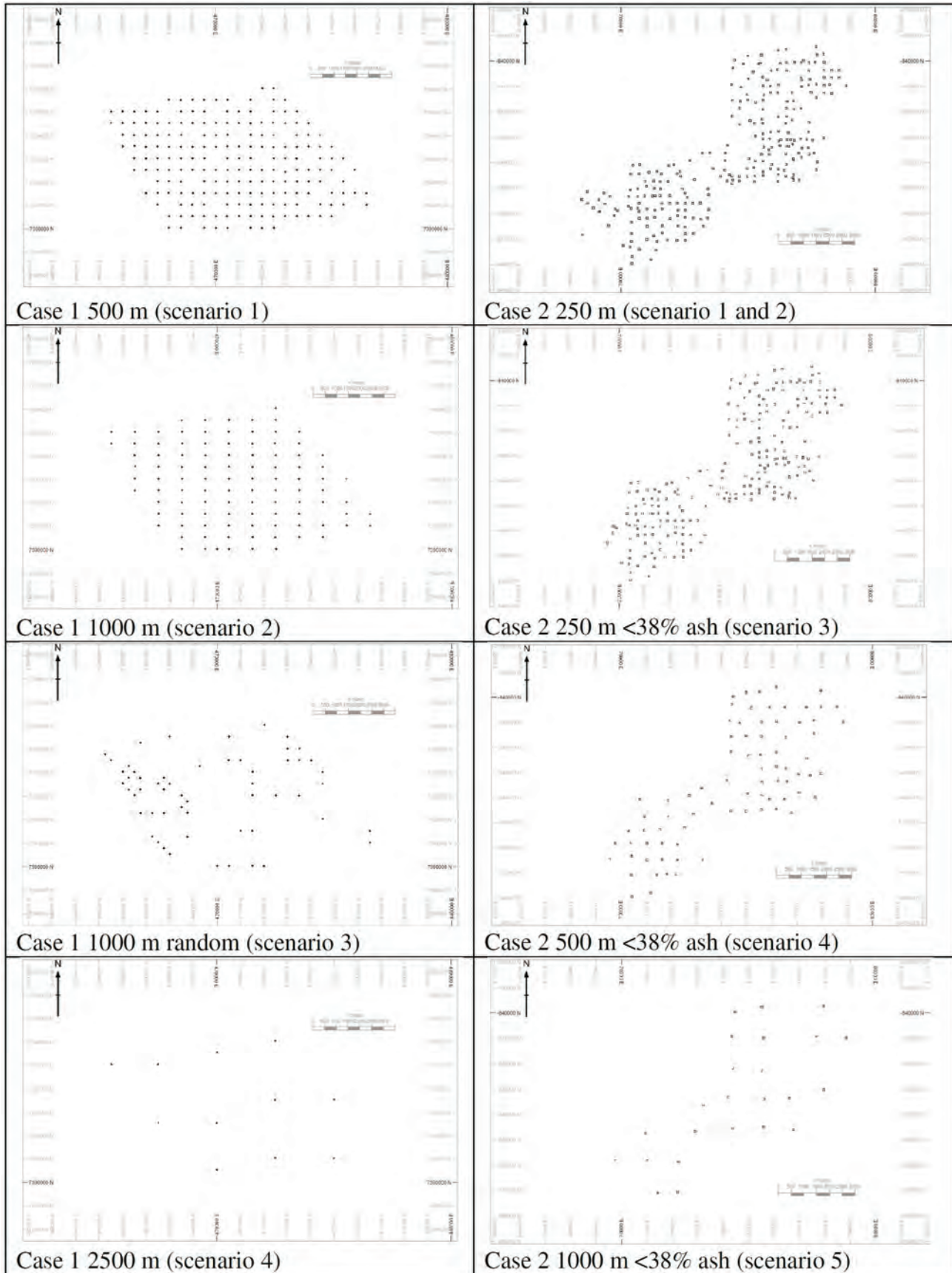


Figure 4: Sample configurations (scenarios) for each of the two test cases

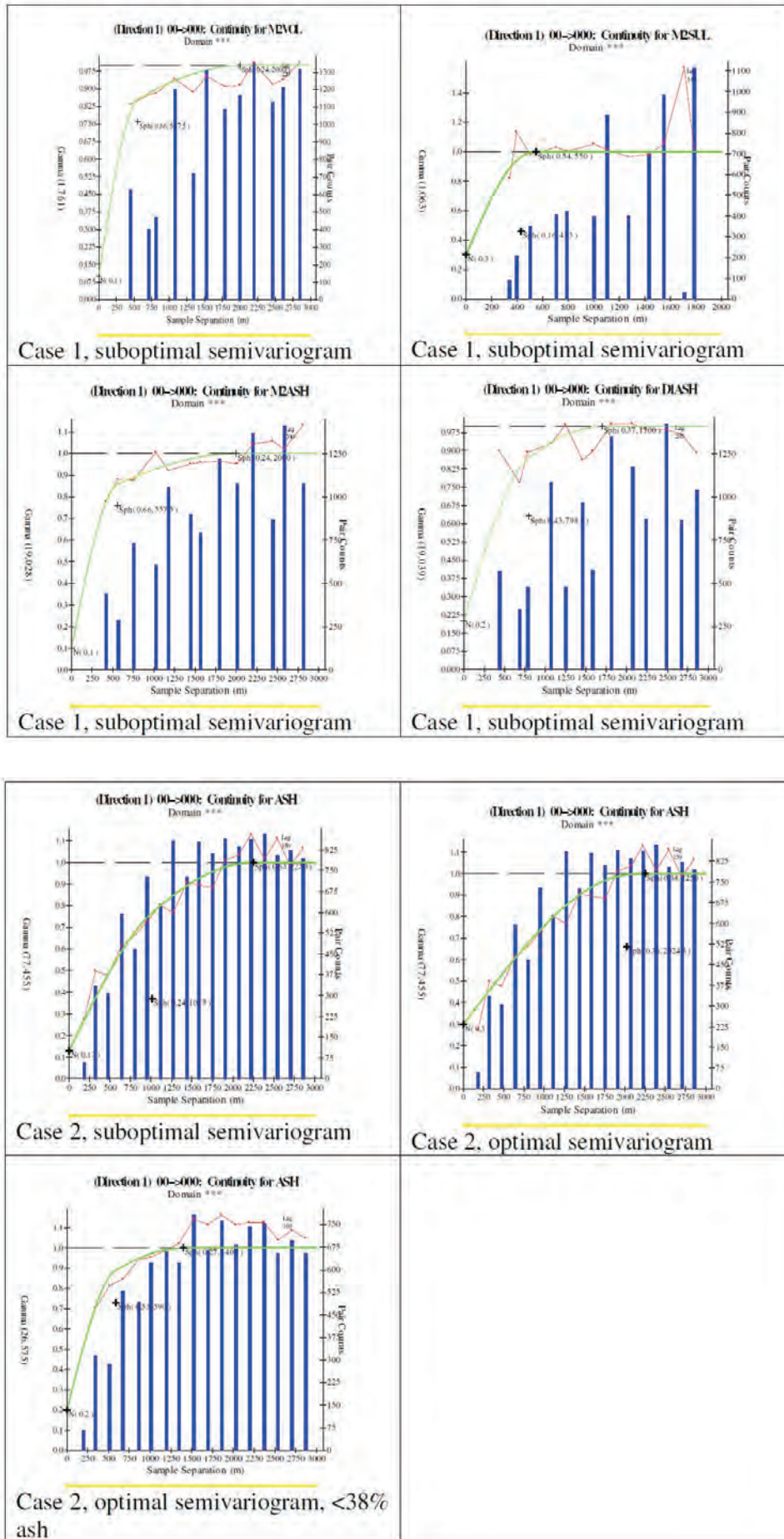


Figure 5: Semivariograms used in OK estimates

using a much larger block size which ranges from the same as to 1/5th of the drill spacing for the successive wider spaced data sets. Despite these issues there are a number of advantages of using OK which need to be considered, namely;

- Provided the estimation parameters and semivariogram model are optimal, OK is designed to obtain the best weighting of samples used in the estimate so as to minimise the MSE.
- A deficiency with IDW, particularly when it comes to resource classification, is that there is no way of determining the actual estimation error. In the case of OK however, the kriging variance (KV) is readily calculated and is a function of the semivariogram model and the data distribution around the block being estimated. Other parameters such as the slope of the regression and kriging efficiency give an indication of the accuracy of the estimate and degree to which the input data has been smoothed, which is not available in the case of IDW.
- The estimation error of the block mean can be calculated from the kriging variance within the 95% confidence interval as follows:
Estimation Error = $\pm 1.96 \cdot (KV)^{0.5}$

This can then be expressed as a percentage of the mean estimated attribute value.

ESTIMATION PARAMETERS

IDW2 was used throughout for all IDW estimates. Flat models were used for estimates with a nominal 1m length in the Z direction. Block sizes in the X-Y plane were set at 50m by 50m except in the case of Case 1 where the second OK estimate for each scenario employed a block size set at 500 m by 500m. A spherical search ellipses was used with the radius set as the range on continuity of the attributes concerned in the case of OK. In the case of IDW, a standard spherical search radius of 5000 m was used in all cases. A minimum of 3 and maximum of 30 samples was used in all cases for both OK and IDW.

RESULTS

The MAPE for the OK estimates (50m blocks) are shown in and Figure 6. The degree of MAPE is strongly related to the population variance of each attribute with M2VOL showing the lowest MAPE for each scenario, followed by D1ASH, M2ASH. M2SUL, which shows the highest estimation error, is the exception to this rule, however its low population variance is related to its low mean value as this is clearly a highly variable attribute. A better measure of variability in this case would be the coefficient of variation for sulphur which is the highest of all the attributes as shown in Figure 3. The strong relationship between MAPE and variance/CV illustrates that the variability of the attribute, expressed by the population variance or CV, is the main driver which determines estimation error.

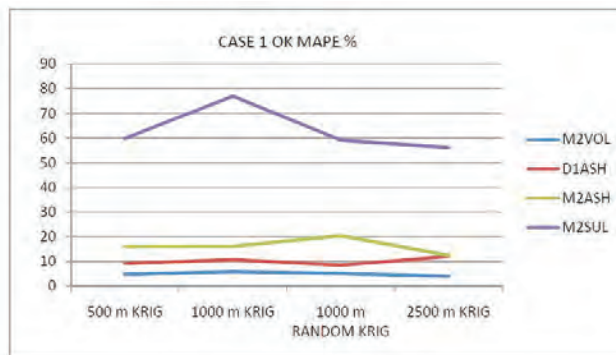


Figure 6: Plot of Case 1 MAPE for the four coal quality attributes showing different degrees of estimation error expressed as a percentage of the mean value

Table 3: Case 1 MAPE for OK

	SCENARIO	M2 VOL (%)	D1 ASH (%)	M2 ASH (%)	M2 SUL
1	500m KRIG	4.7	9.1	16.0	59.8
2	1000m KRIG	5.7	10.8	16.1	77.0
3	1000m RANDOM KRIG	5.0	8.4	20.4	59.1
4	2500m KRIG	3.9	12.1	12.5	56.1

M2VOL shows an essentially flat MAPE curve with no response to grid spacing or regularity. In the case of M2SUL, the highly variable MAPE is also apparently independent of sample spacing. The increase in the variance in the 1000 m random grid scenario for M2ASH causes the MAPE for this estimate to increase and the converse is true for D1ASH. D1ASH is the only attribute to show an increase in MAPE related to grid spacing with a noticeable increase in MAPE for the 2500 m scenario. This is probably due to the fact that this last scenario is well outside the range of continuity for D1ASH whereas the other attributes are still close to their range in the last scenario (except for M2SUL where the highly variable nature of the attribute imparts a very high MAPE which is apparently insensitive to grid spacing).

The trends seen in Table 3 and Figure 6 are mirrored in Table 4 and Figure 7 which shows the results for the IDW estimates. It can be seen from Table 4 that OK shows a slightly better MAPE than IDW for D1ASH and M2ASH. The results are very close for M2VOL and M2SUL however and this is thought to be due to the very low and high variability of these two attributes, cancelling out the slight improvement in estimation error achieved through OK in these two cases. Of note however is the fact the IDW shows a larger percentage increase in MAPE compared to OK when going from scenario 2 to scenario 3 (the random grid example) as highlighted in Table 4. This illustrates IDW's susceptibility to irregular sampling configurations.

Results for Case 2 are shown in Table 5 and Figure 8. Of note here is the visible improvement in MAPE for OK over IDW in the second scenario which used an improved semivariogram for the OK estimate. Also of note is the

Table 4: Case 1 MAPE for IDW

	SCENARIO	M2 VOL (%)	D1 ASH (%)	M2 ASH (%)	M2 SUL (%)
1	500m IDW	4.7	8.5	16.0	55.9
2	1000m IDW	5.5	10.2	16.6	66.0
3	1000m RANDOM IDW	5.2	8.6	21.6	58.0
4	2500m IDW	4.4	15.4	13.8	48.4

Table 5: Case 2 MAPE for two interpolators for raw ash %

SCENARIO	INTERPOLATOR	
	IDW	OK
1. first pass semivariogram	20.3	20.1
2. second pass improved semivariogram	20.3	19.5
3. third pass, domain out high ash	16.3	16.4
4. fourth pass 500m grid	20.1	20.2
5. fifth pass 1000m grid	27.0	26.7

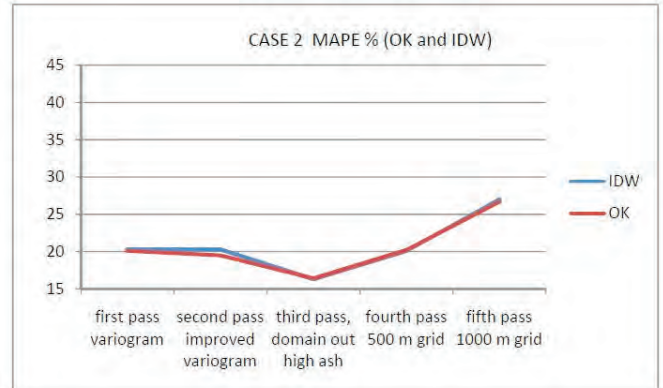
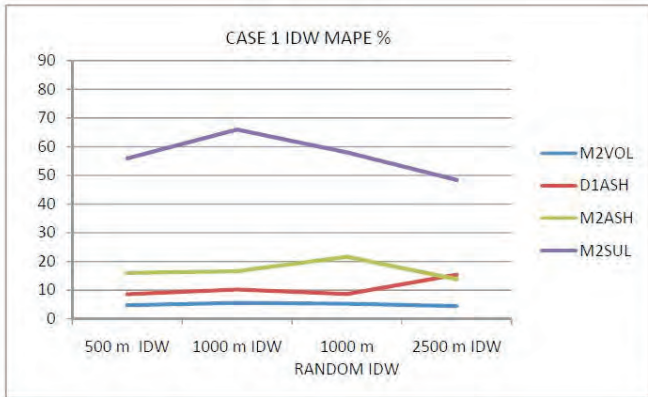


Figure 7: Plot of Case 1 MAPE for the four coal quality attributes showing different degrees of estimation error expressed as a percentage of the mean value

Figure 8: Case 2, MAPE plot for two interpolators for raw ash %, expressed as a percentage of the mean value

significant improvement in MAPE for both interpolators achieved in scenario 3 where the high ash portion of the data set was removed. This illustrates the importance of domaining prior to estimation irrespective of which interpolator is being used. Scenarios 3 to 5 show a steady increase in MAPE for both interpolators related to increasing sample grid size. This feature may not be entirely due to sample spacing alone as the ash variance also increases slightly with increasing grid size (Table 2) which is an indication that non-stationarity in the population and the effect of population variance on estimation error is playing a role here as well.

least as high as those calculated for the OK estimates at the 50 m block size. The estimation errors for the 500 m block size scenarios is reduced as is expected, but those for the highly variable M2 sulphur remain extremely high, even in the case of scenario 1, where the samples are relatively close together in coal terms and the block size compared to the sample spacing is very large.

Table 6 shows the estimation errors of the block means for the Case 1, calculated from the mean kriging variances and the means of the estimated coal quality attributes for OK estimates employing both 50 m and 500 m sized blocks respectively.

Comparison of these actual estimation errors for the OK estimates as shown in Table 6, with the MAPE values shown in Table 3, shows that in the 50 m block case the actual estimation errors are quite high (very close to 30% or more for all attributes except M2 volatiles) and almost double the equivalent MAPE value (as mentioned previously the MAPE is not a real estimation error). Although actual estimation errors cannot be calculated for the IDW Case 1 scenarios, the close correlation between OK and IDW seen in the case of the MAPE values for Case 1, is considered to provide some indication that actual estimation errors for IDW could be at

SUMMARY

The main factors determining the coal quality estimation error, in order from largest to smallest are;

1. Global statistics of the attribute ($\pm 70\%$)
2. Grid spacing/regularity ($\pm 5-10\%$)
3. Mixed domains/stationarity ($\pm 5\%$)
4. Geostatistical properties /continuity / variography ($\pm 5\%$)

The variance of the attribute is the main factor which determines the degree of coal quality estimation error, however as the variance is not comparable for attributes with large differences in mean values, use of the coefficient of variation (CV) is therefore recommended over the variance as it is independent of the mean due to the fact that the CV is calculated by dividing the variance by the mean. Hence the MAPE is strongly correlated with the CV.

Table 6: Estimation error of the block mean for Case 1, expressed as a percentage of the mean estimated attribute value

SCENARIO	OK 50m blocks				OK 500m blocks			
	1	2	3	4	1	2	3	4
MEAN M2ASH ESTIMATE	21.12	21.70	21.20	21.02	21.13	21.7	21.32	21.05
MEAN KV M2ASH	0.55	0.80	0.82	0.96	0.33	0.51	0.53	0.68
M2ASH VAR SAMPLES	18.02	18.02	18.02	18.02	18.02	18.02	18.02	18.02
M2ASH estimation error %	29.22	34.30	35.54	38.91	22.62	27.38	28.41	32.60
MEAN M2VOL ESTIMATE	23.69	23.40	23.60	23.86	23.68	23.40	23.58	23.85
MEAN KV M2VOL	0.55	0.80	0.82	0.966	0.33	0.51	0.53	0.68
M2VOL VAR SAMPLES	1.88	1.88	1.88	1.88	1.88	1.88	1.88	1.88
M2VOL estimation error %	8.42	10.28	10.32	11.08	6.52	8.21	8.30	9.30
MEAN M2SUL	1.96	1.92	2.07	1.60	1.96	1.92	2.09	1.6
MEAN KV M2SUL	0.64	0.83	0.80	0.82	0.38	0.51	0.47	0.49
M2SUL VAR SAMPLES	1.19	1.19	1.19	1.19	1.19	1.19	1.12	1.19
M2SUL estimation error %	87.34	101.54	92.46	121.11	67.30	79.59	70.19	93.62
MEAN D1ASH	23.71	23.8	23.56	25.28	23.7	23.75	23.6	25.31
MEAN KV D1ASH	0.46	0.69	0.77	0.91	0.34	0.52	0.59	0.73
D1ASH VAR SAMPLES	19.45	19.45	19.457	19.457	19.45	19.45	19.45	19.45
D1ASH estimation error %	24.73	30.17	32.20	32.62	21.27	26.25	28.14	29.19

Note: KV values are for semivariograms with sills normalised to 1. Multiply normalised KV by total sample variance (VAR) to get average KV.

In Case 1 there is a strong positive correlation between the CV and the MAPE. Attributes ranked in order from largest to smallest for both CV (see) and MAPE for all scenarios are:

M2SUL

M2ASH

D1ASH

M2VOL

Grid spacing, continuity and stationarity are all dependent on each other i.e. the estimation error (MAPE) is seen to increase for D1ASH by around 5% once outside of its range of continuity (1700m) in the Case 1 scenario 4 which used a grid spacing of 2500 m. However the increase MAPE in Case 2 of about 10% from a grid spacing of 250 m to 1000 m (Case 2, scenario 3 to 5) is linked to a rise in the population variance from 26.58 to 44.51 (i.e. indicative of a certain amount of non-stationarity). A reduction in MAPE of around 5% is seen in Case 2, from scenario 2 to scenario 3, due to the domainning out of high ash samples.

Improvement of the semivariogram model gives rise to a slight reduction in estimation error as seen in Case 2, from scenario 1 to scenario 2.

In almost all cases the difference in terms of MAPE between the OK estimate and IDW proved to be largely indistinguishable. This has been noted before in the literature

in a similar type of study conducted for iron ore by De-Vitry (2003). De-Vitry used the Mean Percentage Difference or MPD (similar to MAPE) between OK and IDW estimated Fe% values, compared against a closely spaced blast hole sample data set which he used as the truth data set. Differences in MPD between OK and IDW2 were around 0.5%.

This paper shows that for very high CV attributes like M2SUL or very low CV attributes like M2VOL, the two interpolators are indistinguishable. For moderate CV attributes like M2ASH and D1ASH, OK performs slightly better than IDW for most scenarios. The advantage of OK over IDW is enhanced at large grid spacings outside of the range of continuity (Case 1, scenario 4, D1ASH) or when an optimal semivariogram is used (Case 2 scenario 2). This is similar to what De-Vitry (2003) found with OK out performing IDW by up to 0.6% MPD when optimal search parameters were used for the OK estimate.

OK is still considered to offer an advantage over IDW due to the fact that statistics can be readily generated which give an indication of the estimation error as shown in where the estimation error around the block mean has been calculated for the OK estimates for two different block sizes.

DISCUSSION

This paper has shown that the global statistics of the coal quality attribute being estimated, in particular the population

variance and the CV, is a main driver in determining the estimation error that will be incurred. This has important implications for Coal Resource classification. The use of standard spacings for the classification of Coal Resources, as outlined in the Coal Guidelines (2003), should be used with caution when looking at a coal quality estimate that contains coal quality attributes which exhibit both low and high population variances and CVs. This is due to the fact that the error of estimation for these two attributes is likely to be significantly different and therefore the classification should consider both the variability and the continuity of the attribute most likely to control the economics of the coal product. As seen in the case of M2 sulphur for Case 1 (Table 6), the estimation error of the block mean is extremely high at 67%, even for the scenario which used large blocks and the closest sample spacing of 500 m. This sample spacing is inside the range of continuity for M2 sulphur. One possible classification methodology outlined by Snowden (1996), whereby Indicated Resources could be defined between two thirds of the semivariogram range and the maximum range of continuity or sill of the semivariogram, is often used to justify radii around points of observation when classifying Coal

Resources. In the case of M2 sulphur, this sample spacing only based resource classification approach would significantly underestimate the resource risk involved for the resource category concerned.

REFERENCES

- AUSTRALIAN GUIDELINES FOR ESTIMATING AND REPORTING OF INVENTORY COAL, COAL RESOURCES AND COAL RESERVES, 2003: The Coalfields Geology Council of New South Wales and the Queensland Mining Council.
- CIC ENERGY CORPORATION, 2006: Mmamabula Energy Project, Southeastern Botswana, Project No. J912, Fourth Technical Report.
- DE-VITRY, C., 2003: Transactions of the Institute of Mining and Metallurgy, **112**.
- SNOWDEN, D.V., 1996: Practical interpretation of resource classification guidelines, AUSIMM 1996 Annual Conference.
- http://en.wikipedia.org/wiki/Mean_absolute_percentage_error

Luis A. Martinez

Strategic coal mine planning project using an integrated real options model approach

INTRODUCTION

Strategic planning and mine design is a complex process. This complexity arises from the large range of variables that need to be considered in order to maximise the value of a mining operation with any confidence.

Despite extensive data gathering exercises primarily focussed on the deposit, many of the inputs into an evaluation process are either unknown or limited (e.g., ash content, washability, coal prices and operating costs, among others) even when the project is at an advanced stage. This typically results in a sequential evaluation process and averaged or factored inputs being applied to the mining operation, with little or no consideration given to the inherent uncertainty associated with such an approach.

Unfortunately, current coal open pit evaluation procedures do not account for all these technical, operational and financial aspects appropriately. One of the main reasons for this is that current mine evaluation techniques are based on the (static) discounted cash flow (“DCF”) and the associated Net Present Value (“NPV”) techniques. However, these techniques are somewhat limited in that they provide a static view of the project based on averages or expected values and, from a valuation perspective, largely disregard cash flows beyond a certain period (as little as five or six years). This is formally referred as the “Flaw of Averages in Mine Project Evaluation”. Another reason is the complexity of the mine evaluation process, i.e., dealing with uncertainty and risk in coal mine project evaluation is not an easy task due to the different sources of uncertainty that a mine project faces during its production life.

In the light of the above, the objective of this paper is twofold. Firstly, it discusses the concept of “flaw of averages in coal mine projects” (Martinez, 2009, 2010). Secondly, it introduces and extends recent investigations using real options theory to the evaluation of a coal mining project. Here the need for building generic frameworks that can facilitate the evaluation process of a coal mine project, in the face of uncertainty and risk, is discussed. The paper introduces a generic framework for coal mine project evaluation, named an integrated model real options approach, which is then applied to a small coal mine operation where coal quality and coal prices are seen as the main sources of uncertainty.

Flaw of averages in coal mine project evaluation

Traditionally, coal mine organisations use various types of quantitative methods to estimate profit and loss associated with a proposed mine project. Among all these measures of profitability, the Net Present Value (NPV), which is based on the Discounted Cash Flow (DCF) technique (see for example Benninga, 2000), is the most widely used in the mining industry. This is because it recognises the time value of money, and accounts for risk *via* an adjusted discount rate, R (see Equation 1), giving the mine analyst a tool for making financial investment and dividend decisions. More formally, the NPV technique consists of subtracting the capital investment, $CapInv$, incurred at the beginning of the mining project (assumed to be period t_0), from the sum of the present value of the expected net cash flows (CF_t) generated throughout the operating life ($t = 1, 2, \dots, T$) of the open pit mine project:

$$NPV = \left[\frac{CF_1}{(1+R)^1} + \frac{CF_2}{(1+R)^2} + \dots + \frac{CF_T}{(1+R)^T} \right] - CapInv \quad 1$$

In practice, the expected cash flows generated at each production period, $t = 1, 2, \dots, T$ are estimated using expected values for the underlying variables such as the coal price, S_t , production costs, $Cost_t$, and coal product quantity, q_t , produced, i.e.,

$$CF_t = q_t \times S_t - Cost_t \quad 2$$

One consequence of using expected values when estimating cash flows is that the resulting NPV value is also assumed to be an expected value, which, as it will shown later on, may not be reflecting the real project’s expected value leading to incorrect decisions.

Although some variations of the Discounted Cash Flow (DCF) technique, such as scenario analysis, have been developed to give mine analysts the flexibility of including different scenarios in the mine evaluation process, they still suffer the same problem of the DCF, i.e., instead of working with the uncertain variables, these techniques work with a single estimated value¹ for each scenario, relying on the adjusted discount rate, R , to account for risk and uncertainty in the entire coal mine project.

¹ Observe that a single estimate in the context of a financial and engineering statement is a single number, often an average or expected value, used to represent the value of an uncertain quantity such as the average coal quality of the deposit, the coal price, and future mine revenues or expenses, among others. An uncertain quantity is normally represented by a probability distribution, or a bar graph, which represents the relative likelihood of various outcomes

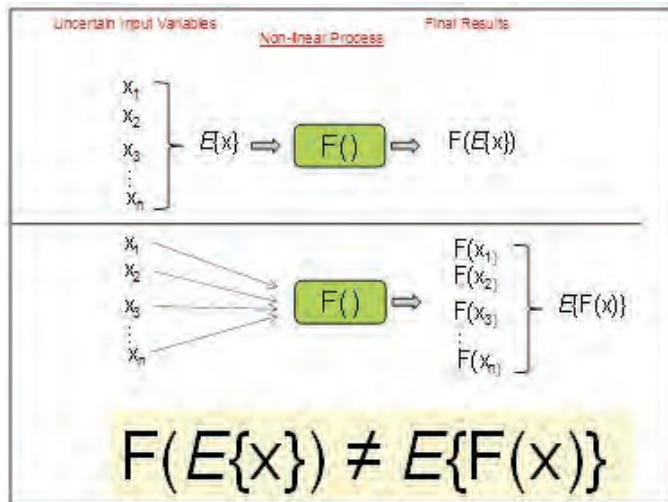


Figure 1: Scheme showing that 'average inputs do not always yield average outputs' when dealing with uncertainty and non-linear processes.

The problem with evaluation techniques based on the DCF is that in cases involving uncertainty and non-linear processes, in our case the mine optimisation/evaluation process, single estimate values are often of little use because of their lack of accuracy in describing an uncertain process. In other words, as it is shown in Figure 1, serious trouble can arise when a single number is substituted for a distribution of probabilities. That is, if the expected value, $E\{X\}$, of the uncertainty variable, X , is input into the non-linear process $F(\cdot)$, the resulting output, $F(E\{X\})$, will not be the same as the expected value of the resulting outputs, $E\{F(X)\}$, generated by inputting the entire distribution of values: i.e. $F(E\{X\}) \neq E\{F(X)\}$.

Professor Savage, from Stanford University, refers to this problem as "the *Flaw of Averages*"² (Savage, 2002a), which states that plugging average values of uncertain inputs into a non-linear process **does not** result in the average value of the process; i.e., $F(E\{X\}) \neq E\{F(X)\}$. He explains this concept with the following example (Figure 2).

"Consider the state of a drunk, wandering back and forth on a busy highway. His average position is the centreline of the highway. Therefore the state of the drunk at his average position is alive. However, it is clear that the average state of the drunk is **dead**".

An analogous situation happens when evaluating a coal mine project using traditional mine evaluation techniques that are based on the DCF. That is, when evaluating a coal mine project it is common to use expected single values for representing all the mine variables³ that are input into the non-linear mine optimisation process (Martinez, 2003; Dimitrakopoulos, 1998). The final output of this practice is a single estimated value for each of the project indicators, such as projected revenues and expenses, coal quality, coal quantities, and mining and processing costs, among others, which are assumed to be the average values to be obtained. Although, it is common to perform a sensitivity analysis that uses spider and tornado diagrams to obtain a sort of interval of

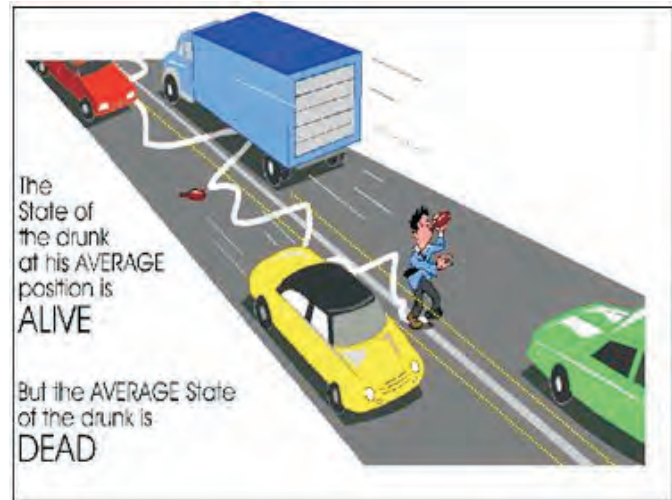


Figure 2: A sovereign example of the flaw of averages (from Savage, 2003).

confidence for the final mine revenues, traditional mine evaluation techniques ignore any possible realistic fluctuations in revenue or expense due to the existing uncertainty of the different input variables over time, and corresponds to the assumption that the drunken guy will be always walking on the centre line (refer to Figure 2).

The problem is that even though sensitivity analysis is supposed to account for variations in the different input variables, it assumes that these changes will happen in a linear fashion, i.e. the same change will occur at each production period, which is not true. See for example Figure 2 above, where the yellow dashed lines represent the $\pm 10\%$ confidence interval that is supposed to account for the drunk's trajectory deviation from the central line. As observed in the figure, this confidence interval does not give a realistic representation of the drunk's trajectory. Another limitation of sensitivity analysis is that it ignores dependence structure between the underlying variables that take part in a mine evaluation process performing changes in an isolated fashion, i.e., changes to a specific variable are performed keeping the other ones constant.

In the case of a coal mining project, coal quality (e.g. % of ash) variations will occur at different locations of a coal seam model, but following a specific correlation structure, i.e., changes at different locations will be generated following a specific correlation structure, which is a non-linear process. Similarly, (export/thermal) coal prices will also vary at each production period but at different rates and also following a correlation structure. Thus, it is important to be cautious when making decisions based on a sensitivity analysis, since it could lead to spurious description of the current financial situation of the mining project.

One of the techniques that has been widely accepted as a unified approach to dealing with uncertainty is the **Monte Carlo Simulation** technique (Glasserman, 2004; Chan & Wong, 2006). This is because instead of hiding behind a

² Also known in finance as the Jensen's inequality, which states that because the value of a project, x , is a random variable and the option value, OV , on the project is a convex function of the project value, then, $OV(E\{X\}) \neq E\{OV(X)\}$.

³ Examples of these input variables are: the seam model, export/thermal coal prices, coal quality, costs, and yields, among others.

single best "estimate" this technique quantifies uncertainty by sampling the probability distribution of the uncertain variable while tracking the resulting outputs. However, despite its benefits when dealing with uncertainty, the application of the Monte Carlo technique to the mine evaluation problem is not straightforward.

The reason for this is that the mine optimisation process is a 3D complex, non-linear procedure where the uncertainties of the input variables are of different natures. For example, the uncertainty of the coal seam model (let's say ash quality) could be classified as static (Martinez, 2007) since it depends on the geology of the coal deposit that is uncertain; not because it changes over time, but because of the limited data (e.g. drill-hole/well data) obtained for its quantification⁴. On the other hand, the uncertainty of future coal prices can be classified as dynamic because it depends on the international coal market, which is affected by different mechanisms such as offer, demand and speculation, and which varies over time. Furthermore, besides the nature of the sources of uncertainty, a coal mine evaluation process also depends on plans that are based on physical designs, such as the ultimate pit and production scheduling limits that obey technical constraints such as slope angles and run of mine ('ROM') coal tonnes, among others.

A road to improvement: Applying an Integrated Real Options Based Coal Mine Project Evaluation Framework (IROCMP)

Different techniques have been developed to overcome the complexity of the mine evaluation problem. Although some of them have been shown to be very efficient in dealing with a specific part of the problem, none of them have been able to solve the complete problem, i.e., considering all sources of uncertainty. The reason that current techniques cannot solve appropriately the mine problem is that these techniques have been developed in isolation. That is, mine evaluation techniques, such as the Upside/Downside Potential, developed to deal with technical uncertainties, such as the orebody model, do not account for the uncertainty of economic variables. Similarly, mine valuation techniques, such as real options (Longstaff & Schwartz, 2001), that deal with economic uncertainties, such as metal prices, do not appropriately account for technical (geological) uncertainty.

The Integrated Real Options Based Coal Mine Project Evaluation Framework ('IROCMP') is a novel techniques which is based on the Integrated Valuation/Optimisation Framework (IVOF⁵) (Martinez, 2008), which is able to account for uncertainty and risk when evaluating a mine project. In this context, the IROCMP sees the coal mine evaluation problem as a multi-stage solution where the problem is broken down into a set of simple building blocks. One important feature of the IROCMP process is that the

flexibility to close the coal mine project at any production period — if operational and economic conditions are adverse — is considered as an embedded option of the evaluation process

In its essence, the IROCMP is composed of the following five general stages:

- Base-case coal mine plan and design, which is built using traditional techniques and used to identify main cash flow drivers. The base-case project indicators also provide a benchmark from where to assess the existing risk and upside potential;
- Integrating and assessing the effect of geological (coal quality) uncertainty on the base-case mine plan and design;
- Integrating and assessing the effect of future (export/Thermal) coal prices in current base-case mine plan design;
- Adding value to the current mine project by adopting different operational and managerial flexibilities such as coal product blending and closing mine operations in the face of future adverse conditions, among others; and
- Estimating the base-case extended net present value (ENPV) and making final strategic decisions.

Observe that key elements for making final decisions when applying real options are i) the perception of the existing uncertainty; and ii) the perception of both the risk and opportunities that can be generated. Consequently, if accurate final decisions are to be made when evaluating a coal mine project using the IROCMP technology, it is important to:

- Quantify the main sources of existing uncertainty, such as the seam model (e.g., coal quality), costs and commodity prices;
- Assess the risk and opportunities that can arise due to the existing uncertainty; and
- Identify the strategies that can be implemented in the face of uncertainty.

The case of a multi-seam coal mine project evaluation

A coal mining corporation is evaluating one of its coal mine projects. The coal mine operation consists of a small multi-seam (three) open pit coal mine project containing an estimated 7.8M tonnes of export coal and additional 3.8M tonnes of thermal coal.

The property has been explored, but there is still some uncertainty over the total tonnage of final export and thermal coal product which depend upon the coal quality within each of the three coal seams — see Figure 3 (there is no washing plant and final yield is considered to be 100%).

⁴ It is possible to minimise the uncertainty of a coal seam model by taking samples on a very small grid. However, this procedure will result in a non-profitable project because the high cost incurred in the data collection.

⁵ The IVOF was developed to deal with mine projects containing precious metals such as gold. It is generic framework which allowed us to adapt it to other real commodities such as coal mine projects

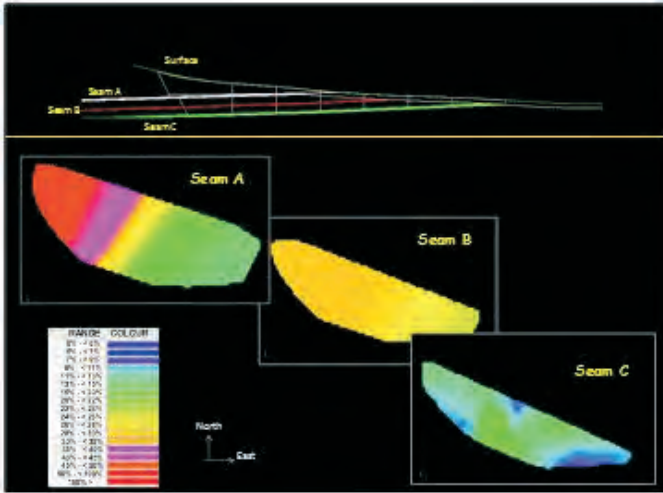


Figure 3: North-East section showing ash variability on Seams A, B, and C. Here, hot/cold colours indicate high/low ash content

Furthermore, the corporate office is interested in assessing the effect of future (export and thermal) coal prices on project cash flow and NPV.

Besides the previous corporate questions, management is also trying to answer the following questions:

- i. What is the value of the coal mine using traditional mine evaluation techniques?
- ii. What is the effect of *in situ* coal quality variability on final export / thermal coal product?
- iii. What is the effect of both *in situ* coal quality and export / thermal coal price uncertainties on final project value?

Coal Mine Operation- Technical/economic inputs

As observed in Figure 4, the coal mine project consists of a mine design, composed of pit limits and *in-pit/ out-pit* dumps.

The production scheduling was built using input economic data; in this case, coal prices for thermal and export coal as well as mine and processing costs and the estimated ash variability for each seam.

The ROM coal material is transported to a plant, which assumes 100% Yield (i.e., input ROM coal equals output final coal product).

The final product is then classified based on its ash content and stockpiled either as export coal (ash content $\leq 20\%$) or local/thermal coal (ash content $> 20\%$) products.

Finally, depending of their final market, the final products are then commercialised at international export/thermal coal prices of AU\$104.6/t and AU\$76.91/t, respectively.

A corporate 10% discount rate is used for cash flow analysis. Also observe that the total ROM production is 3.0Mt per year (stock piling was not considered at this stage).



Figure 4: Schematic of typical coal mining operation.

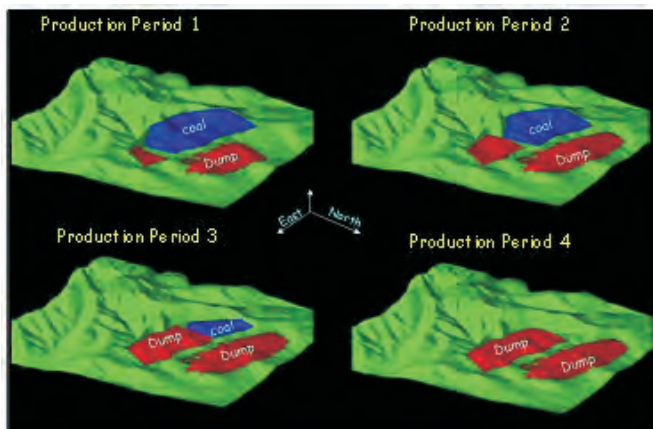


Figure 5: Coal mine design: ultimate pit and long term production scheduling.

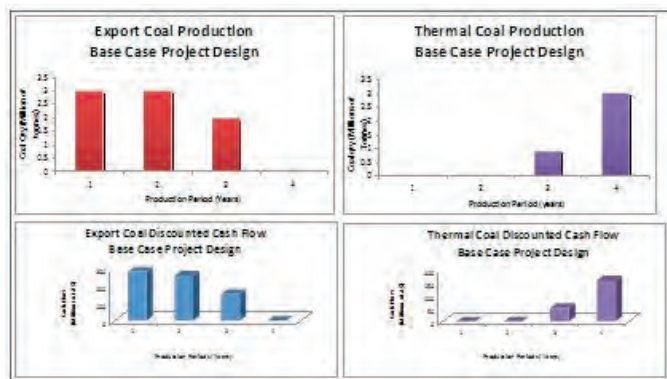


Figure 6: Coal mine project indicators for export/thermal coal production (up) and their respective cash flows (bottom)

To design and plan the production scheduling all (estimated) technical/operational and economic parameters are input into an open pit mine scheduler engine ('OPMSE'), the results from the coal mine production schedule process are depicted in Figures 5, 6 and 7.

Figure 5 shows the production scheduling layout, where it is seen how the coal mine project is depleted over time while the in/out pit dumps are filled in. The results indicate that the coal mine project will have a life of mine ('LOM') of four years. Figure 6 shows the export and thermal coal production (top part), as well as their respective cash flow (bottom part) generated at each production period of the coal mine project.

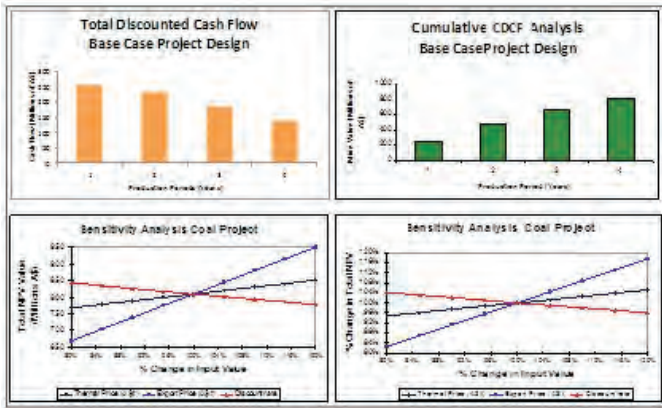


Figure 7: Coal mine project indicators for total discounted cash flow (up) and their respective sensitivity analysis (bottom). The sensitivity analysis was performed by varying export and thermal coal prices, as well as the discount rate by $\pm 20\%$.

As noted, the coal mine project is expected to produce a total of 7.8Mt of export coal during the first second and third year, and around 3.8Mt of thermal coal during the last two production years.

The results shown in Figure 6 (bottom part) also indicated that the total discounted cash flow to be obtained from export and thermal coal production are around AU\$687 M and AU\$208 M, respectively. Observe that the production scheduling engine maximised project value by extracting high quality coal (export coal) during the first, second and third years due to its higher market price than the thermal coal, which was produced during the remaining one and a half years to achieve production targets.

A year by year analysis indicated that the coal mine project is expected to generate the following cash flows: AU\$285 M, AU\$259 M, AU\$125 M, and AU\$17 M, from export coal production and AU\$69 M, AU\$63 M, AU\$80 M, and AU\$127 M, from thermal coal production.

A sensitivity analysis was run to see the sensitivity of project value due to changes in export and thermal coal prices, and discount rates. In this case the value of each parameter considered in the sensitivity analysis was varied in a $\pm 20\%$ of its original value (see Figure 7-bottom). The sensitivity analysis indicated that $\pm 20\%$ variability in export coal prices originated a $\pm 16\%$ variability on project value, and that $\pm 20\%$ variability on thermal coal prices and discount rates did not have a significant effect on project value originating just $\pm 4\%$ variability in project value. These results would be indicating that the value of the coal mine project is highly sensitivity to changes on export coal prices while changes in thermal coal prices and discount rates will not have a significant effect on project value.

Further economic results (shown in Figure 7) indicated that the coal mine project will generate a total (export + thermal) expected project cash flow of AU\$896.4 M throughout its LOM.

What is the effect of coal quality (ash variability) on final project value?

To assess the effect of coal quality variability on final export/thermal coal production, and consequently on project cash flow, the following steps are performed:

- Quantify coal quality variability (uncertainty) on each coal seam. This process is done using the Conditional Simulation technique (geostatistics);
- Assess the effect of coal quality variability on given production schedule. This is done by superimposing each simulation on current production scheduling.
- Analyse results.

Figure 8 shows the inclusion of the *in situ* ash variability on current coal mine production scheduling.

Figure 9 shows the result of integrating coal quality variability on current mine production scheduling. In the figure, the bars with different colours, such as black for coal production (top part) and red for cash flow (bottom part) represent the values estimated for the base-case mine plan and design (refer to Figure 7), while the bars of similar colour represent the effect of coal variability on each variable. For instance, the effect of coal quality variability on export coal production and its

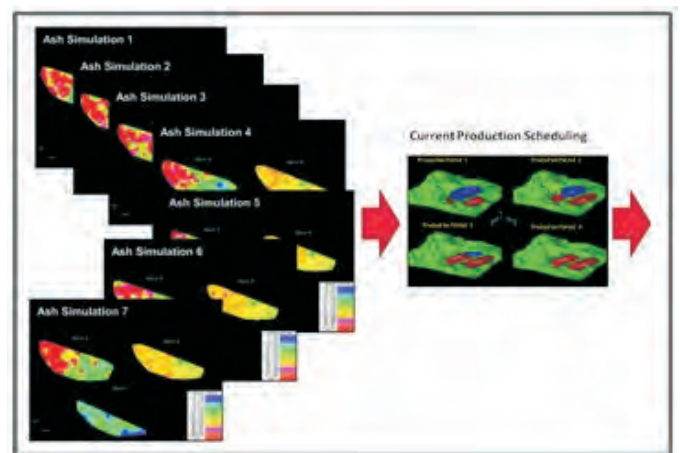


Figure 8: Assessing the effect of coal quality (for Seams A, B, and C) on coal mine production scheduling. Here the ash variability is quantified using the Conditional Simulated seam models.

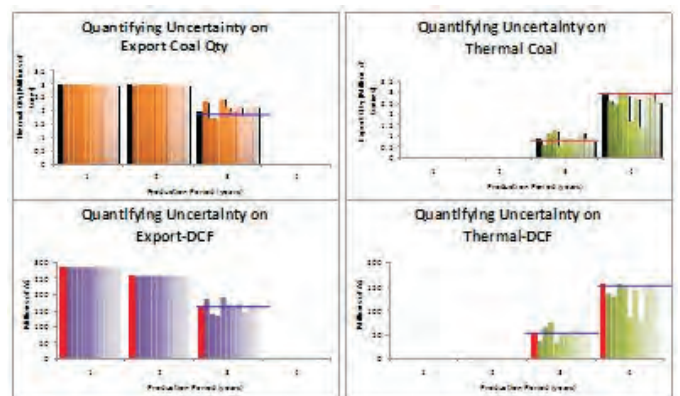


Figure 9: Effect of coal quality variability on project indicators such as export and thermal coal production, and export/thermal cash flow generation.

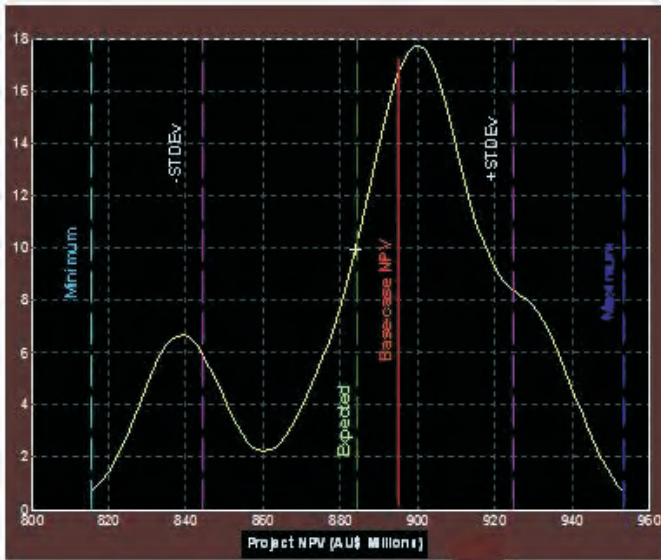


Figure 10: Effect of coal quality variability on final coal mine project NPV

corresponding cash flow generation are indicated by the orange bars, on the top left figure, and purple bars, on the bottom left figure, respectively. As noted, the probability of achieving export coal production of 3Mt, and corresponding cash flow, during the first and second years are very high; i.e., there is not a significant variability on coal quality during the first two years, whereas year three is seen to be the one where coal quality variability will have a significant effect for both export and thermal coal production, and consequently their corresponding cash flows.

Figure 10 shows the effect of coal quality variability on final project NPV. As noted, the results indicates that the project could generate an NPV oscillating between a minimum of AU\$820 M (light blue dashed line) and a maximum of AU\$950 M (dark blue dashed line) with an average of AU\$886 M (green dashed line). Also note that the expected NPV in the face of coal quality variability is less than the base-case NPV (red solid line), i.e., if coal quality variability were not accounted when evaluating the coal mine project, the resulting NPV could be overestimated, as it is the case of this example.

But, what if coal prices change over time?

This is the second question that the corporate and management offices wish to know. That is, once the coal quality uncertainty has been integrated into the coal mine evaluation process and its effect assessed (as shown in Figures 9 and 10), the uncertainty about the effect of future coal prices on the project is another important question that needs to be assessed. In this case, questions such as what if export/thermal coal prices go above/below the assumed prices, i.e., AU\$104.6/t and AU\$76.91/t, for export and thermal coal, respectively, become a mandatory question.

A quick analysis of historical export and thermal coal prices (see Figure 11) indicates that since 2005 export coal prices

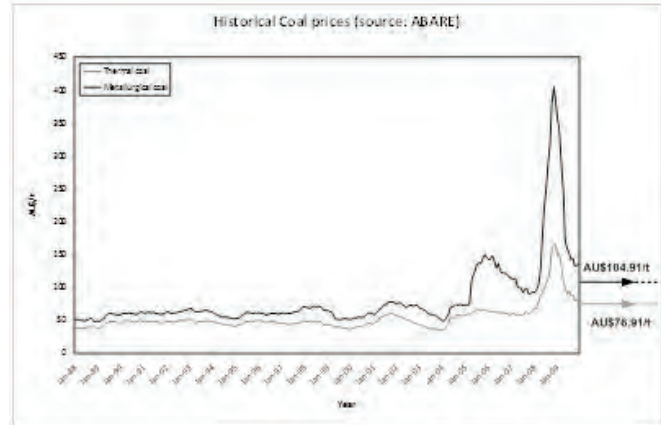


Figure 11: Historical export / thermal coal prices for the period Jan 1988 – Dec 2009.

have had a more erratic behaviour (i.e., a highly volatile) with significant changes in their trends during short periods of time. Although not as critical as export coal prices, thermal coal prices are also seen to have similar erratic behaviour since 2007⁶.

Further information obtained from the historical coal price data (plotted in Figure 11) is that both export and thermal coal prices tend to have a common behaviour, formally called correlation in the financial jargon. In fact, a simple linear correlation analysis indicates that export and thermal coal prices are strongly positive correlated with a factor of 0.97 (a value of ± 1 indicates a perfect positive/negative correlation). This last result suggests that if export coal prices go up/down then thermal coal prices also tends to go up/down with strength of 0.97.

One important outcome from the analysis of historical coal prices is that the modelling of export and thermal coal prices, and consequently their forecast process, has to be done considering their correlation instead of an independent analysis.

Modelling coal prices

In finance, coal prices are commonly modelled as mean reverting ('MR') processes, which indicates that coal prices tends to revert to a long-term stable level, normally given by supply and demand and which normally is assumed to be the long-term mean price⁷. A well known MR model used to model commodities such as coal prices is the Ornstein-Uhlenbeck process (also called arithmetic mean reverting process), which is modelled as

$$dY_t = \eta(\bar{Y} - Y_t)dt + \sigma d_t \quad 3$$

where the coal price, Y_t (with volatility σ), tends to revert to its long-term stable level, \bar{Y} , at a speed of, η . Observe that the MR model depend on the current price. In practice, Monte Carlo ('MC') simulations and discrete trinomial lattices are commonly used to model these processes. In the case of the coal mine project, Monte Carlo simulation (Glasserman,

6 For the period 1988–2004 both export and thermal coal prices were characterised by a stable flat trend of AU\$62/t and AU\$42/t, respectively.

7 For more details about commodity price models the reader is referred to financial and derivative books such as Dixit & Pindyck, 1994.

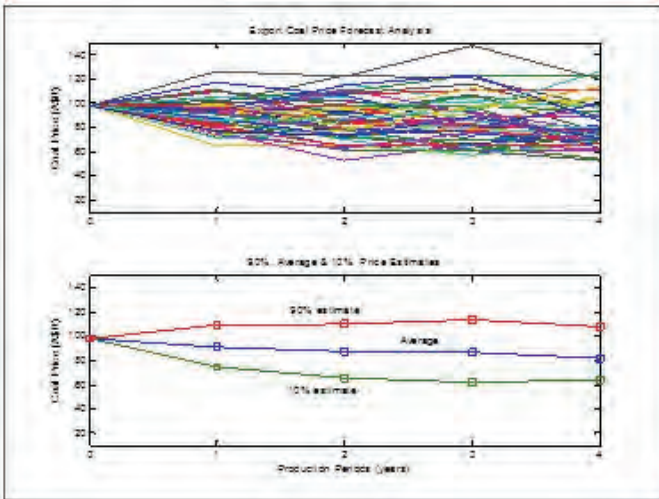


Figure 12: Four years forecast of export coal price (above) with respective 90th, 10th percentiles and long term average (bottom).

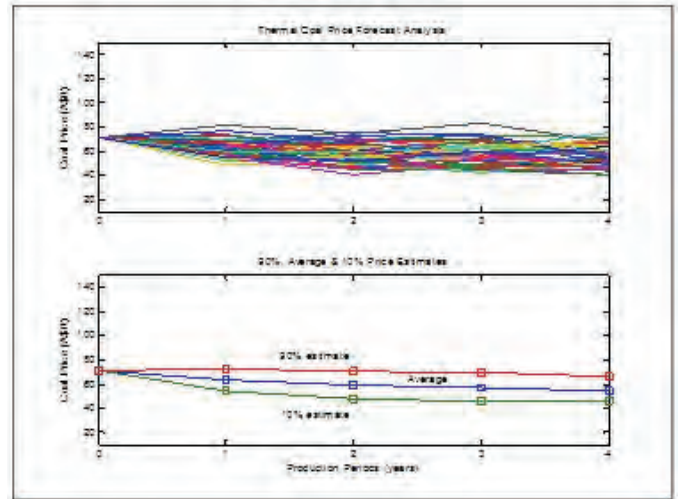


Figure 13: Four years forecast of thermal coal price (above) with respective 90th, 10th percentiles and long term average (bottom).

2004) is used to joint model and forecast export and thermal coal prices; note that the forecasting process is done considering the correlation between both commodities.

The four year forecast for export and thermal coal prices are shown in Figures 12 and 13, respectively. As noted in Figure 12, export coal prices are seen to follow a long-term trend of AU\$98/t (average) with maximum and minimum AU\$115/t (90th percentile) and AU\$80/t (10th percentile), respectively. Similarly, Figure 13 shows that future thermal coal prices tend to follow a long-term price of AU\$59/t (average) with maximum and minimum of AU\$70/t (90th percentile) and AU\$55/t (10th percentile), respectively; note that the estimated export and thermal prices used to model the base-case coal mine project were AU\$104.9/t and AU\$76/t, respectively (see Figure 10).

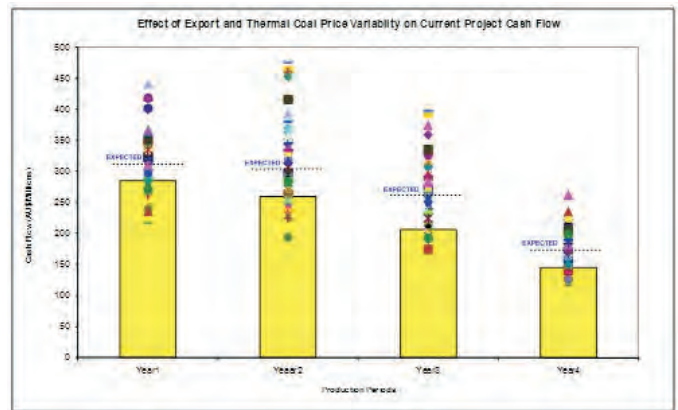


Figure 14: Effect of future export and thermal coal prices on current project cash flow.

Figure 14 shows the effect of future export and thermal coal prices on base-case project cash flow (that already integrates coal quality variability). In the figure, the yellow bars indicate the estimated cash flow for the initial base-case coal mine project (refer to Figure 7- top left) while the colourful shapes indicate the effect of coal prices and coal quality uncertainties on project cash flow generation. As noted, the effect of coal quality and future coal price uncertainties is significant when compared with the initial estimated cash flows (given as yellow bars). The analysis indicates that in the face of coal quality and future coal price uncertainties the coal mine project will generate expected cash flow of AU\$315.6 M, AU\$307 M, AU\$261 M, and AU\$175.8 M for the first, second third and fourth production periods, respectively. Further analysis indicates that the likelihood to achieving cash flow values below the initial estimates are small (around 15%) while the likelihood of achieving values above are significant.

The resulting coal mine project NPV in the face of coal quality and future coal prices is depicted on Figure 15. A quick comparison between Figures 10 and 15 indicates that the inclusion of coal quality and future coal price uncertainties not only increased the downside risk from AU\$820 M to AU\$700 M but also the upside potential from AU\$950 to AU\$1280 M. Furthermore it is noted that the expected project NPV increased from AU\$896 M to AU\$967 M.

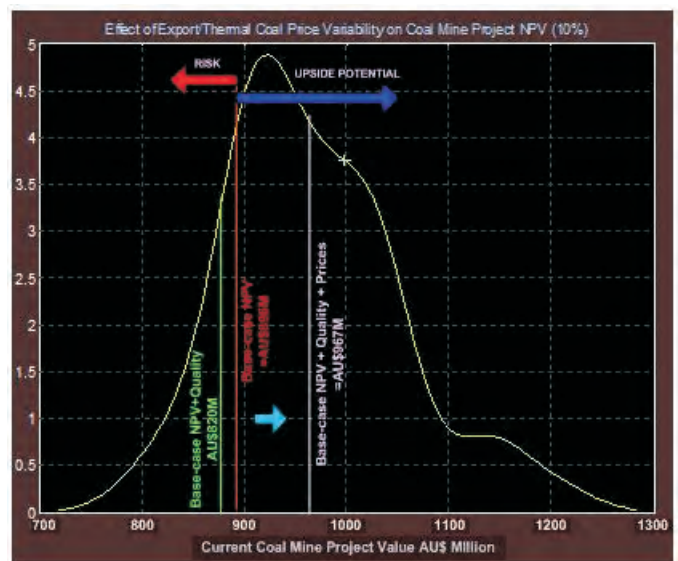


Figure 15: Effect of future export/thermal coal price variability on final coal mine project NPV.

CONCLUSIONS

This paper has discussed the importance of including uncertainty, risk and upside potential in any coal mine project evaluation process. As seen in Figure 15, the value of the coal mining project increased significantly (although it is not always the case) due to managing of uncertainty, risk and upside potential. In fact, the results indicated that the inclusion of coal price uncertainty significantly increased the coal mine value when compared with the base-case scenario which uses a traditional DCF approach.

The results also indicated that the inclusion of coal quality uncertainty on the evaluation process decreased the expected project NPV (see Figure 15) from AU\$896 M to AU\$820 M (approximately 8%). This result is informative for mine planners and mine valuers since it indicates that the initial base-case coal mine plan is overestimating ROM coal quality which also overestimates final export/thermal coal production and consequently their corresponding cash flow.

In conclusion, and based on the previous analysis, the answer to corporate-management questions, formulated at the beginning of the project, are:

- i. The value of the coal mine project estimated using traditional mine evaluation techniques is AU\$896.4 M.
- ii. The effect of *in situ* coal quality variability on final export / thermal coal product does not have a significant effect on export coal product during the first and second year. However the results indicate that during the third year the likelihood of achieving export coal production is less than 50%; this is also seen for thermal coal production during where the likelihood of achieving initial estimated targets during the third and fourth production years is less than 50%.
- iii. The effect of both uncertainties on project value is significant, as seen in Figure 15. The results indicated that the integration of coal quality and future coal price uncertainties not only increased the downside risk of the coal mine project NPV (with a minimum of AU\$700 M) but also its upside potential (with a maximum of AU\$1280 M). Most importantly, it is seen that besides the increment in downside risk and upside potential, the

integration of coal quality and future coal price uncertainties increased the expected project NPV from AU\$896 M to AU\$967 M (approximately 8%). The reason for this is the consideration of the upside potential that coal quality and future coal price uncertainties bring to the process, which otherwise is not considered in a traditional DCF.

Observe that in order to add value to a project an accurate real options analysis should include all mine project sources of uncertainty as well as all operational and managerial flexibilities, such blending and cut-off grade optimisation and the option to close or delay mine operations, among others.

Unfortunately the application of real options to a mine project is not simple, and it demands highly qualified/experienced professionals as well as advanced mine project evaluation tools. These tools have not yet been developed. We hope that this paper can encourage the application of real options in coal mine projects as well as the development of new tools which can facilitate the process.

REFERENCES

- BENNINGA, S., 2000: *Financial Modelling*, 622 pages (The MIT Press: London).
- GLASSERMAN, P, 2004: *Monte Carlo Methods in Financial Engineering*, 596 pages (Springer).
- LONGSTAFF, F. A. & SCHWARTZ E., 2001: Valuing American options by simulation: A simple least-square approach, *Review of Financial Studies*, **14**, 113–147.
- MARTINEZ, L., 2009: Designing, planning and evaluating a gold mine project under *in situ* metal grade and future metal price uncertainties. In Dimitrakopoulos, R. (Editor): *Proceedings of Orebody Modelling and Strategic Mine Planning*, AusIMM, 225–234.
- MARTINEZ, L., 2009: Why accounting for uncertainty and risk can improve final decision-making in strategic open pit mine evaluation. In Proceedings the AusIMM Project Evaluation Conference 2009 - Moving Forward in Challenging Times, 113–124.

Matt Yacopetti and Stephen Mundell

Improving the quality of geoscientific information

“Garbage In - Garbage Out”. Almost everyone has heard this phrase and most would agree with its core message, but in essence it’s a cop out! Why? Because it is used to deflect criticism from systems that return useless or poor quality information and answers.

Today, more than any other time in history, data are business assets. All businesses that collect, store, manage, interrogate, abstract, use and deliver data, especially digital data, need to be mindful of its origins, context, relevance and usage. As a consequence businesses are increasingly turning their attention to data quality issues in order to exploit the value of their data & information assets.

There are numerous data assets in the mining industry. Those to be considered here are the original observations and measurements that represent an understanding of the subsurface (i.e. the geoscientific information). These subsurface data types are used as inputs for modelling (both economic and operational) and are interpreted to provide information upon which decisions will be made.

Therefore the value of the original observations and measurements to a mining business extends well beyond the cost of drilling or sample analyses etc. When compared to other asset classes, geoscientific data have properties that are very different from more tangible assets such as truck fleets, dragline buckets or explosive inventories for example. If we accept that data are business assets, then we should also accept that they should be managed as aggressively as any other asset class.

To illustrate this problem, think of a well known physical mining asset and answer the following questions:

1. How much or how many assets do you have?
2. How much is each asset worth to replace?
3. How much are the assets worth collectively?
4. How many assets are unused?
5. How many assets are unserviceable or otherwise unfit for use?

Now substitute your mine data or your latest drillhole data results for the “asset” and perform the same five-question exercise. Were you able to answer as many questions with similar or greater precision compared to the physical asset class?

As simplistic as this exercise is, it strives to make the point established by Redman (2008) that data are essentially unmanaged assets and that it is easier for businesses to

leverage physical capital and human resources than it is to leverage data and information.

It is a simple thing to say that data quality is important, but how can this statement be assessed? If you do have poor quality data, what is its cost to your business and where should you focus your efforts in order to improve the situation? Typically mining businesses have drilling data, assay data, grade control data, and production data etc., all of which are essential for managing the asset. How difficult therefore, would it be to manage that asset if the data was missing, incomplete, inaccessible or hard to understand?

For a business to successfully leverage the full value of its data and information they must be:

- Accurate (correct)
- Accessible (able to be located quickly and easily)
- Trustworthy (consistent within context)
- Able to be understood (for those it is intended for)
- Useable (by appropriate users)
- Secure (protected against loss, theft, fraud and degradation).

Too often individuals, teams or organisations spend valuable time checking, researching, locating, reconciling and reformatting their own information. In other words they are acting as “data janitors” rather than value adding “knowledge workers”.

The reasons for this are complex and involve both the properties of the data itself and the way that humans interact with those properties, including organisational and political. We will explore some of these issues in order to suggest ways in which the data quality of geoscientific information can be improved.

THE UNIQUE PROPERTIES OF DATA AND INFORMATION

Digital data and information can be shared, almost without limitation. As a consequence they are more difficult to secure and protect. Data have properties that can make it behave like a living organism rather than static information (e.g. long lifetimes and the ability to replicate and change). These properties can also mean that data and information can be more difficult to locate and share. Ever since the advent of digital information and the internet, most of us can attest that more data does not automatically equate to better data.

All systems and activities that use data create more of it. Data volumes in their own right are becoming a difficult problem. The amount of time needed to double the data generated and maintained by a business is estimated to be between 12 and 18 months, Whiting (2006). This is due to the fact that data is not consumed with use and can be re-used time and time again. Logically, the existence of poor quality data may have potentially serious consequences, Lacey (2010). The urgency of dealing with this issue is growing, as is the likelihood that poor quality data will be shared with users, both internally and externally.

Who then, in the organisation is responsible for dealing with these issues? Many mining professionals would nominate the IT Department or the Database Administrator. This is despite the fact that these roles are custodial, that is, they manage the data, but they are unlikely to be accountable for data quality at the point of origin. Data management is not purely a technological issue. It is as much an issue of organisational structure and leadership.

PEOPLE PROCESS AND TECHNOLOGY

When an asset is recognised as valuable to a business, the business will invest in its maintenance and management. Try to imagine a viable mining business today that does not invest in its human resources or capital equipment? Data management is no different. Mining businesses should invest in their data management capabilities in order to leverage and secure their valuable geoscientific information assets. A multifaceted approach that focuses on the interchange between people, process and technology will be fruitful.

People

By far the most important is the human dimension. Mining businesses need to recognise that they own the issue of geoscientific information management and to employ the people responsible. Those people need to have the required Information Management skills to do the job. No technology will improve the situation until people in the organisation have clear data quality goals and the processes in place to support those goals.

Corporate and business trends have also played their part. The cyclical nature of exploration and mining activity that is driven by commodity prices has seen periodic downturns characterised by downsizing, mergers and a move to use external service providers. Broome and Cox (2007) have noted that the increased mobility of exploration expertise has resulted in diminished corporate knowledge of data assets.

The 'people dimension' can be difficult to change. Despite its importance, the topic of 'data management' suffers from a lack of profile. It lacks 'appeal' and frequently fails to capture the attention of management, until there is a problem. Even then, the problem is likely to be associated 'with IT' rather than the lack of an overall data management capability.

Process

Advances in information technology and the need for enterprise-wide computing environments have led to the adoption of more structured data management. For the mining industry the key drivers have been:

- The move away from systems that allow users to manage data as if they own it
- The need to prevent errors at their origin
- The realisation that many errors do not affect the person or group who created them
- The move to systems that support corporate standards and data interoperability.

Processes connect people or groups to tasks. For mining businesses a good process will enable internal and external groups to establish effective data supplier relationships. With geoscientific information in mind, the processes listed below all benefit from an easy connection between people and the task:

- Capture of original observations and measurements to reduce error at the point of origin
- Discovery and access to the captured data
- Differentiation of original data from derivative data
- Identification of metadata (or data about the data)
- Data interoperability — providing the data in variety of standard formats
- Delivery of select data sets to required client systems
- Aggregation and abstraction of data and delivery in desired formats
- Internal data quality alerts and measures.

Redman (2008) estimates that knowledge workers spend on average 30% of their time searching for the data they need, and are unsuccessful at least half of the time. In a mining company where skilled workers are at a premium, the business cannot afford for geoscientists to spend this amount of their time using or creating poorly designed data management systems. This is a major opportunity to improve workplace productivity.

Technology

The challenge for the technology dimension is to connect people to the process. This will encourage the discovery, access and integration of diverse geoscientific information. A well designed Geoscientific Information Management System (or GIMS) will provide an architecture that will enable the geoscientist to capture and access high quality information on demand. To achieve this goal, the business must pay at least as much attention to their work practices and organisational structure as they do to the selection of available solutions.

For mining companies wanting a comprehensive technical solution that supports their individual business requirements, there are a variety of professionally developed, commercial database solutions. These systems may offer all or some of the following enterprise architecture advantages:

- Professionally designed, developed and maintained
- Database hosted by a server based Enterprise Level RDBMS (e.g. Microsoft SQL Server)
- User friendly graphical user interfaces
- Open and persistent data models
- Support for geoscientific data types and interoperability with client systems
- Built-in technology redundancy

MISUSE OF THE HUMBLE SPREADSHEET

One of the most pervasive data management tools available today is the spreadsheet. There is ample evidence from detailed studies to show that error rates in spreadsheets are at levels that would be unacceptable to any organisation, Panko (2005). Despite this, spreadsheets continue to be used in the mining industry for routine data collection and management tasks.

Simply put, spreadsheets are error prone. Very few are created by qualified developers and most organisations lack policies governing their use or development. Many use macros and have links to other spreadsheets or databases and many don't use cell protection. It is common for spreadsheet development to be informal and iterative with extensive revision. Many spreadsheets do not employ modular design principles, and testing with specially designed test data is limited. Many spreadsheets are rushed in development and fewer still are documented.

Why then are they so commonly used? Overconfidence in the accuracy of spreadsheets by the people who create them seems to be one reason why their development appears to be so casual and ubiquitous. Although large levels of overconfidence would seem to be unreasonable, Panko (2005) argues that it is perhaps the most well-established phenomenon in behavioural studies.

Cost and convenience are factors. Selection due to convenience would tend to support informal development controls, whereas cost is a perception problem in as much as businesses may not be convinced of the cost impacts of poor data quality. This is supported by research performed by Eckerson and Sherman (2008) into the main reasons why spreadsheets exist in a range of industries surveyed in North America and Europe. In their ranking, the top five categories were:

1. High degree of local autonomy / control
2. Quick fix to integrating data
3. Inability of the business improvement team to move quickly
4. Low cost option
5. This is the ways it is always done here

Spreadsheets are used due to a perceived lack of viable alternatives.

THE VALUE OF DATA IS MISSING

If mining executives were convinced of the value their own data, then commercial GIMS would be more pervasive than spreadsheets. The fact that this is not the case indicates that many businesses remain unconvinced of the value of their own data or of the costs due to its poor quality. Moseley (2010) reports that in a recent survey by IBM, only 22% of the executive respondents said "data are critical business assets with known value". 27% said "their data are somewhat valuable assets", 16% said "data are an asset with some intrinsic value", 22% said "data are an application resource that always seems broken" and 13% "said data is not even on their radar".

Such analyses indicate that many organisations are content to live in a 'spreadsheet hell' with their inherent disadvantages and are reluctant to adopt a more architectural, enterprise-wide approach. This would seem to indicate therefore that there is a need for more persuasive evidence of direct measures that demonstrate the business value of well managed geoscientific information.

More documented business cases are needed in order to make the connection between people, process and technologies. There is certainly no lack of suitable "war stories" concerning the mismanagement of data in our industry, but very few organisations are prepared air their laundry in public. This then is a challenge for the industry and if embraced; would reflect a growing maturity and understanding of the issues.

THE COST OF DATA QUALITY

The news media is littered with examples of poor quality data causing serious problems. These examples range in scope from lost spacecraft, financial reporting scandals, credit rating errors, military intelligence failures, the unintended release of private information to the public, and the list goes on and on.

These examples demonstrate that data quality is important to all of us and the risks of not getting it right can be higher than we think. Ask yourself the following question. Do poor data management practices occur in my organisation? The logical answer is that it probably does.

Poor quality data can adversely affect businesses on three levels, Operational, Organisational and Strategic, Redman (2008). On an operational level, impacts will be due to the higher cost of production and lower productivity. In a competitive business environment anything that impacts your productivity may erode any competitive advantage you enjoy. On the organisational level, poor data quality can lead to delayed or bad decisions with an attendant increase in risk. It may also affect the trust that other groups place in the data if they need to share it. On the strategic level the affect of poor quality data may be the inability to align people, process and technology within the organisation and make it harder to execute the corporate strategy owing to distracted management attention.

All of these issues have real dollar consequences in both the short, intermediate and longer terms. In addition, there are likely to be significant opportunity costs associated due to inaction or due to the results of poor decisions.

CONCLUSIONS

The original observations and measurements form the basis of all economic and operational decisions made on the future of a mining resource. These data are a business assets and it should be accepted that they be managed like all other significant business asset classes.

For a business to leverage the full value of its data assets, the information must be accurate, accessible, trustworthy, able to be understood, usable and secure. This can be achieved by investing in the people, process and technology components of your business.

People: By far the most important component — technology will never make up for shortcomings in terms or personnel. Data management lacks appeal — raise its profile by understanding and demonstrating its value and importance to the business and investing in the people who collect and manage your data.

Process: Implement rigorous business processes that outline the purpose for the process, have a clear accountability and ownership model, define a standard process and how success of the process can be determined. By having documented and accepted processes, you will minimise the time geoscientists spend using or creating poorly designed data management systems.

Technology: The technology component allows the implementation of the process and makes it accessible and usable by the people — technology does not come first. The technology must be appropriate for the task, support the needs of those who operate it and ensure the accuracy, accessibility, usability and security of the data assets.

These components go hand in hand to ensure the quality of your data. The value of your data to your business goes

beyond the cost of drilling, sampling and assaying — think of the opportunity costs of decisions based on poor quality data.

ACKNOWLEDGEMENTS

The authors would like to thank acQuire for the permission to publish this paper as well as Stephen Alpers and Warren Cook for their helpful comments during the review of the draft.

REFERENCES

- BROOME, J. & COX, S., 2007: Geoscience Information Management and Access: Evolution of a Key Enabler for Exploration Success. *In: Milkereit, 2007: Proceedings of Exploration 07: Fifth Decennial International Conference on Mineral Exploration*, 97–108.
- EKERSON, W. & SHERMAN, R., 2008: Strategies for Managing Spreadmarts, Migrating to a Managed BI Environment, First Quarter 2008 Best Practices Report, TDWI Research. <http://tdwi.org/>
- LACEY, D., 2010: *Improving Data Quality*. Computer Weekly, March 29. http://www.computerweekly.com/blogs/david_lacey/2010/03/imp_roving_data_quality.html
- MOSELEY, M., 2010: The Value of Data, Mastering Data Management, Business Process Management blog, January 21 <http://blog.initiate.com/index.php/2010/01/21/the-value-of-data/>
- PANKO, R., 2005: What We Know About Spreadsheet Errors, University of Hawaii, College of Business Administration, Honolulu, Spreadsheet Research (SSR) Website: <http://panko.shidler.hawaii.edu/SSR/index.htm>
- REDMAN, T. C., 2008: *Data Driven*. Harvard Business Press, Boston.
- WHITING, R., 2006: Hamstrung by Defective Data, Information Week, May 8. <http://www.informationweek.com/news/global-cio/showArticle.jhtml?articleID=187200771>

Abouna Saghafi

A Tier 3 method for estimating fugitive emissions from open cut coal mining: application to Bowen Basin Coalfields

Coal seams and enclosing strata can contain large volumes of methane and carbon dioxide gases which are liberated during mining and post mining. Gas emissions from mining are quantified in terms of specific emission or Emissions Factor (*EF*) which is used in this paper and is the volume of gas (m^3) liberated per tonne of coal mined.

During the last two decades numerous measurement strategies and estimation methods were conceived and applied to coal mines of Hunter and Bowen Basin coalfields. The new proposed method is based on theoretical, laboratory and field measurement work undertaken, particularly during the last decade, to achieve a Tier 3 method of estimation of gas emissions from open cut mining. There are three levels of accuracy associated with estimation of emissions, namely, Tier 1, Tier 2 and Tier 3. Tier 3 is the most accurate method.

The new method considers the coal seams and strata surrounding the mine pit as gas reservoir units which constitute a 'gas release zone'. This zone consists of a column of strata units (layers), starting from the ground surface to a certain depth below the base of mining, affected by coal mining operations. Most gas from the gas release zone is released during mining. In order to assess *EF* value(s) for the mine, the lease is partitioned in a number of gas domains/zones where gas content and gas composition follow a similar pattern (gas content/composition are stationary functions of space). In each gas domain, a limited number of drilling is undertaken to measure the gas content and composition for input to the model. Post mining emissions are also considered in the new method. These are emissions which are produced after mining and during transport and utilisation of coal and would hence form part of the fuel value of coal fired in a power station. These emissions are generally insignificant; however in certain cases the residual gas content can be high and might be required in a carbon constraint economy.

This paper describes the new tier 3 method for gas emissions estimate and its application to a typical open cut coal mine in Bowen Basin.

INTRODUCTION

Coal seams are high capacity gas reservoirs and most coals contain, to some degree, certain volumes of gas. In Australia, at shallow depths (<300 m) the mine gas consists generally of

methane (CH_4) and carbon dioxide (CO_2) but also of nitrogen (N_2).

Mining leads to large disturbance of the coal seam reservoir as the fracturing develops both in coal and rocks. Gas is escaped to the atmosphere via fractures and exposed coal surfaces. The intensity of emissions depends on the flow properties of strata, diffusivity and the matrix permeability of coal. The method of mining affects the extent and density of induced fractures which causes a substantial increase (several orders of magnitude) in the permeability of gas and water. The discharge of water from a mining area leads to a further increase of permeability and acceleration of gas desorption from coal.

CO_2 and CH_4 are greenhouse gases, with CH_4 having high global warming potential (GWP). Its warming potential is evaluated at ~21 to 24 times the potential of CO_2 in terms of mass or ~8 to 9 times in terms of gas volume. However, N_2 is not a greenhouse gas and has a GWP of zero.

The mechanism and sources of emissions from mining are complex. One level of complexity is that most emissions are not sourced from the mined coal seams, but come from other gas bearing strata (including roof and floor seams) in the vicinity of the coal seam mined. This is evidenced by the fact that the volume of emissions is larger by a factor of more than 1 than the *in situ* gas contained in the mined seams. For example, Kissell & others, (1973), who studied the CH_4 emissions for US underground mines, reported that the volumes of gas released from these mines exceeded the *in situ* CH_4 by a factor of 7. For Australian mines, Saghafi & others, (1997) found that this factor to be about 4.

Since early 1990 and following the first IPCC meeting in Washington DC in relation to climate change, CSIRO started investigating methodologies for evaluation of fugitive gas emissions from coal mining which included both underground and open cut mines (Saghafi & Williams, 2002; Williams & Saghafi, 1993; Williams & others, 1996). In developing the models of emissions, the concept of an Emissions Factor (*EF*), or specific emission, was used. The terminology originates from underground mining where specific emission represents the volume of gas released into the coal face for each tonne of coal extracted (see for example Boxho & others., 1980; Creedy, 1993; Creedy & others., 1997). The IPCC (Inter-governmental Panel on Climate Change) has recommended using EF with a tier qualifier.

Tiers present three levels of accuracy, namely tier 1, 2 and 3, with increasing level of accuracy. In this paper the meaning of the three Tiers are as follows,

- Tier 1 *EF* is a generic number for gas emissions from coal mining, Tier 1 numbers are only applied if no data on gas content and emissions are available for the coal basin and country.
- Tier 2 *EF* is used for basin specific emissions. This *EF* value is an average number for one or several basins.
- Tier 3 *EF* is mine specific. It is the emission factor determined by measuring emissions from an individual mine and is therefore the most accurate (see for example the IPCC 2006 report for more official definition of these terms).

In the following sections, after a brief history of the evolution of the method of measurement, the details of the new method and its application to a typical mine in the Bowen Basin are presented.

EVOLUTION OF METHODS OF ESTIMATION OF EMISSIONS FROM COAL MINING IN AUSTRALIA

In the last two decades, several studies have been undertaken in the coalfields of eastern Australia to develop a method for evaluation of emissions from coal mining.

The studies started with a global emission measurement approach. This consisted of measuring plumes for one or several mines in order to determine an average *EF* for a conglomerate of mines. Global measurement of emission undertaken during several campaigns in open cut mines Sydney and Bowen Basins in the early 1990s (Saghafi & Williams, 1992; Williams & others, 1993).

The method of measurement was based on established air pollution techniques. The devised methods assumed a crosswind profile for a CH₄ plume emitted from the mine (number of mines if they were to be measured together). Wind speed was measured directly as well as the concentration of gases in the plume which were measured using a vehicle fitted with instruments (Figure 1).

Assuming a width of w and a height of h for the plume, the mine emissions rate (Q) can be calculated as follows,

$$Q = chwv$$

where c is the CH₄ concentration and v is the wind speed. A vehicle was driven crosswind along available public access roads in proximity to the mine lease.

This work was undertaken at 10 mines in the Bowen Basin and 7 mines in the Sydney Basin (Hunter Coalfield). It led to the definition and quantification of two emission factors for these coal basins. For the Bowen Basin an average emission factor of 1.2 m³/t was calculated (1.2 m³ of CH₄ is emitted if one

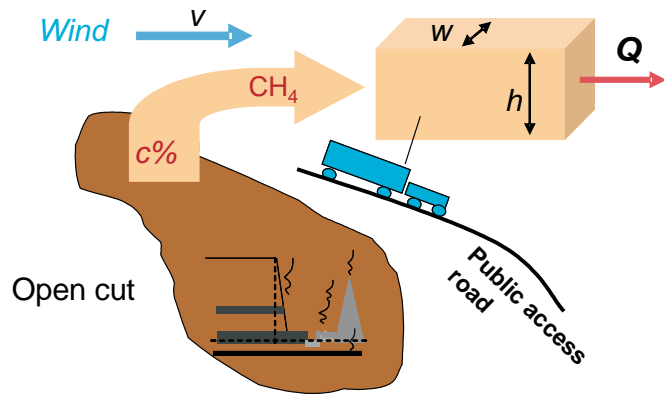


Figure 1: Direct mine emissions measurement using an air pollution technique

tonne of coal is produced), whereas for the Hunter Valley, the average *EF* was calculated to be about 3.2 m³/t. According to the IPCC definition, these factors can be qualified as being coal basin specific and, therefore, they have the accuracy of a Tier 2 method. It should be noted that the measurement of emissions concerned only CH₄ emissions and the volume of possible CO₂ emissions were not included in these numbers. These numbers were in use by the Australian open cuts as their default *EF*s for estimation of their emissions.

In Figure 2, the emissions data measured during the CSIRO field investigation campaign of 1990–1992 in the Bowen Basin are shown. The 10 mines for which the measurement of emissions were undertaken produced between 4 to 12.5 Mt (million tonne) of coal per year. In 1992 the total coal production from these 10 mines was about 68 Mt. The *EF* for individual mines was calculated by dividing the measured emissions from plumes by the mine's production. The

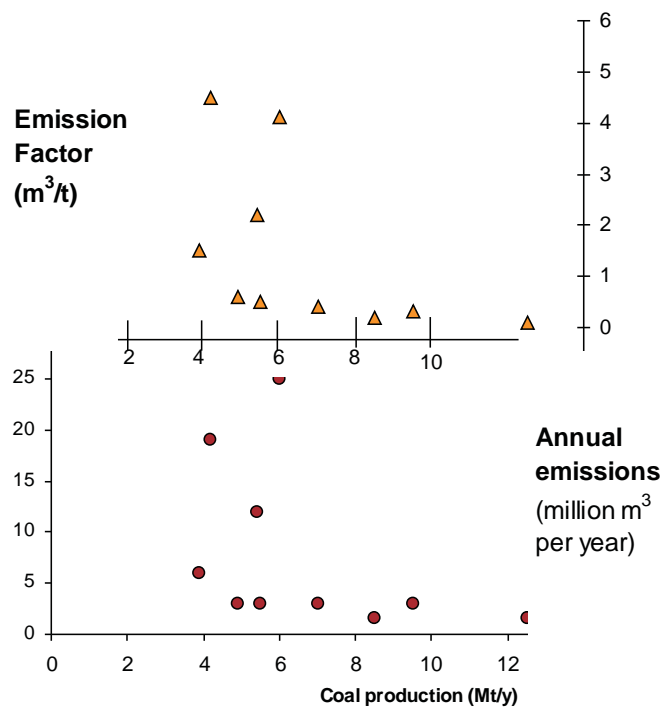


Figure 2: Measured emissions from 10 open cut coal mines of Queensland, CSIRO campaign of 1990–92 (Saghafi & Williams, 1992; Saghafi, 2008)

calculated *EFs* varied from about 0.1m³/t to about 4.5m³/t. The average *EF* of 1.2m³/t for Bowen Basin mines was obtained by adding all emissions and dividing this total by the total coal production from these mines.

Surface emission measurement

Though global emissions from one mine or a number of mines could be obtained from air pollution techniques, this approach was abandoned as they proved to be costly, complex and time dependent. This is because suitable environmental and metrological conditions are required to undertake the measurements. The results were also uncertain as they were very sensitive to meteorological conditions and to assumptions on the shape of the plume and the origin of the emissions. These issues prevented the follow up of the work and further development of the air pollution methodology.

Consequently, more local methods of measurements were designed and applied to coal mines. Methods such as local surface measurement of emissions were introduced. These methods used chamber techniques that were used previously in the study of spontaneous combustion of coal and spoil in open cut mines (for example, see Carras & others, 2000). The results were promising (Saghafi & others, 1995). However, these techniques were also found to be difficult to apply, mainly because of the requirements for staff and equipment to be present at the site of measurement. In many areas of a mine, access is prohibited and safety or production requirements make spot measurements of emissions impossible. However, some important insights were gained through measurement of gas emitted from uncovered and blasted coal.

Since the early 2000s, with funds from CSIRO and ACARP, three major studies have been undertaken to develop a Tier 3 method for estimation of gas emissions from a reservoir point of view of coal and strata in open cut mining (Saghafi & others, 2003; Saghafi & others, 2004; Saghafi, 2008). The aim of this research has been to develop mine-specific (Tier 3) methods whereby the emission factor specific to a mine can be quantified.

DESCRIPTION OF THE NEW TIER 3 METHOD OF MINE EMISSION ESTIMATE

As discussed, the new method the concept of coal and strata as a gas reservoir is used. Coal seams and gas bearing strata initially contain all gas which would be emitted during mining and post-mining. This approach assumes that:

- the total volume of emissions (during and post mining) is equal to the volume of gas initially trapped in the reservoir, and
- assuming the mine advances at a regular pace (over the life of mining), then the annual emission rate from mine is equal to the volume of gas contained in a

‘slice’, or column, of the reservoir removed or fractured during mining.

The approach is illustrated in Figure 3, it assumes,

$$Q = q_1 + q_2 + \dots + q_n \tag{2}$$

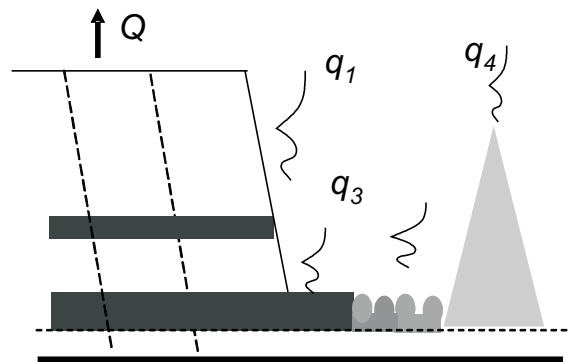


Figure 3. The emissions from various source equals gas contained in a ‘slice’ prior to mining

where *q*₁ to *q*_{*n*} are emissions from various locations such as the highwall, uncovered coal seams, blasted coal, spoil pile and other products in the chain of mining.

It is assumed that coal mining causes the release of seam gas from this column, spanning over the whole height of the overburden (*h*) and to some extra depth (*δh*) into the floor of the pit (Figure 4).

The column is compartmentalised into a number of sedimentary ‘horizon/layer’ units in the overburden and in the underburden (floor of the pit), each with a different gas volume stored and different capacity to hold gas. While all gas bearing layers in the overburden release their totality of gas, the gas bearing layers in the underburden might release only part of their initial gas, depending on their position below the pit base. In this new Tier 3 model, the column of strata above and below the mine pit is called the ‘gas release zone’ or ‘gas emission zone’. In this zone, the release of gas is largely enhanced by mining induced fracturing and the discharge of ground water from the highwall.

Using the new Tier 3 method of estimation requires that a map of the stratigraphic column in the mine lease is built. The stratigraphic column should comprise all sedimentary units including coal seams in the overburden and underburden to depth of *δh* below the deepest pit. In this model, the column of strata is divided into a number of layers. Each layer corresponds to a different emissions regime. A simple way of identifying various layers is to delineate them according to the type of material which they contain. A refinement of the layering strategy is to subdivide them further according to their gas content and/or their gas composition. In Figure 4, the layers are identified based on the type of material.

The total gas volume (*g_i*) contained in layer *i* is,

$$g_i = c_i \rho_i h_i \tag{3}$$

where *c_i*, *ρ_i* and *h_i* are gas content (or *in situ* gas content minus residual content if post mining emissions should be

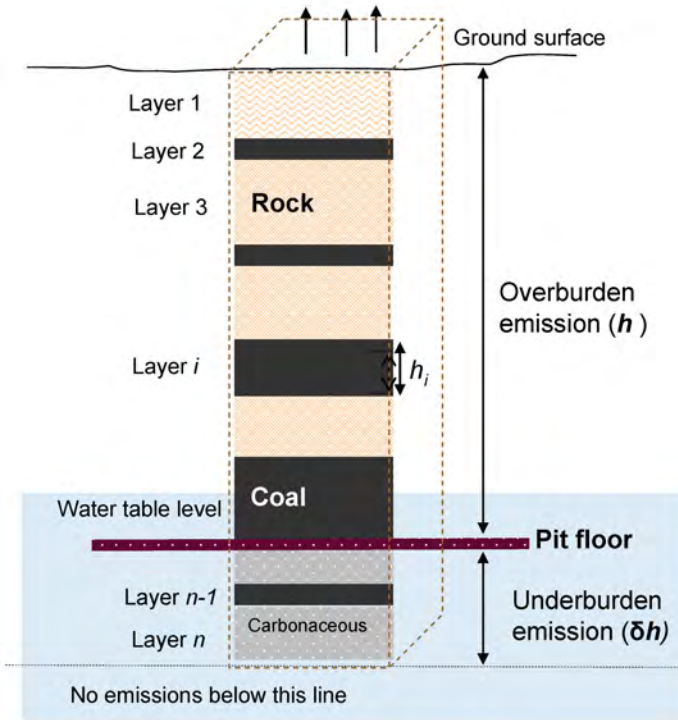


Figure 4. Gas release zone is divided into n layers each with different gas content and thickness (modified from Saghafi, 2008).

considered separate entities), density and thickness of layer i . Emissions of gas from this layer may be complete or partial. It can be assumed that the overburden layers release the totality of their gas during mining. The underburden layers, however, may only partially release their gas. This is expressed by multiplying the volume of gas in place by an emission coefficient (β). The gas emitted for layer i is:

$$q_i = \beta_i c_i \rho_i h_i \quad (4)$$

Assuming that data on gas content, density and thickness are available, the emissions from individual each layers are calculated using Equation (4). Then, all individual emissions are summed up to deliver the total site specific emissions.

$$Q = \sum_1^n q_i \quad (5)$$

The emission has the unit of *volume of gas emitted per unit area of the ground* (in m^3/m^2) which can be called the 'surface emission factor'. This is a useful way of quantifying emissions. Once an average value for the surface emission factor in a mine lease or a gas zone is established, the total emissions can be estimated by multiplying Q by the area of ground which would be mined over a year. Specific emission, or emission factor, is commonly expressed in terms of *volume of gas per tonne of coal produced*. The production of coal from an individual layer is,

$$p_i = \alpha_i \rho_i h_i \quad (6)$$

The coefficient α , which is called the 'production coefficient', takes on a value of either 1.0 or 0. If the layer is a coal horizon and is mined $\alpha = 1$. Otherwise, if the layer is spoiled

$\alpha = 0$. As for emissions, all individual productions are also added up to estimate the *total coal production per unit ground surface area* (t/m^2).

$$P = \sum p_i \quad (7)$$

Finally the emission factor (EF) for the specific site is,

$$EF = \frac{Q}{P} \quad (8)$$

The model is easily amenable to a spreadsheet calculation. The input data are gas content, composition, thickness, density and emission coefficient for various layers. Gas content and composition are the primary parameters to be considered. The emission coefficient β takes on a value of 1 for overburden layers. For underburden, a linear relation with depth can be considered where $\beta = 1$ at the base of the pit and zero at a distance δh below the base. However, if the maximum level of emissions is required then β is assigned the value of 1 for all layers.

Parameter β and residual gas content

The emission coefficient, β , presented in the last section is also an indicator of the residual gas content which remains in coal post-mining. Residual gas content and parameter β are related as follows:

$$\beta = 1 - \frac{c_r}{c_i} \quad (9)$$

where c_r is the residual gas content and c_i is the initial gas content of layer i .

In cases where carbon taxes are applied not only to producers but also to coal users, the residual gas content must be quantified and used in calculation.

Emissions in terms of CO_2 equivalent

For greenhouse gas inventory purposes, gas emissions are generally presented in terms of CO_2 equivalent ($\text{CO}_2\text{-e}$). The CH_4 emissions are converted to $\text{CO}_2\text{-e}$ by multiplying its value by the greenhouse warming potential (GWP_{CH_4}). We assume that the GWP for CH_4 on a volume base is about 8.36. Note that in terms of mass base the GWP for CH_4 would be about 21. In order to convert the mixed emissions to emissions in terms of CO_2 equivalent ($\text{CO}_2\text{-e}$), the following relation can be used,

$$Q_{\text{CO}_2\text{-e}} = \frac{\text{CO}_2\% + \text{CH}_4\% \text{GWP}_{\text{CH}_4}}{100} Q \quad (10)$$

In Equation (10), $\text{CO}_2\%$ is the concentration of CO_2 in volume per cent, $\text{CH}_4\%$ is the concentration of CH_4 and GWP_{CH_4} is the global warming potential of CH_4 . Note that it is assumed that the greenhouse gases emitted from coal seams in open cut mines are basically CO_2 and CH_4 and no higher hydrocarbon gases are emitted.

In this model, an important concept is the 'layer'. Each layer is an individual gas reservoir with a different emission regime. For instance, a gas bearing coal layer can also contain thin

bands of rock and other carbonaceous material. Similarly, a rock layer may contain thin bands of coal. The layers are characterised by their thickness, density, gas content and composition.

Input data required for the Tier 3 model

As discussed, the assumption is that gas is released from gas release zone which also includes the mine floor. The primary data required is the *in situ* gas content of coal and carbonaceous rocks contained within the gas release zone prior to mining. Other data are the thickness and density of coal and rock layers. Gas composition is important as the GWP of CH₄ is much higher than CO₂.

Gas content of coal should be measured directly by using the standard gas content testing method (Australian Standards, 1998). For coal mines where mixed gas conditions dominate, the fast desorption method is preferable. It reduces the risk of underestimation of CO₂ content and errors of gas composition determination (for example, see Saghafī, 1998).

For rock horizons, the direct measurement of gas content is almost impossible as most gas is free gas. Maximum gas content can be estimated by measuring the rock porosity and assuming a certain level of pore water saturation exists.

APPLICATION OF THE NEW MODEL TO A BOWEN BASIN MINE

In this section, we use the Tier 3 model to estimate emissions from a relatively gassy mine in the Bowen Basin where the pit base depth would be about 110m. There are four seams in total, where Seam 1, 2 and 3 are to be mined, while the relatively thinner Seam 4 which is at about 117m below the surface would not be mined. The first step is to divide the column (gas release zone) into layers (Table 1). Emission layers in this example are basically the lithological units.

The next step is to obtain gas content, gas composition and density for the emission layers. In Table 2, the measured data and other parameters of the model are presented. As discussed in previous sections, other parameters required are production coefficient and emission coefficient for various layers. All non-coal layers would have a production coefficient of zero ($\alpha = 0$) while the coal production layers have values of 1 ($\alpha = 1$) and the ones which are not mined are given a value of 0. In this example all coal seams in overburden are mined ($\alpha = 1$) whereas the coal seam in the underburden is not mined ($\alpha = 0$). The Emission coefficient β for layers in the overburden takes on a value of 1.0 indicating that all gas is released during mining. In the underburden, the value of β is assumed to follow a linear function of depth (gas is partially released).

The data for this example mine (given in Table 2) can be implemented in a spreadsheet where *EF* and other emission quantities are calculated using the relationship presented in this paper. Note that the emission coefficient in underburden reduces linearly with depth. No gas is emitted from strata and coal seams located more than 20 m below the base of the mine ($\delta h = 20\text{m}$). In Figure 5, an image of the spreadsheet calculation is shown.

As shown in Figure 5 both CO₂ and CH₄ emissions are calculated separately, i.e., $EF_{CO_2} = 0.09\text{m}^3/\text{t}$ and $EF_{CH_4} = 4.62\text{m}^3/\text{t}$.

In terms of emissions per m² of ground surface the results are $Q_{CO_2} = 1.53\text{m}^3/\text{m}^2$ and $Q_{CH_4} = 78.24\text{m}^3/\text{m}^2$.

As discussed, for greenhouse gas inventory purposes, emissions should be expressed in terms of CO₂-e emissions. Therefore, the emission factor for this mine in terms of CO₂-e would be:

$$EF_{CO_2-e} = 0.09 + 8.36 \times 4.62 = 38.70\text{m}^3/\text{t}.$$

Table 1: Well Logging data are used to layer the gas release zone in emission units

Emission Layer	Material	Position and thickness of each layer (m)			
		Top	Bottom	Mid depth	Thickness
1	Sandstone	30.54	43.07	36.81	12.53
2	Seam 1	43.07	44.74	43.91	1.67
3	Siltstone, sandstone and shale	44.97	67.96	56.47	22.99
4	Seam 2	68.06	69.57	68.82	1.51
5	Siltstone with carbonaceous bands	70.15	108.53	89.34	38.38
6	Seam 3	108.53	111.61	110.07	3.08
Pit floor					
7	Sandstone and siltstone with coal patches	113.05	116.50	114.78	3.45
8	Seam 4	116.52	117.40	116.96	0.88
9	Siltstone	120.10	126.51	123.31	6.41

Table 2: Input data for calculation of emissions

Emission layer		Attributes of each layer (model input data)					
Layer	Nature of the layer	Thickness (m)	Density (t/m ³)	Gas content (m ³ /t)	CH ₄ /[CH ₄ +CO ₂]	Production coeff. α	Emission coeff. β
1	Sandstone	1.00	2.53	0.02	0.90	0	1.00
2	Seam 1	2.00	1.49	0.26	0.90	1	1.00
3	Siltstone, sandstone and shale	3.00	2.28	0.05	0.95	0	1.00
4	Seam 2	4.00	1.39	1.35	0.95	1	1.00
5	Siltstone with carbonaceous bands	5.00	2.30	0.10	0.98	0	1.00
6	Seam 3	6.00	1.40	4.00	0.98	1	1.00
Pit floor							
7	Sandstone and siltstone with coal patches	7.00	2.40	0.11	0.99	0	0.76
8	Seam 4	8.00	1.35	3.00	0.99	0	0.71
9	Siltstone	9.00	2.60	0.09	0.99	0	0.26

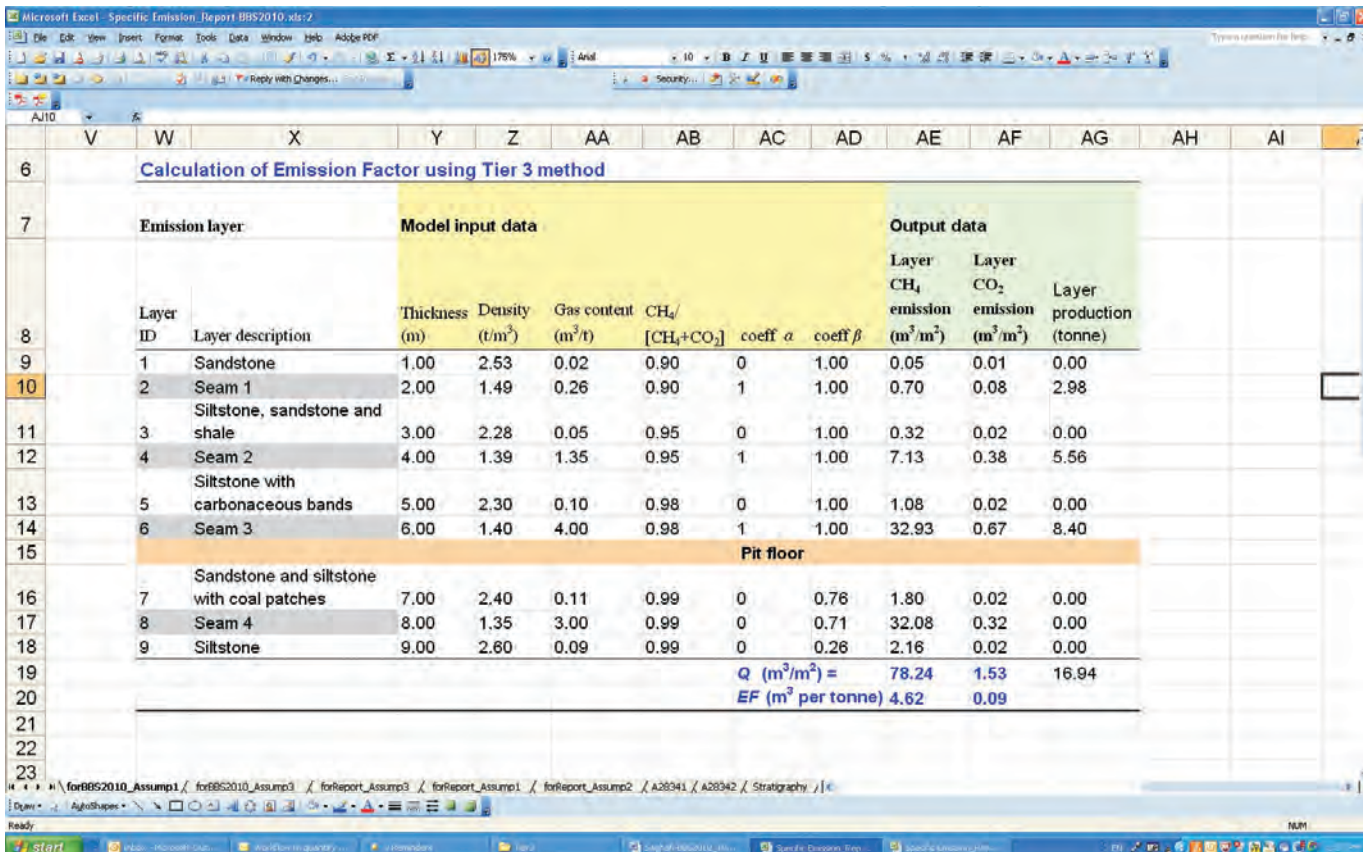


Figure 5. Image of spreadsheet calculation of emission factor for a Bowen Basin mine

GAS ZONE AND GAS DOMAIN CONCEPTS

The data required for this method needs to be measured by drilling a limited number of core holes within the mine lease prior to mining. For this purpose, the mine lease should be divided into a number of regions where the functions defining the main input of the model, such as gas content and composition, are spatially stationary. In other words, *gas content and composition versus depth* do not change significantly within that region. In this paper, these regions are termed ‘gas zones’. Within each gas zone, at least one borehole should be drilled to determine the main parameter of the model required for the calculation of *EF*.

Note that the concept of gas zone used in this method is not necessarily identical to geological domains. The latter delineate a region based on local structural geology and might enclose several gas zones. The main purpose of the concept of gas zone is that, within such zones, a single *EF* value could be used. Therefore, the major identifiers of gas zone are those properties (variables) which strongly affect the value of *EF*. The identifier can be *gas content versus depth* where there is a single gas present or CH₄ is strongly dominant. However, in mixed gas conditions, *gas composition* could be the major identifier of the gas zone (see Figure 6). In very low gas content mines, other properties such as *coal thickness* or *gas saturation* could be the identifiers of gas zones.

Hence, the first step in the evaluation of *EF* is to divide the mine lease into geological compartments (domains), and then try to build the gas zones based on these domains. Direct measurement of the gas composition and content of coal collected from blasted coals can be helpful in an initial delineation of gas zones which can be supplemented by data on previous exploration drilling and hydrological tests (such

as piezometry) within the lease. Note that a gas zone can be delineated vertically as well in a three dimensional volume.

Once gas zones are identified, gas drilling could be undertaken to collect the necessary coal and rock samples. The samples should correspond to the layers in the ‘gas release zone’ in the model. One or two core boreholes may be drilled in each gas zone. These boreholes can be part of the routine exploration program, which reduces the overall cost of *EF* estimates.

Gas zone based on CO₂-e pattern

The most important parameters of the model are the *in situ* gas content and gas composition. Though the rate and intensity of gas release from mining at a given time is primarily a function of the temporal gas content and flow properties of coal and strata, the total volume of gas liberated over the life of mine is a function of the virgin, pre-mining magnitude of gas content of coal seams and gas trapping strata.

COST OF EMISSIONS ESTIMATE USING THE MEW METHOD

The cost of determination of *EF* depends on the level of accuracy required (or degree of uncertainty allowed). More accurate results, however, do not imply more boreholes and more samples are required. A suitable strategy for applying the method should be sought to both reduce the cost and increase accuracy. The main cost involved is the core drilling. This cost can be reduced by correctly delineating the mine lease in gas zones prior to core drilling so that the number of gas boreholes is reduced. The drilling cost can be further reduced by including the gas drilling in the routine

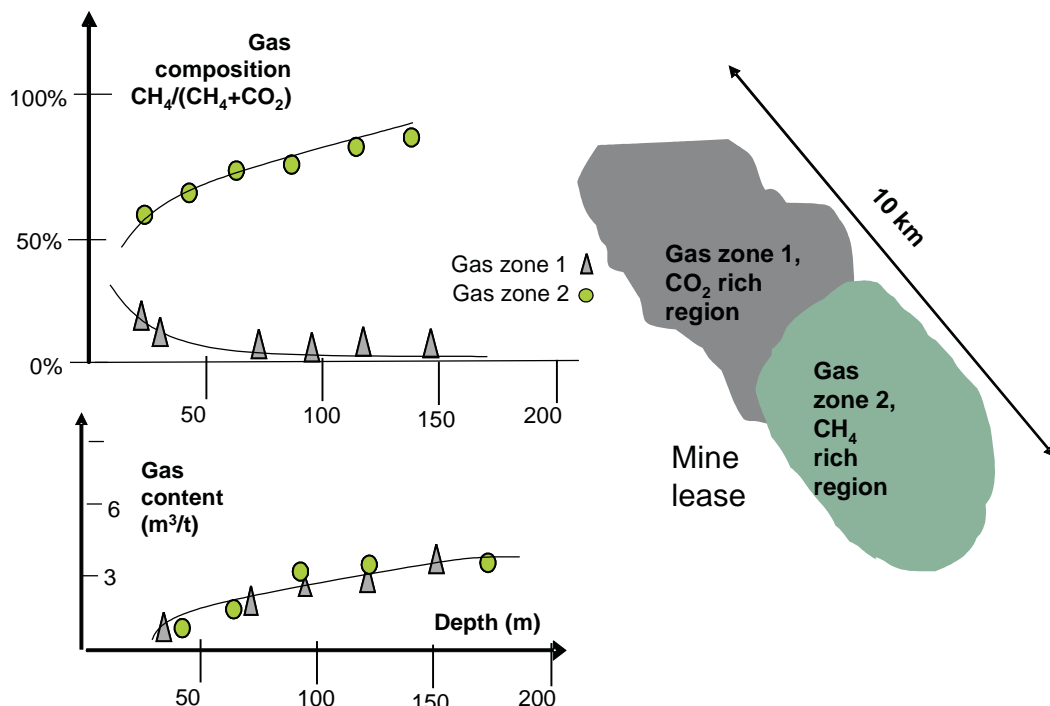


Figure 6. Mines are divided into a number of gas zones where gas composition and gas contents, follow similar patterns with respect to depth.

exploration drilling program. For example, in one drilling program, when emissions-determination drilling was combined with routine exploration drilling, the cost of an equivalent stand-alone emissions determination program was reduced to about 50%.

Other costs involved in EF determination are field sampling and laboratory measurements of gas content and composition. The number of coal samples required depends on the number of coal seams and vertical variability of gas content and composition along the gas release zone. For instance, in some locations in Hunter coalfield there are a multitude of coal seams at shallow depths, each made of numerous splits. If all the splits had to be measured then the cost could be high. In these conditions one strategy could be to combine several thin sections in a single sample to reduce the cost. Furthermore, for thin interburden seams enclosed between two thicker seams, the gas content and composition may be determined by interpolation of the data from these adjacent thicker seams.

At the time of writing this report, investigations were being undertaken (by CSIRO and ACARP) to devise methods of estimation of gas content and other gas parameters in order to reduce the number of samples from a borehole.

CONCLUSIONS

A working Tier 3 model for estimation of coal seam gas emissions from open-cut mining is proposed which should replace the current Tier 2 Emission Factors for Australian open-cuts. The main inputs for the model are gas content and gas composition of coal seams and carbonaceous rocks within the overburden, and within that part of the underburden extending to a certain distance below the base of the pit. The main data should come from direct desorption measurement of core samples collected from a limited number of core drilling in the lease prior to mining.

In order to reduce the number of drilling, it is suggested that the mining area be partitioned in a number of 'gas zones'. *Gas content versus distance* can be a primary identifier of these zones. In mixed gas conditions, gas composition might be the primary identifier of gas zones. The cost of drilling can be reduced by including gas drilling in routine mine exploration drilling programs.

ACKNOWLEDGEMENTS

The author wishes to thank CSIRO and ACARP for providing the necessary funds to undertake this research. The in-kind support provided by numerous coal mines in NSW and Queensland is gratefully acknowledged. I shall also acknowledge the contribution of many of CSIRO staff to the field and laboratory work which was vital for developing the Tier 3 model.

REFERENCES

- AUSTRALIAN STANDARD, AS 3980-1999, 1999: *Guide to the determination of gas content of coal seams - Direct Desorption Method*. Standards Australia.
- BOXHO, J., STASSEN, P., MUCKE, G., NOACK, K., JEGER, C., LESCHER, L., BROWNING, E.J., DUNMORE, R. & MORRIS, I.H., 1980: *Firedamp drainage handbook for the coal mining industry in the European Community*. Coal Directorate of the Commission of the European Communities, Verlag Gluckauf, Essen.
- CARRAS, J.N., DAY, S., SAGHAFI, A. & WILLIAMS, D.J., 2000: Measurement of greenhouse gas emissions from spontaneous combustion in open cut coal mining. ACARP project C8059.
- CREEDY, D.P., 1993: Methane emissions from coal related sources. *Chemosphere*, **26**, 419-439.
- CREEDY, D.P., SAGHAFI, A. & LAMA, R.D., 1997: *Gas Control in Underground Coal Mining*, IEA CR/91, London, UK. IEA Coal Research.
- IPCC, 2006: *IPCC Guidelines for National Greenhouse Gas Inventories, Volume 2, Energy*. NGGIP Publications. Also available at: <http://www.ipcc-nggip.iges.or.jp/public/2006gl/vol2.html>
- KISSELL, F.N., McCULLOCH, C.M. & ELDER, C.H., 1973: The direct method of determining methane content of coalbeds for ventilation design. *U.S. Department of the Interior, Bureau of Mines RI 7767*, NTIS No. PB221628.
- SAGHAFI, A. & WILLIAMS, D.J., 1992: Estimation of methane emission from Australian coal mines. *Symposium on Coalbed Methane Research and Development in Australia, Townsville, Australia*, **5**, 7-13.
- SAGHAFI, A., WILLIAMS, D.J. & LAMA, R.D., 1997: Worldwide methane emissions from underground coal mining. In: Ramani, R.V., (Editor): *Proceedings of the Sixth International Mine Ventilation Congress, Pittsburgh, PA, USA, May 17-22, Society for Mining, Metallurgy, and Exploration, Inc.*
- SAGHAFI, A., WILLIAMS, D.J. & BATTINO, S., 1998: Accuracy of measurement of gas content of coal using rapid crushing techniques: In: *Proceedings of the 1st Australian Coal Operators Conference COAL '98, 18-20 February, Wollongong, Australia*, 551-559, also available from <http://ro.uow.edu.au/coal/273/>
- SAGHAFI, A., DAY, S., WILLIAMS, D.J., ROBERTS, D.B., QUINTANAR, A. & CARRAS, J.N., 2003: Toward the Development of an Improved Methodology for Estimating Fugitive Seam Gas Emissions from Open Cut Mining. ACARP Project C9063.
- SAGHAFI, A., DAY, S.J., FRY, R., QUINTANAR, A., ROBERTS, D., WILLIAMS, D.J. & CARRAS, J.N., 2004: Development of an improved methodology for Estimation of Fugitive Seam Gas Emissions from Open Cut Mining: ACARP Project C1207.
- SAGHAFI, A., DAY, S.J., & CARRAS, J.N., 2005: Gas properties of shallow Bowen Basin coal seams and gas leaks to the atmosphere. In: Beeston, J.W. (Editor): *Bowen Basin Symposium 2005: The Future for Coal: Fuel for Thought: Proceedings, Yeppoon, Qld. Geological Society of Australia Coal Geology Group and the Bowen Basin Geologists Group*, 12-14 October, Qld, Australia, 267-271.

- SAGHAFI, A., ROBERTS, D.B., FRY, R.F., QUINTANAR, A., DAY, S.J., LANGE, T., HOARAU, P. & DOKUMCU, C., 2008: Evaluating a Tier 3 Method for Estimating Fugitive Emissions from Open-cut Coal Mining. ET/IR 1011R, ACARP Project C15076.
- WILLIAMS, D. J., SAGHAFI, A. & LAMA, R., D., 1996: Methane emissions from coal mining. *IEA Greenhouse Gas R&D Programme, Report Number PH2/5, June 1996.*
- WILLIAMS, D.J. & SAGHAFI, A., 1993: Methane emissions from coal mining - A prospective. *The Coal Journal*, **41**, 37–40.

Scott Thomson

Gas layering in the subsurface: implications for greenhouse gas emissions

Recent work has established that gas distribution in subsurface layers follows predictable patterns that have proven to be repeatable throughout many Australian basins. This pattern is a response to tectonic history, the coalification process, biogenesis, groundwater flow and magmatic activity.

This paper identifies the drivers behind variability in gas character in the subsurface, and develops a generalised model that can be used to better understand, and predict gas layering for greenhouse gas (GHG) emission accounting purposes.

The implications of this study are important to open cut mining operations because it provides a firm basis for estimating GHG emissions for National Greenhouse Emissions Report (NGER) accounting purposes. The model can also be applied to economic studies of the incremental worth of coal extraction as gas content increases with depth. The model also has implications for underground mining outburst risk analysis.

INTRODUCTION

The Australian government has developed a national greenhouse reporting scheme that attempts to account for greenhouse emissions across a range of industries. This scheme is incorporated in law through the National Greenhouse and Energy Reporting Act 2007, and the National Greenhouse and Energy Reporting Determination (Measurement) 2008. The ultimate aim is for emission intensive industries to pay a financial penalty which is directly proportional to the amount of gas they release into the atmosphere.

For most industrial and mining activities in Australia, emissions can be directly measured, and this is acknowledged to be essentially the case for underground coal mining (by measuring emissions in the ventilation system, and through the pipe range associated with gas drainage activities). For open cut mining, measuring emissions appears to be much more problematic.

Firstly, open cut miners have (historically) very little actual gas data from their operations and in the past, have had no incentive to gather such data. Secondly, the measurement of actual emissions via empirical techniques (i.e. “sniffers”) is inherently inaccurate. Thirdly, the true story is a complex one exacerbated by gas character variability in the near subsurface which is a product of geological history, and the near term

effects of mining itself. Fourthly, the accurate measurement of low gas content samples is problematic.

The issue of accurately measuring, calculating (and reporting) emissions is currently resulting in a flurry of industry activity, and no fewer than four (4) current ACARP projects are grappling with various aspects of the uncertainty associated with open cut emission accounting at time of writing. A key aspect of these programs is aimed at understanding laboratory error associated with low gas content sampling, and the establishment of guidelines for future sampling.

CURRENT WEAKNESSES IN SAMPLING FOR GREENHOUSE EMISSIONS

The major concerns relating to the accurate measurement of greenhouse emissions from open cut operations pertains to the following uncertainties:

- How accurate is the ‘gas content’ result obtained from actual sampling?
- Is the error bar significantly greater for low gas content samples than high ones? If so, by how much?
- How do we accurately measure gas content in non-coal units, in particular porous sandstones?
- How do we deal with gas compositional data that in many cases is clearly contaminated by air?
- How much sampling is enough?
- How do we account for fluid and gas migration from lower seams, and from areas outside the boundary of the mine?
- How much does the mine itself impact subsurface gas character?

There are a range of nuances associated with low gas content sampling that are the subject of intense research, experimental work, and considered debate. Resolution of many of these questions should be obtained by the successful completion of ACARP research work over the next 12-18 months.

The purpose of this paper is not to attempt to prejudge the outcome of this research, but to provide a universal model that explains variability in the subsurface, and to also offer some suggestions as to how this model can be applied to provide a practical solution to greenhouse gas accounting.

THE MODEL – WHY GAS CHARACTER VARIES IN THE SHALLOW SUBSURFACE

The definition of 'shallow subsurface' here reflects current expectations of the depth of open cut operations, around 300m from surface, however many of the observations contained herein are equally relevant to understanding gas variation in underground mining operations also. By extension, this general model also applies to Coal Seam Gas (CSG) plays, and is pertinent to exploration strategy in the CSG industry (see Thomson, 2008).

The fact that gas character varies in the subsurface is well documented (for example, see Scott & others, 1994, Faiz & others, 2003, Faiz & Henry, 2006, and Thomson & others, 2008). In some cases, open cut operations may contain very little gas at all, and others clearly have a considerable emission footprint. So, what governs the variability? First, it is important to describe what kind of variability there may be.

Variation in gas content

Gas content ostensibly increases with depth. This "truism" is correct, and as a generalisation all coals should show some increase in gas content with depth, however this increase is unlikely to be uniform. The increase in gas content with depth is a direct response to increased reservoir pressure, and an accompanying increase in gas holding capacity for any given coal (coals of the same rank). Effectively, coals obey their isotherm, and as pressure (depth) increases, they store more gas.

So, this simple theoretical relationship should provide the means to predict the gas holding capacity of any given coal. In reality, it rarely does, and this is a function of the extent of gas saturation any given coal may have. If a coal is a 100% saturated, it follows the isotherm. If a coal is undersaturated, the extent of undersaturation will govern the gas content. Other complicating factors include maceral variability, and changes to ash and moisture — all of which will influence the gas holding capacity.

Most near surface coals in the Sydney-Bowen Basin complex are undersaturated. They are undersaturated as a function of their geological history, or as a near term response to the march of a neighbouring open cut operation. Extent of undersaturation significantly adds to the complexity of gas content prediction in the subsurface.

Variation in gas composition

The major coal seam gases found in the near subsurface are effectively CH₄ (methane) and CO₂ (carbon dioxide). Minor amounts of N₂ (nitrogen) and H₂S (Hydrogen Sulphide) may also be present, but are not generally significant. N₂ is a troublesome gas for accurate reporting of gas composition because it is present in substantial quantities in air. N₂ values in gas compositional data above 6% by volume should

generally be treated with suspicion. Results >20% strongly suggest at least some air contamination.

The story is further complicated by the fact that there are two types of methane, isotopically heavy thermogenic methane formed during the coalification process, and the lighter version, formed from biogenic action.

Most of the CO₂ in Australian coals is a by-product of ancient magmatism, and in some areas CO₂ is very significant. In others, there is no CO₂ at all.

The interplay between biogenic and thermogenic methane, and magmatic CO₂ is central to understanding greenhouse emissions in the shallow subsurface.

The model for gas variation in the subsurface

Thomson & others (2008), using data from a Hunter Valley mining operation proposed a model for gas layering that occurred in the subsurface (Figures 1 and 2). For additional context, refer to Hennings & others, 2007.

- Zone 1 — A surface zone extending to a depth of about 150m, which contains negligible gas. The gas that is present is often CO₂. This gas may be present simply due to the 'residual' effect. CO₂, due to its molecular size and affinity with coal, can be very difficult to entirely remove.
- Zone 2 — the 'Biogenic Window' containing shallow methane and extending from a depth of approximately 150m to about 250–350m. The gas content of this zone is usually from 4–12m³/t and increases with depth.
- Zone 3 — A 'Mixed Gas Zone' below Zone 2 and extending to a depth of approximately 600–700m. The gases in this zone are both methane and CO₂ but mostly CO₂.
- Zone 4 — the 'Thermogenic Zone' of high methane below Zone 3.

It is argued herein that the example presented in Thomson & others (2008) occurs consistently, but to varying extents throughout the Eastern Australian coalfields, and not just the Permian ones. The interplay between biogenic and

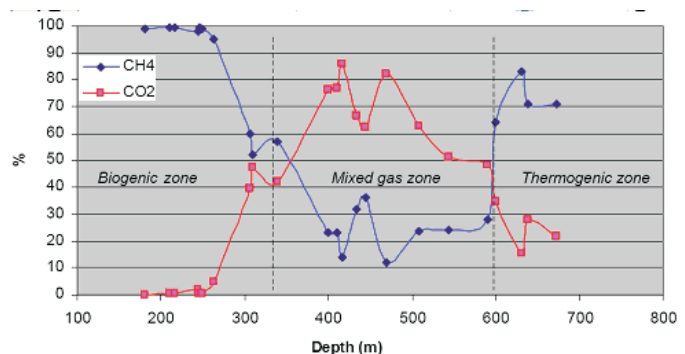


Figure 1: The gas layering present in the subsurface at one Hunter Valley operation (from Thomson & others, 2008). Note relationship between methane and CO₂ with depth, as presented in the upper diagram. As depth increases the influence of CO₂ waxes, then finally, wanes.

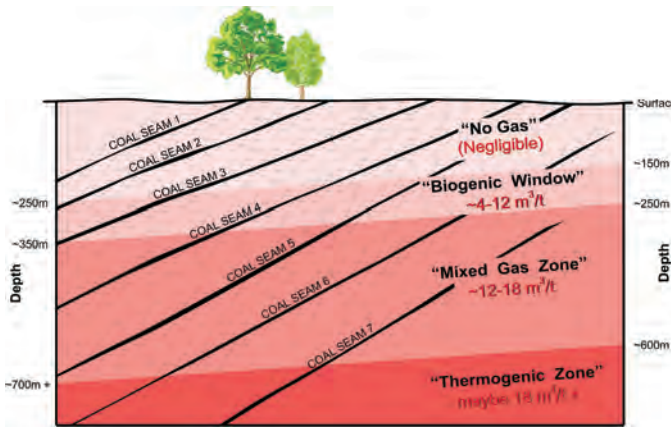


Figure 2: A schematic representation of the gas layering present in the subsurface in a Hunter Valley example (from Thomson & others, 2008). Note that layering is seam independent, and has occurred post-tilting, indicating that the drivers behind the layering postdate the tilting event.

thermogenic methane, and magmatic CO_2 governs subsurface variability, and equally applies to many other Australian basins. Similarly, in the author's experience, the same pattern is evident in many overseas fields. In the end, geological processes are universal.

For more specific details from the Hunter Valley example refer to the original paper, Thomson & others, (2008).

It is argued herein that variants of this same model are present in all the major Australian basins, and this is directly relevant to open cut emission accounting. Sometimes CO_2 is not present at all, and sometimes thermogenic methane gas dominates. For most open cut operations, biogenic methane is the major subsurface gas, and the major contributor to greenhouse emissions.

An example of a variant of the model, with no CO_2 present is presented in Figure 3. This schematic example is based on actual data from a mine site in the Sydney – Bowen Basin complex.

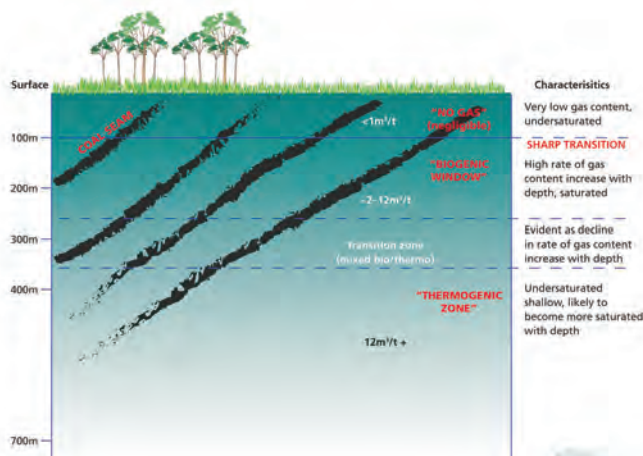


Figure 3: An example of essentially the same, but slightly nuanced, model as Figure 2 — from a widely disparate region, with the notable exception of a lack of CO_2 in the subsurface.

From the perspective of greenhouse emissions, it appears evident that in the simplest terms, the following general patterns apply to all coals of the Sydney – Bowen Basin complex to greater and lesser degrees:

- A gas depleted zone that extends from surface to around 100m depth (actual may vary). Gas contents are almost entirely $<0.5\text{m}^3/\text{t}$, and gas composition is usually dominated by CO_2 .
- A rapid gas increase zone that extends from approximately 100m to 250–300m, dominated by biogenic methane. Gas content increases rapidly generally (trying) to follow the isotherm. Tending towards greater saturation (a product of biogenic 'top up') but rarely succeeding.
- A transition zone where both biogenic and thermogenic methane may occur (may be significantly undersaturated)
- A deep thermogenic zone dominated by methane (tending towards greater saturation with depth).
- In some areas, magmatic CO_2 is juxtaposed on this pattern, and it may be the dominant subsurface gas in shallow coals.

DRIVERS OF THE MODEL

Effectively, the Permian coals of the entire eastern seaboard of Australia have had a very similar tectonic history. In simple terms, the major tectonic phases pertinent to the study of coal seam gas character in the subsurface are as follows:

- Deposition of vast nascent coal seams in the Permian.
- Compressive tectonics initiated during the late Permian and extending into the Mesozoic (Fielding, 1990, Fielding & others, 1990, Ferguson, 1990 and Scheibner & Basden, 1998).
- Burial and coalification, with peak burial probably occurring in the mid Cretaceous. Maximum burial of most Permian coals is estimated to be 2.5–4kms.
- Pull apart tectonics associated with the Tasman Rift, starting from the late Cretaceous.
- Uplift and erosion.
- Various stages of magmatism, with peak periods in the Jurassic, late Cretaceous, and Tertiary (see Carr & Facer, 1980).
- Compressive tectonics starting from about 8My BP to present.
- Various phases of methanogen bearing groundwater flow from subcrop and fracture systems through seam aquifers.

The deep burial of the Permian coals which are the current target for open cut mining in the Sydney – Bowen Basin complex is responsible for the rank of these coals and their gas storage capacity. In addition, this coalification phase would have provided the opportunity for the coals to become saturated with thermogenic gas. The deep coals in the Permian Basin (at 500m+) are effectively fossil representatives of this stage of gas accumulation. The coals have remained too deep to be affected by near surface biogenic activity, and in many cases too deep to be affected

by CO₂, which will not come out of solution at depths (and pressures) greater than ~800m (thus, if the coals were buried deeper than 800m at the time of the introduction of magmatic fluids, no adsorption of CO₂ should be expected).

The rifting phase provided the tensional tectonics which enabled gas migration to the surface and the progressive under saturation of near surface layers. Fracture connection to the surface and through the subcrop also allowed the introduction of methanogen and nutrient bearing water, and provided the opportunity for biogenic gas development. In some cases, the introduction of biogenic methane 'tops up' the undersaturated coals, and may result in gas contents that are reflective of near fully saturated coals.

The evolutionary stages are presented in Figures 4–7.

IMPLICATIONS FOR GREENHOUSE GAS ACCOUNTING

An understanding of what drives gas variability in the surface can be directly applied to the problem of estimating gas emissions from open cut mining. Each site needs to do some basic exploration drilling and gas sampling to establish local subsurface conditions (the amount of boreholes needed to satisfy the indigenous variability will differ from site to site). However, fundamentally the task remains to:

- Establish the depth of 'no gas' — at what point does the essentially meaningless " $<0.5\text{m}^3/\text{t}$ " gas ramp up? In many cases this will occur at around 100m depth.
- Establish the lateral influence of the open cut — at what maximum distance from the highwall does 'real time' desorption cease?
- Determine gas compositional variability in the near surface.
- Determine the rate of increase of gas content with depth (in many cases this will be of the order of $4\text{--}6\text{m}^3/\text{t}$ per 100m depth, starting from 100m+).
- Establish general depth v. gas content relationships that can be extrapolated across the site.
- Insert this data into a static model (such as the local mine planning software).
- Integrate with mine scheduling inputs to produce calculated CO₂ emissions per annum.

The essential inputs needed for such an approach include; gas desorption results, and some isotherms (to reveal the level of undersaturation). Some isotope tests would be beneficial to establish the extent of biogenic influence at each site.

A detailed program of work to achieve these goals is necessary, the specifics of which should be left to another forum.

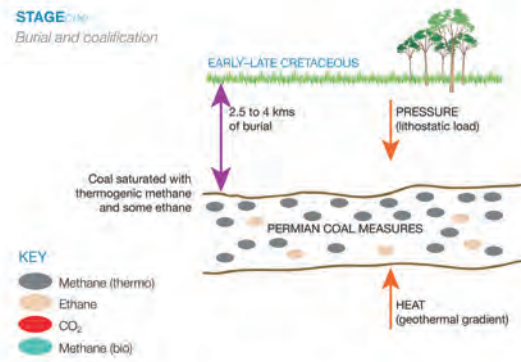


Figure 4: Deep burial in the mid Cretaceous enabled the coals to be charged with methane and some higher hydrocarbons (such as ethane). At this stage, coals were likely to be fully saturated.

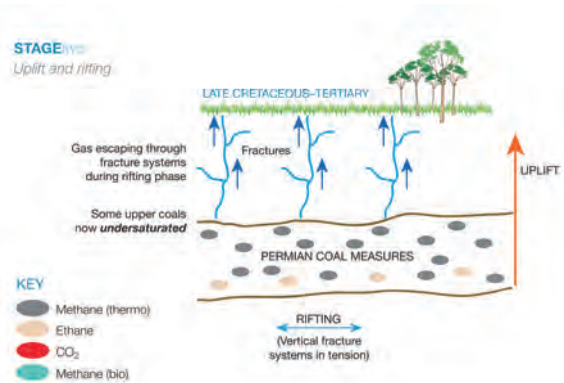


Figure 5: Uplift and rifting provided the opportunity for some gas to escape the system (leading to undersaturation).

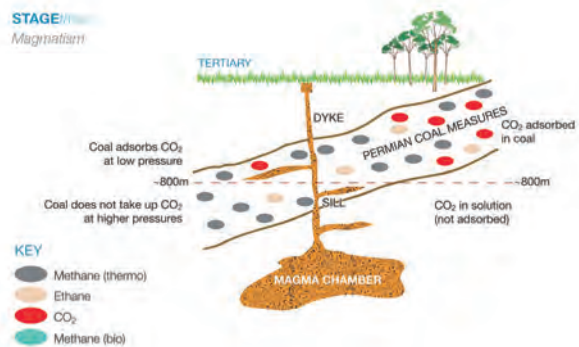


Figure 6: Extensive Tertiary magmatism was the likely catalyst for the introduction of CO₂ laden magmatic fluids, some of which was adsorbed in the coals.

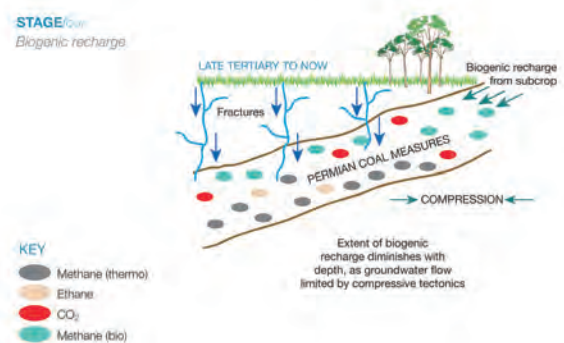


Figure 7: The final phase enabled methanogen bearing groundwater to enter the coal aquifer system, and this has led to the creation of biogenic gas in the shallow subsurface.

CONCLUSIONS

Gas character in the subsurface can be understood, and a predictive model has been developed to account for near surface variability. This understanding can be applied to improve the confidence in greenhouse emission accounting, and reported to the Federal Government as part of the NGER protocol.

REFERENCES

- CARR, P. & FACER, R., 1980: Radiometric ages of some igneous rocks from the Southern and Southwestern Coalfields, New South Wales, *Search*, **11** (11), November, 1980, 382–383.
- FAIZ, M., STALKER, L., SHERWOOD, N., SAGHAFI, A., WOLD, M., BARCLAY, S., CHOUDHURY, J., BARKER, W. & WANG, I., 2003: Bio-enhancement of coalbed methane resources in the southern Sydney Basin, *APPEA Journal*, **43** (1), 595–610.
- FAIZ, M. & HENDRY, P., 2006: Significance of microbial activity in Australian coal bed methane reservoirs – a review, *Bulletin of Canadian Petroleum Geology*, **54** (3), 261–272.
- FIELDING, C., 1990: Tectonic evolution of the Bowen Basin, eastern Australia, *Pacrim 90 Congress, Australasian Institute of Mining and Metallurgy, Brisbane, Proceedings*, 183–189.
- FIELDING, C., FAULKNER, A., KASSAN, J. & DRAPER, J., 1990: Permian and Triassic depositional systems in the Bowen Basin. In *Geological Society of Australia, Queensland Division: Bowen Basin Symposium Proceedings*, 21–25.
- FERGUSON, C., 1990: Thin-skinned thrusting in the Bowen Basin and northern New England Orogen, central Queensland. In *Geological Society of Australia, Queensland Division: Bowen Basin Symposium Proceedings*, 42–45.
- HENNINGS, S., THOMSON, S. & SANDFORD, J., 2007: A Petroleum Industry Approach to Coal Mine Gas Drainage, *American Society for Mining, Metallurgy, and Exploration, Annual Conference*, Presented at the SME Annual Conference, Denver, CO, USA, 25–28 February 2007.
- SCOTT, A.D., KAISER, W.R. & AYERS, W. B., 1994: Thermogenic and secondary biogenic gases, San Juan Basin, Colorado and New Mexico – Implications for Coalbed gas producibility, *AAPG* **78** (8), 186–209.
- SCHEIBNER, E. & BASDEN, H., 1998: Geology of New South Wales – Synthesis, Department of Mineral Resources, *Geological Survey of NSW Memoir Geology* **13**(2), 666 pages.
- THOMSON, S., 2008: Geology and Gas Composition – A Model for the Sydney and Gunnedah Basin, *Proceedings Asia Pacific Coal Bed Methane Conference, Brisbane, 2008*.
- THOMSON, S., HATHERLY, P., HENNINGS, S. & SANDFORD, J., 2008: A Model for Gas Distribution in coals of the Lower Hunter Sydney Basin, *Eastern Australian Basins Symposium III Proceedings, Sydney, September 15-17, 2008*.

Philip Ferenczi

Bowen Basin coal exploration and mine developments 2005–2010

Exploration expenditure (2004/05 – 2009/10) graph (Figure 1) shows a substantial increase Queensland annual exploration expenditure over the past five years. Between 60 and 70% of the expenditure is related to coal projects within the Bowen Basin.

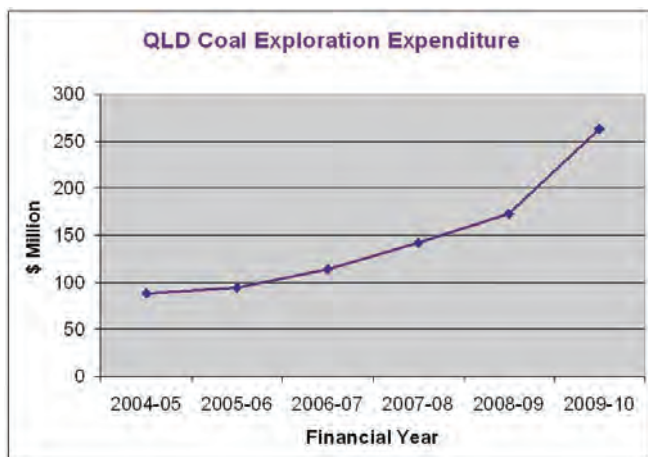


Figure 1: Annual coal exploration expenditure in Queensland between 2004/05 and 2009/10. (Source: Australian Bureau of Statistics, 2010).

Quarterly exploration expenditure for Queensland over the past two and a half years (Figure 2) shows how petroleum (dominated by the coal seam gas sector) has grown rapidly relative to other commodities; coal, base metals (BM) and gold. This growth has been driven by proposed LNG export projects mainly located in Gladstone. The Global Financial Crisis (September Quarter 2008 to September Quarter 2009) had a substantial negative impact on exploration expenditure for metals in Queensland. Declines recorded each year in the March quarter are mainly related to seasonal rainfall across the State reducing off-road access to drilling and survey sites.

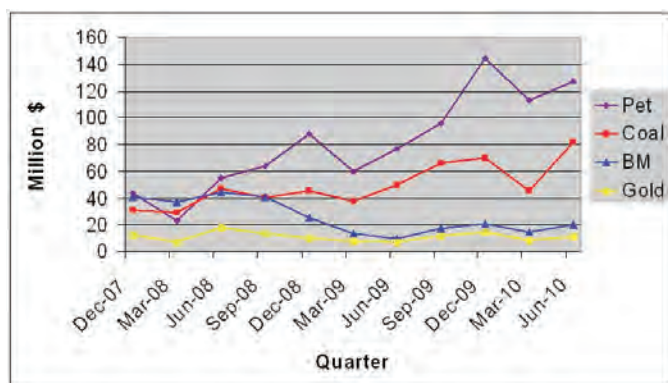


Figure 2: Quarterly Exploration Expenditure on mineral and petroleum commodities in Queensland. (Source: Australian Bureau of Statistics, 2010)

Tenure map comparison (Figure 3) indicates a substantial increase area under Granted EPC (Exploration Permit for Coal) within the Bowen Basin. Large areas of the Galilee and Surat basins are under EPC applications. There has also been a significant increase in the number of companies mining and actively exploring in the Bowen Basin over the past 5 years.

New deposits/resources (25)

Exploration programs over the past five years within the Bowen Basin have identified twenty four new coal resource areas. Some of these deposits have progressed to advanced coal mining projects and are likely to be developed within five years.

Arcturus, Arcadia, Byerwen, Baralaba North, Broughton, Dingo West, Drake, Eagle Downs, Ellensfield, Humbolt, Isaac Plains South, Jax, Lenton, Minyango, Moorvale West, Rocklands, Saraji East, Sarum, Sienna, Springsure Creek, Talwood, Theresa, Washpool, Wilunga and Yamala.

The Bowen Basin contains Measured and Indicated coal resources totalling 20 500Mt (at June 2009). Some 45% of this resource is suitable for open cut extraction and 42% of the resource could produce a coking coal product. Inferred coal resources total 19 600Mt for the basin.

Production

State saleable coal production (Figure 4) has increased 20% over the past 5 years. About 90% of the 208Mt of saleable coal produced in 2009/10 was derived from mines in the Bowen Basin. Exports totalling 159.3Mt worth about \$41 billion (fob) were made to 37 countries in 2008/09. Some 27Mt of predominately thermal coal was supplied to domestic markets. State coal exports for 2009/10 increased by 15% (from the previous year) to 183Mt.

New mines (22)

Underground (6): Newlands Northern, Grasstree, Broadmeadow, Carborough Downs, German Creek Bundoora Colliery and German Creek Aquila Colliery.

Open Cut (16): Suttor Creek, Wollombi, Sonoma, Millennium, Potrel, Minerva, Lake Vermont, Baralaba (re-opened in July 2005), Dawson North (from September 2005 to March 2009), Curragh North, Lake Lindsay, Rolleston, Broadlea North (from May 2007 to December 2009), Isaac Plains, Middlemount and Clermont.

Queensland Coal

Coal exploration tenure expansion 2005 to 2010

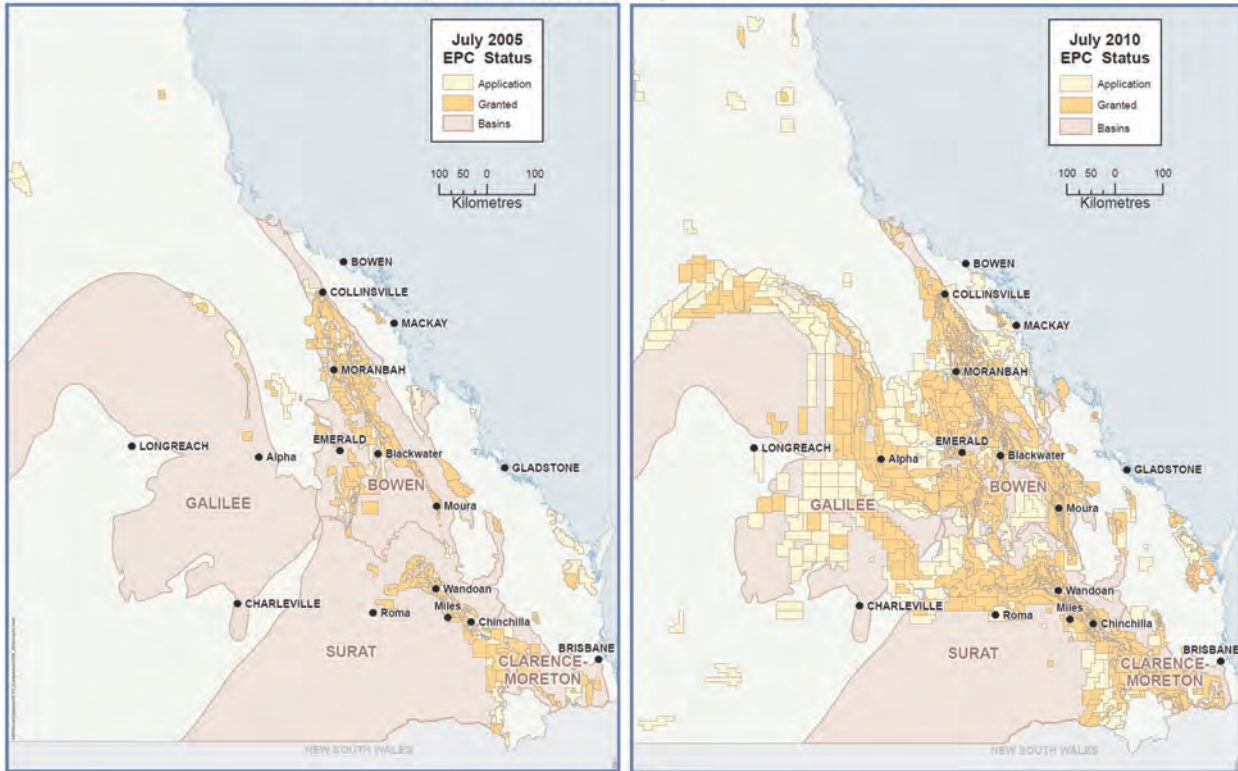


Figure 3: Expansion of coal exploration tenures in Queensland. In July 2005: 183 granted EPCs covering 49 000 km². In July 2010: 671 granted EPCs covering 171 000 km².

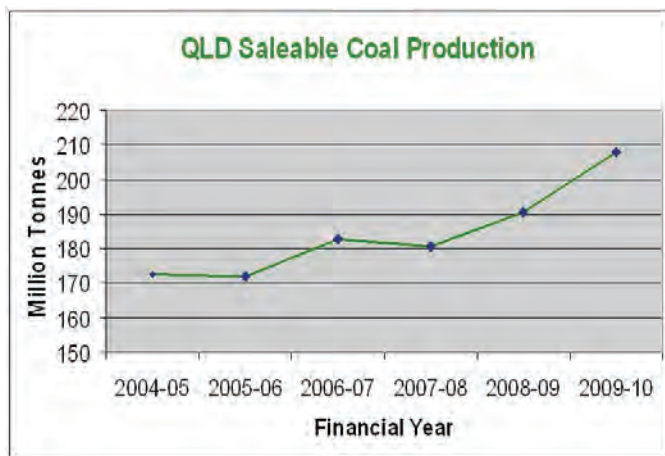


Figure 4: Queensland saleable coal production form 2004/05 to 2009/10.

Details of these new coal mines are provided in Table 1.

Mine Expansions and Extensions (5)

Blackwater, Dawson, Hail Creek, Cook and Foxleigh.

Closures (8)

Riverside, Dawson North, German Creek Central Colliery, German Creek Southern Colliery, Newlands Southern Colliery, Oaky Creek (open cut), Broadlea North and German Creek Aquila Colliery (scheduled to re-open in the December quarter 2010).

New Exploration and Mining Companies (24)

Several corporate acquisitions have taken place over the past five years and many new coal or mixed commodity companies have entered the Bowen Basin exploration scene.

New coal mine operators include: Aquila Resources Ltd (AQA), Caledon Resources PLC (CCD), Cockatoo Coal Ltd (COK), QCoal Ltd, Vale Australia Ltd and Yancoal Australia Ltd.

New exploration companies: Altera Resources Ltd (AEA), Aston Resources Ltd, Bandanna Energy Ltd (BND), Bowen Energy Ltd (BWN), Dragon Energy Ltd (DLE), Eastern Corp. Ltd (ECU), Endocoal Ltd (EOC), Guildford Coal Ltd (GUL), Gullewa Limited (GUL), Linc Energy Ltd (LNC), MCG Resources Ltd, New Hope Coal Ltd (NHC), Newland Resources Ltd (NRL), Northern Energy Corp. Ltd (NEC), Norton Gold Fields Ltd (NGF), Rocklands Richfield Ltd (RCI), Stanmore Coal Ltd (SMR) and Waratah Coal Ltd.

Table 1: Bowen Basin coal development projects

Project	Company	Status	Expected Start-Up	Est. Cap Exp	New capacity
Middlemount open-cut	Macarthur Coal Ltd	New project, under construction	2010	\$140m	1.4Mt coking and PCI (Stage 1)
Isaac Plains open-cut	Aquila / Vale Australia	Expansion, under construction	2010	\$118m	2.8Mt coking, thermal and PCI
Yarrabee open-cut	Yancoal Aust.	Expansion in progress	2010	\$50me	2.8Mt PCI
Baralaba open-cut	Cockatoo Coal Ltd	Expansion, pre-FS underway	2011	na	0.75Mt PCI & thermal
Daunia open-cut	BHP Billiton Mitsubishi Alliance	New project, EIS complete	2011	\$625m	4Mt coking and PCI
Curragh open-cut	Wesfarmers Ltd	Creek Diversion, under construction	2011	\$130m	Extend mine life
Ellensfield underground	Vale Australia Ltd	New project, EIS in progress	2011	\$640m	4.7Mt coking and thermal
Millennium open-cut	Peabody Energy Ltd	Expansion, EIS commenced	2012	US\$150me	Up to 7Mt hard coking
Codrilla open-cut	Macarthur Coal Ltd	New project, EIS & FS underway	2011	\$150m	2.7Mt PCI and thermal
Oaky Creek open-cut (Stage 1)	Xstrata Coal Ltd	Re-development, FS underway	2011	na	1Mt coking
Jax open-cut	QCoal Ltd	New project, Scoping study	2011?	na	1.8Mt (ROM) coking
Curragh open-cut	Wesfarmers Ltd	Expansion, under construction	2012	\$286m	Up to 8.5Mt coking
Ensham Central B&P underground	Ensham Resources	New project, committed	2012	\$166m	1.7Mt thermal
Newlands Northern underground	NCA JV (Xstrata Coal Ltd 55%)	Extension, under construction	2012	US\$130m	7.5Mt thermal
Dawson South II open-cut	Anglo Amer. Met Coal / Mitsui	Extension, EIS complete	2012?	\$80me	3Mt thermal
Eagle Downs underground	Aquila Resources / Vale Australia	New project, EIS & FS in progress	2012	\$988m	4Mt hard coking (Stage 1)
Cook underground	Caledon Resources	Expansion, On-hold	2012?	na	1.8Mt coking and thermal
Middlemount open-cut	Macarthur Coal Ltd	Expansion, FS underway	2012?	\$130m	4 Mt coking and PCI (Stage 2)
Kestrel underground	Rio Tinto Ltd	Expansion, in progress	2012	US\$991m	5.7 Mt hard coking
Byerwen open-cut	QCoal Ltd	New project, pre-FS underway	2012?	\$1000m	Up to 10Mt hard coking
Foxleigh open-cut	Anglo American Metallurgical Coal Ltd	Extension, pre-FS underway	2012	na	3.2Mt PCI
Drake open-cut	QCoal Ltd	New project, pre-FS underway	2013	na	6Mt coking and thermal
Moorvale B&P underground	Macarthur Coal Ltd	Expansion, pre-FS underway	2013	na	1Mt coking and PCI

Source: ABARE April 2010 and DEEDI-Mines Rockhampton August 2010

e= unofficial estimate, na= not available, ROM= run of mine, FS= Feasibility Study, B&P= Bord and Pillar

Table 1: Bowen Basin coal development projects (continued)

Project	Company	Status	Expected Start-Up	Est. Cap Exp	New capacity
Olive Downs North open-cut	Macarthur Coal Ltd	New project, Mining Lease granted	2013	\$20m	1Mt coking and PCI
Peak Downs open-cut	BHP Billiton Mitsubishi Alliance	Expansion, EIS commenced	2013	\$4000m	11Mt hard coking
Caval Ridge open-cut	BHP Billiton Mitsubishi Alliance	New project, EIS in progress	2013		5.5Mt hard coking
Grosvenor underground	Anglo American Metallurgical Coal Ltd	New project, EIS & FS in progress	2013	\$1100m	Up to 5Mt hard coking
Rolleston open-cut	Xstrata Coal Ltd	Expansion, pre-FS underway	2013	US\$450m	Up to 14Mt thermal
Dingo West open-cut	Bandanna Energy Ltd	New project, pre-FS underway	2013?	\$160me	1.9Mt PCI and thermal
Hail Creek open-cut	Rio Tinto Ltd	Expansion, pre-FS underway	2013?	na	17Mt coking and thermal
Wonbindi open-cut	Cockatoo Coal Ltd	New project, pre-FS underway	2013?	\$300me	3.6Mt PCI and thermal
Goonyella-Riverside open-cut & UG	BHP Billiton Mitsubishi Alliance	Expansion, EIS in progress	2013?	\$1000m+	Up to 25Mt hard coking
Washpool open-cut	Aquila Resources Ltd	New project, FS completed	2013	\$320m	1.6Mt coking & PCI
Minyango underground	Caledon Resources	New project, FS underway	2013?	\$400m	3.4Mt coking & thermal
Winchester South open-cut	Rio Tinto Ltd	New project, scoping study	2013?	na	4Mt coking & thermal
Theresa underground	Linc Energy Ltd	New project, scoping study	2013?	na	3.8Mt coking & thermal
Yamala underground	Northern Energy Corp.	New project, pre-FS underway	2013	\$350me	2Mt thermal & PCI
Sarum open-cut and UG	Xstrata Coal Ltd	New project, pre-FS underway	2013	\$700m	5Mt coking and thermal
Eaglefield (Denham) open-cut	Peabody Energy Ltd	Expansion, EIS commenced	2013	US\$400me	Up to 6Mt hard coking
Dysart East open-cut and underground	Bengal coal Ltd	New project, pre-FS underway	2013	\$450m	Up to 4Mt/tpa (ROM) coking
Lake Vermont open-cut	Lake Vermont Resources Ltd	Expansion, pre-FS underway	2014	\$200m	6Mt coking
Curragh South open-cut	Macarthur Coal Ltd	New project,	2014	na	6Mt/tpa coking & PCI
Talwood underground	Aquila Resources Ltd	New project, scoping study	2014	na	2Mt PCI & thermal
Moranbah South underground	Anglo Amer. Met Coal / Exxaro Australia	New project, pre-FS underway	2014	US\$1000m	Up to 4.5Mt coking
Belvedere underground	Aquila Resources/Vale	New project, EIS in progress	2016	\$2800m	Up to 7Mt hard coking
Saraji East Open-cut	BHP Billiton Mitsubishi Alliance	New project, EIS process – terms of reference	2016	\$1000m	5Mt hard coking

Source: ABARE April 2010 and DEEDI-Mines Rockhampton August 2010

UG=underground, na=not available

PROPOSED COAL MINE PROJECTS FOR THE BOWEN BASIN 2010–2015

The Bowen Basin is a world-class mining province. It produces all of Queensland's high-grade coking coal, and much of the export-traded thermal coal. Extensive coal resources within the region also provide the basis for significant coal seam gas development and an emerging LNG export industry.

There are currently 49 coal mines operating in the Bowen Basin. Many of these mines have coal reserves that will enable production beyond 2020. Twenty mines have commenced production over the past five years, and one new mine (Middlemount) is under construction (as at July 2010).

Mining projects under construction (2010): 8 (totalling \$4.0 Bn)

Kestrel Expansion, Carborough Downs Expansion, Moranbah North LW upgrade, Curragh Creek Diversion, Curragh Expansion, Newlands underground Extension, Isaac Plains Expansion and Middlemount.

Mining Projects under consideration: 49 (potential total of \$17 Bn)

Advanced (24)

New mines (12): Ellensfield, Grosvenor, Daunia, Caval Ridge, Olive Downs North, Ensham B&P underground, Eagle Downs, Codrilla, Drake, Sarum, Belvedere and Washpool.

Expansions / extensions (12): Cook, Dawson South Stage 2, Curragh, Oaky Creek O/C (re-development), Yarrabee, Millennium, Rolleston, Eaglefield (Denham), Crinum North, Baralaba, Middlemount (Stage 2) and Foxleigh.

Less advanced (25)

New mines (18): Moranbah South, Yamala, Minyango, Wonbindi, Moorvale underground, Lenton, Saraji East, Jax, Theresa, Arcturus, Byerwen, Dingo West, Hillalong, Winchester South, Talwood, Springsure Creek, Moorvale West and Exevale.

Expansions / extensions (7): Goonyella-Riverside, Hail Creek, Collinsville, Peak Downs, Lake Vermont, Ensham LW underground and Sonoma.

Details of significant coal projects in the Bowen Basin are given in Table 1 and shown in Figure 5.

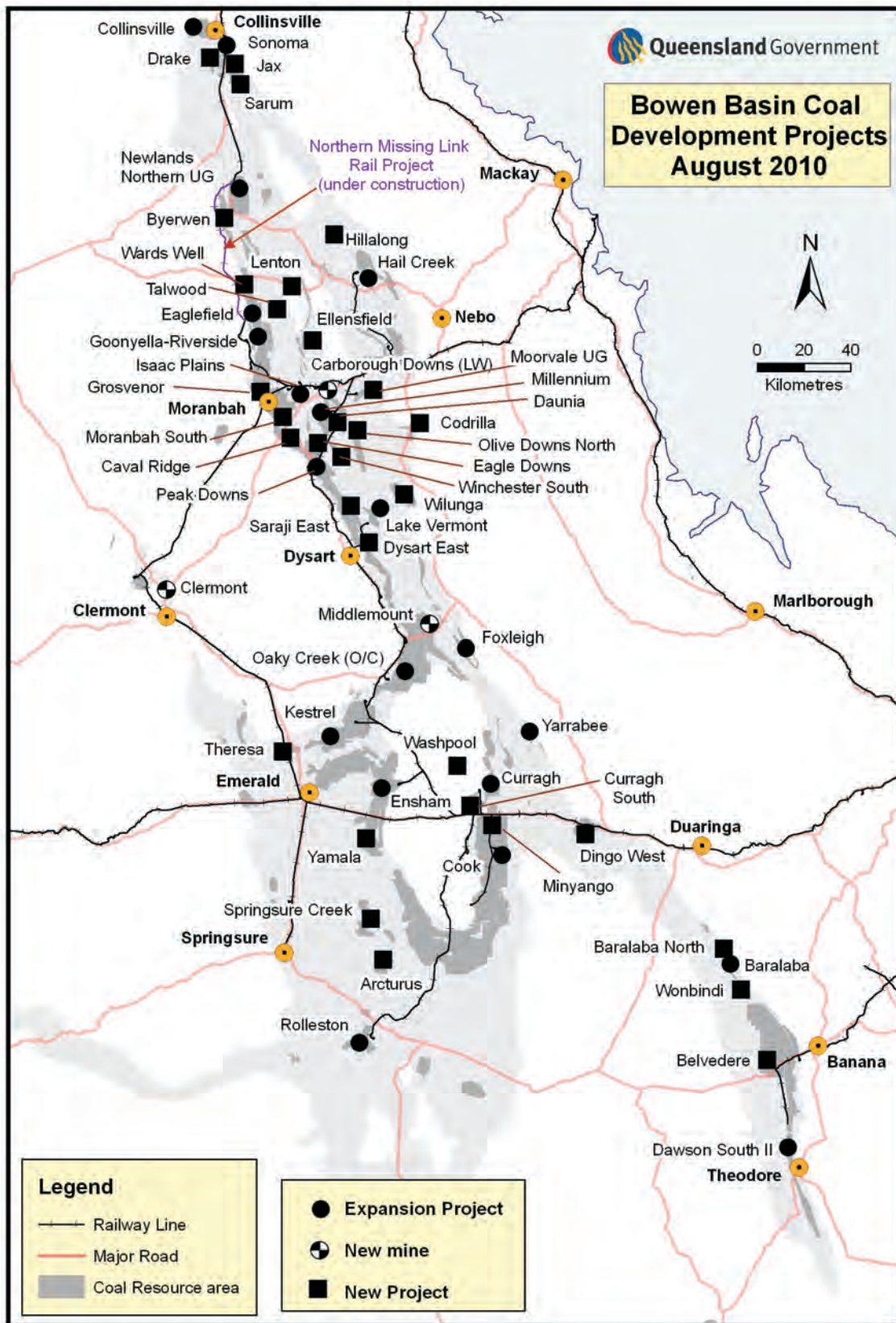


Figure 5: Significant coal projects in the Bowen Basin.

Troy Peters, Nicola Rich and Shaun Strong

Seismic reflection, a useful tool to assist underground coal gasification (UCG)

Carbon Energy have developed the world's first commercial scale oxygen injected Underground Coal Gasification (UCG) facility, based at Bloodwood Creek, 55km west of Dalby in South West Queensland. UCG is an alternative coal utilisation method; it provides an opportunity to access large reserves of otherwise inaccessible coal, via non-mechanical excavation. The process minimises the environmental impact of the mining process, by converting the coal *in situ* to a syngas. This is then extracted through a borehole to be used for low emission power generation, alternatives to oil based fuel and the production of chemicals for agriculture and other businesses.

The successful application of the UCG process requires many key elements: for example; suitable coal quality (up to 50% ash) and thickness, lateral seam continuity and an understanding of the extent of previously gasified coal seams.

Between 2008 and 2009 Carbon Energy undertook the acquisition of firstly a 2D seismic dataset, to test the seismic response, and then a 3D dataset to better understand lateral seam continuity ahead of full scale mining operations.

This paper will firstly examine the results of the 2D (Mini-SOSIE) and 3D (Vibroseis) surveys, comparing the image quality and the characteristics of the two seismic sources. Questions relating to the lateral continuity of the target Walloon Coal Measures will be answered with the presentation of results from the 3D interpretation. Finally, through a combination of both forward modelling and advanced seismic attribute analysis, this paper illustrates that changes in the reflective properties of strata around the UCG cavity can be clearly identified.

INTRODUCTION

Underground Coal Gasification (UCG) involves the gasification of coal *in situ*. To this end it is both a mining process involving the extraction of the raw material and a conversion process whereby the raw material is converted to a synthetic gas comprising elements such as carbon dioxide, carbon monoxide, hydrogen, methane and under pressure, hydrogen sulphide.

The process of Underground Coal Gasification (UCG) was first proposed in 1868 (Siemens, 1868). Since this time the technique has been significantly refined, but its transformation to an industry accepted energy source has been limited to only a few locations throughout the world. Today, coal continues

to be the largest and most affordable source of energy throughout the developed and developing world.

However, the greenhouse gas emission targets proposed by governments and world climate bodies, has placed a new focus on the UCG process as a means of meeting these challenging targets. UCG already has many advantages over traditional coal mining e.g. greater resource – energy conversion and obvious health and safety benefits as the process is conducted remotely. Possibly the greatest of these relates to the fact the process takes place *in situ* and eliminates the problems related to the disposal of solid waste (Shu-qin & Jun-hua, 2002). Therefore, UCG in conjunction with Carbon Capture and Storage (CCS) has the potential for developing into an attractive low emissions energy source.

At Bloodwood Creek (55km west of Dalby, Queensland, Figure 1) Carbon Energy has established a trial program, to explore the successful gasification of thermal coal. The coal utilised is from the Walloon Coal Measures, specifically the Macalister Seam, which sits in within the Surat Basin. This site was selected because it satisfied many of the key ingredients for a successful UCG project. That is, the coal is at a favourable depth and sufficient coal quality for successful gasification.

UCG requires a reasonable water head to assist with the process of gas extraction and the hydrogeology of the area indicates favourable groundwater conditions also exist. Important for the success of the project, but initially not well understood, are the coal seam continuity and structural complexity of the area. To assist with answering these questions, Carbon energy embarked on a 2D seismic survey, which was subsequently followed by the acquisition of a 3D volume.

This paper presents the results for both the 2D and 3D seismic surveys. It then sets out to deliver not only information relating to the lateral continuity and structure of the Bloodwood Creek area, but also how the 3D seismic volume and forward modelling may be used to provide information relating to the coal seam and surrounding sediments post the gasification process.

2D and 3D Seismic Survey Results

For over 30 years the seismic technique has been utilised to assist with coal seam extraction. The technique is considered the only geophysical tool which can produce remote, high resolution, laterally continuous images of a coal seam. For this reason, Carbon Energy considered it the ideal geophysical

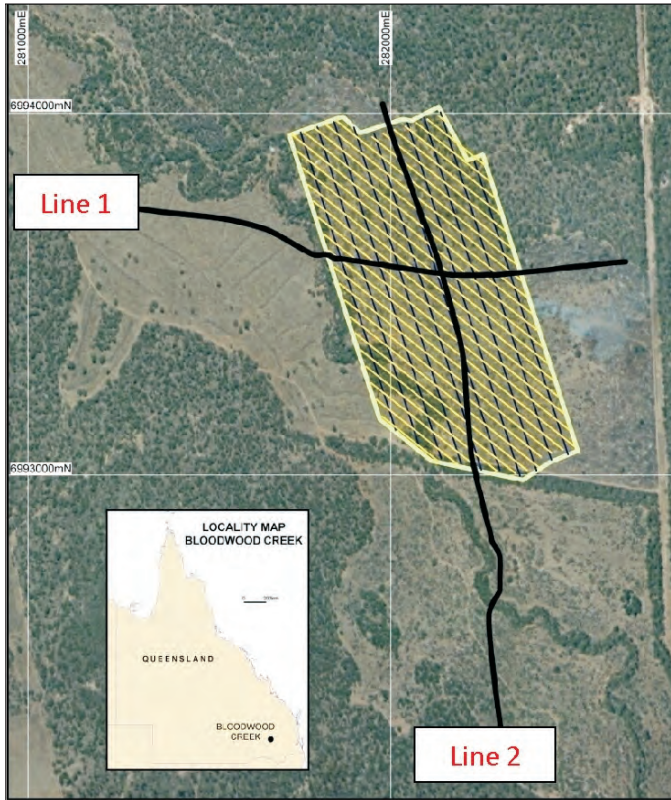


Figure 1: Trial Area Map showing 2D and 3D Locations

tool to assist in understanding the structure and seam topology of the Macalister seam within the Bloodwood Creek area.

2D Seismic Survey

By its nature 2D seismic acquisition is limited to delivering sub-surface imagery in a 2D plane (the plane of acquisition). Therefore, the objective of the 2D seismic survey was limited to testing the seismic response in the Bloodwood Creek Trial area and reporting on any broad scale changes in the seam stratigraphy. Two seismic lines, lines 1 and 2, were acquired in the configuration illustrated by Figure 1.

Two different commercial methods of UCG have evolved over time (UCG Partnership, 2007). The method adopted by Carbon Energy at Bloodwood Creek, uses dedicated in-seam boreholes and oxygen enriched air to produce a mobile controlled retraction injection point or CRIP. Line 2 was planned to follow approximately the line of the in-seam hole used to supply oxygen for the gasification of the trial panel.

During the 2D survey planning stage, two different seismic sources were considered. These were Explosives, and one of the commonly used surface based sources, Mini-SOSIE. Within the survey area the Macalister seam thickness ranges from 8–13m. Therefore, whilst Dynamite provides superior resolution and the ability to detect very subtle changes in the seam structure, the thicker seam means that a surface energy source (lower resolution) may still deliver on the survey objectives of interpreting structure with at least half seam thickness, with significant cost saving to the project.

The acquisition parameters for the 2D and 3D surveys are outlined in Table 1. In both instances the survey parameters

have been optimised for fold and offset to ensure a reliable image is produced at the Macalister seam. As illustrated by Figure 2 (a), the 2D sub-surface image quality is good and the Macalister seam may be easily interpreted across both seismic lines. Whilst signal to noise is one way to evaluate the success of a seismic survey within an area, consideration should also be given to the frequency content of a dataset. The ability to detect subtle changes in structure and the stratigraphy is controlled by the vertical and lateral resolution of the seismic dataset.

There are a number of quasi-theoretical measures of vertical resolution, which may be used to determine the resolving power of P-wave seismic data. Vertical resolution may be calculated by considering both the overburden velocity and seismic frequency, whereas lateral resolution is calculated with the added consideration of reflector depth. Using Appendix A, and substituting a value of 50Hz for the dominant frequency (derived from the frequency spectra Figure (2b)) and 2000m/s as an indicative overburden velocity, the Rayleigh and Widess resolution criteria are calculated as 10m and 5m respectively. Further, the Fresnel Zone, which is an indicator of the lateral resolution, is determined to be 63m at a seam depth of 200m. Whilst the frequency content is lower than similar surveys conducted with a surface source in the Bowen Basin, the resulting resolution limits are comparable given that the average overburden velocity is lower. Therefore, as the thickness of the Macalister seam is between 8–13m, the vertical resolution limit proposed will be sufficient to detect changes in the coal seam stratigraphy with a magnitude of greater than half seam thickness.

3D Seismic

The mine design for the process of UCG is similar to that of Longwall mining. That is, the gasification occurs within defined panels, with rib supports provided to ensure surface subsidence is kept to a minimum. Following the successful completion of the 2D seismic survey, Carbon Energy decided to acquire a 3D seismic survey over an area, which would constitute approximately 3 gasified panels (0.45km²).

Whereas 2D seismic data acquisition is restricted to producing a sub-surface image in the plane of acquisition, 3D data acquisition has the added advantage, in that a grid of receivers records sound waves reflected from a coal seam. Acquiring seismic data in this fashion produces large volumes of spatial data, which when interrogated by modern interpretation systems produces high definition structural maps and laterally continuous coal seam profiles (see Peters, 2005, Hendrick, 2005a, 2005b).

The Bloodwood Creek 3D volume was acquired with source and receiver parameters as indicated by the right side of Table 1. As with the 2D data, the 3D data quality was good and the Macalister seam was easily mapped across the entire survey area. Figure 3a represents the Macalister seam elevation profile and Figure 3b the Macalister seam amplitude map. Attribute maps such as amplitude are excellent indicators of changes in the coal seam stratigraphy. When

Table 1. 2D and 3D Acquisition Parameters.

Item	2D	3D
Geophones	30Hz, Array	
Filter hi-cut	375 Hz	375 Hz
Filter Lo-cut	40 Hz	Out
CDP Interval	2.5m	8m
Survey pattern	In-line	non-orthogonal (slant shot lines)
Live patch	Live patch	18 lines x 50 channels max patch size
Shot line spacing	-	48m
Shot point	5m	29m
Receiver line spacing	-	48m
Receiver point	5m	16m
Receiver array	Receiver array	Single geophones
Fold	60 nominal	20 fold at seam
Energy Source	Mini-Sosie	Vibroseis (Enviro-Vib)
Sweep	-	20-140Hz
Size	60Kg	18000lb

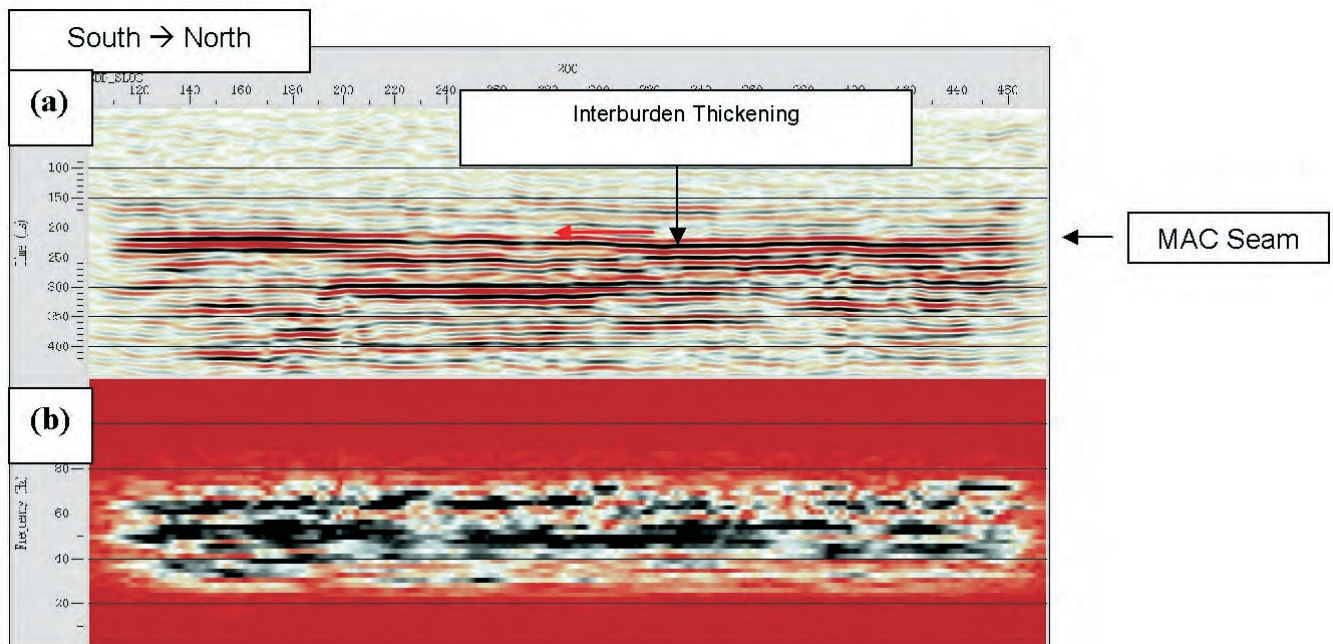


Figure 2: Seismic Line 2 (a) subsurface section (b) frequency vs. offset plot

viewing seismic data by colour section, often a fault plane will be obvious as a line of reduced amplitude.

This is both a result of the destructive interference of the reflection and diffraction off the fault plane and a change in the acoustic properties surrounding the fault.

When amplitude is mapped across a horizon these variations are represented spatially.

The amplitude map for this particular survey has been very effective for the delineation of structure and as will be discussed shortly, excellent as an indicator as to the location of gasified coal.

For the majority of the survey area the Macalister seam exhibits little change in grade (Figure 3a). The exception to this is in the North western corner, where a structure apparent in both attribute maps (Figure 3) is observed. This fault, interpreted with a Normal sense of movement and downthrown to the west, exhibits a maximum displacement of approximately 16m (+2m) and a fault plane dip of approximately 45 degrees. The size of this structure is certainly a boundary to the current UCG resource and will be avoided as mining progresses.

In addition to this major structure, a small anomaly in the Macalister seam amplitude map (red ellipse) is noted in the southern portion of the survey area. This anomaly presents as a distinct zone of low amplitude and by increasing the scale and modifying the colour intensity the anomaly (Figure 4a) becomes more prominent. Further investigation reveals that at this location the Macalister seam has already undergone gasification. The anomaly in amplitude is complemented by the Semblance attribute (Figure 4b). Semblance is a measure of seismic trace similarity, hence the anomaly on this map highlights the dissimilarity in seismic signature between the gasified and no-gasified coal.

The polygon annotated on these images (Figure 4) represents the approximate position of the gasified zone as constructed. The seismic attribute anomaly extends up to 18m around the cavity. While the cavity may vary slightly from the predicted position, changes in the properties of the surrounding strata are likely to impact on the seismic anomaly extent. Therefore the authors have decided to conduct a forward modelling study in the hope of better understand the accuracy of the seismic volume with respect to locating regions of gasified coal.

Fine tuning to identify the small changes between an undisturbed *in situ* coal seam and a gasified coal cavity will enable the use of 3D seismic images as an aid in UCG cavity confirmation.

Forward Modelling

Forward Modelling is the name given to a group of techniques which attempt to estimate the seismic response given a defined geological model. The use of synthetic seismograms to associate coal seams to reflection horizons is the simplest

form of Forward Modelling. Other methods by order of their complexity include Zero Offset and Finite Difference Acoustic *modelling*, and Elastic Finite Difference modelling. Whereas synthetic seismograms are limited to estimating the seismic response at a single borehole, these other methods allow the geological model to vary laterally. Varying the model in this way enables effective modelling of faulted zones, or in this case, zones exhibiting lateral changes in stratigraphy due to the UCG process. By comparing the model produced with the actual seismic data, a greater understanding of the limitations in seismic resolution and the overall accuracy of the seismic to detect these gasified zones may be obtained.

For the purpose of this exercise Zero Offset Acoustic modelling was chosen as a starting point. Carbon Energy provided a geological model representing the most likely seam stratigraphy post gasification (Figure 5). Important characteristics of this model are that within the gasified zone, the majority of the Macalister seam is replaced by both air and fused ash (clinker). In addition to this model, two additional models were constructed. These were identical to that shown by Figure 5 with the exception that the air filled cavity was replaced with a cavity filled with water and goaf respectively. Appropriate sonic and density values were assigned to the rock mass and to the varying cavity materials. The zero offset sections were constructed using a 20–70Hz Ricker wavelet, which is a similar bandwidth to the actual seismic data (Figure 2b). The resulting synthetic sections derived are illustrated by Figure 6. This figure shows the three modelled sections (Figures 6a–6c) alongside a seismic cross line (extracted from the 3D volume), which intersects the zone of gasification.

Comparing the section characteristics (horizon shape and amplitude) at the Macalister seam level, the best correlation is achieved when the actual data (Figure 6d) is compared to the goaf model (Figure 6c). This implies that goaf material has most likely in-filled the cavity post gasification. Whilst the composition of the cavity is likely to be more complex and possibly a combination of all three components presented, this modelling exercise suggests that the cavity fill is dominated by goaf material.

Recall that some discrepancy is observed between the known position of gasified coal and the position suggested through the interrogation of seismic attributes (Figure 4). Limitations in lateral resolution can impact on the seismic datasets ability to reliably position such changes in seam stratigraphy. To investigate the reliability of the seismic data to accurately position the zone of gasified coal, a more rigorous modelling technique has been adopted to that described above. Using the Goaf model as the preferred composition of the cavity, a full Elastic Finite Difference algorithm was implemented to construct the synthetic section shown in Figure 7.

Unlike Zero Offset Modelling, this approach constructs synthetic field records by modelling a variety of seismic wavefields (e.g. noise, P-waves, S-waves, multiples). The geometry of these records may be tailored to match the actual data so that when these synthetic records are processed, the resulting synthetic image is more realistic.

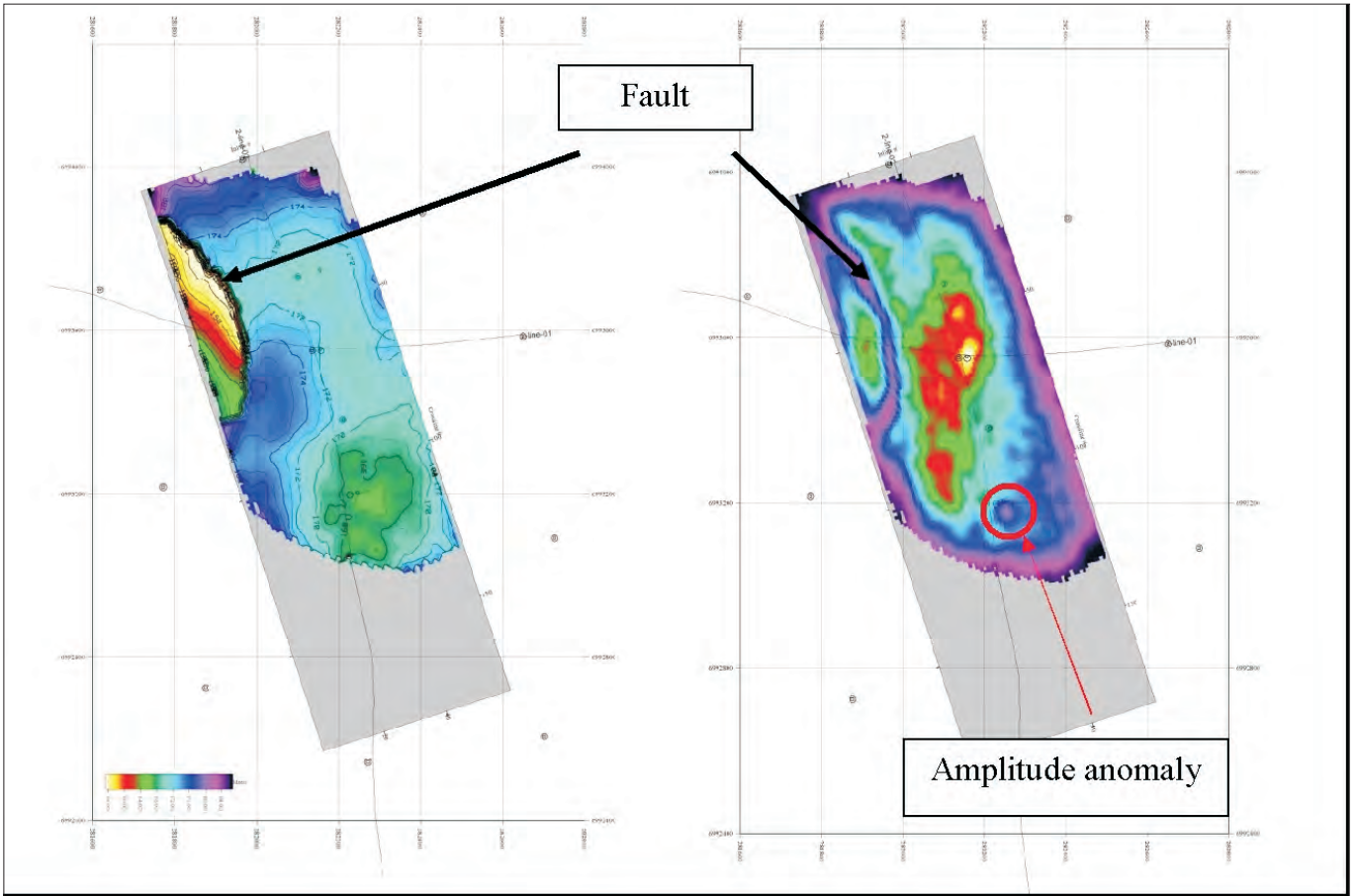


Figure 3: Macalister seam (a) elevation map (b) RMS amplitude

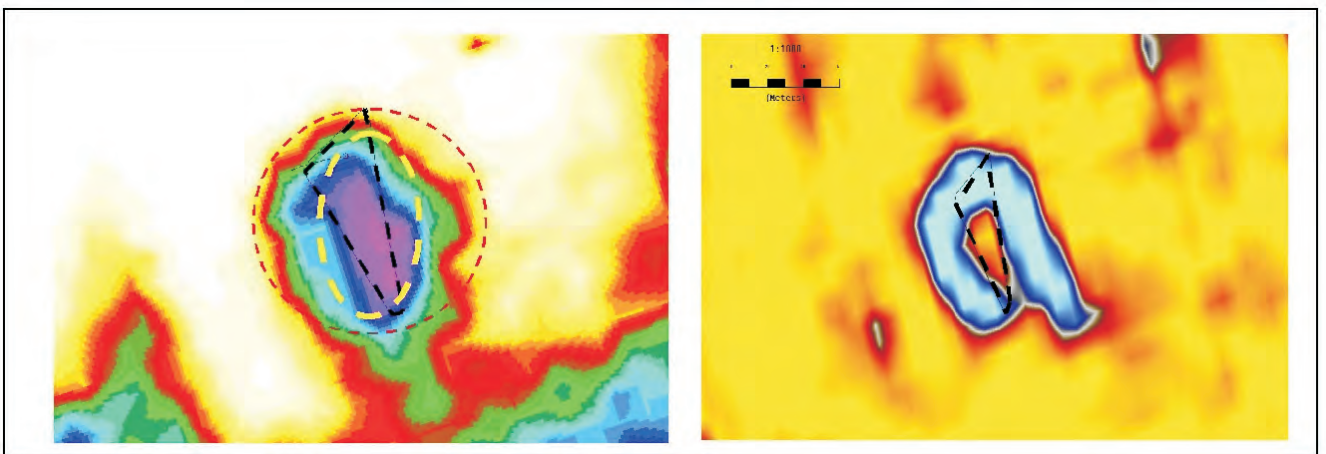


Figure 4: Macalister seam seismic attribute maps. (a) Rms amplitude map (b) Time slice through Semblance volume (220ms). Black polygon represents approximate position of gasified coal and seismic attributes appear to be modified around the cavity for up to 18m some of which may be attributed to resolution limits.

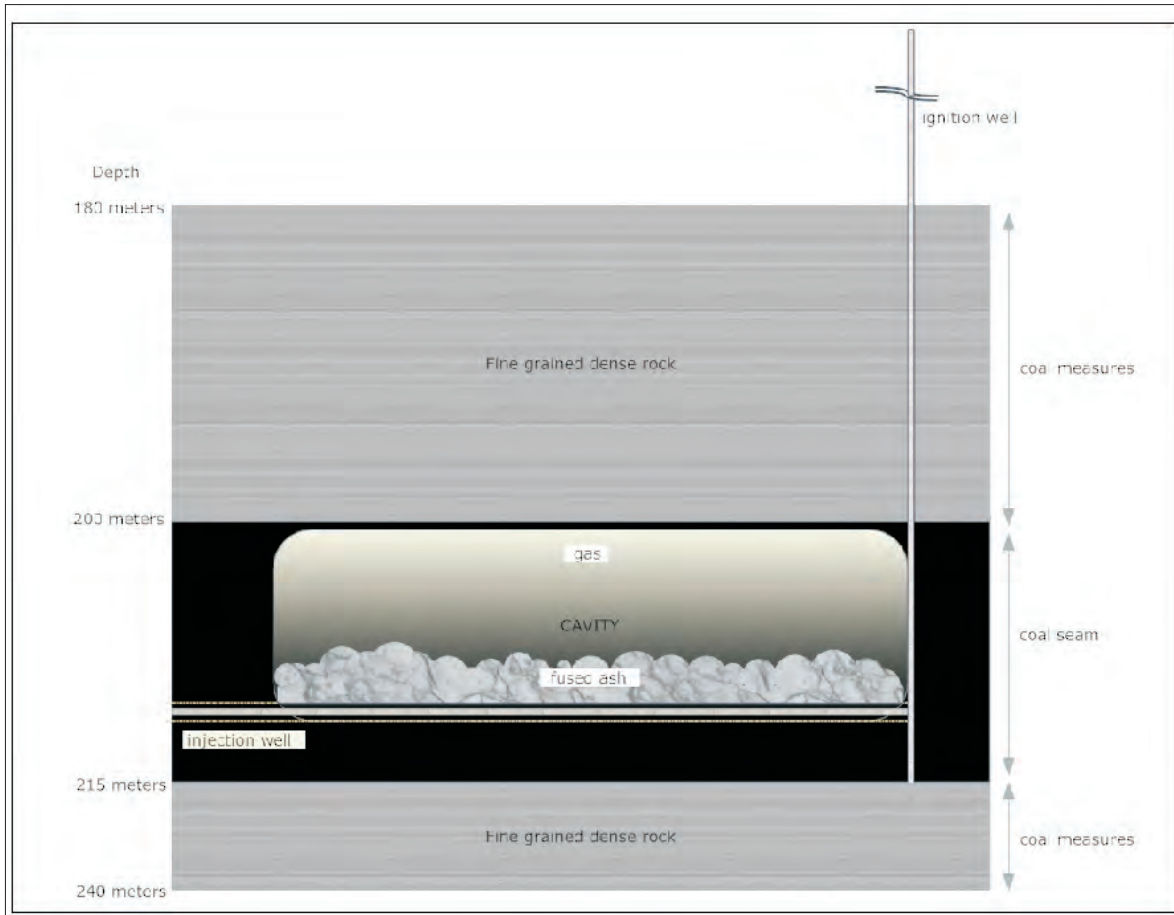


Figure 5: Macalister seam geological model (post gasification)

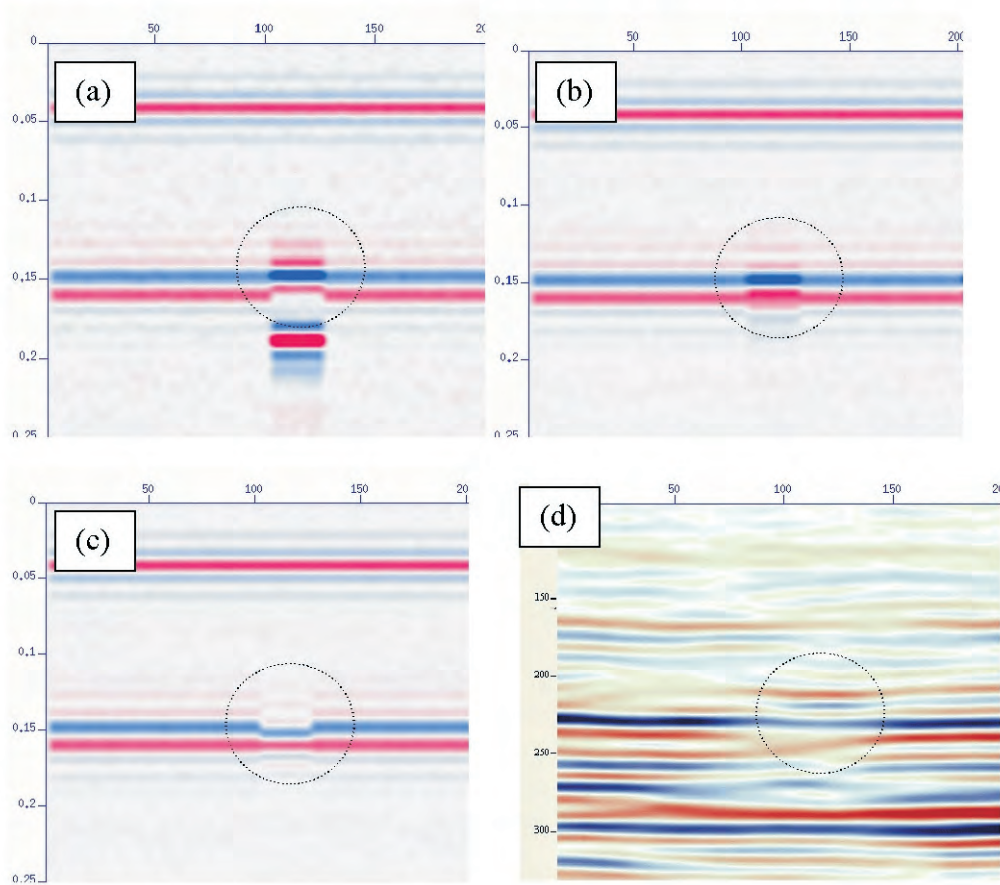


Figure 6: Comparison of Zero Offset Modelling and 3D Cross line intersecting gasified zone. (a) Air filled Cavity model, (b) Water filled Cavity model, (c) Goaf filled cavity model, (d) Representative cross line intersecting gasified zone.

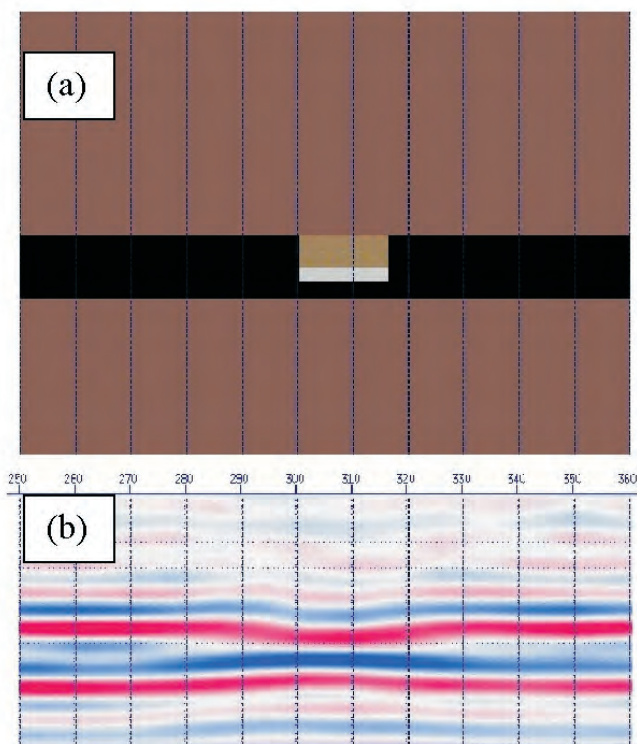


Figure 7: Result of Elastic Finite Difference modelling. (a) Goaf geological model, (b) Resulting synthetic seismic section

As illustrated by Figure 7b, the Finite Difference modelling has been successful in producing a realistic synthetic section. The correlation between the modelled section and that section extracted from the 3D volume, through the zone of gasification (Figure 6d), is excellent and improved when compared to the simplistic zero offset section (Figure 6c). When the spatial position of the cavity from the geological model (Figure 7a) is compared with the synthetic section, an 8m variance in this position is observed. This variance relates to limitations in the spatial resolution of the seismic technique and suggests that the maximum error between the true cavity position, and that which can be determined using the 3D seismic volume, is approximately 8m.

At the site of the UCG reactor, as previously mentioned, the discrepancy between the actual reactor cavity and the anomalies observed in the seismic attributes was approximately 18m. Whilst some of the lateral error is attributed to resolution limitations changes in the rock structure surrounding the cavity could affect seismic attributes, however the anomaly remains centred on the cavity.

CONCLUSION

At Bloodwood Creek, Carbon Energy has developed the world's first commercial scale oxygen-injected UCG Syngas production facility.

When initially proposed, the objectives for both the 2D and 3D seismic surveys were to test the seismic response within the Bloodwood Creek area and to provide information relating

to the structure and stratigraphy of the Macalister seam. This paper has shown that in addition to achieving these objectives, the seismic technique in its 3D form, may be used to deliver valuable information by confirming cavity geometry and location.

Specifically, this study has shown that by interrogating subtle changes in seismic attributes, the location and extent of gasified coal can be obtained with reasonable accuracy. Developing this technique would be advantageous to the growing UCG industry as a tool to track resource recovery and assist with mine planning.

For the management of conventional oil and gas reservoirs, a 4D seismic approach is often adopted. That is, 3D seismic surveys are acquired at the same location and at regular intervals during production, to ensure maximum resource recovery. Whether a 4D approach is adopted at sites like Bloodwood Creek to assist with Syngas production, will ultimately be determined by economics and by the ability to locate these previously gasified zones by other methods.

REFERENCES

- PETERS, T., 2005: The successful integration of 3D seismic into the mining process: Practical examples from Bowen Basin underground coal mines. In Beeston, J.W. (Editor): *Bowen Basin Symposium 2005 – The future for coal – Fuel for thought*. Geological Society of Australia Inc Coal Geology Group and the Bowen Basin Geologists Group, Yeppoon, October 2005, 165–169.
- HENDRICK, N., 2005a: Converted-wave seismic reflection for open-cut coal exploration. In Beeston, J.W. (Editor): *Bowen Basin Symposium 2005 – The future for coal – Fuel for thought*. Geological Society of Australia Inc Coal Geology Group and the Bowen Basin Geologists Group, Yeppoon, October 2005, 129–134 (also on CD).
- HENDRICK, N., 2005b: E preliminary evaluation of integrated P/PS seismic interpretation for improved geological characterisation of coal environments. In Beeston, J.W. (Editor): *Bowen Basin Symposium 2005 – The future for coal – Fuel for thought*. Geological Society of Australia Inc Coal Geology Group and the Bowen Basin Geologists Group, Yeppoon, October 2005, 135–140 (also on CD).
- SHU-QIN, L. & JUN-HUA, Y., 2002: Environmental Benefits of underground coal gasification, *Journal of Environmental Sciences* 12(2), 284–288.
- SIEMENS, W. 1868: *Transactions of Chemical Society*, 21, 279.
- UCG PARTNERSHIP, 2007: Introduction to Underground Coal Gasification.

ACKNOWLEDGEMENTS

The Authors would like to thank Carbon Energy for granting permission to use the results of the seismic surveys conducted at Bloodwood Creek to compile this case study.

APPENDIX A

Vertical Resolution

The commonly used 'Rayleigh resolution limit', defined as the minimum separation of discrete seismic reflectors at which one can ascertain more than one interface is present (Sheriff, 1991), is $\lambda_D/4$. The 'Widess limit' is an alternative, and more optimistic definition, which states that two interfaces are resolvable if their separation is greater than or equal to $\lambda_D/8$ (Sheriff, 1991).

The 'detectable limit' is defined as the minimum layer thickness required to produce an observable seismic reflection (Sheriff, 1991). This is generally taken to be of the order of $\lambda_D/30$, where λ_D is the dominant wavelength of the P wave:

$$\lambda_D = \frac{V_{int}}{f_D} \quad \text{F-1}$$

f_D is the dominant frequency of the seismic wave, and V_{int} is the interval velocity of the geological layer being considered.

Horizontal Resolution

For simplicity it is generally assumed that data recorded at a receiver is reflected from a point on a seismic layer. However,

in reality a circular zone of data contributes to each reflection event recorded at each receiver especially for unmigrated data. This zone of reflection is called the Fresnel zone, the size of which governs the horizontal accuracy of structural information that can be acquired from seismic data. The radius of the Fresnel zone is dependent on the reflection depth, frequency content and seismic velocity.

For a P wave the radius of the Fresnel zone (r_p) can be approximated by:

$$r_p = (z\lambda / 2)^{1/2} \quad \text{F-2}$$

where: z equals the depth and λ is the wavelength which is given by the average P-wave velocity divided by the dominant frequency.

REFERENCE

SHERIFF, R.E., 1991. *Encyclopedic Dictionary of Exploration Geophysics*. SEG, Tulsa, Oklahoma.

James K Dirstein and Gary N Fallon

Automated Interpretation of 3D seismic data using genetic algorithms

Over the past twenty-five years Geoscientists have acquired more than 550,000 square kilometers of 3D seismic data [APPEA statistics] over continental and offshore Australia in the pursuit of mineral and petroleum deposits. Whether the target is hydrocarbons of any phase (solid, liquid or gas) or minerals, the information extracted from the 3D seismic data when integrated with other geological and geophysical data helps form models of the subsurface. These models are the foundation upon which decisions are made, directing future exploration, appraisal and development activities. The success of these activities often depends upon the accuracy of these models.

Many advances in acquisition, processing and interpretation methods have been implemented since the first 3D seismic surveys were acquired in Australia during the 1980s. As a consequence of these advances, the geoscientist today is faced with dramatic increases in the volumes of high quality data available for analysis. However, the time available for the thorough examination, analysis, extraction and integration of the information from these large often multi-volume datasets is always limited and is becoming more problematic. Typically, the geoscientist will spend most of their available time extracting information from small portions of these datasets with a disproportionately amount of time spent thinking about the significance of the results.

Fortunately, Geoscientists are not the only, or the first Scientists, to face challenges associated with the analysis of large amounts of data. Specifically, ideas developed during the course of the thirteen (13) year Human Genome Project (HGP) have been adapted to help interpret seismic data by automatically segmenting and identifying all surfaces within a 3D volume of data; which is then stored into a visual database. Using this technology enables the Geoscientist the ability to analyse large amounts of data in an unbiased manner and thereby incorporate much more data into their models. The details of this patented technology are discussed and demonstrated on several examples including a 3D seismic dataset collected over a Queensland Bowen Basin Coal Mine.

INTRODUCTION

This presentation includes 3D data collected over a Bowen basin coal mine. The actual location and orientation of the data is withheld at the request of the company operating the mine. While limited information has been made available for publishing additional information may be available in the presentation.

The use of 3D seismic data is a fairly common practice for the evaluation of both coal and hydrocarbon exploration. While considerable effort and budget dollars are spent on the planning, collection, processing and interpretation of this data, the majority of seismic, in most cases, is underutilised.

Table 1 shows how the typical interpreter might spend his time working with a 3D seismic volume.

Table 1: Breakdown of 3D seismic interpretation

Activity	Total Project Time
Analysing data	10%
Picking horizons	60%
Creating geological interpretation	20%
Significance of results	10%

For 3D seismic volumes specifically acquired in coal operations the geological interpretation component is a little larger as the effort goes into detailing the characteristics of faults identified in the volume.

The table suggests that the effort required to identify and map individual surfaces within each seismic volume is quite time consuming and limits the amount of data examined within any 3D Seismic dataset. By automating the most time consuming element of the process and looking at all the data in an unbiased manner, more time should be available to develop a better understanding of the significance of the results. Given that many auto-tracking algorithms available in commercial workstations struggle to yield high quality surfaces for single horizons without constant corrections in erroneous event tracking; how will the automatic and simultaneous analysis of all surfaces provide a better solution?

ORIGINS

The new technology outlined in this presentation finds its inspiration, effectiveness and perhaps future refinements from the Human Genome Project (HGP). Therefore it is appropriate to begin with some background information about the HGP. The HGP was the most ambitious task undertaken by biologists and was perceived to be the last effort needed to conclude work in a field founded by Watson and Crick with their publication of the double helix model for deoxyribonucleic acid (DNA) in 1953. Some of the objectives of the HGP were as follows:

- To identify all of the genes in the human DNA (initial expectation of as many as 150,000 genes),
- To determine the sequences of the 3 billion chemical base pairs,
- Store this information in databases and improve tools for analysis,
- Transfer related technologies to the private sector, and
- Address the ethical, legal and social issues (ELSI) that may arise from the project.

Thoroughly conducted scientific investigations generally yield data and insights that were beyond original expectations, and the HGP project is no exception (Baltimore, 2001). A summary of the HGP big surprises were:

- About 24,000 genes were identified in the Human Genome (still not 100% sure).
- Genes are much more complicated than originally imagined (Before the HGP a two hour undergraduate lecture was adequate to describe the gene model; After the HGP three months of lectures are required to explain the concept of a Gene [Darkin, 2006, "What is a Gene?" Nature V 441,25]).
- The initial model developed pre-project used only the DNA (ignoring 50% of the mass which comprised of the encasing protein),
- The "ignored" protein plays a vital role in the Human Genome (new field called Epigenetics),
- The Human Genome has only 2,000 more genes than the simple nematode
- Cautionary insight: An accurate model could not be created using 50% of the data!

Given geoscientists in both the petroleum and coal industry use less than 10% of the surfaces available in 3D Seismic data volumes in their analysis, it would be reasonable to assume that additional insights into the subsurface would be improved upon if all the data could be examined in a timely, accurate and cost effective manner.

METHODOLOGY

The HGP inspired analysis system developed uses an entirely evolutionary process in the form of genetic algorithms to segment the seismic data. Genetic Algorithms are a mathematical process (Grefenstette & others, (1989) and Michalewicz & others, (1992)) that mimic the genetic process of biological evolution. The evaluation of a possible solution depends on the predetermined parameters associated with the "goodness of fit" criteria. The better the fit, the greater the chance of the solution surviving until the next generation of evaluations. Fang & others, (1996) and others have demonstrated the effective use of genetic algorithms in geosciences. By applying this approach to identify unique waveform segments that relate to surfaces or horizons and are referred to as GeoPopulations™ which are then automatically extracted quickly, accurately and in an unbiased manner.

To determine the extent of GeoPopulations™ these evolutionary algorithms apply the principles of natural selection and "survival of the fittest" to grow from disordered

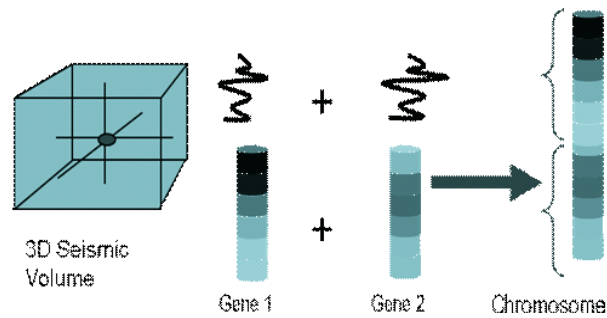


Figure 1: Analogy between Seismic and the Chromosome. Image from Seisnetics LLC unpublished material.

and random seed points to groups of genetically related individuals. A wide range of genetic algorithms have been used and proven to be both powerful and effective for a wide variety of optimization problems, such as medical, airline scheduling, stock market trading, adaptive control, military, and so forth.

The genetic analogy with the seismic volume (Figure 1) can be described as follows:

- A Chromosome is analogous to a seismic trace.
- The seismic volume therefore, consists of many Chromosomes.
- Each Chromosome is made up of a group of Genes just as each seismic trace consists of a group of waveforms. Therefore, a seismic waveform are considered equivalent to Genes.
- Each Gene (waveform) can be characterized by its own unique suite of attributes (i.e. location, amplitude value, neighbour trace shape etc.,).

Initially, the Seismic Volume is first automatically segmented into a population of individual waveforms (Figure 2). Individuals within this collection of waveforms are randomly selected as new populations. This Gene then looks both local and global for other genes with the most similar genetic characteristics (amplitude values, trace shapes, frequency or any combination of attributes that are associated to each sample).

As the populations grow (evolve), the common waveform or genotype changes as selection and reproduction continue according to criteria based on both a local and global parameters.

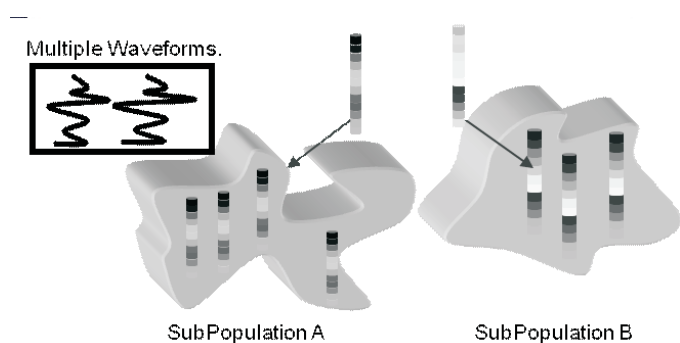


Figure 2: The evolution of a GeoPopulation™. Image from Seisnetics LLC unpublished material.

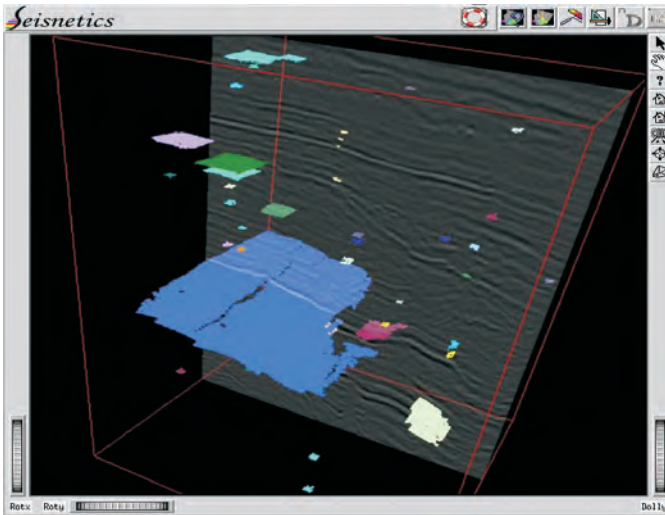


Figure 3: Evolution of GeoPopulations™ (snapshot in time). Some populations evolve faster than others (Blue horizon). Image from Seisnetics LLC.

As the groups of waveforms grow they will eventually encounter other groups. If they are compatible both spatially and genetically they combine forming a new larger Subpopulation (offspring) that inherits the genotype (common waveform) of its two parents. The evolution continues throughout the entire volume until all GeoPopulations™ have been identified and categorised into a database of surfaces.

Like any evolutionary process some elements, as seen in (Figure 3), evolve faster and others fail to evolve at all. At the end of processing, each 3D seismic volume has hundreds of identified GeoPopulations™. This database of surfaces needs to be reviewed, sorted and filtered. Based on the current requirements of the interpreter, a selection of these surfaces will be extracted for further analysis. The most effective means of reviewing all the results is by way of a visual database which enables subsets of the GeoPopulations™ to be reviewed and selected for extraction based on a number of statistical and visual criteria. For example the interpreter

might initially select the largest surfaces to help develop an initial structural model (Figure 3). Later as objectives change, the visual database can be revisited and queried for other objectives such as a stratigraphic zone of interest, specific seam-roof-floor, shallow overburden assessment or fault analysis.

The exportation of selected surfaces into an interpretation, GIS package or modelling software enables further analysis and leaves the integrity of the unbiased GeoPopulation™ database intact.

Within the visual database the identification of GeoPopulations™ which match specific criteria can be realised using a number of different filters and sorting techniques (population size, position, quality, etc.,).

Each GeoPopulation™ has a set of attributes associated with each member of the population. One of these attributes is called “Fitness” which provides a measure of “genetic likeness” for each member in the population when compared to the common waveform (Genotype) of the same population. This Fitness criteria shows individuals that might still be related but are best described as first or second cousins. The best way to assess the genetic variability within a population is to view the Fitness values as a map. The Fitness map shows areas of high fitness (green) with lower fitness values as blues and reds (Figure 5). Investigation of the lower fitness values which form linear and curvilinear features on the map are predominantly caused by subtle faulting with some subtle stratigraphic elements as well. The waveform located in the lower left hand corner of Figure 5 is the common waveform for this GeoPopulation™ and is referred to as the Genotype (shown in red).

A 3D seismic volume is reported to contain many attributes (>150), however most of these attributes are derived from, and dependant on, other attributes e.g. the gradient is from the TWT horizon. Consequently, some seismic attributes are

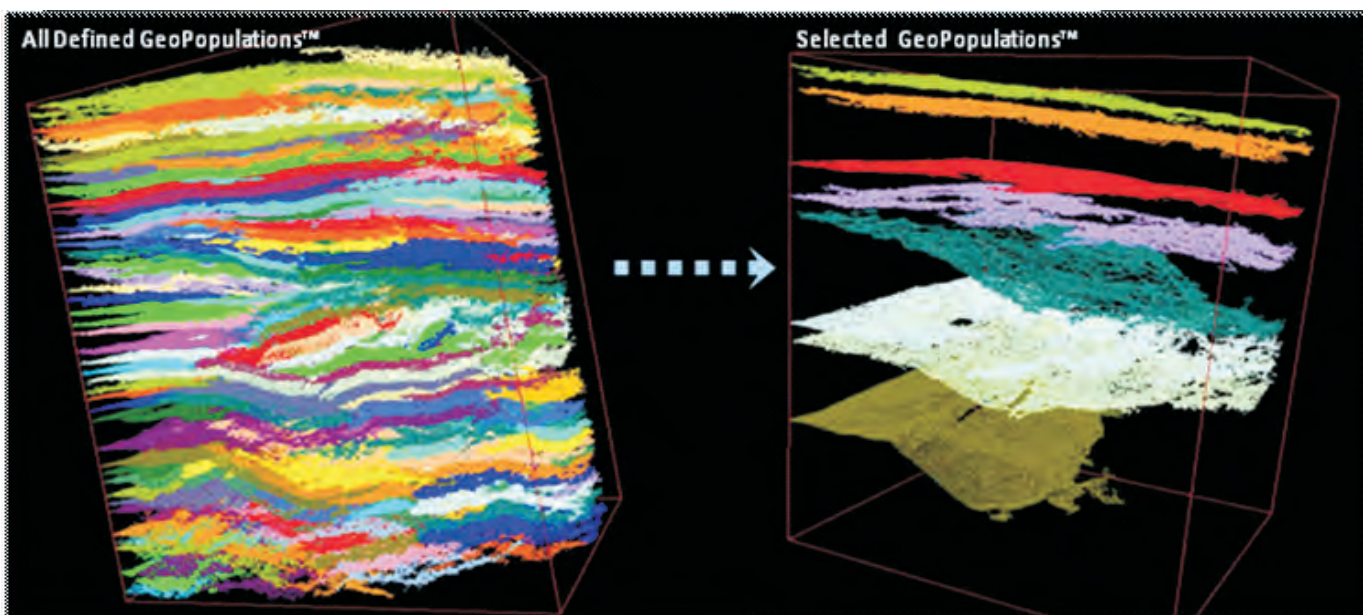


Figure 4: Horizons which address the current task are identified and then exported for import into GIS, interpretation or modelling software. Image from unpublished Seisnetics presentation.

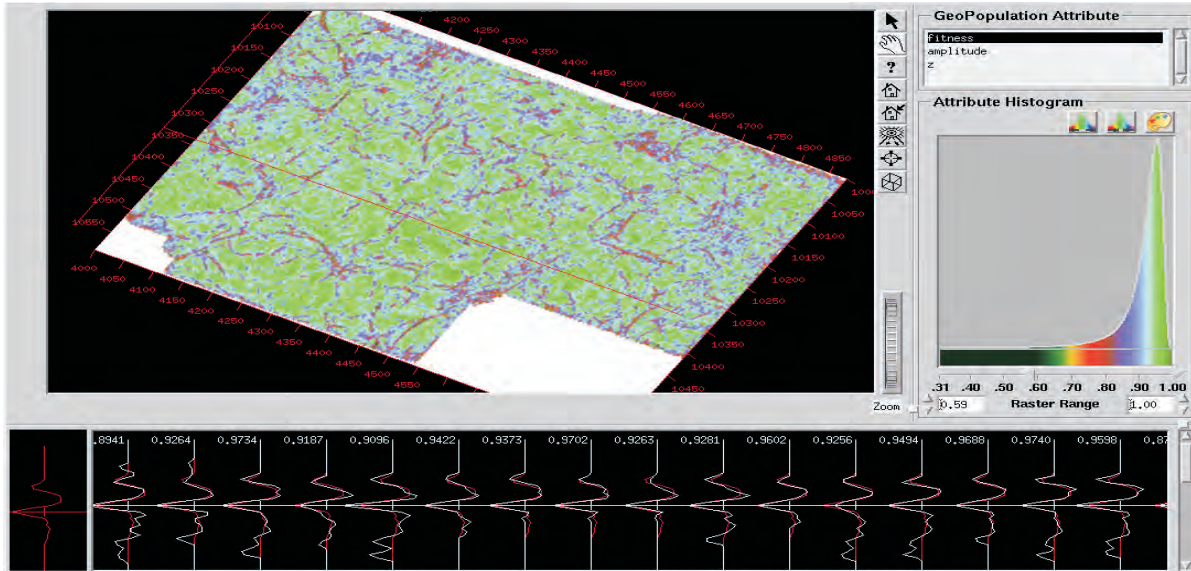


Figure 5: The map shows the “Fitness” of a single GeoPopulation™. The common waveform or Genotype is shown as the red trace in the lower left hand corner of the image. High fitness values are shown as green on the map meaning these traces have the highest degree of similarity with the Genotype. The low fitness values are shown as blue on the map meaning these traces are not necessarily an indication of a poor pick. In this case, the areas of lower fitness values identify subtle structural and stratigraphic features.

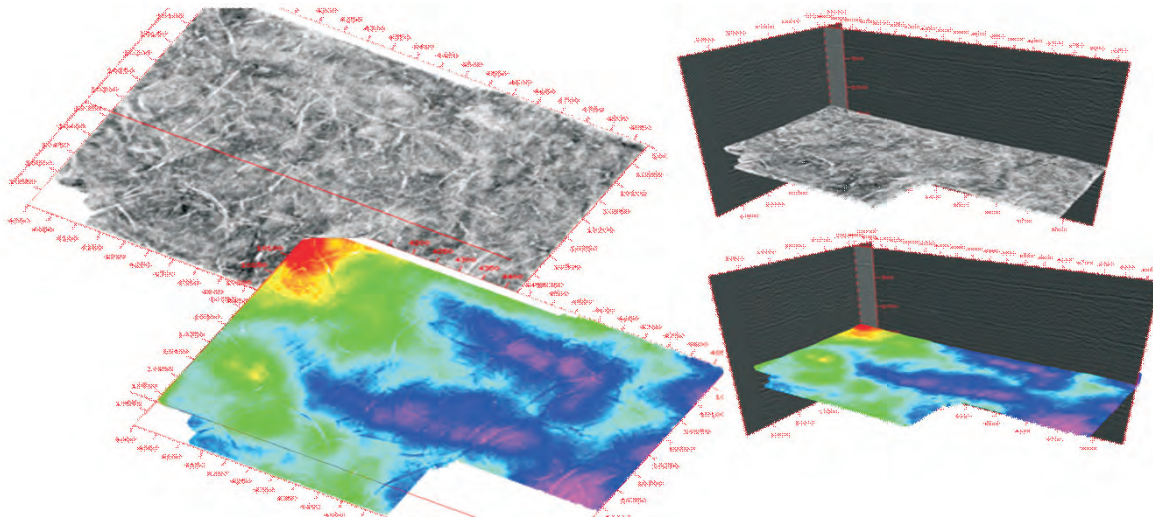


Figure 6: Amplitude and TWT when combined with Fitness provide a rapid visual assessment of the GeoPopulation™.

useful while others will be redundant or useless and can confuse seismic interpretation more than they help. (Barnes Arthur E. 2007) Using attributes which have a greater degree of orthogonality (or independence) provides better discriminatory power and produces more reliable results. This all clearly assumes the seismic volume has been correctly processed in the first place to minimise artifacts and truly represent the signal and image characteristics at each reflective horizon. Other independent attributes identified for each individual in the GeoPopulation™ are Amplitude and Two-Way-Time (TWT) (Figure 6) . High quality surfaces will result in more meaningful horizon amplitudes and TWT structure. TWT with Fitness and Amplitude enables a rapid assessment of the volume surfaces.

RESULTS

The processing algorithm described above has been applied by author Dirstein to thousands of square kilometers of 3D

seismic surveys both onshore and offshore Australia. In addition to final processed TWT volumes, some of the other data types processed in this manner include but are not limited to the following different data types:

- Time, Frequency or Depth Domain
- Post-Stack (angle stacks, AVO and Inversion attributes, Reflectivity, most seismic attributes).
- Spectral attributes volumes such as Spectral Decomposition and Spectral Attenuation
- Pre-Stack (gathers, shots for first break or refraction analysis)

Several examples are shown from across Australia using datasets collected over the Gorgon Project area, the South Australia portion of the Cooper /Eromanga basin and data collected from a coal minesite in Queensland.

Example 1: The Chandon Gas field (Chevron Operation) reservoir level

The Chandon gas discovery was drilled in 2006 in 1,200 metres of water and is located in the North Carnarvon Basin (Figure 7). This field is one of a number of large gas accumulations which form the Gorgon project area. Chevron reports that these fields contain approximately 40 Trillion cubic feet (TCF) of natural gas and Chevron cites this as Australia's largest natural gas resource Chevron Australia (2010). The Seisnetics genetic algorithm was applied to a sub-volume extract from the Chandon 3D seismic volume. The subset processed consists of just under 500,000 traces or about two gigabytes of data. After approximately eight hours of processing more than 700,000 generations of "evolution" identified about 120 million individuals which were assigned to GeoPopulations™. Figure 8 shows a surface near the top of the reservoir section contained in tilted fault blocks. This surface is one of hundreds of high quality surfaces automatically extracted by the Seisnetics processing algorithm. The interpreter then reviews the resulting surfaces to decide which of those surfaces provide the most meaningful geological insight.

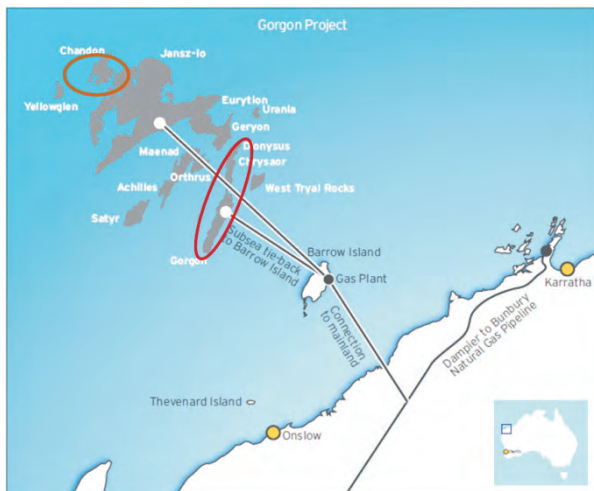


Figure 7: Location map for Chandon and Gorgon gas fields. Extract from Chevron Publication "The Power of Human Energy" a copy can be downloaded from the following link: <http://www.chevronaustralia.com/Libraries/Publications>

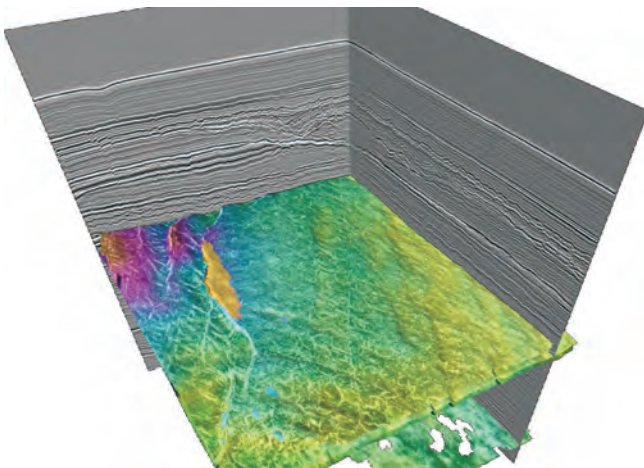


Figure 8: Image taken from visual database of GeoPopulations from the Chandon 3D volume. The GeoPopulation shown is located just above the top of the reservoir section.

Example 2: The Gorgon Gas field (Chevron operation) Outgassing and Geohazard

The Gorgon field was discovered in 1981 and is located in the South East corner of the Gorgon project area. The production lifespan of the project may approach 60 years. In this example the entire sixteen gigabyte dataset was processed for GeoPopulations™ of both peaks and troughs. As with the Chandon example hundreds of high quality surfaces were automatically extracted after several days of processing. Figure 9 shows an extract from the surface associated with the Sea Floor. The round circular patterns are pockmarks which are geomorphologic features which are often indicative of upward fluid flow and the venting of gas. The Gorgon field along with many other gas accumulations offshore Western Australia show evidence of out-gassing and upward fluid flow. This out gassing has, in places, resulted in both small scale and large scale depressions in the sea floor. While some pockmarks can be small and below the imaging resolution of conventional exploration 3D surveys, many (like those shown here) are much larger and can measure 100s of meters in diameter. Regionally, areas of higher density of pockmarks have contributed to slumping and sea-floor instability over large areas during the course of geological time.

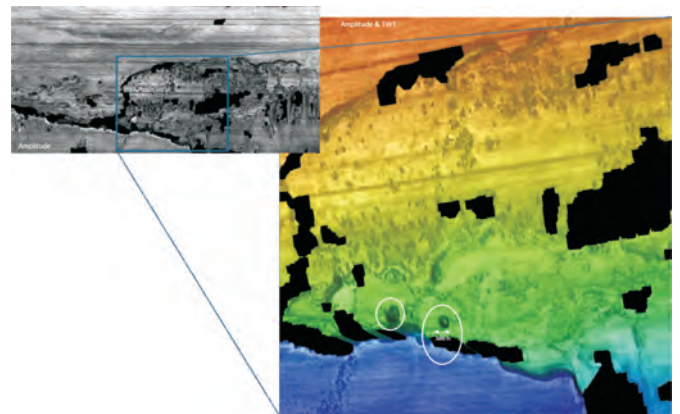


Figure 9: Evidence of Outgassing over the Gorgon Gas Field offshore Western Australia. While zones of outgassing can reduce the exploration risk and demonstrate area of active hydrocarbon migration, they can provide an indication of possible drilling hazards.

Example 3: The Cooper /Eromanga basin (South Australia and Queensland)

The Cooper and Eromanga basins, which span North East South Australia and South West Queensland, form Australia's largest onshore petroleum province. Currently, more than sixty (60) 3D seismic data volumes comprising of about 13,000 square kilometers of seismic data have been processed from this area using the automated genetic algorithm from Seisnetics. The initial phase of the project which processed forty (40) volumes was completed within four calendar months. The integration into GIS applications of these high quality GeoPopulations™ with openfile well control, production data and zones of interest enables both regional and very detailed models to be developed (using much more of the available data). Moreover, these models are entirely data driven and can provide a effective means of extending

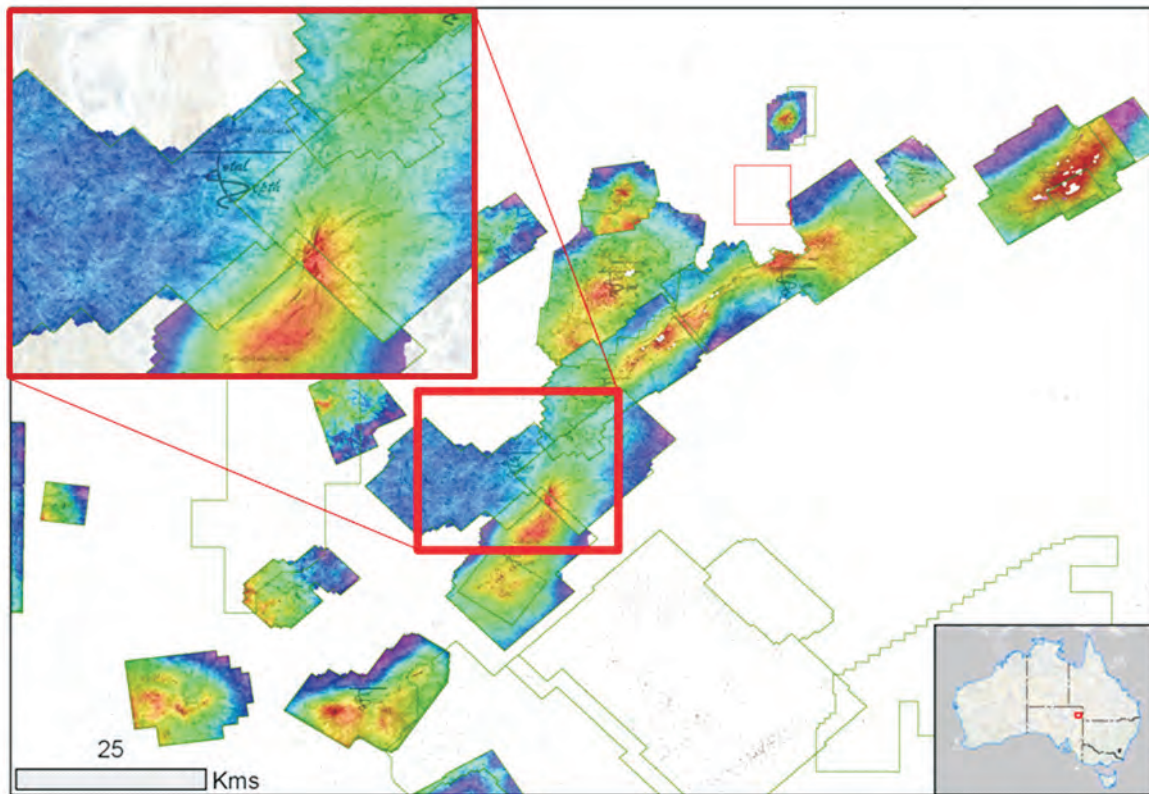


Figure 10: The image shows the location of some of the 3D datasets available from the Cooper Eromanga basin. The coloured images show the TWT attribute for the same horizon on all 3D datasets. From the visual database of GeoPopulations™ similar composites could be made at virtually any surface. Colour bars are scaled independently.

constrained models into areas which have less data coverage. This type of integration is underway offshore and also onshore in every state in the commonwealth as all seismic data collected eventually becomes open-file. While the seismic open-file concept is not legislated in the Queensland minerals act, the industry would benefit in the long term from the integration and incorporation of this type of seismic data analysis into other regional projects.

Example 4: Coal mine from the Bowen Basin

The Bowen Basin in central Queensland is subject to a significant amount of open cut and underground coal extraction. At this site the target coal seam is approximately 210m below the surface. The seam has an average thickness obtained from the 60 core samples of 2.1m and the survey area is 7.6 square km. The coal seam of economic interest is the German Creek seam within the Permian Moranbah Coal Measures. There are several much thinner seams existing above the German creek, however these are not of underground economic interest within the project area. The seismic data are derived from a 3D dynamite source survey acquired on a brick acquisition geometry using six geophones grouped into a 2m array length, spaced 15 m apart, along lines separated by 32 meters. A 150gm PETN booster was used for the charge placed 2m below the base of weathering. The dominate wavelength for the final processed signal is approximately 18 to 20 meters. Higher resolution will generate greater detail at or near the target horizon, but this does not necessarily bring greater clarity or certainty in the

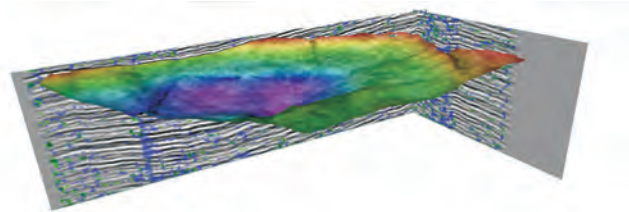


Figure 11: TWT GeoPopulation with Fault zones

interpretation. Figure 11 illustrates one horizon of many that can be used by the interpreter to provide an objective starting point to providing a meaningful geological interpretation.

DISCUSSION AND INTERPRETATION

The ability of an interpreter to provide a geological interpretation that is close to reality depends on a numbers of factors (e.g. experience, survey design, sampling, data quality, noise levels,... etc.) If the interpreter focus is only on one or two horizons then the 3D volume has almost certainly been underutilized. Geological events both syn and post depositional combined with lithification can create a complex environment which requires a thorough assessment of the likely hazards associated with placing people and machinery within that world. For the Biologists their initial model of the Human Genome was very wrong because collectively, they had chosen to ignore half of the data when they stripped away

the encasing protein to study the DNA molecule. Since Geoscientists create models from seismic 3D volumes often using less than 10% of the available data, these models are also likely to be incorrect or heavily biased. To use an often paraphrased quote; “Remember that all models are wrong; the practical question is how wrong do they have to be to not be useful” { Box, George E. P.; Norman R. Draper (1987). While the genetic processing technique described is capable of objectively extracting all the surfaces in a data volume, it is unlikely whether anyone would want to use all data for model construction. However, being able to review all the surfaces in a volume, to develop an understanding of the variability within the dataset, should enable the GeoScientist to develop models that are sufficiently detailed to capture that variability and not overly simplified to render them useless.

From the examples shown, examination of the GeoPopulations™ provided insight into structure, geomorphology, fluid-flow, out-gassing and sea-floor stability at both regional and local scales. These insights can only be made when the volume surfaces can be reviewed in detail (preferably, by a multi-disciplinary team). Often different disciplines are able to extract different types of meaningful information from the results. Therefore, by automating the surface extraction process and providing one or two orders of magnitude more high quality surfaces than conventional interpretation techniques, more time can be spent developing an understanding of the results instead of getting bogged-down by the mechanics of the extraction process. In areas where a horizon is noisy or subject to coherent interference, the ability to rapidly have an objective horizon for critical review by the interpreter can significantly improve the reliability of the interpretation. Moreover, when this analysis is incorporated during the processing of the data, additional information can be used to optimise the processing of the data and get useful data to the interpreter at a much earlier stage. Finally, older legacy data volumes, with the incorporation of geological and engineering data from the sub-surface team into the visual database; will form a knowledge base and provide teaching opportunities for the next project and the next wave of geoscientists. One might also speculate on how this technology would apply to other sets of waveform data collected by the minesite (i.e. analysis of the radar guidance waveforms from the long-wall shearer).

CONCLUSIONS

This paper has described and illustrated a mathematical process for objectively providing a series of automatically picked horizons within a 3D seismic volume. The mathematical process emulates biological evolutionary stages whereby an initial population of individuals are randomly identified and given the opportunity to evolve. At the end of each generation, individuals which match the selection criteria, combine with an existing population forming offspring which inherits the genotype of its two parents. Through the generations, the fittest have more chance to be selected and to reproduce, which enable them to grow faster than less fit individuals. Typically, the more continuous surfaces evolve first with the more complicated surfaces

evolving last. Using this process the authors have illustrated examples where large multi horizons 3D datasets can be assessed at either a micro or macro scale for horizon characteristics. The aim of the process is to provide a method whereby the interpreter can rapidly examine all the data, assess the significant aspects of the data then create a meaningful geological model which has been created based on a review of all the data.

Currently, the authors are building visual databases of GeoPopulations™ for individual and basins of 3D seismic datasets. While there is no formal requirement for the sharing of 3D data over coal mines, perhaps an informal arrangement allowing the exchange of data over areas already mined would offer insights on improving models and incrementally improving best practice for coal mining.

Future development of this technique for the coal mining industry could be to modify the segmentation process to simultaneously target both populations of horizons and faults such that the visual database would contain an automatically created and unbiased model of the entire 3D seismic volume.

ACKNOWLEDGEMENTS

The authors gratefully acknowledge the efforts of the team at Seisnetics LLC (patent holder of this technology). Specifically, the guidance from David Jetelina in the use of the 3D visualization tool used to view the visual database of GeoPopulations™. Finally, the authors would like to thank and congratulate Nabil Tnacheri on the development of this beautiful technology and encourage the Seisnetics team to keep up the good work.

REFERENCES

- BALTIMORE, D., 2001: Our genome unveiled. *Nature*, **409**, 814–816.
- BARNES, A.E., 2007: Redundant and useless seismic attributes. *Geophysics*, **72**, 33.
- BOX, G.E.P. & DRAPER, N.R., 1987: *Empirical Model-Building and Response Surfaces*. 424, Wiley.
- CHEVRON AUSTRALIA, 2010: The Power of Human Energy. http://www.chevronaustralia.com/Libraries/Publications/100510_Chevron_Australia_Corporate_Brochure_2010.sflb.ashx
- FANG, J.H., KARR, C.L. & STANLEY, D.A., 1996: Transformation of Geochemical Log Data of Mineralogy Using Genetic Algorithms. *The Log Analyst*, **March-April**, 26–31.
- GREFENSTETTE, J.J. & BAKER, J.E., 1989: How Genetic Algorithms Work: A Critical Look at Implicit Parallelism. In: Kaufmann, M.: *The Proceedings of the Third International Conference on Genetic Algorithms*. San Mateo - California, 12–19.
- MICHALEWICZ, Z., 1992: *Genetic Algorithms + Data Structure = Evolution Programs*, 3rd edition., Springer-Verlag, New York, 387.
- WATSON, J.D. & CRICK, F., 1953: Molecular Structure of Nucleic Acids: A structure for deoxyribose nucleic acid. *Nature*, **171**, 737–738.

James K Dirstein is the managing director and principal Geoscientist for Total Depth Pty Ltd

Gary Fallon is a director and geoscientist for Geophysical Resources & Services Pty Ltd (GRS)

Binxhong Zhou, Peter Hatherly, Troy Peters and Weijia Sun

Seismic imaging of coal seam structure under basalt cover

Tertiary volcanic basalts (high velocity layers) exist in both the Bowen and Sydney Basins. In these areas, exploration using seismic reflection methods may not produce meaningful results and drilling is difficult and costly. These exploration difficulties make areas with basalt cover significantly less attractive for mining. To gain insights and obtain potential solutions to this important problem, we have investigated the propagation of seismic waves through basalt cover with numerical modelling and the analysis of seismic reflection and borehole vertical seismic profiling data at the North Goonyella Mine and the Moranbah South coal mine lease in the Bowen Basin.

Our investigations show that the main problem with the basalts is the large impedance contrasts that exist within the flows and the surrounding strata. These contrasts lead to the generation of numerous undesirable seismic effects such as reverberations within the basalts, multiple reflections between the basalts and surrounding interfaces – especially the ground surface, and complex diffraction/scattering phenomena at the boundaries of the basalt. When these wave behaviours are excited, simple wavefronts no longer propagate down through the geological sequence. These issues arise again on the return of the reflected waves to the ground surface.

It is observed that the pre-stack depth migration processing has largely improved the reflection continuity for the data set from North Goonyella but not the one from Moranbah South. This is attributed to the effect of surface ground-rolls in these two data sets: the North Goonyella data have much less ground-roll than the Moranbah South one. This is supported by the surface shot gathers and borehole VSP records.

The strong scattered and reverberated surface ground-rolls in the basalt zone seriously mask the relatively weak deep reflections and make coal seam imaging below the basalt very difficult at the Moranbah South Mine. Reducing the surface wave will be the key for improving the imaging under basalt cover, especially when the basalt is shallow.

INTRODUCTION

Near surface volcanic basalts of Tertiary age occur in both the Bowen and Sydney Basins. These basalts often contain vertical cooling joints and other inhomogeneities. In addition, multiple flows may be present with unconsolidated sediments lying between flows. Basalts usually have very high seismic velocities and densities compared to surrounding rocks.

Consequently, wave propagation through basaltic layers is complex. Where basalt flows occur, seismic reflection exploration for underlying coal seams is problematic. In many instances, reflection surveys totally fail to map the coal seams and the absence of good seismic reflection data beneath basalts makes these areas less attractive for coal mining.

These problems with seismic imaging under basalts are not unique to coal mining. In the petroleum industry, the imaging difficulty under basalt cover around the world is well known. For example, two special issues on sub-basalt imaging have been published by Geophysical Prospecting (Williamson, 2003; Christie & White, 2008).

The main problems with seismic surveys are generally thought to be due to the high-impedance contrast with the surrounding rocks and the inhomogeneity of basalts (Ryu, 1997; Fruehn & others, 1998; Ziolkowski & others, 2003; Hobbs, 2002; Behera, 2006). Many modifications to data acquisition and processing have been tested to improve the quality of seismic sections in the basalt covered areas. These techniques include long offset seismic data acquisition (Ryu, 1997; Wombell & others, 1999; Hanssen & others, 2002), low-frequency sources (Ziolkowski & others, 2003) and prestack depth migration (Fruehn & others, 2001; Reshet & others, 2003; Gallagher & Dromgoole, 2008). Improved results have been reported in the petroleum industry.

To understand and research potential solutions to this important problem, we have studied the propagation of seismic waves through basalt cover with numerical modelling and the analysis of seismic reflection and borehole vertical seismic profiling data from surveys at the North Goonyella Mine and the Moranbah South coal mine lease in the Bowen Basin (Zhou & others, 2010).

ANALYSIS OF SEISMIC DATA OVER BASALTS

North Goonyella Data

To study the feasibility of the 3D seismic method in future longwall areas, North Goonyella mine conducted seismic trials to test acquisition parameters. A reverse vertical seismic profile (RVSP) survey and a 2D surface reflection seismic survey were shot in 2002 by Velseis Pty Ltd. Figure 1 shows the locations of the RVSP borehole GN954 and the 2D seismic trial line. The borehole for the RVSP and the northern part of the 2D seismic line are located in an area containing

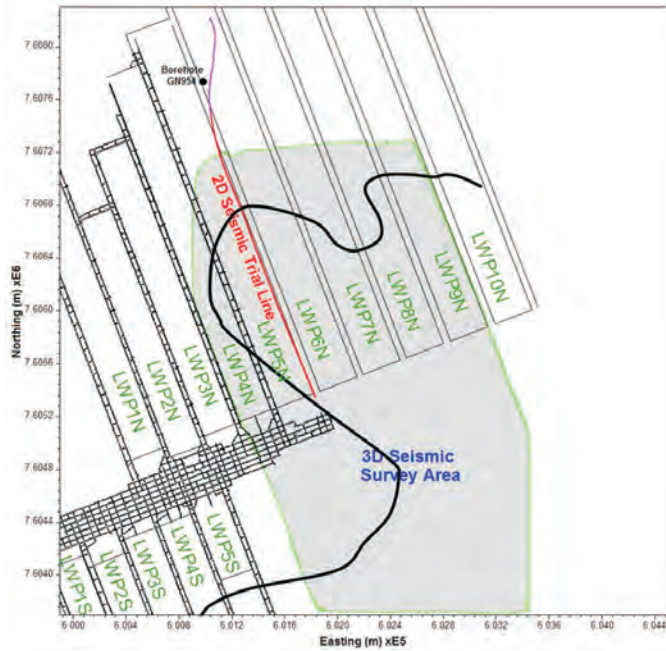


Figure 1: The location of the 2D trial seismic survey line and the borehole used in the reverse VSP survey. The thick black line indicates the southern boundary of thick Tertiary basalt. The northern part of the 2D seismic line is in the area where the basalt affects the seismic data.

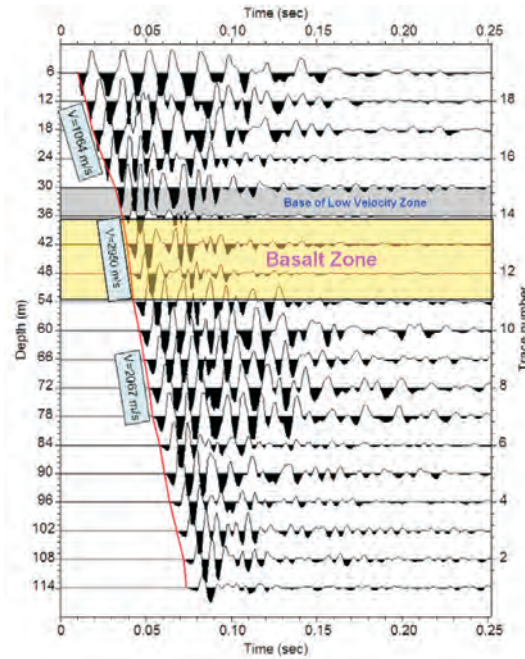


Figure 2: A common receiver gather at receiver 61 from the RVSP shot records. This receiver has an offset of 2 metres from the borehole and the direct ray paths to this receiver from the shots are approximately vertical. This plot indicates that there is a low velocity (~1064m/s) zone above 36m.

Area without Basalt

Basalt Covered Area

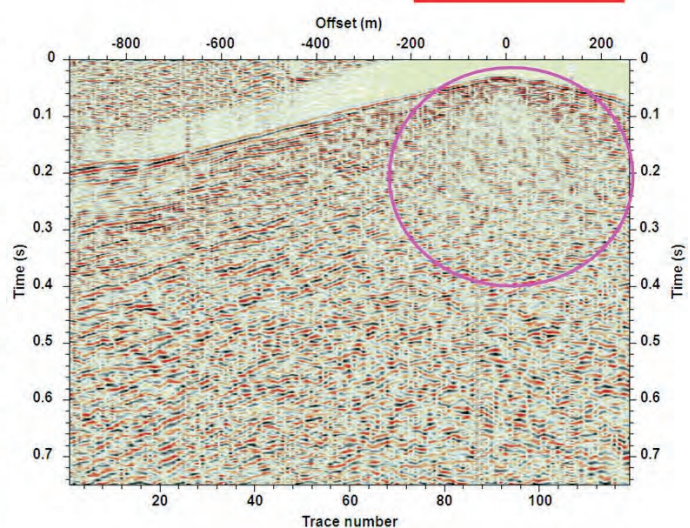
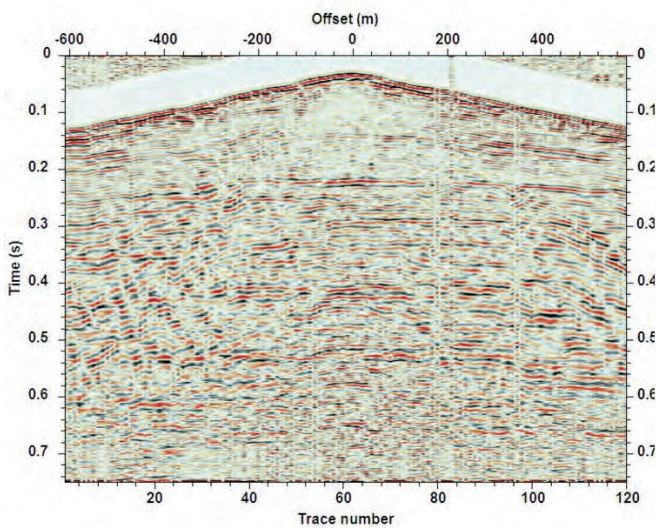


Figure 3: Typical seismic shot gathers from areas with (right) and without (left) basalt cover at North Goonyella Mine.

near surface Tertiary basalt. The source charge used in the RVSP survey was a 2x150g booster for each shot.

The RVSP reveals that the signal-to-noise (S/N) ratio can be significantly improved if the shots are at, or below, 36m depth; otherwise ground roll is generated. From the near-offset RVSP plot in Figure 2, there is a low velocity zone to a depth of 36m below this is basalt to a depth of 54m. The estimated velocity of this basalt is about 2950m/s, suggesting that it is weathered. Another basalt layer was intersected at the base of the hole at 114m depth. This basalt was not drilled because of its strength. It is thought that it is about 20m thick because a 20m thick basalt was encountered at a similar depth in borehole GN644C which is 60m away to the south-east.

Figure 3 presents two shot gathers from the 2D seismic trial survey in the areas with and without basalt cover. The data clearly shows that the basalt-cover seriously affects the signal-to-noise ratio and compromises our ability to image beneath it. Figure 4 shows the processed surface reflection section, with poorly imaged coal seam reflections below the basalt covered area on the right of the section. The section of the line over the basalt with the poor results is the same as that with the poor shot records illustrated in Figure 3. In an effort to improve the results, we investigated the use of automatic gain control (AGC), common reflection stack (CRS) and pre-stack depth migration (PSDM).

Figure 5 shows the reprocessed results after the PSDM procedures. The continuity of the reflections from the coal

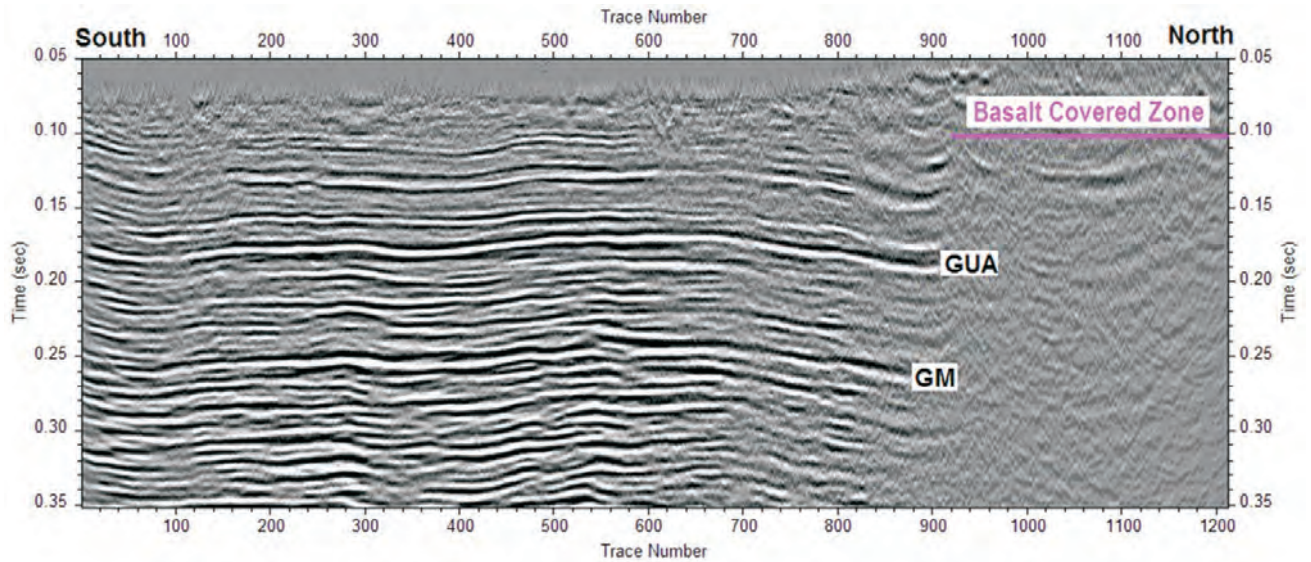


Figure 4: Typical seismic section from basalt covered area at North Goonyella Mine.

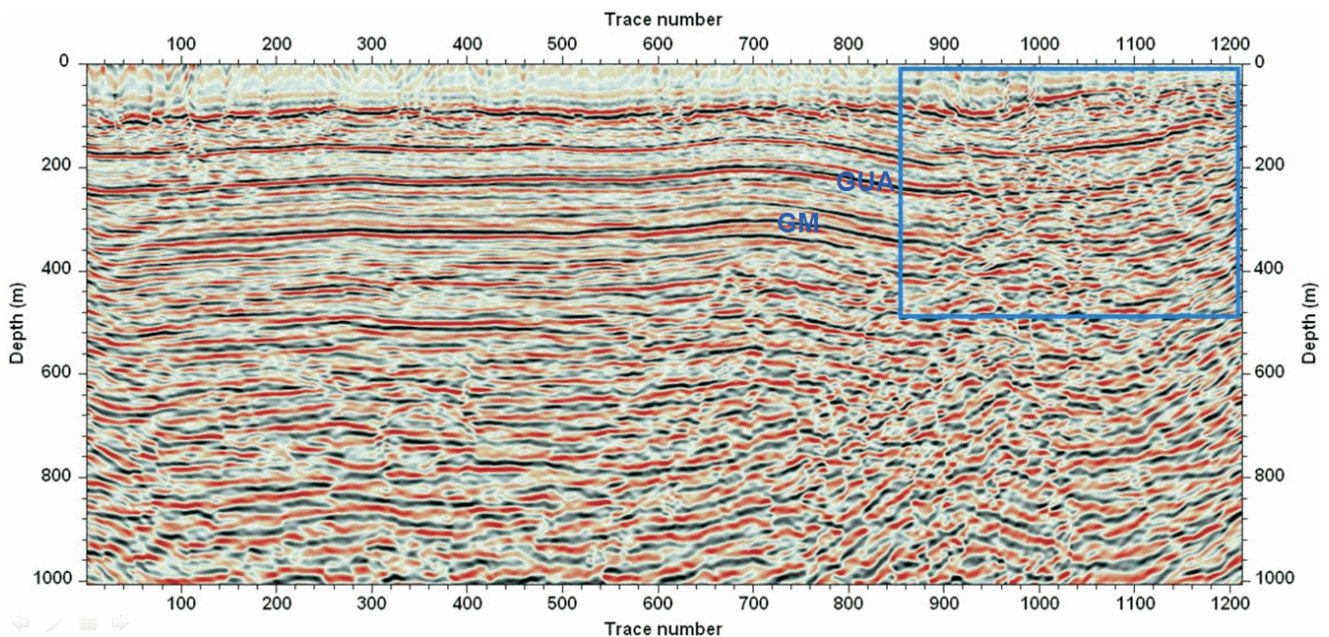


Figure 5: Prestack depth migration section for the North Goonyella 2D seismic line. The continuity of the coal seam reflections is largely improved in the basalt affected area as shown in the blue box.

seams has been improved and they can be traced through the basalt affected area. PSDM therefore can improve seismic imaging in complex situations. It is also consistent with our predictions from a numerical modelling study with two relatively thin basalt layers — one weathered and one fresh. The numerical modelling results suggest that thin layers have less effect on seismic wave propagation and therefore we can expect to image the sub-surfaces in this situation.

Moranbah South Data

With the support of Anglo Coal, seismic data for our sub-basalt imaging investigation were specifically collected as part of Anglo’s Moranbah South 2D seismic program. Figure 6 shows locations of the seismic lines on a total magnetic intensity map. Line MS-04 crosses a sinuous basalt flow and over this section of the line, long offset surface reflection data were acquired. In addition, borehole RMS0107 was drilled in the centre of the basalts to a level below the

target Goonyella Middle (GM) seam, which is at a depth of 307 m. In this hole, geophones were grouted and used for walkaway VSP recording using the shots from the seismic reflection survey as sources. Geophysical logging data from RMS0107 and surrounding boreholes (see Figure 7) suggest that the basalt is about 40m thick and interbedded with unconsolidated sediments (sands and gravels). The magnetic data indicate the basalt is about 360m wide. The seismic data acquisition for the special portion of the line MS04 was conducted by Velseis in August 2008. Compared to a conventional seismic reflection survey, a few parameters have been modified:

- a long-offset configuration with offset ranges from 0 to 4400m has been used in anticipation of imaging the coal seams below the basalt.
- the size of the seismic source was doubled from a standard size of 400gm to 800gm to accommodate the long-offset recording.

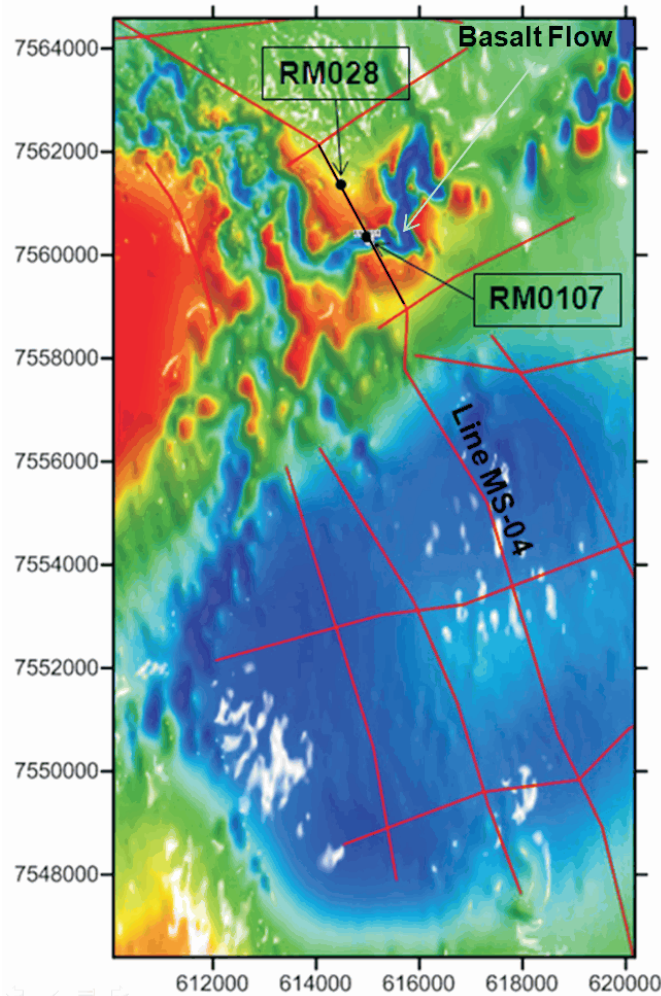


Figure 6: Location of seismic lines at Moranbah South as planned and the total magnetic intensity map (reduced-to-the-pole). The sinuous negative (blue) magnetic anomaly indicates that the basalts have flowed down a pre-existing drainage channel. Long offset reflection recording and a VSP survey were shot where line MS-04 crosses the channel.

- the natural frequency of geophones was lowered from the usual 30Hz to 14Hz to capture low frequency seismic signals with improved penetration characteristics and less sensitivity to near surface inhomogeneities.

This survey at Moranbah South therefore allowed the testing of long-offset seismic recording and an investigation of the characteristics of seismic wave propagation within and below the basalts.

The Moranbah South long-offset seismic data were processed by Velseis using conventional data processing procedures. The post-stack time-migrated section which has had a 50ms AGC applied is presented in Figure 8. It is evident that the coal seams below the basalt zone have not been imaged properly although there is a suggestion that the GM and P seams be traced through. The estimated width of the basalt on this section is about 330m (from traces 310 to 376 with a 5m trace interval).

We also tried F-X prestack depth migration (PSDM) to the long-offset data. Theoretically, prestack depth migration has no restriction to the offsets. However, due to the shallowness

of the target seams, we still need to apply a mute to the data to remove interference with refraction events. The PSDM result with post-stack processing such as inverse Q and time variant filtering is shown in Figure 9. The overall continuity of the reflections, especially for the deep reflections below the GM seam, on the section has been improved. However, the major coal seams below the basalt zone are not resolved.

Coal seam reflections under basalts

The sub-basalt imaging results from North Goonyella and Moranbah South are quite different: one can be improved by PSDM processing but not the other. The question as to why this is so therefore arises.

To answer this question, we compare the VSP data from North Goonyella with those from Moranbah South in Figure 10. At North Goonyella, the structure of the down-going wave is relatively simple and there are clear up-going reflections present later in the records. However, there are no up-going waves which can be identified at Moranbah South. This suggests that there are strong reverberations caused by the basalts at Moranbah South which

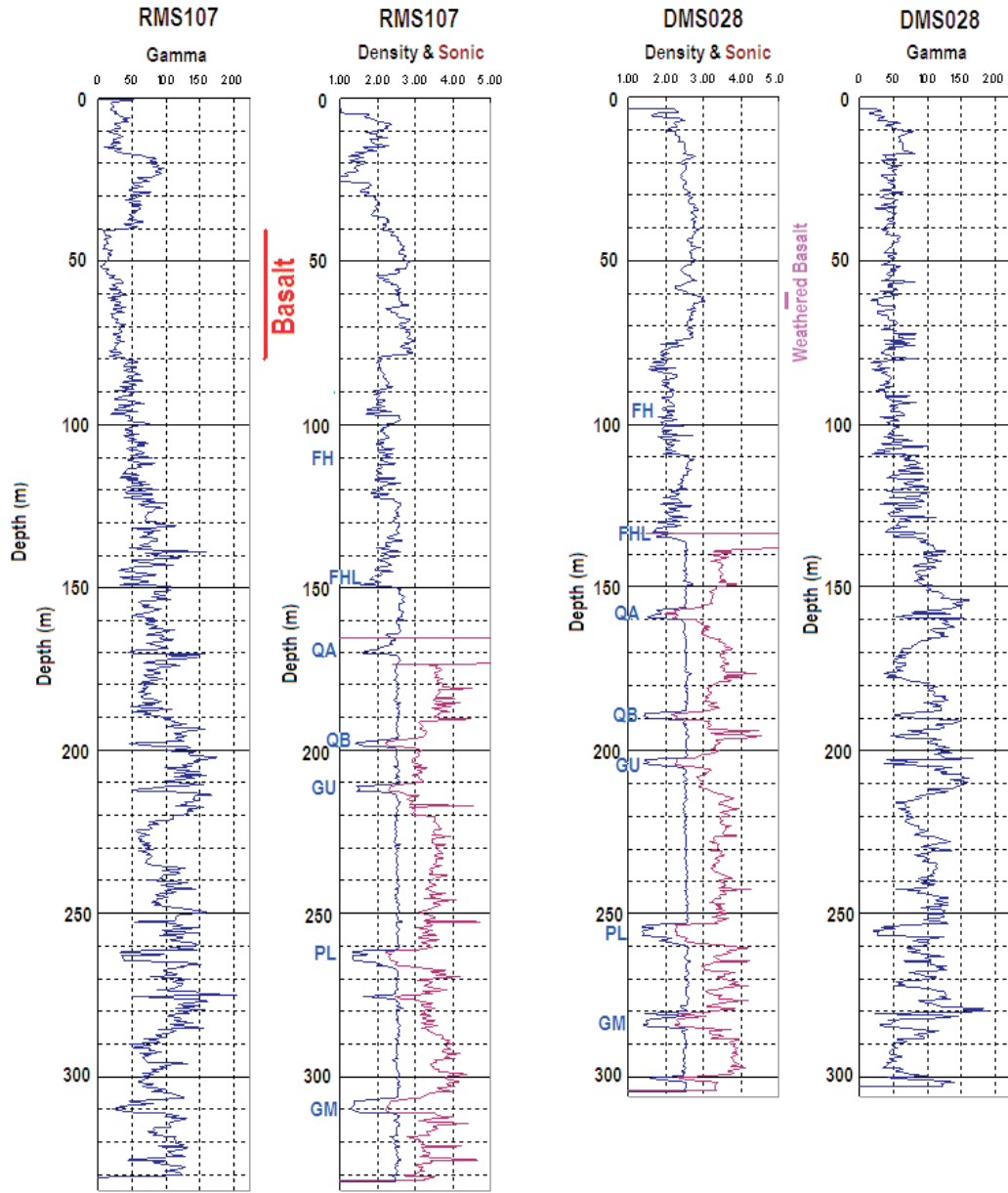


Figure 7: Geophysical logs from borehole RMS0107 (first two columns) and DMS028 (last two columns). **Borehole RMS107:** Fresh Basalt 3–8m, 9–17, 40–80; Clay bands are within. Fair Hill seam 90–122m. Fair Hill Lower seam 134–150m. HWT casing to 174m. Base QA seam at 170m, base of QB seam 198m, base of GU 213m, base of P Lower seam 267m, P tuff 275m, base of GM seam 312m. **Borehole DMS0028:** Weathered Basalt ~6m at 60m. Base of Tertiary 14m. Fair Hill seam 75–109m. Fair Hill Lower seam 124–135 m. Steel casing to 138m. Base QA seam at 160m, base of QB seam 190m, base of GU 205m, base of P Lower seam 260m, P tuff 280m, base of GM seam 284m.

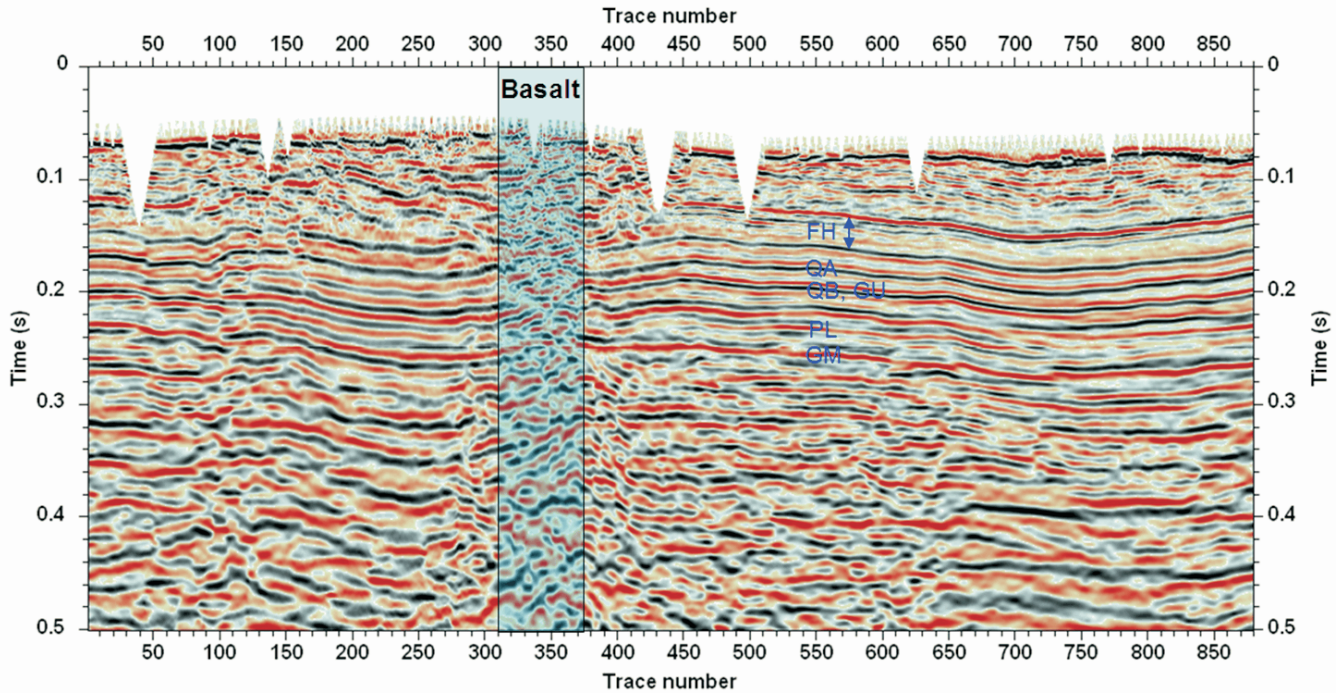


Figure 8: Conventional processed seismic migration section for the Moranbah seismic survey. The trace interval is 5m. The light-blue shaded rectangle is the basalt affected zone with a width about 330m. The reflections corresponding to the major coal seams GM, PL, GU, QB, QA and FH are marked on the plot. A 50ms AGC was applied for display purpose.

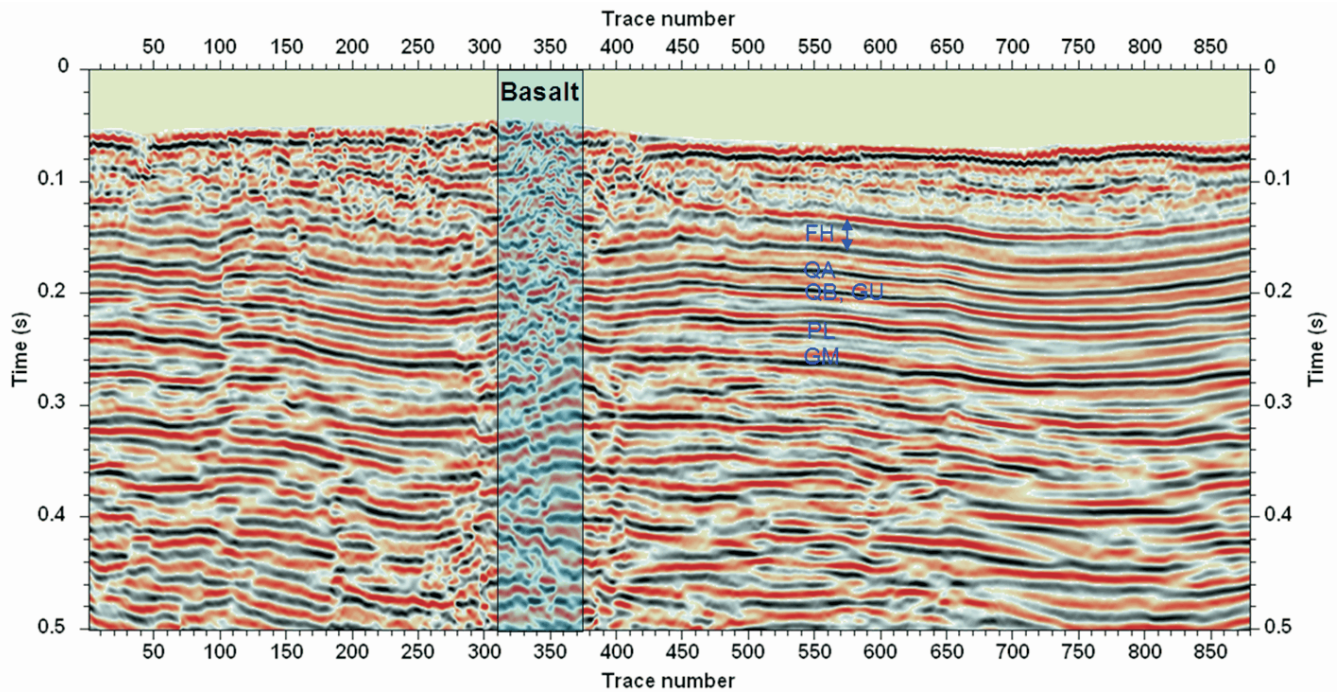


Figure 9: Prestack depth migrated section for the Moranbah South seismic survey

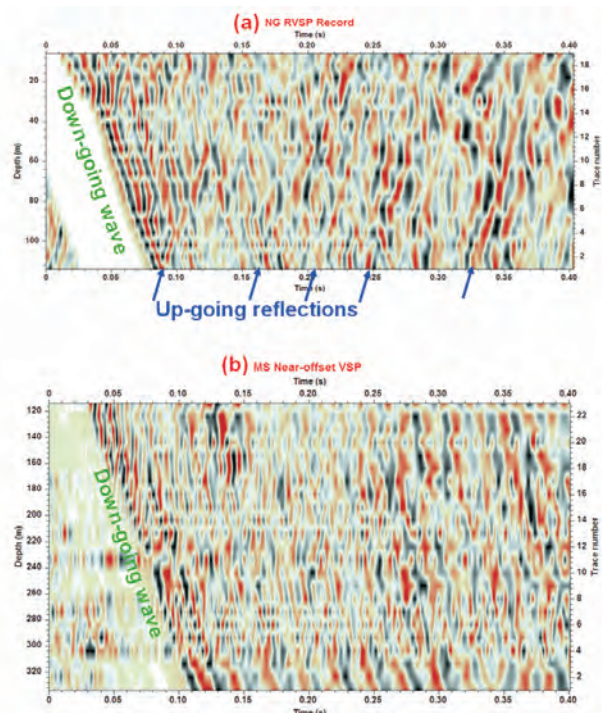


Figure 10: VSP data from the North Goonyella VSP survey showing a clean down-going wave (first arrival) followed by clearly recognisable up-going waves. At Moranbah South (b), the down-going wave is much more complex and no up-going waves are evident.

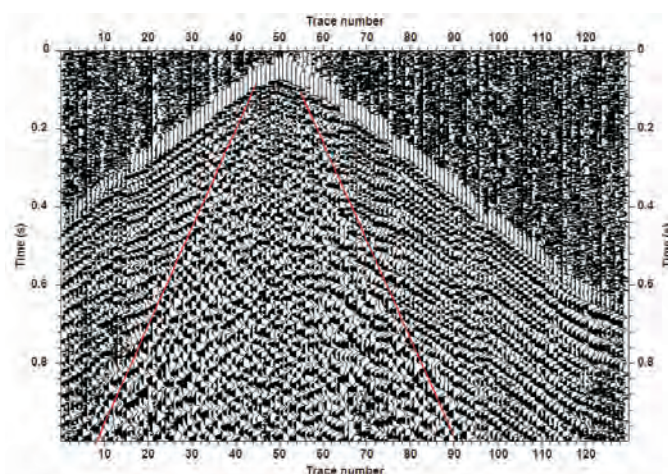


Figure 11: The common borehole geophone gather at a depth of 234m in borehole RMS0107, which is overlaid with the simulated scattered ground wave curve in red. Within this scattered ground waves curve, no coherent reflections can be observed.

degrade the signal-to-noise ratio and make the reflections insignificant compared with the background noise. This is supported by our numerical modelling and the common borehole geophone gathers such as the one shown in Figure 11.

CONCLUSIONS

Significant efforts have been made to understand key features of the wave propagation and to image major coal seams beneath basalt cover. The approaches taken for the imaging

include long-offset data acquisition and pre-stack depth migration. At North Goonyella, we improved the continuity of the coal seam reflections across the zone affected by the basalt through processing and without the need of any special acquisition parameters. However, at Moranbah South, the problem with the basalts proved to be intractable. Neither long-offset data acquisition nor prestack depth migration was able to produce satisfactory results.

Based on our observations, the main issues for seismic surveying in basalt covered areas are (i) the generation of complex down-going and up-going wavefields, which are due to the strong impedance contrasts between the basalt and the surrounding strata, and (ii) the generation of incoherent scattered and reverberated waves from inhomogeneities within the basalts and their rough margins. The reverberation of ground-rolls in the basalt covered area will seriously contaminate the weak reflections and make the sub-basalt imaging difficult. Therefore, reducing the surface wave will be the key for improving the imaging under basalt cover, especially when the basalt is shallow.

ACKNOWLEDGEMENTS

The work reported here was financed by Australian Coal Association Research Program (ACARP) project number C17013. Special thanks go to the following people: Russell Howarth (ACARP project co-ordinator), Andrew Willson (ACARP project monitor, Anglo Coal), Doug Dunn (ACARP project monitor, BMA), Michael Creech (Peabody), Mike Armstrong (BHPB Coal), Todd Harrington (Xstrata) and Henk van Paridon (GeoSolve) for various discussions, suggestions and support to the project. The prestack depth migration processing was conducted by Oil Hunters.

REFERENCES

- BEHERA, L., 2006: Sub-basalt imaging using converted waves: A numerical approach: *76th Annual International Meeting of the Society of Exploration Geophysicists, Expanded Abstracts*, 2318–2322.
- CHRISTIE, P.A.F. & WHITE, R.S., 2008: Imaging through Atlantic Margin basalts: An introduction to the sub-basalt min-set, *Geophysical Prospecting*, **56**, 1–4.
- FRUEHN, J., WHITE, R.S., RICHARDSON, K.R., FLIEDNER, M., CULLEN, E., LATKIEWICZ, C., KIRK, W. & SMALLWOOD, J.R., 1998: Flare – a two-ship experiment designed for sub-basalt imaging: *68th Annual International Meeting of the Society of Exploration Geophysicists, Expanded Abstracts*, 94–97.
- FRUEHN, J., FLIEDNER, M.M. & WHITE, R.S., 2001: Integrated wide-angle and near-vertical subbasalt study using large-aperture seismic data from the Faeroe-Shetland region. *Geophysics*, **66**(5), 1340–1348.
- GALLAGHER, J.W. & DROMGOOLE, P.W., 2008: Seeing below the basalt - offshore Faroes. *Geophysical Prospecting*, **56**, 33–45.
- HANSEN, P., ZIOLKOWSKI, A. & LI, X., 2003: A quantitative study on the use of converted waves for sub-basalt imaging, *Geophysical Prospecting*, **51**, 183–193.

- HOBBS, R., 2002: Sub-basalt imaging using low frequencies, *Journal of Conference Abstracts*, **7**, 152–153.
- RESHEF, M., SHULMAN, H. & BEN-AVRAHAM, Z., 2003: A case study of sub-basalt imaging in land region covered with basalt flows. *Geophysical Prospecting*, **51**, 247-260.
- RYU, J, 1997: Seeing through seismically difficult rocks unconventionally, *Geophysics*, **62** (4), 1177–1182.
- WILLIAMSON, P., 2003: Introduction: *Geophysical Prospecting*, **51**, 167–168.
- WOMBELL, R., JONES, E., PRIESTLY, D. & WILLIAMS, G., 1999: Long offset acquisition and processing for sub-basalt imaging: *69th Annual International Meeting of the Society of Exploration Geophysicists, Expanded Abstracts*, 1429–1432.
- ZHOU, B., HATHERLY, P., PETERS, T. & SUN, W., 2010: Imaging coal seam structure under basalt cover: Final report for ACARP Project C17013.
- ZIOLKOWSKI, A., HANSEN, P., GATLIFF, R., JAKUBOWICZ, H., DOBSON, A., HAMPSON, G., LI, X. & LIU, E., 2003: The use of low frequencies for sub-basalt imaging, *Geophysical Prospecting*, **51**, 169–182.

Peter Hatherly and Terry Medhurst

Additional opportunities for geophysical log analysis

Australian coal geologists have long realised the value that geophysical borehole logging brings to exploration programs and routinely log most exploration holes. Logs are typically studied to identify coal seams and marker horizons, to provide a record of the hole trajectory and to reconcile drillers' depths with actual depths. For geotechnical purposes, sonic logs are often used to estimate UCS. Geophysical logs are also used to qualitatively assess the stratigraphy in uncored intervals.

While these varied applications indicate an acceptance of geophysical logging technology, it is our view that there is more that geologists could be doing at the quantitative level. Quantitative analysis is based on petrophysical rock models which consider the various types of solids present (quartz, clays, carbonaceous materials), the cements that bind the grains, the porosity and the material in the pore spaces. To identify these components, suites of geophysical logs (ideally comprising density, sonic, natural gamma, neutron and resistivity logs) need to be analysed to produce petrophysical models consistent with the log responses.

The complexity of the models varies according to the nature of the rocks, the questions being asked and the suite of geophysical logs available. In an Australian context, quantitative analysis could be undertaken in response to questions on hole-to-hole correlation, depositional environments, the amount of carbonaceous material present, quantification of geotechnical conditions and the presence of gas. 2D and 3D modelling of results is also possible.

To encourage geologists to extend their use of geophysical logs, this paper discusses our approach to quantitative interpretation and provides examples of our work on such questions.

INTRODUCTION

In Australian coal mining, it is accepted practice for exploration boreholes to be geophysically logged on completion of drilling. In addition to providing information on the condition of the borehole and a survey of its path, there are a number of well-established geological uses. From the density log comes the opportunity to locate coal seam margins and to provide depth control, the sonic log allows estimation of UCS, and the natural gamma log allows the mapping of tuff band markers and the demarcation of sandy and clay rich units. These applications require just an intuitive understanding of the geophysical logs and the ability to pick

the depths of features of interest. Most geologists are comfortable performing these tasks.

Geologists also recognise that geophysical logs provide a record of the down-hole geology that can be archived for future consideration. In this paper we discuss the significant benefits to be obtained by realising some of this future potential now.

LITHOLOGY

The main lithological units that can be identified from geophysical logs are:

- Coal — anything with a density value lower than a chosen cut-off, typically 1.9 to 1.95t/m³.
- Other carbonaceous units — anything with a density greater than the coal cut-off but still with relatively low densities, say less than 25% greater than the coal cut-off.
- Siderite — anything with a density significantly greater than the matrix density of the clastic rocks present (typically in the range 2.62 to 2.7t/m³)
- Clastic units — non-carbonaceous and non-sideritic materials with natural gamma values lying between extreme values associated with clean sandy units (low natural gamma values) and clays (high natural gamma values).
- Tuff — anything with a natural gamma value significantly higher than the value selected for clays.

If borehole caving is present, log values may be distorted. Caliper logs should always be examined to check on borehole conditions.

ROCK MODEL

For clastic rocks, a simple volume-balanced rock model is:

$$V_{quartz} + V_{clay} + \phi = 1 \quad (1)$$

Where V_{quartz} is the fractional volume of quartz present, V_{clay} represents the fractional volume of clay (shale), and ϕ is the porosity. The volume of quartz and clay added to the porosity cannot be greater than 1. All fractional volumes should also be consistent with geological expectations.

POROSITY

For clastic rocks, it is a simple matter to determine the porosity from the density log. All that is required is an estimate of the matrix density. Geophysical logging contractors frequently provide a density porosity log as part of the final logging results. These are almost always calculated using a matrix density of 2.65t/m^3 (the density of quartz) but if the true matrix density is greater, use of a value of 2.65t/m^3 can lead to small, even negative porosities. In this and the converse situation when the true matrix density is less than 2.65t/m^3 , the density porosity should be recalculated.

Geophysical logging contractors may also provide porosities from sonic logs which are based on a calculation with assumed velocities for the rock matrix and the pore fluids. The calculation also assumes that a rock model applies whereby the velocity is given by the travel time through a single solid layer representative of the matrix ($V_{\text{quartz}} + V_{\text{clay}}$) plus the travel time through a single liquid layer representative of the porosity. Unfortunately, this simple model is not adequate. The speed of a P-wave (sonic wave) differs in quartz and clay. As well, the grain contacts and packing affect the velocity and the extent of the influence of the pore fluids.

Porosities can also be determined from a neutron log. These values are only applicable for the clastic rocks within the borehole. Before they can be taken to be representative of the true porosity, compensation is required for the bound water resident within any clay minerals present.

CLAY AND CLAY MODELS

From a natural gamma log, the clay content at any point within the clastic section of the hole can be determined by scaling values relative to chosen natural gamma values for clean sand ($V_{\text{clay}} = 0$) and pure clay ($V_{\text{clay}} = 1$). The assumption here is that the natural gamma value is solely due to the amount of clay that is present. This is generally a reasonable assumption but exceptions can arise. For example, kaolinite contains zero or little potassium and as consequence ^{40}K , the required radioactive isotope, is missing and the overall level of natural gamma radiation is reduced. Conversely, some sands containing heavy minerals which can also be rich in thorium. Such sands may have the natural gamma signatures of shales.

If resistivity and/or neutron logs are available, ambiguities such as these can be resolved by making alternative determinations of the clay content. Calculations involving these logs also require estimates of the porosity provided from the density log. The neutron log is probably more commonly acquired but for those mines and sites where neutron logging is not allowed because of the perceived risks associated with the neutron source, resistivity logging may be worth considering as an alternative means for clay estimation.

In addition to determining the clay content, it is possible to establish how the clays are distributed within clastic units. Figure 1 shows that cross-plots of natural gamma values

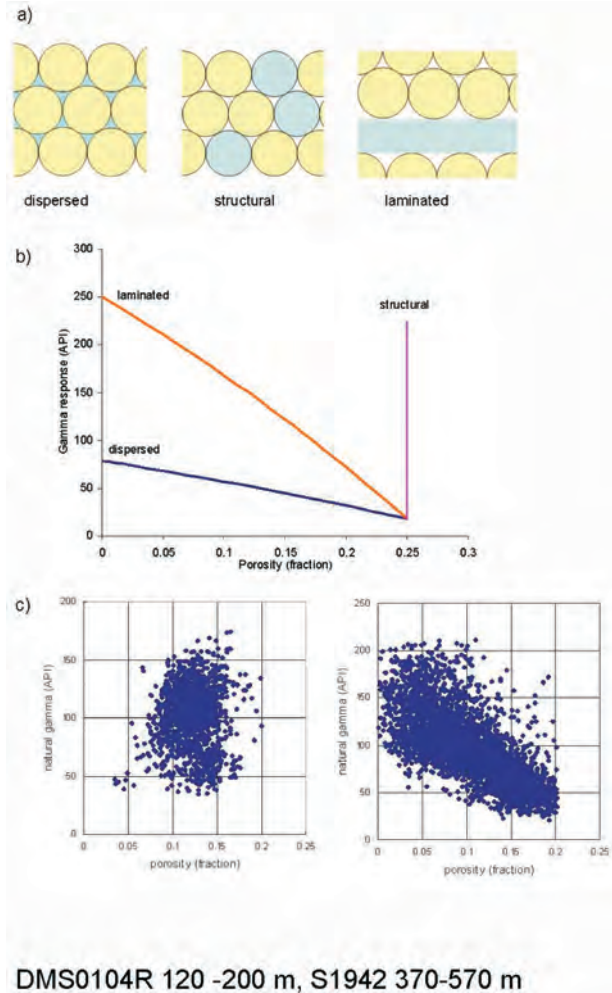


Figure 1: a) Clay models for clastic rocks. Left; dispersed clay occupies the pore spaces between the grains. Centre; structural clay occurs as grains. Right; clay laminations with zero porosity are interspersed between layers of grains. b) A cross plot between the natural gamma response and the porosity indicates which clay model applies. c) Left; in a typical hole from the Moranbah Coal Measures, the structural model appears to apply. Right; In a typical hole from the Narrabeen Group of the Sydney Basin, a dispersed clay model is indicated.

against porosity will indicate whether the clays form laminations separate to the grains (laminated clay), whether they replace the grains (structural clay) or whether they fill the pores (dispersed clay). A laminated clay model appears to hold for the Triassic Narrabeen Group of the Southern Sydney Basin. As shown in Figure 1, the porosity decreases with increasing clay content. In the Moranbah Coal Measures, a structural clay model is often observed with the porosity remaining constant and independent of the clay content.

EMPIRICAL RELATIONSHIP WITH VELOCITY

Eberhart-Phillips & others (1989), provide an empirical relationship between sonic velocity, V_p and ϕ , V_{clay} and effective pressure, p_e (confining pressure minus the pore pressure):

$$V_p = 5.77 - 6.94\phi - 1.73\sqrt{V_{\text{clay}}} + 0.446(p_e - e^{-16.7p_e}) \quad (2)$$

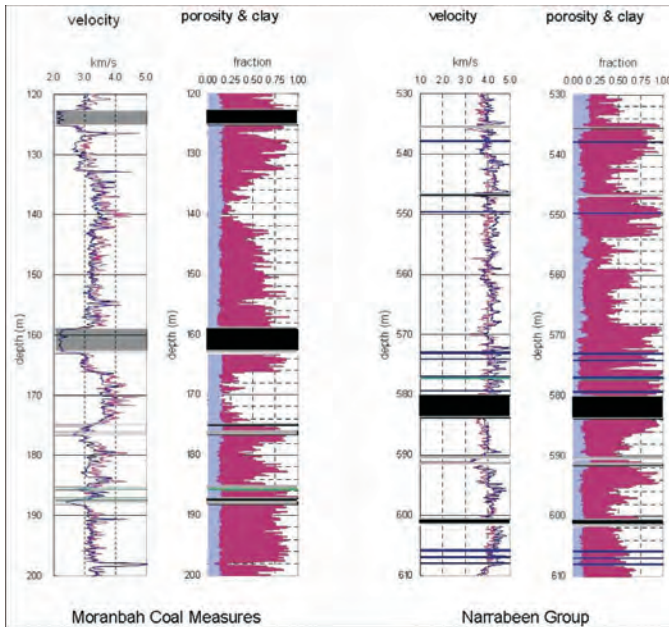


Figure 2: For the boreholes from the Moranbah Coal Measures and Narrabeen Group used in Figure 1, the logs to the right show the calculated porosity (in blue) and clay content (in red). From these are calculated velocities which are compared with observed sonic velocities (in red and blue respectively). The agreement in the velocities is very good. Note also that in the Narrabeen Group, the porosity decreases in the clay rich units (in keeping with the laminated clay model), whereas in the Moranbah Coal Measures, the porosity is independent of the clay content (the structural clay model).

In this equation, V_p is in units of km/s and p_e is in units of bar. This equation was derived from a laboratory study of a variety of clean and dirty sandstones from onshore and offshore areas of the Gulf States of the USA. It allows velocity to be calculated using the values of the porosity and clay content determined from geophysical logs. If these values are reasonably accurate, we have found that the calculated velocity will match the observed velocity, even in clay rich materials. Figure 2 compares the calculated and observed velocities for the boreholes from the southern Sydney Basin and Moranbah Coal Measure shown in Figure 1. The agreement is quite striking.

If the calculated and observed velocities match and if the values of the porosity and clay content are geologically reasonable, an interpretation of the porosity and the clay content that fits with our basic clastic model (Equation 1) has been derived. If the calculated and observed velocities do not agree or the results are not geologically reasonable, further geophysical analysis is required to determine better estimates for the porosity and clay content.

GEOPHYSICAL STRATA RATING

The Geophysical Strata Rating (GSR) is a geotechnical rating scheme based on a quantitative geophysical log analysis such as discussed above. We developed the GSR through three ACARP projects (Hatherly & others, 2004; Hatherly & others, 2008; and Medhurst & others, 2010). It utilises the sonic

velocity and the rock model inferred from the analysis of the geophysical logs. While it is an empirical scheme, it has a physical basis. There are similarities with the CMRR (Mark & Molinda, 2005).

For the clastic sections within a borehole, the GSR is made up of the following scores.

1. Strength score	0 to 55	plus	} Initial (intact) GSR
2. Cohesion score	10 to 25	plus	
3. Porosity score	-15 to 0	plus	
4. Moisture score	-10 to 0	plus	
5. Defect score			
- fracture score	0 to 10	plus	
- bedding score	0 to 10		

The sonic velocity is the major contributor and requires correction for depth (effective pressures of typically 15-25MPa/km depth) which we base on the last term in Equation (2). The porosity and the clay content add detail, mainly through the porosity score, the moisture score and the bedding score. If the velocity lies in the usual range of 2.5 to 5km/s, the GSR lies between 5 and 100.

In carbonaceous units, the same formulation is used with the porosity score set to zero. In the case of coal, dirty coal is stronger than clean coal and we therefore relate the initial GSR to the ash content according to

$$Initial\ GSR = 5 + 45x\ ash \tag{3}$$

where the ash content is determined from the density log using the following empirical relationship:

$$ash = 1 - \frac{\rho_{max} - \rho}{\rho_{max} - \rho_{min}} \tag{4}$$

Here ρ_{max} is the maximum density possible for carbonaceous material, ρ_{min} is the density for clean coal and ρ is the measured density. Comparison of logging densities and laboratory determined ash values suggests that a value of 2.45t/m³ is typical for ρ_{max} and 1.2t/m³ is appropriate for ρ_{min} .

Other empirical relationships for determining ash are also possible.

The fracture and bedding scores for coal are calculated in the usual manner.

COAL QUALITY

A detailed discussion of the use of geophysical logs to estimate coal quality is beyond the scope of this paper. However, Zhou & Esterle (2007) provide an extensive review of the approaches that have been investigated by other workers. For example, there is the potential for conventional neutron-neutron logs to reveal differences in maceral types and resistivity results may be related to volatile matter. Zhou and Esterle also review the application of spectrometric radiometric logs (neutron-gamma and gamma-gamma) for indicating ash composition. In addition they provide a detailed discussion of density logging, including a comparison of

logged density with laboratory measurements of relative density and ash content.

GAS

While a correlation between geophysical log responses and the amount of adsorbed gas contained in carbonaceous materials has yet to be established, it is well known that free gas in the pores of clastic rocks will affect geophysical log responses. Resistivity values become elevated, the porosity values from the density log become larger and those from the neutron log become smaller. These changes in porosity lead to porosity cross-overs, whereby the neutron porosity is significantly less than the density porosity. If full waveform sonic logs are recorded, reduced signal strength may be evident. If gas is flowing into the borehole, the attenuation of the signal within the gassy borehole fluids may be sufficient for the sonic and acoustic scanner logs to record no signal.

These responses provide just qualitative indications for the presence of strata gas. They do not reveal the amount of gas present, its composition nor the permeability. Laboratory measurements and well tests are required to determine these parameters.

SAMPLING INTERVAL

In recent years it has become more common for geophysical logs to be obtained at 0.01m intervals up the borehole, rather than at the 0.1m intervals that previously tended to be used. The reason for this appears to stem from the desire to obtain closely spaced (0.0m) data within the coal seams of interest. Rather than making separate closely spaced logging runs for the seams and then the entire hole at a larger sampling interval, the closely spaced data is now being obtained for the entire hole.

While there is nothing wrong with obtaining closely spaced data, it needs to be appreciated that the conventional geophysical logs respond to a volume of rock somewhat larger than 0.01m in diameter. For example, the sphere of influence for a natural gamma log is likely to be 0.2–0.3m radius and in the case of a sonic log, the receivers are typically 0.2m apart and thus provide an integrated response to thin rock bands. When close to boundaries, density logs are also affected by nearby beds. Zhou & Esterle (2007) suggest that measurements in coal seams need to be at least 0.1m away from boundaries to avoid effects from the bounding strata.

From a geological perspective there is also an argument that the logging of beds in the clastic section of a borehole with 0.01m resolution is not particularly meaningful. Fracture mapping requires such detail but not the mapping of the geological sequence.

To illustrate the issues involved, Figure 3 compares a natural gamma log, a sonic log, an acoustic scanner image and core photography over a 2m section of a borehole. The geophysical logs are shown with sample intervals of 0.01m, 0.05m and 0.1m. At the 0.3m scale, discrete beds can be seen on all logs

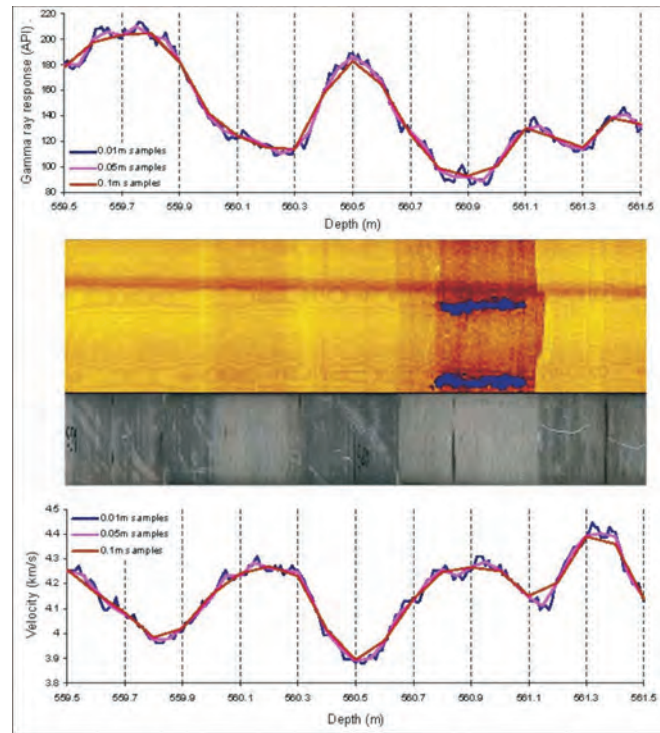


Figure 3: Top to bottom for a 2m section of a borehole, the natural gamma log, an acoustic scanner image, a core photograph and the sonic log. The natural gamma and sonic logs are shown at the 0.01m spacing of the original logs as well as at 0.05m and 0.1m spacings (after smoothing and resampling). The acoustic scanner image and core photograph show beds 0.3m thick as well as thinner beds (e.g. the 0.1m thick bed between 560.65m and 560.75m). The natural gamma and sonic logs respond to the 0.3m thick beds but not the thinner beds. At 0.01m spacing, the geophysical logs are also noisy. The inability to identify the thin beds is due to the combined effects of the size of the region sampled by the logs and the proximity to the boundaries. A spacing of 0.05m appears to offer the best compromise between resolution and signal clarity. At 0.1m spacing, the bed resolution deteriorates.

but there is smoothing at the boundaries. Importantly, close examination will show that there is no additional information in the closely spaced natural gamma and sonic data.

This example suggests that 0.05m spacing is adequate for these geophysical logs and a typical geological section such as this. If closer spaced data is obtained, it is likely to be noisy and it should be smoothed and resampled to 0.05m spacing. Furthermore, data files at 0.05m sampling are significantly smaller.

MODELLING

An analysis of geophysical borehole data based on the procedures discussed above provides numerical measures of rock properties that can be used as input in geological and geotechnical models. Figure 4 shows an example of complementary models of the clay content and the GSR from the Newlands Northern Underground developed in Medhurst & others (2010). These sections are taken from a 3D model derived from the analysis of 13 nearby boreholes. The Upper Newlands Seam is present as the bed with low clay content

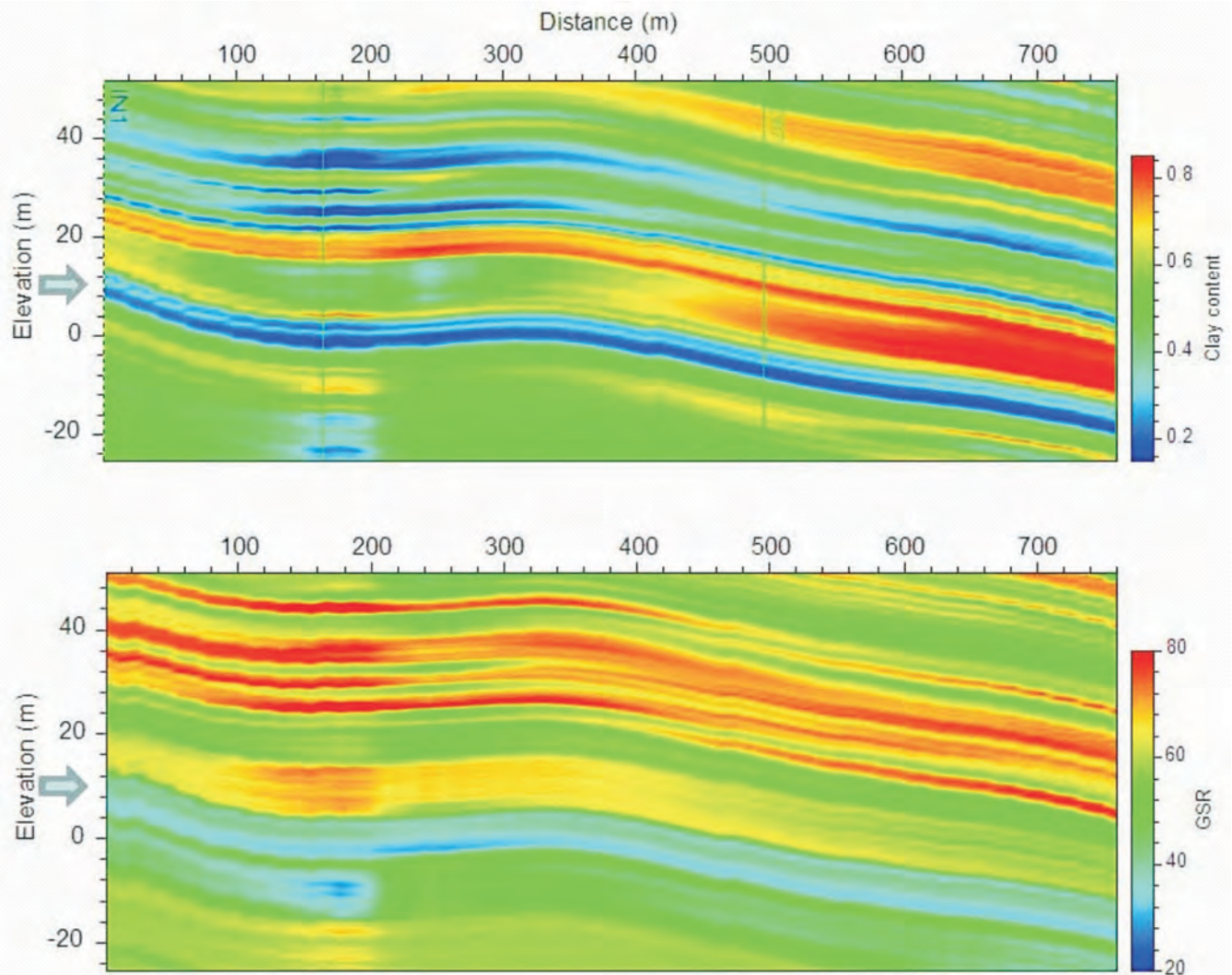


Figure 4: 3D models of clay content (top) and GSR (bottom) calculated from an analysis of geophysical logs from Newlands Northern Underground (Medhurst & others, 2010). The arrows point to the Upper Newlands Seam which has low clay content and low GSR. Above this is the Marker Mudstone which is clay rich to the right but to the left is more sandy at its base. Bands of clean sandstones above the mudstone have clay contents of less than 0.3 (30%) and GSR values of 70 or more. The GSR values for the mudstone and other clay rich units are between 40 and 60 but increase in the sandier section of the Marker Mudstone. Within the Upper Newlands Seam the GSR is lower (about 30) at the base than at the top (about 35).

and low GSR. Above this is the Marker Mudstone which at the left becomes sandy towards its base. Above the Marker Mudstone, there is a series of sandstone and siltstone layers with the sandstones having clay contents of less than 0.3 (30%) and GSR values over 75. The siltstones have higher clay contents and GSR values between 40 and 60.

Mine planning and operational decision making could be improved through the generation of models such as these. The geophysical borehole analysis that we are advocating here provides an excellent opportunity for the integration of geological and geotechnical information.

CONCLUSIONS

Identification of coal, carbonaceous material, clastic rocks, tuff and dense material (siderite) is possible from an assessment of geophysical logs. For clastic rocks, the geophysical logs also allow the amounts of clay and the porosity to be determined. Quartz is assumed to represent the remainder. The accuracy of the derived fractions can be

checked by calculating the velocity and comparing this with the observed sonic velocity. If the match is satisfactory, the derived parameters can be used to determine clay models, check for strata gas and to calculate the GSR. Compositional and GSR data can then be modelled to provide a complete 3D picture of the geological and geotechnical conditions.

For such analyses, the logging suite should contain as a minimum, calibrated density, natural gamma, caliper and sonic logs. However, given the additional information that neutron and resistivity logs provide on the clay content and strata gas, these logs should also be run if possible. Our ACARP reports, Hatherly & others (2004), Hatherly & others (2008) and Medhurst & others (2010) give more information and examples of the log analysis procedures discussed in this paper.

REFERENCES

EBERHART-PHILLIPS, D., HAN, D.-H. & ZOBACK, M.D., 1989: Empirical relationships among seismic velocity, effective

- pressure, porosity and clay content in sandstone. *Geophysics*, **54**, 82–89.
- HATHERLY, P., SLIWA, R. TURNER, R. & MEDHURST, T., 2004: Quantitative geophysical log interpretation for rock mass characterisation. Final Report, ACARP Project C11037.
- HATHERLY, P., MEDHURST, T. & MACGREGOR, S., 2008: Geophysical Strata Rating. Final Report, ACARP project C15019.
- MEDHURST, T., HATHERLY, P., ZHOU, B. & YE, G., 2010: Application of the Geophysical Strata Rating in production settings. Final Report, ACARP Project C17009.
- MARK, C. & MOLINDA, G.M., 2005: The Coal Mine Roof Rating (CMRR) – a decade of experience. *International Journal of Coal Geology*, **64**, 85–103.
- ZHOU, B. & ESTERLE, J., 2007: Improving the reliability of density and grade estimation from borehole geophysical log suites. Final Report, ACARP Project C15036.

Ralf Opperman

A new workflow for high-resolution fault imaging delivers groundbreaking insights into resource operations and recoveries

Fault and fracture networks can have significant effects on drilling, mining and the safety of resource operations. Due to this, various automatic fault extraction techniques have been developed for 3D seismic data in recent years. These techniques aim to support or (partially) replace manual fault mapping efforts, which are typically labour-intensive, time-consuming and subjective.

This paper presents innovative techniques and workflows that have been developed to integrate 3D seismic visualization and highest-resolution image processing results with the detailed calibration and review of various seismic, well and mining data.

From the application of these workflows, groundbreaking insights into the physical description of resources can be gained. Fault and fracture networks can be identified faster, more reliable and at a much higher resolution than achieved by other current seismic methods. With the increased resolution, much higher fault/fracture densities are found than previously mappable or recognised, and a better understanding of structural geometries and fault populations can be achieved.

New workflows developed for Oil & Gas projects have demonstrated that the new techniques can provide a step-change in understanding drilling, production and safety issues in existing wells. They furthermore can be utilised to optimise future resource activities and recoveries, and increase the safety of future operations.

A new workflow for high-resolution fault imaging has been developed for the Coal Mining industry. This workflow helps to push fault resolution down to the true fault resolution from 3D seismic data, not the perceived fault resolution that is typically established by visual (Interpreter) mapping only. The new technique helps in resolving the 'sub-visual' fault domain, and as such helps to bridge the scale gap between seismic data and well & mine data. With 'sub-visual' imaging there is now a means to minimise drilling, production and safety issues that are caused by faults in wells and mines.

Where faults pose geotechnical, production and/or safety hazards in underground mines, high-resolution fault imaging can support Mine Design & Planning and Fault Zone Management activities.

INTRODUCTION

Fault and fracture networks can have significant effects on drilling, mining and the safety of resource operations, and can also significantly impact reserve recovery & productivity. Detailed fault mapping, at highest possible resolution, is therefore important for most resource development projects (Oppermann 2010).

In Oil & Gas reservoirs, it is often critical to improve the understanding, detection, modelling and prediction of fault and fracture networks and their fluid compartmentalizing effects and storage-transmissivity characteristics. These efforts can help to locate connected hydrocarbon volumes and unswept sections of reservoir, and thereby help to optimize field developments, production rates and ultimate hydrocarbon recoveries (Jolley & others 2007).

The successful application of new techniques in automated fault identification in Oil & Gas projects has demonstrated a number of key benefits that can be realised with these techniques (Stephenson, Cassidy & Warrlich 2005; Oppermann 2010).

This paper discusses how these Oil & Gas workflows can be applied in the Coal Mining industry, and likely provide a step-change in understanding and addressing drilling, production and safety issues in current and future wells and mines.

FAULTS AND UNDERGROUND COAL MINING

In underground coal mines, fault and fracture networks can result in significant geotechnical, production and/or safety hazards. As a result of this, ground control strategies typically include mine designs that minimize fault exposure (Molinda & Ingram 1990).

Through coal seam offsets, faults can cause major interruptions to production and can affect the economic viability of a coal mine (Cocker, Urosevic & Evans 1997; Driml, Reveleigh & Bartlett 2001; Kecojevic & others 2005).

Faults can affect floor and roof stability and cause e.g. roof failures, resulting in lost time incidents, or with possibly even lethal consequences.

Faults can also act as trap zones for gas, which can result in outbursts during mining, again posing significant risks to production and the safety of mining personnel. All fatal outbursts in Australia, except Leichhardt Colliery, have occurred on faults (University of Wollongong 2010).

Fault penetrations can also lead to incidents related to fluid losses or gains, gas kicks or geomechanical problems in boreholes (wellbore instability, breakouts, casing damage due to slippage along reactivated fault planes etc.).

FAULT DETECTION

Fault (i.e. hazard) identification from seismic and well data plays a key role in coal mining. It is of key interest to improve the prediction and confidence in fault mapping from seismic, as this can help in avoiding costly production issues or life-threatening incidents in underground mines.

In recent years, various seismic processing techniques and software packages focused on 3D fault visualisation, auto-extraction and also semi-automated fault picking have been developed and are increasingly being applied in the Oil & Gas industry. Various attributes are in use for imaging discontinuities in seismic data, e.g. coherence, semblance, curvature, similarity, dip & azimuth, frequency variability, seismic texture etc. These attributes typically identify and enhance spatial discontinuities that are computed at every data point within a seismic data cube. For a description of attributes and a detailed account of the advances made in the automation of seismic fault interpretation, reference is made to the publication by Pepper & Bejarano (2005).

Automated fault detection techniques have been developed to support or (partially) replace manual fault mapping efforts, which are labour-intensive and time-consuming (Admasu, Back & Toennies, 2006), but also largely subjective, and with this imprecise and often biased. The application of fault extraction workflows in Oil & Gas projects around the world has shown that properly calibrated

fault & fracture network volumes typically can deliver faster, more reliable and fully objective fault evaluations (Oppermann, 2010). Automated fault extraction is based on the physical measurement of spatial variation in amplitude, phase and/or frequency content of 3D seismic data (Figure 1), and is as such free of bias and interpretation. Fault extraction therefore allows making a distinction between measurement and the interpretation of this measurement, as e.g. manifested in visual reflector offset mapping. A further benefit of fault extraction is that the significance of faults and the confidence in fault presence can be objectively evaluated.

Extraction leads to a better understanding of structural geometries and more comprehensive sampling of fault populations, due to a marked increase in fault resolution, and a resultant dramatic increase in the number of faults that are identified from seismic. With the increased structural resolution, much higher fault & fracture densities are found than previously mappable or recognised. The very latest fault imaging technology pushes fault resolution down to the true

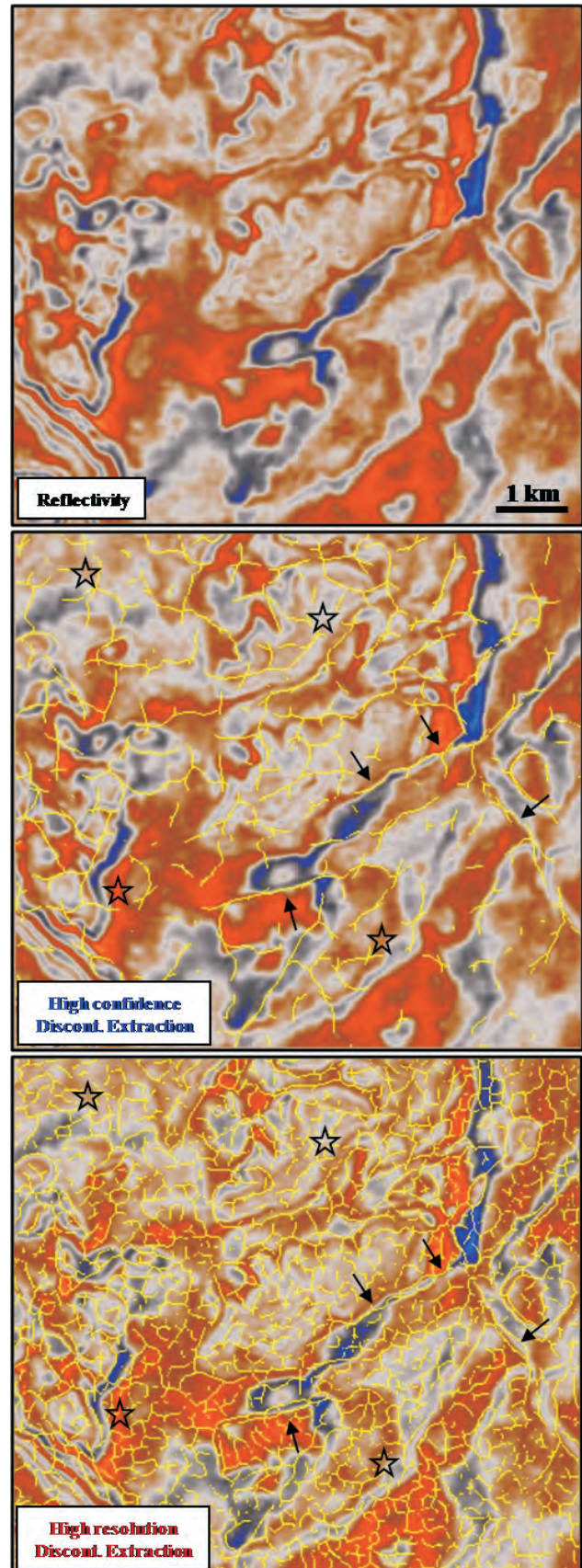


Figure 1: Visual comparison of time slices (at 1,398ms) through a reflectivity volume, a high **confidence** discontinuity extraction and a high **resolution** discontinuity extraction. Faults that show clear offsets are picked (arrows), and smaller scale faults are picked in both extraction volumes that only the analysis of spatial variation in amplitude, phase and frequency resolves (stars). Extraction data generated from Myall Creek 3D Land Seismic Survey 2004 (Surat Basin/Queensland; open file data, Queensland Govt. DEEDI).

fault resolution of a particular data set, not the perceived fault resolution that is typically established by visual (Interpreter) mapping only. Most 3D surveys in the resource industries are therefore currently under-utilized, as an entire medium-sized, 'sub-visual' (but not sub-seismic) fault population could be extracted from already existing data with relatively little effort (Oppermann, 2010). Overall, much improved and multiple 3-dimensional fault & fracture network models can be generated from fault extraction data.

PROPOSED NEW WORKFLOW

New workflows developed for Oil & Gas projects have demonstrated that the new techniques can provide a step-change in understanding drilling, production and safety issues in existing wells. They furthermore can be utilised to optimise future resource activities and recoveries, and increase the safety of future operations. The following new workflow is proposed, which integrates new Oil & Gas fault extraction methods with established coal mining workflows. The workflow has been designed to be applicable to a new coal mining project, but can be adapted for the evaluation of an existing coal mine. The presented workflow will likely require refinement in future applications to coal mining assets.

Generally, most discontinuity processing workflows follow a similar approach - volume conditioning with noise cancellation, followed by automatic discontinuity delineation, conversion into 3D objects and calibration and analysis of these objects.

1. Discontinuity Processing / Fault Extraction

Processing of 3D seismic data and visualisation of 3-dimensional fault networks at different extractable resolution levels.

- 1.1 Generation of *structural attribute volumes*: Dip, Azi, DipAzi volumes.
- 1.2 Discontinuity highlighting using a number of different methods/algorithms. Generation of a *first set of fault volumes*, for each utilised algorithm: Fault Network (FN), Fault Network Reflectivity (FNR; e.g. Figure 1), Fault Density (FD), Fault Density Network (FDN), Fault Trend (FT) volumes.
- 1.3 Generation of *sensitivity volumes*, to assess the impact that different parameterisations have on results, and to assess fault picking confidence.

2. Calibration of initial Discontinuity Volumes

Seismic discontinuities do not necessarily represent fault surfaces, but can be also related to other geologic features (channel edges, dykes, hydrocarbon contacts etc.) or noise (acquisition/processing artefacts). It is of key importance to confirm that the discontinuity extractions represent structural features, rather than artefacts. There are a number of key steps to help with this validation process:

- 2.1 Calibration by *visual inspection* on sections, time slices and in volume view. Key questions to address: Are fault patterns & geometries meaningful and have horizon offsets been identified (Figure 1)? Are features being consistently identified when comparing different algorithm results? Any obvious noise pollution or artefacts? And is structure-oriented filtering required?
- 2.2 Calibration against *other structural highlighting data*. Often a good match is observed between seismic discontinuities and features indicated by other structural highlighting data (e.g. Dip, Azi, DipAzi, Semblance, Coherence, etc). Fault auto-extraction, however, usually delivers a much higher resolution than other structural highlighting tools (Figure 2).

3. Reflectivity Data Conditioning with Noise Reduction / Structural Smoothing

Noise-contamination of seismic data can be addressed by running spatial filters that attenuate or remove a possible noise contamination but retain the geometric detail such as small-scale fault breaks (Chopra & Marfurt 2007). Noise reduction can e.g. be achieved without degradation to the fault expression by data conditioning with structure-oriented smoothing utilising edge preservation (Hoecker & Fehmers 2002).

- 3.1 Structural smoothing of reflectivity data.
- 3.2 Generation of a *second set of fault volumes* (as in 1.2)
- 3.3 Generation of a *second set of sensitivity volumes* (as in 1.3)
- 3.4 *Comparison* of the unsmoothed, first volume set with the smoothed, second volume set, to assess and quantify how smoothing has modified the data and possibly affected fault identification, e.g. by sharpening discontinuities.

4. Optimally Placing Wells for the Pre-Drainage of In Seam Gas

The degasification of coal prior to mining is an important commercial and safety-increasing activity (Cocker, Urosevic & Evans 1997). The early detection of faults on 3D seismic data can allow coal companies to more effectively degasify the coal seam in advance of mining operations (Gochioco & Cotten 1989). The new seismic fault network volumes provide detailed fault information, which can be used to optimise well locations and with this, the pre-drainage of mine gas.

5. Further Calibration of Fault Volumes with Faults identified from Log Correlation, Cores and Image logs in Pre-Drainage Wells

New fault information acquired in pre-drainage wells can be used to further calibrate fault extractions. Image logs can play a key role in proving that seismic discontinuities represent faults (e.g. Richard & others 2005; Stephenson, Cassidy & Warrlich 2005; Warrlich & others 2009; Oppermann 2010).

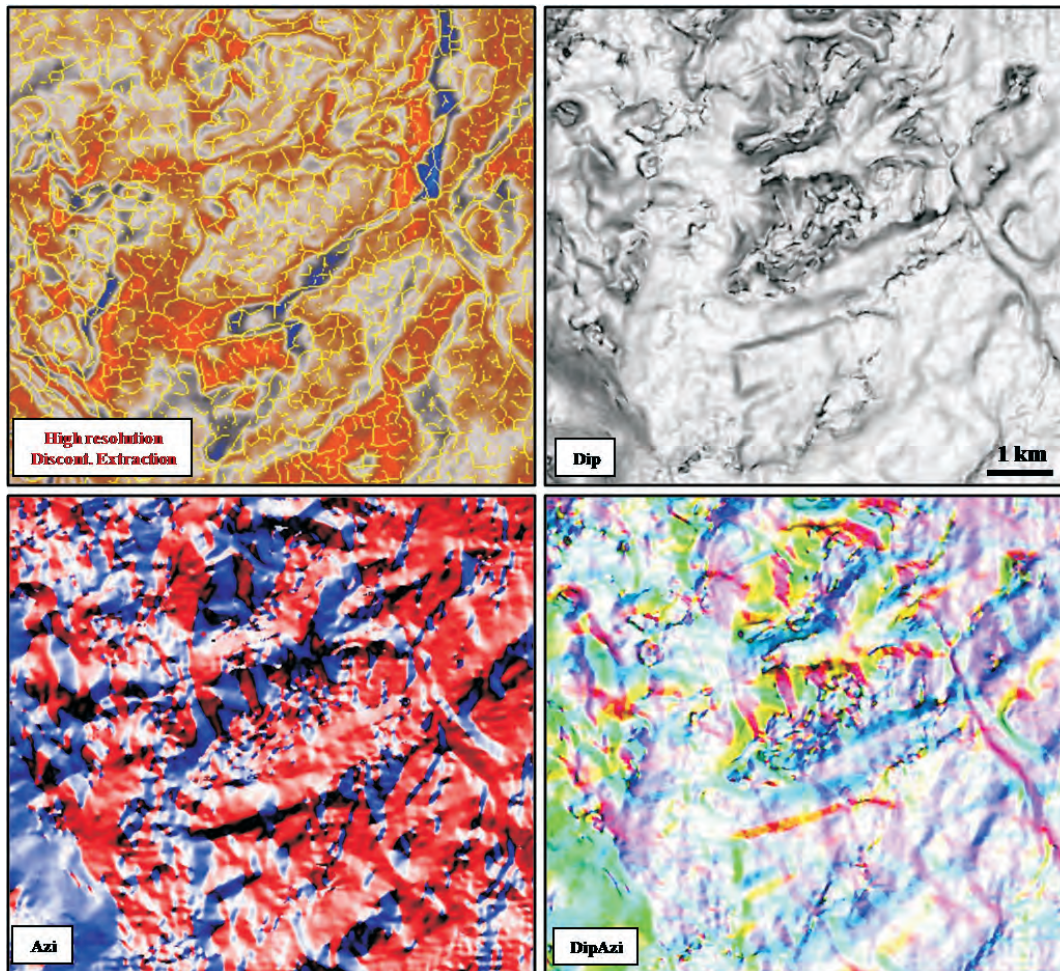


Figure 2: Comparison of high-resolution fault extraction results with other structural highlighting data (Dip, Azi, DipAzi). Structural volume data generated from Myall Creek 3D Land Seismic Survey 2004 (Surat Basin/Queensland; open file data, Queensland Govt. DEEDI).

6. Detailed Mine Design & Planning and Fault Zone Management activities

Currently, manually interpreted faults are integrated with well data and considered during mine design and detailed mine planning, as well as during coal extraction (Peters & Hearn 2001). Faults encountered in the subsurface during mining are evaluated in detail and compared with faults mapped from 3D seismic to calibrate and improve fault prediction capabilities of the (manual) seismic interpretation effort.

The use of calibrated seismic fault network, fault density and fault trend volumes for general and detailed mine planning has the potential to significantly improve Mine Planning and Fault Zone management efforts.

- 6.1 Initial focus on the *prediction of larger full seam faults* (with offsets larger than the seam thickness), to identify faults that could be major production or safety hazards ('mine stoppers'). Inventorisation of key faults and their parameters (location, depth, throw, strike and dip direction, etc.).
- 6.2 Subsequent focus on the *prediction of smaller-scale faults*, to identify faults that also could have geotechnical and/or safety relevance (e.g. coal seam correlation, roof collapse, outbursts).

- 6.3 Evaluation of *fault mapping confidence* (or uncertainty), using fault network sensitivity volumes (run for each algorithm).
- 6.4 For existing mines: comparison of seismic fault extractions with *previous efforts to map faults* (manual fault mapping, curvature, similarity, gradient, dip/azi, semblance, etc.), or with *faults encountered during drilling and mining*.
- 6.5 *Comparison of seismic fault predictions with actual fault penetrations* in wells and mines (full calibration): assessment of true seismic fault resolution that is achieved with different fault extraction algorithms and parameterisations; calibration of fault confidence (or uncertainty) assessments.
- 6.6 *Comparison of seismic fault predictions with possible drilling and mining issues*: assessment of links between faults and possible fluid losses or gains, gas kicks, outbursts, geomechanical problems (wellbore instability, breakouts, casing damage, floor and roof failures), incidence reports etc. *Incidence inventorisation and analysis* with respect to faulting, with the aim to improve gas compliance, outburst and roof stability control.
- 6.7. Assessment of the *variability* in results from the running of different fault extraction algorithms, with the aim to identify a *Base Case method* (after full calibration).

- 6.8. Application of volume interpretation tools for the prediction of other production hazards, e.g. dykes, sills, basalt channels, sandstone channels, etc.
- 6.9. Continuous integration of latest results and possible re-calibration of the model throughout mining operations ('feedback loop').

7. Planning and Optimisation of Post Drainage of Gas

CONCLUSIONS

Fault and fracture networks can have significant effects on drilling, mining and the safety of resource operations, and can also significantly impact reserve recovery & productivity.

In recent years, various automatic fault extraction techniques have been developed for 3D seismic data. These techniques aim to support or (partially) replace manual fault mapping efforts, which are typically labour-intensive, time-consuming and subjective.

The application of automated fault extraction workflows in Oil & Gas projects around the world has shown that groundbreaking insights into the physical description of resources can be gained. Properly calibrated fault & fracture network volumes deliver faster and more reliable and objective fault interpretations, and a better understanding of structural geometries and fault populations. Due to a marked increase in fault resolution, automated fault extractions also provide a more comprehensive sampling of fault populations and an in fact dramatic increase in the number of faults that are identified from seismic.

A new coal mining workflow has been developed which integrates 3D seismic visualization and highest-resolution image processing results with the detailed calibration and review of various seismic, well and also mining data.

The application of this new workflow in the Coal Mining industry could provide a step-change in understanding and addressing drilling, production and safety issues in current and future wells and mines.

Where faults pose geotechnical, production and/or safety hazards in underground mines, high-resolution fault imaging has the potential to significantly improve mine design & planning and fault zone management activities.

ACKNOWLEDGEMENTS

A number of people have introduced the author into the Coal Mining industry and the challenges that can be brought about by faulting. I'd like to thank the following for their helpful comments and also interest in the transfer of Oil & Gas technology into Coal Mining:

Andrew Willson (Anglo American Metallurgical Coal Pty Ltd), Barry de Wet (BDW Geophysics Consulting Pty Ltd),

Doug Dunn (BHP Billiton Mitsubishi Alliance), Hugo Kaag and Clive Pickering (BHP Billiton Illawarra Coal), Gary Fallon (Geophysical Resources & Services Pty Ltd), Henk van Paridon (GeoSolve Pty Ltd), Mark Johnston and Richard Mills (PIMS Group), Jürgen Schaeffer (Shenhua Watermark Coal Pty Ltd), Troy Peters and Karel Driml (Velseis Processing Pty Ltd) and Todd Harrington (Xstrata Coal Pty Ltd).

REFERENCES

- ADMASU, F., BACK, S. & TOENNIES, K., 2006: Autotracking of faults on 3D seismic data, *Geophysics*, **71** (6), A49–A53.
- CHILDS, C., WALSH, J.J. & WATTERSON, J., 1990: A method for estimation of the density of fault displacements below the limits of seismic resolution in reservoir formations. In Trotman, G. (Editor): *North Sea oil and gas reservoirs, The Norwegian Institute of Technology*, **2**, 309–318.
- CHOPRA, S. & MARFURT, K.J., 2007: Volumetric curvature attributes add value to 3D seismic data interpretation, *The Leading Edge*, **July 2007**, 856–867.
- COCKER, J., UROSEVIC, M. & EVANS, B., 1997: A high resolution seismic survey to assist in mine planning. In Gubins, A.G. (Editor): *Proceedings of Exploration 97: Fourth Decennial International Conference on Mineral Exploration*, 473–476.
- DRIML, K., REVELEIGH, M. & BARTLETT, K., 2001: Mini-SOSIE — Successful shallow 3D seismic data acquisition in an environmentally sensitive area, Extended Abstracts ASEG 15th Geophysical Conference and Exhibition, August 2001, Brisbane.
- GAUTHIER, B.D.M. & LAKE, S.D., 1993: Probabilistic modelling of faults below the limit of seismic resolution in Pelican Field, North Sea, offshore United Kingdom, *Bulletin of the American Association of Petroleum Geology*, **77**, 761–777.
- GILLESPIE, P.A., HOWARD, C., WALSH, J.J. & WATTERSON, J., 1993: Measurement and characterisation of spatial distributions of fractures, *Tectonophysics*, **226**, 113–141.
- GOCHIOCO, L.M. & COTTEN, S.A., 1989: Locating faults in underground coal mines using high-resolution seismic reflection techniques, *Geophysics*, **54** (12), 1521–1527.
- HEARN, S. & HENDRICK, N., 2001: Bandwidth requirements for shallow, high-resolution seismic reflection, Extended Abstracts ASEG 15th Geophysical Conference and Exhibition, August 2001, Brisbane.
- HOECKER, C. & FEHMERS, G., 2002: Fast structural interpretation with structure-oriented filtering, *The Leading Edge*, **March 2002**, 238–243.
- JOLLEY, S.J., BARR, D., WALSH, J.J. & KNIPE, R.J., 2007: Structurally complex reservoirs, *Geological Society Special Publication* **292**.
- KECOJEVIC, V., WILLIS, D., WILKINSON, W. & SCHISLER, A., 2005: Computer mapping of faults in coal mining, *International Journal of Coal Geology*, **64** (1-2), 79–84.
- LOHR, T., KRAWCZYK, C.M., TANNER, D.C., SAMIEE, R., ENDRES, H., THIERER, P.O., ONCKEN, O., TRAPPE, H., BACHMANN, R. & KUKLA, P., 2008: Prediction of subseismic

- faults and fractures: Integration of three-dimensional seismic data, three-dimensional retrodeformation, and well data on an example of deformation around an inverted fault, *AAPG Bulletin*, **92** (4), 473–485.
- MAERTEN, L., GILLESPIE, P. & DANIEL, J.M., 2006: Three-dimensional geomechanical modeling for constraint of subseismic fault simulation, *AAPG Bulletin*, **90** (9), 1337–1358.
- MOLINDA, M. & INGRAM, D.K., 1990: Effects of structural faults on ground control in selected coal mines in southwest Virginia, *International Journal of Mining and Geological Engineering*, **8** 332–347.
- OPPERMANN, R., 2010: Application of hi-res fault imaging technology in the resource industries. In Hutton, A., Ward, C. & Bowman, H, (Editors): Thirty-seventh Symposium on the Geology of the Sydney Basin, Hunter Valley, Pokolbin, NSW May 6-7, 2010 (Abstracts).
- PEPPER, R. & BEJARANO, G., 2005: Advances in seismic fault interpretation automation, *Search and Discovery Article*, **40169**, 1–16.
- PETERS, T. & HEARN, S., 2001: The influence of coal-mine geology on seismic data quality in the Bowen Basin. *Extended Abstracts ASEG 15th Geophysical Conference and Exhibition, August 2001*, Brisbane.
- RICHARD, P., RAWNSLEY, K., SWABY, P. & RICHARD, C., 2005: Integrated fracture characterisation and modeling in PDO carbonate fields using novel modeling software and sandbox models, *International Petroleum Technology Conference, Doha, Qatar, 21-23 November 2005, IPTC 10428*.
- STEPHENSON, B., CASSIDY, P. & WARRLICH, G., 2005: Novel use of seismic volume interpretation for fracture detection and modelling: examples from field in the Philippines and the Middle East, *14th SPE Middle East Oil & Gas Show and Conference, Bahrain, 12-15 March 2005, SPE 93759*.
- UNIVERSITY OF WOLLONGONG, 2010: Coal Mine Outburst Factors, viewed 1 July 2010, <http://undergroundcoal.com.au/outburst/faults.html>.
- WARRLICH, G.M.D., RICHARD, P.D., JOHNSON, T.E., WASSING, L.B.M., GITTINS, J.D., AL-LAMKI, A., ALEXANDER, D.M. & AL-RIYAMI, M., 2009: From data acquisition to simulator: fracture modeling a carbonate heavy-oil reservoir (Lower Shuaiba, Sultanate of Oman), *2009 SPE Middle East Oil & Gas Show and Conference, Bahrain, 15-18 March 2009, SPE 120428-PP*.
- YIELDING, G., WALSH, J.J. & WATTERSON, J., 1992: The prediction of small-scale faulting in reservoirs, *First Break*, **10**, 449–460.

Zach Casley, Oli Bertoli, Clare Mawdesley and Doug Dunn

Drill hole spacing analysis for coal resources

This paper focuses on the use of geostatistical techniques to support classification of mineral resources. The objective is to either optimise the drilling budget to attain a specific resource category over a fixed ground coverage, or optimise the ground coverage per resource category for a fixed drilling budget.

Geostatistical drill hole spacing analysis ('DHSA') based on global estimation variance is a method which provides a quantitative measure of the global estimation precision with which a given variable for a given seam/domain combination may be estimated at a particular drilling spacing.

The use of DHSA results requires corporate decisions to be made on the applicable key variables and time periods that will be the drivers for classification decisions. Resources may then be broadly 'classified' according to the drilling coverage defined once precision intervals have been established for the different resource categories. BMA have decided that Thickness and Raw Ash, and global estimation precisions over 5 year periods will be the key criteria used for applying DHSA results.

Geostatistics provides the tools to consider issues related to resource classification at an industrial scale, but as always, the limitations and assumptions behind this framework must be understood and controlled to allow for a reliable implementation of the methods.

This paper gives a brief explanation of the background theory, with particular emphasis on the caveats that must be borne in mind by the end user. Following this, the paper covers the implementation of DHSA, and gives a comparison of the results of classification using the Coal Guidelines versus classification using the geostatistical method for Measured and Indicated resources for a selection of BMA's operating mines.

INTRODUCTION

Coal resource classification is a multivariate problem and the resource classifications assigned by the competent person need to encompass their confidence in a range of factors that affect the resource.

Drill Hole Spacing Analysis ('DHSA') using the global estimation variance method is a geostatistical technique that provides quantitative measures of the global precision with which quality and tonnage variables can be estimated. It does not provide any information with respect to geological structure and other factors which must be allowed for when assigning classification categories, and designing exploration programs.

DHSA provides a quantitative input to the classification process, that is, it provides a quantitative measure of global estimation precision, driven by the real in situ variability of key attributes in the classification process.

Finally the DHSA technique is based on the utilisation of a variogram model that is generated from a rigorous geostatistical analysis that is useful in ensuring the integrity of the data being processed.

Exploratory Data Analysis ('EDA')

The first stage of any geostatistical analysis is Exploratory Data Analysis ('EDA'). Two of the main purposes of the EDA process are:

1. Check the validity of domaining decisions, with respect to the underlying assumptions of statistical homogeneity of the spatial distribution of the coal characteristics; and,
2. Identify outliers in the data, that is, sample values that are inconsistent with the underlying spatial distribution for the variable of interest and may impact the calculation of the experimental variograms.

The development of appropriate geological domains is an integral part of the decision making process concerning the definition of 'domains of stationarity'. The term stationarity is linked in a sense to the statistical homogeneity within a given domain. Domains of stationarity are generally closely related to geological, structural and/or weathering units.

EDA can be performed for each variable in each seam/domain combination by analysing linked:

- Location map of samples;
- Histogram of sample values;
- Scatter Diagram between the variable of interest and Northing;
- Scatter Diagram between the variable of interest and Easting; and,
- Experimental omnidirectional or directional variograms obtained from the selected samples.

The examination of the linked scatter diagrams between the variable of interest and the spatial coordinates is particularly helpful in evaluating the level of statistical homogeneity within a given domain and rapidly identifying potential sub-domains, and/or the presence of outliers.

Variography

The variogram is the basic diagnostic tool for spatially characterising a regionalised variable, and is central to

geostatistical estimation/interpolation methods (kriging) and the more advanced methods such as conditional simulation as it characterises spatial continuity.

Note that experimental variography for 2D coal seams is usually affected by:

- The presence of outliers (extreme values – high or low), which are isolated or atypical with regards to the underlying sampling pattern, and may unduly affect the apparent spatial variability. Because of this, their temporary exclusion for variographic analysis may be warranted; and,
- A property that is referred to in geostatistics as a ‘drift’. Drifts occur when the spatial variations (at a certain scale) of data values within a domain are no longer compatible with a stationary model. For a 2D dataset, what this means is that a variable shows a strong dependence (linear or not) with one or both coordinates.

A significant point to note is that the impact of the drift on the experimental variograms obtained for coal parameters is usually only significant at a scale larger than the scale of the study being undertaken. In these situations a stationary model may be safely modeled to fit the experimental variograms, as the departure from stationary conditions does not impact on the problem at hand.

Global Estimation Variance Methodology

A simple method is presented here (‘Global Estimation Variance’, see Journel & Huijbregts, 1978 for mathematical details) which allows robust and rapid optimisation of drilling grid spacing’s for coal deposit data.

Example

Suppose we want to estimate the average insitu Ash content over an area that corresponds to a mining period of 1 year, and characterise the precision of estimation through an estimation variance. This estimation variance depends on:

- The variogram model chosen for the variable (*in situ* Ash), domain and seam being modelled;
- The ‘geometry of the data’, that is, the particular data locations used for estimation; and,
- The block size and geometry (the area to be estimated).

Once a variogram model is available for a given variable (insitu Ash) the following general methodology can be implemented:

1. Select grid mesh dimensions Easting (X) and Northing (Y) corresponding to the nominal drill spacing being investigated;
2. Calculate the elementary estimation variance σ_e^2 when a block of size X (m) by Y (m) is estimated using one central sample (using the variogram model established previously);

3. Calculate the number N of blocks required to cover the area of interest corresponding to the envisaged mining period (this number N corresponds to the number of samples required to achieve sampling of the area of interest at the desired drill spacing);
4. Calculate the theoretical variance of estimation of the mean *in situ* Ash value of the entire area as $\sigma_E^2 = \frac{\sigma_e^2}{N}$ (combination of elementary variances);
5. Calculate the equivalent standard deviation (square root of the variance calculated above). Then, as a first approximation of relative precision, calculate the ratio of two times this standard deviation to the global mean of *in situ* Ash, i.e. $\frac{2\sigma_E}{m}$.
6. Plot this relative precision (expressed in percent) versus the sampling grid defined in Step 1.

This equates to an approximate 95% confidence interval versus a drilling spacing for the corresponding area.

The following caveats apply to global estimation precisions derived from DHSAs. The global precisions:

- Apply only to the deposit, seam, domain and variable considered;
- Can only be used to assign a precision to estimation of the mean of an attribute of interest for a global area equivalent to a certain production period, assuming a fixed mining rate; and,
- Are not applicable to any other area than the one implicit in the calculations and, in particular, are not suited to assigning local confidence intervals.

Should local confidence intervals be required subsequently, other geostatistical techniques may be applied. Conditional simulations (Lantuéjoul, 2002) rely on the application of more powerful models, which require adherence to stronger hypotheses, and more importantly are much more involved. When the objective is to derive global precision intervals for resource classification, methods based on conditional simulations require unnecessary amounts of extra work to be properly implemented, for essentially an identical result.

Another solution when trying to build local Confidence Intervals is to use techniques relying on the application of the Discrete Gaussian Model of change of support (Rivoirard, 1994), which is more adapted, but again, this is likely to be unnecessary if the problem at hand is only dealing with resource classification issues.

Operational Issues

For the DHSAs method to be implemented, an annualised area for the global precisions to be applied to is required for the calculations. The results from the drill hole spacing analysis are tabulated and plotted accordingly to multiples of this annual mining area equating to periods of, for example, 1, 2, 5 and 10 years.

The mean value for each variable is estimated at the start of the DHSA process. Following test work on the different potential methods, the authors of this paper have been using the estimation of the mean via point kriging of regularly spaced points on a regular basis.

Implementing DHSA within BMA — Establishing Guidelines for DHSA

In order to interpret the results from DHSA, guidelines must be established regarding:

- The variables to base the classification decisions upon;
- The method of deriving the annual area on which DHSA is to be calculated;
- The relevant time period for which classification decisions will be made; and,
- The relation of appropriate global precision ranges to resource categories.

Following consideration of the different attributes derived from DHSA, and their applicability to business planning from a classification standpoint, it was decided that the variables to be used for resource classification would be Seam Thickness ('TK') and *in situ* raw ash content ('RA').

The annual area over which DHSA is to be applied is subject to further scrutiny. BMA's decision for its open cut operations was to use the average annual 'area disturbed'. This is the area stripped each year, from which coal can theoretically be extracted by the open cut operation. For underground operations, the area has been set at the average annual area mined by the longwall(s) for the particular site.

The time period to be considered can, for example, be taken as the payback period for the project under consideration. BMA have established that the time period for classification decisions for their operations will be five years, as this ties into their business planning cycle.

The final guideline to be established is that relating to the linking of global estimation precisions to resource classification categories. This is a matter for each company, and competent person to decide on a case by case basis, as it relates to not only the certainty of the resource in the ground, but also the level of risk which a company is prepared to have associated with it's resources. Current practice within BMA relates resource classification categories to global estimation precisions derived from DHSA as detailed in Table 1.

An example of a DHSA graph obtained for an area equating to a mining period of 5 years is given below for Raw Ash

Table 1 : Relationship of resource classification categories to global estimation precision ranges

Classification Category	Global Estimation Precision
Measured	<10%
Indicated	>10% and <20%
Inferred	>20% and <50%

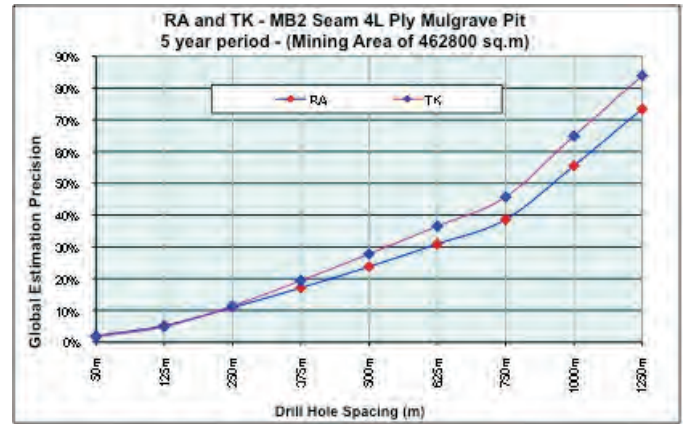


Figure 1: DHSA Results for RA and TK – MB2 Seam, 4L Ply, Mulgrave Pit – South Walker Creek Mine

(‘RA’) and Thickness (‘TK’) of the 4L ply in the MB2 Seam, in the Mulgrave Pit at South Walker Creek Mine.

The results for this ply are that the spacing derived from DHSA for a global estimation precision which equates to the Measured Resource category would be of the order of 250 metres, while the spacing for an Indicated Resource would be approximately 375 metres. Currently, the drill spacings for the various resource classification categories at South Walker Creek Mine are derived for the full seam packages and are equivalent to the minimum spacing recommended in the Coal Guidelines.

Approximations/Limitations

1. Assumption regarding the yearly reference area may be first pass approximations.
2. The approximation formula $\sigma_e^2 = \frac{\sigma_e^2}{N}$ used to calculate global estimation variances requires a minimum number of samples ('N') to yield meaningful results (typically N should be no less than say 8 samples). For shorter mining periods (e.g. 1 year) the areas considered are smaller and 'N' may take on values (1 or 2 samples) that are pushing the envelope for the validity of the results. Coal allocation decisions over these periods should be based on closer spaced information (collected at the development mining stage) or at least on a model of local *in situ* values estimated by ordinary kriging (OK) using a moving neighbourhood of informing samples.

Given the limitations described above, which are inherent to the approximation formula used in the global estimation variance methodology, the results for longer time periods (i.e. the five and 10 year timeframes) are more reliable than those for the shorter time periods.

It must be noted that DHSA only provides a quantitative measure with regard to global estimation precisions, that is, the variability of the attributes Raw Ash and Thickness for the seam and domain under study. Drilling may still be required to define geological structure and continuity, define faulting, *in situ* gas, geotechnical parameters and a range of other mining parameters that need to be considered in resource classification decisions.

Table 2: Increase in Measured and Indicated Resource Tonnage — Geostatistical Classification versus ‘Coal Guidelines’ Method

Site	Increase/Decrease versus Non-Geostatistical Method (%)
Goonyella Riverside	+18%
Gregory Crinum	+17%
Norwich Park	+26%
Peak Downs	+17%
Poitrel	+9%
Saraji	+24%
South Walker Creek ⁽¹⁾	+10%
TOTAL⁽²⁾	+19%

1. SWC study only covers a small portion of the SWC Mine
2. Figures may not tally exactly due to rounding

DHSA provides the Competent Person with an additional, quantitative, tool for resource classification. The Competent Person must still make the classification decision taking into account not only DHSA results, but also, all other geological and economic considerations for the deposit.

Benchmarking Exercise

Prior to implementing the DHSA process described in this paper, BMA undertook a comparison exercise for its operations, comparing the results from classification using DHSA versus the recommended minimum spacing as per the Coal Guidelines.

The resource categories were classified using the parameters detailed previously, using the drilling information in place at the time of the benchmarking exercise (2009).

The exercise was conducted at seven sites, Goonyella Riverside, Gregory Crinum, Norwich Park, Peak Downs, Poitrel, Saraji and South Walker Creek. The general results in terms of percentage change are shown in Table 2.

CONCLUSION

DHSA using global estimation variance techniques produces global confidence intervals that are geostatistically based, which means they are the result of a process that incorporates a detailed data analysis (including treatment of outliers and characterisation of spatial variability through variogram modeling).

They offer a significant advantage over non-geostatistical guidelines, as the technique is tailored to the individual variability of each deposit, and it is fully transparent and auditable.

In the example shown for the seven BMA sites where DHSA has been implemented, the application of this geostatistical technique to resource classification resulting in an increase in the resource tonnages classified as either Measured or Indicated approximately 19% when compared to classification using the Coal Guidelines.

Quantifying the variability of the key parameters used for classification for a deposit through DHSA provides the Competent Person with an additional, quantitative, tool, which may be of assistance when making decisions regarding resource classification..

The final advantage of adopting the geostatistical framework to run DHSA is that there is not a large amount of extra work required to produce geostatistical estimates through kriging. As illustrated in (Casley & others, 2009) this can provide significant improvements in the accuracy and precision of resource estimates for all variables showing non-negligible spatial variability.

REFERENCES

- CASLEY, Z, BERTOLI, O, MAWDESLEY, M, DAVIES, G, DUNN, D. 2009: Benchmarking Estimation Methods for Coal Resource Estimation. *AusIMM 2009 International Mine Geology Conference*, Perth.
- LANTUÉJOL, C., 2002: *Geostatistical Simulation, Models and Algorithms*. Springer-Verlag, Heidelberg.
- RIVOIRARD, J., 1994: *Introduction to Disjunctive Kriging and Non-Linear Geostatistics*. Oxford University Press, Oxford.

Zach Casley, Oli Bertoli, Clare Mawdesley, Grenville Davies and Doug Dunn

Benchmarking estimation methods for coal resource estimation

The coal industry in Australia has been actively working in recent years towards the (re-) integration of geostatistical techniques to the process of coal resource estimation. The benefits of using geostatistical techniques, over the current interpolation algorithms in use in coal modeling packages used to generate the grid estimates, need to be illustrated for the methodology to gain a broader acceptance in the coal industry.

This paper focuses on the benefits gained at BHP Billiton Mitsubishi Alliance’s Saraji mine for the estimation of the total product yield value at a 9.7% product ash cutoff of a particular seam of the Saraji deposit.

In order to perform this comparison, the results of the alternative estimation methodologies need to be benchmarked, which in most situations is achieved through the reconciliation of the estimates against production and/or process plant reconciliation data. Unfortunately, this benchmarking was not possible as no reconciliation data for the area of interest in the chosen seam was available, as it has not been mined at the time of the study.

Where no reconciliation data is available, an alternative method is to use conditional simulations as the benchmark for comparison. The simulated values can be regarded as ‘reality’, and the alternative estimation methodologies, based on a sampling of the underlying ‘reality’, can then be compared using the simulated ‘reality’ as the benchmark for comparison.

INTRODUCTION

BHP Billiton Mitsubishi Alliance (BMA) are currently mining the Saraji Mine in Central Queensland, producing coking coal products and a small amount of thermal coal. The two coking coal products produced by the mine are a ‘normal’ coking coal and an Ultra Low Volatile (‘ULV’) specification coking coal. Thermal coal is sourced from coal which has been heat effected, or which is not of sufficient quality for sale as coking coal (typically either having too high a phosphorous or ash content).

Saraji Mine is located 213km south west of the Hay Point coal export terminal on the Whitsunday Coast. The following geological summary is paraphrased from Broome (2005).

The main coal bearing unit at Saraji is the Late Permian marine influenced Moranbah Coal Measures which overlies the German Creek Formation. The Moranbah Coal Measures contain six coal bearing horizons with seam splitting and



Figure 1: Map showing the location of the Saraji Mine.

coalescing common. The German Creek Formation contains abundant quartzose sandstone with lesser lithic sandstone, siltstone and mudstone.

Five coal seam groups are present over the mining area. The P seam series, The Harrow Creek Upper, Harrow Creek Lower, the Dysart K seam and the Dysart seam are all contained in the Moranbah Coal Measures. All five seams split and coalesce over the length of the lease to around 15 seam splits.

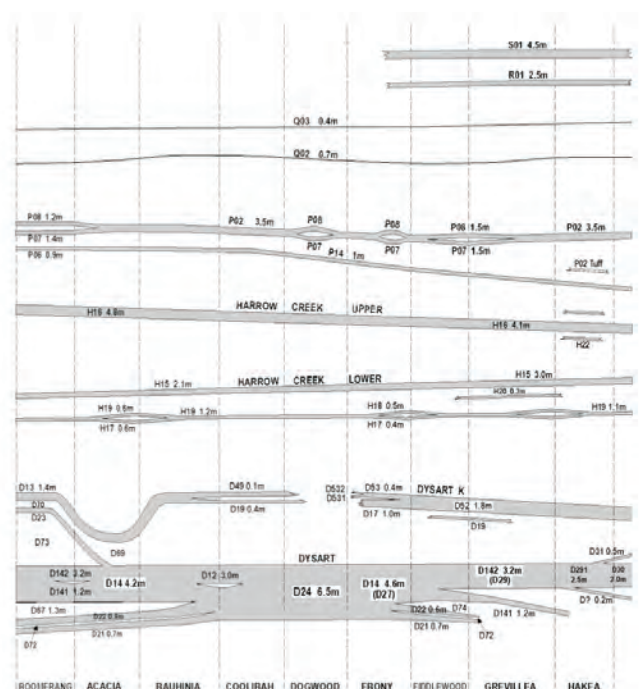


Figure 2: Saraji Seam Correlation Diagram.

The Permian sequence is unconformably overlain by up to 45m of poorly consolidated Tertiary and unconsolidated Quaternary sediments consisting predominantly of sand and clay with irregular gravel beds.

Three stratigraphic sequences are worked at Saraji, the Harrow Creek seams, the Dysart seams and the P seams. Coal is uncovered by open cut methods utilising four draglines supplemented by a truck/shovel stripping operations. Coal is mined in the pits using a hydraulic excavator and front end loaders, and then hauled to the mine preparation plant by 8 x 160 tonne capacity coal haulers, where it is processed to customers' specifications. One such coking coal product has a specified product ash of 9.7%. The variable of interest in this case is the total product yield at this 9.7% product ash cutoff (TP YIELD 9.7%), which is a measure of the coal recovery through the coal processing plant.

The benefit of using ordinary kriging (OK) estimates over the inverse distance (ID) methodology currently applied by BMA was investigated for TP YIELD 9.7% in the P14 seam. The purpose of the comparison of the OK and ID estimates was to establish the existence of an appreciable improvement in the precision of local estimates to be gained through the implementation of ordinary kriged estimates for seams and variables that have non-negligible spatial variability.

With the absence of available reconciliation data, it is necessary to use conditional simulations (CS) as the benchmark for comparing the OK and ID estimates. The conditionally simulated values are regarded as 'reality' in lieu of reconciliation data, and the OK and ID estimates can be compared using the simulated 'reality' as the benchmark for comparison.

Background

In addition to reproducing the data histogram, geostatistical simulations also honour the spatial variability of data, usually characterised by a variogram model. If the simulations also honour the data values themselves, they are said to be conditional simulations.

A key property of geostatistical simulation models is that a series of images, or 'realisations' that presents a range of plausible possibilities is produced. If the underlying assumptions are acceptable and adapted to the problem at hand, then the resulting images can be considered as equally plausible possibilities to represent the unknown reality.

Study Area

The comparison study was conducted on a subset area of the P14 seam, which contains a mixture of well drilled and less

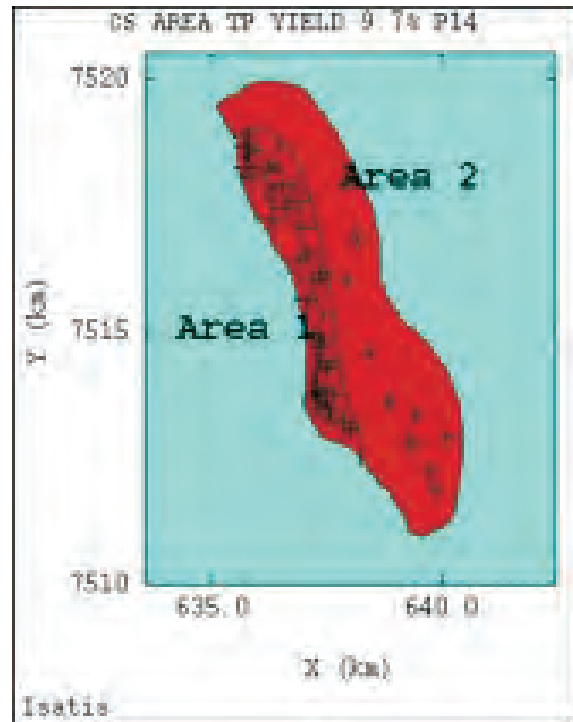


Figure 3: Area used for conditional simulation study (shaded in red) - P14 Seam, TP Yield 9.7%.

well drilled areas. Samples situated in a known coked region to the north were separated from the remaining P14 seam data (the remaining P14 seam data is shown in Figure 3). The final P14 subset contains 54 samples and the raw statistics are listed in Table 1 below. The final subset for comparison contained two areas of vastly differing sampling density. These are defined as Area 1, which is a well drilled area where the data density provides conditions for robust quality of estimation and strong conditioning for the simulations and Area 2, a sparsely drilled area offering much poorer conditions for estimation and in which the conditioning of the simulations is weaker.

Ordinary Kriging Methodology

Estimation was performed by ordinary kriging of naïve (un-accumulated) variables for coal quality parameters. Tests showed that the difference between estimating naïve variables or accumulation variables for quality variables was insignificant. That is, for quality variables in seam P14 the choice to krig the variables directly has limited impact on the outcome of the estimation procedure. This is due in part to the high continuity exhibited by the thickness of seam P14 (the omnidirectional thickness variogram reaches a sill of 0.03 at 2km for an average thickness of 1.05m).

The resource estimates were performed using ordinary kriging of the variables on a 250 mE x 250 mN grid.

Table 1: Raw statistics for P14 seam for variable TP YIELD 9.7%.

Domain	Count	Minimum	Maximum	Mean	Variance	CV
P14	54	63.10	99.83	82.18	104.21	0.124

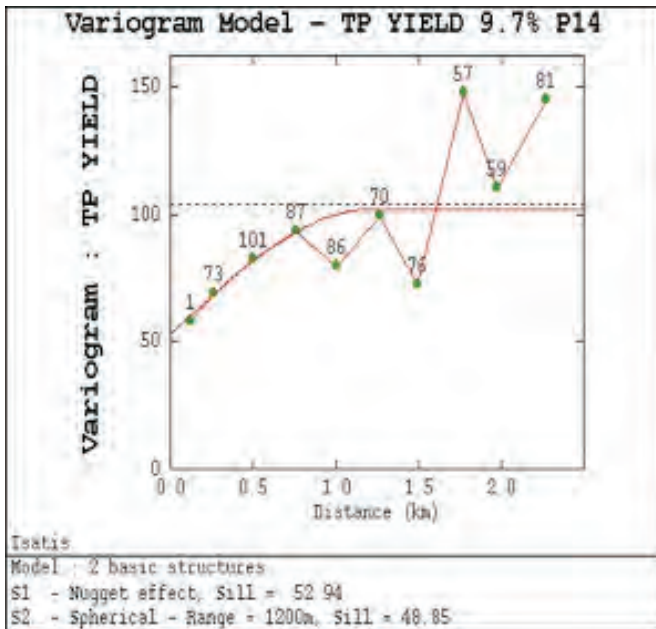


Figure 4: Omnidirectional variogram model fitted to the P14 seam TP YIELD 9.7% experimental variogram.

An omnidirectional variogram model was fitted, with a 52% nugget effect and a range of 1200 metres (shown in Figure 4).

Kriging neighborhood analysis (KNA) (see Vann, Jackson and Bertoli, 2003) was performed by running multiple kriging tests with different neighbourhoods for TP YIELD 9.7% in the P14 seam, and the following kriging parameters were selected:

- 3 sectors;
- Minimum of 8 samples;
- Optimum of 10 samples per sector; and,
- Search distance 900 metres (omnidirectional).

Results from KNA are shown in Table 2.

Table 2: KNA Results for areas of differing sampling density (Area 1 & Area 2)

KNA results	Area 1	Area 2
Weight of the simple kriged mean	0.3	0.3
Slope of the regression of true on estimated block value	0.9	0.4
Correlation Coefficient between true and estimated value	0.7	0.2

Inverse Distance Methodology

For the same 250 mE x 250 mN grid used for the OK estimate, an inverse distance estimate was also calculated for TP YIELD 9.7% in the P14 seam.

The inverse distance estimation (which at the time of the test work was the current BMA estimation process) was undertaken with the distance between the sample locations and the grid nodes raised to a power of 1 (i.e. ID¹), using all the samples falling within the neighbourhood defined in the KNA process (i.e. within a 900m radius).

Conditional Simulation Process

Conditional simulations were conducted for TP YIELD 9.7% seam using the Gaussian-based turning band method (Lantuéjoul, 2002)

The following procedure was followed for each variable:

- Transformation into Gaussian values using declustering weights (representative histogram);
- Variography on Gaussian values;
- Conditional simulation of Gaussian transforms (using 500 bands, 100 realisations were generated);
- Back transformation into raw (YIELD) space; and,
- Post-processing (averaging, sampling, estimation and statistical calculations).

The variogram model for the Gaussian transforms is shown in Figure 5.

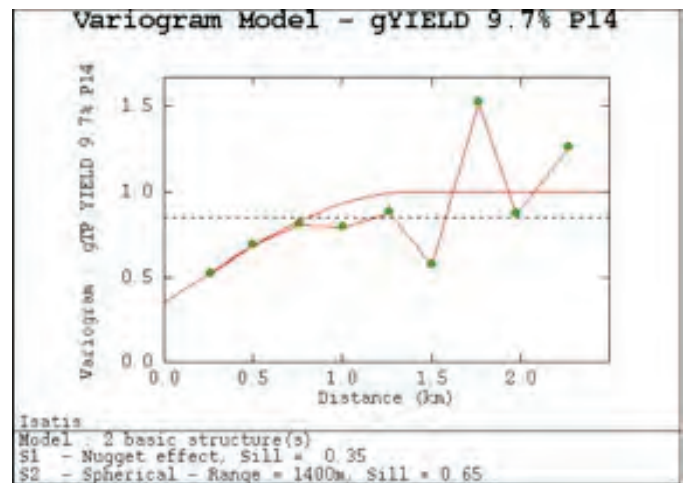


Figure 5: Variogram model for Gaussian transformed variable gYIELD 9.7% for the P14 Seam.

Benchmarking Process

The comparison of the OK and ID estimates was performed assuming the set of conditionally simulated points is the unknown 'reality'.

The methodology used to generate the conditional simulations and estimates can be separated into the following stages:

- 1 Conditional simulation of the variable (TP YIELD 9.7%) within the seam (P14) under study was performed using the turning bands algorithm, based on 500 bands, with a 25m x 25m simulation grid. The simulated values were then regrouped (averaged) into a 125m x 250m cell sized grid, which approximates a mining block at Saraji. In this sized cell, 50 simulated nodes are used to generate the block simulated value, so fluctuations linked to the discretisation of the block should be marginal;
- 2 Sampling of the simulated nodes was based on a 250m x 250m sampling grid with a variable grid origin. Nine sampling grids were defined and used to test the

sensitivity of the results to changes in the origin of the sampling grid;

- 3 For each grid and simulation, the closest simulated values were migrated to the output grid node, offering an initial sampled distribution of reality. Geostatistical estimation was then performed using ordinary kriging with the estimation parameters (i.e. variograms, neighbourhoods, etc) defined during the study;
- 4 The OK and ID estimates were then compared to the simulated 'reality' to compare the accuracy and precision of each estimation method.

A systematic, fixed sampling grid was used to sample the simulations and these results were statistically compared to the OK and ID estimates.

Sampling Configuration

A systematic fixed sampling geometry (refer to Figure 6) was used with the origin of the sampling grid being changed to get nine different sets of samples. The coordinates of the origin of grid 1 are 625000m East and 7500000m North. Grids 2, 3, 4, 5 have the X origin (Easting) shifted by increments of +25m, and grids 6, 7, 8, and 9 have the Y origin (Northing) shifted by increments of +25m.



Figure 6: Diagram illustrating a systematic fixed sampling grid.

For each sampling grid and simulation, a comparison between estimates and 'reality' is directly accessible. The following information can be accessed from the grids:

- Bivariate statistics between the CS 'reality' and the estimates. This allows the retrieval of spatial correlation coefficients between reality and estimates; and,
- The calculation of the error (the difference between the 'reality' and the estimate) and the calculation of the mean and variance of that error per realisation and subsequently the average of these statistics over the 100 realisations.

For the nine sampling grids utilised the average results for the mean of the error, the variance of the error and the correlation coefficient are shown in the table in the following section.

Table 3: Comparison of the global estimation performance for the nine sampling grids

Grid number	Estimation methodology	Average mean of error	Average variance of error	Average correlation coefficient with simulated reality
1	OK	-0.01	12.80	0.88
	ID	0.06	18.59	0.85
2	OK	0.2	13.17	0.86
	ID	0.28	18.75	0.80
3	OK	-0.03	12.15	0.88
	ID	0.05	17.70	0.83
4	OK	0.1	12.26	0.87
	ID	0.2	18.33	0.82
5	OK	0.02	13.01	0.86
	ID	0.11	18.65	0.80
6	OK	-0.04	12.97	0.87
	ID	0.04	18.50	0.81
7	OK	0.04	12.71	0.88
	ID	0.1	17.37	0.83
8	OK	-0.08	12.06	0.88
	ID	-0.02	16.60	0.85
9	OK	-0.2	13.23	0.86
	ID	-0.15	17.23	0.82

Results

The comparison of the global estimation performance for ID and OK estimates, for the nine sampling grids is summarised in Table 3.

The results from the benchmarking indicate that;

- For all grids, ordinary kriging has no bias. The inverse distance method, in this case, has an average bias of ~0.05;
- The variance of the error between the estimate and reality is reduced on average by 35% by using ordinary kriged estimates; and,
- The correlation coefficient between reality and the estimate is increased by approximately 4% by using ordinary kriging.

The consequences of the above results on misclassification through erroneous estimation are tabulated in Table 4 using various target Yields at the coal processing plant. The results are averaged for all realisations and for the 9 sampling grids. They quantify the actual precision gains through implementing ordinary kriging as the estimator rather than

Table 4: Comparison of the proportions of blocks misclassified at the coal processing plant at various target yields (average proportion for the different sampling grids over all simulations)

Misclassification Category	Estimation Methodology	Target Yield		
		75%	80%	85%
Wrong Acceptance	OK	5.8%	9.0%	6.5%
	ID	8.2%	11.5%	6.7%
False Rejection	OK	1.8%	5.0%	7.3%
	ID	0.7%	4.4%	10.1%
Total Misclassification	OK	7.6%	14.0%	13.8%
	ID	8.9%	15.9%	16.8%

inverse distance when dealing with variables with spatial variability comparable to TP YIELD 9.7% in the P14 seam.

The seam used for this study displayed a moderate level of spatial variability as defined by the variogram (50% nugget effect, range of 1200m). The errors through lack of precision due to using inverse distance methods will be magnified as the spatial variability of the seam and/or variable increase.

CONCLUSIONS

The purpose of the comparison of the OK and ID estimates was to establish if there is an appreciable improvement in the precision of local estimates to be gained through the implementation of ordinary kriged estimates for seams and variables that have non-negligible spatial variability.

The results of this benchmarking study suggest that for variables with spatial variability comparable to TP YIELD 9.7% in the P14 seam, misclassification through erroneous estimation would be reduced at least by an order of approximately 10% through implementing ordinary kriging as the estimator rather than inverse distance. The seam used for this study displayed a moderate level of spatial variability as defined by the variogram (50% nugget effect, range of 1200m). The errors through lack of precision due to the use of inverse distance methods will be magnified as the spatial variability of the seam and/or variable increase.

A significant opportunity for improving material classification and resource optimisation exists if geostatistical estimates are

applied (as an alternative to inverse distance) for seams and variables that display non-negligible spatial variability. The corresponding gains in revenue through improved material misclassification and optimal utilisation of the coal resource are significant.

ACKNOWLEDGEMENTS

The authors would like to thank BHP Billiton Mitsubishi Alliance Ltd for its support in publishing this paper, and for allowing the authors to use data and findings from ongoing work at its Saraji Mine. The contribution of the geologists who have worked at Saraji, and contributed to the understanding of the resource is gratefully acknowledged.

REFERENCES

- BROOME & DUNN, 2005: Resource Estimation Report as at 30th June 2005. Confidential JB Mining Services Report for BHP Billiton Mitsubishi Alliance Coal, dated 30th August 2005.
- LANTUÉJOUL, C, 2002: *Geostatistical Simulation: Models and Algorithms*. Springer-Verlag, Berlin.
- VANN, J. JACKSON, S. & BERTOLI, O., 2003: Quantitative Kriging Neighbourhood Analysis for the Mining Geologist — a description of the method with worked examples In: *5th International Mining Geology Conference, Bendigo, Victoria, 17-19 November, 2003*: 215–223. The Australasian Institute of Mining and Metallurgy: Melbourne.

Zach Casley, Principal - Mine Geology and Resource Evaluation, Tenzing Member of the AusIMM and AIG, Tenzing, PO Box 979, Wynnum, QLD 4178, zach@tenzing.net.au

Oli Bertoli, Principal - Geostatistics and Resource Evaluation, Tenzing, Member of the AusIMM and GAA, Tenzing, PO Box 979, Wynnum, QLD 4178, oli@tenzing.net.au

Clare Mawdesley, Senior Consultant - Resource Evaluation, Member of the AusIMM and AIG, Tenzing, PO Box 979, Wynnum, QLD 4178, clare@tenzing.net.au

Grenville Davies, Principal Resource Evaluation Geologist - Resource Development Group, BHP Billiton Mitsubishi Alliance Coal, GPO Box 1389, Brisbane QLD 4001, Australia, Grenville.Davies@bmacoal.com

Doug Dunn, Manager Geological Services, BHP Billiton Mitsubishi Alliance Coal, GPO Box 1389, Brisbane QLD 4001, Australia, Doug.L.Dunn@bmacoal.com

Paper has been previously published in the proceedings of the Seventh International Mining Conference 2009, Perth Australia.

Kevin Rosengren, John Simmons, A. Paul Maconochie and Thomas Sullivan

Geotechnical investigations for open pit mines — 250m and beyond

In 1981, Rosengren published guidelines for geotechnical investigations for Bowen Basin open pit dragline mining to depths of '45m and beyond'. Now, open pit coal mining to depths in excess of 250m has been achieved or is being planned, with and without draglines. This paper updates Rosengren's guidelines for geotechnical investigations to reflect investigation requirements for future generations of open pit slopes.

With increasing depth of mining, geotechnical factors assume increasing importance in the design and operation of open pit coal mines. Dragline strip mines are particularly sensitive to stability conditions since the dragline is a relatively inflexible machine, particularly in relation to its limited dumping radius for overburden disposal. Geotechnical factors relevant to open pit mine design include:

- spoil pile stability, including operating bench stability,
- wall stability,
- floor stability,
- excavation characteristics, and
- groundwater conditions.

A basic geotechnical investigation program suitable for new mine feasibility studies and projects to extend the life of current mines is described. This includes:

- terrain evaluation,
- geotechnical drilling and logging,
- geophysical logging of drillholes,
- materials testing,
- seismic refraction and other wide-field geophysical surveying, and
- groundwater studies.

Such a program will give an overall geotechnical assessment of the site and highlight any areas which may require further, more detailed investigations. It is likely to be carried out in parallel with a wide range of environmental impact and baseline investigations, where the project will benefit from coordination and cooperation with these other disciplines.

INTRODUCTION

With increasing depths of mining, geotechnical parameters assume increasing importance in the design and operation of strip coal mines. The principal geotechnical parameters are:

- spoil pile stability,
- operating bench stability,

- wall stability,
- floor stability,
- excavation characteristics, and
- groundwater conditions.

The great variety of geological conditions, seam geometries and mining methods occurring in open pit mines ensures that each of the above parameters will have a variable degree of importance in each specific deposit.

Although all types of open pit mining are sensitive to geotechnical factors to some degree, it is in dragline strip mines that they assume their greatest importance. This situation arises from the basic geometric limitation of the dragline, specifically its dumping radius, which is basically a function of its boom length. Thus, while the dragline is unchallenged in its ability to remove overburden from a coal seam at minimum cost, it requires favourable stability conditions to be fully effective. It can still be used where stability conditions are not favourable, but only at the expense of modified geometry (longer boom/smaller bucket) or high rehandle volumes, either of which will inevitably erode its basic economic advantages. Thus, the dragline may not always be the optimum overburden removal method, even for overburden depths <100m.

In Australia, the importance of geotechnical factors in efficient dragline operations was first highlighted by the severe problems encountered in the Goonyella mine (Boyd & others, 1978). Similar issues have been experienced at many of the other mines in the Bowen Basin. In the first decade of dragline stripping, extensive research was carried out to gain an understanding of these geotechnical problems and to seek optimum methods for their solution (Gonano, 1980). During the second decade, increasing use of in-pit benches and multiple-pass stripping techniques generated a new class of geotechnical problems, for which optimum methods for management have been developed in-house, particularly by BMA Coal (Simmons, 1995; Simmons & McManus, 2004). Within the past decade, the rapid price-driven expansion of the industry has generated a new class of geotechnical problems, involving very high excavated walls and even higher spoil dumps, for which optimum solutions are still being developed.

This paper summarises the various geotechnical parameters important in open pit coal mining and discusses methods of obtaining the necessary geotechnical data for mine design, with particular reference to so-called greenfield sites. The major emphasis is placed on dragline stripping, but reference is also made to other mining methods, where relevant.

SPOIL PILE STABILITY

Spoil pile stability is usually the most critical geotechnical parameter in open pit mining, since the spoil pile is basically an uncontrolled, uncompacted heap of disturbed overburden, which can only be placed a limited distance from where it is excavated. Spoil pile heights are generally in the range 80–110m for current maximum dragline digging depths of around 60m, but pre-strip surcharge commonly extends current overall dump heights to between 150m and 200m. At the time of writing, the highest truck dumps are in the order of 350m high and there are plans for dump heights of close to 500m.

When dumped, the overburden will rill to its angle of repose, which may range from 33° or less for some sand and clay materials, to 40° or more for hard rock. Most commonly it is in the range 35–40°. The angle of repose applies only to the dynamic movement of loose material on the free surface of the pile and is not the same as the angle of internal friction for the material mass. Dumped spoil material is essentially rockfill with fines that is subjected to self-weight compaction. As a consequence, its angle of internal friction varies with confinement and it is therefore possible to re-excavate dumped spoil at slopes steeper than the angle of repose. For example, the lower part of the spoil profile is commonly cut to angles of 40° to 45° when the dragline bench is rehandled during in-pit bench stripping procedures.

Spoil pile failure can occur in three ways:

- relatively superficial slumping of the face of the pile due to inadequate strength of the spoil material when the face is over-steepened,
- large-scale instability of the spoil mass due to inadequate strength of the spoil material, and
- large-scale instability due to translational failure of the dump foundation, which usually includes floor heave at the toe.

Large-scale failures are by far the most important, both in frequency and volume of material (Gonano, 1980).

Considerable research has been carried out on both the theoretical (Dunbavan, 1980) and observational (Cox & Dunbavan, 1981) aspects of spoil pile stability. To a first approximation, virtually all large-scale failures can be represented by a simple bi-linear wedge mechanism (Figure 1). Before the widespread availability of computer-based stability analysis, stability charts were commonly used for slope design purposes and an example from Rosengren (1981) is shown in Figure 2.

Irrespective of the method used for design, it is well established that the stability of the pile is not very sensitive to spoil material strength, but it is highly sensitive to floor dip and foundation strength. Because infiltrating water is likely to collect and flow through the basal layer of dumped spoil, this zone typically becomes saturated and its strength state is therefore reduced from the unsaturated condition. This means that the weakened strength of the basal spoil or a weak layer

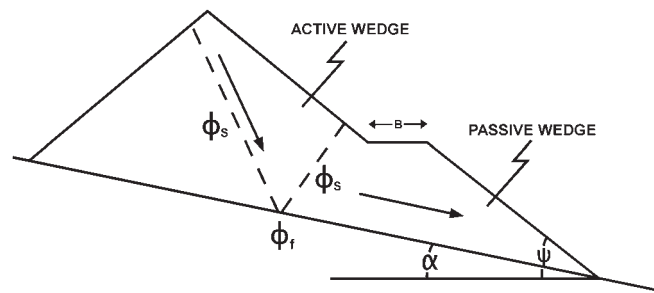


Figure 1: Spoil pile geometry and failure mechanism (Rosengren, 1981)

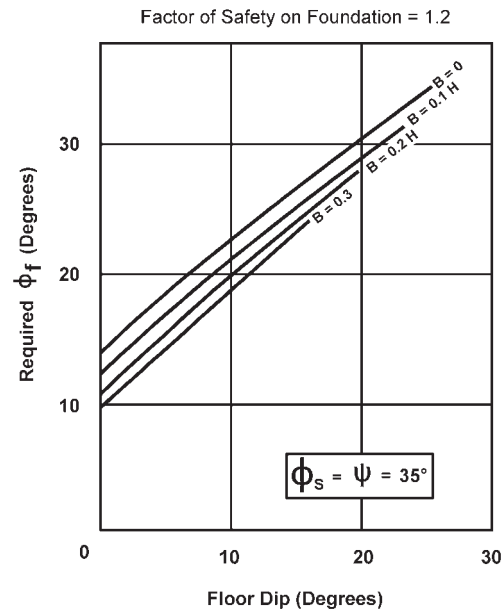


Figure 2: Spoil pile stability analysis chart (Rosengren 1981).

within the foundation will control the stability of the dump. It is critically important during investigations to determine whether foundation layers are likely to exist with strengths less than the weakened strength of the basal spoil.

For a typical dragline spoil dump profile, the required foundation angle of friction (ϕ_f) ranges from 14° for a horizontal foundation to 26° for a foundation dipping at 15°. The minimum shear strength horizon may be located either in the immediate floor or in the spoil, depending on the relative strength properties of each material and therefore the relevant foundation angle of friction may be determined by the floor or the spoil properties.

If the immediate floor stratum consists of sheared mudstone or claystone then the likely floor strength will approximate the residual angle of friction (ϕ_r). This is typically found to be in the range of 12°–17° with zero cohesion. If the sheared horizon is particularly rich in montmorillonite ϕ_r may be as low as 7° to 9°.

In the case of spoil, because of the potentially large shearing deformations generated in wet and weak spoil foundation materials during dumping of the spoil pile, it is considered that the residual angle of friction with zero cohesion for the

foundation material are appropriate for stability analyses in the following situations:

- weak, slaking prone material placed in the base of the pile,
- weak material lying on the previous floor of the pit, and
- weak layers beneath the floor of the pit.

Water is also a major contributor to foundation failure, in the form of:

- water on the floor of the pit prior to placing the pile,
- surface water ponding in the spoil pile peaks and seeping through the pile and along the floor, and
- groundwater seeping upwards from the floor. As well as the effect of water softening of slaking-prone material, pore water pressures can develop in the pile, leading to a further reduction in stability.

The maximum residual friction angle that can be expected in Bowen Basin conditions is around $\phi_r = 18^\circ$ (Simmons & McManus, 2004). From Figure 2, it can be seen that stability will be questionable with floor dips greater than about 7° and that exceptionally good materials ($\phi_r = 27^\circ$) will be required to ensure spoil pile stability on floor dips greater than 15° .

Spoil pile stability can be increased by leaving benches either at operating bench height of dragline spoil piles or at one or more dumping levels for truck or spreader-dumped spoil piles. Figure 2 shows that the degree of stabilisation is rather limited for practically achievable benches. For example, with a floor dip of 10° and a 100m high spoil pile, a 30m wide bench decreases the required foundation strength from $\phi_r = 23^\circ$ to $\phi_r = 19^\circ$ only.

In contrast to the relative inflexibility of dragline spoil piles, waste dumps built from transported material have the following advantages with respect to stability:

- they can be placed some distance from the coal face so that dump failures, if they do occur, will not disrupt coal mining operations, and
- they can be placed in layers which will receive some benefit from compaction (particularly in the case of scraper placement) and which can be offset to form a lower overall slope. A stability analysis for a layered waste dump shows that, for example, stability can be ensured on a 10° dipping foundation with $\phi_r = 20^\circ$ by reducing the overall dump slope to 28° . This increased flexibility and stability will be achieved usually at additional cost, compared with dragline stripping.

In dipping seams, there are important differences in stability conditions between advancing down dip and advancing along strike. A conventional dragline operation advances down dip and the spoil pile must support itself on a dipping foundation, as discussed above. On the other hand, if the strip is oriented down dip and advances along strike, the spoil pile is buttressed against the final down dip wall and stability problems are substantially reduced. This so-called haulback method can be used with draglines under certain conditions,

but it is generally more suited to shovel/truck or similar operations. Haulback methods have become more widely used in Australia for accessing steeply-dipping coal seams that were considered to be too difficult for open pit mining until the 1990s.

In summary, geotechnical data required for an assessment of spoil pile stability are:

- foundation dip,
- strength of materials on and immediately below the pit floor,
- strength of overburden spoil materials, particularly those which will be placed in the lower part of the pile, and
- groundwater conditions.

OPERATING BENCH STABILITY

As pits have progressed deeper, dragline stripping has been increasingly adapted to multiple-seam, multiple-pass operations. Economic imperatives have also driven dozer-assisted digging methods that minimize chopping, but often at the expense of poorer, looser excavated faces and increased dozer exposure to rockfalls. Operating bench stability is critical to the success of dragline stripping and requires appropriate investigations.

Operating bench stability is also a significant consideration for excavator or shovel stripping but these machines, being much smaller than draglines, place lesser loading demands on benches. The same geotechnical principles apply to all machine loads on operating benches, but the following discussion is concentrated on draglines.

Dragline bench failures can occur in many ways:

- uncontrolled tub slip or tub sink at operating bench level,
- collapse of the bench due to inadequate strength of spoil or previous void backfill material, and
- sliding on weak surfaces within the blast-damaged, but still contiguous, rock mass stratigraphy underlying part of the bench profile. These weak surfaces may exist within seam roof or floor strata, as well as within the seam or ply sequence.

In principle, uncontrolled tub movements on operating benches should not occur when standard operating procedures are followed. These include sound construction techniques, maintaining grade control and providing a clean working surface free of wet, soft material.

Bench collapse due to inadequate strength of spoil material is a matter for design, recognising the loading applied by the dragline tub and identifying the spoil strength using the same methodologies that have been developed for spoil dumps. For various reasons (none of which are endorsed by geotechnical specialists), water or mud may accumulate in a previous void and be covered by a blast profile or by dumped pre-strip material. Under such conditions, the effects of water and/or

mud cause softening and remoulding of spoil materials, for which the residual friction angle becomes appropriate for stability design. The dragline tub loading is equivalent to a surface spread footing, and the potential collapse mechanisms that may develop are known from the principles of foundation engineering to be either arc-shaped or multi-linear wedge-shaped.

Weak surfaces within the geological profile have several origins. Low-strength clay layers are formed by subaqueous or subaerial deposition of suspended sediments, including tuffs. In horizons subjected to long-term weathering with wetting and drying cycles, fissuring can develop in clay-rich intervals and the fissures may reduce the strength of the mass to the residual friction angle. Tectonism may induce weak surfaces which tend to follow bedding partings or clay layers, as well as low-angle intraformational shearing associated with bending deformations. Faulting obviously creates principal displacement surfaces, but often consists of complex structural zones, including complementary shears and Riedel shears (Morgenstern & Tchalenko, 1967; Atmaoui & others, 2006).

In many circumstances, blasted ground may be loosened and fractured but still retain continuity of weak surfaces.

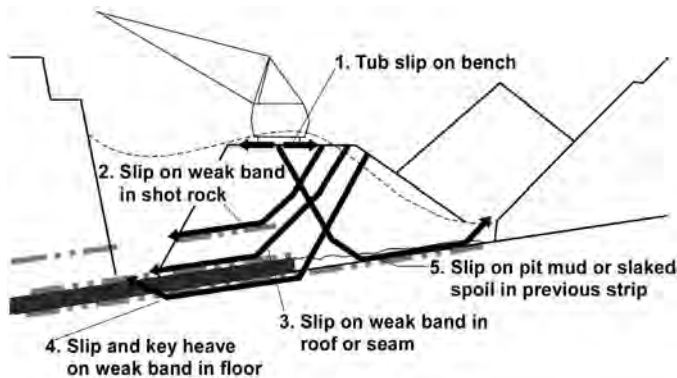


Figure 3: Potential failure modes for a dragline (Simmons 2000)

Operating benches may include a component of 'prime' dirt where dragline loading may create potential failure mechanisms that exploit pre-existing weak surfaces. Figure 3 shows examples of potential dragline-induced bench instability caused by overstressing of pre-existing, geologically weak surfaces. Each of these examples is based on events that have been experienced. Clearly, the scope of investigations must include adequate information about whether or not such surfaces are likely to be present during mining and, if so, there must also be adequate information regarding the strength of such surfaces.

A special case of operating bench is the tiphead, where truck loads are dumped. At the tiphead, tipped materials slide and roll down the exposed face and some segregation of particle sizes results. As a consequence, all dump profiles have a complex internal structure and it takes some time for freshly placed material to settle and gain its full mass strength. The actions of trucks reversing, braking to a halt, and tipping results in a dynamic loading situation, where most of the mass of the loaded truck is supported on the rear axle at its closest

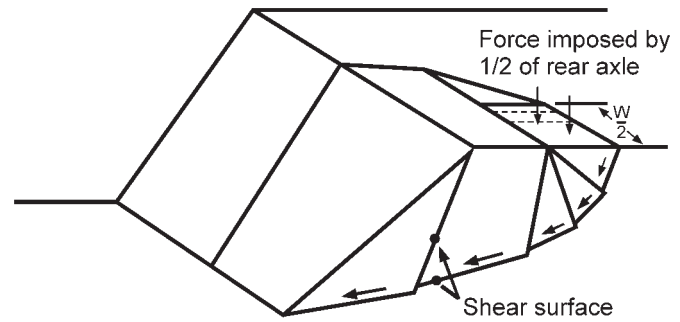


Figure 4. Symmetrical half of 3D failure mechanism with five blocks (May 1991)

approach to the tiphead (Figure 4). Specialised assessment procedures are required for assessing tiphead stability (May, 1991) and these rely upon reliable assessment of shear strength of the dumped spoil materials.

WALL STABILITY

In a strip mining operation, two long excavated walls are formed in the initial boxcut. One of these, the lowwall, remains and is eventually covered by spoil. The other, the highwall, is progressively excavated and occupies a new position within each strip. The maximum highwall batter height in a dragline operation is usually of the order of 45–60m, depending on the dig depth of the machine, with a variable depth of chopping or pre-stripping above the operating bench level. In open pit coal mining using truck or conveyor transport, there is virtually no limit to mining depth and benched walls, with total heights of greater than 300m becoming common.

Potential failure mechanisms for excavated walls fall into three categories with some overlap. When the material strength is weak enough, as in soils, alluvium, and weakly cemented sediments, the mobilised strength is the shear strength of the material, and soil-like instability develops without any geometric control by bedding partings, fissures, or other structural features. Excavated wall failure in such materials will occur by slumping along a curved slip surface through the material.

Secondly, in materials and slope conditions where intact material strength is high enough, failure can only occur by slippage and opening along simple or complex surfaces, formed by pre-existing defects in the rock mass. These structure-controlled mechanisms of failure are the most common and involve the greatest volumes of material under Bowen Basin conditions (Gonano, 1980). Under such conditions, bedding dip is again an important factor in wall stability, and specific design procedures are required for steeply dipping seams (Walton & Atkinson, 1978).

Thirdly, composite failure mechanisms, in which the failure path follows existing fracture paths and extends these through intact rock bridges, become more likely as pits become deeper and s_1 increases, while s_3 remains low. In the past, simple empirical methods such as RMR, Q and GSI have been used

to estimate the rock mass strength. Numerical modelling of composite failure mechanisms provide a much better simulation of composite failure mechanisms, but is computationally intensive. An alternative approach is to generate composite failure paths statistically and to determine the average shear strength for each path. Such a scheme was first formulated by McMahon working in Bougainville and has been developed and implemented in the program STEPSIM4 by Baczynski (Baczynski, 2000; Dight & Baczynski, 2009).

For the stronger, harder materials, back-break from overburden blasting can have an important influence on wall stability. For this reason, the use of angled blastholes and initiation sequences designed to minimize back-break is highly recommended (Scott, 1996).

Damage in the near-field region includes the shattering and crushing of rock near the blasthole, and the creation of a fractured zone further away from the blasthole (Scott, 1996). Controlling the extent and severity of near-field damage in open cut blasting involves understanding the relevant damage mechanisms and designing the blast to minimize damage beyond the nominal blast volume. The principal mechanisms of damage to walls in open pit blasts are:

- back-break,
- burden relief, and
- confinement.

In strip mining operations, pre-split blasting is the most effective method of controlling such damage. In order to achieve this, sufficient geological data is required, in particular joint spacing and orientation, and rock strength.

Effective pre-split blasting can reduce highwall geotechnical hazards, e.g. rock falls, overhanging blocks, etc.

Groundwater pressures can have an influence on stability if high pressures exist close to the face of the wall. Most coking coal seams in Australia have reasonably high permeabilities and will act as underdrains for the walls, but steaming coal seams tend to be less permeable and may not be as effective in this regard. Recent versions of slope stability software, including Slide and SLOPE/W, incorporate finite element groundwater modelling modules. These can generate sophisticated steady and transient pore pressure profiles for the slope stability analyses. An example of a non-intuitive pore pressure profile is shown in Figure 5. Clearly, this has a significant effect on the calculated FOS compared with more simple profiles. Some degree of back-break from blasting can, in fact, be beneficial in increasing overburden permeability and thus permit larger-scale, natural depressurisation to occur.

If adequate natural dewatering/depressurisation of walls cannot be reliably achieved, it may be necessary to use artificial methods, usually in the form of horizontal drains or pumped wells behind the wall. Such measures are currently not common in open pit coal mines and are more usually applied to deeper, benched hard rock mines. However, there are also incentives for wall dewatering to reduce the incidence

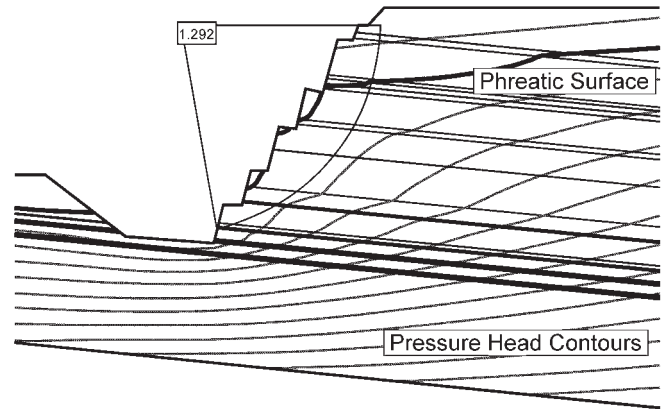


Figure 5: Combined seepage and slope stability analysis output from the program Slide (Simmons, 2010, personal communication)

of wet blastholes and thus reduce blasting costs (Hagan, Friday & Lemberg, 1981).

As mines have progressed deeper, the assumptions that are normally made regarding adequacy of groundwater pressure drawdown become less reliable, and analytical models are increasingly being used for predicting pressure distributions. However, the reliability of such models is dependent on the reliability of inputs, including the geological model, permeabilities, and boundary conditions that are applied. Figure 5 shows an example of output from such a model, in terms of total head contours (the level to which water would rise in a standpipe piezometer). In this model, the geological model was generated from exploration data, anisotropic permeabilities were inferred from back analysis of multiple piezometer installations, and boundary conditions were obtained from piezometer data, assuming bedding-parallel flow at depth.

Boxcut lowwall stability requires additional stability considerations because the majority of the exposed excavation face will be weakened by weathering effects, as well as the effects of adverse seam structure dip. Boxcut toes are typically located at the up-dip limit of economically recoverable coal. However, unless the coal measures rocks are truncated by geological unconformities or pre-strip excavations, the seam structure will continue up-dip until it subcrops. Coal seams typically weather to form soots and clays, which can be very weak.

Pre-existing bedding-parallel weakness will also continue up-dip until truncated. Under such conditions, the loading imposed by a boxcut spoil pile may contribute to an unacceptably high risk of boxcut lowwall collapse, leading to coal losses and unplanned capital costs. For this reason, adequate information must be obtained from investigations to enable specific stability assessments to be carried out. For adverse sedimentary or seam structure dips greater than 10°, it may be necessary to place the boxcut spoil clear of the seam subcrop.

Rockfall hazards are likely to be present for any excavated wall. Risks can be minimized to acceptable levels through combinations of design controls (batter angles, blasting

techniques, benching, windrows, and access-restricted zones) and operations controls (effective blast execution, adequate trimming to remove loose material, continual inspections, and barricading etc.).

FLOOR STABILITY

Floor stability problems can arise from:

- floor buckling, as a result of spoil pile failure by sliding on a weak floor layer, and
- heaving, as a result of water pressure in a confined aquifer beneath the pit floor level.

The first mechanism has been discussed above. It may generate operating problems with coal extraction, as well as sudden and rapid ground movement that can damage or trap equipment and personnel. Heaving due to subfloor water pressures is potentially even more serious, since uncontrolled floor heave could also lead to rupture of the aquiclude layer and flooding of the open pit.

An imbalance of water pressure and overburden pressure will occur in all cases when excavation proceeds below the local piezometric surface (water table). These pressures will tend to dissipate by natural drainage and will not cause a problem unless a high permeability aquifer occurs beneath the floor, which will permit a recharge of water pressure at a greater rate than it is dissipated by drainage. In this situation, it is necessary to depressurise the aquifers, either by free-flowing or pumped boreholes. The rate of depressurisation must ensure that, at all times, there is an adequate factor of safety against floor heave. This situation occurs at the brown coal mines in the Latrobe Valley in Victoria (Rosengren & Krehula, 1965). Failure to control the groundwater was responsible for the reduction in sliding resistance that resulted in the Latrobe River breaching the Yallourn Open Cut in 2007 (Sullivan, 2008).

Water pressures can also be critical, even where there are no significantly permeable layers, in situations where the floor or footwall of the pit is formed by a steeply dipping seam pavement. Water pressure relief holes are often considered in such cases (Walton & Atkinson, 1978) and have been implemented for the Abbey Green South pit at Mount Thorley Warkworth Mine. Lack of adequate footwall depressurisation has contributed to very large footwall failures in open pit coal mines in Indonesia.

EXCAVATION CHARACTERISTICS

Overburden removal costs are usually the major cost element in open pit coal mines and it is therefore essential that this operation be optimised. A major question is whether the primary overburden or the seam partings will require blasting, since ripping and dozing is often a convenient method of excavation, particularly for thin partings. The application of

bucket wheel excavators is also highly dependent on material hardness.

If blasting is required, as is most often the case, it is essential to optimise:

- blasthole diameter,
- blasthole pattern,
- blasthole inclination,
- powder factor,
- initiation sequence, and
- type of explosive.

These aspects are discussed in detail by Scott (1996) and require knowledge of:

- material types and strengths,
- bedding and jointing orientations and spacings, and
- groundwater conditions.

GROUNDWATER CONDITIONS

Water pressures have a most important influence on the stability of pit walls and waste dumps, as discussed above. Detailed information is therefore required on:

- groundwater levels in relation to the proposed mine geometry, and
- permeabilities of the overburden, coal and floor strata.

This information can be used to assess the influence of water pressures on stability and, if necessary, to design depressurisation procedures to reduce water pressures to acceptable levels.

In addition to the influence on stability, groundwater has a further influence on pit design, in relation to:

- occurrence of wet blastholes and influence on blasting costs (Scott, 1996), and
- anticipated inflows to the pit and required pumping capacity.

Both of these factors can be estimated once water levels and strata permeabilities are known. In some cases, it may be necessary or economical to dewater an area by borehole pumping prior to the commencement of mining. A vital part of pre-mining investigations is therefore measurement of existing groundwater pressures. In addition, hydrogeological investigations should include *in situ* permeability testing. Drawdown tests using multiple wells are of particular value when they enable estimates to be made of non-uniform permeability in different strata and anisotropic permeability within key strata, particularly coal seams.

GEOTECHNICAL INVESTIGATIONS

In order to provide data on the geotechnical parameters discussed above, information is required on the following:

- seam structure dip and preferably also sedimentary structure dip,
- seam thickness,
- overburden thickness,
- nature and properties of overburden,
- nature and properties of coal seams,
- nature and properties of floor materials, and
- groundwater conditions.

Data on the first three aspects are usually available from the geological exploration program. However, data on the remaining aspects are usually inadequate when coal deposits are explored using open holes, with coring of coal seams only.

The additional data usually requires a specific geotechnical study program, which would include some or all of the following elements:

- terrain evaluation,
- geotechnical drilling and logging,
- geophysical logging,
- materials testing,
- seismic refraction traversing, and
- groundwater studies.

Terrain Evaluation

Engineering terrain evaluation is a technique for classifying surface materials, in which an area of interest is divided into a number of terrain units, each with its own specific characteristics. The method is based mainly on stereoscopic examination of aerial photographs, but other relevant information and, ideally, a field inspection, are used as well. The resulting terrain evaluation is then used as a basis for more detailed investigations for specific engineering purposes. The recognition of different terrain units can be based on a variety of criteria, such as topography, geological boundaries, vegetation, and drainage patterns.

A major advantage of the method is that a large area can be described in a minimum of time and used as a basis for selecting specific areas for more detailed investigations. In addition, it is often possible, using aerial photographs, to observe features and their relationship to one another when they are not obvious on the ground or even from low level aerial reconnaissance.

Terrain evaluation is an essential part of any geotechnical investigation for open cut mining, since it is the only practical method of gaining a general appreciation of a large area, which will form an overall perspective for planning and optimising the more specific investigations discussed below. It is particularly useful for identifying surface materials which

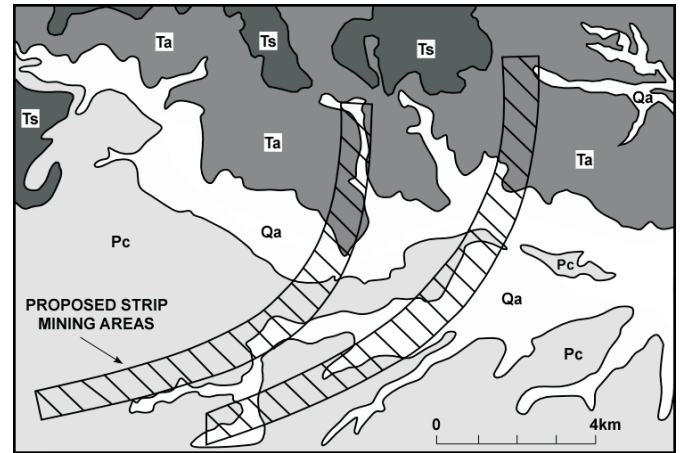


Figure 6: Typical terrain evaluation (Rosengren, 1981)

could have a deleterious effect on spoil pile stability and which will therefore require selective stripping and spoiling.

A typical terrain evaluation is shown in Figure 6. Features of this particular evaluation are:

- extensive Recent alluvium (unit Qa) around the main drainage channels. These cross the proposed mining areas and may generate stability and groundwater problems, which will require further, more detailed investigation,
- extensive deposits of an older, possibly pre-Tertiary alluvium (unit Ta) in the northern part of the mining area. Subsequent cored drilling showed this to consist of up to 30m of unconsolidated sand and clay, which will require modified spoiling techniques and flatter high wall slopes to ensure stability,
- remnants of a Tertiary land surface (unit Ts), consisting of poorly consolidated sandstones and siltstones, and
- outcropping Permian coal measures (unit Pc) with alternating hard and soft bands. Subsequent seismic traverses showed that the hard bands were unrippable close to the surface and would be significant obstacles to pre-stripping ahead of the dragline.

Geotechnical Drilling and Logging

Most exploration programs for strippable coal are based on open hole drilling, with geophysical logging and limited coring of the coal seams only, to provide samples for quality analysis. It is therefore usually necessary to drill a number of fully cored boreholes to determine the nature of the overburden and floor strata and to provide samples for materials testing. Requirements for geotechnical drilling are:

- boreholes must be cored from as close as practical to surface, through the overburden and coal seam, to at least 10m below the floor of the seam. If there is any suspicion of permeable zones at a greater depth below the floor, the boreholes should be extended,
- cores should preferably be at least 'HQ' size (61mm diameter) and drilled with triple tube, split inner tube core barrels, to ensure minimal core disturbance. Wireline coring techniques are preferred because of

minimized trip time but may have disadvantages when bit wear, bit damage, or changed ground conditions cause problems with core recovery quality, and

- in many cases, it may be desirable to drill inclined rather than vertical holes for the purposes of:
 - » orienting the core, either from the bedding traces or by the use of a core orienter,
 - » intersecting, steeply dipping joints, which are common in flat-lying sediments and which are poorly sampled by vertical boreholes, and thereby obtaining reliable information on joint orientations prior to mining, and
 - » unfortunately, the drilling industry that supports coal mining has not developed widespread competency in drilling inclined holes in sometimes low-strength and water-sensitive overburden materials. This has resulted in a cost premium for inclined holes and a perception that the added benefits are not justifiable. This has led to numerous projects where inadequate investigations have resulted in unplanned development costs that far exceeded the costs of inclined drilling.

The density of geotechnical drilling will be dependent primarily on the degree of variability of the materials over the proposed mining area. In our experience, it is necessary to drill holes initially at 1 to 2km spacing along strike in the initial mining areas (usually subcrop) and further down dip, with emphasis on the former. Additional infill holes may be required, depending on the results obtained. If the terrain evaluation shows a wide variation in surface materials, it may be desirable to drill additional shallow boreholes or to dig test pits to fully define these materials.

Drilling must be supervised by an experienced person, preferably a geologist with specific geotechnical training, to record hole depths, core losses and any other significant aspects (e.g. water losses) during drilling. As each core run is recovered, it should be carefully transferred to the core tray and allowed to dry before being:

- photographed in colour, ensuring that the core trays are adequately labelled,
- logged in detail for the following features:
 - » rock type,
 - » degree of weathering,
 - » rock substance strength,
 - » description of soft or weak zones (or accurate identification and description of drilling characteristics for loss intervals, which usually represent soft or weak zones), and
 - » location, description and orientation of any breaks in the core.
- sampled for laboratory testing.

Core photographs are an invaluable record of the original core condition. The core, even if available at a later date, may have deteriorated or be incomplete as a result of sampling. Tools are available for assembling and presenting core photographs for interpretation purposes, such as the CSIRO developed CoreProfiler (Sliwa, Dean & Poropat, 2007).

Logging should be carried out in accordance with national standards. Terminology used in the logs should be objectively defined e.g. strength descriptors should relate to specified strength value ranges.

Geological data should be presented in graphical form to highlight the similarity or variations in properties across the proposed mining area. Rock substance, strength and bedding or joint frequency can be plotted in histogram form along the borehole paths. Such plots are usually made with an exaggerated vertical scale to give adequate detail, but it is also important to plot natural scale sections to place the data into its actual physical context.

Geophysical Surveys and Logging

Geophysical surveys are usually undertaken for resource definition purposes. Airborne methods that are useful for coal exploration include gravity, resistivity, and magnetic surveys. For geotechnical purposes, such surveys are of limited value other than delineating igneous intrusions or the extent and potential depth of volcanic deposits. Ground-based surveys can be more specifically useful for fault delineation (resistivity or seismic techniques in 2D and 3D).

Geophysical logging is an essential part of coal exploration in relation to:

- minimizing time and expense by drilling open rather than cored boreholes, although a proportion of cored boreholes is still required to provide samples for analysis and testing,
- seam correlation, particularly in areas of complex sedimentology or in areas of structural disturbance,
- identification of lithology and sedimentary facies, and
- correlation with geotechnical parameters.

Emphasis has often been placed on delineation of coal plies and seams, using the calibrated density log. Other geophysical logs, including neutron, natural gamma, and caliper logs, also provide valuable data for geotechnical studies, including:

- correlation of non-coal strata and facies variations,
- tracing of claystone beds, which can be significant weak layers,
- identification of fault traces from hole width changes, and
- identification of saturated water level, which may not be the same as standing water level due to flows induced by drilling connections between layers of different permeabilities and pressures.

Sonic velocity (or its inverse, interval travel time) log can provide valuable data on rock substance strength when appropriate correlations are used. Although much less frequently used, neutron or density logs may provide strength correlations of equal or superior reliability (Elkington, Stouthamer & Brown 1982). Resistivity logs can provide additional information in lithology contrasts, and insights into groundwater flow regimes. Spontaneous potential logs are underutilised in coal exploration, but provide insights into

groundwater flow conditions and are more widely used for groundwater investigations.

It is highly desirable that the cored geotechnical boreholes be geophysically logged to provide a direct correlation between cores and the various logs. This information can then be used to extrapolate the data to open boreholes between the more widely spaced cored boreholes. Verticality logs should always be run in holes greater than about 50m depth to maintain depth accuracy because of inevitable departures caused by drilling through ground that is influenced by inclined bedding and jointing structures.

Acoustic scanner logs and dipmeter logs have gained widespread acceptance because they provide direct information on rock mass defect orientations. Vertical drillholes bias data collection to flatter seam, bedding, and sedimentary structure orientation rather than steeper joints or faults, which may be more relevant for excavation stability assessment.

At the BBS 2005, in the workshop conducted by Peter Hatherly, concerns were expressed that the coal industry did not have access to affordable software to process the large amounts of data being generated by the routine geophysical logging of boreholes. That situation has not changed in the ensuing five years.

Materials Testing

A basic program of materials testing is required to determine significant material properties and to confirm visual estimates made during core logging. Relevant testing for proposed strip mines includes:

- slaking and classification tests on weathered or suspected weak materials, which could influence spoil pile stability, and on likely pit floor materials for trafficability assessment,
- shear strength tests on soft or weak layers, particularly in the floor, and on overburden materials showing strong slaking behaviour, for use in analysis of spoil pile or wall stability, and
- compressive strength, point load strength and drillability tests to provide information for estimation of overburden excavation characteristics.

Seismic Refraction Traversing

Shallow seismic refraction traversing is a very convenient and rapid method of measuring *in situ* rock mass strength, with particular reference to excavation without blasting.

This information is particularly valuable when it is required to pre-strip ahead of the stripping fleet. To provide the best information, it is preferable to carry out ripping trials along the seismic traverse lines to provide a direct correlation between seismic velocity and rippability for the particular site. A generalised correlation for sedimentary rocks is given in Table 1.

Table 1: General correlation of seismic velocity with rippability for coal measures rocks (Caterpillar Inc., 2000)

Seismic Velocity	Strata Characteristics
Less than 1700m/s	Easily ripped by D9
1700–2000m/s	Rippable by D9
2000–2400m/s	Rippable by D10
2600–3100m/s	Rippable by D11R
Greater than 2400m/s, depending on rock type	Requires blasting

While it is often possible to rip materials with higher seismic velocities, though only with difficulty, it is rarely an economic proposition where large volumes are involved.

Groundwater Studies

Essential data for any assessment of the influence of groundwater on mining operations are:

- water levels across the proposed mining areas, and
- permeabilities of the various strata to be mined.

Water Levels

The first stage is to measure standing water levels in all available open boreholes. For this purpose, it is good practice to install PVC collar pipes in all exploration boreholes, to ensure that they remain open for water level measurement. It is also important to leave boreholes for at least 24 hours after drilling to ensure water level equilibration.

The water levels should be plotted and contoured to define the overall level and shape of the water table in the proposed mining area. Comparison of these levels with proposed pit floor levels will indicate to what extent mining will extend below the water table and at what stage groundwater problems could be expected to become evident.

Open hole water levels can show only a simple hydrostatic distribution of water pressure and cannot define any zones of higher or lower pressure in the strata. For this reason, piezometers should be installed in selected boreholes to check on actual pressure distributions to define any abnormal pressure zones. Particular attention should be paid to any obviously permeable zones, if present, which are likely to be subject to recharge.

Strata Permeability

The most complete information on strata permeability is obtained from full scale pumping tests, in which water is extracted from a borehole by pumping and drawdown is measured in a network of observation boreholes. Such tests can be analysed by standard techniques and *in situ* strata permeabilities determined. These data are then used to calculate groundwater inflows at various stages of mining, and the influence of water pressures on stability.

ACKNOWLEDGEMENTS

The authors are grateful to their colleagues and to their clients for their assistance in developing the ideas presented in this paper.

REFERENCES

- ATMAOUI, N. & others, 2006: Initiation and development of pull-apart basins with Riedel shear mechanisms: insights from scaled clay experiments. *International Journal of Earth Sciences*, **95**, 225–238.
- BACZYNSKI, N., 2000: STEPSIM4 Step-path method for slope risks. In *Proceedings of Geo Eng 2000 international conference on geotechnical and geological engineering*, 19–24 November 2000, Melbourne, **2**, 86 (and on CD).
- BOYD, G., KOMDEUR, W. & RICHARDS, B., 1978: Open strip pitwall instability at Goonyella mine — causes and effects. In *Proceedings of AusIMM conference, North Queensland*, 139–157.
- CATERPILLAR INCORPORATED, 2000: *Handbook of ripping — 12th edition*, Peoria, Illinois.
- COX, R. & DUNBAVAN, M., 1981: A study of the instability of a spoil pile in an open strip coal mine, Geomechanics of Coal Mining Report No. 23, CSIRO. Division of Applied Geomechanics, Melbourne.
- DIGHT, I. & BACZYNSKI, N., 2009: Rock bridges and their influence on slope stability. In *Proceedings of slope stability 2009*, Santiago.
- DUNBAVAN, M., 1980: Two-wedge stability analysis based on energy principles, Geomechanics of Coal Mining Report No. 17, CSIRO. Division of Applied Geomechanics, Melbourne.
- ELKINGTON, P., STOUTHAMER, P. & BROWN, J., 1982: Rock strength predictions from wireline logs, *International Journal of Rock Mechanics, Mining Sciences and Geotechnics Abstracts*, **19**, 91–97.
- GONANO, L., 1980: An integrated report on slope failure mechanisms at Goonyella — November 1976, Technical Report No. 114, CSIRO Division of Geomechanics, Melbourne.
- HAGAN, T., FRIDAY, R. & LEMBERG, D. 1981: Drilling and blasting to achieve lower costs for deeper stripping. In *Proceedings of AusIMM Symposium on Strip Mining — 45m and beyond*, Rockhampton, Queensland, 201–211.
- MAY, J., 1991: INSLOPE3: A computer code to analyse the effect of haulage truck operation on dump point stability: user's guide. US Bureau of Mines Information Circular IC 9291, 20.
- MORGENSTERN, N. & TCHALENKO, J., 1967: Microscopic structures in kaolin subjected to direct shear, *Géotechnique*, **17**, 309–328.
- ROSENGREN, K., 1981: Geotechnical investigations for new strip mines. In *Proceedings of AusIMM symposium on strip mining — 45m and beyond*, Rockhampton, Queensland, 11–23.
- ROSENGREN, K. & KREHULA, F., 1965: Earth Movements and Batter Stability in the Latrobe Valley Open Cuts. In *Proceedings*

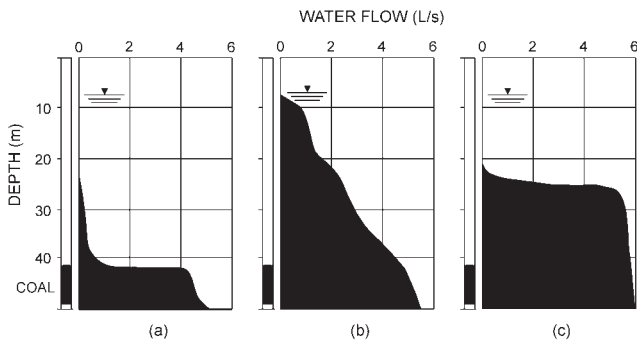


Figure 7. Typical air lift pumping profiles (Rosengren 1981)

Full scale tests are relatively time consuming and expensive and can usually be performed in only a small number of locations. For this reason, simpler index tests are used to cover larger areas. Common index tests are:

- air lift pump tests, and
- borehole packer tests.

Air lift pump tests utilise the air lift capability of a standard air flush rotary drill. The flow of water from a borehole at various depths is measured by a V-notch weir and the distribution of water flow with depth provides information on the relative permeabilities of the strata. Figure 7a shows virtually impermeable overburden and a highly permeable coal seam. Figure 7b shows uniformly permeable overburden and coal strata, and Figure 7c shows a high permeability fissure in the overburden.

Packer tests involve isolating a given section of borehole with inflatable packers and measuring the rate of intake to the section under a given pressure head, or the rate of head loss in a falling head test. Results of these semi-quantitative tests can be used to select the most representative sites for full scale pumping tests.

CONCLUSION

Geotechnical investigations are an integral part of any open pit mine feasibility study. They have particular importance to dragline stripping operations, since such operations are more generally sensitive to geotechnical factors than are most other forms of open pit mining. Such investigations give rise to design recommendations which are, in effect, the primary controls for mining risks to health and safety of personnel, reliability and availability of equipment, production rates and plans, and rehabilitation costs.

The basic program of geotechnical studies discussed above is based on experience from a large number of open pit coal mining studies and from actual experience in operating mines. It will give an overall appreciation of the geotechnical characteristics of a particular site and will highlight any specific problem areas which may require further, more detailed investigations.

- of eighth Commonwealth Mining and Metallurgical Congress, Australia and New Zealand*, **6**, 573–585.
- SIMMONS, J., 1995: Slope stability for open pit coal mining, *Australian Geomechanics*, No.29, 45–57.
- SIMMONS, J., 2000: Coal mine open pit geotechnical hazards – In-pit bench stability, safety training presentation.
- SIMMONS, J. & McMANUS, D., 2004: Shear strength framework for design of dumped spoil slopes for open pit coal mines. In, Jardine J., Potts, D. & Higgins, K., (Editors): *Advances in geotechnical engineering: proceedings of the Skempton conference*, March 2004, London, Thomas Telford Limited, **2**, 981–991.
- SLIWA, R., DEAN, P. & POROPAT, G., 2007: CoreProfiler — Tool for rapid and consistent capture of drill core observations, CSIRO Report No 2007/446 and accompanying software. ACARP Project No C15037.
- SULLIVAN, T., 2008: *Mining Warden Yallourn Mine Batter Failure Inquiry*. Victorian Government Printer.
- SCOTT, A. (Editor), 1996: *Open Pit Blast design Analysis and Optimisation*, Julius Kruttschnitt Mineral Research Centre Monograph Series in Mining and Mineral Processing, The University of Queensland.
- WALTON, G. & ATKINSON, T., 1978: Some geotechnical considerations in the planning of surface coal mines, *TransIMM Section A*, **87**, A147–A171.

A. Paul Maconochie, Philip Soole and John Simmons

Validation of a simple one person method for structural mapping using Sirovision

A simple, one-person digital photogrammetric method is described for mapping highwall structure using Sirovision software, without the need for detailed survey support. Comparative data are presented from the stand alone method and an alternative standard method supported by site based differential GPS positioning of camera locations. The results from the two methods are, for practical purposes, identical.

INTRODUCTION

Various laser and digital camera based photogrammetry systems are used in the Bowen Basin for geological mapping. Suppliers have often focussed on the spatial accuracy and precision of their systems. However, in many situations it is the speed of delivery of structural data and the ability for an operator to work completely independently in collecting orientated geological data of adequate accuracy that is of greater importance than locating the geological structures in 3D space with centimetre precision.

Sirovision enables a user to carry out structural mapping using survey controls provided by handheld GPS positioning of one reference camera position and taking an initial reference photograph in which the camera is set to be flat and level. No additional ground control points are needed. Thereafter, additional 3D models can be created by taking hand held stereo pair photographs that are aligned to the reference images. All that is needed for the hand held photographs is that a suitable baseline distance has been paced out between the camera locations so as to support 3D image creation and there is sufficient image overlap to create the 3D images.

Because of the convenience of the method and the speed with which results can be obtained it has been dubbed Stand Alone Sirovision.

This note describes the method and presents data obtained from recent mapping carried out using the stand alone method and a conventional method in which the camera locations or ground control points were defined using a site based differential GPS.

METHOD

When carrying out photogrammetric mapping of highwalls, there are various methods of providing georeferencing controls in the images to achieve sufficient spatial and geometric accuracy in the final 3D models. These methods generally require a minimum of three surveyed control points

within each image that forms part of a stereo pair. This will often require access to toes and crests of highwalls and survey support.

This note describes a technique that is available in Sirovision (2010) which allows a single person, using fully portable equipment, to quickly photograph and create 3D models of a highwall. The method is demonstrated to produce results that are well within the range of error that would be expected from traditional mapping methods or that would be required for structural analysis.

The equipment that is required for this method is:

- a digital SLR camera and fixed focal length lens: a Nikon D300 with an $f = 24$ mm lens were used in the work reported here,
- a sturdy tripod and head to capture the reference image: a Manfrotto model 074B tripod and model 405 head were used,
- a custom levelling base plate,
- a simple hand held GPS: a Garmin Etrex Summit GPS was used,
- a handheld compass: a Suunto compass was used,
- a laser range finder to measure the distance to the highwall: a Bushnell Yardage Pro Sport 450 model was used,
- a tape measure.

All of these items can be easily carried by one person.

The stand alone method involves creating one or more reference 3D models and then, through a process of software based image matching, daisy chaining additional 3D models aligned to the reference model(s). The additional models are based on stereo pair photographs that can be taken by hand. The only constraint is that there must be sufficient overlap and an appropriate baseline separation between each pair of photographs to create a 3D image from each stereo pair.

Field Procedure

An initial reference stereo pair of photographs is acquired. The first, conventionally the left, photograph is taken using a camera that is level in both elevation and tilt. Figure 1 shows a camera mounted on a custom plate that incorporates two spirit levels to achieve maximum levelling accuracy. Reliance on circular bubble levels as typically used on tripods and off-the-shelf levelling heads will introduce 1° to 3° inaccuracy which renders the stand alone method unusable.



Figure 1: Camera mounted on custom levelling plate

The photographs do not need to be taken perpendicular to the highwall. If the initial left hand photograph does not include the area of interest, then the line of sight of the camera can be elevated and a second photograph taken that does include the area of interest. An overlap of at least 30% in the two 3D images is required so that the software can accurately georeference the positions of all of the pixels in the second 3D image.

The position of the camera where the first image of the reference pair is acquired is measured using a handheld GPS typically with a positional accuracy in the horizontal plane of $\pm 5\text{m}$ based on satellite availability. Experience shows that the actual accuracy often is better than the value indicated by the GPS. Care is required to ensure that when recording eastings and northings or transferring them to other programs that the coordinate reference datum is known.

The direction of the camera is measured by taking a compass reading of the direction of the optical axis (the line of sight) of the camera. This is a critical measurement for application of the stand alone method and must be made with the best accuracy possible. Compass readings may need to be corrected for local magnetic declination. As a rule of thumb, in the Bowen Basin region this will usually mean adding between 5 and 12 degrees to the magnetic reading to obtain a reading relative to grid north.

The right hand image of the reference pair can be taken with a hand held camera but it is preferable to use a tripod. The distance between the left and right camera locations should be between $\frac{1}{6}$ and $\frac{1}{9}$ of the distance to the highwall as measured using the range finder. The distance between the two camera locations should be measured as accurately as possible and is best measured using a tape measure, properly tensioned. Using a tripod when taking the right hand image makes this measurement easier.

Subsequent stereo pairs of photographs can be taken by hand. Each pair should overlap with the previous pair by 30% to 40%. As with the reference stereo pair, the baseline separation should be between $\frac{1}{6}$ and $\frac{1}{9}$ of the distance to the highwall. It is sufficient to pace out the baseline.

In the work reported here the time required to take the reference photographs including all necessary measurements was 15 minutes. The time needed to take the additional 12 pairs of hand held photographs to cover 750 linear metres of highwall was an additional 20 minutes.

DATA PROCESSING

The field data was processed using the Sirovision version 4.1 software. A detailed description of the process is beyond the scope of this note. The methods used are described in detail in the Sirovision manual (CSIRO, 2010a).

Using field data always involves some overheads in data transfer and management but, including downloading the images from the camera, the first two 3D models, suitable for geological mapping were produced within 40 minutes of returning to the office. The complete, 750m long georeferenced 3D mosaic ready for structural mapping using the Sirojoint component of Sirovision was completed within 2 hours of creating the reference 3D image.

The data processing could have been carried out in the field within a similar period using a current, mid-level notebook computer.

RESULTS

Standard GPS versus differential GPS

To undertake the comparison reported here the camera position of the camera for the first image of the reference pair was obtained using a hand held GPS receiver and a differential GPS receiver. The results from each method used are shown in Table 1. The easting and northing values show only small differences that are less than the 'accuracy' indicated by the hand held GPS receiver. The elevation values are quite different. This arose because the particular hand held GPS used in this case calculates elevation from barometric pressure, and was not calibrated to a known height datum before deployment. However, errors in elevation have no impact on the calculated geometry of geological structures.

Table 1: Comparison of hand held and differential GPS location results for left hand reference camera

Method	Stand alone (m)	Differential (m)	Difference (m)
Easting	~605	~603.295	1.705
Northing	~749	~749.879	0.879
Elevation	379	433.543	54.543

Distance measurement from differential GPS versus tape measure

The distance between the left and right camera positions of the reference image pair was measured using the differential GPS and a fibreglass tape measure.

Table 2 shows the difference in the measurements of the baseline between the two camera locations used to take the photographs of the reference image pair.

Table 2: Comparison of measured distances using a tape measure and differential GPS

Method	Tape (m)	Differential GPS (m)	Difference (m)
Distance	15.35	15.38	0.03

Normally the tape measurement would be expected to show the greater distance as tapes sag. Tape stretch is one explanation for the observed difference, an error in the differential GPS measurement is another. Nevertheless, the apparent error is less than 0.2%. Such an error would have a negligible impact on the calculated dimensions of geological structures and does not affect the calculation of the orientation of structures.

Coordinate measurements from differential GPS versus Sirovision

Although not required, a second set of reference photographs was taken, approximately 157m NE from the first reference. The two camera positions were located using the differential GPS. Their positions were also calculated using Sirovision on the basis of the hand held measurements that were made when establishing the initial reference model. The results for the left hand camera position of reference set 2 are shown in Table 3.

The results show that there is a drift in the horizontal positional data as the distance from the reference model increases. The cause of this is inaccuracy in the compass measurement of the direction in which the initial left hand reference image was taken.

There are two ways to treat this error. The first is if there is a feature of known orientation then all the models can be transformed to align with the known feature. The second is to establish reference models every 100 to 200 m, as previously described, and to use them to pin the models created with the photographs taken with the hand held camera.

Table 3: Calculated and measured coordinates for reference position 2, left hand camera

	Sirovision	Diff GPS	Difference
E(m)	~733.382	~722.746	10.636
N(m)	~871.310	~853.019	18.291
EI(m)	431.001	430.859	0.142

No significant drift was observed in the elevation values. This is further evidence that the drift is due to inaccuracy in the initial reference model set up rather than any fundamental defect in the method.

Highwall Orientation

The highwall bearing and batter angle were measured on the reference model using the Sirojoint component of Sirovision (CSIRO, 2010b). The results were compared with the latest pit survey and mine design and the results are shown in Table 4.

The results are identical.

Table 4: Comparison of highwall bearing and batter angle obtained from Sirojoint and the mine survey

Method	Siro joint	Mine Survey	Difference
Bearing (°)	049	049	0
Batter angle (°)	70	70 (design)	0

Structural Measurements

Two prominent geological structures, shown in Figure 2, were measured for orientation. Three methods were used: Sirojoint based on a 3D model created using the stand alone method, a 3D model created using differential GPS generated data, and the estimate of one of the authors (JVS) based on his site observations and database built up over a number of years. The results are shown in Table 5.

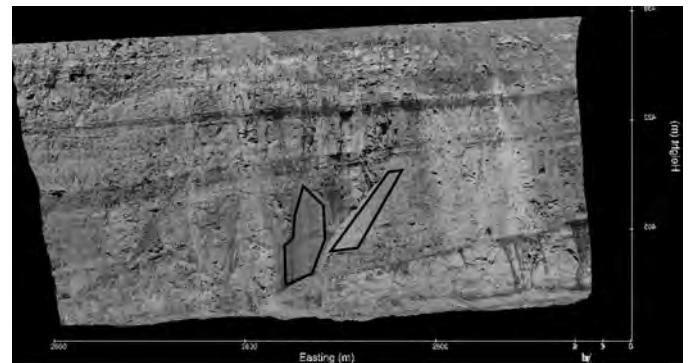


Figure 2: A 3D model of a section of the 45 m high highwall showing the two structures referred to in the text

Table 5: Orientation of selected geological structures using 3 different methods

Structure	Sirovision Stand alone	Sirovision Diff GPS	JVS
J1 D/DDN	87/293	86/294	82/283
J2 D/DDN	48/021	45/025	49/020
Intersection Plunge/Trend	46/021	45/020	42/009

D/DDN = dip/dip direction

The structural measurement results show that there is little practical difference in the calculated orientations for planes that were selected regardless of whether the survey data for the Sirovision models came from hand held tools or the differential GPS. It is also remarkable to note how close the field estimates of the orientations of the structures are to the Sirovision values. This is despite observing the required stand off from the highwall and the difficulties of measuring structural orientations from various viewing points.

It is recognised that the comparisons of location accuracies and structural orientations presented here are for a very small data set. However, they are typical of the results that the authors have obtained from using the stand alone method. It is expected that future work will demonstrate for larger data sets that the accuracy and repeatability obtained using the stand alone method is comparable to that obtainable by traditional face mapping techniques under field conditions.

CONCLUSIONS

The results of the work presented in this note demonstrate that a 750m long, 45m high highwall can be photographed in about an hour and all of the models processed within 3 hours ready for structural geological interpretation. This can be done by a single operator using hand held tools.

The accuracy of the orientations obtained using the hand held tools is comparable to results obtained when a differential

GPS is used to establish camera positions. It is judged that the accuracy is well within what can be obtained in the field using tape and compass, particularly given exclusion zone and access restrictions that are mandatory in Australian open cut coal mines. The work reported provides validation of a rapid method for measuring structure where the spatial position of the structures is not critical enough to require the accuracy of a differential GPS unit. The orientation and spacing of structures can be obtained by the stand alone method with the accuracy required to undertake meaningful geotechnical analysis of the structures.

ACKNOWLEDGEMENTS

The authors acknowledge the support and permission of the mine owner and operator in preparing and presenting this technical note.

The authors also acknowledge Dr Bruce Hobbs and Dr Alison Ord, formerly of the CSIRO, who, 20 years ago, had the vision for a fully portable geological mapping system. This technical note documents that the current Sirovision team has developed such a tool and that it is accurate enough for all practical purposes.

REFERENCES

- CSIRO, 2010a: Siro3D Sirovision 3D Imaging Mapping System Manual Version 4.1.
- CSIRO, 2010b: Sirojoint Sirovision structural mapping and analysis system – User manual Version 4.1, CSIRO.

Duncan Thomson

Imaging systems for geotechnical boreholes – Slim Borehole Scanner

The Slim Borehole Scanner (SBS) is a useful tool for enhancing the capability of Australian underground mine operators to assess roof conditions. The SBS is a significant advance on existing qualitative assessment methods such as the Borescope, and is complementary to existing direct measurement methods such as Tel-tales and Gel-extensometers.

The system can be easily deployed by 1-2 individuals and is best applied on a discretionary basis by geotechnical engineers as an investigative tool. A clear advantage of the SBS is the ability to develop a database of roof conditions in digital form that can easily be contrasted and compared between sites and over time.

The SBS could provide a useful aid to the implementation of the CMRR system through the provision of reliable fracture intensity data.

The use of the SBS system is likely to deliver the following benefits to the Australian underground coal industry.

- Improved means of carrying out quantitative analysis of roof behaviour;
- Improved understanding of roof properties and changes through time;
- Advance notice of potential roof stability issues;
- Reduced risk of unexpected gateroad failure; and
- Provide an objective digital record of roof properties.

The SBS system is currently available in Australia, and is planned to undergo intrinsic safety approval in late 2010. Once approved, this tool should be adopted as a routine part of the geotechnical engineer's arsenal in assessing roof control issues in Australian mines.

INTRODUCTION

An optical imaging system for geotechnical boreholes (Figure 1) has been developed in Germany by Deutsche Montan Technologie (DMT). It is called the Slim Borehole Scanner (SBS), previously known as the Anchor Borehole System (ABS). This enables optical scanning and imaging of a borehole, similar to that of a televiewer. The system is Intrinsically Safe (IS) in Germany. It is the only IS imaging system suitable for use in underground coal mines and is therefore fundamentally different to other commercially available imaging tools used in exploration boreholes. The SBS has the following key features:



Figure 1: The digital video module of the SBS system.

- 23mm diameter, length 120cm;
- 360° optical scanning in short and slim drill holes;
- Digital image storage;
- Oriented acquisition of fractures;
- Multiple monitoring tool to detect fracture widths; and
- Software for quantitative analysis.

The physical investigation of roof strata through geotechnical logging has been actively pursued in the mining industry for many years. The purpose of geotechnical investigations for underground mines is to identify and compile a proper record of those parameters that are most likely to influence the stability of a particular roadway. Parameters of interest when collecting detailed geotechnical data include chemical, geological and physical properties of rock (including structural features).

Current tools commonly used to identify geotechnical properties include borescopes, tell-tales, gel and sonic extensometers. The DMT SBS tool is a direct replacement for some of these tools.

CURRENT PRACTICE

Current Status of Geotechnical Logging

Tools used to establish the physical parameters of roof lithologies are broadly categorised as 'geotechnical logging tools'. Standard tools for the Australian underground coal mining industry include borescopes, tell-tales, GEL

extensometer and the sonic extensometer; the purpose of each is outlined below:

Borescope – The borescope is a tubular periscope. Typically a 27mm or 28mm hole is drilled to a depth of 6m to allow for the insertion of the flexible coaxial cable attached to a viewing area. This viewing area offers a 360 degree view of the varying levels in the strata. The borescope light cannot penetrate past its immediate surroundings so therefore it will not illuminate the cracks and fissures. This means that displacements in the lithologies are observed as ‘black’ areas. Measurements of these displacements can be combined with the known lithologies to create borescope plots.

Unfortunately, borescope data is subjective and somewhat laborious. It relies heavily on the skill and observational integrity of the user. The subjectivity of borescopes is the main shortcoming of this geotechnical tool. With no scale shown for reference in the viewing window, the size of cracks and fissures is often overestimated or exaggerated.

Other disadvantages include:

- a small viewing area;
- limited borehole depth;
- fragility of the coaxial cable; and
- cumbersome operation.

The introduction of camera borescope tools (such as the ‘SeeSnake’) has been successfully trialed at several mines in Australia. This tool is a significant improvement to the traditional borescope methods; however, it still does not offer the imaging capability or data manipulation of the SBS.

Tell-tales – A simple means of assessing the integrity of the immediate roof horizon. Tell-tales measure movement in two horizons to an accuracy of $\pm 2\text{mm}$ (Figure 2). Tell-tales are the most common form of monitoring devices in use in Australian underground mines. As a standard, routine instrumentation in a mine consists primarily of tell-tales installed at each intersection during development.

- Tell-tales have a clear advantage over all other current forms of geotechnical logging. They are:
- Low cost – Tell-tales typically cost $< \$150$ each. This is relatively inexpensive when compared to other geotechnical logging tools.



Figure 2. Tell-tale unit.

- Easy installation – Tell-tales are fast and simple to install. They are installed from the continuous miner. This is convenient, safe and efficient.
- Data quality is high – An accuracy of $\pm 2\text{mm}$
- Instant visual readings – Tell-tales have a visual display that allows for the crew at the face to identify changes quickly without needing to confer with other parties.
- Due to the advantages outlined above, it is likely that tell-tales will always be the frontline geotechnical logging tool that is used as a benchmark to determine what future action is required. This future action may include the introduction of other tools to provide additional data.

Gel Extensometer – An advanced version of tell-tales; gel extensometers offer more accurate and detailed measurements through the use of five electronic anchors. Gel extensometers are typically installed to supplement information obtained from tell-tales.

Sonic Extensometer – The sonic extensometer uses a flexible sonic probe constructed in the form of a wand that is inserted into the access tube of a prepared hole. An electronic pulse in the head of the probe drives current up the length of the wand. Interaction with the field produced by the magnet induces a signal that travels back to the head in a wave guide. This acoustic signal is converted into an electrical signal and the time between pulses resolves the differences in position of the anchors, effectively allowing for inter-anchor displacement readings. The readout box displays these displacements and all the data is recorded and added to a database to produce appropriate plots (Figure 3).

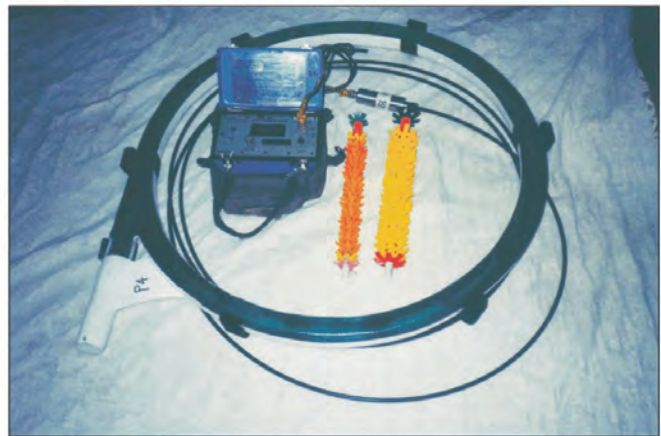


Figure 3: A sonic extensometer, anchors and readout box.

The advantage of the sonic probe over all other current geotechnical logging tools is the ability to have up to 20 anchors per hole, giving extremely high accuracy and sensitivity. However, like borescopes, the flexible probe makes this tool expensive, fragile and cumbersome.

The Slim Borehole Scanner (SBS)

The SBS (Figure 4) provides a digital image of the borehole wall. This provides objective information that can be used for future comparative purposes, and provide a permanent digital



Figure 4: The digital video module of the SBS. A schematic of the tool appears above the main image.

record of roof conditions at any point in time. The images can be orientated in 3-D and provide the basis for structural analysis of bedding, joints and faults. The images can be further assessed using advanced software developed by DMT (SBS-Vision, Figure 5).

The SBS is 23mm in diameter and thereby useful for most bolt holes used in Australian mining. The probe is 120cm in length, and can be extended indefinitely into the roof using PVC conduit on a reel or progressively joined. The limitation is the level of physical comfort of the operator. From the work carried out in Australian mining operations, images to 6m depth were performed without difficulty.

The unit has 360° optical scanning capability in short and slim drill hole, and can be orientated. It is therefore possible to determine the strike and dip of oblique features intersecting the borehole wall. This information is stored digitally, and can be further reviewed using the visual optimisation software that accompanies the tool.

The tool is lightweight and mobile. One person can carry the unit in a case that is light and portable. Two personnel are preferred for the operational procedure but it is physically possible for it to be done by one individual.

The SBS is approved in Germany for use in their mines, and is therefore designed to be intrinsically safe (Ex I M1 EEx ia D). It is planned that the SBS system undergoes intrinsic safety approval in Australia in late 2010.

The chief advantages of using the SBS system, relative to existing competitors available to the Australian coal industry is the objectivity of the measured results and the suitability of these digital images for permanent record and comparative purposes. It will be possible to use these images for forensic analysis of failed roof intersections, and thereby improve general understanding of failure mechanisms and likely ways to avoid a repeat in the future (leading to an optimisation of borehole spacing and length). Repeated observations in the same borehole are likely to provide the opportunity for time based analysis of deformation (for example, see Figure 6). The character of digital image storage implies that it will be possible to review and reinterpret the data at any time.

APPLICATIONS FOR THIS TOOL – PRACTICAL DEPLOYMENT

The obvious applications for the SBS tool include:

- An objective means of detecting changes in fracture partings over time.
- Lithological identification of roof material.
- Providing a means of investigating roof strata using advanced visualisation tools.

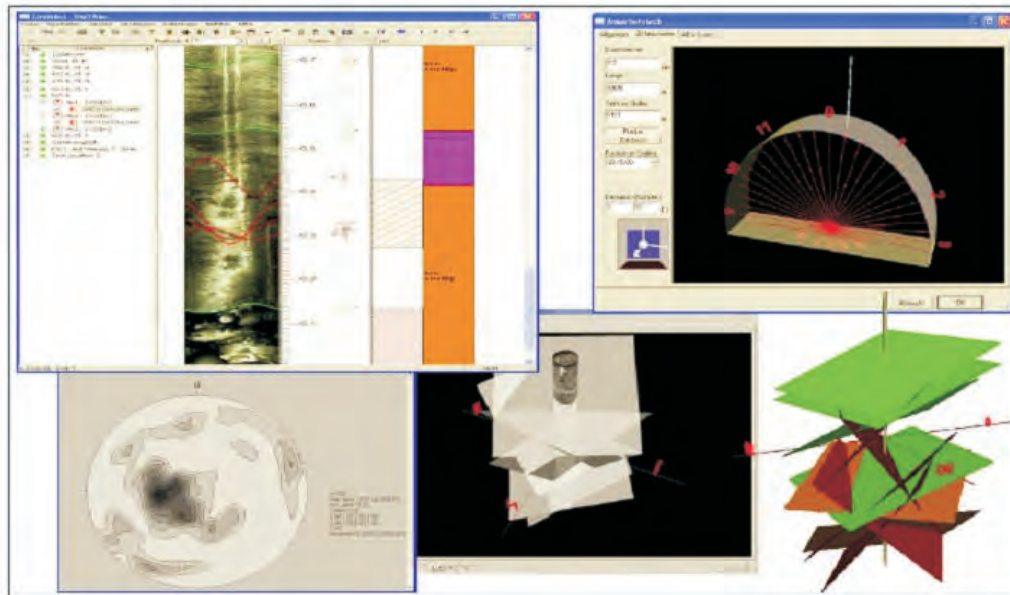


Figure 5: Examples of the detailed visual analysis and presentation possible using imaging software associated with the SBS.

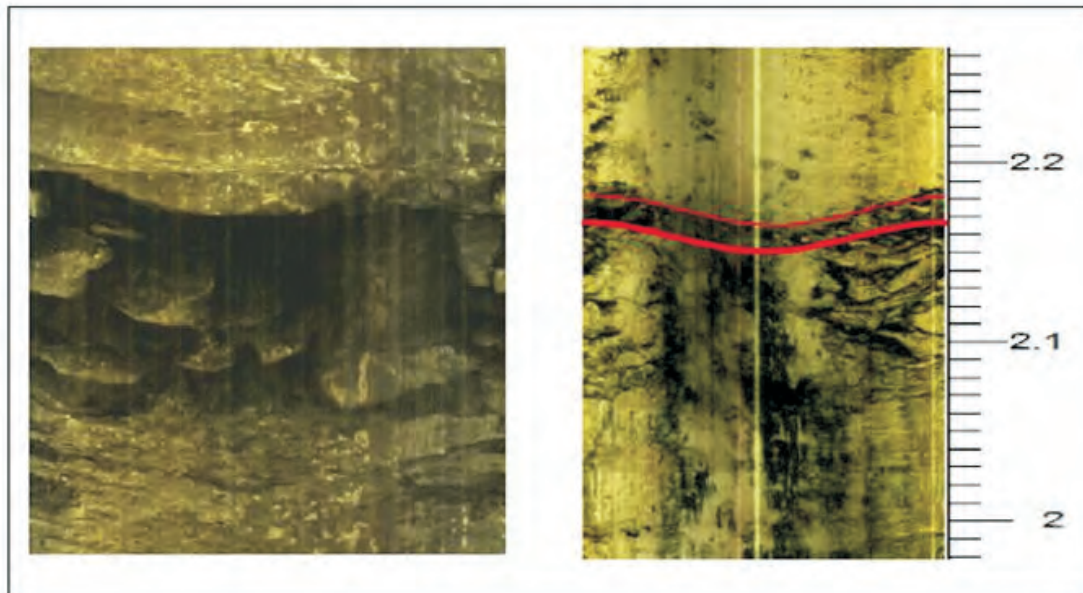


Figure 6: Examples of a parting, or shatter zone in a roof borehole.

INTEGRATION OF SBS WITH CMRR SYSTEMS

The Coal Mine Roof Rating (CMRR) is a roof classification system that was first introduced to the mining community in 1994. The CMRR system was designed to evaluate the properties of the coal mine roof rock mass which contribute to its weakness and convert them into a relative strength rating from 0-100. These properties include the cohesion and frequency of discontinuities like bedding, slips, shears, and joints, UCS, and moisture sensitivity. With simple laboratory and field tests and observation, the CMRR can be calculated by technical and operating personnel with a minimum of training.

The SBS system can complement the CMRR classification process by providing greater confidence in the reporting of fracture spacing variation. Coupled with physical measurements from core (UCS, Point Load tests), the SBS tool should improve CMRR standards at operating mine sites.

CONCLUSIONS

The SBS is a useful tool for enhancing the capability of Australian underground mine operators to assess roof conditions. The SBS is a significant advance on existing qualitative assessment methods such as the Borescope, and is complementary to existing direct measurement methods such as Tel-tales and Gel-extensometers.

A clear advantage of the SBS is the ability to develop a database of roof conditions in digital form that can easily be contrasted and compared between sites and over time.

The SBS could provide a useful aid to the implementation of the CMRR system through the provision of reliable fracture intensity data.

The tool is light, mobile, robust and practical and is immediately useful to Australian mining operations. It is anticipated that the SBS will become a routine part of the geotechnical engineer's arsenal in assessing roof control issues in Australian mines.

Currently, the SBS system is available in Australia, and is planned to undergo intrinsic safety approval in late 2010.

ACKNOWLEDGEMENTS

The availability of the SBS in Australia has been achieved thanks to an ACARP funded project carried out by CRC Mining.

REFERENCES

- HATHERLY, P., MEDHURST, T. & MCGREGOR, S., 2008: Geophysical Strata Rating, ACARP Project C15019, Final Report, July 2008.
- MARK, C., MOLINDA, G. & BARTON, M., 2002: New developments with the coal mine roof rating. *In: Peng, S.S., Mark, C., Khair., A.W. & Heasley, K.A., (Editors): Proceedings of the 21st International Conference on Ground Control in Mining. Morgantown, WV: West Virginia University, August 2002, 294–301.*
- MOLINDA, G. & MARK, C., 1993: The Coal Mine Roof Rating (CMRR)—A Practical Rock Mass Classification for Coal Mines. *In Proceedings, 12th International Conference on Ground Control in Mining, Morgantown, WV, 1993, 92–104.*
- MOLINDA, G. & MARK, C., 1994: *The Coal Mine Roof Rating (CMRR)—A Practical Rock Mass Classification for Coal Mines.* USBM IC 9387, 83 pages.
- THOMSON, S. & ADAM, S., 2009: Imaging Systems for Geotechnical Boreholes, ACARP Project C16019, Final Report, 2009.

Christopher Harding, German Hernandez and Michael Fleming

A geological solution at Cerrejón, Colombia

Carbones del Cerrejón Limited (Cerrejón) operates one of the world's largest open-pit coal mines with a deposit spread over a strike length of 50 kilometres. The coal deposit contains up to 175 coal seams with a cumulative thickness of approximately 100 metres and extends over an area of approximately 300 square kilometres. The Cerrejón Formation is Tertiary (Late Paleocene) in age and is a paralic siliciclastic unit in the confluence of the Cocos, South American and Caribbean plates. The entire sequence is approximately 1,000 metres thick, exposed along a southeast-dipping (18° on average) folded and thrust faulted monocline. Total coal resources are approximately five billion tons with average *in situ* qualities of 11 846Btu/lb heat content, 3.7% Ash, 0.5% Sulphur and 34% Volatile Matter. Cerrejón's mining fleet comprises 30 shovels and more than 220 haul trucks removing approximately 244 million cubic meters of waste and 32 million tons of export coal per annum. Due to the large scale, structurally complex coal deposit, Cerrejón's greatest challenge is to mine the coal seams safely and in harmony with the environment and the surrounding communities, whilst optimizing coal recovery.

The Geology Department at Cerrejón consists of 14 geologists, who provide multiple services that range from exploration through geological drilling and geophysics, modeling, daily mine operation support, resource estimation, and long-term planning. Among other activities, the field geologists use hand-held GPS units to map the geological features exposed by each mining bench and acquire a wide range of data to aid in the structural interpretation and support to mining operations. This data includes: seam roof and floor traces; seam thickness; structural observations including strata dip and strike, fault planes and fold characteristics. This data is stored, processed and analyzed in a Geographical Information System (GIS) package, generating high precision 2-D micromodels, updated and utilized daily in conjunction with geological sections and under-seam blast hole information. As a measure of coal recovery performance, a detailed coal reconciliation exercise is carried out monthly; measuring the mining parameters and Run-of-Mine (ROM) coal recovery achieved versus the geological model in-situ predictions. Field experiments carried out under the supervision of the Geology Department are regularly performed to identify and address any short-falls in the coal recovery process.

Micromodel maps produced on a daily basis providing up to date, actual stratigraphic and structural conditions in the operating pits, are used by the field geologists for structural support and by the coal mining supervisors. An additional function of the micromodel maps is to project seam traces into the advancing benches, allowing for improved weekly planning and minimisation of coal losses due to incorrect loading positions. Since 2006, the total

coal recovery at Cerrejón (actual production vs. geological model) has improved steadily from 84% to over 94% in 2009, culminating in a 2010 target recovery of 95% for all coal seams irrespective of pit depth and seam structure complexity. The in-pit stakes experiment showed an average seam head loss of 45 centimeters irrespective of mining height, with some variations per operating pit. This and other experiment findings have led to the further improvement of the coal mining procedures used during operations and the continuing quest for increased coal seam recovery.

Keywords: cerrejón; reconciliation; recovery; macromodel; micromodel; stakes experiment.

INTRODUCTION

Carbones del Cerrejón Limited (Cerrejón) is Colombia's largest mining operation, and one of the largest open-pit coal mines in the world. Cerrejón is a privately-owned, equally participated Joint Venture between Anglo American PLC, BHP Billiton and Xstrata Coal. The mine currently employs 5120 permanent staff and more than 4000 contractors. The operation has an established infrastructure system capable of transporting approximately 133 000 passengers per month between the mine, the mine residential village and the surrounding towns via bus. Additionally, the company transports by air some 7330 passengers monthly between Barranquilla, Bogotá, the Mine and Puerto Bolivar. The company also has housing facilities in the private mine village of Mushaisa, which includes an internationally recognized school, medical and recreational facilities.

A brief history

The current Cerrejón coal mining operation is the result of a number of exploration programs, mining ventures and amalgamations. In 1983, Carbocol (the government coal mining agency, Carbones de Colombia) and Exxon, in an equal joint venture known as Intercor (International Colombia Resources), commenced mining in the North Zone. In 1997, a joint venture was created between Anglo American PLC, Glencore International AG and Rio Tinto (operating as CdelC) to mine the Comunidad and Oreganal leases in the Central Zone. BHP Billiton acquired the interest in CdelC previously owned by Rio Tinto in 2000. The South Zone was successfully bid for by CdelC in December 1997. The CdelC Consortium acquired Carbocol's 50% interest of Intercor in July 2001. Intercor successfully bid for the adjacent Patilla Norte lease from Carbocol shortly before the Consortium acquired the remaining 50% share of Intercor from Exxon in February 2002. This final integration created Cerrejón as it exists today.

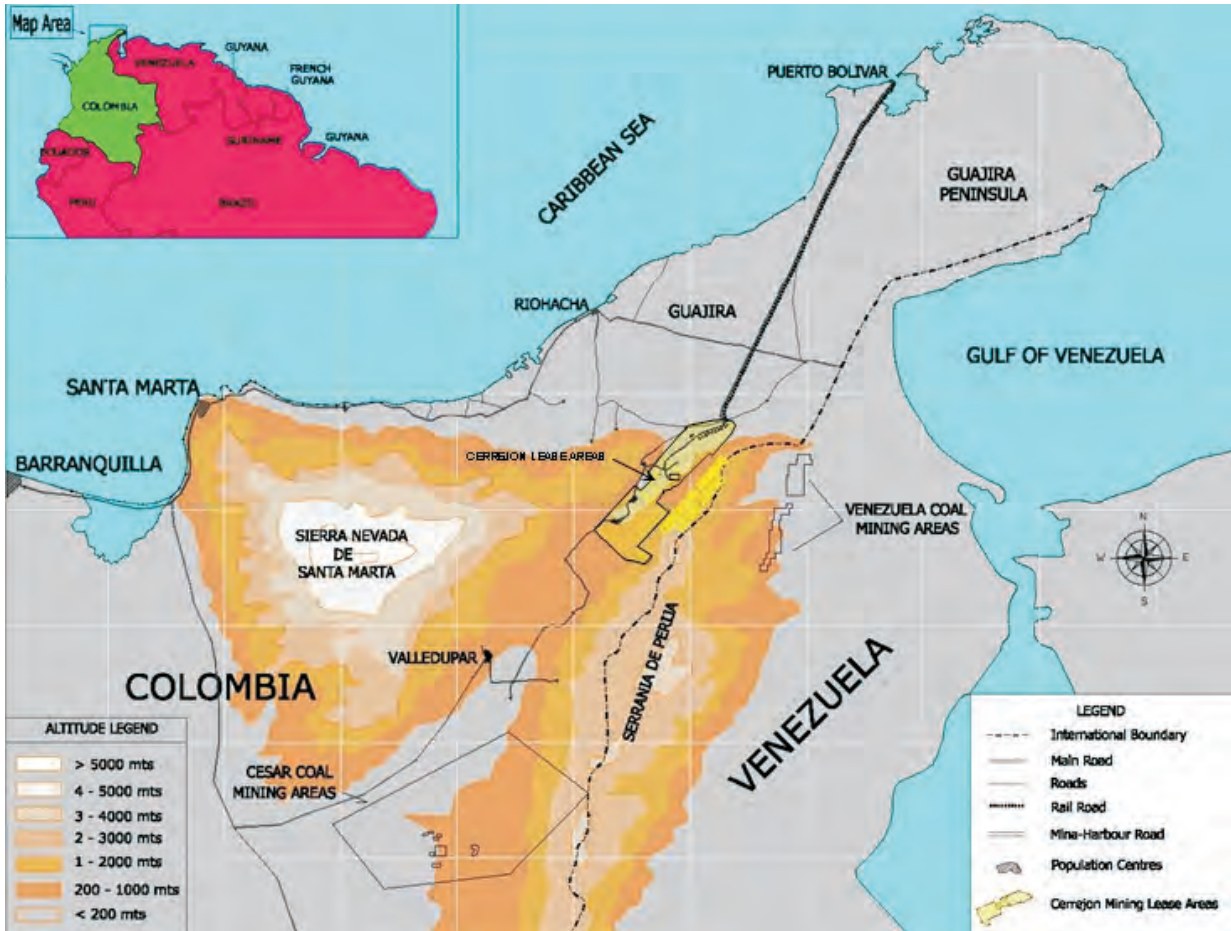


Figure 1: Location map of Carbones del Cerrejón in La Guajira Department, Colombia.

Location

Cerrejón is situated in the La Guajira Department in northern Colombia, South America (refer to Figure 1), approximately 980 kilometres north of the capital city Bogotá. It is adjacent to the Venezuelan border and occurs within the municipalities of Barrancas, Fonseca, Hato Nuevo and Albania.

The coal deposit extends over a strike length of 50 kilometres and covers an area of approximately 300 square kilometres. The Cerrejón lease area is made up of three discrete zones: North, Central and South (Figure 2).

The North Zone is situated north of the Rancheria Fault and includes the active Tabaco, Puente, and Patilla mining pits as well as the inactive Expanded West Pit (EWP). The Central

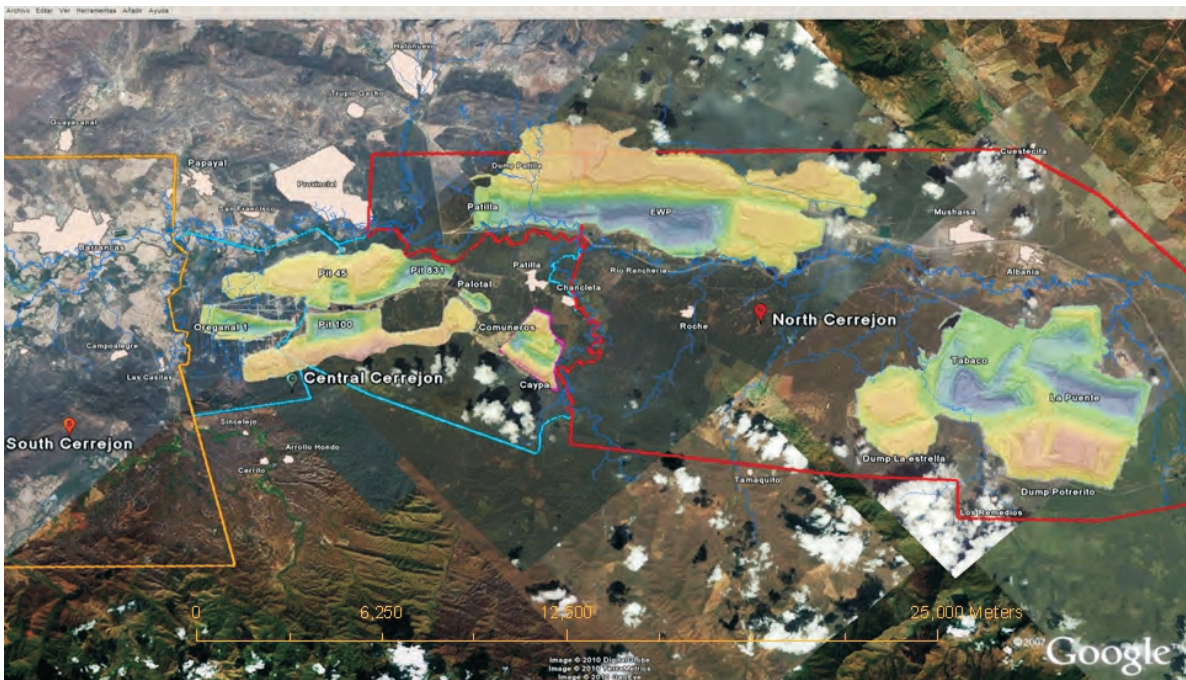


Figure 2: Active mining pits and waste dumps at Cerrejón, as at the end of 2009.

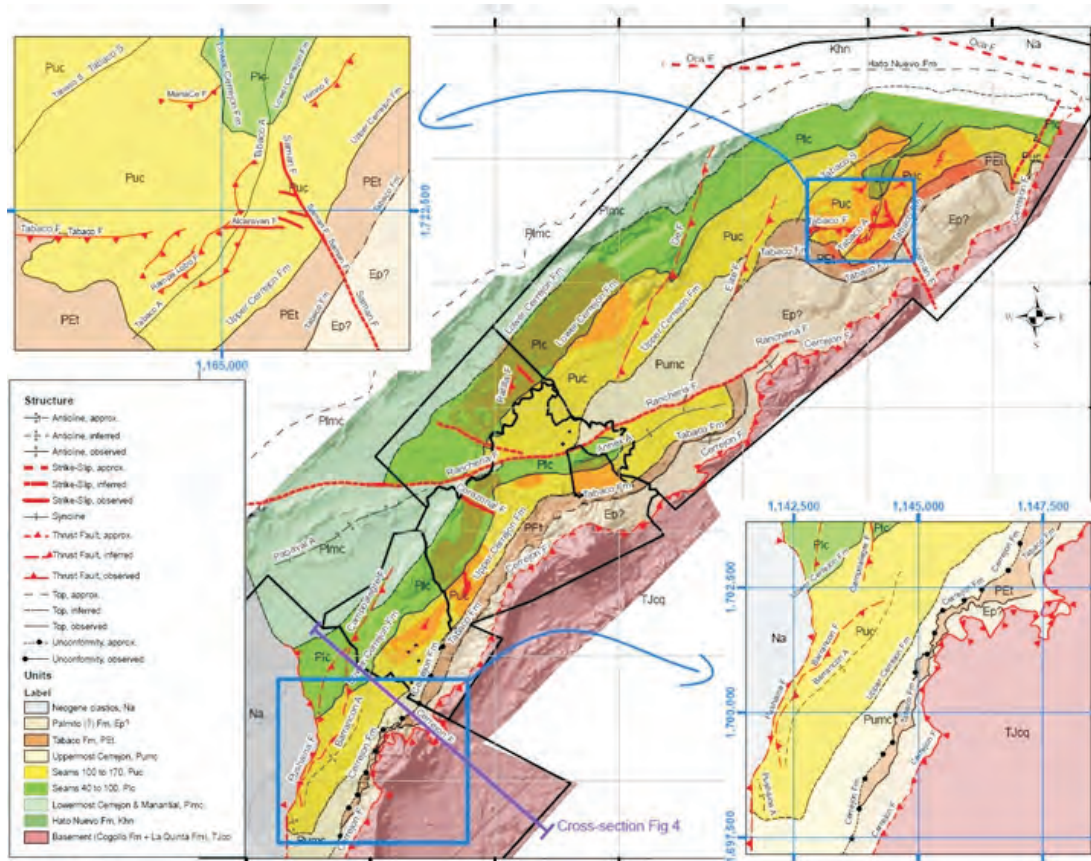


Figure 3: Regional geological setting of the Cerrejón coal deposit, with some of the major thrust-slip faulting indicated on the map. Including the Oca Fault, the Cerrejón Thrust Fault and the Rancheria Fault.

Zone comprises Pit 100, Comuneros and Oreganal mining pits. The South Zone comprises the undeveloped Campo Alegre and Conejo deposits south of Palomino Creek.

Regional geology

The mine operates in an overall southeast-dipping monocline crossed by thrust and strike-slip faults oblique to its strike. The deposit is bound to the north by the right-lateral Oca Fault and to the southeast by the northwest-verging Cerrejón Thrust Fault. Both faults are crustal-scale tectonic structures (Figure 3). The coal seams continue for at least six kilometers beneath the Perijá Range up to the footwall cut-off of the Cerrejón Thrust Fault. Structural deformation in the Cerrejón lease area is mostly brittle and related to the regional emplacement of the Cerrejón thrust sheet (Figure 4).

Three major faults that define the coal deposit are the Rancheria Fault, the Oca Fault and the Cerrejón Thrust Fault (Figure 3). The Rancheria Fault duplicates the deposit, and is a left-lateral strike-slip fault with a horizontal displacement of over five kilometres. The Oca Fault is part of the southern Caribbean deform belt and is an east-west trending fault. The Cerrejón Fault is a crustal scale thrust structure, which thrusts rocks of Cretaceous age onto Paleocene-Eocene rocks and defines the edge of the Perijá Mountains.

Various other large-scale thrust fault systems have been recognized during exploration and in-pit geological mapping, and include the following: the Campoalegre fault system; D Fault; East Fault; Tabaco Fault; Rampa Lobo; and the La

Chapa thrust fault systems. Major strike-slip faults include the Corazonal, Pit 100 and Samán strike-slip faults.

Stratigraphy

The coal-bearing Cerrejón Formation is a siliciclastic unit of late Paleocene age approximately 1,000 meters thick and continuous for over 50 kilometres along the strike in the northern part of the Rancheria River valley (Figure 5). The Formation accumulated in an oscillating paralic environment under very high precipitation (approximately 300cm/yr), and a tropical climate (Cerrejón Expansion to 40mtpa, 2009.). This thick and compositionally immature clastic sequence records an overall regressive cycle that starts with Late Cretaceous carbonate platform rocks and culminates with the fluvial sandstone and conglomerate of the Late Paleocene-Eocene Tabaco Formation. The Cerrejón Formation has been dated at 58 million years and accumulated over a period of approximately two million years. It contains up to 175 coal seams with a cumulative thickness of approximately 100 metres.

Coal seams are correlated and named sequentially from bottom to top, with the major seams occupying the multiples of five, and minor seams, or splits occupying the available spots in-between. Even though only 49 major coal seams are modeled, more than 100 coal horizons occur in the entire thickness of this unit. Total coal thickness in the stratigraphic column is about 100 metres, with seam thickness ranging from less than one metre to greater than 10 metres. The interval that contains the bulk of the economic coal extends

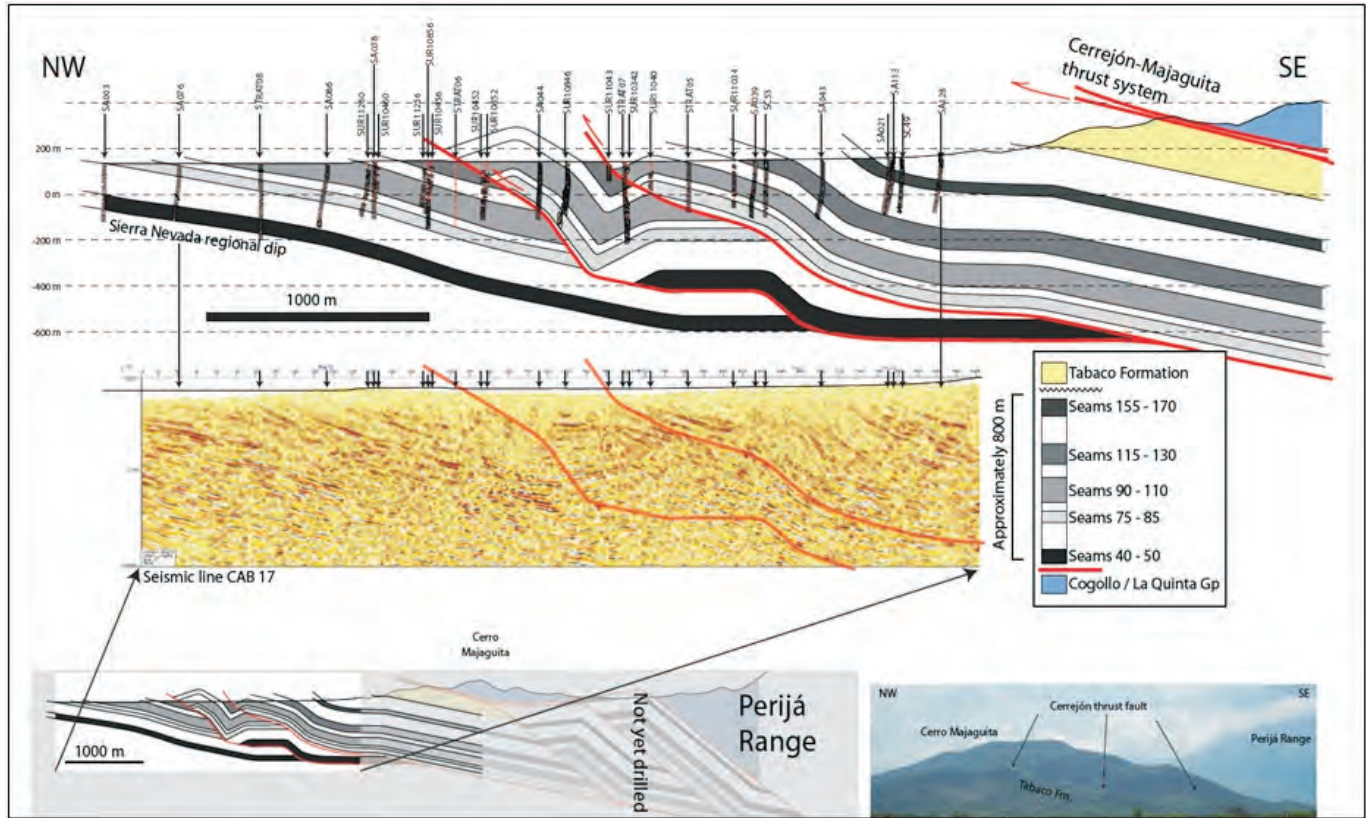


Figure 4: Interpreted cross-section through the Cerrejón deposit.

from Seam 40 (basal) up to Seam 183. The ‘bachelor zone’ is a 60 metre thick, stratigraphic interval, between Seams 80 and 100 where the coal seams are relatively thin (cumulative coal thickness ~3.5 metres) and consequently lead to high stripping ratios. This bachelor zone separates the Cerrejón Formation into the upper (Seams 100 to 183) and lower (Seams 40 to 80) open cut zones.

Resources and coal quality

Total coal resources within the shell have been estimated at 4.9 billion tons (Hernandez, unpublished). Coal reserves are estimated at 744 million tons within the 32 million-ton-per-annum practical pit mining shell.

The coal seams in the Cerrejón deposit are very uniform in terms of quality. In-situ ash content is 3.7% on average, with seam to seam variation related to thickness. Total moisture increases systematically upwards in the stratigraphy and from north to south in the coal deposit. On average, the *in situ* total moisture is 12.9%. Consequently, there is a general decrease in inherent Calorific Value (CV) and increase in Volatile Matter as the total moisture increases. *In situ* average CV for the deposits is 11 846Btu/lb.

Mining Method

Cerrejón is an open-pit mine, with six pits currently in production; Tabaco, Puente, Patilla, Pit 100, Oreganal and Comuneros (Figure 2). Cerrejón's mining fleet, one of the largest in the world, comprises over 30 shovels and more than 220 haul trucks, which haul on average 650 000 cubic meters

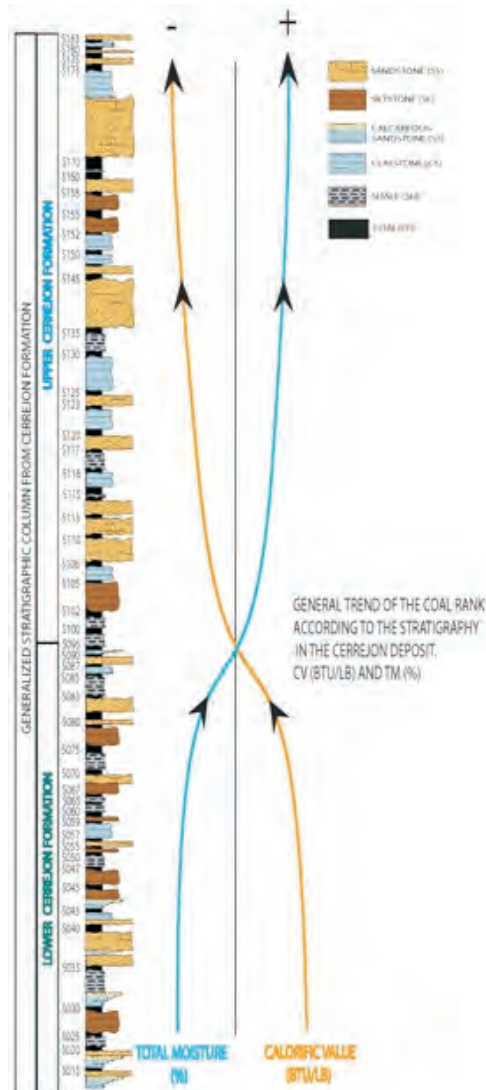


Figure 5: Stratigraphic column of the Cerrejón Formation.



Figure 6: A series of photographs of the main components at Cerrejón. A: Mining operations, B: Coal transportation via Train, and C: Ship loading at Puerto Bolívar.

of waste material and 88 000 tons of coal every day. Annually, production levels of 244 million cubic metres of waste and 32 million tons of coal are achieved. This accounts for almost half of Colombia's annual coal exports (Key World Energy Statistics, 2009).

The mining process starts with the removal and storage of the topsoil layer; whenever possible it is taken directly to its final location in the rehabilitation areas. Fortich (2008) contends that the under-seam blasting method, used since 1989, aims to fragment the waste material located above and below the dipping seams in a single operation. The waste material is loaded by electrical rope shovels and electrical or diesel hydraulic shovels in 10 meter benches. Mechanical Caterpillar 793 trucks and electrical Euclid Hitachi 5000 trucks are used for the waste hauling.

According to the Coal Mining Operating Procedure (2010) at Cerrejón, the mining of a coal seam should be done safely and without risk to the operation, avoiding losses of volume and quality of coal by addition of out-of-seam contamination or

water. Therefore, it is the responsibility of the coal mining supervisor to mark in the pit, with fluorescent orange-colored stakes, all the parameters or limits to ensure clean coal mining (such as the dimensions of the waste and coal safety buffers). The coal seam head should be defined throughout the block, where cleaning is done along strike and coal stockpiled to be mined later as plant feed. In order to minimize losses of coal during the seam roof cleaning stage, track dozers or a Liebherr long boom excavator ('giraffe') in seams with dip $>25^\circ$ are used.

During waste material removal, approximately eight centimetres, 5cm and 3cm in the seam roof and floor respectively, of material comprised of a mixture of coal and waste is mined separately as 'interface' coal and sent to the coal wash plant. In addition, high-ash coal zones are identified and mined separately for plant feed material. The plant is used to de-stone approximately 3.3Mt of feed per year.

The clean coal is loaded predominantly by front-end loaders into Caterpillar 789 trucks. The majority of the clean coal,

upwards of 65%, is loaded and transported directly from the pits to main crushing plants and then conveyed into the train loading silos. The remaining clean coal is placed onto raw coal stockpiles and the interface coal is sent to the wash plant feed stockpiles.

All of the production is exported with only minimal beneficiation, with three main products ranging in Calorific Value from 10 600Btu/lb to 11,300Btu/lb exported to customers. Cerrejón transports the coal on a 150 kilometer long railway to a dedicated port facility, Puerto Bolivar, both of which are owned by Cerrejón. The mine operates five coal transportation train sets, each pulling between 88 and 125 wagons of 110 tons each (Figure 6). The port facilities are capable of loading ships of up to 175 000 ton capacity.

METHODS — GEOLOGICAL FUNCTIONS

The geology department within Technical Services at Cerrejón consists of 14 geologists grouped into three sub-sections: Exploration, Modeling and Mine Geology. Through the work of these sections, the geology group aims to provide a quality service to both internal customers within the Technical Services group, and external customers such as the production and coal quality departments. These services are core to solving the problems of high production mining on a massive scale in a structurally complex geological environment.

Exploration

Cerrejón has a long history of exploration activity (Figure 7), and since 1976, has utilized both open and core borehole diamond drilling techniques, supported by down hole geophysical wireline logging. Drilling depth has increased

substantially from an average of 200-300 metre depth holes in the 70s and 80s to over 500 metres in depth in the current drilling programs. In 2009, over 25 000 metres of open and cored boreholes were drilled and logged using geophysics by in-house personnel as well as contractors. Geological drilling and exploration standard procedures include logging and detailed core descriptions and core photography. Top and bottom coal seam contacts are identified with the aid of the geophysical logs. Non-core drill hole coal intersections are also picked using the suite of down-hole geophysical logs which include caliper, temperature, survey/borehole deviation, gamma, density and dip-meter.

Geological Computer Modeling

The current modeling methodology consists of measuring the roof and floor depth from geophysical logs, and the assignment of a seam name. This correlation is empirical and based on marker seams or groups of seams that have been demonstrated to be relatively continuous. Once the sequence has been established, the information is loaded into a geological database and fed into the geological modeling software (Minex) and a model is generated. The geological model is locally referred to as a macromodel as, due to its size and complexity, the model incorporates macro scale geological features and geological drilling such as the major faults systems, base of weathering and clinker areas. The geological database currently contains more than 7000 boreholes comprising over 1140 kilometres of core and non-core drilling.

The macromodel is reviewed during the year, with an official geological model provided to various customers (short and long-term planning and geology) annually. When considering geological and mining parameters to be used in the geological modeling process, various points of data are considered; best

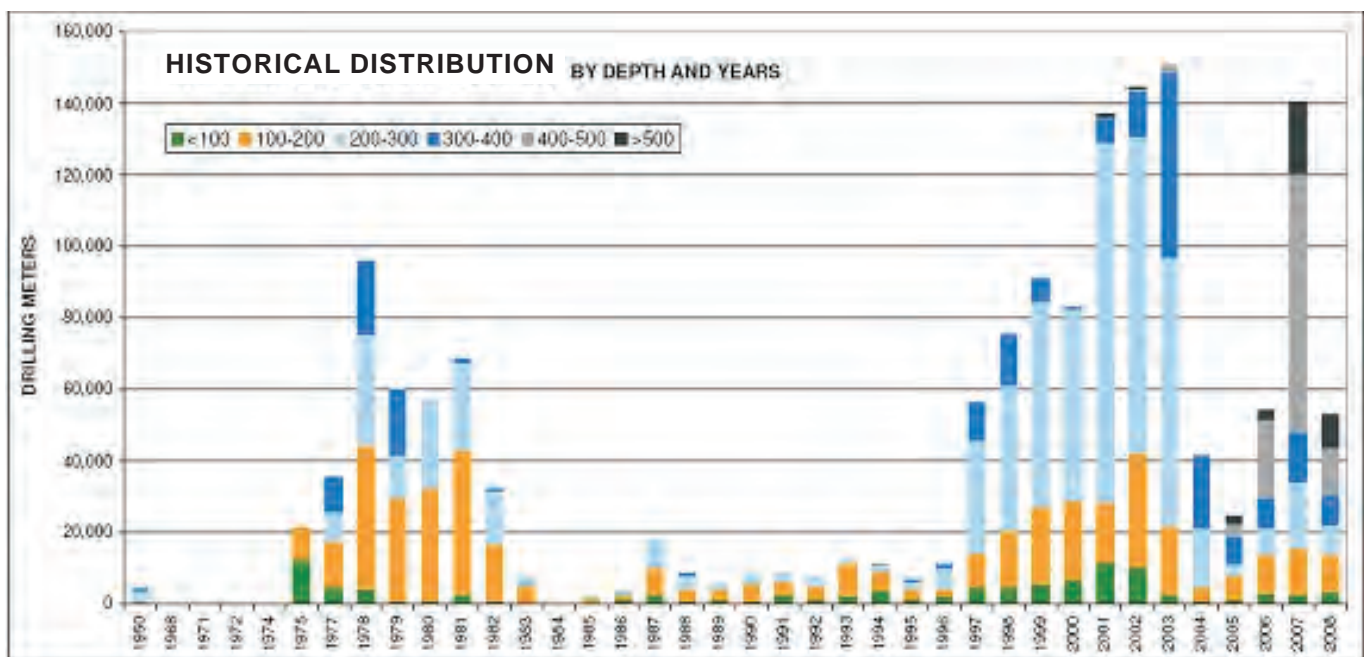


Figure 7: Historical drilling at in the Cerrejón deposit, showing the split by depth (1950 to 2008).

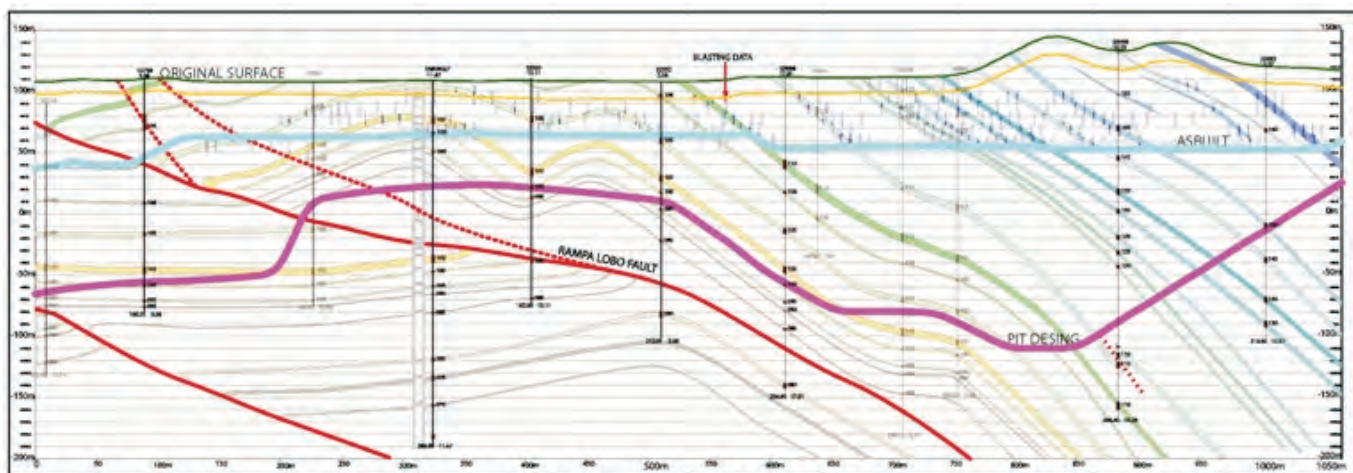


Figure 8: Typical geological cross section of the Tabaco anticline as depicted in the geological macromodel.

practice, historical performance, theoretical assumptions, in-pit measurements and controlled field experiments.

Mine geology

The macromodel, used for production planning and Life-of-Mine exercises does not sufficiently predict the day-to-day or micro scale geology required. In order to facilitate high coal seam recoveries in a structurally complex, thrust faulted environment, and over 50 coal seams, structural support and daily field mapping on a mining bench scale is essential. This is due to the irregular nature of the stratigraphy and structural environment, over relatively short distances. At present, there is a structural geologist assigned to each of the operating pits, collecting field data, providing in-pit assistance to the coal mining supervisors and aiding in the daily mining operations.

In order for the in-pit geologist to provide reliable information, daily seam roof and floor traces are mapped, structural data observations (including dip and strike) and seam thickness measurements are recorded (Figure 9). Geological mapping takes place before and after a coal face has been mined, delineating seam roof and floor, using a differentially-corrected handheld GPS. Additional to the in-pit mapping, the geologist observes and in some cases records the adherence to the coal mining standards or procedure. These standards include seam head cleaning, size of the waste and coal safety strips; procedures for cleaning high-dipping seams; and positioning of colored stakes to delineate authorized mining blocks. Traditional geological mapping is also carried

out ex-pit, when required assisting the geologist in the understanding and modeling of the structural style and geological landscape.

Once the geological points of observation have been recorded, the data is loaded into a GIS database where the seam roof and floor traces and structural observations are used to interpret and project the coal seams and relevant structure into advancing levels. This is currently being done in ArcGIS software. Geological cross sections are also generated from the macromodel, in Minex, where manual structural interpretations are done. These manual interpretations make use of blasting under-seam (BUS) data, which is also plotted on the section. BUS data is obtained from the geophysical logging of the blast holes in-pit, which gives a clear indication of seam traces and structure on a much smaller scale, as this blasting is done on a bench by bench basis.

Coal reconciliation

A production reconciliation exercise is carried out monthly, measuring actual production achieved against the geological model predictions (macromodel) both in terms of model Gross-Tons-In-Situ (GTIS) and Run-of-Mine (ROM). The reconciliation process involves taking monthly field measurement of advancing surfaces or areas with topographic survey, measuring the official coal production with dispatch records, as well as through inventory movements, and finally calculating the recovery and quality between the measured topographic surfaces. This information is garnered from or through the Minex macromodel. Recovery comparisons are



Figure 9: Series of photographs, illustrating the functions of the in-pit geologist (Ramón Daza). A: Structural points of observation, (dip and strike), B: Certified thickness measurements, and C: Seam traces with GPS.

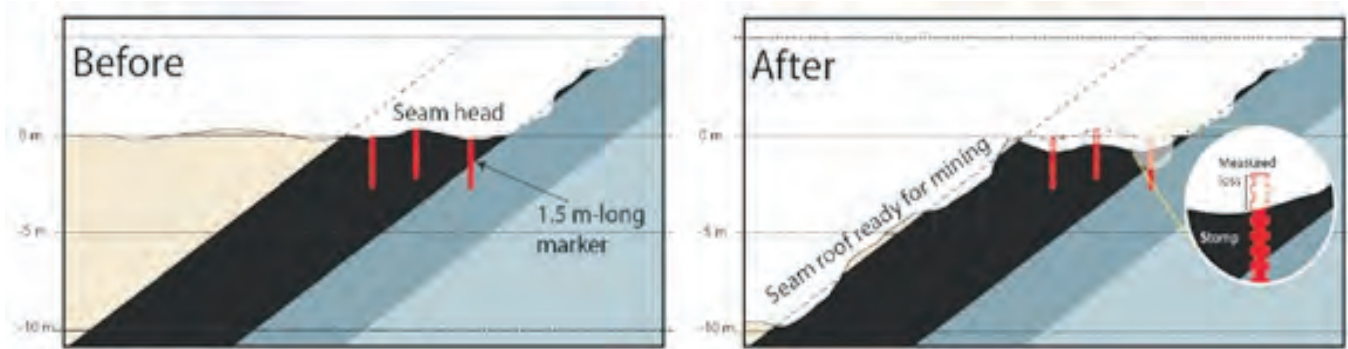


Figure 10: A schematic illustrating the position of the stakes placed in the coal seam head, before and after coal block exposure and cleaning.

then done on a seam-by-seam and pit-by-pit basis and summarized as an overall mine recovery. This recovery is tracked monthly and statistically by using the month actual, 3-month, 12-month and year-to-date averages.

In-pit experiments

Various in-pit experiments have been carried out at Cerrejón to better understand mining losses and recovery factors. Two primary experiments are the stakes and seam recovery experiments. The stakes experiment looks at the mining losses due to grading, cleaning the coal head, and road preparation which are particularly difficult to measure because blasting displaces all references. The seam recovery experiment serves two functions; one to check the accuracy of the macromodel on a smaller scale, and the second, to record, analyze and evaluate the mining practices used.

The stakes experiment was performed using wooden stakes, specially designed to break at 10 centimeter intervals, drilled into coal seam heads immediately after the mining equipment completed the loading of the coal seam at a mining face. The stakes were 1.5 metres long, painted with reflective colors and their position marked by GPS to facilitate easy recovery before mining the prepared coal block. The stakes thus record the losses that take place from the time the coal seam head was first exposed on the mining floor until the coal seam was fully exposed and ready to be mined (Figure 10).

The seam recovery experiment involved the accurate measurement of a prepared coal mining block from start to finish. Using topographic survey, structural points of data (dip and strike), certified thickness measurements, and recording all mining processes (equipment used, truck loads and timing). Coal trucks are weighed and the dispatch system, based on truck factors, is used for production tonnages, which are compared against the macromodel for recovery percentages.

Samples of clean coal, floor and roof interface are also taken and compared to the macromodel information. An interpreted version of the macromodel (using under-seam blasting information) is also used to compare to the actual production, providing a more accurate reflection of true recovery. This experiment thus gives an insight into the effectiveness of the

mining standards as well as macromodel accuracy on a small scale.

RESULTS — VALUE ADDED???

Micromodel

The 2-D micromodel, generated in ArcGIS from daily field mapping and observations, more accurately reflects the daily in-pit conditions and seam variation on a micro-scale when compared to the macromodel, which is used for modeling the deposit. As of the end of 2009, there were over 1,600 kilometres of seam traces in the database, and an example of the 2D micromodel map for one of the operation pits - Tabaco, is given in Figure 11. Maps, such as those shown in Figure 10, are distributed monthly as poster maps, and daily to relevant personnel as smaller field hand-outs. On a monthly basis, typical field traces and observation (per operating pit) amount to >2500 metres of seam traces, >50 points of structural observation and approximately eight certified thickness measurements.

Coal reconciliation and recovery

Since 2006, the overall annual recovery for all coal seams mined has increased from approximately 84% to more than 94% in 2009 (Figure 12). Due to this improvement and the continual improvement in the coal mining processes at Cerrejón, the coal seam recovery target for 2010, for all coal seams, is 95%, irrespective of pit depth and structural complexity.

In-pit experiments

The results of the stakes experiments showed, on average, a seam head loss of 45 centimetres irrespective of mining bench height, with some variations per pit: Tabaco high dip with 44 centimetres; Puente with 66 centimetres; Patilla with 32 centimetres; and Tabaco Extension with 37 centimetres. These losses were due to cleaning the seam head, traffic, grading and dozing in preparation for mining the seam block. In a 10 meter bench, this loss alone represents approximately 5% of all the available coal. Recent stake experiments in Patilla pit have shown an improvement, with seam head losses ranging between 10 and 30 centimetres.

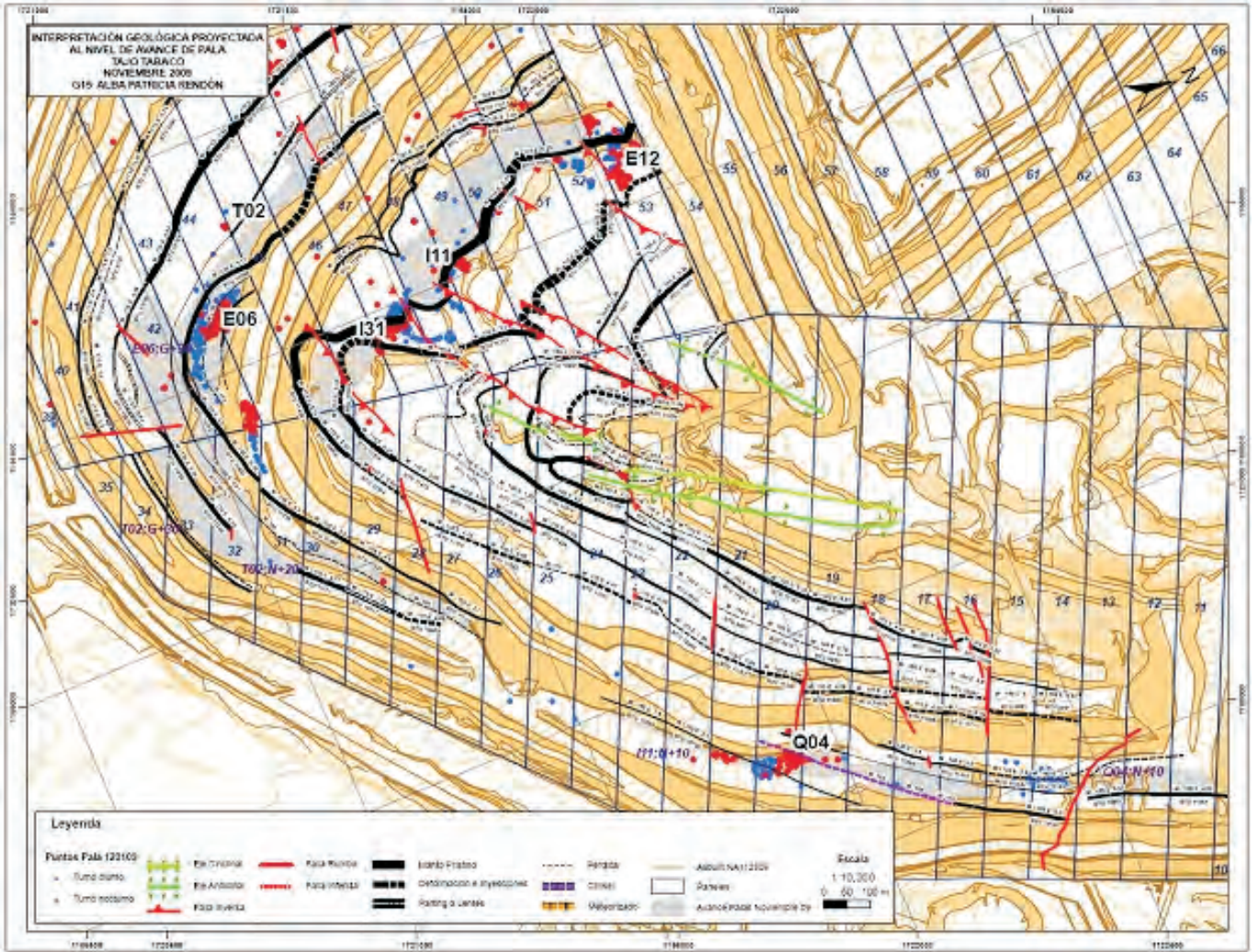


Figure 11: An example of the 2-D geological micromodel map of the Tabaco Pit.

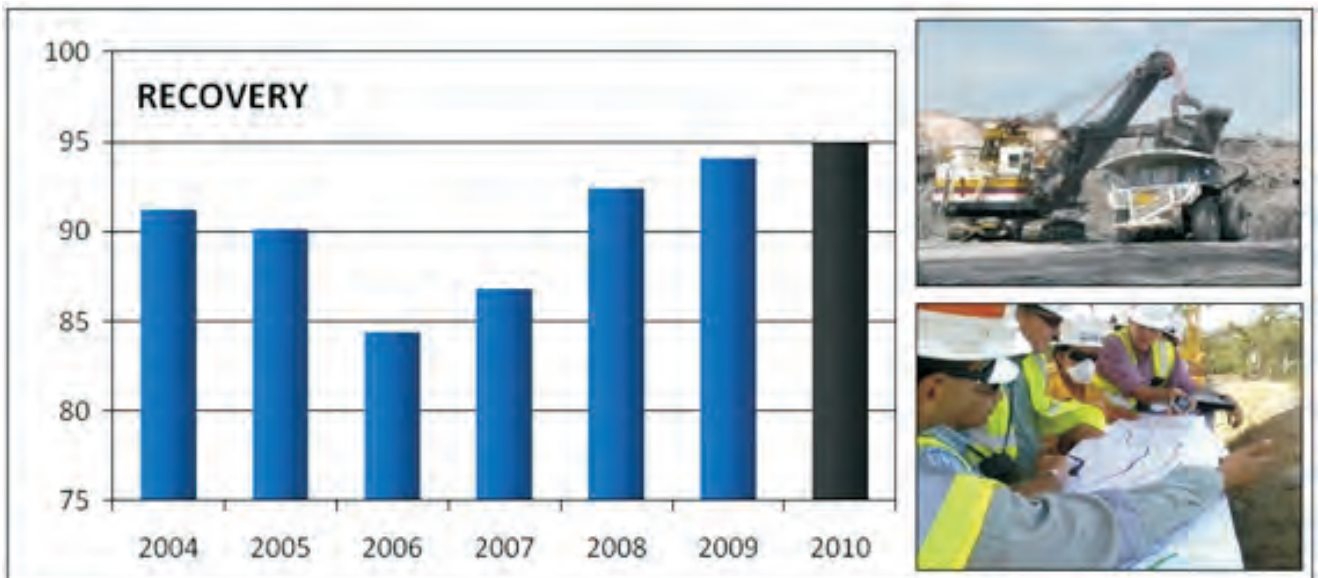


Figure 12: Graph showing the overall increase in recovery from 2006 to 2009, with the 2010 target indicated as the final black column.

Results from the seam recovery and model accuracy experiments are varied. Some field experiments show a relative accuracy in the macromodel and others show a marked difference. However, these differences are generally either stratigraphic or structural in nature. When analyzing the effectiveness of the mining standards, the overall importance of interface recovery is always highlighted.

DISCUSSION

Cerrejón is characterized by dipping coal seams, structurally complex geological domains, numerous coal faces, and mining on a large scale. In order to ensure optimal coal seam recovery in such a complex environment, the geology department at Cerrejón has found that following the process of macro geology to micro geology, though in-pit mapping and support has yielded the most beneficial results. This is most evident in the success of using the micromodel geological maps daily for structure support by the in-pit geologist and for coal mining by the coal mining supervisor. There has been an increased focus on getting the understanding of the smaller scale structures communicated to the relevant groups and departments to further realize the seam recovery and to also understand the implication on seam quality.

The Geology Department at Cerrejón assists the mining operation through the following:

- continual in-pit data gathering on a bench scale and the correct interpretation and communication of this information,
- resource estimation on an annual basis for the three Shareholders and continual improvement of the Minex geological macromodel,
- continual and accurate measurement and tracking of coal seam recovery performance,
- continuous checking of mining standards or procedures and factors through various in-pit experiments, and
- flow of information between Geology - Mine Planning - Mining - Coal Quality departments.

Through these fundamental steps, seam recovery can increase significantly, particularly in a structurally complex, massive mining operation such as Cerrejón.

FUTURE DIRECTIONS

A project is currently underway to further develop the micromodel data into a functional 3D geological model, with associated tonnages and seam qualities (similar to the macromodel, but capturing the micro-scale information). This project is dependent on identifying a suitable software platform able to handle the type of information currently used in the various platforms. A number of options are currently being evaluated.

The coal reconciliation process is constantly under review and analysis, to ensure the accurate measurement of pit features and mining parameters. Part of this review is to understand the implications of seam-by-seam variance on the accuracy of the macro and micromodels.

In-pit field experiments will be broadened in future to incorporate both mine planning adherence and down-stream quality process flow. An analysis of historical information is also currently under review.

REFERENCES

- CARBONES DEL CERREJÓN LIMITED, 2009: The Cerrejón Expansion to 40 MTPA Feasibility Study, in-house report, 2009.
- CARBONES DEL CERREJÓN LIMITED, 2010: Coal Mining Procedure, Cerrejón Standard, in-house report, 2010.
- FORTICH, H., 2008: Coal Recovery at Cerrejón, In *Anglo American Mining Conference*, Johannesburg.
- HERNANDEZ, G., 2009: Resource and Reserve Statement Report as of 31st December 2009. In, Carbones del Cerrejón Limited, in-house report, 2009.
- INTERNATIONAL ENERGY AGENCY, 2009: *Key World Energy Statistics*, 15.

Wes Nichols

Implementing a Stepchange in Safety Culture — a Case Study in Managing Safety

This paper documents the change process that occurred in the safety culture of team of people who provide the geological functions for a medium-sized company. The challenge was to take a geology and exploration team of around 45 people from their existing position of non-compliant safety culture (well below industry best practice) to a position of being, at least, equal with the leaders in the industry. This case study is a diary of events from my perspective that outlines the odyssey of applying the work process model to implement a step-change in safety practices.

1. INTRODUCTION

When I started working as Senior Geologist for the company, it owned two top-head-drive drill rigs, each with a water/rod truck and crew-cab F250 support vehicles. At the time, one of the drill rigs was 18 years old and the other was 4 years old.

There were three 3-person drill crews operating the two drill rigs on an 18-days-on/9-days-off hitch roster with 12 hour shifts. Some of the personnel had certificate 2 drilling qualifications, but none of the drillers had the required certificate 3 qualifications. Investigation into a process to upgrade these qualifications had been instigated prior to my taking over the position, but this process was not being actively progressed.

The drill rigs were in a less-than-desirable state. Guards were missing from components on the older drill rig. Neither rig had side-access platforms and the older rig had no access ladder for the rig deck. The deck on this older rig was being accessed by using a 20 litre drum as the step-up mechanism to climb onto it. The rotating drill rods in the mast were openly accessible while drilling — no safety cage was in place.

A maintenance plan was not in place — the rigs were being maintained when they broke down. Hydraulic leaks were tolerated and some of the essential daily lubrication was not being performed.

Incidents occurred regularly and there were a number of these with high potential ramifications, with one resulting in hospitalisation of an offsider for a few days.

While there was a lagging indicator process in place, not all incident reports were being completed. Toolbox meetings were not being conducted at regular intervals. SLAM books were available but were not being used.

The geology team was made up of disparate subsets (crews) that worked as discrete and separate units. The crews only met each other when they were working in the same area and staying at the same accommodation complex. Even then, they preferred to keep within their crews and tended not to mingle. To my knowledge, the crews had never all met together as an entire geology team. The team's morale required some work.

On the 11th of August 2008, I became Geology Manager and undertook the challenge to implement a process of change.

2. THE CHANGE PROCESS

I became aware of the the Work Process Model, also known as the Nertney wheel (Nertney & Bullock, 1976), during a generic surface induction that I completed in April 2008 (Anon, 2007). I recognised this as being a powerful tool and one that I could use to implement the changes required to improve the safety culture in the team.

The process I employed to manage the change was:

- a) treat each of the team individuals as an important member of a larger team; and
- b) use the work process model to implement the changes required.

3. BUILDING THE TEAM

On the 23rd of August 2008, I called a full team meeting. This was the first time that everyone in the geology team had been together in the same place to meet, converse and discuss issues together. The atmosphere was fairly tense and the individuals were cautious in their interactions with each other and expectations of what the outcomes would be.

The meeting consisted of a formal presentation session, with the final 3 hours of the day set aside for open discussion. During the meeting, the team members were told they were a team, the work process model was explained, a communication process/protocol was issued, the upcoming exploration plan was outlined and several corporate office personnel were invited to talk about issues ranging from the purchasing process to some of the corporate HR policies.

The atmosphere at the beginning of the afternoon session was electric. However, once the session started and people realised that it was an open-floor event where there were no restrictions and no recriminations, a myriad of issues manifest themselves, such as:

- low morale
- no systems in place (safety, cost management, maintenance, reporting, communication between crews/head office)
- distrust of management

It was amazing, but it set the starting position for my job ahead. This meeting was the catalyst for building a coherent team that worked towards safe production outcomes.

4. EFFECTING CHANGE

To effect change, buy-in must be obtained from the target audience. This is where applying the Work Process Model is important. This model sets out the requirements for people, equipment and work practices and the critical factor in making this work is support from upper management, especially for the costs that the process will involve.

At its core, the Work Process Model (WPM — Figure 1) has, and the desired target is, production — but it has to be safe production. This safe production is achieved by ensuring that the three key components that contribute to this core in the model (competent people, safe work practices and fit-for-purpose equipment) are maintained. The all-encompassing requirement surrounding the entire model is to ensure that there is a controlled and managed work environment (Anon, 2007).

So, as per the first component of the WPM, how did I ensure the team were competent (Anon, 2007)? I embarked on a process of:

- Identifying what each job entails (what skills and knowledge were required as well as any physical requirements) and developed procedures for these jobs
- Selecting the most suitable person for the job
- Determining what competencies each person had, what they needed to meet the requirements of their role, and identifying any gaps
- Providing training, and assessing the person's competence to fill the gaps
- Having the person authorised by the Site Senior Executive (SSE) to do the task
- Monitoring and evaluating performance
- Providing high quality supervision and support
- Identifying changes in the job that required further training and assessment

Implementing safe work practices (Anon, 2007), the second component of the WPM, is not an easy task. This requires a culture that includes safety as a way of doing work with the attitudes to match. If that culture does not already exist, it must be built. The key word in "safe work practices" is "practices". This means more than just "procedures". "Practices" requires procedures to be put into action and this must be maintained. I did this by allowing a culture of ownership to develop where the workers created and followed their own job instructions.



Figure 1: The Work Process Model

These job instructions (Standard Operating Procedures and Safe Work Procedures) came from two sources (Anon, 2007):

- at the work site level, via a formal risk assessment conducted by the work crew of the risks involved in the task (particularly Job Safety Analyses and Workplace Risk Assessment & Controls); and
- via the Safety & Health management System.

How is fit-for-purpose equipment (the third component in the WPM) achieved? For any given task, equipment should be suitable to carry out the job for which it is intended. Equipment should be designed, tested, installed, operated and maintained in a way that allows it to complete the task safely and efficiently (Anon, 2007).

For example, Figure 2a shows one of the drill rigs prior to upgrade. There were guards missing, there was no ladder to access the rig deck, there was no cage around the spinning rods at the rear of the rig and hoses were left lying in the work area.

Figure 2b shows the same rig after it was upgraded with the safety features in place (platforms with rails, rear deck access steps and rod cage at the rear) and a much tidier work area.

There are two aspects to achieving a planned and controlled work environment (this is the all-encompassing aspect of the WPM). The first is understanding and controlling the applicable physical parameters involved, such as the boundary of the work area (this can be achieved at the drill site by erecting a boundary) and the physical working conditions (e.g. temperature, weather, noise, dust, vibration and structure). The second is to understand and manage the critical components of the work cycle, such as work schedules, communication processes, cooperation, work allocations and work locations (Anon, 2007).



Figure 2a: Rig 2 before (August 2008)



Figure 2b: Rig 2 after upgrade (May 2009)

5. APPLYING THE WPM THEORY

To apply the theory, the company had to be convinced to address the three components of the WPM — all were identified as being deficient. To their credit, they did provide the resources to address them.

The repair and upgrade of the equipment, (drill rigs, support vehicles, etc.) to compliance level was the controlling factor. This took eight months where there was no production from that equipment!

During that eight month period, all personnel were involved in developing the required procedures. Also, their training gaps were identified and they were trained in the theory components of their courses to the required certificate levels. The practical component of their training could only be completed once the equipment came back online and this was implemented as soon as production recommenced.

6. MAINTAINING A SAFETY CULTURE

In my opinion, there are two aspects to safety. The first aspect, the most important aspect, is to develop the practices that ensure your team members go home at the end of the day in the same shape, or better, as when they turned up for work that morning.

The other aspect to safety is the evidential, “cover-your-back”, data collection (paperwork) side where evidence needs to be produced for proving, or disproving, a case in a court of law. This is important aspect of safety, and the data is generally used to define trends with incidents and safety performance. But, it is the aspect of safety that most people find to be laborious, interruptive, a nuisance and time-consuming. The implementation, monitoring and maintenance of a paperwork system requires a great deal of effort by way of explanation, example-setting, supervision and showing the users the benefits of such a system. One way to show the benefits is to provide feedback of the results from analysis of the data collected. This is done at our quarterly meetings.

To help change and maintain safety culture, a leader must be genuine and lead by example. Again, this is not an easy task. Shutting production down for eight months to do this is not advisable, but it definitely helped my cause in showing the team that I was genuine. I have facilitated their fit-for-purpose equipment, modelled safe work practices and helped them to gain their required competencies. As a consequence, the team is continuing to work cooperatively towards a controlled and managed work environment, and to perform to the appropriate standard.

Team leaders (supervisors and drillers) should be challenged as often as possible about the quality of their safety effort and how they are working towards developing a higher level of safety consciousness. Further, supervisors must be provided with the resources they need to allow them to provide high quality supervision. Supervisors should not be desk-bound which keeps them focusing on the evidential side of safety instead of being workplace-focused and working with, monitoring and managing their people. It took me quite a while to resolve this, but it’s progressing well now.

It’s important to applying realistic safety Key Performance Indicators (KPIs). Again, safety KPIs are implemented to data for analysis of trends in safety performance and to provide evidence that the safety system is working. Care must be taken to ensure that workplace safety recording is not seen purely as a chore. There is particular the danger for tick-and-flick systems such as SLAMs. However, if used correctly and continuously, these daily-use systems are an important driver of raising safety awareness levels and developing a good safety culture.

Establishing a Safety & Health Management System (SHMS) is mandated under that Coal Mining Safety & Health Act (1999). However, aside from the act, it simply makes good sense. A good system supports and promotes safe work

practices and is be able to establish, monitor and review itself to facilitate continuous improvement. I am still in the process of setting this system up. At the outset, I decided it was more important to focus on the culture of the team and to make sure they were able to look after themselves in the field so that they could return home safely each day. However, this is not to be at the expense of establishing a good SHMS — this is now my focus.

7. CONCLUSION

The Work Process Model played a key part in the in working towards safe production and developing a good safety culture in the workplace. I introduced the team members to this process and they incorporated it into their routine. As a result, the team has certainly matured a lot since we started the process back in August 2008.

At our quarterly geology team meeting, it is now standard practice that each of my drillers report their quarterly performance statistics (including safety statistics) in a powerpoint presentation. I believe that this is a level of professionalism that is unequalled in the industry. For example, I believe that it's the equivalent of a digger operator in charge of a mine pit crew making a presentation to management.

Moreover, my drillers understand what these statistics mean and are beginning to use them as a management tool to achieve safe production. The safety results are starting to highlight the marked improvement in our geology team's performance.

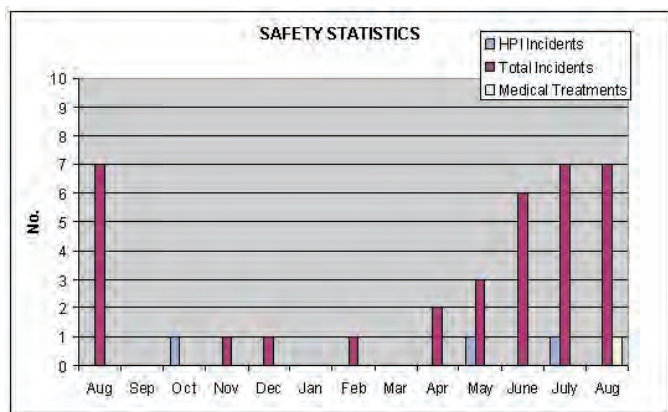


Figure 3: Safety statistics August 2009 – August 2010-09-21 (one year LTI free)

Table 1: Incident list August 2010 showing over-riding non-injury reporting

Unit	Incident Description
Drill Rig #3	<ul style="list-style-type: none"> Medical Treatment Injury (MTI) offsider twisted knee Oil Leak from hydraulic fittings on top head drive Haul plug on rod on trailer worn out
Drill Rig #4	<ul style="list-style-type: none"> Oil filler cap dislodged from engine on Rig 4 water truck Grab cylinder not locking in correctly and cracks detected in A frame of mast
Light Vehicles	<ul style="list-style-type: none"> Flat tyre on a logging truck Small crack on the windscreen of logging truck

In August 2010, the team of 45 people (including full-time staff and contracting staff) have achieved one year lost time injury free and are maintaining this position at present. Their incident reporting is now at a level where non-injuries outnumber injury-related reports. Further, the crew members are now demanding a higher level response of me and my management team.

Another significant outcome has been the result of an audit by a government Inspection Officer in December 2009. It was the first time he did not have to shut a rig down. In his report, he commended our efforts and was impressed by both the condition of the equipment and with the standard of safety practices in place.

The challenge from here on is to strive for continuous improvement in our safety culture and our level of professionalism. The danger is to become complacent. There's been a good start and a step-change in safety culture has occurred. However, there's still a lot of work to do.

REFERENCES

- NERTNEY, R.J. & BULLOCK, M.J., 1976: *Human Factors in Design*. US Dept of Energy, Systems Safety Development Centre: EG&G Idaho Falls USA.
- ANON, 2007: Topic 11: Summing up – The Work Process Model. In: *Generic Induction – Coal Core*, Mining Industry Skills Centre Inc., Brisbane (www.miskillscentre.co.au).
- Queensland Government, 2010: *Coal Mine Safety and Health Act 1999*. Reprint 3D, Queensland Government Printer (GoPrint), Brisbane.

BOOK IN THE BLACK

PARADISE

ISBN 978-0-646-54347-5